

Insular adaptations in the appendicular skeleton of Sicilian and Maltese dwarf elephants

Matthew Edward Scarborough

A thesis presented for the Degree of

DOCTOR OF PHILOSOPHY

In the Department of Biological Sciences

Faculty of Science

University of Cape Town

October 2020



The copyright of this thesis vests in the author. No quotation from it or information derived from it is to be published without full acknowledgement of the source. The thesis is to be used for private study or non-commercial research purposes only.

Published by the University of Cape Town (UCT) in terms of the non-exclusive license granted to UCT by the author.

The copyright of this thesis vests in the author. No quotation from it or information derived from it is to be published without full acknowledgement of the source. The thesis is to be used for private study or non-commercial research purposes only.

Published by the University of Cape Town (UCT) in terms of the non-exclusive license granted to UCT by the author.

This research was supported by the South African National Research Foundation (Grant no. 83352).

The only scientific man I saw in London was Falconer, who goes to Sicily in October. He was very full about a tiny new species of Elephant from Malta not much larger than a calf!

- Charles Darwin

(Letter to Sir Charles Lyell, 28 August 1860)

Falconer has made out clearly the former existence of a small elephant, the size of a Shetland pony, in the small island of Malta. They have also found a hippopotamus there, and a gigantic dormouse the size of a rat...

- Charles Lyell

(Letter to Sir John William Dawson, 27 October 1860)

Three fossil elephants were determined by Dr. Falconer and Professor Busk, from the remains sent home by Mr. Adams. The largest of these would have stood about 7 feet high...while the smallest was not more than 2 feet 6 inches to 3 feet! ...We have here a very striking exception to the rule of extinct being larger than existing species.

- Alfred Russel Wallace

(Review of *Notes of a Naturalist in the Nile Valley and Malta*, 1 July 1871)

This thesis describes original research undertaken towards the degree of
DOCTOR OF PHILOSOPHY
at the University of Cape Town, which has not been submitted in any form
towards a degree at another university. I submit it as my own work and
acknowledge all assistance received.

Supervised by

Anusuya Chinsamy-Turan and Maria Rita Palombo

October 2020

Declaration

Thesis title: Insular adaptations in the appendicular skeleton of Sicilian and Maltese dwarf elephants

I, Matthew Edward Scarborough hereby

- . (a) Grant the University of Cape Town free license to reproduce the above thesis in whole or in part for the purpose of research;
- . (b) Declare that:
 - (i) The above thesis is my own unaided work, both in concept and execution, and that apart from the normal guidance from my supervisors; I have received no assistance except as stated in the Acknowledgements.
 - (ii) Neither the substance nor any part of the above thesis has been submitted in the past, or is being, or is to be submitted for a degree at this university or at any university.

I am now presenting the thesis for examination for the Degree of PhD.

Signed: [MES]

Signed by candidate

Date: 3 October 2020

Abstract

This thesis investigates the evolution of Pleistocene insular proboscideans from the central-western Mediterranean (*Palaeoloxodon* species from Sicily, Malta, Favignana) and a mammoth (*Mammuthus lamarmorai*) from Sardinia, with a particular emphasis on the anatomy of the limbs. Differences in the morphology of the limbs are examined across a ten-fold reduction in mass (from 3,5m-tall *P. antiquus* from Germany to 1,2 m-tall *P. ex gr. P. falconeri* from Spinagallo Cave, Sicily), revealing insights into significant morphological changes in the long and foot-bones, particularly appendicular changes evident in Siculo-Maltese *P. ex gr. P. falconeri*. Notable morphological differences between *P. antiquus* and its insular descendent *P. ex gr. P. falconeri* include the functional morphology of the ankle-joint (especially the calcaneus' articular facet for the tibia). Furthermore, morphological similarities found between the femur of young continental elephants (*P. antiquus* and *L. africana*) and adult insular dwarfs (*P. ex gr. P. falconeri* and its probable ancestor *Palaeoloxodon* sp. from Luparello Fissure, Sicily) suggest evidence of paedomorphism in the limbs. Similarly, comparisons of the ontogenetic allometry of the tibia in *L. africana* and *P. ex gr. P. falconeri* include changes which are also consistent with paedomorphism, although other factors could not be ruled out. In the humerus large differences are evident in the morphology of the deltoid tubercle between co-generic insular *Palaeoloxodon* species, suggesting interspecific differences in the musculo-skeletal system. Furthermore, on the basis of dimensions, morphology and stratigraphy, the large *Palaeoloxodon* sp. remains from Luparello Fissure, north-western Sicily are suggested to belong to the ancestral chronospecies of *P. ex gr. P. falconeri* from Sicily, which may have subsequently colonized Malta during the reduced sea-levels of a Middle Pleistocene glacial lowstand (following a corridor with reduced distances between the two islands). Additionally, morphological differences in the calcanei of elephants from Luparello Fissure, Sicily, and Benghisa Gap, Malta may be the result of allopatric speciation between similar-sized elephants during the Middle Pleistocene, or alternatively relate to ecomorphology. These findings suggest that the morphology of the calcaneus may be more informative than hitherto recognised for resolving systematics and taxonomy among the Elephantini. Furthermore, although the absolute chronology of Siculo-Maltese elephants remains poorly constrained, preliminary U-Th dating at Alcamo Quarry, western Sicily suggests a tentative early Middle Pleistocene age for *Palaeoloxodon* sp.

Acknowledgements

Over the past eight years I have been fortunate to receive the generous and much-needed support of friends, family and colleagues, including many new acquaintances; all of whom contributed in their own way to the successful completion of this thesis:

To my supervisor Anusuya Chinsamy-Turan (University of Cape Town) I would like to say a huge thank-you for encouraging me to undertake a PhD in the first place, and being a constant source of encouragement and support. Your mix of cheerful breeziness and shrewdly skilled guidance never ceased to amaze me. Thank you for the many hours spent in discussion, entertaining dinners at your home and for somehow always managing to find time in a busy schedule - your generosity is appreciated more than you know. To my co-supervisor Maria Rita Palombo (La Sapienza University, Rome) I am extremely grateful for entertaining a request out of the blue to study dwarf elephants by a complete stranger. Your kindness in patiently and skilfully guiding me through the research, breadth of scientific knowledge and the many days spent in your Rome office poring over fossil specimens together in animated discussion are among the most memorable experiences - thank you so much.

Three examiners were kind enough to provide detailed feedback on the thesis. These criticisms and comments were extremely valuable for improving the scientific integrity of its conclusions. Thank you so much for giving your time and sharing your hard-won expertise and experience.

This research would not have been possible without the kind support of the collections managers who gave so generously of their time during research trips: Francesco Sciuto and Antonietta Rosso (Department of Geological Sciences, University of Catania) for your kindness and warm hospitality during three visits. Thanks goes to Carolina Di Patti (Gemellaro Museum, Palermo) and all the museum staff for your kindness during two visits, the tours of local caves, help dismantling museum displays, and making my two visits to Palermo particularly enjoyable. In Paris thanks goes to Stéphanie Renault (Muséum national d'Histoire naturelle) for assistance in locating and cataloguing specimens in the bowels of your museum and making my visit a very enjoyable experience. In Rome thanks goes to Linda Riti (Museo di Palaeontologia, La Sapienza) for your kindness in locating specimens during five productive visits to Rome.

In London thanks goes to Pip Brewer (Department of Earth Sciences, Natural History Museum) for generously giving your time during my visit, and to Adrian Lister and Victoria Herridge for instructive and very interesting discussion. Across the channel my gratitude also goes to Loïc Costeur and Martin Schneider (Naturhistorisches Museum Basel) for your very gracious willingness to help during three visits. In Germany thanks especially goes to Harald Meller and Roman Mischker (Landesmuseum für Vorgeschichte, Halle), for hospitality and the kind offer to use the museum's guest-room, which made the experience of studying your collections very profitable and enjoyable. In Kenya thanks goes to Ogeto Mwebi and museum staff (National Museums of Kenya, Nairobi) for your constant willingness to be of assistance

during an extended visit. Finally, thanks also to Denise Hamerton (Iziko Museums, Cape Town) for locating and loaning comparative material.

No PhD would be complete without its own unique set of challenges: although it was meant to take 3-4 years, it ended up being a mammoth eight years (!) because of what started out as an annoyingly incurable sore-throat, that slowly developed into full-blown fibromyalgia - a poorly understood medical condition which causes inflammation in the brain and nervous system, making it impossible to concentrate for any length of time without becoming nauseous. I am particularly grateful to those who supported me during this period. During this stretch I became well-acquainted with a somewhat experimental (and mostly off-label) cocktail of antivirals, antibiotics, antidepressants, antihistamines, anti-seizure and diabetes medication, *Cannabis sativa* oil, Transcranial Magnetic Stimulation (a large electromagnet which sends pulses through your brain), 73 and a half hours of Hyperbaric Oxygen Therapy (picture being squeezed into a coffin-shaped Perspex tube which is pumped full of pressurised air), and a tonsillectomy. I am particularly grateful to the people who supported me during this period: in particular my wife Lina, who earned us an income, supported and nursed me on countless occasions; and the particularly generous and nameless friend who covered the very considerable medical bills (you know who you are); as well as the many doctors without whose expert treatment I would not have been able to have complete the project. I shall forever be grateful for your support.

On the numerous research trips to Rome Federica Marano and Roberto Rozzi provided excellent company on many long days in the office and museum. Emanuela Di Martino (formerly the University of Catania, now the Natural History Museum, London) was kind enough to assist in cataloguing and measuring tibiae from the Spinagallo Cave assemblage. For accommodation during trips overseas I would also like to express my thanks to Elena Strehler, Joel, Bea and Joshua Meier (Switzerland), and Alecia, Jamie and Robbie Dawson (England) for their hospitality during extended trips. A big thank-you also goes to Peter and Barbara Anderson for allowing me the run of your home and caravan during the years of my PhD - much appreciated. To Thomas and Ester Scarborough I would also like to say thank-you for your wisdom and moral support throughout the PhD, it meant a lot. Lina Scarborough, my Sweetheart - I met you half way through, and it wouldn't have been half as enjoyable without you by my side! I hope you derived some enjoyment from the experience too.

Expert input was provided by Robyn Pickering (formerly School of Earth Sciences, University of Melbourne, now the Department of Geological Sciences, University of Cape Town) and John Hellstrom (University of Melbourne) for generous assistance in U-Th dating; Petrus Le Roux (Department of Geological Sciences, UCT) for expert input and introduction to experts in different fields. Thanks also goes to Ebru Albayrak (American Museum of Natural History) and Federica Marano for making photographs and measurements of *P. antiquus* from Neumark-Nord, Germany available. For technical assistance and help in producing anatomical illustrations thanks goes to Jens Gerntholz, Florian Reiner, Nikki Horn and especially Angela Moore for skilfully assisting with Photoshop.

For assistance with statistics my gratitude goes to Ushma Galal, Reshma Kassanje and Anneli Hardy (Statistical Consulting Services, Department of Statistical Sciences, UCT for countless consultations and your patient and instructive help (none of whom accept responsibility for the correctness of results). Sugnet Lubbe (Department of Statistical Sciences, UCT) was kind enough to make her R code for PCA and CVA biplots available. Thanks also to Bongiwe Ndamane of UCT's Postgraduate Funding Office who was kind enough to handle all matters relating to funding. This research was made possible by the generous assistance of the National Research Foundation which provided financial support over three years and a travel grant to attend the *6th International Conference on Mammoths and their Relatives* in Greece (Grant no. 83352).

Last but not least, my grateful thanks goes to the friends and family who provided the financial, moral and practical support during twelve years of study in South Africa and England from Bachelors to PhD. They say you've never lived until you've done something for someone who can never repay you. May you be richly blessed.

Table of contents

Declaration.....	i
Abstract.....	ii
Acknowledgements.....	iii
Table of Contents.....	vi
List of Figures.....	x
List of Tables.....	xix

Chapter 1: The pattern and process of elephant evolution on the Siculo-

Maltese Palaeo- archipelago.....	1
1.1 Introduction.....	2
1.2 Origins of the Elephantidae and island biogeography of <i>Mammuthus</i> and <i>Palaeoloxodon</i>	2
1.3 Phylogeny and palaeogeographic context of Siculo-Maltese elephants.....	7
1.4 Insular environments as a key for investigating adaptive mechanisms.....	9
1.4.1 The causes of dwarfism in insular elephants.....	10
1.5 Rationale and aim of the study.....	13
1.5.1 Appendicular changes in Siculo-Maltese elephants.....	13
1.6 Hypotheses.....	14
1.7 Thesis layout.....	19

Chapter 2: Materials and methods.....20

Part 1: Materials.....	21
2.1 <i>Palaeoloxodon antiquus</i> (FALCONER and CAUTLEY 1847).....	22
2.1.1 <i>Palaeoloxodon antiquus</i> from Neumark-Nord Lake 1, Sachsen- Anhalt, Germany.....	22
2.2 Siculo-Maltese <i>Palaeoloxodon</i> species and their biochronology	23
2.2.1 <i>Palaeoloxodon</i> sp. 1 from Luparello Fissure, Sicily.....	27
2.2.2 <i>Palaeoloxodon</i> ex gr. <i>P. falconeri</i> (BUSK 1867) from Luparello Fissure, Sicily.....	29
2.2.3 <i>Palaeoloxodon</i> ex gr. <i>P. falconeri</i> from Spinagallo Cave, Sicily.....	29
2.2.4 Size variation in the <i>Palaeoloxodon</i> spp. assemblage from Spinagallo Cave.....	30
2.2.5 Spinagallo Faunal Complex.....	31
2.2.6 <i>Palaeoloxodon</i> ex gr. <i>P. mnaidriensis</i> from Puntali Cave, Sicily.....	33
2.2.7 Maccagnone and Grotta San Teodoro-Pinanetti Faunal Complexes.....	34
2.2.8 <i>Palaeoloxodon</i> sp. 2 from Faraglione Cave, Favignana Island.....	36
2.3 <i>Mammuthus lamarmorai</i> (MAJOR 1883) from Gonnese, Sardinia.....	36
2.4 <i>Loxodonta africana</i> (BLUMENBACH 1797) from Kenya.....	37
2.5 Materials studied.....	38
Part 2: Methods.....	43
2.6 The study of allometry in proboscidean evolution.....	43
2.6.1 Statistical methods in the study of allometry.....	44

2.6.2	Selection of measurement locations.....	48
2.7	Measurement of the shoulder and long bones.....	49
2.7.1	Measurement of the tibia.....	49
2.7.2	Measurement of the scapula's glenoid fossa.....	50
2.7.3	Measurement of the humerus.....	50
2.7.4	Measurement of the ulna.....	50
2.7.5	Measurement of the femur.....	50
2.8	Measurement of the carpals.....	51
2.8.1	Measurement of the ulnar carpal.....	51
2.8.2	Measurement of the intermediate carpal.....	52
2.8.3	Measurement of the radial carpal.....	52
2.8.4	Measurement of the os carpale III.....	53
2.9	Measurement of the tarsals.....	53
2.9.1	Measurement of the astragalus.....	53
2.9.2	Measurement of the calcaneus.....	54
2.9.3	Morphometry of the tibio-fibular facet.....	54
2.9.4	Measurement of the central tarsal.....	55
2.9.5	Measurement of the os tarsale IV.....	55
2.10	Measurement of the metapodials.....	56
2.10.1	Measurement of the metacarpal III.....	56
2.10.2	Measurement of the metacarpal IV.....	56
2.10.3	Measurement of the metatarsal IV.....	56
Chapter 3: Insular adaptations in the feet.....		57
3.1	RESULTS.....	62
3.1.1	Ulnar carpal.....	62
3.1.1.1	Intraspecific variability in the ulnar carpal of <i>P. ex gr. P. falconeri</i> from Spinagallo Cave.....	63
3.1.1.2	Interspecific comparison of the ulnar carpal.....	66
3.1.2	Intermediate carpal.....	68
3.1.3	Radial carpal.....	70
3.1.4	Os carpale III.....	73
3.1.4.1	Intraspecific variability in the <i>P. ex gr. P. falconeri</i> os c. III from Spinagallo Cave.....	74
3.1.4.2	Interspecific comparison of the os c. III.....	74
3.1.5	Astragalus.....	80
3.1.6	Calcaneus.....	85
3.1.6.1	Variation in the presence/absence of the tibial facet.....	87
3.1.6.2	PCA of the <i>Palaeoloxodon</i> spp. calcaneus.....	90
3.1.6.3	Dimensional and morphological differences between the calcaneus of <i>Palaeoloxodon</i> sp. 1 from Luparello Fissure and <i>P. ex gr. P. falconeri</i>	94
3.1.6.4	Possible ontogenetic allometry in the calcaneus of <i>P. antiquus</i> and <i>L. africana</i>	96

3.1.7	Central tarsal.....	98
3.1.8	Os tarsale IV.....	104
3.1.9	Metapodials.....	108
3.1.9.1	Metacarpal III.....	108
3.1.9.2	Metacarpal IV.....	111
3.1.9.3	Metatarsal IV.....	112
3.2	DISCUSSION.....	112
3.2.1	Evolution and functional significance of the calcaneus' tibio-fibular facet.....	113
3.2.2	Adaptive mechanisms in the tarsals of insular <i>Palaeoloxodon</i> spp.....	114
3.2.3	Limitations of classifying developmental stages in foot bones.....	115
3.2.4	Gross manual and pedal functional morphology and possible autapomorphies.....	115
3.3	CONCLUSIONS.....	119
Chapter 4: Insular adaptations in limb musculoskeletal anatomy.....		121
4.1	RESULTS.....	123
4.1.1	Bivariate allometry of the scapula's glenoid fossa.....	123
4.1.1.1	Intraspecific variability in <i>P. ex gr. P. falconeri, P. antiquus</i> and <i>L. africana</i>	123
4.1.1.2	Interspecific bivariate allometry.....	126
4.1.2	Anatomy of the humerus.....	126
4.1.2.1	Cranial profile of the humerus.....	127
4.1.2.2	Morphology of the deltoid fossa.....	133
4.1.2.3	Interspecific bivariate allometry.....	135
4.1.3	Anatomy of the ulna-radius.....	138
4.1.3.1	Radio-ulnar synostosis.....	139
4.1.3.2	Interspecific bivariate allometry	143
4.1.4	Anatomy of the femur.....	143
4.1.4.1	Cranial and medial profiles.....	150
4.1.4.2	Position and morphology of muscle scars.....	151
4.1.4.3	Interspecific bivariate allometry.....	152
4.1.5	Anatomy of the tibia.....	155
4.1.5.1	Interspecific variation in the tibia.....	155
4.1.5.2	Cranial profile and external characteristics.....	155
4.1.5.3	Bivariate allometry in adult <i>Palaeoloxodon</i> spp.....	164
4.1.5.4	Contrasting ontogenetic series in <i>P. ex gr. P. falconeri</i> and <i>L. africana</i>	167
4.1.5.5	Intraspecific variability in <i>P. ex gr. P. falconeri</i> from Spinagallo Cave.....	168
4.2	DISCUSSION.....	174
4.2.1	Scapula's glenoid fossa.....	174
4.2.2	Humerus.....	175

4.2.3	Ulna and radius.....	178
4.2.4	Femur.....	178
4.2.5	Tibia.....	180
4.2.6	Scaling.....	183
4.3	SUMMARY AND CONCLUSIONS.....	183
Chapter 5: Discussion		185
Part I: DISCUSSION ABOUT HYPOTHESES.....		186
5.1	Hypothesis III in the scapula.....	186
5.2	Hypotheses II and III in the long bones.....	186
5.2.1	Morphology of the humerus.....	187
5.2.2	Morphology of the ulna-radius.....	189
5.2.3	Morphology of the femur.....	190
5.2.4	Morphology of the tibia.....	192
5.3	Hypothesis II in <i>P. ex gr. P. falconeri</i> from Spinagallo Cave.....	193
5.4	Hypothesis III in the carpals and tarsals.....	195
5.4.1	Tarsal morphology in relation to body mass.....	196
5.4.2	Low-gear locomotion in the feet of <i>P. ex gr. P. falconeri</i>	199
Part II: DISCUSSION ABOUT CHRONOLOGY AND SYSTEMATICS.....		200
5.5	Preliminary U-Th dating of <i>Palaeoloxodon</i> sp. from Alcamo Quarry, Sicily.....	200
5.6	New insights into <i>Palaeoloxodon</i> sp. 1 from Luparello Fissure, Sicily.....	200
5.6.1	The uncertain chronological position of <i>Palaeoloxodon</i> sp. 1.....	200
5.6.2	Morphological differences between <i>Palaeoloxodon</i> sp. 1 and <i>P. ex gr. P. falconeri</i>	201
5.6.3	Systematics and taxonomy of <i>Palaeoloxodon</i> sp. 1.....	201
5.6.5	Concluding remarks on <i>Palaeoloxodon</i> sp. 1.....	203
Chapter 6: Conclusions		204
6.1	Concluding remarks.....	204
6.2	Proposals for further research.....	207
6.3	The major findings of this study.....	210
References cited		211
Appendix A: Systematics and taxonomy		239
A1	Partial synonymy of Siculo-Maltese taxa with notes on systematic uncertainties.....	241
A1.1	<i>Palaeoloxodon mnaidriensis</i> (ADAMS 1874) from Mnaidra Gap, Malta.....	241
A1.2	<i>Palaeoloxodon falconeri</i> (BUSK 1867) from Malta and Sicily.....	242
A2	Partial synonymy of Siculo-Maltese taxa of uncertain systematic position.....	243
A2.1	<i>Palaeoloxodon antiquus leonardi</i> (AGUIRRE 1969a) from Via Libertà, Sicily.....	244

A2.2	<i>Palaeoloxodon</i> ex gr. <i>P. mnaidriensis</i> (ADAMS 1874) from Puntali Cave, Sicily.....	244
A2.3	<i>Palaeoloxodon</i> sp. 1 from Luparello Fissure, Sicily.....	245
A 2.4	<i>Palaeoloxodon</i> sp. 2 from Faraglione Cave, Favignana Island.....	246
A3	Phylogeny of Siculo-Maltese elephants.....	246
A4	Partial synonymy of <i>Mammathus lamarmorai</i> (MAJOR 1883) from Gonnese, Sardinia.....	248
Appendix B: Uranium-Thorium dating at Alcamo Quarry, Sicily.....		249
Appendix C: Insular endemic mammals with alleged evidence of low-gear locomotion.....		253
Appendix D: Preliminary catalogue of the unaccessioned <i>Palaeoloxodon</i> sp. remains from Luparello Fissure, Sicily in the Vaufrey collection.....		255
Appendix E: Regression table.....		260
Appendix F: Scaling in <i>Palaeoloxodon</i> long bones.....		264

List of figures

Figure 1.1	Mediterranean islands with <i>Palaeoloxodon</i> and <i>Mammuthus</i> spp.....	6
Figure 1.2a)	Palaeogeography of Sicily and Calabria during the Late Pliocene- Early Pleistocene.....	7
b)	Approximate palaeogeography of the Siculo-Maltese Palaeoarchipelago during the Last Glacial Maximum.....	7
Figure 1.3	Tentative phylogeny of proboscideans included in this study.....	8
Figure 1.4	Tibiae of adult Sicilian <i>Palaeoloxodon</i> spp. in cranial aspect.....	18
Figure 2.1	Sicilian and Maltese localities with elephant remains studied in this thesis.....	24
Figure 2.2	Luparello Fissure, Palermo, Sicily.....	28
Figure 2.3	Standing section of Vaufrey's excavation of Luparello Fissure, Sicily.....	28
Figure 2.4	Mounted composite skeletons of <i>P. ex gr. P. falconeri</i> from Spinagallo Cave, Sicily.....	30
Figure 2.5	Composite reconstruction of <i>P. ex gr. P. falconeri</i> from Spinagallo Cave, Sicily.....	31
Figure 2.6a)	Entrance to main chamber of Spinagallo Cave, escarpment of the Hyblean Plateau, south-eastern Sicily.....	32
b)	Spinagallo main chamber and entrance to the excavated lower cavern.....	32
c)	View from the interior of the excavated lower cavern.....	32
Figure 2.7	Mounted composite <i>P. ex gr. P. mnaidriensis</i> skeleton from Puntali Cave, Sicily.....	34
Figure 2.8a)	Entrance to Puntali Cave, Carini, north-western Sicily.....	35
b)	Interior view of the first chamber, facing the entrance.....	35
Figure 2.9	Isometry, positive and negative allometry as defined in relation to the generalized allometric equation $y = ax^b$	47
Figure 2.10	Measurements on the tibia.....	49

Figure 2.11	Measurements on the scapula.....	50
Figure 2.12	Measurements on the humerus.....	50
Figure 2.13	Measurements on the ulna.....	50
Figure 2.14	Measurements on the femur.....	50
Figure 2.15	Measurements on the ulnar carpal.....	51
Figure 2.16	Measurements on the intermediate carpal.....	52
Figure 2.17	Measurements on the radial carpal.....	52
Figure 2.18	Measurements on the os c. III.....	53
Figure 2.19	Measurements on the astragalus.....	53
Figure 2.20	Measurements on the calcaneus.....	54
Figure 2.21	Measurement of the fibular and tibial articular facets on the calcaneus.....	54
Figure 2.22	Measurements on the central tarsal.....	55
Figure 2.23	Measurements on the os t. IV.....	55
Figure 2.24	Measurements on the mc III.....	56
Figure 2.25	Measurements on the mc IV.....	56
Figure 2.26	Measurements on the mt IV.....	56
Figure 3.1	Articulated manus of:	
	A) <i>P. antiquus</i> from Riano, Italy.....	59
	B) <i>P. ex gr. P. falconeri</i> from Spinagallo Cave, Sicily.....	59
	C) <i>M. lamarmorai</i> from Gonnese, Sardinia.....	59
Figure 3.2	Articulated pes of:	
	A) <i>P. antiquus</i> from Neumark-Nord 1, Germany.....	60
	B) <i>P. ex gr. P. falconeri</i> from Spinagallo Cave, Sicily.....	60
	C) <i>M. lamarmorai</i> from Gonnese, Sardinia.....	60
Figure 3.3	Figure legend for species studied in Chapters 3 and 4.....	61
Figure 3.4	Size-frequency histograms of the ulnar carpal of <i>P. ex gr. P.</i> <i>falconeri</i> from Spinagallo Cave.....	63
	a) Max anterior height (pr-d)	63
	b) Ratio of the breadth (m-l)/length (a-p) of the articular facet for the ulna.....	63
Figure 3.5a)	Principal Component Analysis of the ulnar carpal of <i>P. ex gr. P.</i> <i>falconeri</i> from Spinagallo Cave.....	64
	b) Log-transformed principal Component Analysis of the ulnar carpal of <i>P. ex gr. P. falconeri</i> from Spinagallo Cave.....	65
Figure 3.6	Scatterplots of the dimensions of the ulnar carpal.....	67
	a) Max breadth (m-l) vs. max anterior height (pr-d)	67
	b) Max breadth (m-l) vs. max length (a-p) of articular facet for the ulna.....	67
	c) Dimensions of the articular facet for the accessory carpal.....	67
	d) Ratio of the dimensions of the articular facets for the accessory carpal and ulna.....	67
	e) Max cranial height (pr-d) vs. allometry of the articular facet for the ulna.....	68

Figure 3.7	Box-and-whisker plot of the ratio of the ulnar carpal's articular facet for the ulna (max breadth (m-l)/max length (a-p))	68
Figure 3.8	Scatterplots of the dimensions of the intermediate carpal.....	69
a)	Breadth (m-l) of the articular facet for the radius vs. max thickness (a-p).....	69
b)	Symbol legend.....	69
c)	Max breadth (m-l) vs. breadth (m-l) of the articular facet for the radius.....	69
d)	Max breadth (m-l) vs. max thickness (a-p)	69
Figure 3.9a-e)	Radial carpal in medial aspect, illustrating differences in the angle between the articular facet for the radius and the articular facet for the os c. II.....	71
f)	Scatterplot of the max length (pr-d) vs. angle between articular facets for the radius and os c. II.....	71
Figure 3.10	Scatterplots of the dimensions of the radial carpal.....	72
a)	Distal thickness (a-p) vs. max height (pr-d) with distal end horizontal.....	72
b)	Distal thickness (a-p) vs. max length (pr-d) of anterior side of radial carpal.....	72
c)	Distal thickness (a-p) vs. max length (pr-d) of proximal articular facet for intermediate carpal.....	72
d)	Breadth (m-l) of articular facet for radius vs. length (a-p) of articular facet for radius.....	72
e)	Max breadth of articular facet for os c. II continuous with distal articular facet for intermed. carpal vs. max length (a-p) of art. facet for the os c. II.....	73
Figure 3.11	Intraspecific morphological variability in the os c. III of <i>P. ex gr. P. falconeri</i> from Spinagallo Cave.....	74
a)	Scatterplot of the cranial breadth (m-l) vs. max thickness (a-p).....	74
b)	Os c. IIIs in dorsal aspect.....	74
Figure 3.12	Os c. III of Elephantinae species.....	75
1)	<i>P. ex gr. P. falconeri</i> from Spinagallo Cave, Sicily.....	75
2)	<i>P. mnaidriensis</i> from Mnaidra Gap, Malta.....	75
3)	<i>P. ex gr. P. mnaidriensis</i> from Puntali Cave, Sicily.....	75
4)	Young <i>P. antiquus</i> from Neumark-Nord 1, Germany.....	75
5)	Adult <i>P. antiquus</i> from Neumark-Nord 1.....	75
6)	<i>M. lamarmorai</i> from Gonnesa, Sardinia	75
Figure 3.13	Scatterplot of the os c. III cranial height (pr-d) vs. max thickness (a-p).....	76
Figure 3.14	Scatterplots of the dimensions of the os c. III.....	77
a)	Max cranial breadth (m-l) vs. max thickness (a-p)	77
b)	Max cranial breadth (m-l) vs. max cranial height (pr-d)	77
c)	Max cranial breadth (m-l) vs. max caudal breadth (m-l)	77

	d)	Max length (a-p) vs. max breadth (m-l) of the articular facet for the mc III.....	77
Figure 3.15		Astragalus in dorsal, plantar and medial aspects.....	81
	1)	<i>P. ex gr. P. falconeri</i> from Spinagallo Cave, Sicily.....	81
	2)	<i>Palaeoloxodon</i> sp. 1 from Luparello Fissure, Sicily.....	81
	3)	<i>Palaeoloxodon</i> sp. from Benghisa Gap, Malta.....	81
	4)	<i>P. ex gr. P. mnaidriensis</i> from Puntali Cave, Sicily.....	81
	5)	<i>P. antiquus</i> from Neumark-Nord 1, Germany.....	81
	6)	<i>L. africana</i> from Kenya.....	81
	7)	<i>M. lamarmorai</i> from Gonnesa, Sardinia.....	81
Figure 3.16		Scatterplot of the dimensions of the astragalus including <i>P. antiquus</i>	82
Figure 3.17		Scatterplots of the dimensions of the astragalus.....	83
	a)	Max breadth (m-l) vs. max length of articular facet for the central tarsal in <i>P. ex gr. P. falconeri</i> from Sicily and Malta.....	83
	b)	Max breadth (m-l) vs. max length of articular facet for the central tarsal in insular dwarfs.....	83
	c)	Max breadth (m-l) vs. max thickness (pr-d)	
	d)	Max length (a-p) on lateral side vs. max length (a-p) on medial side.....	83
Figure 3.18		Box-and-whisker plot of the ratio of the astragalus max breadth (m-l)/ max thickness (pr-d).....	84
Figure 3.19		Box-and-whisker plot of the calcaneus' ratio of the max length of distal end of tuber/max length (a-p) of fibular facet.....	86
Figure 3.20		Calcaneus of <i>P. ex gr. P. falconeri</i> from Spinagallo Cave, Sicily in lateral aspect.....	87
Figure 3.21		Calcaneus of <i>Palaeoloxodon</i> spp. and <i>M. lamarmorai</i> in fontal, lateral and superior aspects.....	88
	1)	<i>P. ex gr. P. falconeri</i> from Spinagallo Cave, Sicily.....	88
	2)	<i>Palaeoloxodon</i> sp. 1 from Luparello Fissure, Sicily.....	88
	3)	<i>Palaeoloxodon</i> sp. 1 from Luparello Fissure, Sicily.....	88
	4)	<i>Palaeoloxodon</i> sp. from Benghisa Gap, Malta.....	88
	5)	<i>P. ex gr. P. mnaidrneisis</i> from Puntali Cave, Sicily.....	88
	6)	<i>P. antiquus</i> from Neumark-Nord 1, Germany.....	88
	7)	<i>P. antiquus</i> from Neumark-Nord 1, Germany.....	88
	8)	<i>M. lamarmorai</i> from Gonnesa, Sardinia.....	88
Figure 3.22		Scatterplots of the dimensions of the calcaneus.....	89
	a)	Max length of lateral articular facet for astragalus vs. max articular breadth of the fibular facet.....	89
	b)	Max breadth vs. max length of the distal end of tuber.....	89
	c)	Max length vs. max breadth of the lateral articular facet for the astragalus.....	89
	d)	Max breadth (a-p) of fibular facet vs. max breadth of distal end of tuber.....	89
Figure 3.23a)		Principal Component Analysis of the calcaneus.....	90

Figure 3.23b)	Standardized and log-transformed Principal Component Analysis of the calcaneus.....	91
Figure 3.24	Morphology of the calcaneus' articular facet for the tibia and fibula.....	92
a)	Scatterplot of the dimensions of the articular facet for the tibia.....	92
b)	Three individuals of <i>P. ex gr. P. falconeri</i> illustrating intraspecific variability in the morphology of the tibial and fibular facets.....	92
c)	Box-and-whisker plot of the ratio of the tibial facet length/distal tuber length.	92
d)	Calcaneus of <i>P. tiliensis</i> from Tilos, Island, Greece in lateral aspect.....	92
Figure 3.25	Calcaneus intra- and inter-specific differences between the morphology of the tibial and fibular facets.....	93
Figure 3.26	Scatterplots of the dimensions of the calcaneal tibial and fibular facets in <i>P. ex gr. P. falconeri</i> and <i>Palaeoloxodon</i> sp. 1 from Luparello Fissure and Spinagallo Cave, Sicily.....	95
a)	Max length (a-p) of fibular facet vs. min length (a-p) of the tibio-fibular bridge.....	95
b)	Max length (a-p) of fibular facet vs. max length (a-p) of tibial facet.....	95
c)	Max length (a-p) of articular facet for the tibia vs. max length of tibio-fibular bridge.....	95
d)	Max length of distal end of tuber vs. max length (a-p) of tibial facet minus min length of tibio-fibular bridge (a-p).....	95
Figure 3.27	<i>L. africana</i> calcaneus from Kenya in frontal aspect.....	97
a)	Juvenile with unfused tuber.....	97
b)	Adult with fused tuber.....	97
Figure 3.28a)	Box-and-whisker plot of the ratio of the central tarsal's max breadth (m-l)/breadth (m-l) of articular facet for astragalus.....	99
b)	Box-and-whisker plot of the ratio of max breadth of the central tarsal/cranial height (pr-d).....	99
Figure 3.29	Box-and-whisker plot of the central tarsal's breadth (m-l) of the articular facet for the astragalus/length (a-p) of the articular facet for the astragalus.....	100
Figure 3.30	Box-and-whisker plot of variability in the central tarsal's articular facet for the calcaneus (ratio of m-l breadth/a-p length).....	100
Figure 3.31	Central tarsal in superior, inferior, cranial and caudal aspects.....	101
1)	<i>P. antiquus</i> from Neumark-Nord 1, Germany.....	101
2)	<i>L. africana</i> from Kenya.....	101
3)	<i>M. lamarmorai</i> from Gonnese, Sardinia.....	101
4)	<i>P. ex gr. P. falconeri</i> from Spinagallo Cave, Sicily	101
Figure 3.32	Scatterplot of the central tarsal max breadth (m-l) vs. max breadth (m-l) of articular facet.....	102
Figure 3.33	Morphology and dimensions of the central tarsal.....	103
a)	Variability of the central tarsal's articular facet for the calcaneus in <i>P. ex gr. P. falconeri</i> from Spinagallo Cave, Sicily.....	103

	b)	Scatterplot of the max breadth (m-l) of articular facet for the calcaneus vs. max length (pr-d) of articular facet for calcaneus.....	103
	c)	Scatterplot of the max breadth (m-l) vs. thickness (pr-d).....	103
	d)	Scatterplot of the breadth (m-l) of articular facet for astragalus vs. length (a-p) of articular facet for astragalus.....	103
Figure 3.34		<i>P. ex gr. P. falconeri</i> os t. IV from Spinagallo Cave, Sicily.....	105
	1)	Large specimen with separated articular facets for the central tarsal and calcaneus.....	105
	2)	Small specimen with contiguous facets for the central tarsal and calcaneus.....	105
Figure 3.35		Os t. IV in superior, inferior, cranial, medial and lateral aspects.....	106
	1)	<i>P. ex gr. P. falconeri</i> from Spinagallo Cave, Sicily.....	106
	2)	<i>Palaeoloxodon</i> sp. 1 from Luparello Fissure, Sicily.....	106
	3)	<i>Palaeoloxodon</i> sp. from Benghisa, Malta.....	106
	4)	Young <i>P. antiquus</i> from Neumark-Nord 1, Germany.....	106
	5)	Adult <i>P. antiquus</i> from Neumark-Nord 1, Germany.....	106
	6)	<i>M. lamarmorai</i> from Gonnesa, Sardinia.....	106
	7)	<i>L. africana</i> from Kenya.....	106
Figure 3.36		Scatterplot of the os t. IV interspecific comparisons anterior breadth (m-l) vs. max thickness (a-p).....	107
Figure 3.37		Mc III in cranial aspect.....	109
	a)	<i>M. meridionalis</i> from the Oosterschelde Estuary, Netherlands.....	109
	b)	<i>Anancus arverensis</i> from the Oosterschelde Estuary, Netherlands.....	109
	c)	<i>M. lamarmorai</i> from Gonnesa, Sardinia.....	109
Figure 3.38		Scatterplots of the dimensions of the mc III.....	110
	a)	Diaphysis breadth (m-l) at midshaft vs. max length (pr-d).....	110
	b)	Diaphysis breadth (m-l) at midshaft vs. diaphysis thickness (a-p).....	110
	c)	Min diaphysis thickness (a-p) vs. max length (pr-d).....	110
	d)	Max height (pr-d) vs. diaphysis dimensions.....	110
Figure 3.39		Mc IV in medial aspect.....	111
	a)	<i>M. lamarmorai</i> from Gonnesa, Sardinia.....	111
	b)	<i>P. ex gr. P. mnaidriensis</i> from Puntali Cave.....	111
	c)	Young <i>P. antiquus</i> from Neumark-Nord 1, Germany.....	111
Figure 3.40		Scatterplot of the dimensions of the mc IV.....	111
Figure 3.41		Box-and-whisker plot of the ratio of the MC IV max height (pr-d) /min diaphysis thickness (a-p).....	111
Figure 3.42		Scatterplot of the min breadth (m-l) vs. max height (pr-d) of the mt IV.....	112
Figure 4.1		Dimensions of the scapula's glenoid fossa in <i>P. ex gr. P. falconeri</i> from Spinagallo Cave, Sicily.....	124
	a)	Size-frequency histogram of the max breadth of the glenoid fossa.....	124
	b)	Scatterplot of the chord breadth (m-l) vs. surficial length (a-p).....	124
	c)	Scatterplot of the chord length (a-p) vs. chord breadth (m-l).....	124
	d)	Scatterplot of the chord length (a-p) vs. surficial length (a-p).....	124

Figure 4.2	Scatterplots of the dimensions of the scapula's glenoid fossa.....	125
a)	Surficial length (a-p) vs. chord breadth (m-l).....	125
b)	Chord length (a-p) vs. surficial length (a-p).....	125
c)	Chord length (a-p) vs. chord breadth (m-l).....	125
Figure 4.3	Humerus of juvenile <i>L. africana</i> from Kenya.....	127
Figure 4.4	Humerus of <i>P. ex gr. P. falconeri</i> humerus from Spinagallo Cave, Sicily.....	128
Figure 4.5	Humerus of <i>Palaeoloxodon</i> sp. 1 from Luparello Fissure, Sicily.....	129
Figure 4.6	Humerus of <i>P. ex gr. P. mnaidriensis</i> humerus from Puntali Cave, Sicily.....	130
Figure 4.7	Humerus of young <i>P. antiquus</i> from Neumark-Nord 1, Germany.....	131
Figure 4.8	Humerus of adult <i>P. antiquus</i> from Neumark-Nord 1, Germany.....	132
Figure 4.9	Humerus of juvenile <i>P. ex gr. P. falconeri</i> from Spinagallo Cave in lateral aspect.....	133
Figure 4.10	Box-and-whisker plot of the ratio of the humerus' max diaphysis height (pr-d)/min diaphysis breadth (m-l).....	135
a)	Pooled samples of unfused and fused epiphyses.....	135
b)	Samples divided into groups with fused and unfused epiphyses.....	135
Figure 4.11	Figure legend for taxa in Fig. 4.12.....	136
Figure 4.12	Scatterplot of the dimensions of the humerus.....	137
a)	Min diaphysis breadth (m-l) vs. max diaphysis height (pr-d).....	137
b)	Min diaphysis breadth (m-l) vs. max height (pr-d) including epiphyses.....	137
c)	Min diaphysis circumference vs. circumference at deltoid tuberosity.....	137
d)	Min diaphysis breadth (m-l) vs. diaphysis breadth (m-l) at deltoid tuberosity.....	137
Figure 4.13	Box-and-whisker plot of the ratio of the humerus' diaphysis breadth (m-l) at deltoid tubercle (m-l) vs. min diaphysis breadth (m-l).....	138
Figure 4.14	Distal ulna-radius of <i>P. ex gr. P. falconeri</i> from Spinagallo Cave.....	139
Figure 4.15	Comparison of the ulna in cranial aspect.....	140
a)	Juvenile <i>L. africana</i> from Kenya.....	140
b)	Adult <i>L. africana</i> from Kenya.....	140
c)	<i>P. ex gr. P. falconeri</i> from Spinagallo Cave, Sicily.....	140
d)	<i>Palaeoloxodon</i> sp. 1 from Luparello Fissure, Sicily.....	140
e)	Adult <i>P. ex gr. P. mnaidriensis</i> from Puntali Cave, Sicily.....	140
f)	Adult <i>P. antiquus</i> from Neumark-Nord 1, Germany.....	140
Figure 4.16	Comparison of the ulna in medial aspect.....	141
a)	Juvenile <i>L. africana</i> from Kenya.....	141
b)	Adult <i>L. africana</i> from Kenya.....	141
c)	<i>P. ex gr. P. falconeri</i> from Spinagallo Cave, Sicily.....	141
d)	<i>Palaeoloxodon</i> sp. 1 from Luparello Fissure, Sicily.....	141
e)	Adult <i>P. ex gr. P. mnaidriensis</i> from Puntali Cave, Sicily with synostotic radius.....	141

f)	Adult <i>P. antiquus</i> from Neumark-Nord 1, Germany.....	141
Figure 4.17	Scatterplots of the dimensions of the ulna.....	142
a)	Min diaphysis breadth (m-l) vs. max height (pr-d) including epiphyses.....	142
b)	Min diaphysis breadth (m-l) vs. diaphysis height (pr-d).....	142
c)	Min diaphysis breadth (m-l) vs. min diaphysis thickness (a-p).....	142
d)	Min diaphysis thickness (a-p) vs. diaphysis height (pr-d).....	142
Figure 4.18	Femur of juvenile <i>L. africana</i> from Kenya.....	144
Figure 4.19	Femur of adult <i>L. africana</i> from Kenya.....	145
Figure 4.20	Femur of <i>P. ex gr. P. falconeri</i> from Spinagallo Cave, Sicily.....	146
Figure 4.21	Femur of <i>Palaeoloxodon</i> sp. 1 from Luparello Fissure, Sicily.....	147
Figure 4.22	Femur of <i>P. ex gr. P. mnaidriensis</i> femur from Puntali Cave, Sicily	148
Figure 4.23	Femur of <i>P. antiquus</i> from Neumark-Nord 1, Germany.....	149
Figure 4.24	Ontogeny and phylogeny in the femur diaphysis (medial aspect).....	151
Figure 4.25	Scatterplot of the femoral diaphysis dimensions (medio-lateral breadth vs. antero-posterior thickness).....	152
Figure 4.26	Scatterplots of the dimensions of the femur.....	153
a)	Diaphysis midshaft breadth (m-l) vs. max height (pr-d) including epiphyses.....	153
b)	Diaphysis midshaft thickness (a-p) vs. max height (pr-d) including epiphyses.....	153
c)	Diaphysis midshaft breadth (m-l) vs. breadth (m-l) of femoral head.....	153
d)	Diaphysis midshaft thickness (a-p) vs. breadth (m-l) of femoral head.....	153
Figure 4.27	Box-and-whisker plot of the ratio of the femur's diaphysis midshaft breadth (m-l)/diaphysis midshaft thickness (a-p).....	154
Figure 4.28a)	Box-and-whisker plot of the ratio of the femur's max height (pr-d) including epiphyses vs. min diaphysis breadth (m-l).....	154
b)	Box-and-whisker plot of the ratio of the femur's max height (pr-d) including epiphyses vs. thickness (a-p) of diaphysis midshaft.....	154
Figure 4.29	Tibia of juvenile <i>L. africana</i> from Kenya.....	157
Figure 4.30	Tibia of adult <i>L. africana</i> from Kenya.....	158
Figure 4.31	Tibia of <i>P. ex gr. P. falconeri</i> from Spinagallo Cave, Sicily	159
Figure 4.32	Tibia of <i>Palaeoloxodon</i> sp. 1 from Luparello Fissure, Sicily.....	160
Figure 4.33	Tibia of <i>P. ex gr. P. mnaidriensis</i> from Puntali Cave, Sicily.....	161
Figure 4.34	Tibia of young <i>P. antiquus</i> tibia from Neumark-Nord 1, Germany.....	162
Figure 4.35	Tibia of adult <i>P. antiquus</i> from Neumark-Nord 1, Germany.....	163
Figure 4.36	Synostotically fused tibia-fibula of <i>P. ex gr. P. falconeri</i> from Spinagallo Cave.....	164
Figure 4.37	Scatterplots of the dimensions of the tibia.....	165
a)	Max breadth (m-l) of proximal epiphysis vs. max height (pr-d) including epiphyses.....	165
b)	Max breadth (m-l) of distal epiphysis vs. max height (pr-d) including epiphyses.....	165

	c)	Max thickness (a-p) of proximal epiphysis vs. max height (pr-d) including epiphyses.....	165
	d)	Diaphysis midshaft breadth (m-l) vs. max height (pr-d) including epiphyses.....	165
Figure 4.38a)		Scatterplot of the tibial max height (pr-d) including epiphyses vs. diaphysis midshaft breadth (m-l).....	166
	b)	Box-and-whisker plot of the tibia's max height (pr-d) including epiphyses/diaphysis midshaft breadth (m-l).....	166
Figure 4.39		Distal tibia of <i>P. ex gr. P. falconeri</i> from Spinagallo Cave, illustrating morphological variability in the <i>Cochlea tibiae</i>	168
Figure 4.40		Scatterplots of the dimensions of the <i>P. ex gr. P. falconeri</i> tibia diaphysis from Spinagallo Cave.....	169
Figure 4.41		Scatterplots of the interspecific bivariate allometry of the tibia.....	170
	a)	Max breadth (m-l) of distal end of diaphysis vs. max diaphysis height (pr-d).....	170
	b)	Max breadth (m-l) of proximal end of diaphysis vs. max diaphysis height (pr-d).....	170
	c)	Max breadth (m-l) of distal end of diaphysis vs. max breadth (m-l) of proximal end of diaphysis.....	170
	d)	Breadth (m-l) at diaphysis midshaft vs. max diaphysis height (pr-d).....	170
Figure 4.42		Box-and-whisker plot of the ratio of the tibia's diaphysis height (pr-d)/breadth (m-l) of the proximal end of diaphysis without the epiphysis.....	171
	a)	Pooled samples of unfused and fused epiphyses.....	171
	b)	Samples divided into groups with fused and unfused epiphyses.....	171
Figure 4.43		Box-and-whisker plot of the ratio of the tibia's diaphysis height (pr-d)/breadth (m-l) of the distal end of diaphysis without the epiphysis.....	172
	a)	Pooled samples of unfused and fused epiphyses.....	172
	b)	Samples divided into groups with fused and unfused epiphyses.....	172
Figure 4.44		Box-and-whisker plot of the ratio of the tibia's breadth (m-l) of the proximal end of diaphysis without the epiphysis/max breadth (m-l) of distal diaphysis end without epiphysis.....	172
	a)	Pooled samples of unfused and fused epiphyses.....	172
	b)	Samples divided into groups with fused and unfused epiphyses.....	172
Figure B1a)		Alcarno Quarry sampling location, with the author pointing to the exposed tusk.....	250
	b)	Close-up of exposed tusk in section, with sample removed from immediately to the left of the tusk.....	250

List of Tables

Table 1.1	Mediterranean islands with representatives of the genus <i>Mammuthus</i>	4
Table 1.2	Mediterranean islands with representatives of the genus <i>Palaeoloxodon</i>	5
Table 1.3	Factors hypothesized to influence the evolution of body mass in Siculo-Maltese <i>Palaeoloxodon</i> spp. and Sardinian <i>Mammuthus lamarmorai</i>	10
Table 2.1	Elephantinae taxa sampled, their geographic provenance, approximate adult skeletal height, geological age and collections provenance.....	21
Table 2.2	Published geochronological ages of Siculo-Maltese elephants.....	25
Table 2.3	Sicilian Pliocene to Holocene vertebrate faunal complexes as classified according to Marra (2013).....	26
Table 2.4	Long bones of insular <i>Palaeoloxodon</i> spp. sampled in the present study.....	39
Table 2.5	Metapodials sampled in the present study.....	39
Table 2.6	Carpals sampled in the present study.....	40
Table 2.7	Tarsals sampled in the present study.....	41
Table 2.8	<i>Loxodonta africana</i> long bone metadata (KNM collection).....	42
Table 2.9	Categories of studies for comparing proboscidean allometry based on choice of sample and the elements sampled in this thesis.....	44
Table 3.1	Carpal and tarsal terminology and their commonly-used synonymms.....	61
Table 3.2	<i>P. ex gr. P. falconeri</i> ulnar carpal specimens from Spinagallo Cave, belonging to modes B and C in Figure 3.4b.....	64
Table 3.3a)	Principal Component Analysis of the ulnar carpal of <i>P. ex gr. P. falconeri</i> from Spinagallo Cave.....	65
Table 3.3b)	Standardized and log-transformed Principal Component Analysis output for the ulnar carpal.....	66
Table 3.4	Angle between the radial carpal's articular facets for radius and os c. II.....	71
Table 3.5	Mann-Whitney U-test pairwise comparison in the os c. III.....	78
Table 3.6	Interspecific morphological differences in the os c. III.....	79
Table 3.7a)	Principal Component Analysis output for the calcaneus.....	90
Table 3.7b)	Standardized and ln-transformed Principal Component Analysis output for the calcaneus.....	90
Table 3.8	Differences in the articular facet for the tibia on the calcaneus between species (or morphotypes).....	94
Table 3.9	MWU-test pairwise p-values of <i>Palaeoloxodon</i> sp. 1 from Luparello Fissure and <i>P. ex gr. P. falconeri</i> from Spinagallo Cave, Sicily.....	94

Table 3.10	Summary observations comparing the morphology of select carpals in <i>P. antiquus</i> from Neumark-Nord 1, Germany and <i>P. ex gr. P. falconeri</i> from Spinagallo Cave, Sicily.....	116
Table 3.11	Summary observations comparing tarsal morphology in <i>P. antiquus</i> from Neumark-Nord 1, Germany and <i>P. ex gr. P. falconeri</i> from Spinagallo Cave, Sicily.....	117
Table 4.1	Hypotheses and predictions tested in Chapter 4.....	122
Table 4.2	Mann-Whitney U-test p-values on interspecific bivariate allometric comparisons of the scapula's glenoid fossa.....	126
Table 4.3	Interspecific differences in the morphology of the deltoid fossa	134
Table 4.4	Pair-wise Mann-Whitney U-test results for the humerus' diaphysis height (pr-d) vs. min diaphysis breadth (m-l).....	136
Table 4.5	Mann-Whitney pairwise p-values of allometric differences in the tibia of <i>P. antiquus</i> from Neumark-Nord 1, Germany and <i>P. ex gr. P. falconeri</i> from Spinagallo Cave, Sicily.....	167
Table 4.6	Allometry of the tibia in <i>L. africana</i> and <i>P. ex gr. P. falconeri</i>	173
Table 4.7	Scaling in the long-bones of <i>Palaeoloxodon</i> spp.....	171
Table 4.8	Summary of results from Table 4.6 comparing the allometry of the tibia.....	182
Table 5.1	Outcomes of the Hypotheses as stated in Chapter 1.....	186
Table 5.2	Summary of the qualitative morphological differences in the long bones between Sicilian <i>Palaeoloxodon</i> spp. and European <i>P. antiquus</i>	188
Table 5.3	Summary of the results from Table 4.6 comparing the allometry of the tibia in <i>L. africana</i> and <i>P. ex gr. P. falconeri</i>	193
Table 5.4	The presence/absence of pedomorphic features in Siculo-Maltese <i>Palaeoloxodon</i> spp. and <i>M. lamarmorai</i> from Sardinia.....	194
Table 5.5	Summary of the metric and qualitative morphological differences in the tarsals between <i>P. antiquus</i> , Sicilian <i>Palaeoloxodon</i> spp., and Sardinian <i>M. lamarmorai</i>	197
Table 5.6	Features in the appendicular skeleton demonstrating both morphological differences and close similarities between <i>Palaeoloxodon</i> sp. 1 and <i>P. ex gr. P. falconeri</i>	201
Table A1.1	Type-series of insular <i>Palaeoloxodon</i> spp. studied in this thesis.....	241
Table A1.2	Published reference material of <i>Palaeoloxodon</i> spp. from Sicily and Favignana Island for which the taxonomic status may require revision.....	243
Table B1 a)	U-Th results from the Alcamo Quarry travertine deposit, western Sicily associated with an <i>in situ</i> <i>Palaeoloxodon</i> sp. tusk.....	252
Table B1 b)	U-Th results from the Alcamo Quarry travertine deposit, western Sicily associated with an <i>in situ</i> <i>Palaeoloxodon</i> sp. tusk.....	252
Table C1	Insular endemic mammals displaying alleged evidence of low-gear locomotion.....	254

Table D1	Preliminary identification of unaccessioned <i>Palaeoloxodon</i> spp. remains from Luparello Fissure, Sicily, excavated by Raymond Vaufrey in 1925/1926.....	256
Table E1	Regression table.....	261

CHAPTER 1

**The pattern and process of elephant evolution on the
Siculo-Maltese Palaeo-archipelago**

1.1 Introduction

Among the clade Afrotheria, the Proboscidea ILLIGER 1811* are a morphologically diverse phylum encompassing all taxa with tusks and trunks (Latin *proboscis*). Although currently limited to just one extant family (the Elephantidae), more than 42 genera including 175 taxa are currently reported from the fossil record (Shoshani and Tassy, 2004; 2005). As such, the order Proboscidea reveals important insights into the pattern and process of evolutionary adaptation, particularly due to the fact that (i) Proboscideans were adapted to an extremely diverse range of environments, from tropical Africa to arctic Siberia (Osborn, 1936; 1942; Lister and Bahn, 2009); (ii) An exceptionally diverse range in body mass is represented within the Proboscidea (Fig. 1.4), including members belonging to the same genus weighing between 0,3 and 22 tons (Larramendi and Palombo, 2015) providing insights into anatomical changes in relation to mass; (iii) Finally, the massive changes undergone in scale and allometry enable us to identify the heterochronic mechanisms underpinning their evolution (Palombo, 2001a). Considering that these factors are all manifested in insular endemic Proboscidea, Pleistocene elephants and mammoths from the Mediterranean islands are a nexus for studying major themes in proboscidean evolutionary biology (Palombo, 2007; Herridge, 2010).

The purpose of this chapter is therefore to provide background and a detailed literature survey on the evolution of insular elephants from the western-central Mediterranean, from which numerous insular species are known, and to summarize the current state of knowledge of the effects of island environment, body mass and heterochrony on their evolution, with a particular emphasis on the appendicular skeleton. Finally, this chapter outlines the hypotheses to be tested and layout of the thesis.

1.2 Origins of the Elephantidae and island biogeography of *Mammuthus* and *Palaeoloxodon*

The order Proboscidea originated in Africa during the early Cenozoic (Gheerbrant and Tassy, 2009), and dispersed repeatedly into Eurasia from the Late Oligocene onwards (Antoine *et al.*, 2003). From the Early Miocene onwards numerous taxa became established outside Africa (Osborn, 1934; 1936; 1942; Maglio, 1973; van der Made and Mazo, 2003; Kalb *et al.*, 2004a; 2004b; Todd and Roth, 1996; Shoshani, 1998), adapting to an extremely diverse range of environments (Lister and Sher, 2001; van der Made, 2010; Todd and Roth, 1996; Shoshani, 1998). The Elephantidae GRAY, 1821, a family that radiated into Europe, Asia and North America during the Pliocene and Pleistocene, is today represented by three species, the African bush elephant *Loxodonta africana* (BLUMENBACH 1797)*, and woodland

*Following taxonomic convention, where the original taxon name has been modified the names of binomial authorities accompanying them are placed in parentheses (). Due to much taxonomic confusion in the literature, all binomial authorities are placed in capital letters to distinguish them from other references. Also note references are cited with page numbers where a specific topic is being referred to. However, when a general topic is under consideration page numbers are omitted.

elephant *Loxodonta cyclotis* MATSCHIE 1900, and the Asian elephant *Elephas maximus* LINNAEUS 1758. A further two genera are represented in the fossil record of Eurasia, the genera *Mammuthus* BROOKES 1828 and *Palaeoloxodon* MATSUMOTU 1924 (Albayrak, 2012: 366; Shoshani and Tassy, 2004; Todd and Roth, 1996; Palombo and Ferretti, 2005; Saegusa and Gilbert, 2008). Mammoths (genus *Mammuthus*) first appeared in Europe during the Pliocene (Lister *et al.*, 2005; Saegusa and Gilbert, 2008) and through a complex process of anagenetic and cladogenetic speciation the Pliocene ancestral species *Mammuthus rumanus* ȘTEFĂNESCU 1924 gave rise to numerous species (Lister *et al.*, 2005; Lister and Bahn, 2009). The genus persisted as the woolly mammoth *Mammuthus primigenius* (BLUMENBACH 1799) until it became extinct on Wrangel Island in north-eastern Siberia some 3,600 years ago (Vartanyan *et al.*, 2008; Arppe *et al.*, 2009). The genus *Palaeoloxodon* in contrast, is represented by only one species within continental Europe, the straight-tusked elephant *P. antiquus* (from ca. 900-34 ka in Europe, see Stuart, 2005; Braun and Palombo 2012: Fig. 24; Palombo, 2017). This species is typically associated with interglacial fauna during the late Middle to Late Pleistocene and adapted to mild humid/temperate climates with wooded or mixed vegetation in central Europe (Stuart, 1982; 2005; Pushkina, 2007: 226-230; Mania, 2010a; Mania and Mai, 2010), persisting in southern Europe during glacial stages (Tsoukala and Lister, 1998; Stuart, 2005; Marra, 2009). Its earliest presence in Europe likely dates to approximately 0,9 Ma (Palombo, 2014: 65; Palombo, 2017), by which time the species may already have been present on the Italian peninsula (Palombo, 1994).

Mammuthus spp. and *P. antiquus* later colonized numerous Mediterranean islands from the southern shores of Europe or the Near East, sometimes even repeatedly colonizing the same island. At present, there are two species of named endemic mammoths on Mediterranean islands (Table 1.1) and eight species of named insular endemic palaeoloxodont elephants (Table 1.2). In rare cases islands may have briefly been connected to the continent during low sea-levels (van der Geer *et al.*, 2014: 140-141; see also Anastasakis and Dermitzakis, 1990: 12-13; Herridge, 2010: 56; van der Geer *et al.*, 2014: 139; Sen, 2017: 88), although most islands were reached by swimming. It has been speculated that proboscideans were attracted to islands by the scent of vegetation, quite possibly while there were food shortages on the mainland (see Johnson, 1980: 389 and references therein).

The remarkable ability proboscideans have to swim to and become established on Mediterranean islands is explained by at least eight factors. These include (i) their ability to use their trunks as snorkels (Johnson, 1980), and (ii) the ability to breathe easily while almost completely submerged due to the absence of a pleural space and unusual anatomy of their lungs (West, 2001; West *et al.*, 2003). (iii) Further, their low surface area to body mass ratio results in elephants dissipating heat slowly to the surrounding ocean. Factors which allegedly also increase the buoyancy of proboscideans are gasses produced by cecal fermentation (Sondaar and van der Geer, 2002: 2; van der Geer *et al.*, 2010: 24) as well as the presence of highly-pneumatized cranial sinuses (Athanassiou *et al.*, 2015; see van der Merwe *et al.*, 1995: Fig. 2B), although no empirical data exists on the significance of these two factors. Other important factors for reaching islands likely include (iv) their excellent sense of smell which may have enabled proboscideans to tell the direction of an island by using their trunks as a

kind of olfactory periscope (see Johnson, 1980: 389). (v) Proboscideans also have a wide dietary tolerance which likely contributed to successful colonization (see Lawlor, 1982; Ehrlich, 1986 for insular dietary generalists) and (vi) unlike many other mammals proboscideans also have a tendency to swim in herds (Sondaar and van der Geer, 2002: 2). In addition to the excellent swimming abilities of proboscideans, Pleistocene sea level fluctuations likely played a significant role in making islands more accessible, by increasing island size and decreasing the distance from the European mainland during lowstands, both factors which increase the probability of successful colonization (see MacArthur and Wilson, 1967: 123-144; Johnson, 1980; Herridge, 2010: 54-60).

Due to all the abovementioned factors, endemic and non-endemic Pleistocene-Holocene proboscideans occurred on more than 60 islands from around the world, including the islands of the Mediterranean¹, north-east Asia², southeast Asia³; Japan⁴, Bering Sea islands⁵, the California Channel Islands⁶ (¹Theodorou, 1983; Doukas and Athanassiou, 2003; Caloi *et al.*, 2004; Palombo, 2007; Herridge, 2010 and references therein; Sen, 2017; Athanassiou *et al.*, 2019; ²Vartanyan *et al.*, 1993 *inter alios*; ³van den Bergh, 1999; van den Bergh *et al.*, 2004; van der Geer *et al.*, 2010: 172-215; Liscaljet, 2012; ⁴Takahashi *et al.*, 2001; Aiba *et al.*, 2010; van der Geer *et al.*, 2010: 229-243; ⁵Veltre *et al.*, 2008; Graham *et al.* 2016; ⁶Roth, 1982; 1993; Agenbroad *et al.*, 1999; Agenbroad, 2001; 2003; van der Geer *et al.*, 2010: 263-267; Muhs *et al.*, 2015). On many of these islands proboscideans continued to evolve along evolutionary trajectories separate from their mainland ancestors.

In the Mediterranean Sea, endemic species derived from the straight-tusked elephant *P. antiquus* are represented on Sicily, Malta, Cyprus and Crete (which all included multiple species either due to repeated colonisation or anagenesis), and several islands on which single palaeoloxodont endemic species are reported (Favignana, Tilos, Rhodes, Delos and Naxos) (see Table 1.2). On Crete and Sardinia endemic mammoths are also reported (Table 1.1), and sparse (presumably Pleistocene) proboscidean remains have also been reported from Milos, as well as Kythnos (possibly dating to the Early Holocene) (Honea, 1975; Doukas and Athanassiou, 2003: 102; Shoshani and Tassy, 2004: 238; Sen, 2017) and Kalymnos (Athanassiou *et al.*, 2017). Despite this extensive diversity in insular proboscideans, there are

Island	Species	Authority	Chronology	Sample literature
Gökçeada	<i>M. meridionalis</i> ?	(NESTI 1825)	Early Pleistocene	Deperet and Mayet, 1923; Theodorou, 1983: 23
Kos				Major, 1887; Airaghi, 1928; Doukas and Athanassiou,
Lesbos				de Vos <i>et al.</i> , 2002; Doukas and Athanassiou, 2003
Euboea				Doukas and Athanassiou, 2003
Kythra				Doukas and Athanassiou, 2003
Sardinia	<i>M. lamormarai</i>	(MAJOR 1883)	Late Middle Pleistocene?	van der Geer <i>et al.</i> , 2010 and references therein; Palombo <i>et al.</i> , 2012; Palombo <i>et al.</i> , 2017
Crete	<i>M. creticus</i>	(BATE 1907)	Late Pliocene/Early Pleistocene?	Poulakakis <i>et al.</i> , 2002a; van der Geer <i>et al.</i> , 2010; Herridge and Lister, 2012

Table 1.1 Mediterranean islands with representatives of the genus *Mammuthus* BROOKES 1828. Note that where the original taxon name has been modified the binomial authority appears in parentheses () following taxonomic convention.

Island	Species	Authority	Chronology	Sample literature
Sicily	<i>P. antiquus</i>	(FALCONER and CAUTLEY, 1847)	Middle Pleistocene	Basile and Chilardi, 1996
	<i>P. antiquus leonardi</i>	AGUIRRE 1969a	Late Middle Pleistocene	van der Geer <i>et al.</i> , 2010 and references therein
	<i>P. ex gr. P. mnaidriensis</i> from Puntali Cave	-	Late Middle Pleistocene to Late Pleistocene	Ferretti, 2008; Herridge, 2010
	<i>Palaeoloxodon</i> sp. 1 from Luparello Fissure	-	early or middle Middle Pleistocene	Scarborough <i>et al.</i> , 2016
	<i>P. ex gr. P. falconeri</i>	(BUSK 1867)	Late Middle Pleistocene - early Late Pleistocene	van der Geer <i>et al.</i> , 2010 and references therein
Favignana	<i>Palaeoloxodon</i> sp. 2	-	Late Middle Pleistocene	Capasso Barbato <i>et al.</i> , 1989; this thesis
Malta	<i>Palaeoloxodon</i> sp.	-	Late Middle Pleistocene	Herridge, 2010
	<i>P. falconeri</i>	(BUSK 1867)	Late Middle Pleistocene - early Late Pleistocene	van der Geer <i>et al.</i> , 2010 and references therein
	<i>P. mnaidriensis</i>	(ADAMS 1874)	Late Middle Pleistocene	Herridge, 2010
Giglio	<i>P. antiquus</i>	(FALCONER and CAUTLEY 1847)	Late Pleistocene	Masseti, 1994 and references therein
Crete	<i>P. ex gr. P. antiquus</i>	(FALCONER and CAUTLEY 1847)	Pleistocene	Mol <i>et al.</i> , 1996; cf. Symeonidis <i>et al.</i> , 2000
	<i>P. creutzburgi</i>	(Kuss 1965)	?Late Pleistocene	Poulakakis <i>et al.</i> , 2002a
Cyprus	<i>P. cypriotes</i>	(BATE 1903)	Late Pleistocene	Davies and Lister, 2001; Dirks <i>et al.</i> , 2012
	<i>P. xlophagou</i>	ATHANASSIOU <i>et al.</i> 2015	late Middle Pleistocene	Athanassiou <i>et al.</i> , 2015
Astypalaea	? <i>Palaeoloxodon</i> sp.	-	Pleistocene?	Athanassiou <i>et al.</i> , 2017
Tilos	<i>P. tiliensis</i>	(THEODOROU <i>et al.</i> , 2007)	Late Pleistocene - Late	Theodorou <i>et al.</i> , 2007; Poulakakis <i>et al.</i> , 2002b
Delos	<i>Palaeoloxodon</i> sp.	-	Pleistocene	Cayeux 1908; Vaufrey, 1929; Doukas and Athanassiou, 2003; Sen <i>et al.</i> , 2014; Sen, 2017: 79-81
Naxos	<i>P. lomolinoi</i>	VAN DER GEER <i>et al.</i> , 2014	Pleistocene	Mitzopoulos, 1961; van der Geer <i>et al.</i> , 2014
Rhodes	<i>Palaeoloxodon</i> sp.	-	Late Pleistocene?	Symeonidis <i>et al.</i> , 1974; see also van der Geer <i>et al.</i> , 2014; 2016; Sen, 2017: 83
Kassos	<i>Palaeoloxodon</i> sp.	-	Pleistocene	Sen <i>et al.</i> , 2014; Sen, 2017: 81
Sérifhos	<i>Palaeoloxodon</i> sp.	-	Pleistocene	Doukas and Athanassiou, 2003: Table 4
Páros	<i>P. antiquus?</i>	(FALCONER and CAUTLEY 1847)	Pleistocene	Doukas and Athanassiou, 2003: Table 4
Kýthera	<i>P. antiquus</i>	(FALCONER and CAUTLEY 1847)	Pleistocene	Tsoukala and Lister, 1998: Table 9; Athanassiou <i>et al.</i> , 2017; Sen, 2017: 81, 83; Athanassiou <i>et al.</i> , 2019
Kephallenia	<i>P. antiquus</i>	(FALCONER and CAUTLEY 1847)	Pleistocene	Athanassiou <i>et al.</i> , 2019
Kalymnos	<i>P. antiquus?</i>	(FALCONER and CAUTLEY 1847)	Pleistocene	Masseti, 2009; 2012; Van der Geer <i>et al.</i> , 2014; Sen, 2017: 81

Table 1.2 Mediterranean islands with representatives of the genus *Palaeoloxodon* (MATSUMOTU 1924). Note that where the original taxon name has been modified the binomial authority appears in parentheses (). Islands with unidentified *Palaeoloxodon* sp. may include endemic species.

The open nomenclature terminology *ex gr.* (*ex grege*) is used where Maltese taxonomy was later applied to Sicilian material, reflecting the uncertainty in conspecificity between islands (see Appendix A for details).

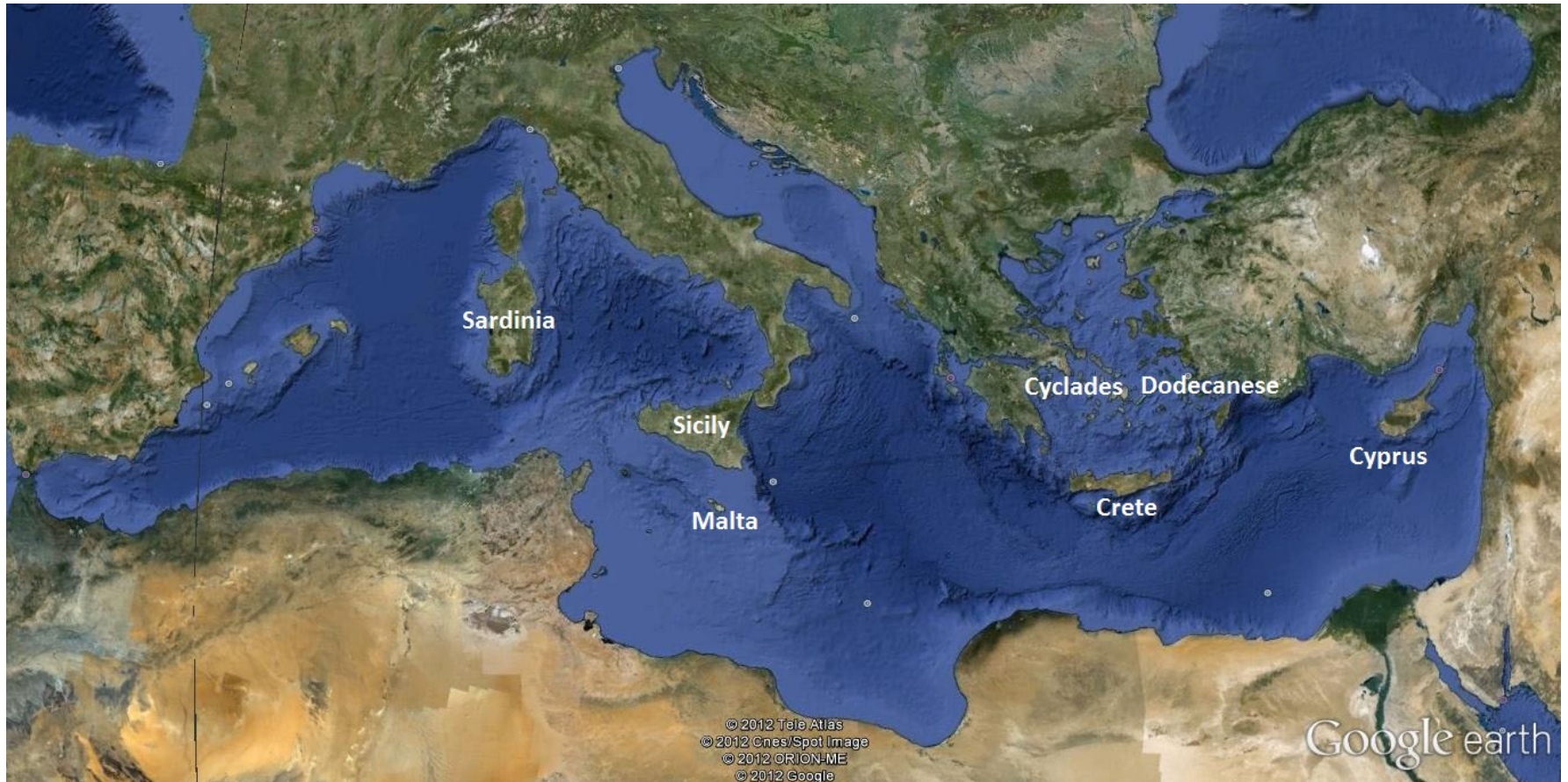


Fig. 1.1 Mediterranean islands with *Palaeoloxodon* and *Mammuthus* spp. Refer to Tables 1.1 and 1.2 for minor islands with proboscideans in the Cyclades and Dodecanese.

nonetheless few studies that systematically compare the anatomy of proboscideans from different islands (see Palombo, 2007; Herridge, 2010 for exceptions). Since Mediterranean islands differ greatly in their environmental characteristics, and were repeatedly colonised by the same ancestral species, islands serve as excellent natural ‘laboratories’ for investigating evolution (cf. Herridge, 2010), and provide a unique opportunity for investigating the effects of numerous selection pressures on the pattern and process of proboscidean evolution.

1.3 Phylogeny and palaeogeographic context of Siculo-Maltese elephants

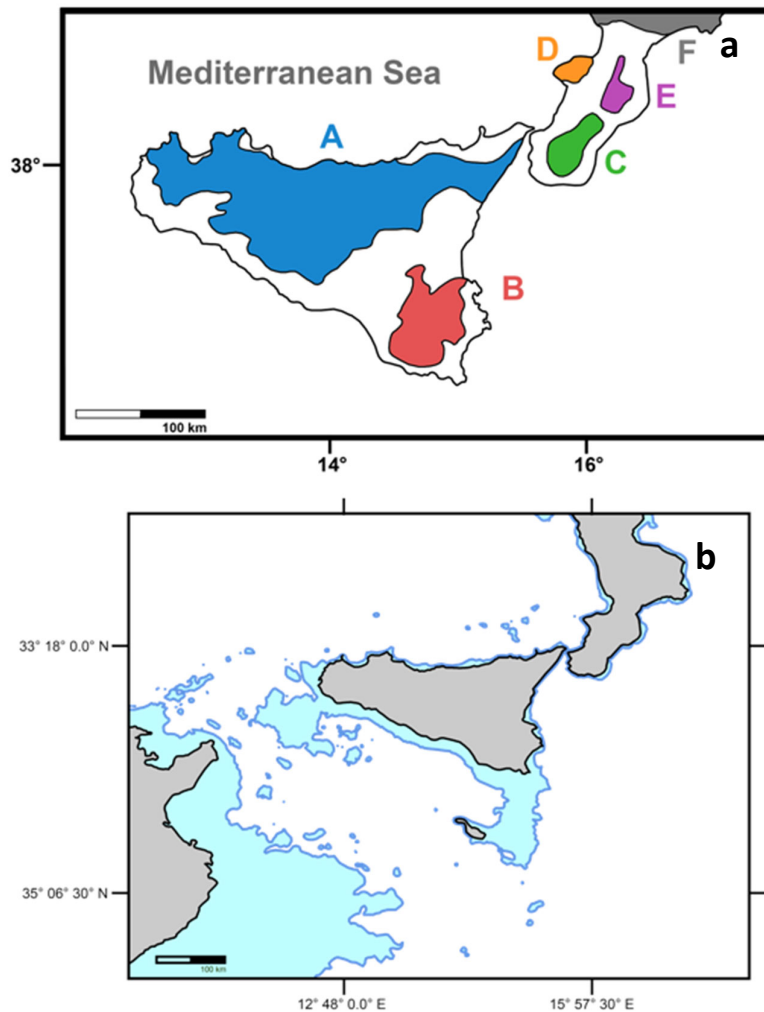
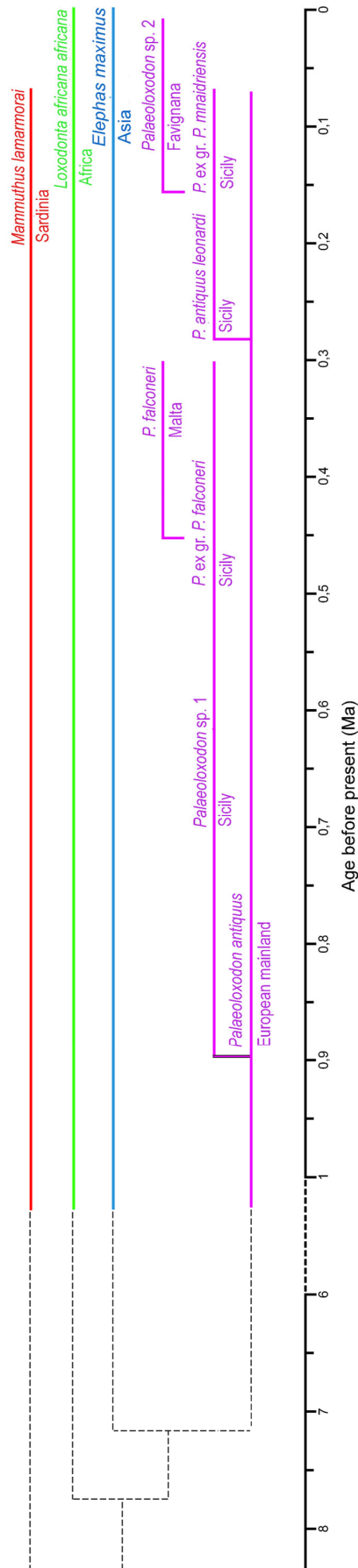


Fig. 1.2(a) Palaeogeography of Sicily and Calabria during the Late Pliocene-Early Pleistocene (after Bonfiglio *et al.*, 2002). A) Northern-Central Sicily B) Hyblean Plateau; C) Aspromonte Massif D) Cape Vaticano E) Serre M F) Northern Calabria. (b) Approximate palaeogeography of the Siculo-Maltese Palaeoarchipelago during the Last Glacial Maximum (light blue represents -130m, after Furlani *et al.*, 2013).

Among the 20 islands known to have been colonised by Pleistocene proboscideans in the Mediterranean, the phylogeny of elephants is particularly complex on the Siculo-Maltese palaeo-archipelago. This is largely due to the fact that the island of Sicily (or its palaeo-islands)

was separated from the Italian mainland by a relatively short distance via the Strait of Messina (currently less than 4 km, see Antonioli *et al.*, 2016), thus enabling *P. antiquus* to reach the island repeatedly during the Middle-Late Pleistocene. The dispersal, evolution and likely also extinction of elephants on the Siculo-Maltese palaeo-archipelago is closely linked to the palaeo-geographic evolution of this region, which was shaped both by tectonics and glacio-eustatics (Yellin-Dror *et al.*, 1997; Di Maggio *et al.*, 1999; Furlani *et al.*, 2013; Marra,



2009; Marra, 2013; Antonioli *et al.*, 2016; Palombo, 2018; van der Geer *et al.*, 2010). Due to the fact that Sicily falls within a tectonically and volcanically active zone where the African plate is being subducted under the Eurasian plate (Yellin-Dror *et al.*, 1997; Argani, 2009), the palaeo-geography of Sicily and its relationship with Calabria (southern peninsular Italy) underwent several significant changes from the Early Pleistocene to Middle Pleistocene (Grasso and Lentini, 1982; Sprovieri 1982; Bonfiglio and Burgio, 1992; Bonfiglio and Piperno, 1996; Bonfiglio *et al.*, 2000: 172; Bonfiglio *et al.*, 2002; Herridge, 2010: 60).

During the Early Pleistocene Calabria consisted of a series of palaeo-islands (Fig. 1.2a), whereas Sicily consisted two main palaeo-islands, a smaller one in the region of what is now the Ragusa Plateau in the south-eastern part of Sicily, and a larger one in what is now northern Sicily (Bonfiglio and Piperno, 1996; Bonfiglio *et al.*, 2002; Herridge, 2010: 58-61; Marra, 2009; 2013). Between 800-500 ka the geography of Sicily has been hypothesized to approximate that of the two-island scenario of Fig. 1.2a (Di Patti and Mannino, 2006: 25) although there is uncertainty with regard to the exact timing of the coalescence of the two palaeo-islands which later formed Sicily.

During the Pleistocene Sicily also underwent significant geomorphological and topographic changes, particularly in the Mt. Etna region which experienced tectonic uplift and volcanism (Gvirtzman and Nur 1999). The submarine eruptions which eventually formed Mt. Etna began around roughly 500 ka (Branca *et al.*, 2008; Branca *et al.*, 2011: 309, 315; De Beni *et al.*, 2011). However the majority of Etna's orogeny occurred during the last 200 ka (Gvirtzman and Nur 1999). Thus the early Middle Pleistocene in particular experienced major geomorphological change (Yellin-Dror *et al.* 1997, Gvirtzman and Nur 1999, Serpelloni *et al.*, 2007). In

Fig. 1.3 (left) Tentative phylogeny of proboscideans included in this study. The chronological placement of nodes for *Loxodonta*, *Elephas* and *Palaeoloxodon* follows Lister (2013: Fig. 1).

contrast to Sicily, Maltese topography during the Pleistocene experienced less significant topographic changes due to orogeny, although Malta tilted towards the north-east along with a general subsidence of the archipelago which is likely still on-going (Magri, 2006). Thus the topography was influenced by subaerial weathering (Pedley, 2011) and especially changes in sea-level, with large areas of relatively flat continental shelf being exposed during glacio-eustatic low-stands (Micallef *et al.*, 2012; Foglini *et al.*, 2016; Prampolini *et al.*, 2017), with the island of Gozo being joined to Malta during lowstands (Foglini *et al.*, 2016).

The early phyletic ancestors of *P. ex gr. P. falconeri* however evolved as a ghost lineage, likely on one of the palaeo-islands of Italy (Fig. 1.2a; see Appendix B), whereas at the time of the *P. ex gr. P. falconeri* deposit at Spinagallo Cave the palaeogeography of Sicily likely more-or-less assumed its present shape (Palombo, 2018). In contrast to the small distance between Sicily and Calabria during the late Middle till Late Pleistocene, the distance between Sicily and Malta (at present 93 km) likely fluctuated more dramatically in response to glacio-eustatic sea level changes due to the presence of a shallow submarine bank (the Hyblean-Malta plateau) extending southwards from Sicily (Fig. 1.2b; Herridge, 2010: Fig. 3.3; Pedley, 2011: Fig. 1b; Antonioli *et al.*, 2016).

Thus it was possible for elephants (and other coeval fauna) to reach Malta from Sicily multiple times from the Middle Pleistocene onwards, most likely during glacial lowstands when a relatively narrow strait separated the two islands (see bathymetric reconstructions in Herridge, 2010: 56-60; Furlani *et al.* 2013; Antonioli *et al.*, 2016). Hence Sicily, Favignana (Aegadian Archipelago) and Malta were isolated to a greater or lesser degree by rises and falls in sea levels during the Pleistocene, affording the opportunity for both anagenetic and cladogenetic speciation among elephants. The phylogeny and systematics are further elaborated in Chapter 2 and discussed in Appendix A; however, a tentative phylogeny of elephants from the Siculo-Maltese palaeo-archipelago is presented in Fig 1.3 in the interim.

1.4 Insular environments as a key for investigating adaptive mechanisms

Patterns of adaptation, colonization and extinction in island endemics play a seminal role in understanding evolution and speciation (Darwin, 1859; Mayr 1963, Kadmon and Pulliam 1993). This is particularly evident with regard to the study of specific adaptations that can be related to the characteristics of different insular environments, or with regard to convergent features on different islands (Table 1.3; McNab, 1994; Diamond, 1991; Palombo, 2007; Lomolino *et al.*, 2012 *inter alios*). This also particularly applies to monophyletic taxa that undergo adaptive radiation on island archipelagos (e.g. Losos *et al.*, 1997; Losos *et al.*, 1998; Grant, 1999; Schuller, 2000; Chiba, 2004; van der Geer *et al.*, 2010). Islands also play a seminal role in understanding many ecological processes and extinction (MacArthur and Wilson, 1967; Case 1978; Herridge, 2010: 19). Since islands provide ‘replicates’ in natural ‘experiments’ for the testing of evolutionary hypotheses (Herridge, 2010 citing MacArthur and Wilson, 1967), they are often justifiably described as the ‘laboratories of evolution’ (MacArthur and Wilson 1967; Whittaker and Fernandez-Palacios, 2006; Losos and Ricklefs, 2009; 2010; van der Geer *et al.*, 2010; Herridge, 2010; Herridge, 2010: 19).

1.4.1 The causes of dwarfism in insular elephants

Insular proboscideans are one of the most conspicuous and oft-cited examples of the *island-rule* (after Foster, 1964; Van Valen, 1973), both for the frequency with which dwarfism occurs, and the dramatic percentage changes evidenced in body mass with respect to the mainland ancestor. The island-rule is a generalization of a tendency for large terrestrial vertebrates to become dwarfed on islands, and small animals to evolve giant forms, and has been observed among a wide range of insular taxa (MacArthur and Wilson, 1967; Lomolino, 2005; Raia and Meiri, 2006; Benton *et al.*, 2010). The rule is however not always as predictable as has sometimes been alleged (see Meiri *et al.*, 2004; 2006; Meiri *et al.*, 2011; Meiri and Raia, 2010), and much debate surrounds the generality and causality of the size-shifts encompassed by the island-rule (see Köhler and Moyà-Solà, 2010; Lomolino *et al.*, 2012; 2013). These shifts are however usually ascribed to a combination of three factors, including (i) resource limitation, (ii) release from predation pressure, or a decrease in inter- and intra-guild competition, and (iii) selection for a faster life-history. The island-rule is however an emergent pattern, and all of these factors may contribute in varying degrees towards the phenomenon of dwarfism in proboscideans (Roth, 1992; Palombo, 2007: 108-109; Palombo, 2009b). The next section provides an overview of the hypothesized causes for dwarfism in insular proboscideans with particular attention to the islands of the western Mediterranean.

Taxon	Island	Present-day island size (km ²)	Duration of isolation from mainland	Predators	Competitors
<i>P. antiquus</i> from Contrada Fusco	Sicily	25,711	Likely short period	Unknown, possibly species in cell below	Unknown, possibly species in cell below
<i>P. ex gr. P. mnaidriensis</i> from Puntali Cave		25,711	Tens or hundreds of thousands of years	<i>Panthera leo</i> , <i>Crocota crocuta</i> cf. <i>spelaeon</i> , <i>Canis lupus</i> , <i>Nesolutra trinacriae</i> , <i>Ursus</i> cf. <i>arctos</i>	<i>Hippopotamus pentlandi</i> , <i>Cervus elaphus siciliae</i> , <i>Dama carburangelensis</i> , <i>Bos primigenius siciliae</i> , <i>Bison priscus siciliae</i>
<i>P. ex gr. P. falconeri</i>		25,711	Hundreds of thousand years	-	-
<i>Palaeoloxodon</i> sp. 1 from Luparello Fissure	Sicily or its palaeo-island(s)	?	Unknown	-	-
<i>P. mnaidriensis</i>	Malta	316	Unknown	None?	-
<i>M. lamarmorai</i>	Sardinia	24,09	At least several tens of thousands of years	<i>Cynotherium sardous</i>	“ <i>Praemegaceros</i> ” <i>cazioti</i>

Table 1.3 Factors hypothesized to influence the evolution of body mass in Siculo-Maltese *Palaeoloxodon* spp. and Sardinian *Mammuthus lamarmorai* (cf. Palombo, 2007). Faunal assemblages after Bonfiglio *et al.*, 2002; Marra, 2005 and Palombo, 2006. Refer to Table 2.1 for species shoulder heights and see also Palombo, 2018 regarding duration of isolation.

(i) Resource limitation

Due to islands being confined areas with finite resources, endemic insular taxa are often faced with resource shortages favouring the evolution of dwarfs that require less food or water in order to survive and reproduce. Studies of extant elephants indicate they consume large amounts of food (Clauss *et al.*, 2007: 212) and frequently move around, sometimes migrating long distances to avoid depleting any one area as they track changes in the local seasonal abundance in food and water (McKay, 1973; Viljoen, 1989; Christiansen, 2004: 534). Daily movement distances averaging 27,5 km are reported in *L. africana* from arid environments, with elephants moving up to 38 km over a 12-hour period (Viljoen and Bothma, 1990, see also Garland, 1983: Table 1 and references therein for other environments), and African elephants also sometimes migrate several hundred kilometres annually (Thouless, 1995; 1996; Nowak, 1999). When an inability to migrate long distances on small islands is coupled with seasonal shortages such as likely in the context of a highly-seasonal Mediterranean-type climate (which was likely already established around 3.2 Ma in the western Mediterranean, see Suc, 1984; Suc *et al.*, 1995), resource limitation is likely to have been a significant factor in the evolution of reduced body mass. Additionally, it is possible that evolution on strongly isolated palaeo-islands between mainland Italy and Sicily may have played a role in the evolution of reduced size (Herridge, 2010: 347, see also Bonfiglio *et al.*, 2002: 34) although there is currently no empirical evidence for this.

(ii) Predation and competition

Insular faunas are typically impoverished and unbalanced in terms of their diversity in comparison to the faunal composition of the adjacent mainland, as is particularly evident among the Pleistocene fauna of Sicily, Malta and Sardinia (Table 1.3). The presence/absence of competitors and large predators on islands is also hypothesized to have influenced the degree of body mass reduction in insular endemics (Raia and Meiri, 2006; Palombo, 2007: 108; van der Geer *et al.*, 2016) due to ecological release (resulting in more pronounced changes in body-size on islands lacking mammalian competitors or predators, see Lomolino *et al.*, 2012; 2013). In Sicilian elephants this is perhaps illustrated by the disparity between the Middle Pleistocene ca. 1m-tall *P. ex gr. P. falconeri* which inhabited the same island as the Middle-Late Pleistocene ca. 2m-tall *P. ex gr. P. mnaidriensis*. However *P. ex gr. P. falconeri* evolved in the absence of predators and competitors (Table 1.3; Bonfiglio *et al.*, 2002: Table 1; Marra, 2013: 122-124). In contrast, *P. ex gr. P. mnaidriensis* evolved in the presence of non-endemic or slightly-endemic predators and competitors, and hyenas scavenged or preyed on the species (Mangano and Bonfiglio, 2012: 59) suggesting large body size still held an advantage for evading predators. Competition also plays an important role in influencing body size evolution as animals maintain different diets by maintaining or evolving to different sizes to avoid competitive exclusion (*sensu* Hardin, 1960; see also Lomolino *et al.*, 2013; van der Geer *et al.*, 2016). Furthermore, niche occupancy may often shift significantly on islands in the absence of similar-sized ecological competitors (Palombo, 2007).

(iii) Accelerated life-history

In the more recent literature attention has also been drawn to the fact that selection on body size in insular endemics may act on life-history traits influencing body size, rather than acting on body size directly (Palkovacs, 2003; Raia *et al.*, 2003; Palombo, 2007; Dirks *et al.*, 2012; Larramendi and Palombo, 2015; Long *et al.*, 2019). Smaller body mass is typically associated with large litters, rapid maturation, short gestation periods, early reproduction and high population densities (Bourliere, 1975; Gould, 1977; Blueweiss *et al.*, 1978; Wassersug *et al.* 1979; Western, 1979; Boyce, 1988; Promislow and Harvey, 1990; Stearns, 1992; Charnov, 1993; Clauss *et al.*, 2014).

Evidence of an accelerated life history is allegedly seen in the age-mortality profile of *P. ex gr. P. falconeri* assemblage which indicates high juvenile mortality at Spinagallo Cave (contrast the four modes of the mortality profiles in Ambrosetti, 1968 with Haynes, 1985; 1987; 1991), and dental remains also suggest higher juvenile mortality in *P. ex gr. P. falconeri* than in the larger *P. ex gr. P. mnaidriensis* (Simonelli, 1995) as is typical in r-selected species (Guenther, 1988). Furthermore, the apparent bilateral tusklessness in *P. ex gr. P. falconeri* females (Ambrosetti, 1968: 295-296) has also been cited as evidence of a more r-selected life-history as this implies increased investment in reproduction relative to growth and somatic maintenance (Raia *et al.*, 2003: 303; Larramendi and Palombo, 2015, see also Marano and Palombo, 2014).

However, the applicability of allometric equations predicting life-history variables in relation to mass based on studies of closely related continental taxa with different body mass is questionable, and histological studies of incremental tissues indicate that dwarf fossil insular endemics often had slower life-histories than expected (Köhler and Moyà-Solà, 2009; Köhler, 2010; van der Geer, 2014: 175-176; Jordana *et al.*, 2012; Kolb *et al.*, 2015). Preliminary analysis of the histology of *P. ex gr. P. falconeri* from Spinagallo Cave provides an estimate of sexual maturity of approximately 9 years, which is within the range of extant elephants and much later than predicted from body mass (Köhler *et al.*, 2013). Further, taphonomic bias resulting in skewed mortality profiles is known in proboscidean assemblages, such as a case of the extreme over-representation of young males attributed to behavioural patterns in *M. columbi* FALCONER 1857 (Lister and Bahn, 2009: 100; 102).

It has been proposed that *P. ex gr. P. falconeri* attained sexual maturity early (at 3-4 years). This estimation is based on the allometric relationship between body mass and physiological time (where $t = M^{0.25}$, using an estimated body mass of 100 kg, see Köhler *et al.*, 2013). This is much earlier than in extant elephants such as *L. africana* (range 7-12 years). However, mass estimates for *P. ex gr. P. falconeri* have since been revised upwards (ranging between 165-300 kg, see Larramendi and Palombo, 2015: 104). Furthermore, although numerous studies demonstrate that K-selection is favoured in low extrinsic mortality environments, and r-selection is favoured under conditions of high extrinsic mortality (Palkovacs, 2003), the specific causes as to why insular elephant populations were subject to high extrinsic mortality are often not explicitly identified. The possibility that reduced body mass in insular

proboscideans evolved in response to selection for a different life history therefore requires further validation.

(iv) Additional factors

Assuming directional selection for increasingly reduced body size over time, one would expect proboscideans that were isolated for longer periods of time (particularly on islands without predators) to be smaller than those that had been on islands for a shorter duration in time. A further consideration with regard to the degree of dwarfism in insular proboscideans is therefore the duration of isolation, which differed greatly on different islands (Lister, 1996a; Tikhonov *et al.*, 2003; Herridge, 2010: 56-58, 355; Lomolino *et al.*, 2013). Interestingly, as might be assumed, insular body size of large mammals is not positively correlated with island area (Lomolino *et al.*, 2012). Thus the degree of dwarfism is influenced by a combination of selective forces whose relative importance and nature of influence are contextual (Lomolino *et al.*, 2012).

1.5 Rationale and aim of the study

The dramatic changes in size and mass of insular proboscideans are also accompanied by numerous allometric changes with respect to their continental ancestors. These are particularly evident in the dwarf species from Sicily and Malta that display numerous highly-derived allometric changes in the teeth and appendicular skeleton (Ambrosetti, 1968; Palombo, 2001a; Ferretti, 2008; Herridge, 2010). These changes however remain only partly-documented and poorly understood in the appendicular skeleton, and require further study in order to explain the large morphological differences between species. The aim of this study is therefore to describe the changes in the appendicular skeleton of dwarf elephants and to investigate their specific causes.

1.5.1 Appendicular changes in Siculo-Maltese elephants

The most important appendicular changes in insular proboscideans that appear in the literature include features that are similar or allegedly homoplastic on separate islands with respect to their continental ancestors (e.g. van der Geer *et al.*, 2010: 362-363). These features include (i) short limbs in relation to body length in *P. ex gr. P. falconeri* from Sicily and *Stegodon aurorae* MATSUMOTO, 1918 from Japan (van der Geer *et al.*, 2010: 313), as well as (ii) the relative shortening of the distal limbs (Ambrosetti, 1968: 308-316) and (iii) increased robusticity such as in *Stegodon aurorae* (Matsumoto, 1918; Konishi, 2000; van der Geer, 2014: 171) and *P. ex gr. P. mnaidriensis* from Puntali Cave, Sicily (Ferretti, 2008: 101). Synostotic fusion is also reported with varying, but much higher frequencies compared to continental proboscideans in the ulna-radius of *P. ex gr. P. falconeri* (Ambrosetti, 1968: 311), *Stegodon florensis insularis* VAN DEN BERGH *et al.*, 2008 from Flores (van den Bergh, 1999; van den Bergh *et al.*, 2008), *P. ex gr. P. mnaidriensis* from Puntali Cave, Sicily (Ferretti, 2008: 101), as well as the Sardinian dwarf mammoth *Mammuthus lamarmorai* (MAJOR 1883) (Caloi and Palombo, 1994: 153; Palombo *et al.*, 2012: 164). Synostosis is further also

reported in the tibia-fibula of *P. ex gr. P. falconeri* (Ambrosetti, 1968: 316) and *Stegodon florensis insularis* VAN DEN BERGH *et al.* 2008 (van der Geer, 2014: 172).

Although highly-derived postcranial anatomies in Maltese and Sicilian elephants were first described a long time ago (Falconer in Murchison, 1868: 303-306; Busk, 1867: 243-251, 254-272, 279-283; Adams, 1874: 49-107, 113-116; Ambrosetti, 1968 *inter alios*), their causes remain poorly understood. These anatomies have however been hypothesized to result from (i) a reduction in body mass, (ii) heterochrony, (iii) low-gear locomotion and (iv) genetic drift. Genetic drift has only been mentioned in the literature without attributing specific allometric changes to its presence (Hooijer, 1967, see also Roth, 2001: 508) so that it is not considered in the next section. This thesis however explores Hypotheses I-III to investigate changes in appendicular anatomy as outlined in this next section.

1.6 Hypotheses

Hypothesis I: background

The feet of insular endemics have often been found to differ considerably in their morphology in comparison to their mainland ancestors and contemporaries. Possible reasons for this may include: (i) allometric scaling, (ii) changes in gait, (iii) paedomorphism and (iv) ‘low-gear locomotion’*

(i) *Allometric scaling relative to body mass* - Seeing the dwarf elephants are dramatically reduced in body-mass, this may have resulted in morphological changes to the feet. Although the effects of scaling are much better studied in the long- than the foot-bones, allometric changes in the articular facets of foot-bones have been observed to scale with body-mass in several taxa. Positive allometry has been observed in some samples (Yapuncich and Boyer, 2014; Yapuncich *et al.*, 2015), and isometry (or close to it) has also been reported in other samples (Tsubamoto, 2014; Yapuncich and Boyer, 2014). It has been suggested that depending on whether mass-induced or muscle-induced forces drive articular facet scaling is probably dependent on sample body-size range and function of the particular facet (Yapuncich and Boyer, 2014).

(iii) *Changes in gait* - In large proboscideans the skeleton is often described as being graviportal, i.e. adapted for bearing weight with a tendency to favour axially-compressive and simple lateromedial bending forces over more complex bending and torsional secondary moments during locomotion (Christiansen, 2007: 424). *P. ex gr. P. falconeri* in contrast, has been hypothesized to be more cursorial than its ancestor *P. antiquus* on the basis of its functional morphology and reduced mass (Palombo, 2003: 288; Larramendi and Palombo, 2015: 4,7), changes in locomotion which may also be reflected in the feet. (iv) Finally, since paedomorphism in *P. ex gr. P. falconeri* has been identified in the cranium (Palombo, 2001), possibly the brain (Benoit, 2015; Larramendi and Palombo, 2015), long-bones (Ambrosetti, 1968: 308-309; Palombo, 2003: 288), and intermembral proportions (Larramendi and Palombo, 2015), it may also have resulted in modifications in the feet.

*Genetic drift, while not discussed further here, may also be a cause for differences.

(iv) *Low-gear locomotion* - Since islands are environments with finite resources where food and water are more limited, and shortages cannot be made up by migrating long distances as they are among extant elephants in seasonal environments (see Section 1.4.1), any mechanisms which enabled dwarf elephants to expand their ecological niche by improving their ability to climb would likely have been an advantage (Appendix C; cf. Leinders and Sondaar, 1974: 112; Caloi and Palombo, 1990; 1994: 157), fitting a broader ecological pattern of niche shifts in endemic island vertebrates (Lomolino, 2005; Palombo, 2007). *P. ex gr. P. falconeri* has also been hypothesized to have shifted its size and niche occupancy towards the mixed-feeder cervid species of the mainland, due to the absence of any intra-guild competition (Palombo, 2007: 113; Palombo, 2009b: 345).

Since the island of Sicily is currently 86% hilly or mountainous (Benedetto and Giordano, 2008: 120), and *P. ex gr. P. falconeri* evolved in the absence of predators, it is therefore highly likely that there was selection for increased stability during locomotion. (refer to Appendix E). Furthermore, it has also been pointed out that many of the morphologies described in Section 1.5.1 would likely increase stability and decrease the likelihood of injury by twisting ankles (see e.g. Sondaar, 1977; Caloi and Palombo, 1994; 1995; Köhler and Moyà-Solà, 2001; van der Geer *et al.*, 2010: 361-363), a pattern often referred to as ‘low-gear locomotion’ (Sondaar, 1977: 683-686). Evidence of possible low-gear locomotion has also been suggested in *P. ex gr. P. falconeri* on the basis of the long-bones (Appendix C).

Thus, due to the fact that the foot-bones of numerous other insular endemics are often highly derived, and for the three reasons outlined above, one would also expect the foot-bones of insular endemic *Palaeoloxodon* species differ compared to *P. antiquus*.

Hypothesis I: The feet of elephants from Sicily (particularly those of *P. ex gr. P. falconeri*) differ significantly in terms their morphology compared with their ancestral species (and co-generic contemporary) *P. antiquus*.

If this hypothesis is correct, it is predicted that:

- There will be significant differences in the allometry of the articular facets of the carpals and tarsals of insular *Palaeoloxodon* spp. compared with continental *P. antiquus*.
- There will be large differences between *P. antiquus* and its smallest, highly derived insular descendent (and contemporary) *P. ex gr. P. falconeri*.

The predictions of Hypothesis I are tested in Chapter 3 (*Insular adaptations in the feet*).

Hypothesis II: background

Large extant and fossil proboscideans are among the longest-lived terrestrial mammals (Roth, 1984), often living into their 70s in the case of extant wild African elephants. This suggests that dwarfism in insular proboscideans may have resulted from different

developmental processes, including (i) a shorter growth period, (ii) a lower growth rate, or (iii) the delayed onset of growth relative to the ancestral species. These differences in growth between the ancestral and descendant species are collectively the result of a process referred to as *heterochrony*, which is defined as *changes during ontogeny in the relative times of appearance and rates of development of characters which were already present in ancestors* (Abercrombie *et al.*, 1990: 268; see also McKinney *et al.*, 1990; McKinney and McNamara, 1991; 1997; 2002; Chatwin, 2016: 259).

Heterochrony may result in dwarfism with no changes in shape, in which case dwarfism is said to be *isometric*. However, the likelihood of concomitant changes in shape (*allometric* changes in the skeleton) occurring as a result of heterochrony is high. Allometric changes in insular endemics are sometimes described as being the result of *paedomorphosis*, which is defined as *the acquisition in mature descendants of ancestral juvenile characteristics* (Godfrey and Sutherland, 1995: 405; see also Gould, 1977: 2)*.

Evidence of paedomorphism is seen in several insular endemic dwarf mammals, allegedly including *Homo floresiensis* (van Heteren and de Vos, 2007), Madagascan lemurs (Cheirogaleidae, see Masters *et al.*, 2014), the pig *Sus nanus* (van Heteren and de Vos, 2007: 78), the goat *Myotragus balearicus* (van Heteren and de Vos, 2007: 78), possibly in the canid *Cynotherium malatestai* (Madurell-Malapeira *et al.*, 2015), and (though not clearly identified as such) possibly in *Hippopotamus minutus* (cf. Major, 1902: 108; Boekschoten and Sondaar, 1966). Paedomorphism has also been documented in dwarf proboscideans (Ambrosetti, 1968: 308-309; Accordi and Palombo 1971; Maglio, 1973; see also van den Bergh, 1999: 201; Roth, 1992; Lister, 1996a; Palombo, 2001a; 2003; van Heteren and de Vos, 2007; Herridge, 2010: 325). Paedomorphism is for example reflected in *P. ex gr. P. falconeri* from Spinagallo Cave, which has been described as possessing a highly paedomorphic cranium closely resembling juvenile *L. africana* (Palombo, 2001a; Palombo and Giovinazzo, 2005), as well as a possibly paedomorphic brain (Benoit, 2015; Larramendi and Palombo, 2015).

With the exception of brief qualitative descriptions (see Ambrosetti, 1968: 308-309; Palombo, 2003: 288; Larramendi and Palombo, 2015: 4), evidence of paedomorphism in the appendicular skeleton of dwarf elephants has never been rigorously examined. Furthermore, the presence of paedomorphism in the limbs of *P. ex gr. P. falconeri* has recently been rejected (van der Geer, 2014: 174). Nevertheless, this rejection made no explicit reference to metric analyses, and no metric comparisons between the limbs of adult *P. ex gr. P. falconeri* and neonate or juvenile continental proboscideans were made. Considering the strong evidence for paedomorphism in the cranium of *P. ex gr. P. falconeri* (Palombo, 2001a; Larramendi and Palombo, 2015: 2), and the global reduction in size in this species, one might therefore expect evidence of paedomorphism in the limbs (*contra* van der Geer, 2014: 174).

*When comparing elephant taxa in order to study heterochrony, particularly with low sample-sizes or disarticulated material (where it is often difficult to determine an individual's ontogenetic stage), it is important to distinguish between a) ontogenetic scaling and b) interspecific scaling. In order to avoid confusing a) and b) it is therefore necessary to constrain ontogenetic equivalence as tightly as possible between different taxa (see Chapter 2; Herridge, 2010: 199-246; 290).

Furthermore, rapid and drastic changes in size and shape during phylogeny (such as in Siculo-Maltese elephants) are often effected through heterochrony resulting in paedomorphism (Gould, 1977). A more rigorous test of the hypothesis that paedomorphism is reflected in the limbs of *P. ex gr. P. falconeri* is therefore warranted.

Hypothesis II: Heterochrony causing dwarfism resulted in paedomorphic morphologies in the limbs of *P. ex gr. P. falconeri* from Spinagallo Cave.

If this hypothesis is correct, it is predicted that:

- The long bones and calcaneus of *P. ex gr. P. falconeri* more closely resemble juvenile *L. africana* than adult *L. africana* in terms of bivariate allometry and overall morphology.
- The degree of paedomorphism increases with decreasing body size in Sicilian dwarf elephants.

The predictions of Hypothesis II are tested in Chapters 3 and 4.

Hypothesis III: background

During a ca. 30-million year period in the first half of the Tertiary there is a clear trend towards increasing mass in proboscideans (Smith *et al.*, 2010), a trend often referred to as *Cope's Rule* (Raia *et al.*, 2012), after the American palaeontologist Edward Drinker Cope (1840-1897). Over the course of this period, proboscideans evolved highly-derived, graviportal (see below) appendicular apomorphies for coping with the anatomical (especially postural) requirements of support (e.g. Herridge and Hutchinson, 2007; Hutchinson *et al.*, 2011). In contrast, insular proboscideans underwent body mass changes of a similar order of magnitude, such as from ca. 11-ton *P. antiquus* to ca. 300 kg *P. ex gr. P. falconeri* (see mass estimates in Larramendi and Palombo, 2015; Larramendi, 2016) (a ca. 88% reduction in body mass) over much shorter timescales, spanning hundreds of thousands years, or perhaps much less. How was such a large difference in mass and morphology achieved? And to what extent are the appendicular differences in the skeleton of dwarf elephants a reflection of the reduced requirements of support? Furthermore, does the location and attachment area of muscle scars in the long bones of insular dwarf elephants differ in comparison with their continental ancestors?

A critical limit of ~300 kg has previously been identified above which mammals are required to sacrifice much of their cursorial performance to the demands of support (Biewener, 1989; 1990). Comparing species slightly below and slightly above this limit should therefore provide a means of assessing to what extent body mass and morphological features are related. Under conditions of so-called *geometric similarity* (also known as *isometric similarity*), shape does not change with scaling. However, dwarf elephants are not scaled-down versions of their ancestors. Since function is scale-dependent, and volume, mass and many other properties do not scale linearly with shoulder height (McGowan, 1994;

Biewener, 2003: 10), a change in absolute size often necessitates modifications by which the mechanical consequences of greater size can be avoided.

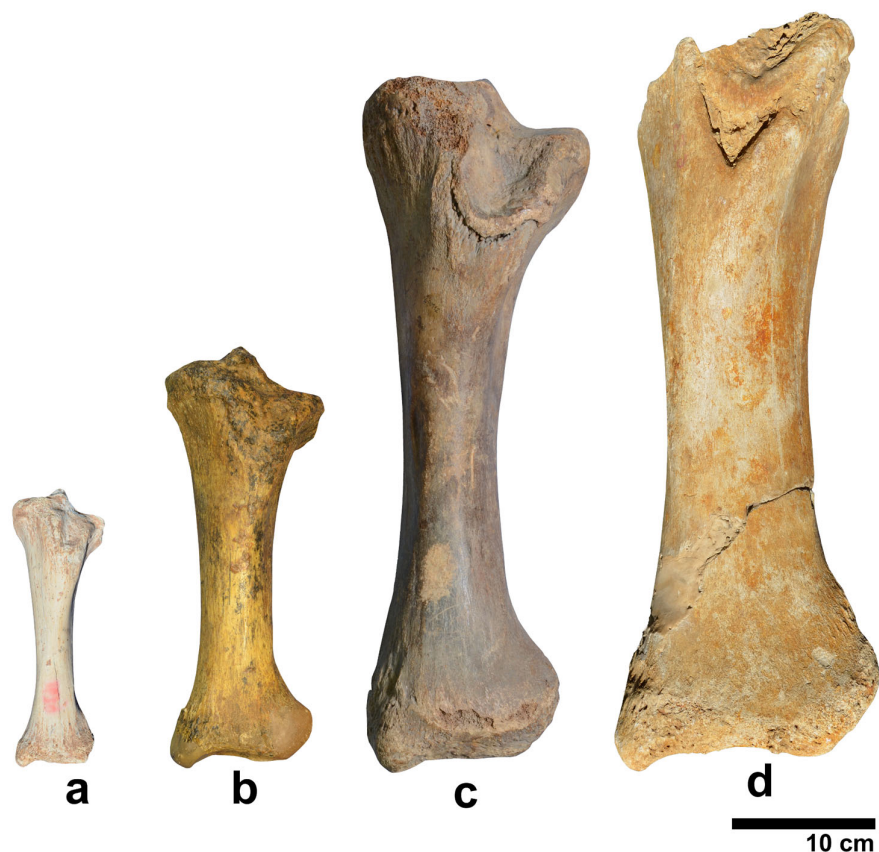


Fig. 1.4 Tibiae of adult Sicilian *Palaeoloxodon* spp. in cranial aspect a) *P. ex gr. P. falconeri* from Spinagallo Cave (UCat-T64)^{dex} b) *Palaeoloxodon* sp. 1 from Luparello Fissure (IPH-F2928)^{dex} c) *P. ex gr. P. mnaidriensis* from Puntali Cave (GMP-GPM12)^{sin} d) *P. antiquus* of uncertain Sicilian provenance (UCat)^{dex}. Refer to Fig 2.1 for site locations.

Frequently, an animal's bauplan reflects so-called *elastic similarity* to allow for scale-dependent functional requirements (Hildebrand, 1988: 466-467; Bertram, 2016). Such a close relationship between mass and anatomy has for example been demonstrated in studies of closely-related quadrupedal taxa with a wide range in mass (Biewener, 2003; Hildebrand, 1988). Furthermore, not only anatomy, but also the type of locomotor system correlates closely with mass, esp. with regard to so-called *graviportal locomotion* (adapted for large body mass support) vs. *cursorial locomotion* (adapted for endurance and speed). Additionally, *P. ex gr. P. falconeri* may also have had a more agile gait than its mainland ancestor in order to forage in more inaccessible regions, expanding its niche (see Caloi and Palombo, 1994: 154; Larramendi and Palombo, 2015: 2). However, as has been previously pointed out, little effort has been made to quantify 'low-gear' and 'frisky' locomotion as biomechanical models, making it difficult to assess their adaptive value (Herridge, 2010: 259). The diverse range in mass among Elephantidae and Siculo-Maltese *Palaeoloxodon* spp. in particular therefore provides an excellent context in which to test hypotheses about the relationship between mass and appendicular anatomy.

Hypothesis III: As mass decreases in dwarf elephants gait becomes more agile in the antero-posterior direction.

If this hypothesis is correct, it is predicted that:

- There is greater flexion in the limbs in insular dwarf proboscideans.
- *P. ex gr. P. falconeri* was more cursorial than *P. antiquus*, and this would be reflected in the greater depth and antero-posterior length of the glenoid fossa of the of the scapula, which would increase the range in rotation of the humeral head.

The predictions of Hypotheses III are tested mainly in Chapter 4 (*Insular adaptations in limb musculoskeletal anatomy*).

1.7 Thesis layout

A literature survey on the evolution of insular elephants is provided in Chapter 1. Chapter 2 (*Materials and Methods*) introduces the materials, describes and illustrates the measurements taken, and also briefly describes the anatomy of each individual species studied from Sicily, Malta, Favignana, and Sardinia, as well as the mainland comparators. Chapter 3 (*Insular adaptations in the feet*) examines the evolution of the feet of insular dwarf proboscideans from Sicily, Malta and Sardinia. The chapter especially investigates the functional morphology of the calcaneus of elephants from Sicily and Malta, as well as to what extent differences between the islands may elucidate systematics and taxonomy. Chapter 4 (*Insular adaptations in limb musculo-skeletal anatomy*) examines the musculoskeletal adaptations in the long bones of insular proboscideans, and compares the appendicular skeleton of Siculo-Maltese taxa with *P. antiquus* and *L. africana*. This chapter also examines heterochrony in the appendicular skeleton, with an emphasis on pedomorphism in *P. ex gr. P. falconeri* from Spinagallo Cave which is compared with the ontogenetic allometry of *P. antiquus* and especially *L. africana*.

Chapter 5 (*Summary of research findings*) discusses the main conclusions of chapters 3-4, and makes suggestions for future research. Chapter 6 (*Conclusions*) highlights the major findings of the study. In Appendix A (*Systematics and taxonomy*) an up-to-date taxonomy of proboscideans from Sicily, Malta, Favignana and Sardinia is provided and in Appendix B (*Preliminary results of Uranium-Thorium dating at Alcamo Quarry, Sicily*) new absolute ages for *Palaeoloxodon* sp. remains are reported. Appendix C (*Insular endemic mammals with alleged evidence of low-gear locomotion*) surveys the literature relating to insular locomotion, and Appendix D (*Preliminary catalogue of the unaccessioned Palaeoloxodon sp. remains from Luparello Fissure, Sicily in the Vaufrey collection*) lists important fossil specimens re-located in Paris during this research. Finally Appendix E (*Regression table*) provides statistical details relating to MWU-tests, and Appendix F (*Scaling in Palaeoloxodon long-bones*).

CHAPTER 2

Materials and methods

Part 1: Materials

The purpose of this chapter is to describe the materials and methods, and is divided into two parts: Part 1, which introduces the materials consisting of four likely *Palaeoloxodon* spp. from Sicily, two species from Malta, one species from Favignana, as well as the Sardinian dwarf mammoth and comparative continental material. Part 1 additionally provides background on the provenance and biochronological framework of fossiliferous assemblages from the Siculo-Maltese palaeo-archipelago. Part 2 of this chapter describes the methods used, including the mathematical and statistical methods and their particular relevance to the study of postcranial allometry. Table 2.1 shows the species that will be investigated, their geographic provenance, shoulder height and chronology, and is followed by an outline of the *P. antiquus* material to which insular proboscideans are being compared. The rest of the chapter provides brief descriptions of each of the insular species, ordered from the oldest to most recent based on their tentative geo-chronological age.

Species	Provenance	Shoulder height (m)	Chronology	Collections
<i>Palaeoloxodon antiquus</i> (FALCONER and CAUTLEY 1847)	Neumark-Nord 1, Germany	3-4	late Middle (MIS 7) or early Late Pleistocene (MIS 5e)	LVH
	Riano, Italy		Middle Pleistocene	MPRU
	Riganano Flaminio, Italy			MPRU
	Uncertain, Sicily		Pleistocene	UCat
<i>Palaeoloxodon antiquus leonardi</i> (AGUIRRE 1969a)	Via Libertà, Sicily	2,9	Middle Pleistocene	GMP
<i>Palaeoloxodon</i> ex gr. <i>P. mnaidriensis</i> (ADAMS 1874)	Puntali Cave, Sicily	2	late Middle-early Late Pleistocene	GMP, NHMB
<i>Palaeoloxodon mnaidriensis</i> (ADAMS 1874)	Mnaira Gap, Malta	~1,7	Pleistocene	NHMUK
<i>Palaeoloxodon</i> sp. 1	Luparello Fissure, Sicily	~1,8	late Early or early Middle Pleistocene	IPH, GMP
<i>Palaeoloxodon</i> sp. 2	Faraglione Cave, Favignana	~1,7	Late Pleistocene	GMP
<i>Palaeoloxodon falconeri</i> (BUSK 1867)	Benghisa Gap, Malta	1-1,2	Middle Pleistocene	NHMUK
	Spinagallo Cave, Sicily	1-1,2	Middle Pleistocene	UCat, MPRU, NHMB
	Luparello Fissure, Sicily	1	Middle Pleistocene	IPH, GMP
<i>Loxodonta africana</i> (BLUMENBACH 1797)	Kenya	2.2-4.0	Extant	KNM
<i>Elephas maximus</i> LINNAEUS 1758	Zoo elephant	2,2-2,6	Extant	SAM
<i>Mammuthus lamarmorai</i> (MAJOR 1883)	Morimonta region, Sardinia	1,4	Late Pleistocene?	NHMB

Table 2.1 Elephantinae taxa sampled, their geographic provenance, approx. adult skeletal height, geological age and collections provenance. Refer to Section 2.5 for collections abbrev. Shoulder heights are based on references listed in Tables 1.1-1.2. and personal observations.

2.1 *Palaeoloxodon antiquus* (FALCONER and CAUTLEY 1847)

Species diagnosis: The species is represented by numerous individuals and all skeletal elements, with a skeletal shoulder height of 4m and estimated mass from ca. 6,000-12,000 kg in bulls and 3m height and mass from ca. 4500-6000 kg in cows (Mania, 2010b: 218; see Larramendi, 2016 for mass estimates). The tusks are comparatively straight; usually curving upwards or slightly inwards, and the molars are relatively narrow and high-crowned with lozenge-shaped enamel loops and medial expansions on the occlusal surface (Herridge, 2010: 91). The long bones are robust and the ulna massive (Palombo et al., 2010: 233) and the humerus has a wide deltoid tuberosity with a deep deltoid fossa (Kroll, 1991: 20; Kevrekidis and Mol, 2015). Geographic distribution: Widespread during interglacial stages of Europe (Lister, 2004: 57), inhabiting the British Islands, parts of continental Eurasia from Spain to the Urals, including Asia Minor, the Levant and the Mediterranean islands (Halámková, 2006: Table 4; Pushkina, 2007; Palombo et al., 2010: 223; Albayrak and Lister 2012; Kevrekidis and Mol, 2015: Fig. 1; see also Table 1.2). Chronological distribution: late Early to Late Pleistocene in Europe (roughly 900–34 ka, see Stuart, 2005; Palombo, 2015).

2.1.1 *Palaeoloxodon antiquus* from Neumark-Nord Lake 1, Sachsen-Anhalt, Germany

The Neumark-Nord 1 (NN-1) assemblage studied in this thesis derives from a late Middle Pleistocene or Late Pleistocene lacustrine deposits which evidences interglacial climatic conditions (Mania, 2010a; Mania and Mai, 2010). The age of the main fossiliferous deposits are controversial, either being ascribed to MIS 7 (243-191 ka), or alternatively MIS 5 (130-71 ka) (see Palombo, 2012: 81 and references therein for discussion). The site was excavated between 1985-1996 and has produced the richest *P. antiquus* assemblage from any single locality to date. The stratigraphic provenance of each fossil is known (Mania, 2010b: 201-218), and the associated diverse plant and animal remains have enabled a detailed reconstruction of the palaeoenvironment (Böttinger, 2010; Mania, 2010a; Mania and Mai, 2010; Mai and Hoffman, 2010; Schoch, 2010; Seifert-Eulen, 2010 *inter alios*).

Several elephants were also found in articulation, and in several individuals both the dental stage (following Laws, 1966; Roth and Shoshani, 1988) and sex have been ascertained using pelvic allometry (Marano and Palombo, 2013: Table 3; however see also Larramendi *et al.*, 2017), making the assemblage highly suitable for comparison with insular *Palaeoloxodon* spp. Although the sample-size is large, the Neumark-Nord 1 assemblage includes no well-preserved juveniles, and only one well-preserved young individual (with an estimated age of 26 years, NN-E22), and therefore has a strong bias towards adult individuals (Marano and Palombo, 2013: Table 3). Due to time constraints and accessibility limitations because of storage, the NN1 collection was only subsampled. However, data were also obtained in 2008-2009 by Maria Rita Palombo (Sapienza, University of Rome), at the kind invitation of Harald Meller (Landesmuseum für Vorgeschichte, Halle), assisted by Federica Marano (Sapienza, University of Rome) and Ebru Albayrak (M.T.A. Natural History Museum, Ankara), and are here included (referred to as Palombo *et al.*, unpublished) with the kind permission of Maria Rita Palombo. Although this adds an element of inter-observer variability, any uncertainties as to how measurements were obtained were queried directly with Maria Rita Palombo, and

in some cases a subsample of measurements was compared in order to verify consistency between observers. Note that unless otherwise stated in the figure captions all data is original.

Although *P. antiquus* is hypothesized to be ancestral to all Siculo-Maltese elephants (Palombo, 2003), it is important to bear in mind that *P. antiquus* from Neumark-Nord 1 postdates the arrival of the ancestor of *P. ex gr. P. falconeri* on Sicily (probably by several hundred thousand years, see Appendix B). In contrast, the NN-1 assemblage may temporally overlap with *P. ex gr. P. mnaidriensis* from Puntali Cave. There are however supposedly no evolutionary morphological trends evident in European *P. antiquus* through time, and *P. antiquus* populations may be considered as equivalent taxonomic entities (Herridge, 2010: 254 citing Davies, 2002). According to Davies (2002) there is also little evidence of temporal and geographical patterns in dental morphology (Herridge, 2010: 108 citing Davies, 2002). However, Davies' sample was heavily biased towards British and German specimens (Herridge, 2010: 108), and other researchers have argued in favour of evidence for anagenetic change in *P. antiquus* (Osborn, 1931; Halámková, 2006: 21), though a more extensive examination of evidence is currently lacking. Furthermore, while morphological differences have been noted between German and Italian *P. antiquus* populations (particularly in the skull), no significant differences have been observed in the postcranial skeleton (see Saegusa and Gilbert 2008; Palombo and Ferretti, 2010; Anzidei *et al.*, 2012: 177 Palombo *et al.*, 2017 *inter alios*). However, to avoid any potential sample bias and include possible geographic variation, *P. antiquus* remains from other European sites and from the published literature are also included in this study, as well as new measurements obtained from an adult individual from Riano (Latium), Italy, from the late Middle Pleistocene (see Maccagno, 1962a: Plate XV; Accordi and Maccagno, 1962).

2.2 Siculo-Maltese *Palaeoloxodon* species and their biochronology

The absolute chronology of Siculo-Maltese proboscideans is generally poorly established (Herridge, 2010: 62-85). Although the earliest arrival of elephants on Sicily is currently unreported in the fossil record, their arrival presumably postdates the earliest evidence of *P. antiquus* in southern Italy (at Notarchirico) around ca. 740-600 ka (see Piperno *et al.*, 1998), although some have favoured an earlier arrival on Sicily, though without fossil evidence (Marra, 2013: Fig. 3). In contrast, a more recent age post-dating 32,000±4,000 ka was reported for *P. ex gr. P. mnaidriensis* from San Teodoro Cave based on U-Th dating (Mangano and Bonfiglio, 2012: 55; see also Antonioli *et al.*, 2016).

Mediterranean insular faunas nonetheless have a tendency to undergo periods of isolation often leading to endemism, intermitted by rapid compositional turnover as waves of new taxa arrive from the mainland (Bonfiglio *et al.*, 2000; Bonfiglio *et al.*, 2002; Sondaar and van der Geer, 2002; Marra, 2005; Masini *et al.*, 2008; Palombo, 2009a; van der Geer *et al.*, 2010). These turnovers are probably related to glacio-eustatic sea-level changes (Palombo, 2003: 275; Palombo, 2007: 113) and perhaps also to tectonics in some instances (van der Geer *et al.*, 2010: 88; Antonioli *et al.*, 2016). In the case of Sicily, the faunal composition of fossil assemblages has enabled a fairly detailed biochronological framework to be established based

on (i) the arrival of new taxa, their (ii) co-occurrence and (iii) extinction. Here, the Plio-Pleistocene biochronology is divided into five distinct faunal complexes (FCs) on the basis of vertebrate-bearing deposits (see Table 2.3). These FCs are further correlated with marine deposits and ancient shorelines (Di Maggio *et al.*, 1999; Bonfiglio *et al.*, 2002: 30; Bonfiglio *et al.*, 2003) and Marine Isotope Stages (Palombo, 2003; 2007; Marra, 2013).

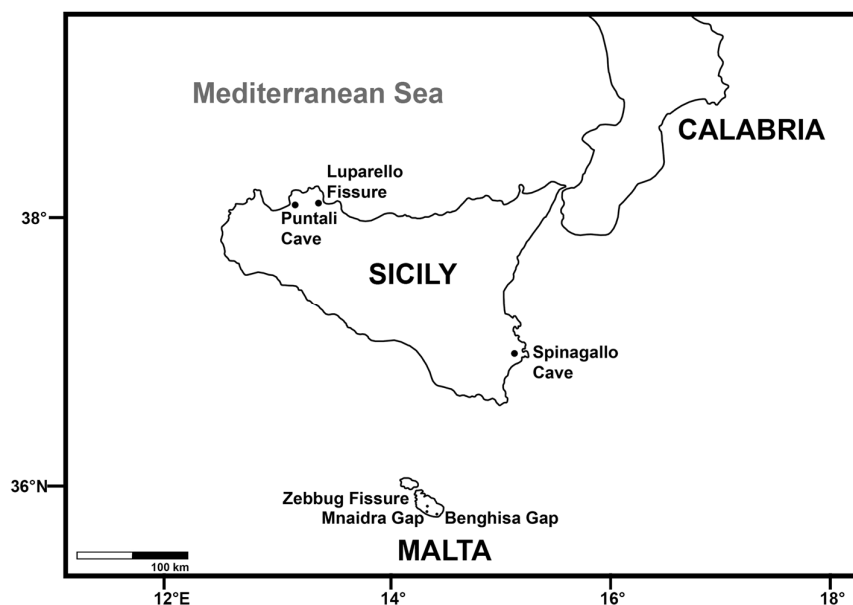


Fig. 2.1 Sicilian and Maltese localities with elephant remains studied in this thesis.

Several Sicilian biochronological schemes have been developed and modified over the years, dividing the Late Pliocene to Holocene into five or more Faunal Complexes (FCs) (Kotsakis, 1979; Burgio, 1997; Bonfiglio *et al.*, 2000; Bonfiglio *et al.*, 2002; Masini *et al.*, 2008; Marra, 2013). Two of these FCs were formally named after the elephant species present on Sicily at the relevant time (the early Middle Pleistocene *Elephas falconeri* FC and the late Middle Pleistocene - early Late Pleistocene *Elephas mnaidriensis* FC see Bonfiglio *et al.*, 2002; Masini *et al.*, 2008: Fig. 4). This approach was however recently abandoned in favour of naming FCs after the localities at which numerous coeval vertebrate taxa are best represented, a change undertaken in part due to taxonomic revisions (Marra, 2013; Table 2.3)*.

*Several legitimate concerns with the paper by Marra have been highlighted (Bonfiglio, 2013). For example the name *Elephas mnaidriensis* was formerly applied to the Puntali Cave elephant material, and is now considered as *Palaeoloxodon mnaidriensis*, and the species may in fact belong to a new, as yet unnamed species different to *P. mnaidriensis* from Malta (see Herridge, 2010). It would thus be inappropriate to continue referring to a FC using a binomial in which the generic and specific epithets are dubitative and likely to be subject to further change, while noting the limitations of Marra and that faunal complexes may not be wholly equivalent between Marra and previous FCs (Bonfiglio *et al.*, 2002; Masini *et al.*, 2008).

Sicily			Malta				Favignana	Pleistocene sub-division	Marine Isotope Stage (Shackleton, 1995)	Marine isotope stage start date
<i>P. antiquus leonardi</i> from Via Libertà, Palermo	<i>P. ex gr. P. mnaidriensis</i> from Puntali Cave	<i>Palaeoloxodon</i> sp. 1 from Luparello Fissure	<i>P. ex gr. P. falconeri</i>			<i>P. falconeri</i>	<i>P. mnaidriensis</i> from Mnaidra Gap			
		Luparello Fissure	Alcamo Quarry	Spinagallo Cave	Benghisa Gap	Zebbug Fissure				
								Holocene	1	14
	(9)						6	Late Pleistocene	2	29
									3	57
									4	71
	(1)								5a	82
	(1)								5b	87
	(1)								5c	96
	(1)								5d	109
	(1)								5e	123
	?					?		Middle Pleistocene	6	191
			?	5	?	?	?		7	243
			?	5	?	?	?		8	300
			?	5			?		9	337
			?	5			?		10	374
			?						11	424
			?						12	478
		1	?	7					13	533
		1							14	563
		1							15	621
		1							16	659
									17	676
								18	712	
								19	761	
								20	790	
								Early Pleistocene	21	814

Table 2.2 Published geochronological ages of Siculo-Maltese elephants. Uncertain ages without published dates are indicated with a question mark. Chronology sources: ¹Rhodes, 1996; ²Bonfiglio *et al.*, 2003; ³Palombo, 2003; ⁴Marra, 2013; ⁵cf. Herridge *et al.*, 2014; ⁶Palombo, pers. comm.; ⁷Appendix A; see also ⁸Scarborough *et al.*, 2016; ⁹Mangano and Bonfiglio, 2012). Parentheses () indicate published dates were obtained from sites different to those listed, but likely from the same species.

Chronology	Faunal Complex (Marra, 2013)	<i>Palaeoloxodon</i> spp. on Sicily	Select associated taxa (Marra, 2013)	Common names of notable associated taxa	Nature of FC composition	
Holocene	-	Absent	<i>Erinaceus europaeus</i> , <i>Terricola savii</i> , <i>Crocidura</i> cf. <i>sicula</i> , <i>Apodemus</i> cf. <i>sylvaticus</i> , <i>Oryctolagus cuniculus</i> , <i>Arvicola terrestris</i> ^[SEP] , <i>Glis glis</i> , <i>Canis lupus</i> , <i>Vulpes vulpes</i> ^[SEP] , <i>Sus scrofa</i> ^[SEP] , <i>Equus hydruntinus</i> , <i>Martes</i> sp. ^[SEP] , <i>Mustela</i> cf. <i>nivalis</i> , <i>Cervus elaphus</i> , <i>Bos primigenius</i> , <i>Felis silvestris</i> , <i>Lutra lutra</i>	Equid, deer, bovid, dog, pig, fox, wildcat, otter, rabbit, hedgehog, vole, Sicilian shrew	Balanced, mildly impoverished	
Pleistocene	Late	Castello	<i>P. antiquus</i>	<i>Crocidura sicula</i> . Non-endemic: <i>Erinaceus europaeus</i> , <i>Canis lupus</i> , <i>Sus scrofa</i> , <i>Vulpes vulpes</i> , <i>Cervus elaphus</i> , <i>Bos primigenius</i> , <i>Equus ferus</i> , <i>Lepus europaeus</i> , <i>Apodemus</i> cf. <i>sylvaticus</i> , <i>Terricola savii</i>	Deer, horse, bovid, pig, European hare	Low diversity, endemites mainly absent, unbalanced
	Late Middle	San Teodoro	<i>P. ex gr. P. mnaidriensis</i>	<i>Crocidura sicula</i> , <i>Cervus elaphus siciliae</i> , <i>Bos primigenius siciliae</i> . Non-endemic: <i>Erinaceus europaeus</i> , <i>Crocota crocuta spelaea</i> , <i>Canis lupus</i> , <i>Ursus arctos</i> , <i>Sus scrofa</i> , <i>Vulpes vulpes</i> , <i>Equus hydruntinus</i> , <i>Apodemus</i> cf. <i>sylvaticus</i> , <i>Terricola savii</i>	Deer, bovid, horse, steppe bison, pig, bear, hyena, dog, fox, wood mouse, Sicilian shrew, vole, hedgehog	Mildly impoverished, species ranging from endemic to marginally endemic
	Early-Middle Middle	Maccagnone		<i>Lutra trinacriae</i> , <i>Leithia melitensis</i> , <i>Crocidura esuae</i> , <i>Maltamys wiedincensis</i> , <i>Hippopotamus pentlandi</i> , <i>Cervus elaphus siciliae</i> , <i>Dama carburangelensis</i> , <i>Bos primigenius siciliae</i> , <i>Bison priscus siciliae</i> (?), Non-endemic: <i>Crocota crocuta spelaea</i> , <i>Panthera leo</i> , <i>Canis lupus</i> , <i>Ursus arctos</i> , <i>Sus scrofa</i> , <i>Terricola</i> sp.	Lion, hyena, dog, bear, hippo, bovids, equids, deer, pig	Balanced and slightly impoverished, mildly endemic to endemic
	Late Early	Spinagallo	<i>P. ex gr. P. falconeri</i>	<i>Testudininei indet.</i> , <i>Lutra trinacriae</i> , <i>Crocidura esuae</i> , <i>Maltamys gollcheri</i> , <i>Leithia melitensis</i> , <i>Leithia cartei</i>	Giant tortoise, giant otter, Sicilian shrew, giant dormice	Highly unbalanced, oligotypic, highly endemic
?Pliocene–Early Pleistocene	Monte Pellegrino	Absent	<i>Hypolagus peregrinus</i> , <i>Pannonictis arzilla</i> , <i>Asoriculus burgioi</i> , <i>Apodemus maximus</i> , <i>Maltamys</i> sp., <i>Leithia</i> sp., <i>Pellegrinia panormensis</i>	Hare, giant field mouse, giant dormouse	Unbalanced, impoverished, endemic	

Table 2.3 Sicilian Pliocene to Holocene vertebrate faunal complexes as classified according to Marra (2013) (excepting the Holocene which is based on Masini *et al.*, 2008: Fig. 4). The FC composition is described in comparison to coeval Italian mainland communities, following terminology in van der Geer *et al.* (2010) and excludes avifauna. For caveats regarding Marra (2013) see Bonfiglio (2013) and also discussion on p. 24.

With regard to the biochronology of Malta, although different terminology has been applied (see Savona-Ventura and Mifsud, 1998; 1999; Hunt and Schembri, 1999; Furlani *et al.* 2013 and references therein), the Zebbug Fissure fauna (such as the giant dormouse *Leithia*) shares several elements with the *P. ex gr. P. falconeri* fauna from Sicily (Bonfiglio, 1992). There are however also compositional differences in fauna between allegedly coeval Maltese and Sicilian FCs, particularly with regard to the absence of association between *P. mnaidriensis* and *Hippopotamus* sp. on Malta (with exception of Għar Dalam Cave and possibly Gandia Fissure) (see Bonfiglio, 1992; Savona-Ventura and Mifsud, 1999; Hunt and Schembri, 1999). In contrast, late Middle Pleistocene to Late Pleistocene *P. ex gr. P. mnaidriensis* is associated with *Hippopotamus pentlandi* on Sicily (Herridge, 2010: 77; *ibid.*, Table 3.11). These differences in FCs may be due to the greater difficulty hippos had in reaching Malta than elephants, or alternatively due to the taxonomic lumping of similar-sized *Palaeoloxodon* spp. from Sicily and Malta represented at different periods in time (see discussion below; Chapter 5).

The dwarf elephants studied in this thesis from Sicily and Malta were excavated from cave or fissure deposits, many of which contain phenomenally rich fossil assemblages (Ambrosetti, 1968; Di Patti *et al.*, 1995). The reasons for elephants being found in caves likely include accidents or natural deaths while in search of mineral salts which often precipitate on the walls of caves (Accordi and Colacicchi, 1962: 219; Redmond, 1982; Howell *et al.*, 1996; Lundquist and Varnedoe, 2006). In *P. ex gr. P. mnaidriensis* there may also have been predation by hyenas (Mangano and Bonfiglio, 2012: 59), or alternatively scavenging after a natural death (*ibid.*). Additionally, caves may have also provided temporary or permanent shelter. Finally, flash floods and rivers may also have washed remains into caves and fissures (Adams, 1865: 489-490; Zammit Maempel, 1989: 59; Herridge, 2010: 359).

2.2.1 *Palaeoloxodon* sp. 1 from Luparello Fissure, Sicily

Species diagnosis: *Partially represented ca. 2m-tall elephant that likely includes both more primitive and derived representatives at Luparello Fissure, likely representing the ancestral chronospecies of P. ex gr. P. falconeri (Scarborough et al., 2016). The teeth are high-crowned with low lamellar frequency. The calcaneus has a tibial facet that is separated to a greater or lesser degree from the fibular facet (Scarborough et al., 2016).* Geographic distribution: *Sicily or possibly its northern palaeo-island.* Chronological distribution: *?Middle Pleistocene.*

Palaeoloxodon sp. 1, although previously attributed to the same taxon as Maltese *E. (recte P.) melitensis* (ANONYMOUS, 1862) (see Vaufrey, 1929) or Maltese *P. mnaidriensis* (see Herridge, 2010), has a different functional morphology in the calcaneus, either due to different ecomorphology on Sicily and Malta, or because it is a separate species from similar-sized Maltese *Palaeoloxodon* sp. (Scarborough *et al.*, 2016). The anatomy of *Palaeoloxodon* sp. 1 has thus far only been described from Luparello Fissure (Vaufrey, 1929; Piccoli and Del Pup, 1967; Abbate, 1974; Herridge, 2010; Scarborough *et al.*, 2016), a site which has been excavated several times (De Gregorio, 1899; Vaufrey, 1929; Imbesi, 1956). Although there is



Fig. 2.2 Luparello Fissure, Palermo, Sicily. The deposit was formerly emplaced where Giovanni Surdi is standing (see Vaufrey, 1929: Fig. 6, Fig. 7).

overlap between the size range of *Palaeoloxodon* spp. at Luparello Fissure (including the larger *Palaeoloxodon* sp. 1 and smaller *P. ex gr. P. falconeri*) on the one hand and *P. ex gr. P. falconeri* from Spinagallo Cave on the other, to avoid confusion any material from Luparello Fissure that has a size exceeding the largest examples of *P. ex gr. P. falconeri* from Spinagallo Cave is here provisionally referred to *Palaeoloxodon* sp. 1 until the systematics of the material is further clarified. Although there is currently no absolute dating of *Palaeoloxodon* sp. 1 and the stratigraphic provenance of specific elephant fossils has never been published (see Herridge, 2010: 369), Vaufrey reported excavating larger *Palaeoloxodon* sp. 1 remains underlying smaller *P. ex gr. P. falconeri* (Vaufrey, 1929; Fig. 2.4).

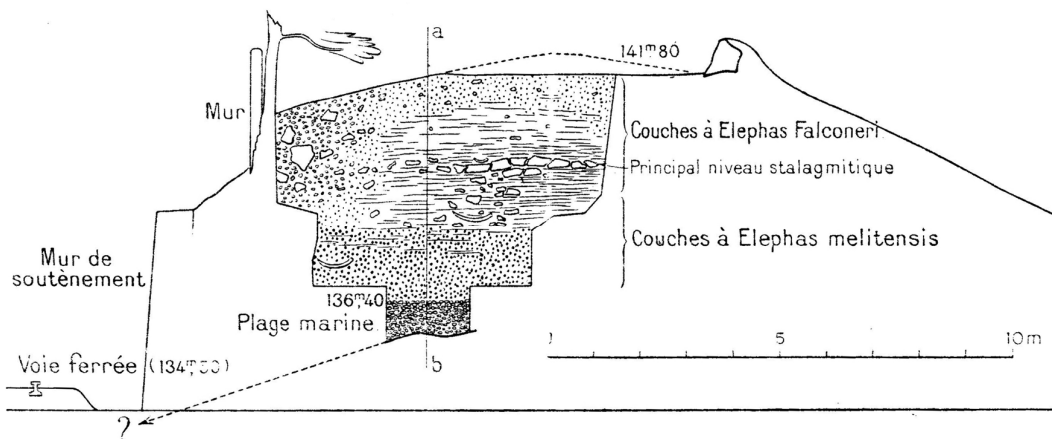


Fig. 2.3 Standing section of Vaufrey's excavation of Luparello Fissure, Sicily, illustrating the stratigraphic superposition of *P. ex gr. P. falconeri* (= *Elephas antiquus falconeri* in Vaufrey, 1929) and *Palaeoloxodon* sp. 1 (= *Elephas antiquus melitensis* in Vaufrey, 1929) (After Vaufrey, 1929: Fig 7).

Additionally, this author re-located a collection of ± 200 hitherto unpublished (excepting Scarborough *et al.*, 2016) and unaccessioned *Palaeoloxodon* sp. 1 and *P. ex gr. P. falconeri* remains in the IPH (Appendix D). The material includes specimens with hand-written fractions on their labels likely corresponding to the depth below the surface figured in Vaufrey's publication (Vaufrey, 1929: Fig 2.4; see Fig. 2.3). The stratigraphic provenance is unknown for most of the associated fauna from Luparello Fissure: deer and *P. ex gr. P. falconeri* co-occurred in superficial reworked deposits (Vaufrey, 1929), but likely belong to the Maccagnone and *P. falconeri* FCs respectively. Based on the faunal associations at other Sicilian sites (see Bonfiglio *et al.*, 2002) it is likely *Leithia cartei* belongs to the Spinagallo FC, and *Cervus elaphus sicilae*, dwarf *Ursus* cfr. *U. arctos*, *Bos* sp. and *L. melitensis* belong to the Maccagnone FC. Likely representatives of the Castello FC include *Sus scrofa*, dwarf *Vulpes* sp., and the Grotta San Teodoro FC members likely include *Equus* sp., Aves sp. (Vaufrey, 1929); *Crociodura* sp., bats and amphibians (Fabiani, 1928; Burgio *et al.*, 2002; Vaufrey, 1929; Burgio and Costanza, 1999; Pavia, 2004; Abbate, 2007: 12-13; Herridge, 2010: 369; Colomba *et al.*, 2011). It should nonetheless be emphasized that with the exception of Pavia (2004), the associated fauna have not been described in detail, and may include ancestral chronospecies of taxa belonging to the Spinagallo FC.

2.2.2 *Palaeoloxodon ex gr. P. falconeri* (BUSK 1867) from Luparello Fissure, Sicily

P. falconeri, after first being described from Zebbug Fissure, Malta (Anonymous, 1862; Busk, 1867; Spratt, 1867) was first identified on Sicily at Luparello Fissure by Vaufrey (1929), although many of the remains are still undescribed (with only selected appendicular and dental remains described by Vaufrey, 1929 and the latter dental stages by Herridge, 2010). The undescribed part of the Luparello Fissure collection re-located by the author (Appendix D) also includes *P. ex gr. P. falconeri* appendicular remains which appears upon first examination to belong to a proportionately high percentage of juveniles. The *P. ex gr. P. falconeri* assemblage from Luparello Fissure has also been shown to evidence phenetic differences compared to remains from Spinagallo Cave (Herridge, 2010), including adult remains that are often towards the smaller size range typically represented at Spinagallo Cave (see Herridge, 2010; see also Scarborough *et al.*, 2016). Whether size and morphological differences are related to different environmental conditions between ectomorphs from north-west and south-east of Sicily, or the Luparello Fissure material includes representatives of a different (perhaps more derived chronomorph) is however unknown.

2.2.3 *Palaeoloxodon ex gr. P. falconeri* from Spinagallo Cave, Sicily

Species diagnosis: *Shoulder height in the flesh ca. 95 cm in bulls, and 80 cm in cows, with estimated body mass ca. 280-300 and 165 kg respectively (Larramendi and Palombo, 2015: 104) or perhaps slightly less (Romano et al., 2019). The tusks curve upwards, and the teeth are high and narrow-crowned with low lamellar frequency, thick enamel, with enamel loop in early wear consisting of long central enamel loops and small median expansions on the occlusal surface (Ambrosetti, 1968: plates V-VIII; see also Maglio, 1973: 94; Herridge, 2010: 122). The molars demonstrate a modest reduction in the plate number and the teeth are proportionally large for body size (Palombo, 2004: 362, see also Ambrosetti, 1968: 303-304).*

The legs appear short in relation to body size (Larramendi and Palombo, 2015: 105) and the torso long (Larramendi and Palombo, 2015: 105, Fig. 5), with short distal limbs and the presence of an often synostotically fused ulna-radius (Ambrosetti, 1968: 308) and (though less frequently fused) tibia-fibula (cf. Ambrosetti, 1968: 316).



Fig. 2.4 Background: Mounted composite skeleton of adult *P. ex gr. P. falconeri* from Spinagallo Cave, Sicily (MPRU). Foreground: 28cm-tall partially-reconstructed neonatal skeleton likely belonging to a single individual (see Accordi and Colacicchi, 1962: 221).

The humerus is characterized by a deep deltoid fossa (see Chapter 4). The hip region is higher than the shoulder, contrasting with *P. antiquus* in this regard (Larramendi and Palombo, 2015: 105, Fig. 1, Fig. 2). The globular and single-domed cranium is pedomorphic (Palombo, 2001a). The calcaneus has a more-or-less continuous tibio-fibular facet (Scarborough et al., 2016). Geographic distribution: Malta (as *P. falconeri*) and Sicily (as *P. ex gr. P. falconeri*) Chronological distribution: Remains from Spinagallo Cave were dated between 366 and 233 ka (OSL, U-series, see preliminary abstract of Herridge et al., 2014). A late Early Pleistocene age has been ascribed to Sicilian strata allegedly containing *P. ex gr. P. falconeri* in the Comiso area of the Vittoria Plain, though without anatomical description (Pedley, 2011: 919). Although the absolute chronology of Pleistocene Malta is also poorly resolved, it has been suggested that Maltese *P. falconeri* is not younger than the Sicilian Stage (Lower Middle Pleistocene) (Bonavia, 1999).

Although the type-series of *P. falconeri* is derived from Malta, the most abundant collections are reported from Sicily (Bonfiglio and Insacco 1992; Bonfiglio et al., 2000). The largest *P. ex gr. P. falconeri* assemblage by far is however from Spinagallo Cave, a raised sea cave on the escarpment of the Hyblean Plateau in south-eastern Sicily, where a minimum of 104 individuals were excavated between 1958-1960 (Accordi et al., 1959; Accordi and Colacicchi, 1962; Accordi, 1962; Fanelli, 1963; Ambrosetti, 1968). Most of the Spinagallo Cave remains were excavated from a fissure deposit and the so-called Lower Cavern (Fig. 2.6b-c), which is a clino-stratified deposit recently dated to the late Middle Pleistocene (cf. Herridge et al., 2014).

2.2.4 Size variation in the *Palaeoloxodon* spp. assemblage from Spinagallo Cave

Being one of the largest proboscidean fossil assemblages from any one site in the world, the Spinagallo Cave assemblage includes a significant range in sexual, ontogenetic and idiosyncratic variability (see Ambrosetti, 1968; Herridge, 2010). The *P. ex gr. P. falconeri* assemblage has also been the subject of several biometric studies (Fanelli, 1963; Accordi and

Palombo, 1971; Palombo and Giovinazzo, 2005; Herridge, 2010), including that of Ambrosetti (1968) who highlighted the existence of four noticeable modes in the size-frequency distribution of *P. ex gr. P. falconeri* teeth and long bones which he attributed to young juveniles (mode A), cows (mode B), bulls (mode C) and infrequently represented old, large bulls (mode D) (Ambrosetti, 1968: 329ff). The *P. ex gr. P. falconeri* assemblage was more recently restudied and again found to be a size-dimorphic elephant taxon on the basis of dental and postcranial remains (Herridge, 2010: 396).

In addition to the presence of four modes referred to ontogenetic and sexual variability in *P. ex gr. P. falconeri*, a large vertebra (from the residual deposit attached to the wall of the eroded main chamber) was ascribed to *E. mnaidriensis* (Ambrosetti, 1968: 281, herein referred to as *P. ex gr. P. mnaidriensis*), as well as a large scapula and femur diaphysis with the proximal and distal epiphyses missing (both from excavated deposits infilling the cave) which were excluded from Ambrosetti's biometric analyses because he believed them to belong to a different Faunal Complex to the one *P. ex gr. P. falconeri* was associated with, and therefore of less relevance to his study (Maria Rita Palombo, pers. comm., 2014). The large vertebra falls within the size-range of *P. ex gr. P. mnaidriensis*, while the femur and scapula are nearly identical in size to *Palaeoloxodon* sp. 1 from Luparello Fissure. Furthermore, other authors have also drawn attention to the presence of remains from Spinagallo Cave larger than typical for *P. ex gr. P. falconeri* but smaller than *P. ex gr. P. mnaidriensis* from Puntali Cave (Palombo, 2001b: 487), although without secure stratigraphic provenance (see Section 6.2).

2.2.5 Spinagallo Faunal Complex



Fig. 2.5 Composite reconstruction of *P. ex gr. P. falconeri* from Spinagallo Cave, Sicily (UCat).

It is not known when the ancestor of *P. ex gr. P. falconeri* first colonized Sicily or its palaeo-islands, but colonization may have occurred around the Early Pleistocene/Middle

Pleistocene boundary at the time of one of the cold stages correlated with OIS 24-22-20 (Palombo, 2001b: 487; Palombo, 2003: 275; Bonfiglio *et al.*, 2003: 109; Marra, 2013: Fig. 3), or possibly at a later lowered sea level around 690 ka

(Hunt and Schembri, 1999: 32). However, the Spinagallo FC has been described from the large faunal assemblage at Spinagallo Cave, and consists of an oligotypic, compositionally

unbalanced and highly endemic fauna of which *P. ex gr. P. falconeri* is the only large mammal (Table 2.3; Bonfiglio *et al.*, 2002).



Fig. 2.6 a) Entrance to main chamber of Spinagallo Cave, escarpment of the Hyblean Plateau, south-eastern Sicily. b) Spinagallo main chamber (above), and entrance to the excavated lower cavern (below). c) View from the interior of the excavated lower cavern.

The only other large terrestrial animal included is a large giant tortoise (slightly smaller in size than *P. ex gr. P. falconeri*) as represented at Alcamo Quarry. The faunal assemblage at Spinagallo Cave also includes a diverse avifauna including a giant owl, as well as bats, amphibians, reptiles and small mammals and includes a giant dormouse (Petronio, 1970; Kotsakis, 1977; Kotsakis and Petronio, 1980; Kotsakis, 1984; Pavia, 1999; 2000; 2004).

Species diagnosis: *Partially-represented ca. 1,7m-tall species with fragmentary long bones and partially represented footbones (Adams, 1874; Lydekker, 1886: 138-151). Two separate morphotypes appear to be distinguishable in the molars, 'pachyganal (large, slightly folded molars with thick enamel: lower laminar frequencies; laminae slightly to markedly subtriangular) and endoganial (thinner, more folded enamel, higher laminar frequencies: reduced loxodontoid expansion', see Caloi et al., 2004: 234). Geographic distribution: Malta (also Sicily according to many authors including Vaufrey, 1929; Imbesi, 1956; Herridge, 2010, although see Scarborough et al., 2016). Chronological distribution: Uncertain, possibly Middle Pleistocene although the type-locality of Mnaidra Gap (see Adams, 1870) is now destroyed (Herridge, 2010: 359-360). Associated fauna: Palaeoloxodon 'melitensis' (sensu ADAMS 1870; 1874), with *P. 'melitensis'* and *P. mnaidriensis* stratigraphically associated in layers A, C and F (Adams 1870, 1874; Herridge, 2010: 359-360); *Leithia melitensis*, *Cygnus falconeri*, and giant tortoise.*

2.2.6 *Palaeoloxodon ex gr. P. mnaidriensis* from Puntali Cave, Sicily

Species diagnosis: *Almost completely represented, 1,8 m tall, estimated mass ranging from ca. 1,100-2500 kg (Palombo, 2007: 113). The cranium has a prominent supra-orbital torus (Fig. 2.7). Inward-spiralling tusks, teeth with narrow and high crown, densely folded enamel, relatively thicker enamel than *P. antiquus*, a higher lamellar frequency and slightly lower plate number with relative width and hypsodonty similar to that of *P. antiquus*. (Ferretti, 2008: 101). The deltoid fossa on the humerus is deep. The calcaneus likely has a wide fibular facet and the tibial facet is absent (Scarborough et al., 2016). Geographic distribution: Sicily (and possibly Malta). Chronological distribution: late Middle Pleistocene to Late Pleistocene (Ferretti, 2008: 92 and references therein).*

Although the species name *E. (recte P.) mnaidriensis* was originally applied to Maltese material only (Adams, 1874), it was later applied to the material from Puntali Cave (Vaufrey, 1929). According to Herridge the Puntali Cave elephant is however a separate species to Maltese *P. mnaidriensis* (Herridge, 2010: 195; *ibid.*, Table 7.1). According to Ferretti (2008) however, cranial autapomorphies are required to reliably settle the question as to the integrity of the Siculo-Maltese *P. mnaidriensis* hypodigm. Acknowledging the uncertainty with regard to the possible existence of a new species best-represented from Puntali Cave, Sicilian material is here provisionally referred to as *P. ex gr. P. mnaidriensis* and large-sized Maltese *Palaeoloxodon mnaidriensis* (ADAMS 1874) from Mnaidra Gap, Malta material from the type-locality of Mnaidra Gap as *P. mnaidriensis*.

The sample of *P. ex gr. P. mnaidriensis* studied in this thesis derives almost entirely from Puntali Cave, which is a large cave system with abundant elephant remains excavated during the 19th century (Pohlig, 1893; Di Patti *et al.*, 1995: 3-20, 33-35 and references therein; Ferretti, 2008; Herridge, 2010). The species is likely also represented at San Teodoro Cave, Sicily where a partially articulated skeleton was recently excavated (Mangano and Bonfiglio, 2012).

2.2.7 Maccagnone and Grotta San Teodoro Faunal Complexes

The fauna associated with *P. ex gr. P. mnaidriensis* from Puntali Cave, Sicily belongs to the Maccagnone FC (Marra, 2013: 133), which is a balanced and slightly impoverished FC



Fig. 2.7 Mounted composite *P. ex gr. P. mnaidriensis* skeleton from Puntali Cave, Sicily (GMP).

with respect to the Italian mainland (Table 2.3). Typically associated taxa include *Hippopotamus pentlandi*, *Cervus elaphus siciliae* and *Dama carburangelensis*, as well as several large carnivores and suids (Palombo, 2007: 113). Dominant species in the preceding Spinagallo FC are absent suggesting dramatic environmental change. The *P. antiquus* representatives ancestral to *P. ex gr. P. mnaidriensis* may have reached Sicily during one of the sea level drops in the late Middle Pleistocene (MIS 10, 8 and 6, see Palombo, 2003: 275; Palombo, 2007: 113). Temporary connections with Calabria may have occurred at this time as suggested by the species composition and moderate endemization. The associated fauna that colonized Sicily around this time are nonetheless typical for a warm period (van der Geer *et al.*, 2010: 88) so that the possibility of dispersal due to tectonic activity in the region of the Messina Strait rather than glacio-eustatic sea level changes should not be ruled out. *P. ex gr. P. mnaidriensis* is not exclusive to the Maccagnone FC, and is also represented

in later Grotta San Teodoro-Pinaetti FC assemblages (Marra, 2013: 120). At Puntali Cave a ²³⁰Th/²³⁴U date from a concretion of 32,000±4,000 ka predates elephant remains (Bonfiglio *et al.*, 2008; Mangano and Bonfiglio, 2012).



Fig. 2.8 a) Entrance to Puntali Cave, Carini, north-western Sicily. b) Interior view of the first chamber, facing the entrance.

2.2.8 *Palaeoloxodon* sp. 2 from Faraglione Cave, Favignana Island

Species diagnosis: *Partially-represented, consisting of several foot bones; a partial left manus, an ulnar carpal, intermediate carpal, metatarsal, phalange I and phalange II. ?D³/D⁴ tooth, (Capasso Barbato et al., 1989) several rib fragments and complete 1st rib with fused distal epiphysis. The two phalanges are likely both digit IV phalange I, suggesting 2+ individuals.* Geographic distribution: *Favignana Island or the Palaeo-Aegadian Islands (see palaeogeography in Antonioli et al., 2016: Figs 16 and 17).* Chronological distribution: *Late Pleistocene (Palombo, pers. comm.).*

Palaeoloxodon sp. 2 from Favignana Island is comparable in size to *Palaeoloxodon* sp. 1 from Luparello Fissure. The Favignana remains were however recovered from surficial deposits (Capasso Barbato et al., 1989) of Faraglione Cave (see Malatesta, 1957), suggesting a more recent age, which is further supported by radiocarbon dating (Palombo, pers. comm.), thereby possibly indicating a relict fauna on the island. Although not excavated under controlled circumstances, the *Palaeoloxodon* sp. 2 remains are reported to have been found in association with several vertebrates, notably *Dama carburangelensis* (Capasso Barbato et al., 1989), which belongs to the *P. mnaidriensis* and San Teodoro FCs of Sicily. A molar and other remains belonging to the species are however smaller than *P. ex gr. P. mnaidriensis* from Puntali Cave, suggesting the possibility that the remains from Favignana Island may belong to a taxon endemic to Favignana (or the Palaeo-Aegadian Islands) descended from *P. ex gr. P. mnaidriensis* from Sicily. Due to the scarcity of remains and absence of clearly identifiable autapomorphic features however, the identification of *Palaeoloxodon* sp. 2 from Favignana Island as a separate species from Sicilian *Palaeoloxodon* spp. remains tentative, being based on chronological, palaeogeographic and metric observations (Palombo, pers. comm.).

2.3 *Mammuthus lamarmorai* (MAJOR 1883) from Gonnese, Sardinia

Species diagnosis: *Partially-represented, known mainly from the largely incomplete Morimonta individual and several isolated teeth and a distal tibia (Malatesta, 1954; Ambrosetti, 1972; Palombo et al., 2005; Palombo et al., 2012; Palombo et al., 2017: Fig. 1; Zoboli et al., 2018). Shoulder height ca. 1,4 m and estimated body mass in the range between 400-700 kg (based on humerus length), and somewhere between 1300-1500 kg based, on minimum circumference (Palombo et al., 2012: 167). Ulna-radius synostotically fused, humerus characterized by a relatively narrow proximal end, and by a much less developed deltoid tuberosity compared with *P. ex gr. P. mnaidriensis* from Puntali Cave. The tibia was likely somewhat robust (Palombo et al., 2017). Wide os c. III; os c. IV differs from *Mammuthus meridionalis* (NESTI 1825) in being relatively wider and lower (Palombo et al., 2012) and the calcaneus has a very narrow facet for the fibula.* Geographic distribution: *Sardinia.* Chronological distribution: *Middle-Late Pleistocene, possibly persisting until 57–29 ka as suggested by OSL dating (see Palombo et al., 2017). The exact location of the type-locality is now uncertain, but in the Gonnese vicinity of south-western Sardinia (Melis et al., 2002; Palombo et al., 2012).*

M. lamarmorai remains are rare, and primarily represented by a partial individual excavated in the Morimonta region of south-western Sardinia, as well as several isolated teeth (Palombo *et al.*, 2012) and a distal tibia (Palombo *et al.*, 2017). The chrono-stratigraphic distribution of the species is poorly constrained although the Morimonta remains may be of Middle or Late Pleistocene age (Melis and Palombo, 2002; van der Geer *et al.*, 2010: 130; Palombo and Rozzi, 2014). A ^{14}C date of $43,000 \pm 1,400$ was obtained from charcoal apparently associated with the skeleton (Melis *et al.*, 2002; Palombo *et al.*, 2005) and should be treated with caution due to the uncertain provenance of the fossils and the nearness of the date to the limit of ^{14}C dating (see Pettitt *et al.*, 2003). The species is probably descended from an advanced representative of *M. meridionalis* or archaic *Mammuthus trogontherii* (POHLIG 1885) that colonized Sardinia (or perhaps Corsica) at the Early to Middle Pleistocene transition (Caloi *et al.*, 2004: 239; Palombo, 2004: 364; Palombo, 2006: 55; Palombo and Rozzi, 2014: 141; Palombo *et al.*, 2017).

2.4 *Loxodonta africana* (BLUMENBACH 1797) from Kenya

Species diagnosis: *L. africana* is represented by numerous individuals including all skeletal elements. Average shoulder height in mature bulls is above 3,0m in the flesh with mass 5,000 kg, and cows averaging 2,5m with mass 3,000 kg (Estes, 2012:259). The tusks curve upwards, and the molar morphology has a distinctive loxodont shape on the occlusal surface. The long bones are more gracile when compared with *P. antiquus*. Current geographic distribution: Parts of central, western and southern Africa associated with lowland and montane forests, all woodland types, and scattered tree savannas (Estes, 2012: 259-260). Chronological distribution: Divergence from its closest relative *L. cyclotis* likely occurred at or after 2,6 Ma (Rohland *et al.*, 2007; Lister, 2013: 333).

The adult *L. africana* material studied in this thesis mainly includes wild elephants from different parts of Kenya. Juvenile *L. africana* in contrast were from the David Sheldrick Wildlife Trust, where they died after being orphaned by poachers. *L. africana* was primarily studied to assess ontogenetic allometry in order to further investigate potential evidence of heterochrony in insular dwarf taxa. There are both advantages and disadvantages to using *L. africana* ontogenetic allometry as an analogue for investigating heterochrony in insular dwarf elephants, the biggest disadvantage being that *L. africana* is a more derived taxon than *Palaeoloxodon* spp. which diverged from *Loxodonta* during the Late Miocene (Lister, 2013: Fig. 1). There are however several distinct advantages in comparing the ontogenetic allometry of *L. africana*, as well as that of *P. antiquus* with insular *Palaeoloxodon* spp.: (i) *L. africana* has a larger sample size; (ii) the KNM *L. africana* collection has a greater range in ontogeny than the *P. antiquus* sample, particularly with regard to the very young ontogenetic stages; (iii) The skeletal anatomy of *L. africana* has been described in greater detail (Smuts and Bezuidenhout, 1993; 1994; Ramsay and Henry, 2008), and the soft tissue may be studied. Furthermore, skeletal morphology may be linked with experimental *in vivo* data on biomechanics and locomotion (Herridge, 2010: 29; (iv) More is known about the habitat of *L. africana* so that it is potentially possible to identify ecophenotypic morphologies, and (v) *L.*

africana skeletons are typically articulated, and well-preserved; (vi) Finally, data on sex, ontogenetic stage and body mass are in many cases accurately recorded (cf. Roth, 1984: 135).

2.5 Materials studied

Abbreviations: Italian collections

GMP	Gemellaro Museum, Palermo (Museo di paleontologia e geologia Gaetano Giorgio Gemmellaro, Università di Palermo)
MPRU	Museo di Paleontologia, Sapienza, University of Rome
UCat	Geological Museum, University of Catania

Abbreviations: Non-Italian collections

IPH	Institut de Paléontologie Humaine, Paris
KNM	National Museums of Kenya (Nairobi)
LVH	Landesmuseum für Vorgeschichte, Halle, Landesamt für Denkmalpflege und Archäologie Sachsen-Anhalt
NHMB	Naturhistorisches Museum, Basel
NHMUK	Natural History Museum, London
SAM	Iziko SA Museum, Cape Town

Species	Provenance	Humerus		Ulna		Femur		Tibia	
		N	Specimens	N	Specimens	N	Specimens	N	Specimens
<i>P. antiquus</i>	Neumark-Nord 1, Germany	4	LVH	12	LVH	13	LVH	10	LVH
<i>P. ex gr. P. mnaidriensis</i>	Puntali Cave, Sicily	2	GMP-Inventario no. 560, collection no. 99, pezzi no. 1; GMP-No. 100	0	-	2	GMP-L.M.O. 782 (left mounted specimen); Right mounted specimen	13	GMP-GPM12, GMP-Inv. No 555, coll. No. 88, pezzi no. 1, GMP-Inv. No 555, coll. No. 87, pezzi no. 1, GMP-GPM13; two unaccessioned mounted specimens
	San Teodoro Cave, Sicily	0	-	1	IPH-F2868	0	-	0	-
<i>Palaeoloxodon</i> sp. 1	Luparello Fissure, Sicily	1	IPH-F2932	1	IPH-F2929	1	IPH	2	IPH-F2928, IPH-F2927
<i>P. ex gr. P. falconeri</i>	Spinagallo Cave, Sicily	64	UCat; MPRU (Ambrosetti, 1968: 364)	42	UCat; MPRU (Ambrosetti, 1968: 365)	25	UCat; MPRU (Ambrosetti, 1968: 365)	110	UCat; MPRU (original data)

Table 2.4 Long bones of insular *Palaeoloxodon* spp. sampled in the present study. For collections abbreviations refer to p. 38. For binomial authorities see Appendix A.

Species	Provenance	Mc III		Mc IV		Mt IV	
		N	Specimens	N	Specimens	N	Specimens
<i>P. antiquus</i>	Neumark-Nord 1, Germany	12	LVH	11	LVH	9	LVH
<i>P. ex gr. P. mnaidriensis</i>	Puntali Cave, Sicily	-	-	1	NHMB-G. 234i and 1938	-	-
	Malta, unprovenanced	0	-	1	NHMUK-44413	3	NHMUK-44474; NHMUK-44476; NHMUK-44477
<i>Palaeoloxodon</i> sp. 1	Luparello Fissure, Sicily	1	IPH-F2995	-	-	2	IPH-F2969; IPH-F2967
<i>P. melitensis</i>	Mnaidra Gap, Malta	0	-	0	-	1	NHMUK-44478
	Benghisa Gap, Malta	0	-	0	-	1	NHMUK-44547
<i>P. ex gr. P. falconeri</i>	Spinagallo Cave, Sicily	30	MPRU	17	MPRU	30	MPRU
<i>M. lamarmorai</i>	Gonnesa, Sardinia	1	NHMB-Tyi207i	0	-	1	NHMB-Tyi207i
<i>L. africana</i>	South Africana	2	SAM-M126	0	-	0	-

Table 2.5 Metapodials sampled in the present study. For collections abbreviations refer to pp. 38. For binomial authorities see Appendix A.

Species	Provenance	Ulnar carpal		Intermediate carpal		Radial carpal		Os c. III	
		N	Specimens	N	Specimens	N	Specimens	N	Specimens
<i>P. antiquus</i>	Riano, Italy	1	MPRU	1	MPRU	1	MPRU	1	MPRU
	Blanzac, France	0	-	1	NHMB-SI.147	0	-	0	-
	Neumark-Nord 1, Germany	13	LVH	14	LVH	5	LVH	13	LVH
<i>P. ex gr. P. mnaidriensis</i>	Puntali Cave, Sicily	1	NHMB	2	GMP, NHMB-G.2340	0	-	1	GMP-RSGP168
	Malta Zà Minica Cave, Sicily	0	-	2	GMP-RSZM141, GMP-RSZM88	1	GMP-RSZM87	-	-
<i>P. mnaidriensis</i>	Mnaidra Gap, Malta	0	-	-	-	0	-	1	NHMUK-44394
<i>Palaeoloxodon</i> sp. 1	Luparello Fissure, Sicily	4	IPH, IPH-F2985	-	-	1	IPH-F2987	0	-
<i>Palaeoloxodon</i> sp. 2	Faraglione Cave, Favignana	1	GMP	-	-	-	-	1	GMP
' <i>P. melitensis</i> '	Mnaidra Gap, Malta	0	-	0	-	0	-	1	NHMUK-44405
	Benghisa Gap, Malta	2	NHMUK-44468, NMHUK-44466	1	NHMUK-44403	0	-	0	-
<i>P. ex gr. P. falconeri</i>	Spinagallo Cave, Sicily	36	MPRU-SpC-UC specimens	36	MPRU	9	MPRU	21	MPRU
	Luparello Fissure, Sicily	1	IPH-F2884	0	-	0	-	0	-
	Zebbug Fissure, Malta	0	-	0	-	0	-	1	NHMUK-49352
<i>M. lamarmorai</i>	Gonnesa, Sardinia	-	-	-	-	0	-	2	NHMB-Tyi207i
<i>L. africana</i>	South Africa	-	-	0	-	2	SAM-M126 (left and right)	1	SAM-M126
<i>E. maximus</i>	Uncertain	-	-	0	-	1	SAM-ZM39031	1	SAM-ZM39031

Table 2.6 Carpals sampled in the present study. For collections abbreviations refer to p. 38
For binomial authorities see Appendix A.

Species	Provenance	Astragalus		Calcaneus		Central tarsal		Os t. IV	
		N	Specimens	N	Specimens	N	Specimens	N	Specimens
<i>P. antiquus</i>	Riano, Italy	0	MPRU	1	MPRU	1	MPRU	0	-
	Neumark-Nord 1, Germany	5	LVH	7	LVH	8	LVH	5	LVH
<i>P. ex gr. P. mnaidriensis</i>	Puntali Cave, Sicily	1	NHMB-G.2344	3	NHMB-2343, GMP	-	0	0	-
	Mnaidra Gap, Malta	1	NHMUK-44453	-	-	0	-	0	-
<i>P. ex gr. P. mnaidriensis</i>	Zà Minica Cave, Sicily	1	GMP-ZM72	0	-	0	-	0	-
<i>Palaeoloxodon</i> sp. 1	Luparello Fissure, Sicily	6	IPH	5	GMP-GL103, IPH	-	0	1	IPH-F2963
' <i>P. melitensis</i> '	Mnaidra Gap, Malta	1	NHMUK-44452	0	-	1	NHMUK-44532	0	-
	Benghisa Gap, Malta	-	-	2	NHMUK-44451 NHMUK-44456	0	-	1	NHMUK-44470
<i>P. ex gr. P. falconeri</i>	Spinagallo Cave, Sicily	51	MPRU, NHMB	50	MPRU, NHMB	19	MPRU	9	MPRU-SpC-TIV specimens
	Luparello Fissure, Sicily	0	-	2	GMP-GL97, IPH	0	-	0	-
	Zebbug Fissure, Malta	1	NHMUK-49263	-	-	0	-	0	-
	Mnaidra Gap, Malta	1	NHMUK-44531	-	-	0	-	1	0
<i>M. lamarmorai</i>	Gonnesa, Sardinia	1	NHMB-Tyi207i	1	NHMB-Tyi207i		NHMB-Tyi207i		NHMB-Tyi207i
<i>L. africana</i>	Kenya (various localities)	0	-	13	KNM	2	KNM-OM8655 LT; KNM-OM8655 (same label, but different individual)	0	-
	South Africa	2	SAM-M126	-	SAM-M126	2	SAM-M126 (left and right)	0	-
<i>E. maximus</i>	Uncertain	1	SAM-ZM39031		SAM-ZM39031	1	SAM-ZM39031	1	SAM-ZM39031

Table 2.7 Tarsals sampled in the present study. For collections abbreviations refer to p. 38. For binomial authorities see Appendix A.

Accession #	Sex	Dental stage	Humerus prox.	Humerus dist.	Humerus lateral (supracondylar)	Ulna prox.	Ulna dist.	Femur head	Femur dist.	Tibia prox.	Tibia dist.
KNM-OM3460	-	-	0	0	0	0	0	0	0	0	0
KNM-OM3460	-	-	0	0	0	0	0	0	0	0	0
KNM-OM7481	-	?	0	0	0	0	0	0	0	0	0
KNM-OM7481	-	?	0	0	0	0	0	0	0	0	0
KNM-OM3561	-	-	0	0	0	0	0	0	0	0	0
KNM-OM3561	-	-	0	0	0	0	0	0	0	0	0
KNM-OM3563	-	?	0	0	0	0	0	0	0	0	0
KNM-OM3563	-	?	0	0	0	0	0	0	0	0	0
KNM-OM2212	M	III	0	0	0	0	0	0	0	0	0
KNM-OM2212	M	III	0	0	0	0	0	0	0	0	0
KNM-OM2211	M	-	0	0	0	0	0	0	0	Missing	Missing
KNM-OM2211	M	-	0	0	0	0	0	0	0	Missing	Missing
KNM-OM4551	M	III	0	0	0	0	0	0	0	0	0
KNM-OM4551	M	III	0	0	0	0	0	0	0	0	0
KNM-OM6100	-	-	0	Y	Y	Missing	-	0	0	0	0
KNM-OM6100	-	-	1	Y	Y	Missing	-	0	0	0	0
KNM-OM8659	-	?	0	Y	Y	Missing	-	0	1	Missing	Missing
KNM-OM8659	-	?	0	Y	Y	Missing	-	0	1	Missing	Missing
KNM-OM7010	-	-	0	0	0	4	0	Missing	Missing	0	0
KNM-OM7010	-	-	0	2	0	4	0	Missing	Missing	0	1
KNM-OM8655	-	?	Y	5	5	4 or 5	5	Y	5	5	5
KNM-OM8655	-	?	-	-	-	5	5	Y	5	5	5
KNM-OM7846	-	-	-	-	-	0	0	0	0	0	0
KNM-OM7846	-	-	0	0	0	0	0	0	0	0	0
KNM-OM8656	-	-	1	5	Y	5	0	0	2	5	5
KNM-OM8656	-	-	Broken	-	-	5	0	0	3	5	5
KNM-OM6098	-	-	Missing	Missing	Missing	4	0	0	3	3	3
KNM-OM6098	-	-	Missing	Missing	Missing	4	0	0	3	3	3

Table 2.8. *Loxodonta africana* long bone metadata (Kenyan National Museum collection). Epiphyseal fusion stages are scored following Herridge, 2010: Fig. 5.2 (0=epiphysis unfused and separate, 1=epiphysis fused internally and epiphyseal line 100% open; 2=epiphyseal line part fused <50%; 3=epiphyseal line part fused >50%; 4=epiphysis 100% fused, but line is still visible; 5=epiphyseal line is 100% fused and line obliterated).

Part 2: Methods

2.6 The study of allometry in proboscidean evolution

Allometry is defined as the proportion of part of an organism relative to the whole. Since there are very significant differences in the scale and shape of different proboscidean taxa (Osborn, 1936; 1942; Christiansen, 2004; 2007; Kokshenev and Christiansen, 2010; Larramendi, 2016), particularly with regard to insular forms (Roth, 1992; Palombo, 2007; Herridge, 2010; Larramendi, and Palombo, 2015), the study of allometry plays an important role in understanding proboscidean evolution. In order to describe and understand the causes of ontogenetic and interspecific differences various allometric and statistical approaches are utilised. These statistical and allometric approaches are outlined below, followed by an explanation of the choice of measurement locations, and finally descriptions of the measurements taken on individual bones. To begin with however, I outline different scaling hypotheses relating to proboscidean allometry.

Scaling in proboscidean allometry

A change in absolute size without any change in shape is known as *geometric similarity* (sometimes also referred to as isometry) (Schmidt-Nielsen, 1984). But animals cannot remain geometrically similar from small to the large, because the cross-sectional area of their limbs increases as the square of body dimension L , while required to support a mass which increases as L^3 (McMahon, 1973: 1202). There are a number of ways in which animals might be expected to accommodate for these increases in mass. Among these are a modification of the (i) material properties of bones and muscles, (ii) geometric shape of bones, (iii) way bones are loaded, (iv) architecture of skeletal muscles, or simply (v) slower locomotion (Dick and Clemente, 2017).

Studies have shown that over a wide range in body size bending-strength in vertebrate bone varies little (Biewener, 1982). Thus it is often necessary for a change in absolute size to be accompanied by a change in shape in order to allow for scale-dependent functional requirements (McMahon, 1973: 1202; Alexander, 1977; Hildebrand, 1988: 466-467; see also Alexander *et al.*, 1979a). Thus if a long-bone's thickness increases proportionately more than its linear height does, proportionately greater bone stresses in large animals are reduced.

According to McMahon's loading hypothesis, this requires *elastic similarity*, a model of scaling in which animals alter their shape to compensate for increases in loading (McMahon, 1973; 1975; 1984; McMahon and Bonner, 1983). The theory of *elastic similarity* predicts that long-bone length scales to diameter to the two-thirds power, or that $l \propto F_{\omega}^{0.25}$ and $d \propto F_{\omega}^{0.38}$, so that an animal's robusticity increases with size (Biewener, 1982). Support for the predictions of *elastic similarity* has been observed, for example in the humerus of various mammal long-bones (Dick and Clemente, 2017) including Bovidae ranging from 4,4-500 kg (McMahon, 1975; Alexander, 1977), with long-bones become slightly thicker in larger taxa

(Christiansen, 1999; Carrano, 2001; Dick and Clemente, 2017). However, this is not always the case: other studies demonstrate that when a large size range of mammals is considered, bone dimensions scale closer to isometry (Dick and Clemente, 2017 and references therein).

Thus numerous studies have been devoted to testing the merits of the different scaling hypotheses (geometric vs. elastic similarity) in different skeletal elements and taxa across a diverse range in body mass (Alexander *et al.*, 1979b; Maloiy *et al.*, 1979; Biewener 1982; 1983; 2000; Silva, 1998; Kokshenev, 2003; Kokshenev *et al.*, 2003; Garcia and da Silva, 2006; Herridge, 2010; Campione and Evans 2012; Jones, 2015 *inter alios*). However, it is now recognized that scaling exhibits a large amount of variation, and there is likely not a universal scaling theory available to describe all terrestrial vertebrates (Campione and Evans, 2012).

2.6.1 Statistical analysis of allometry

In order to examine allometry in this thesis bivariate and multivariate statistical approaches (including principal components analysis) are used to compare extant and fossil members of the Elephantidae. Before comparing proboscidean allometry however it is further useful to define three kinds of comparisons based on the choice of sample (Table 2.5). These are referred to as (i) ontogenetic allometry, (ii) static allometry (usually *static-adult* allometry), and (iii) evolutionary allometry (Klingenberg and Zimmermann, 1992; Klingenberg, 1996). These three categories of allometric comparisons are further distinguished on the basis of their biological emphasis (following Cock, 1966). Static and ontogenetic allometric studies examine intraspecific scaling, while evolutionary allometry examines interspecific differences between taxa (Klingenberg, 1996).

Type of allometry	Ontogenetic stages compared	Taxa compared	Species sampled	Elements compared
Ontogenetic	Range in ontogeny	Within one taxon	<i>L. africana</i> , <i>P. antiquus</i> (more limited sample-size in the latter species)	All appendicular elements sampled
Static	Both adult	Multiple taxa	<i>P. antiquus</i> , <i>P. ex gr. P. mnaidriensis</i> , <i>P. ex gr. P. falconeri</i> , <i>L. africana</i>	Long bones and calcaneus
Evolutionary	Same ontogenetic stage	Multiple taxa	<i>P. antiquus</i> , <i>P. ex gr. P. mnaidriensis</i> , <i>Palaeoloxodon</i> sp. 1, <i>P. ex gr. P. falconeri</i> , <i>L. africana</i>	

Table 2.9 Categories of studies for comparing proboscidean allometry based on choice of sample (following Cock, 1966) and the elements sampled in this thesis. The taxa studied are limited re. ontogenetic allometry by small sample-size.

(i) Ontogenetic allometry - Among placental mammals proboscidean ontogeny is unusual in that proboscideans have an extended growth period, which asymptotically slows as somatic maturity is approached. Among extant elephants the skeleton continues to grow until about

the age of 25 in females when the last long bones fuse, and by about 40 years in males (Roth, 1984; Haynes, 1991). In proboscidean osteology, ontogenetic stage is principally determined using three methods: Firstly, a determination of dental stage (Laws, 1966; Jachmann, 1988; Roth and Shoshani, 1988; Haynes, 1991: Appendix), or secondly by observing within-bone fusion stage, or thirdly, by observing associated intra-skeletal fusion sequence. The within-bone and intraskeletal fusion sequence for the limbs has been investigated in *L. africana* BLUMENBACH 1797 (Roth, 1984; Haynes, 1991: Appendix; Lister, 1999; Herridge, 2010: Table 5.4), *M. primigenius* (BLUMENBACH 1799) (Lister, 1999; Herridge, 2010: Table 5.5; 202-204; 212-242), *E. maximus* LINNAEUS 1758 (Roth, 1984; Herridge, 2010: Table 5.3), and (albeit preliminarily) in *P. antiquus* (Roth, 1984; Lister, 1999; Herridge, 2010: Table 5.6). Furthermore, the within-bone fusion patterns in the limbs of *P. ex gr. P. falconeri* have also been ascertained (Herridge, 2010: Table 5.18).

The precision with which the ontogenetic stage may be determined depends largely on which of the above three methods are available: Odontochronology usually offers the most precise estimate of ontogenetic stage, and is useful for *L. africana* collections in which appendicular bones and teeth are typically associated (Table 2.8). This is due to the fact that proboscidean teeth are replaced horizontally in a conveyor-belt fashion, with six consecutive pairs of maxillary/mandibular teeth erupting from the back of the mouth, and migrating towards the front where they eventually flake off, so that an individual may be assigned a dental stage based on the sequence of tooth eruption and degree of wear. In *P. ex gr. P. falconeri* and other fossil assemblages in which the morphology is compared with *L. africana*, ontogenetic allometry is often necessarily determined separately in disassociated teeth and bones. For disassociated long bones, calcanei and metapodials which possess epiphyses which fuse over the course of ontogeny, it is possible to obtain some measure of ontogenetic stage (following the five epiphyseal fusion stages of Herridge, 2010: Fig 5.2):

- 0 - Epiphysis unfused and separate
- 1 - Epiphysis fused internally, epiphysis line 100% open
- 2 - Epiphyseal line less than 50% fused
- 3 - Epiphyseal line more than 50% fused
- 4 - Epiphysis 100% fused, but line is still visible
- 5 - Epiphyseal line 100% fused and line obliterated

(ii) Static allometry - Also called size allometry, this is studied in a sample of individuals originating from the same species and population, and with the same developmental stage (Cock, 1966: 135-136; Pélabon *et al.*, 2013: 195). Typically in fossil elephants measurements relevant to the study of static allometry might be taken on individuals with the same epiphyseal fusion stage or the same dental stage (e.g. Herridge, 2010). For the insular proboscideans studied in this thesis there are unfortunately no recorded examples of reliable association between dental and appendicular remains, so that epiphyseal fusion stages and dental stages can only be studied independently. Nonetheless, in the *P. ex gr. P. falconeri* assemblage from Spinagallo Cave, Sicily, there is a correlation between the size-frequency distribution of appendicular remains and the frequency of molars I-VI. This has enabled a

rough estimate of the associated dental stage for the appendicular remains (Ambrosetti, 1968: 327-329). Additionally, the sequence of within-bone epiphyseal fusion has been determined in *P. ex gr. P. falconeri* (Herridge, 2010: Table 5.17; *ibid.*, p. 208). In the *L. africana* sample from Kenya and also the *P. antiquus* sample from Neumark-Nord 1, Germany there is often association between dental and appendicular remains so that developmental stages may be compared using both dental and epiphyseal fusion stages.

(iii) Evolutionary allometry - Evolutionary allometry compares size and shape variation between different taxa with the same ontogenetic stage (Cock, 1966; Klingenberg, 1996), and is used to investigate underlying evolutionary mechanisms or processes (Spence, 2009; Herridge, 2010: 249). In practice however it may not always be possible to distinguish reliably between aspects of ontogenetic and evolutionary allometry in insular proboscideans, particularly for disarticulated skeletons where the associated dental stage is unknown. For static and evolutionary allometry in appendicular elements, comparisons are necessarily limited to the long bones, calcaneus and metapodials in which ontogenetic stage may be classified based on epiphyseal fusion stage (see Herridge, 2010: Fig. 5.2). In this thesis subsamples of *P. ex gr. P. falconeri* and *L. africana* long bones with unfused (Fig. 4.29) and fused (Fig. 4.30) proximal and distal epiphyses are grouped and compared. This has the disadvantage that ontogenetic categories are only broadly categorized, although it is possible to distinguish between individuals in which growth is more rapid and individuals in which growth is slowing, as longitudinal growth asymptotes during later ontogeny (Herridge, 2010: Fig. 5.4).

In the carpals and tarsals in which there are no epiphyses, a determination of ontogenetic equivalence between taxa being compared is problematic, especially considering it has previously been shown that patterns of intraspecific limb-bone allometry are consistently affected by the age profile of the sample, with ontogenetic allometry characterised by isometry and static-adult allometry by negative allometry (Herridge, 2010: 350).

Measurements on the foot bones were taken using callipers (accuracy $\pm 0,01$ mm), focusing on dimensions suitable for identifying any differences in functional morphology (Figs 2.15-2.20). In addition to these measurements, we propose a new method for describing and quantifying interspecific differences in the morphology of the fibular and tibial facets of the calcaneus. This method measures the antero-posterior length of the facets at 1mm intervals, revealing large differences in the size and shape of these facets (see Supplementary Information). We further illustrate the usefulness of the method by comparing the functional morphology in representative specimens. Due to the data being non-normally distributed, allometric differences between pairs of species were tested for statistical significance using Mann-Whitney U tests that compare the distribution of variables without adjusting for any other factors. Infrequently distributions were also compared using t-tests when the data was normally distributed. Spearman correlations were also used to assess associations between continuous variables, and linear trendlines were fitted using Microsoft Excel to visually compare trends correlating x and y between species.

Mathematical description of allometric functions

One of the most useful ways of mathematically describing bivariate allometry is using a power-law ($y = ax^b$) where x and y are the morphological variables of interest: x is here used as a proxy for size, a is the allometric coefficient and b is the allometric exponent (following Schmidt-Nielsen, 1984: 15; Packard and Boardman, 2008; see also Biewener, 2000).

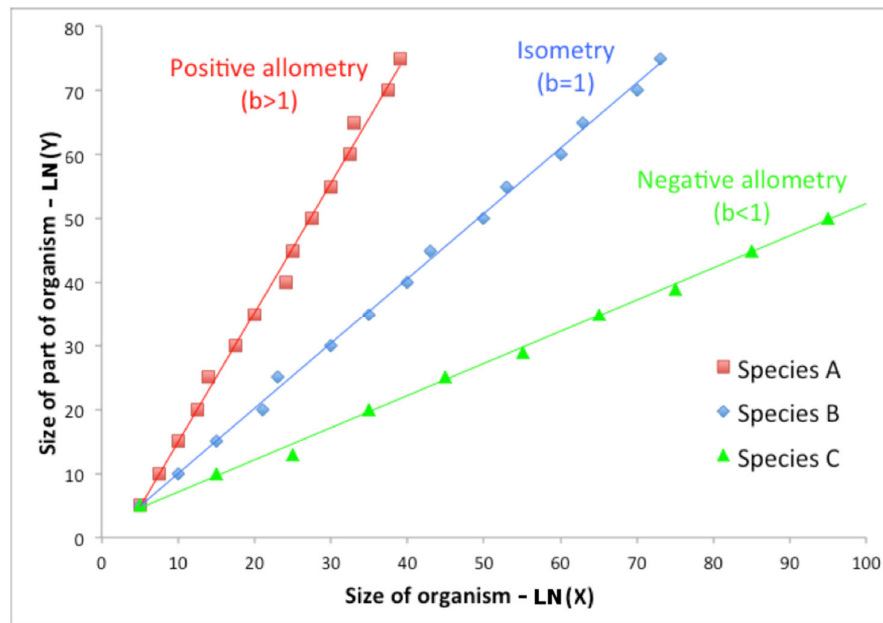


Fig. 2.9 Isometry, positive and negative allometry as defined in relation to the generalized allometric equation $y = ax^b$ (following Huxley and Teissier, 1936).

The different values of b and the associated type of bivariate allometry are illustrated in Fig. 2.9. This equation may be expressed logarithmically as:

$$\log(y) = \log(a) + b \log(x)$$

Where $\log(a)$ is the intercept and $\log(b)$ is the slope, which is easy to interpret visually and mathematically. This may also be expressed as:

$$Y = A + bX$$

where $\log(y) = Y$, $\log(x) = X$, and $\log(a) = A$. From the output, the y-intercept will be the value reported for $\log(a)$ or 'A' and the co-efficient of $\log(x)$ will be 'b'. Furthermore, this equation may be used to test the predictions of isometry vs. elastic similarity (*sensu* McMahon, 1973; 1975) in the long-bones. This is undertaken by regressing $\log(y)$ vs. $\log(x)$ in (SPSS 19.0 or later) with a straight line (scaling relationships were evaluated using Reduced Major Axis regressions). An isometric relationship would generate a slope equal to 1.0 (with negative and positive allometry exhibiting slopes less and greater than one, respectively). In contrast, according to the predictions of *elastic similarity* one would expect a slope gradient = 0,67. Thus, if a line plotted through all the data-points (including multiple

species with different body-masses during adulthood) falls within the 95% confidence interval of a gradient of = 0,67, elastic similarity may apply.

Bivariate regression - All Mann-Whitney U-tests were performed in SPSS (version 19.0). In the regression table (Appendix E) sample-sizes, slopes, intercepts, confidence intervals, correlation coefficients, p-values and t-values were calculated using ln-transformed data in SPSS. *Principal components analysis* - Principal Components Analysis was performed on data obtained from the ulnar carpal and calcaneus, for which data from numerous variables were obtained. PCA was undertaken using the program R (see Fig. 3.5; Fig. 3.23) and PCA plots are presented both on raw data, and as log-transformed, scaled data (i.e. variables are divided by standard deviations), which is more suitable for investigating allometry. All axes were included in order to explore how closely variables are correlated (especially articular facets).

2.6.2 Selection of measurement locations

Measurements were selected based on several criteria:

- Their usefulness for testing hypotheses in Section 1.6.
- Measurements were narrowed down from an exhaustive list derived in part from the literature.
- Based on which measurements were most reliably repeatable, and including measurements that were compatible between species, given (the sometimes large) morphological differences in homologous elements.
- In order to enable metric comparisons with the published literature.
- Where these were likely to best inform upon biomechanics.
- Where large morphological differences were obvious and had been identified visually.

In order to include novel measurements. All measurements on the long bones were obtained using an osteometric board, measuring tape (precision $\pm 1\text{mm}$) and digital callipers (precision $\pm 0.01\text{ mm}$). Due to the extensive travel involved in collecting data (in Germany, Switzerland, England, France, Italy, Kenya and South Africa) osteometry was limited to two-dimensional bivariate measurements obtained using the equipment mentioned above. This has the advantage of being easily transportable and readily repeatable, but also limits the study of certain features that are more suitable for 3D morphometrics (see discussion in Chapter 6, Section 6.2).

In investigating the possible presence of paedomorphism in *P. ex gr. P. falconeri* special attention is given to the tibia (see Chapter 3). Because young individuals lack epiphyses, measurements were obtained on the proximal and distal ends of the diaphysis, both in juveniles with no epiphyses and adults with epiphyses. This contrasts with most studies of proboscidean ontogeny where only the diaphysis height (pr-d) is measured (e.g. Christiansen, 2004; 2007). Obtaining more measurements on the diaphysis, including on the medio-lateral breadth of the ends therefore has the advantage of enabling a more detailed study of

ontogenetic allometry than in many previous studies, particularly when comparing *L. africana* ontogeny with *P. ex gr. P. falconeri* adult morphology.

In the footbones all measurements were taken using callipers, paying particular attention to the articular facets, and focusing on dimensions suitable for identifying any differences in functional morphology. In addition to simple linear measurements, a new method for describing and measuring the articular facets of the calcaneus is presented in section 2.10.1. In order for interosseous joints to prevent overloading, joints that transmit higher stresses require larger articular facets (Yapuncich and Boyer, 2014). Furthermore, facet area may either scale with (i) mass-induced forces or (ii) muscle-induced forces. If mass-induced forces dominate, one would expect facet area to scale with positive allometry to body mass. In contrast, if muscle-induced forces dominate, one would expect facets to scale isometrically with body mass (Yapuncich and Boyer, 2014), thus providing a potential means for investigating the causes of allometric scaling in the feet.

2.7 Measurement of the shoulder and long bones

2.7.1 Measurement of the tibia

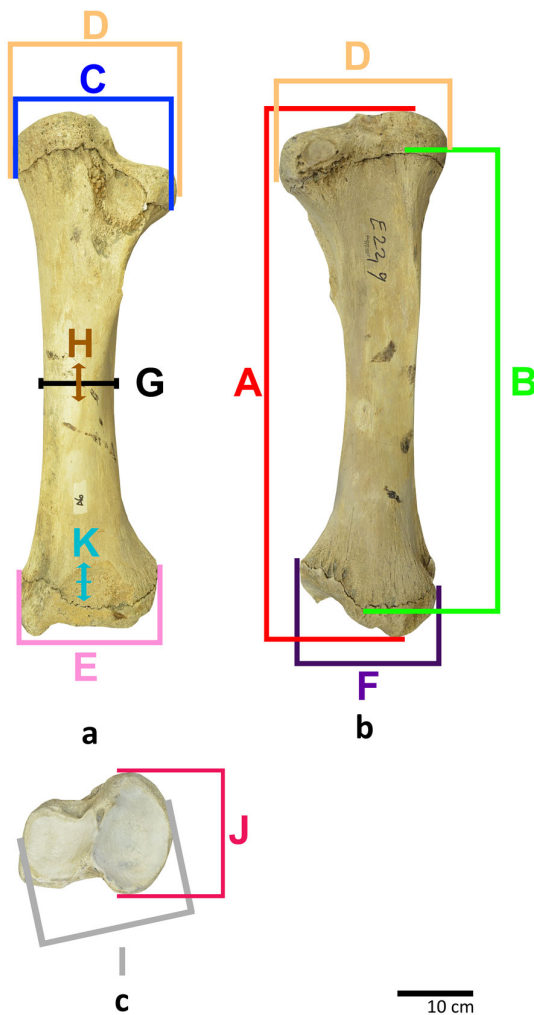


Fig. 2.10 Measurements on the tibia a) cranial b) caudal c) superior aspect. A) Max height (pr-d) including epiphyses. B) Max height (pr-d) of diaphysis. C) Max breadth (m-l) of the proximal diaphysis end without epiphysis (Note: in specimens with fused proximal epiphysis the epiphysis is ignored, and the epiphyseal fusion stage recorded following Herridge, 2010: Fig. 5.2). D) Max breadth (m-l) of proximal epiphysis. E) Max breadth (m-l) of distal end without epiphysis (as above). F) Max breadth (m-l) of distal epiphysis. G) Min breadth (m-l) of the diaphysis (Note: this is measured at the midshaft in all species except *P. ex gr. P. falconeri*, in which the measurement is taken at a slightly more distal position due to the different position of the minimum diaphysis breadth). H) Min thickness (a-p) of the diaphysis (taken at same position as H). I) Breadth of proximal articulation (m-l) (measured with calliper jaws touching edges of medial and lateral condyles). J) Max thickness (a-p) of proximal epiphysis. K) Max thickness (a-p) of distal epiphysis. Illustrated on *P. antiquus* from NN1, Germany.

2.7.2 Measurement of the scapula's glenoid fossa

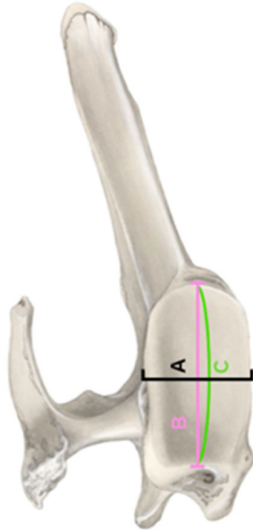


Fig. 2.11 Measurements on the scapula (inferior aspect with lateral side on top and medial at bottom). A) Max chord breadth (m-l) of glenoid fossa (measured using 30-cm digital callipers) B) Max chord length (a-p) of glenoid cavity (measured using 30-cm digital callipers). C) Max surficial length (a-p) of glenoid cavity (using measuring tape placed on concave articular surface). Illustrated on *L. africana*.

2.7.3 Measurement of the humerus

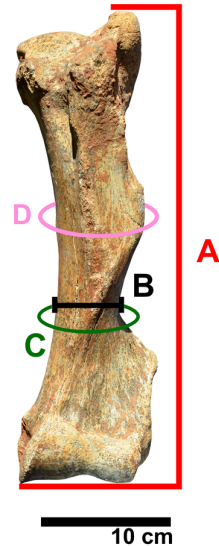


Fig. 2.12 Measurements on the humerus. A) Max height (pr-d) including epiphyses. B) Min diaphysis breadth (m-l). C) Min diaphysis circumference. D) Circumference at deltoid tubercle (where the deltoid fossa is deep the tape passes above the depression). Illustrated on *P. ex gr. P. falconeri* from Spinagallo Cave, Sicily (cranial aspect).

2.7.4 Measurement of the ulna

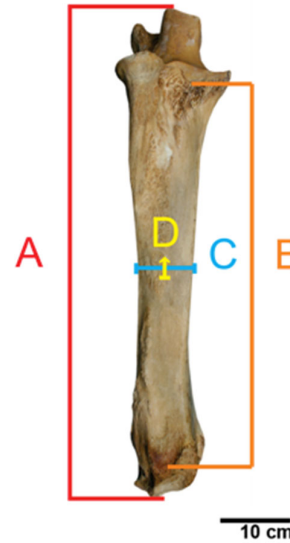


Fig. 2.13 Measurements on the ulna. A) Max height (pr-d) including epiphyses. B) Max diaphysis height (pr-d). C) Min diaphysis breadth (m-l). D) Min diaphysis thickness (a-p). Illustrated on *L. africana* from Kenya.

2.7.5 Measurement of the femur

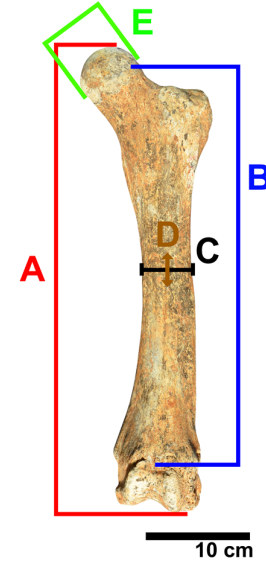


Fig. 2.14 Measurements on the femur (cranial aspect). A) Max height (pr-d) including epiphyses. B) Max diaphysis height (pr-d). C) Min diaphysis breadth (m-l) (taken at position of midshaft). D) Min diaphysis thickness (a-p) (taken in same position as C). E) Breadth (m-l) of the femoral head. Illustrated on *P. falconeri* from Spinagallo Cave, Sicily.

Although interspecific bivariate and multivariate allometry are important for investigating the appendicular anatomy of different species (Herridge, 2010: 281-310 ff.), photography also has the potential to reveal important morphological differences, particularly with regard to overall shape of the long-bones, including differences in musculature, and also differences in the articular facets of the carpals and tarsals.

2.8 Measurement of the carpals

Foot bones are considerably under-represented in the Spinagallo Cave assemblage relative to the long bones (contrast Ambrosetti, 1968: Table VIII with Ambrosetti, 1968: Table II), particularly for carpals and tarsals with a large surface area/volume ratio suggesting that taphonomic processes account for their under-representation (including the central tarsal, os t. I, II, III, IV and radial carpal). The Spinagallo Cave carpal assemblage nonetheless originally included a large sample of 244 carpals, 244 tarsals, 190 metacarpals and 180 metatarsals (Ambrosetti, 1968: Table II), most of which were available for study (Table 2.5; Table 2.6; Table 2.7). In the *P. ex gr. P. mnaidriensis* assemblage from Puntali Cave there are even fewer examples of foot bones despite the often excellent state of preservation (Table 2.5; Table 2.6; Di Patti *et al.*, 1995), suggesting most foot bones may have been lost or dispersed (possibly during the 19th or early 20th century when it was common practice to share material among private collectors and museums). Due to the extreme rarity of select tarsal bones in fossil assemblages, the os c. I, os c. II and os t. I, os t. II and os t. III were excluded from this study. Measurements on the carpals, tarsals and metapodials are described in the next section (refer to Table 3.1 for synonyms used for carpals and tarsals)

2.8.1 Measurement of the ulnar carpal

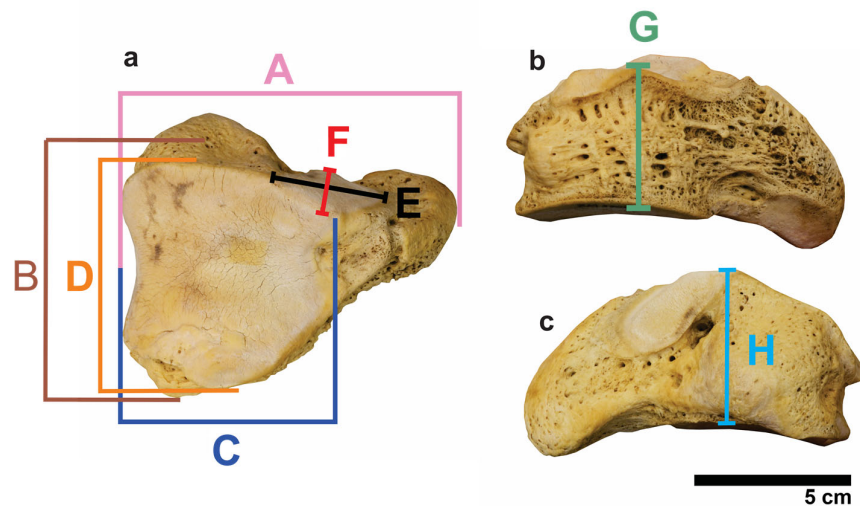


Fig. 2.15 Measurements on the ulnar carpal a) dorsal b) cranial c) caudal aspect. A) Max breadth (m-l) of ulnar carpal (measured with distal articular facet for the intermediate carpal parallel to calliper jaw). B) Max thickness (a-p) of ulnar carpal. C) Max breadth (m-l) of the articular facet for the ulna. D) Max length (a-p) of the articular facet for the ulna. E) Max breadth (m-l) of the articular facet for the accessory carpal. F) Max length (pr-d) of the articular facet for the accessory carpal. G) Max anterior height (pr-d). H) Max posterior height (pr-d). Illustrated on *E. maximus*.

2.8.2 Measurement of the intermediate carpal

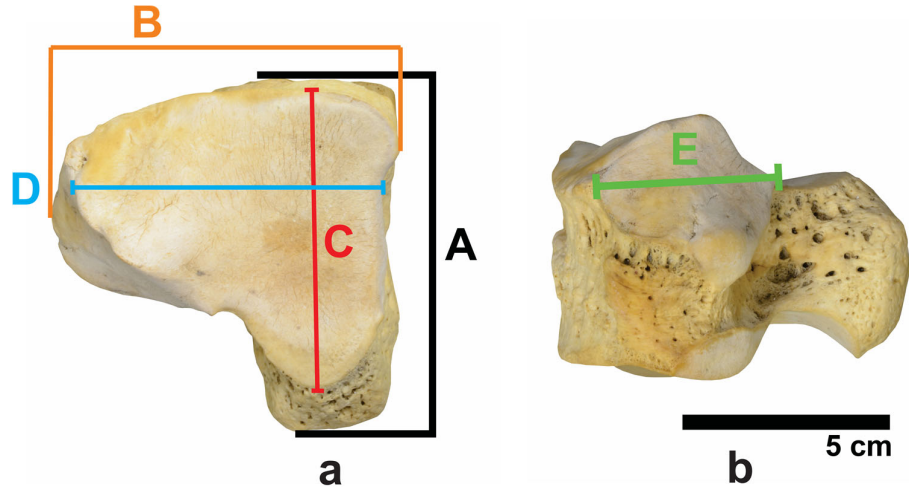


Fig. 2.16 Measurements on the intermediate carpal a) dorsal aspect b) lateral aspect. A) Max thickness (a-p) of intermediate carpal. B) Max breadth (m-l) of intermediate carpal. C) Length (a-p) of articular facet for the ulna. D) Breadth (m-l) of articular facet for the ulna. E) Breadth (m-l) of the articular facet for the radius. Illustrated on *E. maximus*.

2.8.3 Measurement of the radial carpal

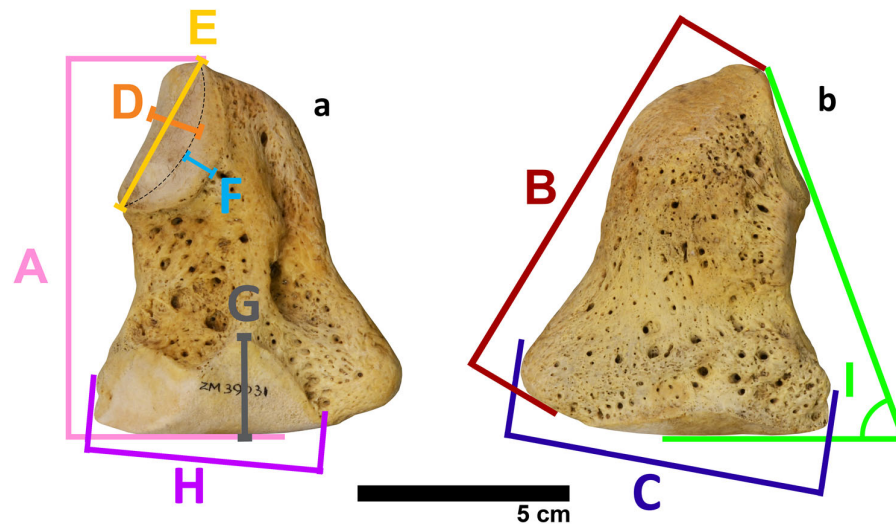


Fig. 2.17 Measurements on the radial carpal. a) lateral b) medial aspects. A) Max height (pr-d) with distal end horizontal. B) Max length (pr-d) of posterior side. C) Distal thickness (a-p). D) Breadth (m-l) of articular facet for radius. E) Length (a-p) of articular facet for radius. F) Max length (pr-d) of proximal articular facet for intermediate carpal. G) Max length (pr-d) of distal articular facet for the intermediate carpal. H) Max breadth of articular facet for os c. II continuous with distal articular facet for intermediate carpal. I) Angle between the articular facet for the radius and the articular facet for the os c. II. Illustrated on *E. maximus*.

2.8.4 Measurement of the os carpale III

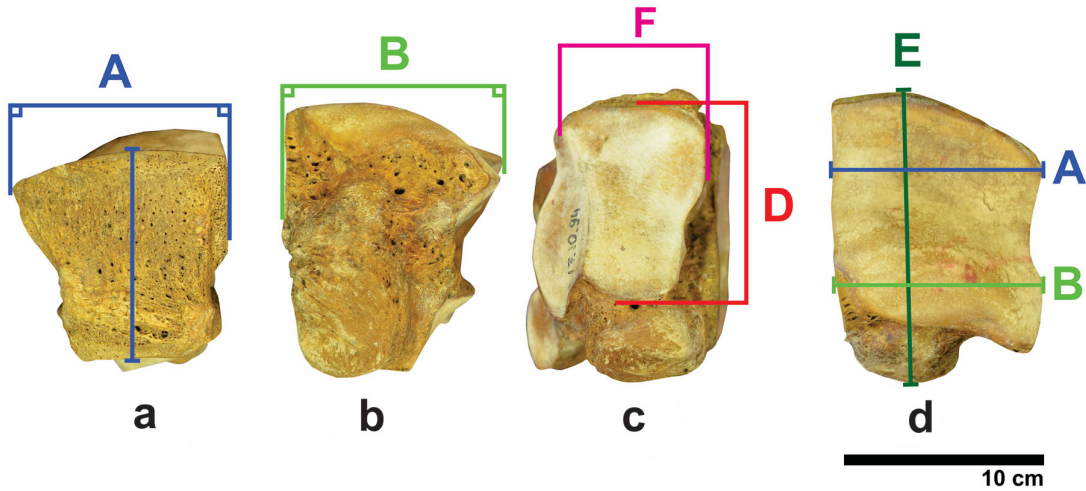


Fig. 2.18 Measurements on the os c. III. a) cranial b) caudal c) plantar and d) dorsal aspects. A) Cranial breadth (m-l) (measured with one calliper jaw parallel to medial facet). B) Caudal breadth (m-l) (measured with one calliper jaw parallel to medial facet). C) Cranial height (pr-d) (measured with the callipers long-axis held vertical and jaws pointing from left to right (m-l)). D) Length (a-p) of articular facet for the mc III. F) Breadth (m-l) of articular facet for mc III (measured on cranial side of facet with calliper jaws pointing parallel to long axis (a-p) of bone). E) Max thickness (a-p) (measured with long-axis of callipers held parallel to the antero-posterior length, with the calliper jaws facing downwards). Illustrated on *P. antiquus* from Neumark-Nord 1, Germany.

2.9 Measurement of the tarsals

2.9.1 Measurement of the astragalus

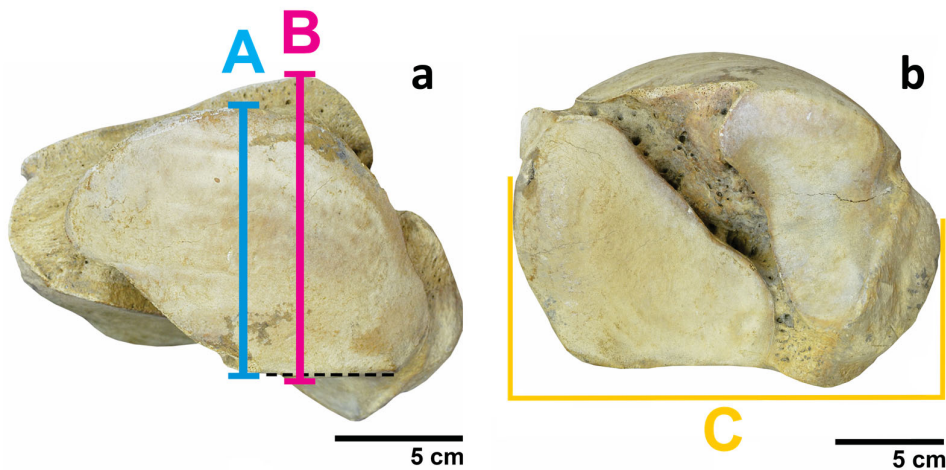


Fig. 2.19 Measurements on the astragalus. a) plantar b) distal aspect. A) Max length (a-p) of the astragalus' articular facet for the central tarsal. B) Max thickness (pr-d) (measured with calliper jaw on the medial facet, parallel to edge of facet). C) Max breadth (m-l) of the astragalus. Illustrated on *P. antiquus* from Neumark-Nord 1, Germany.

2.9.2 Measurement of the calcaneus

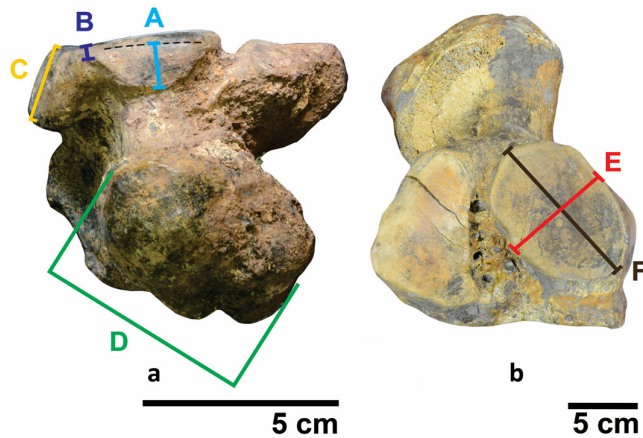


Fig. 2.20 b) Measurements on the calcaneus a) frontal b) superior aspect. A) Max length (a-p) of the tibial facet. B) Min length (a-p) of the tibio-fibular bridge. (Where the tibio-fibular bridge is continuous rather than v-shaped as in *P. ex gr. P. falconeri* this measurement is taken where the tibial and fibular facets meet as identified by a change in slope, see Fig. 3.20, see p. 85 for anatomical definitions). C) Max length (a-p) of fibular facet. D) Max length of distal end of *Tuber calcaneus*. E) Max breadth of lateral articular facet for the astragalus. F) Max length of lateral articular facet for the astragalus. Illustrated on a) *Palaeoloxodon* sp. 1 from Luparello Fissure, Sicily and b) *P. antiquus* from Neumark-Nord 1, Germany.

2.9.3 Morphometry of the tibio-fibular facet

In order to describe differences in the calcaneus morphology, a new method for capturing the 2D geometry of the tibial and fibular articular facets was developed (Scarborough *et al.*, 2016: Supplementary Information). The method measures the antero-posterior length of the articular facets at 1mm intervals, and requires stickers with marked 1mm intervals and callipers. The measurements are obtained using the following procedure:

1. The labels with 1mm intervals are attached to the articular facet for the fibula (and tibial facet where present) as illustrated in Fig. 2.21. The 0 point is situated exactly at the point where the edge of the fibular facet meets the edge of the lateral articular facet for the astragalus.

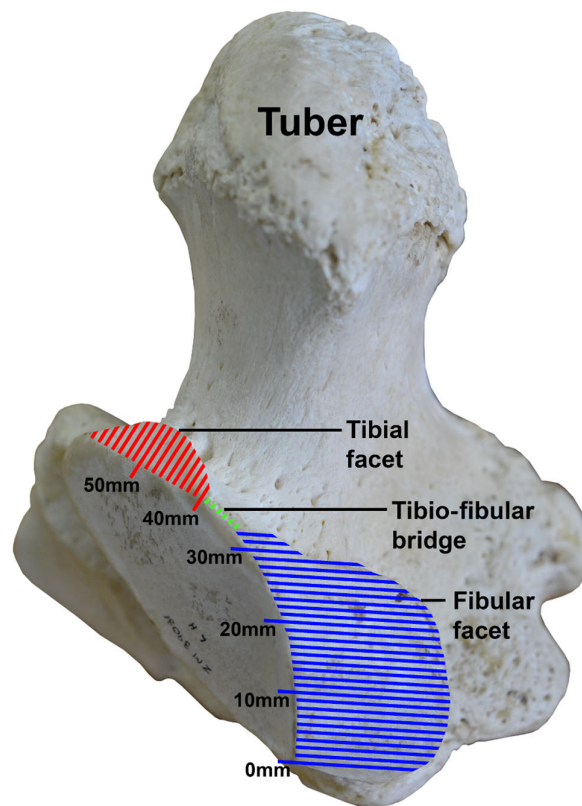


Fig. 2.21 Measurement of the fibular and tibial articular facets on the calcaneus. Illustrated on *E. maximus*.

- Due to the curvature of the edge of the fibular or tibial facets (curvature where the edge meets the lateral articular facet for the astragalus), the labels are cut into shorter strips as required to maintain measurement along the edge of the fibular/tibial facets.
- Using a callipers, the antero-posterior length of the fibular facet (and tibial facet where present) is measured at 1mm intervals, beginning at the 0 point as described above, and ending at the medial end of the fibular facet (or at the medial end of the tibial facet where present). The antero-posterior length of the facet(s) is measured tangentially to the surface of the fibular/tibial facet.
- The data is represented in Microsoft Excel as follows: X-axis: the distance from the lateral side of the fibular facet to the medial side of the fibular facet (or the medial side of the tibial facet where present). Y-axis: the antero-posterior length of the fibular/tibial articular facet(s).
- Some calcanei have (i) a fibular facet only, (ii) separated fibular and tibial facets, or (iii) a continuous fibular-tibial facet. Regardless of the differences in morphology, measurements are taken as described above. In specimens with complete separation between the fibular and tibial facets the antero-posterior length in the region between the facets (the tibio-fibular bridge) is recorded as 0.
- The data is represented as a scatterplot and the data points joined using a moving average trendline (Fig. 3.25). The area beneath the trendline (representing the area of the articular facets) may further be used to compare functional morphology.

2.9.4 Measurement of the central tarsal

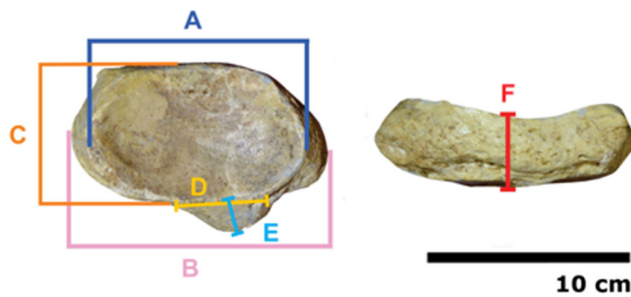


Fig. 2.22 Measurements on the central tarsal a) dorsal aspect b) cranial aspect. A) Max breadth (m-l) of articular facet for astragalus. B) Max breadth (m-l) of central tarsal. C) Max length (a-p) of the articular facet for the astragalus. D) Max breadth (m-l) of articular facet for calcaneus. E) Max length (a-p or pr-d depending on morphology, see

Fig. 3.33a) of articular facet for calcaneus. F) Height (pr-d) on middle of cranial side. Illustrated on *M. lamarmorai* from Gonnese, Sardinia.

2.9.5 Measurement of the os tarsale IV

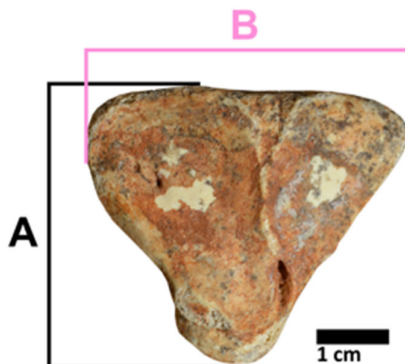


Fig. 2.23 Measurements on the os t. IV (dorsal aspect). A) Max thickness (a-p). B) Max cranial breadth (m-l). Illustrated on *P. ex gr. P. falconeri* from Spinagallo Cave, Sicily.

2.10 Measurement of the metapodials

2.10.1 Measurement of the metacarpal III

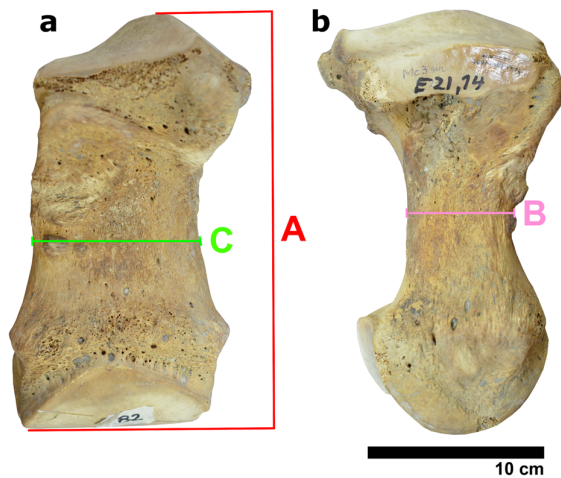


Fig. 2.24 Measurements on the mc III. a) cranial b) medial. A) Max height (pr-d). B) Min diaphysis midshaft thickness (a-p) (Measured with outside jaws gripping diaphysis tightly). C) Diaphysis breadth (m-l) at midshaft. Illustrated on *P. antiquus* from Neumark-Nord 1, Germany.

2.10.2 Measurement of the metacarpal IV

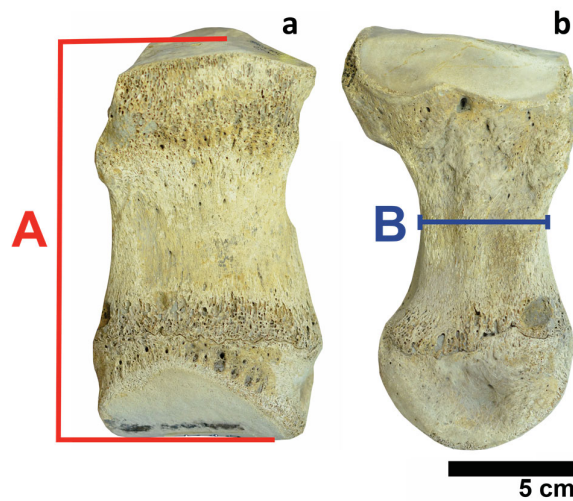


Fig. 2.25 Measurements on the mc IV a) cranial b) medial. A) Max height (pr-d). B) Min diaphysis thickness (a-p) (Note: Measurement is taken with calliper jaws gripping diaphysis tightly). Illustrated on *P. antiquus* from Neumark-Nord 1, Germany.

2.10.3 Measurement of the metatarsal IV

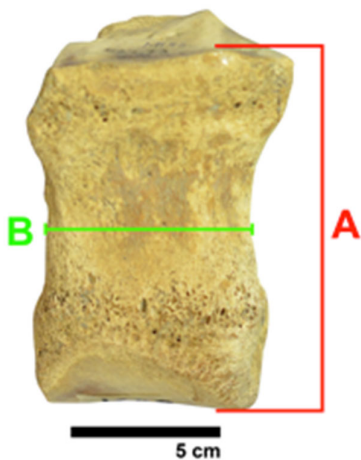


Fig. 2.26 Measurements on the mt IV (cranial aspect). A) Max height (pr-d) (measured with calliper jaw touching, but not necessarily parallel to the distal end). B) Min diaphysis breadth (m-l). Illustrated on *P. antiquus* from Neumark-Nord 1, Germany.

CHAPTER 3

Insular adaptations in the feet

The purpose of this chapter is to test Hypothesis I (*The feet of elephants from Sicily differ significantly in terms their morphology compared with their ancestral species and contemporary P. antiquus*), and its associated predictions. These include the predictions that the morphology and bivariate allometry of the articular facets of insular *Palaeoloxodon* spp. are significantly different to those of *P. antiquus*, and that *P. ex gr. P. falconeri* in particular will evidence large morphological differences. In order to evaluate this hypothesis, the morphology of select carpals and tarsals is described and measured using bivariate and multivariate allometry in numerous Elephantinae species (see Materials in Table 2.1). Particular attention is given to the morphology of articular facets, since these are significant for weight-bearing and influence mobility, and the morphology in different species of widely differing body mass are compared. Additionally, intra-population variation is evaluated in order to understand variability. This Chapter therefore begins with a brief description of proboscidean foot anatomy and an outline of previous osteological studies of feet belonging to Elephantinae species, especially insular species. Following this outline, the morphology of the carpals and then tarsals are described and individually compared between different taxa (alleged species or subspecies), and the manual and pedal metapodials are examined. These results further form the basis of a discussion on the gross anatomy of the manus and pes in each of the insular species studied. Finally, this chapter ends with a brief discussion of the results as they relate to the predictions of Hypothesis I.

Anatomy and osteology of the proboscidean foot

Among the subfamily Elephantinae foot morphology is highly derived, and both fore and hind-feet display numerous autapomorphies relating to the requirements of supporting large body mass. Both the manus and pes are wide compared with most perissodactyls, and the bones most robust laterally. The metapodials of both the fore and hindfoot are robust and digitigrade or subunguligrade, although the manus has the more upright orientation of the two. Collagenous tissues tightly bind the digits together, and predigits made of cartilage are bound into the foot-pad (Weissengruber *et al.*, 2006; Miller *et al.*, 2008: 466). The toes to radiate outwards during footfalls due to the presence of a large digital cushion (consisting of fat and connective tissue) that acts as a compressible shock-absorber (see Weissengruber *et al.*, 2006: Fig. 4; Panagiotopoulou *et al.*, 2012: Fig. 1).

In the manus, the carpals are block-like, and positioned in a column with the metacarpals arranged nearly vertically (Miller *et al.*, 2008: 466). The forefoot consists of a proximal row of carpals (the radial, intermediate and ulnar carpals), which sit atop a row of distal carpals, the os c. I to IV (see Fig. 3.1-1). In the pes, the astragalus-calcaneus robust (see Hutchinson *et al.*, 2008: Fig. 3.6). The pes consists of the astragalus that articulates proximally with the *Cochlea tibia*, plantarly with the calcaneus and distally with the central tarsal (Fig. 3.2; Smuts and Bezuidenhout, 1994: 59). The central tarsal articulates plantarly with the os t. I to IV (Fig. 3.2; Fig. 3.31-B) and the os t. IV articulates with the central tarsal and calcaneus, and distally with the mt III, mt IV and mt V (Fig. 3.2) and medially with the os t. III (Fig. 3.2; Smuts and Bezuidenhout, 1994: 61). Digits II, III and IV act like the three supports of a tripod, in

contrast with the manus, which forms a more unified column. The calcaneus is supported by the digital cushion (Miller *et al.*, 2008: 466).



Fig. 3.1 Articulated manus of A) *P. antiquus* from Riano, Italy (MPRU). B) *P. ex gr. P. falconeri* from Spinagallo Cave, Sicily (MPRU, likely including bones from multiple individuals). C) *M. lamarmorai* from Gonnesa, Sardinia (with reconstructed phalanges) (NHMB-Ty-i207i)^{sin}. 1) cranial 2) medial and 3) lateral aspects. a) Radial carpal b) Intermediate carpal c) ulnar carpal d) Os c. I e) Os c. II f) Os c. III g) Os c. IV.

With regard to their orientation, each of the metatarsals are differently orientated, with digits I and V being the most vertical, and digit III being the most horizontal (Miller *et al.*, 2008: 466).

In addition to the osteology the musculature and kinematics of the fore and hindfoot are also well-documented in extant elephants (Weissengruber and Forstenpointner. 2004; Miller *et al.*, 2008; Nagel *et al.*, 2018). Ankles dorsiflex, then plantarflex during the stance phase,

demonstrating typical spring-like kinematics (Ren *et al.*, 2008). Most of the tendons are quite robust, and act on multiple elements, in part due to the tightly bound foot-bones which form a hoof-like unit. The tendons responsible for pronation and supination are reduced, and their insertions indicate that they are consistent with flexor/extensor functions. The short muscles of the hand together with specific dorsal tendons enable precise movements of specific toes (Nagel *et al.*, 2018). Short flexor, abductor, adductor, lumbricales and interossei muscles are present on the palmar aspect of the carpus, metacarpus and digits. Supinator muscles in contrast are absent. In comparison to most other animals the Achilles tendon (*tendo calcaneus communis*) is very small (Miller *et al.*, 2008: 466).

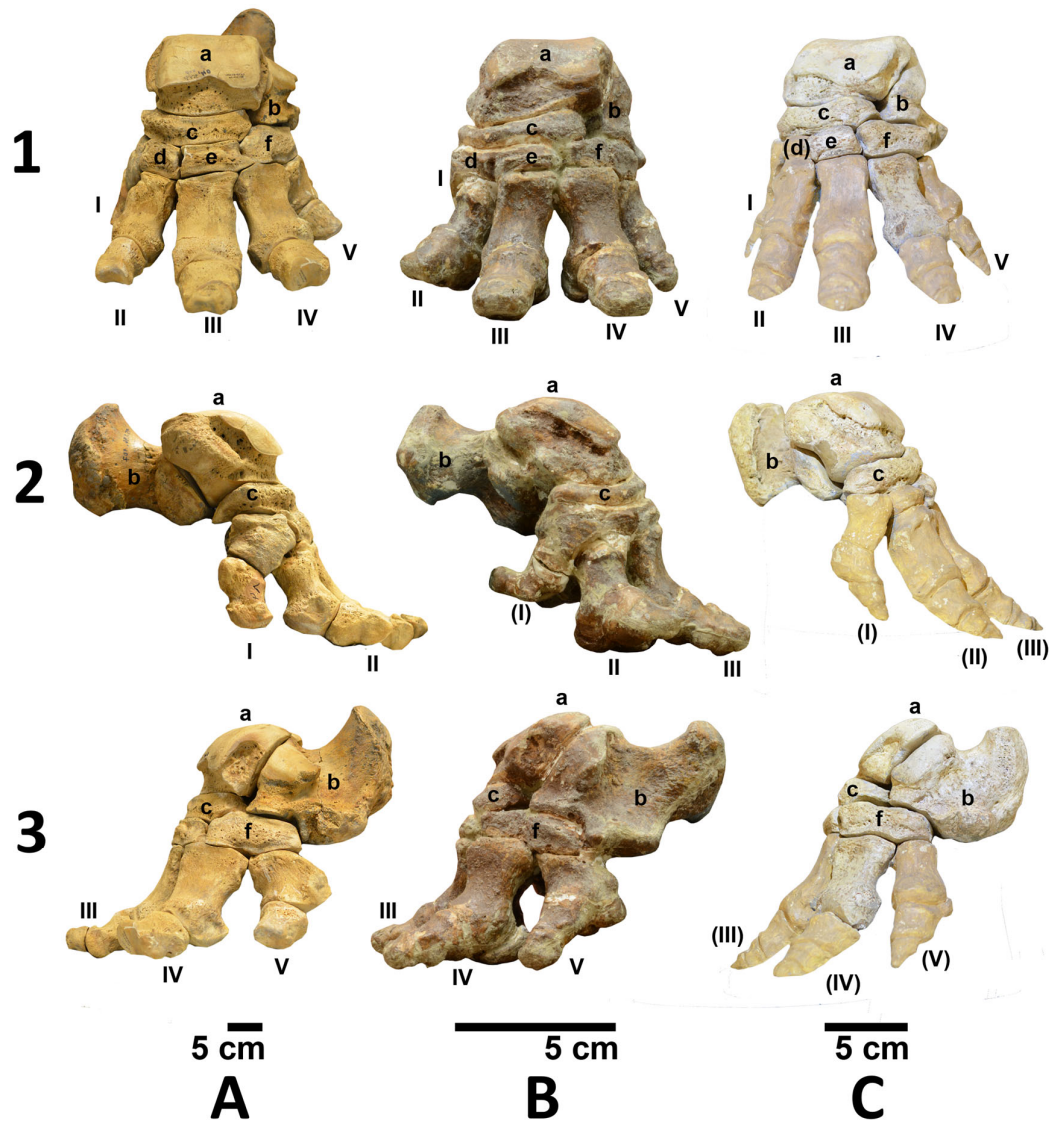


Fig. 3.2 Articulated pes of A) *P. antiquus* from Neumark-Nord 1, Germany (LVH-NN-E15.1.96 and 2007: 25.280,40)^{dex}, B) *P. ex gr. P. falconeri* from Spinagallo Cave, Sicily (MPRU, likely including bones from multiple individuals)^{dex}, C) *M. lamarmorai* from Gonnessa, Sardinia (NHMB-Ty-i207i, partially complete)^{sin}. 1) cranial 2) medial and 3) lateral aspects. a) astragalus b) calcaneus c) central tarsal d) os t. II e) os t. III f) os t. IV.

Terminology	Synonyms
Ulnar carpal	Triquetral, triquetrum, pyramidal, three-cornered bone, triangular bone, cuneiform bone, ulnare
Radial carpal	Scaphoid, navicular
Intermediate carpal	Lunar, lunatum, Ic
Accessory carpal	Os pisiforme, lentiform bone, Ac carpal
Os c. III	Magnum, s. capitatum
Os c. IV	Unciform, os hamatum
Astragalus	Astragalus
Central tarsal	Navicular
Os t. IV	TIV, ectocuneiform, cuboideum, cuboid
Calcaneus	Heel bone

Table 3.1 Carpal and tarsal terminology (following Smuts and Bezuidenhout, 1993; 1994) and their commonly-used synonymms (see Trevisan, 1948; Maccagno, 1962a; Ambrosetti, 1968).

Among Pleistocene representatives of the subfamily ELEPHANTINAE (GRAY 1821, following Shoshani *et al.*, 2007, see Appendix A), the osteology of the feet has been described/figured in *Palaeoloxodon recki* (DIETRICH 1915) by Schaurer (2010: Fig. 9) and *Palaeoloxodon antiquus* (FALCONER and CAUTLEY 1847) by Andrews and Cooper (1928: 7-18, plates III-VIII; see also Trevisan, 1948; Maccagno, 1962a; Dubrovo and Jakubovski, 1988; Kroll, 1991: 22-26; 41-42; Basile and Chilardi, 1996; Palombo and Villa, 2003; Halámková, 2006: 56-78, 96-113; Tsoukala *et al.*, 2011: Fig. 15; Kevrekidis and Mol, 2016: Fig. 16, Fig. 19; Scarborough *et al.*, 2016: Fig. 6, Fig. 7-1, Fig. 9-1). Dwarf *Palaeoloxodon* species thus far

described include *Palaeoloxodon falconeri* (BUSK 1867) from Malta (Busk, 1867: 268-272; Adams, 1874: 66-107; Liscaljet, 2007; 2012), *Palaeoloxodon* sp. from Benghisa Gap (Adams, 1874; Scarborough *et al.*, 2016) and *P. mnaidriensis* (ADAMS 1874) from Mnaidra Gap. Additionally *Palaeoloxodon* spp. from Sicily include *P. ex gr. P. falconeri* from Spinagallo Cave (Ambrosetti, 1968: 317-319; Scarborough *et al.*, 2016), *P. ex gr. P. mnaidriensis* from Puntali Cave (Palombo *et al.*, 2012; Scarborough *et al.*, 2014; 2016) and *Palaeoloxodon* sp. 1 from Luparello Fissure (Vaufrey, 1929: 67-68, plate VIII Fig. 9, Fig. 12; Scarborough *et al.*, 2016).

- *Palaeoloxodon antiquus* from Neumark-Nord 1, Germany
- *Palaeoloxodon antiquus* from Riano, Italy
- △ *Palaeoloxodon tiliensis* from Charkadio Cave, Tilos
- *Palaeoloxodon* sp. 2 from Faraglione Cave, Favignana
- ◆ *Palaeoloxodon ex gr. P. mnaidriensis* from Puntali Cave, Sicily
- ◆ *Palaeoloxodon ex gr. P. mnaidriensis* from Zà Minica Cave, Sicily
- ◆ *Palaeoloxodon ex gr. P. mnaidriensis* from San Teodoro Cave, Sicily
- × *Palaeoloxodon* sp. 1 from Luparello Fissure, Sicily
- ▲ *Palaeoloxodon ex gr. P. falconeri* from Luparello Fissure, Sicily
- ▲ *Palaeoloxodon ex gr. P. falconeri* from Spinagallo Cave, Sicily
- ▲ *Palaeoloxodon falconeri* from Malta
- × *Palaeoloxodon 'melitensis'* from Malta
- + *Mammuthus lamarmorai* from Gonnese, Sardinia
- *Loxodonta africana* from Kenya
- *Elephas maximus* from South Africa

Fig. 3.3 Figure legend for species studied in Chapters 3 and 4. For species binomial authorities refer to Appendix A.

Palaeoloxodon sp. 2 has also briefly been described from Favignana Island (Capasso Barbato *et al.*, 1988). In the central and eastern Mediterranean *Palaeoloxodon* spp. thus far described

include multiple species from Crete: *Palaeoloxodon 'chaniensis'* (SYMEONIDIS *et al.*, 2000) from Vamos Cave, *P. creutzburghi* from Simonelli Cave (Kotsakis, 1980: 118) and Simonelli Cave II (Mol *et al.*, 1996: 87-90). From the Dodecanese Islands *Palaeoloxodon tiliensis* (THEODOROU *et al.*, 2007) has been described from Tilos (Theodorou, 1983: 88-128; 148-179) and *Palaeoloxodon* sp. from Rhodes (Symeonidis *et al.*, 1974).

Among mammoths the osteology of the feet has been described in Early Pleistocene *Mammuthus meridionalis* (NESTI 1825) by Reggiani (1999; 2001; see also Halámková, 2006; Popescu, 2011), Middle Pleistocene *Mammuthus trogotherii* (POHLIG 1885) by Athanassiou (2012; see also Baygusheva *et al.*, 2012), late Middle Pleistocene to mid-Holocene *M. primigenius* (Andrews and Cooper, 1928: plates III-VII; Mol, 1984; Mol and de Vos, 1995; Halámková, 2006; Maschenko *et al.*, 2006: Fig. 5B; Fehlmann and Brinkmann, 2014), North American *Mammuthus columbi* (FALCONER 1857) by Mol and Agenbroad (1994) and the Sardinian dwarf mammoth *Mammuthus lamarmorai* (MAJOR 1883) by Palombo *et al.* (2012). Among extant elephants the foot osteology has also been described in *L. africana* (Smuts and Bezuidenhout, 1993; 1994; Ramsay and Henry, 2008) and *E. maximus* LINNAEUS 1758 by Andrews and Cooper (1928: plates III-VIII). In addition to these osteological studies, the soft-tissue of *E. maximus* has also been described (Shindo and Mori, 1956a; 1956b; Hutchinson *et al.*, 2011).

However, despite the considerable variability in the morphology of the foot bones among the Elephantinae demonstrated by the above studies, there are few in-depth studies comparing mainland with insular species, or different insular species (although see Adams, 1874; Liscaljet, 2007; Scarborough *et al.*, 2016). Furthermore, most of the above studies are purely descriptive or taxonomic in their approach, and do not examine how topography, environment, ontogeny or body mass has influenced the morphology of the feet. These studies nonetheless demonstrate the taxonomic importance and range of morphological diversity in foot bones among the Elephantinae with which dwarf insular species may be compared in order to better understand the evolution of morphologically derived features.

3.1 RESULTS

The results on the carpals are presented below (in Sections 3.1-3.4), followed by the tarsals (Sections 3.4-3.8) and metapodials (Section 3.9).

3.1.1 Ulnar carpal

The ulnar carpal is the largest proximal carpal, located on the lateral side of the foot (Fig. 3.1). Proximally, the articular surface is saddle-shaped for articulation with the ulna and distally the articular surface consists of a quadrilateral medial part, also saddle-shaped, for articulation with the os c. IV. A prominent elongation points palmarly and laterally and an oval articular facet occurs for the accessory carpal on the palmar surface of the base of this projection. The ulnar carpal also articulates with the intermediate carpal via two medially-facing articular facets, one proximal, the other distal, separated by a groove, while a small

elongated facet facing dorsopalmarly articulates with the mc V (Smuts and Bezuidenhout, 1993: 8).

3.1.1.1 Intraspecific variability in the ulnar carpal of *P. ex gr. P. falconeri* from Spinagallo Cave

A wide range in absolute size is evident in the *Palaeoloxodon* assemblage from Spinagallo Cave, including multiple species (see Chapter 2). However, most specimens are referable to *P. ex gr. P. falconeri*. The size-frequency distribution of the maximum anterior height of the ulnar carpal is represented in Fig. 3.4a, demonstrating substantial variability. Additionally, the frequency-distribution of the ratio of the breadth/length of the articular facet for the ulna is figured, displaying two modes with one outlier with an unusually wide facet (MPRU-SpC-UC35; Fig. 3.4b; Table 3.2).

Eight variables were measured in order to investigate possible correlations between the allometry of articular facets using PCA (Fig. 3.5a-b; Table 3.3a-b). In the PCA output the grey lines represent the variables (Fig. 3.5a; Fig. 3.5b) and the side of the line with the label is the positive/increasing side, and variables that move together are correlated. Specimens appear to form broad clusters, except for one specimen appears to be an outlier (MPRU-SpC-UC33, see discussion in 3.10). The table also indicates the standard deviation and proportion of variance explained for each principle component (Table 3.3a-b). The first component explains 82% of the variation in this case with the remaining principle components individually explaining little of the remaining variation. The second part of the table indicates the factor loadings (how much each variable contributes to each principle component). This is not important here as we are not using this data for further analysis and is thus only presented for completion.

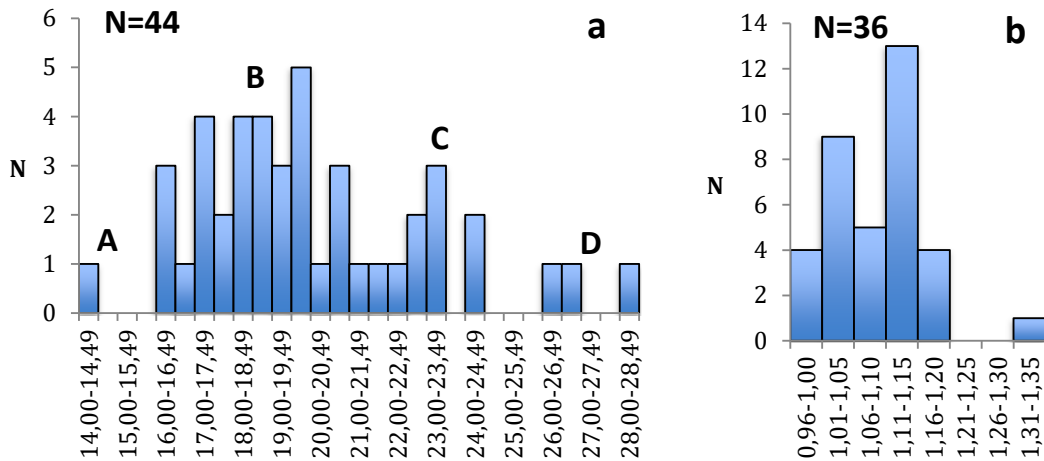


Fig. 3.4 Size-frequency histograms of the ulnar carpal of *P. ex gr. P. falconeri* from Spinagallo Cave (in mm). a) Max anterior height (pr-d). b) Ratio of the breadth (m-l)/length (a-p) of the articular facet for the ulna.

Dimensions of the articular facet for the ulna (m-l/a-p)	Specimens (MPRU collection)
Mode B (1,01-1,05)	SpC-UC14, SpC-UC18, SpC-UC19, SpC-UC22, SpC-UC24, SpC-UC29, SpC-UC30, SpC-UC34 SpC-UC41
Mode C (1,11-1,15)	SpC-UC1, SpC-UC2, SpC-UC9, SpC-UC11, SpC-UC16, SpC-UC20, SpC-UC21, SpC-UC31, SpC-UC32, SpC-UC35, SpC-UC39, SpC-UC40, SpC-UC43

Table 3.2 *P. ex gr. P. falconeri* ulnar carpal specimens from Spinagallo Cave, belonging to modes B and C in Fig. 3.4b.

UC1 and UC2 [ulnar carpal max thickness (a-p) and breadth (m-l) respectively] are highly correlated as they are close together, and both are also correlated (though to a lesser extent) with UC8 (a-p length of the articular facet for the ulna). UC4 [max anterior height (pr-d)] and UC5 [max posterior height (pr-d)] are also highly correlated. There is a lesser degree of correlation between UC14 [diameter (m-l) of the articular facet for the accessory carpal] and UC15 [length (pr-d) of the articular facet for the accessory carpal] which are moving in another direction from the variables mentioned previously, almost perpendicular, indicating that these two are unrelated to the other variables. Finally, UC9 [breadth (m-l) of the articular facet for the ulna] is moving in a direction of its own and is thus unrelated to any of the other variables.

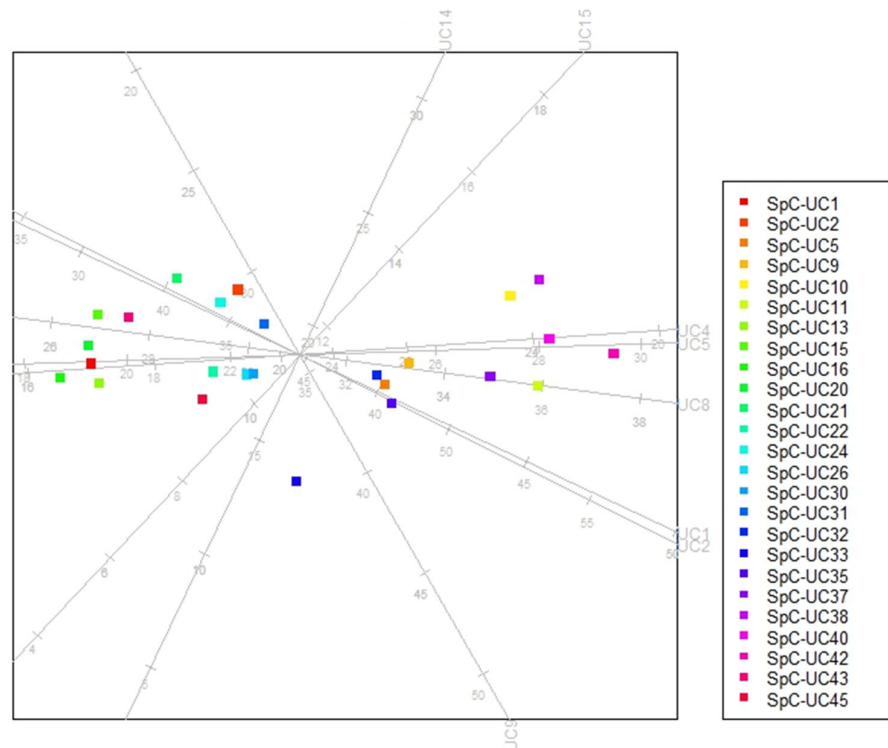


Fig. 3.5a Principal Component Analysis of the ulnar carpal of *P. ex gr. P. falconeri* from Spinagallo Cave (specimens are identified by MPRU-SpC accession numbers).

UC1 [max thickness (a-p)] and UC2 [max width (m-l)] are moving closely together in the same direction. UC14 [Diameter of articular facet for accessory carpal (m-l)] and UC15 [diameter of articular facet for accessory carpal (pr-d)] are roughly at 90° to the previous, and also moving in the same direction. UC4, 5 and 8 [Max anterior height (pr-d)]; [Max posterior

height (pr-d)]; [Length (a-p) of the articular facet for the ulna], are similar in direction. Only UC9 [breadth (m-l) of articular facet for ulna] moves independently in its own direction. PC1 and PC5 have the greatest loadings for UC1. Seeing as there are only relatively small intraspecific differences in the absolute size of the *P. ex gr. P. falconeri* ulnar carpal, there are also only slight differences between the scaled and log-transformed PCA (Fig. 3.5b). As might be expected, length/breadth measurements on the same articular facets are more closely correlated than measurements on different facets.

Principal component	PC1	PC2	PC3	PC4	PC5	PC6	PC7	PC8
Standard deviation	2.56	0.70	0.57	0.50	0.43	0.32	0.27	0.20
Proportion of Variance	0.82	0.06	0.04	0.03	0.02	0.01	0.01	0.00
Cumulative Proportion	0.82	0.88	0.92	0.95	0.97	0.99	1.00	1.00
Rotation:								
UC1 - Max thickness (a-p) of the ulnar carpal	0.37	-0.17	0.18	-0.22	0.31	-0.47	-0.45	-0.49
UC2 - Max breadth (m-l) of the ulnar carpal	0.35	-0.18	-0.33	-0.39	-0.71	0.11	-0.25	0.07
UC4 - Max anterior height (pr-d)	0.36	0.02	0.36	0.61	-0.13	0.04	-0.43	0.40
UC5 - Max posterior height (pr-d)	0.37	0.01	0.01	0.36	-0.33	-0.39	0.63	-0.29
UC8 - Length (a-p) of art. f. for the ulna	0.37	-0.05	0.01	-0.37	0.31	-0.28	0.29	0.68
UC9 - Breadth (m-l) of art. f. for the ulna	0.34	-0.59	0.08	0.05	0.26	0.62	0.22	-0.16
UC14 - Breadth (m-l) of art. f. for accessory	0.32	0.68	0.41	-0.30	-0.02	0.37	0.10	-0.18
UC15 - Length (pr-d) of art. f. for accessory	0.33	0.35	-0.75	0.26	0.33	0.12	-0.12	-0.06

Table 3.3a Principal Component Analysis output for the ulnar carpal of *P. ex gr. P. falconeri* from Spinagallo Cave (see Fig. 3.5a).

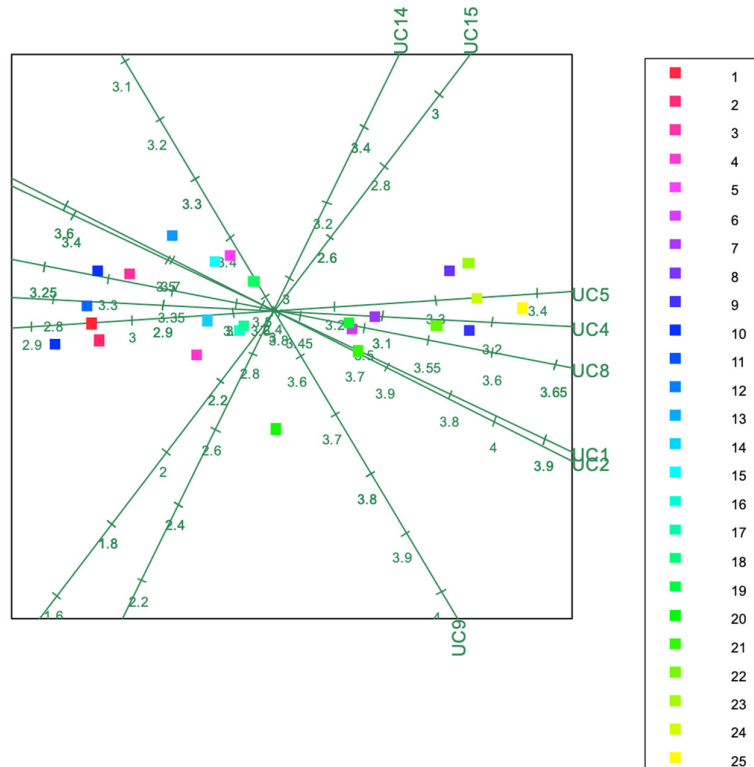


Fig. 3.5b Standardized and log-transformed Principal Component Analysis of the ulnar carpal of *P. ex gr. P. falconeri* from Spinagallo Cave, Sicily. Refer to Table 3.5b for axes variable labels and component loading.

Principal component	PC1	PC2	PC3	PC4	PC5	PC6	PC7	PC8
Standard deviation	2.55	0.73	0.56	0.48	0.42	0.34	0.28	0.19
Proportion of Variance	0.81	0.07	0.04	0.03	0.02	0.01	0.01	0
Cumulative Proportion	0.81	0.88	0.92	0.95	0.97	0.99	1	1
Rotation:								
UC1 - Max thickness (a-p) of the ulnar carpal	0.37	-0.18	0.18	-0.15	0.28	-0.47	-0.36	-0.59
UC2 - Max breadth (m-l) of the ulnar carpal	0.35	-0.18	-0.28	-0.47	-0.67	0.1	-0.26	0.08
UC4 - Max anterior height (pr-d)	0.36	-0.02	0.22	0.66	-0.16	-0.11	-0.42	0.41
UC5 - Max posterior height (pr-d)	0.37	0.02	-0.06	0.31	-0.35	-0.24	0.71	-0.28
UC8 - Length (a-p) of the articular facet for the ulna	0.37	-0.07	0.09	-0.39	0.36	-0.3	0.3	0.62
UC9 - Breadth (m-l) of the articular facet for the ulna	0.34	-0.57	0.05	0.1	0.27	0.67	0.12	-0.1
UC14 - Breadth (m-l) of the articular facet for the accessory carpal	0.32	0.65	0.53	-0.2	-0.04	0.38	0.01	-0.11
UC15 - Length (pr-d) of the articular facet for the accessory carpal	0.33	0.43	-0.74	0.13	0.33	0.11	-0.12	-0.04

Table 3.3b Standardized and log-transformed Principal Component Analysis output for the ulnar carpal (see Fig. 3.5b).

3.1.1.2 Interspecific comparison of the ulnar carpal

In terms of absolute size distribution *Palaeoloxodon* sp. 1 from Luparello Fissure and *Palaeoloxodon* sp. 2 from Favignana Island evidence comparable size, and there is also overlap between *Palaeoloxodon* sp. 1 from Luparello Fissure, Sicily and *Palaeoloxodon* sp. from Malta (Fig. 3.6a, b). *Palaeoloxodon* sp. from Benghisa Gap, Malta (= *Elephas melitensis* Adams, 1874: 70, Pl. xviii Fig. 8-9, NHMUK-44533; 44468; 44466) includes one sample within the size range of *P. ex gr. P. falconeri* from Spinagallo Cave, and two that are slightly larger than this species (Fig. 3.6a). Finally, the single specimen of *P. ex gr. P. falconeri* from Luparello Fissure falls within the lower size limit of *P. ex gr. P. falconeri* from Spinagallo Cave (Fig. 3.6a-c). In terms of allometry there are several noticeable interspecific differences in the ulnar carpal (Fig. 3.6a-e). These include the (i) Allometry of the articular facet for the ulna; (ii) Ratio of the breadth of the ulnar facet (m-l)/length (a-p) of the ulnar facet; (iii) Max breadth (m-l) of ulnar carpal (m-l)/max anterior height (pr-d), and (iv) The dimensions of the articular facet for the accessory carpal.

(i) Allometry of the articular facet for the ulna - The greatest difference in allometry is evident between *Palaeoloxodon* sp. 1 from Luparello Fissure, Sicily (Fig. 3.6b) and *Palaeoloxodon* sp. from Benghisa Gap, Malta (= *Elephas melitensis* Adams, 1874: 70, Pl. xviii Fig. 8-9). Although the sample-size is small for Maltese *Palaeoloxodon* sp. and Sicilian *Palaeoloxodon* sp. 1, the articular facet is narrow in the former and wide (m-l) in the latter (Fig. 3.6b). The single *P. ex gr. P. falconeri* individual from Luparello Fissure, although of comparable cranial height to examples from the Spinagallo Cave sample, falls towards the extreme range of its variability in terms of the allometry of the articular facet for the ulna (Fig. 3.6e).

(ii) Ratio of the breadth of the ulnar facet (m-l)/length (a-p) of the ulnar facet - This is not significantly different between *P. antiquus* vs. *Palaeoloxodon* sp. 1 (Fig. 3.6b; MWU $p=0,785$). However statistically significant differences exist between *P. antiquus* vs. *P. ex gr. P. falconeri* (MWU $p=0,000$) and between *Palaeoloxodon* sp. 1 vs. *P. ex gr. P. falconeri* (MWU $p=0,000$), indicating a relatively less wide articular facet in *P. ex gr. P. falconeri*.

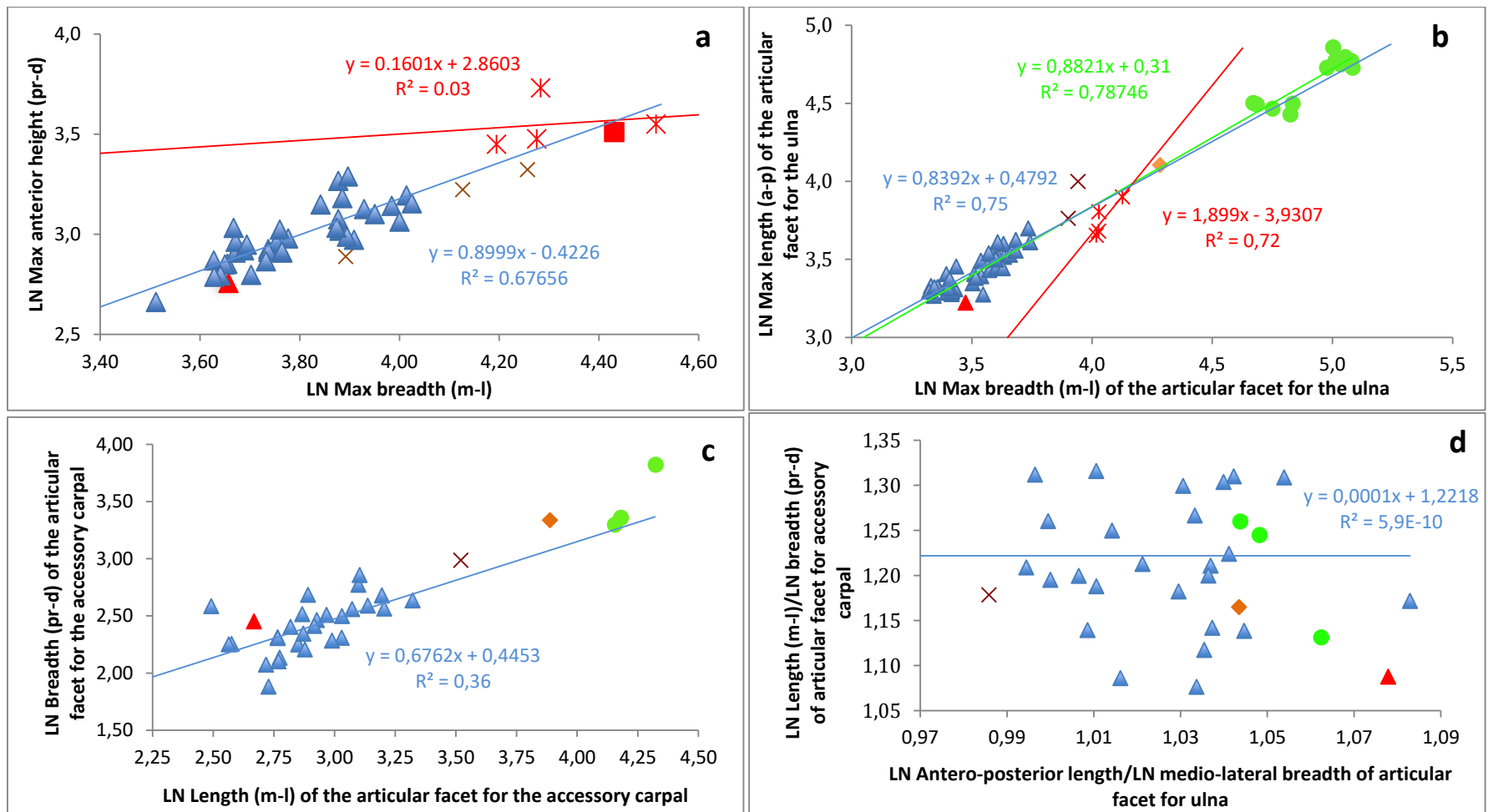


Fig. 3.6 Scatterplots of the dimensions of the ulnar carpal a) Max breadth (m-l) vs. max anterior height (pr-d). b) Max breadth (m-l) vs. max length (a-p) of articular facet for the ulna c) Dimensions of the articular facet for the accessory carpal d) Ratio of the dimensions of the articular facets for the accessory carpal and ulna. Refer to Fig. 3.3 for symbol legend. [Data in Fig. 3.6b: *P. antiquus* from Palombo *et al.*, unpublished. Note that unless otherwise acknowledged in figure legends or captions all data is original].

(iii) Max breadth (m-l) of ulnar carpal (m-l)/max anterior height (pr-d) - Differences are

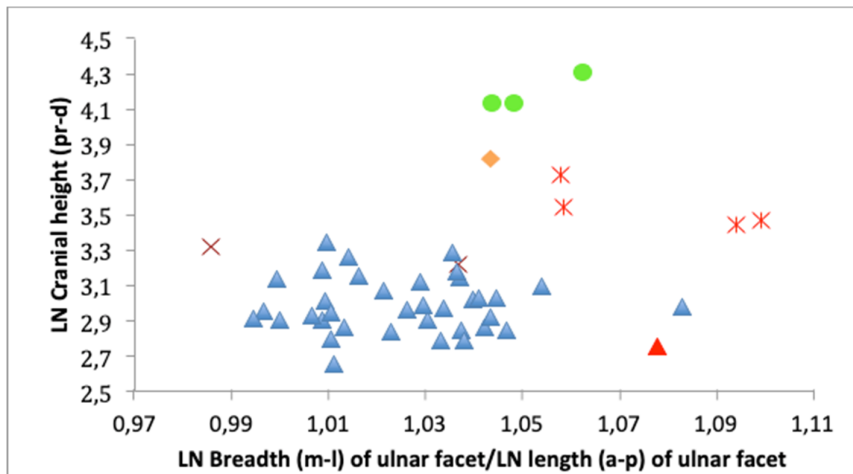


Fig. 3.6e Max cranial height (pr-d) vs. allometry of the articular facet for the ulna. Refer to Fig. 3.3 for symbol legend.

not statistically significant between *Palaeoloxodon* sp. 1 from Luparello Fissure vs. *P. ex gr. P. falconeri* from Spinagallo Cave (MWU $p=0,499$). There is however one tall specimen belonging to *Palaeoloxodon* sp. 1 from Luparello

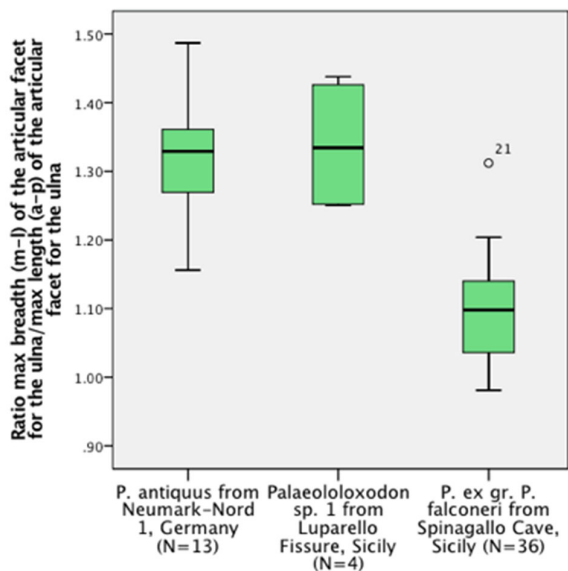


Fig. 3.7 Box-and-whisker plot of the ratio of the ulnar carpal's articular facet for the ulna (max breadth (m-l)/max length (a-p)).

Fissure (Fig. 3.6a). (iv) The dimensions of the articular facet for the accessory carpal - Only three *P. antiquus* individuals were sampled, but one individual has an unusually long facet relative to the other *P. antiquus* individuals, and also relative to the insular *Palaeoloxodon* spp. (Fig. 3.6c). The small sample-size nevertheless demonstrates the presence of intraspecific variability in *P. antiquus*.

3.1.2 Intermediate carpal

The intermediate carpal is situated proximally and articulates with the radius via its proximal, saddle-shaped surface (Fig. 3.1). Dorsolaterally there is an oblique continuation of this surface, articulating with the ulna and ulnar carpal. Along the distal border of the lateral surface there is a parallel area for articulation with the contiguous surface of the ulnar carpal (Smuts and Bezuidenhout, 1993: 7-8). There are two facets for the radial carpal over the medial surface, one proximally, the other distally. The distal articular surface is saddle-shaped, but curvatures are far greater, and it articulates with the os c. III (Smuts and Bezuidenhout, 1993: 8).

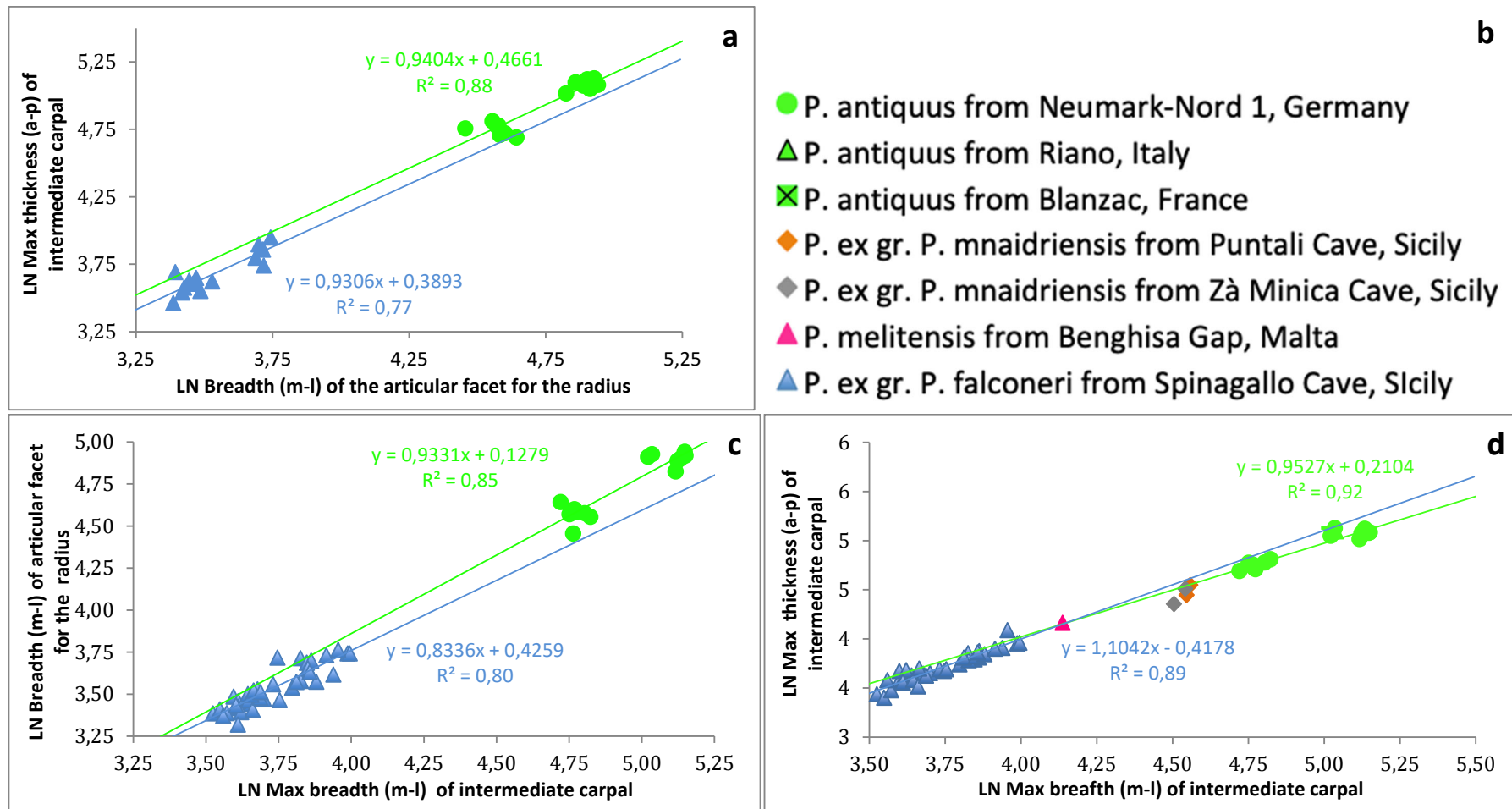


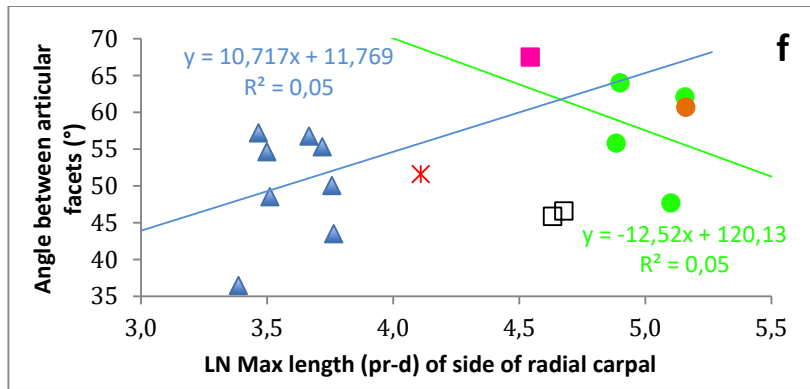
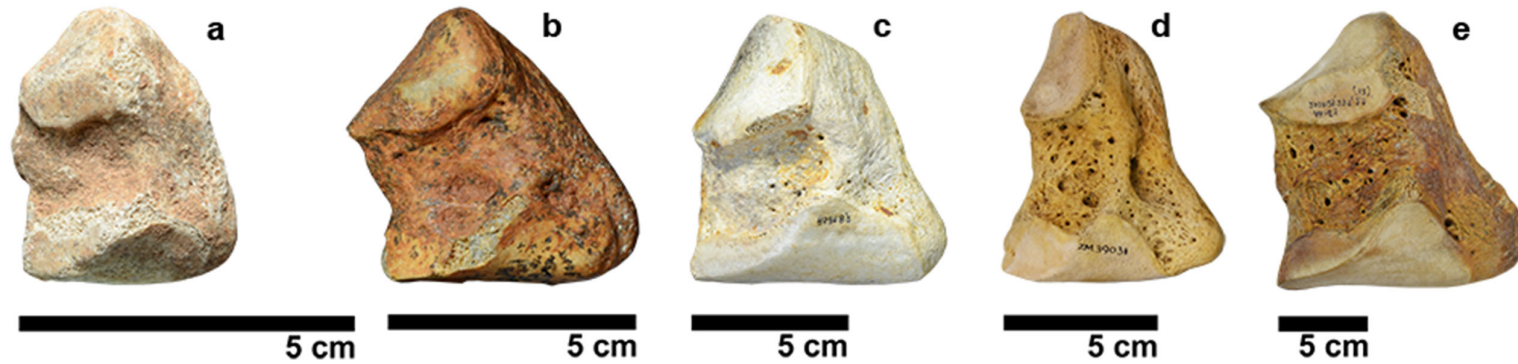
Fig. 3.8 Scatterplots of the dimensions of the intermediate carpal. a) Breadth (m-l) of the articular facet for the radius vs. max thickness (a-p). b) Symbol legend. c) Max breadth (m-l) vs. breadth (m-l) of the articular facet for the radius d) Max breadth (m-l) vs. max thickness (a-p). [Data: *P. antiquus* from Palombo *et al.*, unpublished]

In terms of bivariate allometry, three ratios were compared between species: (i) Ratio max breadth (m-l)/max thickness (a-p) - There is no significant difference between *P. antiquus* vs. *P. ex gr. P. mnaidriensis* (Fig. 3.8d; MWU $p=0,277$), or between *P. antiquus* vs. *P. ex gr. P. falconeri* (MWU $p=0,762$), or between *P. ex gr. P. falconeri* vs. *P. ex gr. P. mnaidriensis* (MWU $p=0,346$). (ii) Max thickness (a-p) of intermediate carpal/breadth (m-l) of the articular facet for the radius - Differences are non-significant between *P. antiquus* vs. *P. ex gr. P. falconeri* (Fig. 3.8a; MWU $p=$). (iii) Ratio of max breadth (m-l) of intermediate carpal/breadth (m-l) of the articular facet for the radius - Finally, there is no difference between the breadth of the articular facet for the radius between *P. antiquus* and *P. ex gr. P. falconeri* (Fig. 3.8c; MWU $p=0,592$).

3.1.3 Radial carpal

The radial carpal is the most medial bone of the proximal row of carpals and is flattened (Fig. 3.1-A1). Proximally it articulates with the radius, and laterally via a proximal and distal articular facet with the intermediate carpal (Fig. 3.9a-e). Distally it also articulates with the os c. II and os c. III (Smuts and Bezuidenhout, 1993: 7). Although the sample-size is small, there are several morphological features of interest, including: (i) The size of the proximal articular facet for the intermediate carpal; (ii) The max length (a-p) of articular facet for the os c. II/max breadth (m-l) of articular facet for os c. II continuous with distal articular facet for intermediate carpal; (iii) The angle between the articular facet for the radius and the articular facet for the os c. II.

(i) Ratio distal thickness/length (pr-d) of proximal articular facet for intermediate carpal - There is much variation among the species in the length (pr-d) of this facet, which is virtually absent in the two examples of *P. ex gr. P. mnaidriensis* examined from Zà Minica Cave (GMP-RSZM87 and GMP-ZM73, see Fig. 3.9c; for details on the site see Fabiani, 1932b), and clearly present in *P. antiquus* from Neumark-Nord 1 (Fig. 3.9e), *Palaeoloxodon* sp. 1 from Luparello Fissure (Fig. 3.9b) and in *P. ex gr. P. falconeri* from Spinagallo Cave (Fig. 3.6a). However, differences are not statistically significant between *P. antiquus* vs. *P. ex gr. P. falconeri* (Fig. 3.10c; MWU $p=0,257$). (ii) Max length (a-p) of articular facet for the os c. II/max breadth (m-l) of articular facet for os c. II continuous with distal articular facet for intermediate carpal - Differences are statistically significant between *P. antiquus* and *P. ex gr. P. falconeri* (Fig. 3.10e; MWU $p=0,010$), indicating a long (a-p) articular facet for the os c. II in *P. ex gr. P. falconeri*.



Species	Min angle	Max angle	N
<i>P. antiquus</i> from NN 1 and Riano	47,7	64,0	5
<i>P. ex gr. P. mnaidriensis</i> from Zà Minica Cave, Sicily	59,5		1
<i>Palaeoloxodon</i> sp. 1 from Luparello Fissure, Sicily	51,6		1
<i>P. ex gr. P. falconeri</i> from Spinagallo Cave	36,5	57,2	9

Fig. 3.9 Radial carpal in medial aspect, illustrating differences in the angle between the articular facet for the radius and the articular facet for the os c. II. a) *P. ex gr. P. falconeri* from Spinagallo Cave, Sicily (MPRU)^{dex}. b) *Palaeoloxodon* sp. 1 from Luparello Fissure, Sicily (IPH-2987)^{sin} c) *P. ex gr. P. mnaidriensis* from Zà Minica Cave, Sicily (GMP-RSZM87, slightly damaged)^{dex} d) *E. maximus* (SAM-ZM39031)^{sin} e) *P. antiquus* from Neumark-Nord 1, Germany (LVH-NN-2.1.96,110)^{dex} f) Scatterplot of the max length (pr-d) vs. angle between articular facets for the radius and os c. II. Refer to 2.16 for measurement protocol and Fig. 3.3 for symbol legend. Table 3.4 Angle between the radial carpal's articular facets for radius and os c. II. Refer to Fig. 2.17 for the identification of articular facets and measurement protocol.

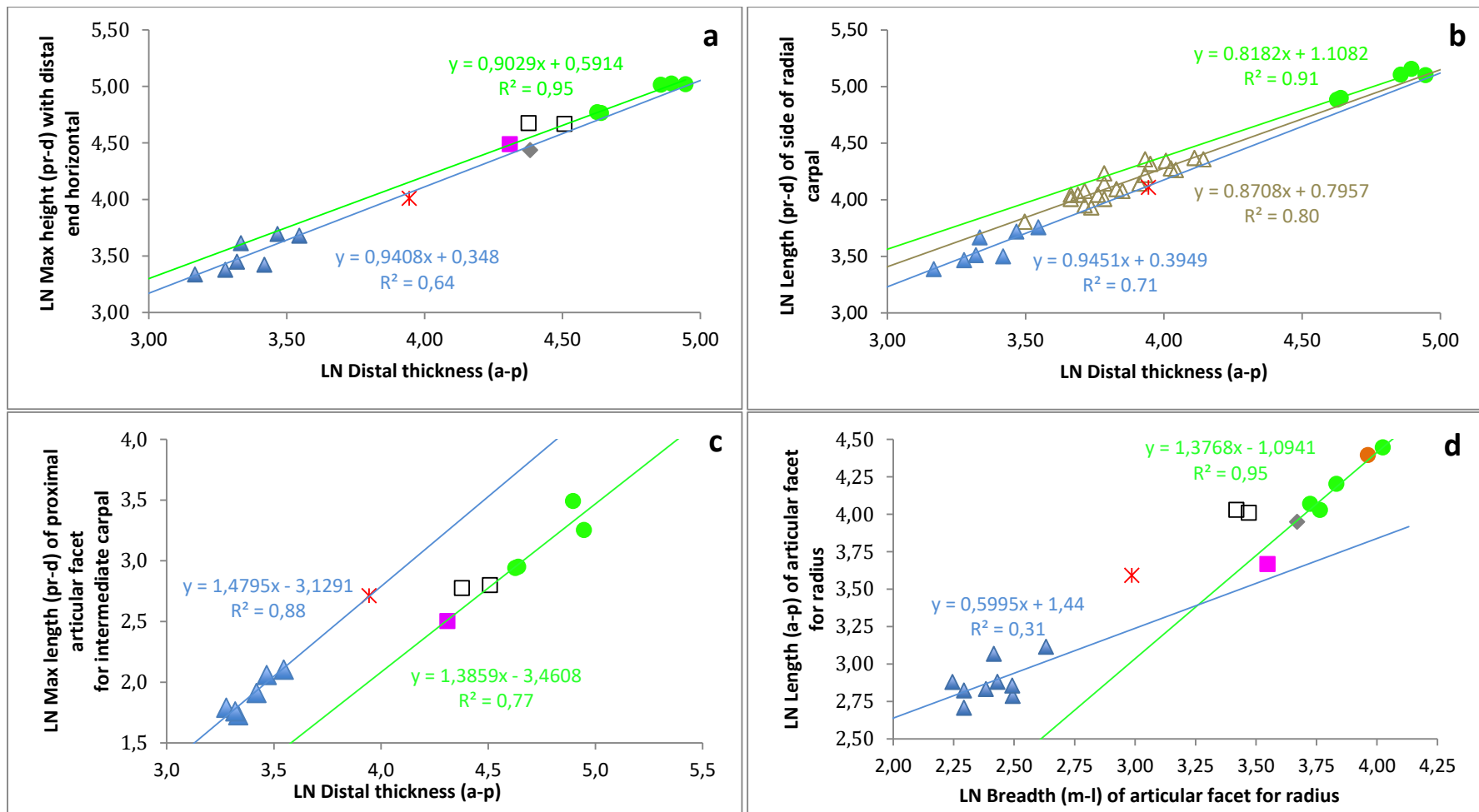


Fig. 3.10 Scatterplots of the dimensions of the radial carpal. a) Distal thickness (a-p) vs. max height (pr-d) with distal end horizontal b) Distal thickness (a-p) vs. max length (pr-d) of anterior side of radial carpal. c) Distal thickness (a-p) vs. max length (pr-d) of proximal articular facet for intermediate carpal. d) Breadth (m-l) of articular facet for radius vs. length (a-p) of articular facet for radius. Refer to Fig. 3.3 for symbol legend.

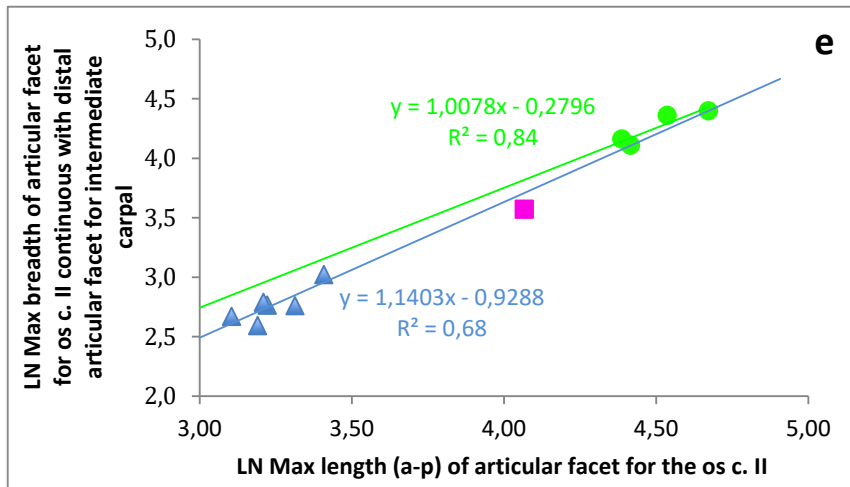


Fig. 3.10e Max breadth of articular facet for os c. II continuous with distal articular facet for intermed. carpal vs. max length (a-p) of art. facet for the os c. II. Refer to Fig. 3.3 for symbol legend.

(iii) Angle between the articular facet for the radius and the articular facet for the os c. II - In the sample studied the angle varies from a minimum of 36,5° in *P. ex gr. P. falconeri* to 67,5° in *E. maximus* (Fig. 3.9a-f; Table 3.4). This angle is known to vary intra- and interspecifically (Maccagno, 1962a; Saunders, 1999), with a more acute angle allegedly reflecting a plantigrade posture, and a more obtuse angle reflecting a digitigrade posture (Maccagno, 1962a: 111; *ibid* Fig. 25). The angle is however not significantly different between *P. antiquus* and *P. ex gr. P. falconeri* (MWU p=0.093) although the angles observed in *P. ex gr. P. falconeri* include individuals which were likely more plantigrade in the forefoot than some *P. antiquus* individuals. Additionally, MWU ratios were compared in: (iv) Length of articular facet for radius (a-p)/breadth (m-l) of articular facet for radius - The facet has a tendency to be wider (m-l) in *P. ex gr. P. falconeri* than in *P. antiquus* (Fig. 3.10d) although differences are not statistically significant (MWU p=0,083). A single *L. africana* individual also evidences a relatively less wide facet than in *P. ex gr. P. falconeri* (Fig. 3.10d). (v) Max height (pr-d) with distal end horizontal/distal thickness (a-p) - Differences are not statistically significant between *P. antiquus* and *P. ex gr. P. falconeri* (Fig. 3.10a; MWU p=0,639). (vi) Length (pr-d) of anterior side of radial carpal/distal thickness - Differences are not statistically significant between *P. antiquus* and *P. ex gr. P. falconeri* (Fig. 3.10b; MWU p=0,343).

3.1.4 Os carpale III

The os c. III is a distal carpal (Fig. 3.1) and is roughly rectangular or trapezoidal in dorsal aspect (Fig. 3.11b; Fig. 3.12-E), with a saddle-shaped proximal articular surface for the intermediate carpal (Fig. 3.12-C; Fig. 3.12-D). In cranial aspect it appears square or rectangular with numerous foramina on the ventral surface (Fig. 3.12-A). The dorsal surface is rough and has a more-or-less projecting tuber situated distally (Fig. 3.12-B). The medial surface has a deep central concavity, surrounded proximally, dorsally and distally by articular surfaces for the os c. II and mc II (Fig. 3.12-C5), although the articular facets vary significantly in their morphology (Fig. 3.12-C). The lateral aspect displays a large articular surface proximally and a small distal facet for os c. IV (Fig. 3.12-D). Palmarly the bone is flat proximally, but bears a tuberosity distally (Fig. 3.12-F), and the surface is divided sagittally

into a small medial facet for the mc II, and a large lateral facet for the mc III (Fig. 3.12-F) (Smuts and Bezuidenhout, 1993: 9).

3.1.4.1 Intraspecific variability in the *P. ex gr. P. falconeri* os c. III from Spinagallo Cave

Several morphological features in the os c. III are noticeably variable, including (i) the max cranial breadth (Fig. 3.11a, b), (ii) the degree of separation between the articular facets: in medial aspect the bone presents an articular facet for the os c. IV (situated proximally) and mc II (situated distally, see Fig. 3.12-5C). In some individuals the two articular facets are joined via an hour-glass shaped articular surface and in other examples the two articular facets are completely separated by a rough horizontal groove for a tendon. (iii) The tuber is also variable and is small in some specimens while projecting dorsally in others, and in some specimens the articular facet for mc II also projects dorsally on the plantar surface of the tuber. iv) Finally, viewed caudally (Fig. 3.12-1B) the orientation of articular facet for the mc II varies between more vertical in some specimens vs. more inclined in other specimens (similar to in *P. antiquus*, Fig. 3.12-4B, 5B).

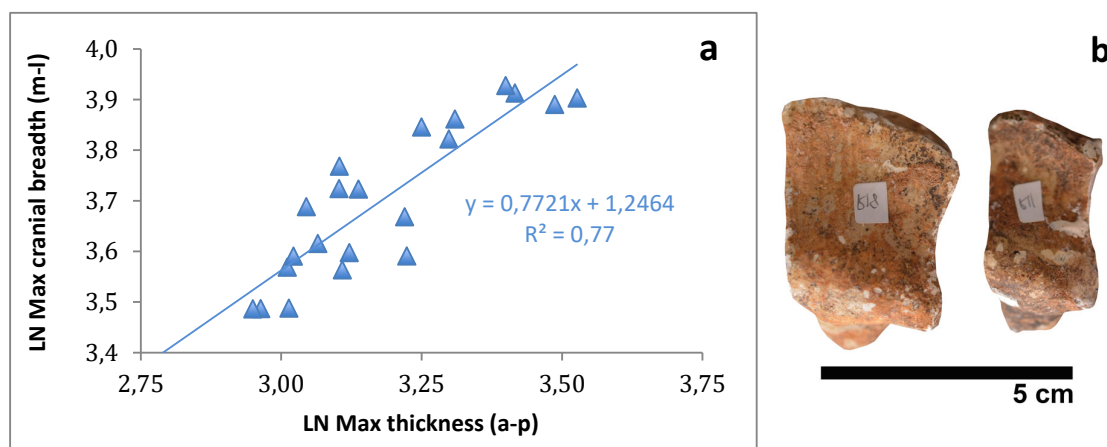


Fig. 3.11 Intraspecific morphological variability in the os c. III of *P. ex gr. P. falconeri* from Spinagallo Cave, including 20 of the 39 specimens identified previously (Ambrosetti, 1968: Table VIII). a) Scatterplot of the cranial breadth (m-l) vs. max thickness (a-p). b) Os c. IIIs in dorsal aspect (MPRU)^{dex}.

3.1.4.2 Interspecific comparison of the os c. III

Size distribution and interspecific morphology in the os c. III - In terms of absolute dimensions similar size is evidenced in *P. ex gr. P. mnaidriensis* from Puntali Cave, Sicily, *P. mnaidriensis* from Malta, *Palaeoloxodon* sp. 2 from Favignana Island and *M. lamarmorai* from Sardinia (Fig. 3.14a; Fig. 3.14b). Morphologically, the os c. III differs in several respects between species. These include the ratios of (i) the max thickness (a-p) vs. cranial breadth (m-l), (ii) the max length (a-p) vs. max breadth (m-l) of the articular facet for the mc III, (iii) the cranial (m-l) vs. caudal (m-l) breadth, and (iv) the inclination of the articular facet for the os c. II. (v) Ratio of the max cranial height (pr-d)/max thickness (a-p), and (vi) the

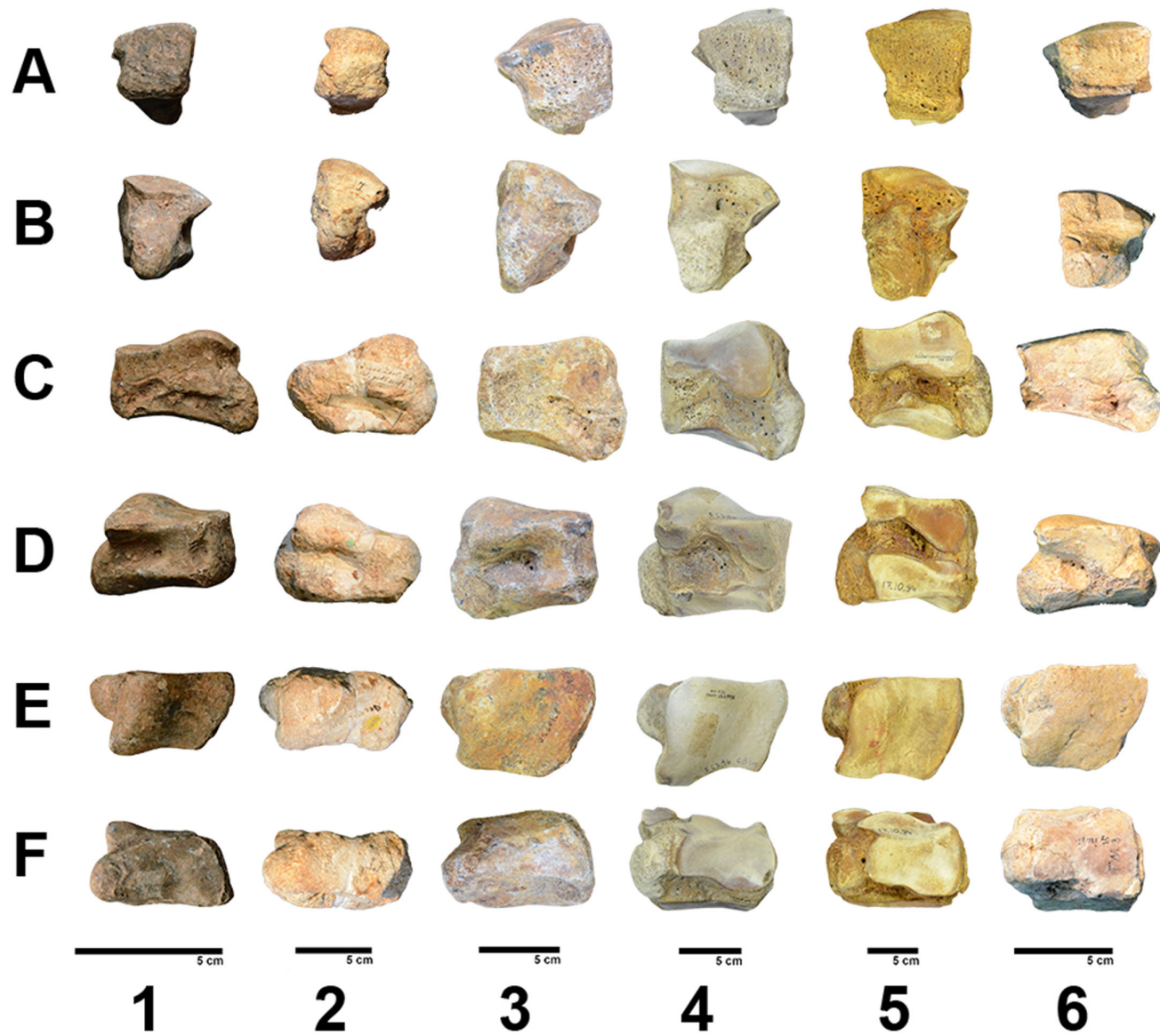


Fig. 3.12 Os c. III of Elephantinae species 1) *P. ex gr. P. falconeri* from Spinagallo Cave, Sicily (MPRU)^{dex}. 2) *P. mnaidriensis* from Mnaidra Gap, Malta (NHMUK-44394)^{sin} 3) *P. ex gr. P. mnaidriensis* from Puntali Cave, Sicily (GMP-RSGP-168)^{sin} 4) Young *P. antiquus* from Neumark-Nord 1, Germany (LVH-NN-E22)^{sin}. 5) Adult *P. antiquus* from Neumark-Nord 1 (LVH-NN-E9 17.10.94)^{sin} 6) *M. lamarmorai* from Gonnessa, Sardinia (NHMB-Ty-i207i)^{sin} A) cranial B) caudal C) medial D) lateral E) dorsal and F) plantar aspects.

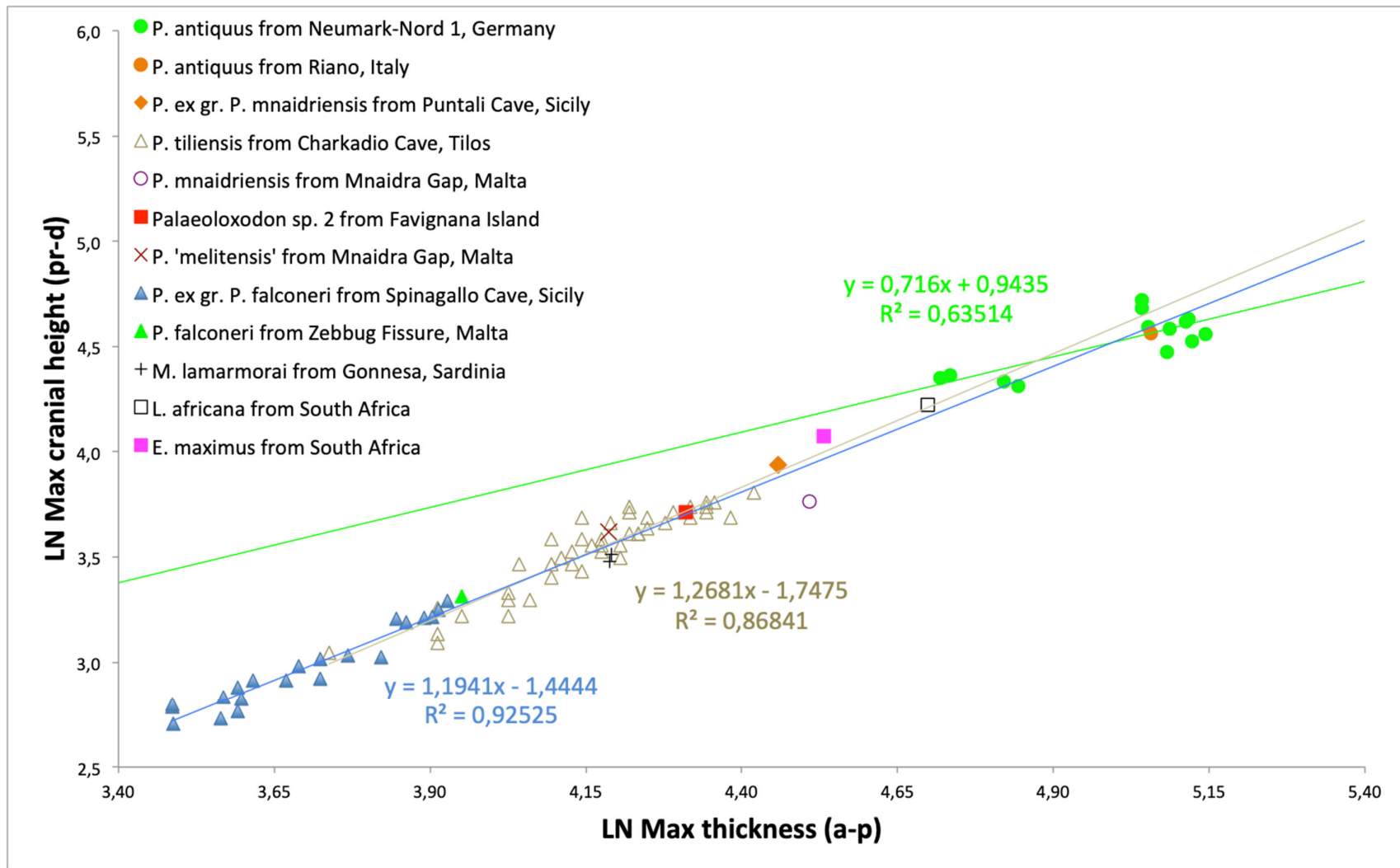


Fig. 3.13 Scatterplot of the os c. III cranial height (pr-d) vs. max thickness (a-p). [Data: *P. tiliensis* from Theodorou, 1983: 207, *P. antiquus* from Palombo *et al.*, unpublished].

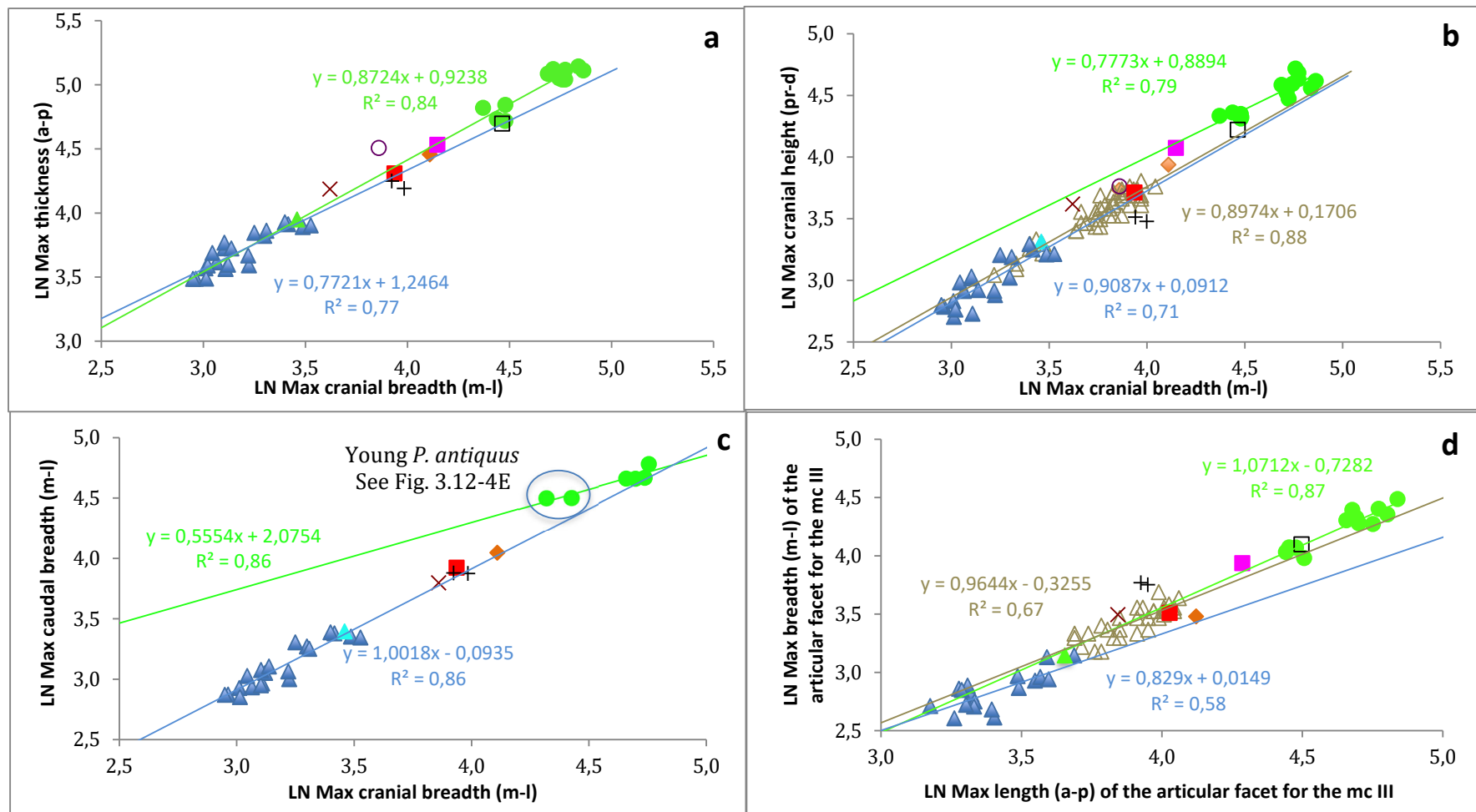


Fig. 3.14 Scatterplots of the dimensions of the os c. III. a) Max cranial breadth (m-l) vs. max thickness (a-p). b) Max cranial breadth (m-l) vs. max cranial height (pr-d). c) Max cranial breadth (m-l) vs. max caudal breadth (m-l). d) Max length (a-p) vs. max breadth (m-l) of the articular facet for the mc III. Refer to Fig. 3.3 for symbol legend. [Data for Figs b, d: *P. tiliensis* from Theodorou, 1983: 207, *P. antiquus* from Palombo *et al.*, unpublished excepting Fig. 3.14c].

	Max thickness (a-p) /cranial breadth (m-l)	Max thickness (a-p)/ cranial height (pr-d)	Art. f. for mc III: max length (a-p)/ max breadth (m-l)	Cranial breadth (m-l)/ cranial height (pr-d)	Cranial breadth (m-l)/ caudal breadth (m-l)
<i>P. antiquus</i> vs. <i>P. tiliensis</i>	-	0,000*	0,010*	0,005*	-
<i>P. antiquus</i> vs. <i>P. ex gr. P. falconeri</i>	0,000*	0,000*	0,000*	0,129	0,009*
<i>P. ex gr. P. falconeri</i> vs. <i>P. tiliensis</i>	-	0,000*	0,002*	0,484	-

Table 3.5 Mann-Whitney U-test pairwise comparison in the os c. III. Statistically significant p-values are indicated with an asterisk (*).

morphology of the articular facet for the intermediate carpal. (vii) The morphology of the articular facets for the os c. II and os c. IV.

In terms of allometry, differences were compared in terms of (i) Ratio of max thickness (a-p)/max cranial breadth (m-l) - The cranial breadth varies considerably, being wide in *M. lamarmorai* relative to *P. ex gr. P. falconeri*, and narrow in *P. mnaidriensis* from Mnaidra Gap, Malta (Fig. 3.14a). With regard to *P. mnaidriensis* however, it is possible that the single specimen (which displays signs of abrasion) was more damaged than was realized, and that its narrow breadth is partly explained by damage (see Fig. 3.12-2). Differences are statistically significant between *P. antiquus* and *P. ex gr. P. falconeri*, which is relatively less thick (a-p) (Fig. 3.14a; MWU $p < 0,000$). (ii) Ratio max length (a-p)/max breadth (m-l) of the articular facet for the mc III - Differences between species are statistically significantly different, being broader in *P. antiquus* than in *P. ex gr. P. falconeri* (Fig. 3.14d; MWU $p < 0,000$) and than *P. ex gr. P. mnaidriensis* (Fig. 3.14d). *M. lamarmorai* is notable for possessing a broad articular facet for the mc III compared with all other *Palaeoloxodon* spp. (Fig. 3.14d). There are also significant differences between *P. antiquus* and *P. tiliensis* (Fig. 3.14d; MWU $p=0,011$), and *P. ex gr. P. falconeri* and *P. tiliensis* (MWU $p=0,002$).

(iii) Ratio of max cranial breadth (m-l)/max caudal breadth (m-l) in relation to ontogenetic allometry - Seen in superior aspect, the os c. III is widest anteriorly in *M. lamarmorai* (Fig. 3.12-6E) and *P. ex gr. P. mnaidriensis* (Fig. 3.12-3E), whereas the bone tends to be widest posteriorly in *P. ex gr. P. falconeri* (Fig. 3.12-1E) and *P. antiquus* (Fig. 3.12-4E; Fig. 3.12-5E). Viewed in dorsal aspect, in young *P. antiquus* () the caudal breadth is noticeably wider than in adult *P. antiquus* (contrast Fig. 3.12-4E with Fig. 3.12-5E; see annotation in Fig. 3.14c). Similarly, the bone widens noticeably in the caudal region of juvenile *L. africana*, suggesting that a wide caudal breadth is related to ontogenetic allometry in these two species. Differences are also statistically significant between *P. antiquus* and *P. ex gr. P. falconeri* (Fig. 3.14; MWU $p=0,009$), indicating a tendency towards a greater cranial breadth in *P. ex gr. P. falconeri*. (iv) Inclination of the articular facet for the os c. II in caudal and cranial aspects - Likely associated with the expanded caudal breadth (m-l) in young *P. antiquus* (Fig. 3.12-4E) is a change in the inclination of the articular facet for the os c. II, which is more obtuse (clockwise from vertical) in young *P. antiquus* (Fig. 3.12-4A; Fig. 3.12-4B) and more acute (clockwise from vertical) in adult *P. antiquus* (Fig. 3.12-5A; Fig. 3.12-5B). The inclination is also slightly obtuse in the figured *P. ex gr. P. falconeri* (Fig. 3.12-1B) and *P. ex*

Ratio max thickness (a-p)/max cranial breadth (m-l)	Ratio max length (a-p)/max breadth (m-l) of articular facet for the mc III	Ratio max cranial breadth (m-l)/max caudal breadth (m-l)	Ratio max cranial height (pr-d)/max thickness (a-p)	Morphology of articular facet for intermediate carpal	Separation between articular facets for os c. II and os c. IV
Cranial breadth is wide in <i>M. lamarmorai</i> relative to <i>P. ex gr. P. falconeri</i> . Differences are statistically significant between <i>P. antiquus</i> and <i>P. ex gr. P. falconeri</i> , which is relatively less thick (a-p).	Broader in <i>P. antiquus</i> than in <i>P. ex gr. P. falconeri</i> and <i>P. ex gr. P. mnaidriensis</i> . <i>M. lamarmorai</i> is notable in possessing a wide articular facet for the mc III.	Widest anteriorly in <i>M. lamarmorai</i> and <i>P. ex gr. P. mnaidriensis</i> , whereas tends to be widest posteriorly in <i>P. ex gr. P. falconeri</i> and <i>P. antiquus</i> . Differences are statistically significant between <i>P. antiquus</i> and <i>P. ex gr. P. falconeri</i> , indicating tendency towards greater caudal breadth in <i>P. antiquus</i> .	Taller in <i>P. antiquus</i> than the other Elephantinae species.	Single specimens belonging to <i>M. lamarmorai</i> and <i>P. ex gr. P. mnaidriensis</i> have a less saddle-shaped articular facet for the intermediate carpal than the other species.	Facet for os c. II (situated proximally) separated from facet for mc IV (situated distally) by rough groove in the figured <i>P. antiquus</i> , contrasting with continuous articular facet in the figured <i>P. ex gr. P. falconeri</i> , <i>P. ex gr. P. mnaidriensis</i> , and likely also <i>M. lamarmorai</i> .

Table 3.6 Interspecific morphological differences in the os c. III. Refer to Fig. 3.12 for photographic illustrations and Figs 3.13-3.14 for bivariate scatterplots.

gr. *P. mnaidriensis* (Fig. 3.12-3B; Fig. 3.12-3A) relative to the figured adult *P. antiquus* (Fig. 3.12-5B). v) Ratio of the max cranial height (pr-d)/max thickness (a-p) - There are several differences between species in this regard, most notably in *P. antiquus* from Neumark-Nord 1 which has a tendency to be taller than the other Elephantinae species (Fig. 3.13). Differences between *P. ex gr. P. falconeri* and *P. antiquus* are statistically significant (MWU p <0,000), and statistically significant between *P. tiliensis* and *P. antiquus* (MWU p <0,000). Differences between *P. ex gr. P. falconeri* and *P. tiliensis* are also statistically significant (MWU p <0,000). *P. antiquus* also displays considerable allometric variability, perhaps partly relating to ontogeny. (vi) The morphology of the articular facet for the intermediate carpal - The single specimens belonging to *M. lamarmorai* (Fig. 3.12-6C) and *P. ex gr. P. mnaidriensis* (Fig. 3.12-3C) have a less saddle-shaped articular facet for the intermediate carpal than the other species (Fig. 3.12-C), also suggesting a less curved distal articular surface in the intermediate carpal of these two species.

(vii) The morphology of the articular facets for the os c. II and os c. IV - Viewed laterally, there are also differences in the morphology of the articular facets (Fig. 3.12-D). The articular facet for the os c. II (situated proximally) is separated from the articular facet for the mc IV (situated distally) by a rough groove in the figured *P. antiquus* (Fig. 3.12-4D, Fig. 3.12-5D), contrasting with the continuous articular facet between the os c. II and os c. IV in the figured *P. ex gr. P. falconeri* (Fig. 3.12-1D), *P. ex gr. P. mnaidriensis* (Fig. 3.12-3D), and likely also *M. lamarmorai* (Fig. 3.12-6D). In the figured *P. mnaidriensis* specimen from Malta there may also have been a continuous facet although abrasion makes it difficult to be certain (Fig. 3.12-2D). These differences in articular facets also suggest that there may have been differences in the tendons joining the os c. II and os c. III: a) In the figured *P. ex gr. P. falconeri* there are likely to have been two tendons joining the os c. II and os c. III (one situated cranially, the other caudally), whereas in b) the figured *P. ex gr. P. mnaidriensis* there was likely only one tendon situated caudally. It is still important to consider that intraspecifically the morphology of the lateral articular facets for the os c. II and os c. IV are highly variable within *P. tiliensis* (Theodorou, 1983: Fig. 21), so that it is at present difficult to know if variability in the articular facets for the os c. II and os c. IV reflects *bona fide* interspecific variation or intraspecific variability within *Palaeoloxodon* species.

Possible autapomorphies of the os. III - Species displaying statistically significant differences in allometry, particularly those with larger sample-sizes (*P. antiquus*, *P. tiliensis* and *P. ex gr. P. falconeri*) may include autapomorphies. These (possibly autapomorphic) differences include the ratio of the max thickness (a-p)/cranial height (pr-d), which has highly significant statistical differences between species (Table 3.5). Also the allometry of the articular facet for the mc III appears to differ significantly between species (Table 3.5), and might possibly be an autapomorphic feature in insular dwarfs.

3.1.5 Astragalus

The astragalus is the most proximal tarsal of the hindfoot (Fig. 3.2) and is proximodorsally convex for articulation with the tibia (Fig. 3.15-A), and flat plantarly for articulation with the calcaneus via two articular facets separated by a rough fossa for the calcaneo-astragaloid ligament (Fig. 3.15-C). Distally a convex facet occurs for articulation with the central tarsal (Fig. 3.2; Fig. 3.15-A), and laterally there is a small facet for articulation with the fibula (Smuts and Bezuidenhout, 1994: 59).

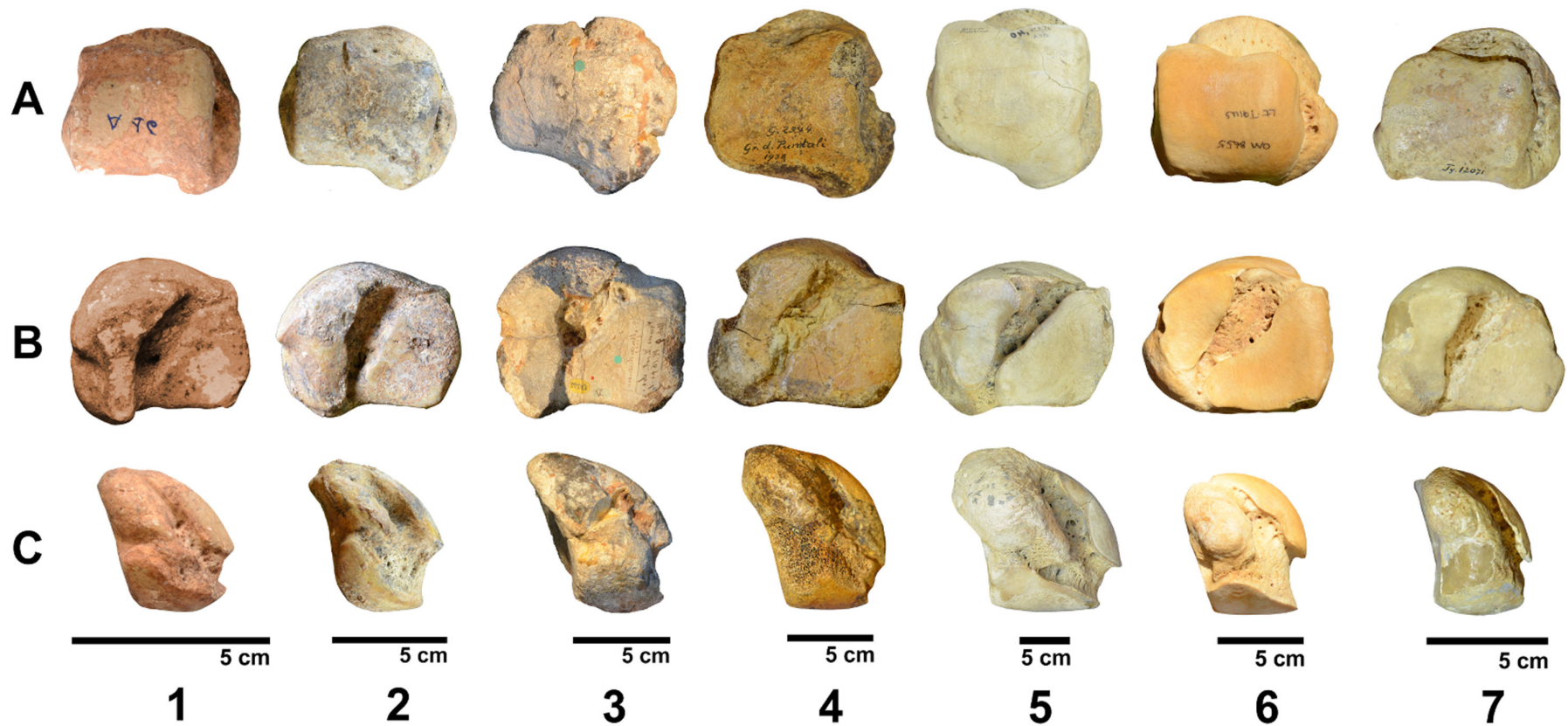


Fig. 3.15 Astragalus of 1) *P. ex gr. P. falconeri* from Spinagallo Cave, Sicily (MPRU)^{dex}. 2) *Palaeoloxodon* sp. 1 from Luparello Fissure, Sicily (IPH)^{sin}. 3) *Palaeoloxodon* sp. from Bnghisa Gap, Malta (NHMUK-44453)^{dex}. 4) *P. ex gr. P. mnaidriensis* from Puntali Cave, Sicily (NHMB-G2344)^{sin}. 5) *P. antiquus* from Neumark-Nord 1, Germany (LVH-NN-E15.1.96 and 2007: 25.280,40)^{dex}. 6) *M. lamarmorai* from Gonnese, Sardinia (NHMB-Tyi207i)^{sin}. 7) *L. africana* from Kenya (KNM-8655)^{sin}. A) lateral B) dorsal and C) plantar aspects.

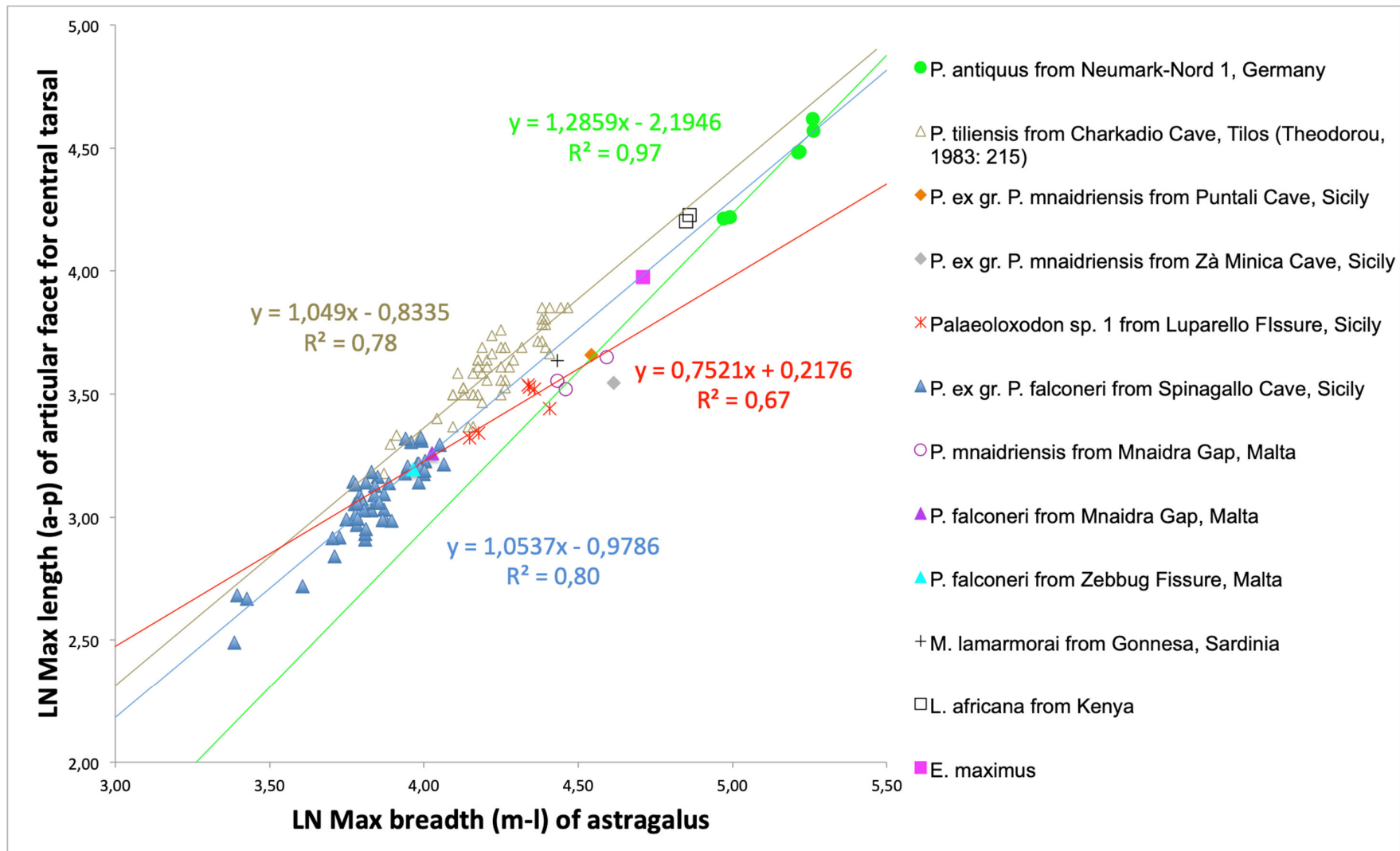


Fig. 3.16 Scatterplot of the dimensions of the astragalus including *P. antiquus*.

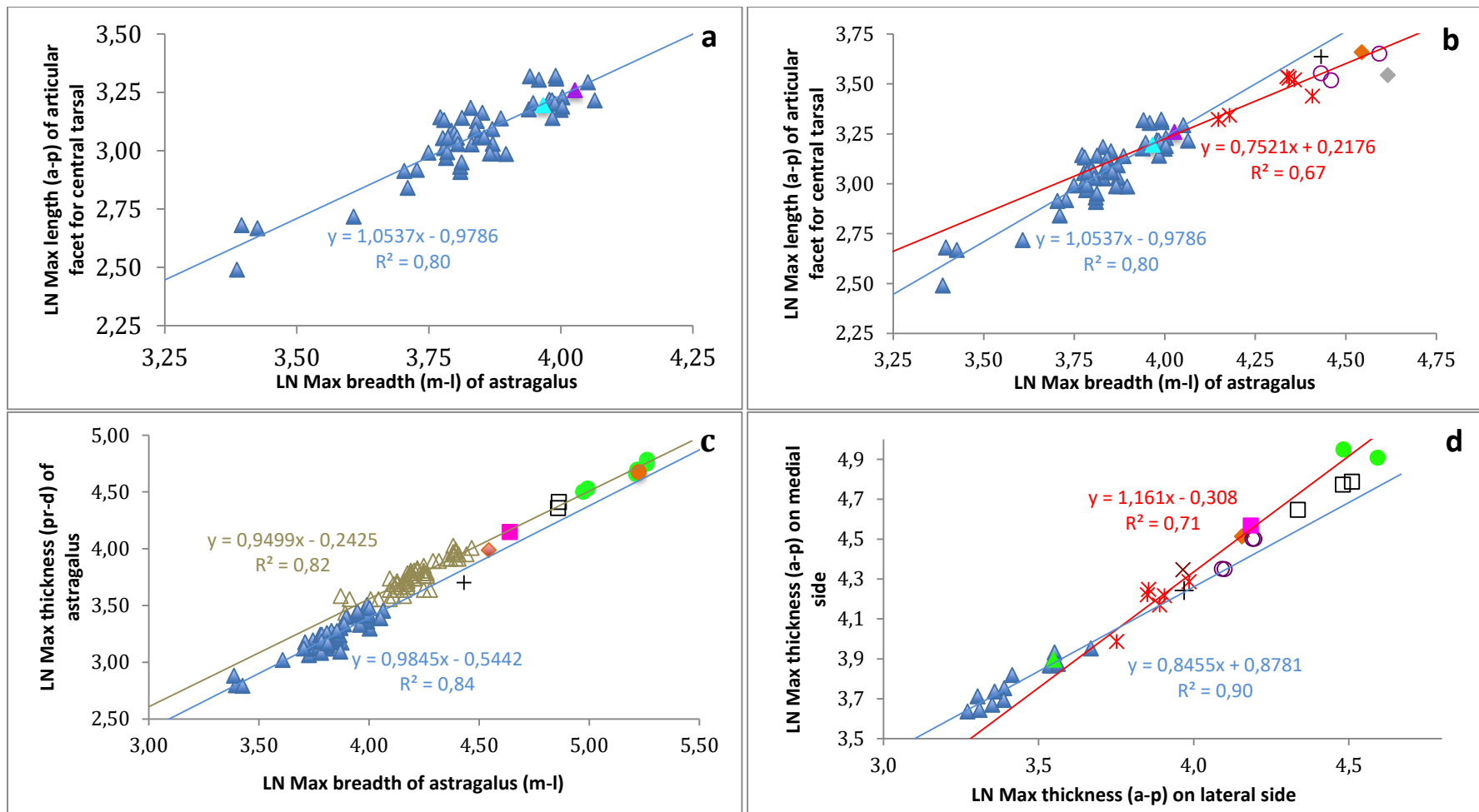


Fig. 3.17 Scatterplots of the dimensions of the astragalus. a) Max breadth (m-l) vs. max length of articular facet for the central tarsal in *P. ex gr. P. falconeri* from Sicily and Malta b) Max breadth (m-l) vs. max length of articular facet for the central tarsal in insular dwarfs c) Max breadth (m-l) vs. max thickness (pr-d). d) Max length (a-p) on lateral side vs. max length (a-p) on medial side. Refer to Fig. 3.3 for symbol legend. [Data: *P. tiliensis* from Theodorou, 1983: 215].

Compared with other quadrupedal mammals, the astragalus is medio-laterally wide, and rotation of the hindfoot is reduced due to the flatter articulation between the astragalus–tibia (Paul, 2009: 152; see also Bonnan, 2005; Hutchinson *et al.*, 2011). This contrasts with the roller-type joint typical of non-proboscidean mammals where lower body mass permits a greater range of movement.

In the sample studied, intra- and inter-specific ranges in the dimensions of the astragalus have a nearly overlapping distribution (Fig. 3.16; Fig. 3.17), so that changes in morphology may be investigated across a nearly continuous range in body mass. The sample also includes ontogenetic and sexual variation, particularly for the large sample of *P. ex gr. P. falconeri* from Spinagallo Cave (Fig. 3.17a; see also Ambrosetti, 1968: 321-327). In comparing species, the most conspicuous morphological differences are seen in (i) the size of the articular facet for the central tarsal. (ii) The angle formed between the central tarsal and calcaneal facets of the astragalus varies between species, suggesting there are also differences in the posture of the toes. (iii) Furthermore, there is also variation in the size of the astragalus' lateral articular facet for the calcaneus.

(i) Ratio max breadth (m-l) of astragalus/length (a-p) of articular facet for the central tarsal - Large interspecific differences exist, and the facet for the central tarsal is generally narrower in the dwarf species in the antero-posterior direction than in *P. antiquus* (Fig. 3.15-5A; Fig. 3.16). Pairwise comparisons are significant for *P. antiquus* vs. *P. mnaidriensis* (MWU $p=0,024$), and *P. antiquus* vs. *P. tiliensis* (MWU $p=0,005$) and *P. antiquus* vs. *Palaeoloxodon* sp. 1 from Luparello Fissure (MWU $p=0,002$) and *P. ex gr. P. falconeri* vs. *P. tiliensis* (MWU $p=0,000$) and *P. ex gr. P. falconeri* vs. *Palaeoloxodon* sp. 1 (MWU $p=0,025$). The articular facet also has a tendency to be thicker in *P. tiliensis* than in similar-sized Sicilian and Maltese *Palaeoloxodon* spp. (Fig. 3.16). Differences are however not statistically significant for *P. antiquus* vs. *P. ex gr. P. falconeri* (MWU $p=0,094$).

(ii) Ratio max breadth (m-l) of astragalus/max thickness (pr-d) - Similar to interspecific allometry in the size of the articular facet for the central tarsal is the max thickness of the bone (Fig. 3.17c), which is significantly thicker in *P. antiquus* than in *P. tiliensis* (MWU $p=0,008$) and *P. antiquus* than *P. ex gr. P. falconeri* (MWU $p=0,000$). Differences are also significant between *P. tiliensis* and *P. ex gr. P. falconeri* (MWU $p=0,000$).

(iii) The angle between the central tarsal and calcaneal facets of the astragalus - This varies between species,

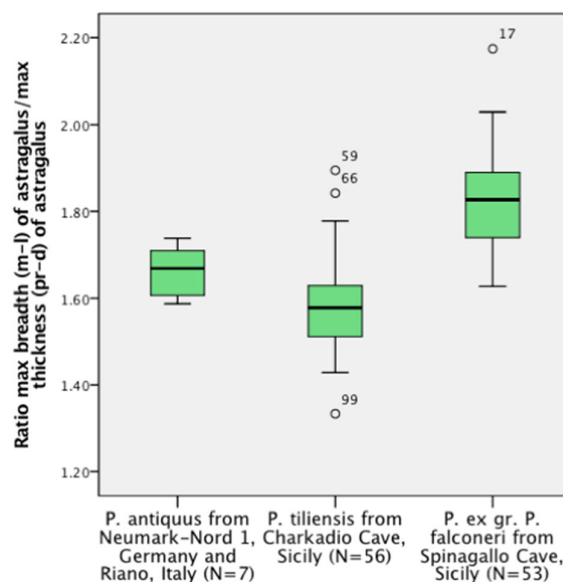


Fig. 3.18 Box-and-whisker plot of the ratio of the astragalus max breadth (m-l)/ max thickness (pr-d).

suggesting there are also differences in the posture of the toes: a more obtuse angle such as in *Palaeoloxodon* sp. from Benghisa Gap, Malta (Fig. 3.15-3A) suggests a more digitigrade posture (more tip-toed), and a more acute angle as in *Palaeoloxodon* sp. 1 from Luparello Fissure, Sicily (Fig. 3.15-2A) suggests a more semi-plantigrade posture (more flat-footed toes) (cf. Maccagno, 1962a: 115).

iv) The astragalus' lateral articular facet for the calcaneus - There is also variation in the size of the astragalus' lateral articular facet for the calcaneus, suggesting that body mass is supported to a greater or lesser degree on the lateral side of the hindfoot by different morphotypes/species. In *P. antiquus* from Neumark-Nord 1, Germany and Riano, Italy the lateral articular facet for the calcaneus tends to be small and have a convex edge, as seen in plantar aspect (e.g. Fig. 3.15-5C). In other *Palaeoloxodon* spp. the astragalus' lateral articular facet for the calcaneus is more expanded, and has a more triangular shape, including in Sicilian *P. cf. antiquus* (from Zà Minica Cave (GMP-ZM72, see Fabiani, 1932b), and Miniera Tabuna, Ragusa (GMP-TB166), *Palaeoloxodon* sp. from Benghisa Gap, Malta (Fig. 3.15-3C) and *P. ex gr. P. mnaidriensis* from Puntali Cave, Sicily (Fig. 3.15-4C), although the sample-size is much smaller in these two insular species (Table 2.7). Although less triangular-shaped, an expanded articular facet is also seen in *P. ex gr. P. falconeri* (Fig. 3.15-1C). A greatly expanded articular facet is seen in *M. lamarmorai* from Sardinia (Fig. 3.15-6C) compared with either of its putative ancestral species, as seen in *M. meridionalis* from Italy (Maccagno, 1962b), *M. trogontherii* from Greece (Athanassiou, 2012: Fig. 18f), England (Lister and Stuart, 2010: Fig. 7b) and China (Tong, 2012: Fig. 6-G2; Chen and Tong, 2017: Fig. 1). The *M. lamarmorai* articular facet is also far more expanded than in all other Elephantinae species compared in this thesis (Fig. 3.15-B), suggesting an expanded articular facet may be autapomorphic in *M. lamarmorai*. Nonetheless, it should be borne in mind the fossil record of *M. lamarmorai* includes only one astragalus belonging to the holotype, so that the amount of species variability is unknown.

3.1.6 Calcaneus

The calcaneus bone is positioned beneath the astragalus (Fig. 3.2) and articulates with the astragalus via a small medial and larger lateral facet, which are separated by a depression (Fig. 3.21-C; Fig. 3.27; Smuts and Bezuidenhout, 1994: 9-60). Distally to the smaller medial facet, and at an angle to it, there is a small, flat facet for the central tarsal. A large, and sometimes slightly concave facet on the distal aspect is for articulation with the os t. IV. Laterally the calcaneus has a convex articular facet for the fibula (Fig. 3.20; Fig. 3.21), and in some species there is also an articular facet for the tibia (Fig. 3.21-A), forming an angle with the lateral articular facet for the astragalus (Fig. 3.20; Fig. 3.21-B). The calcaneal articular facet for the fibula constrains medio-lateral motion during locomotion (or during any joint motion), and the presence and size of the articular facet for the tibia regulates motion in the sagittal plane, likely having a significant influence on the range of antero-posterior mobility during locomotion. The calcaneus also has a prominent tuber for the attachment of tendons and muscles, which is smooth proximally but expanded and rugose distally. Between species differences in the calcaneus include (i) the proportions of the lateral articular facet for the

astragalus, (ii) the relative size and morphology of the articular facet for the fibula. (iii) The presence/absence of the articular facet for the tibia; (iv) The length vs. breadth of the distal end of the tuber; (v) The degree of separation between the fibular and tibial facets (where the latter is present).

(i) The proportions of the lateral articular facet for the astragalus - Between the species studied, the proportion of the length/breadth of the lateral articular facet for the astragalus on the calcaneus (see Fig. 3.21-C) approximates isometry (Fig. 3.22c), although small differences between species may be identified using a linear regression model. Pairwise comparisons are not statistically significant between *P. antiquus* vs. *P. ex gr. P. mnaidriensis* (MWU $p=0,667$), *P. antiquus* vs. *P. tiliensis* (MWU $p=0,240$), and *P. antiquus* vs. *Palaeoloxodon* sp. 1 (MWU $p=0,648$), *P. ex gr. P. falconeri* vs. *P. ex gr. P. mnaidriensis* (MWU $p=0,081$), *P. ex gr. P. falconeri* vs. *Palaeoloxodon* sp. 1 (MWU $p=0,886$). In contrast, there are significant differences between *P. antiquus* vs. *P. ex gr. P. falconeri* (MWU $p=0,025$), and *P. tiliensis* vs. *P. ex gr. P. falconeri* (MWU $p=0,000$).

(ii) The relative size and morphology of the articular facet for the fibula - The ratio of the breadth of the fibular facet/length of the distal end of the calcaneal tuber indicates the fibular facet is significantly wider in *P. ex gr. P. falconeri* from Spinagallo Cave than in *P. antiquus*

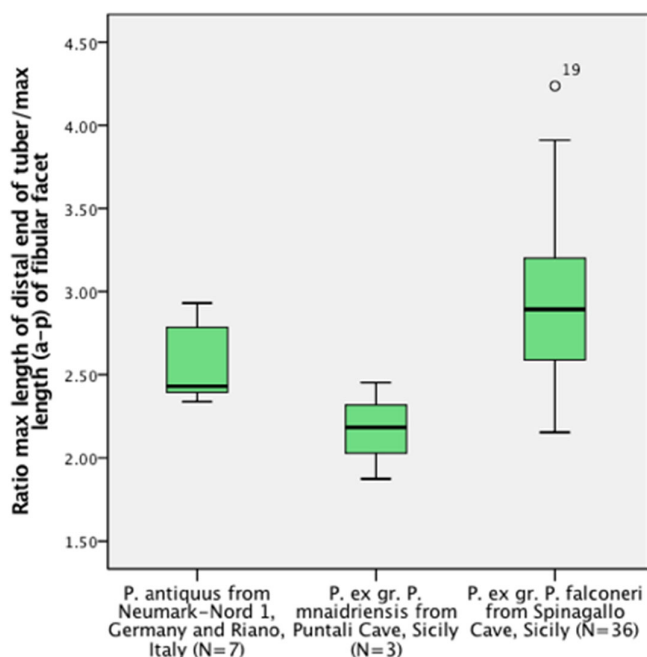


Fig. 3.19 Box-and-whisker plot of the calcaneus' ratio of the max length of distal end of tuber/max length (a-p) of fibular facet.

(MWU $p=0,038$), whereas there is no significant difference between *P. ex gr. P. mnaidriensis* from Puntali Cave and *P. antiquus* (MWU $p=0,183$). However there are only three observations for *P. ex gr. P. mnaidriensis*, and the available evidence suggests the fibular facet was relatively wide in this species (Fig. 3.22d). In contrast to the likely increased range in (antero-posterior) flexion in the *P. ex gr. P. falconeri* hindfoot suggested by the large tibial facet, the medio-lateral displacement of the astragalus-calcaneus was likely restricted by synostosis of the distal tibia-fibula (see Ambrosetti, 1968: 316) and the wide fibular facet in this species. In contrast to *P. antiquus*, in *P. ex gr.*

P. falconeri the fibular facet is usually discernible as two facets oriented in slightly different directions (labelled 'b' and 'c' in Fig. 3.20), with an angle of up to ca. 100 degrees between the facets, although the angle and distinctiveness between the two facets is variable. These two fibular facets are here termed the *superior fibular facet*, which slopes downwards in the medio-lateral direction (Fig. 3.20-b) and the *inferior fibular facet*, on the lateral side, which

slopes latero-medially (Fig. 3.20-c). The allometry of the fibular facet is also significantly different between *P. ex gr. P. mnaidriensis* and *P. ex gr. P. falconeri* (Fig. 3.19, MWU $p=0,007$), bearing in mind the small sample-size for *P. ex gr. P. mnaidriensis*. With regard to the fibular facet of the single *M. lamarmorai* calcaneus specimen, this is very narrow (Fig. 3.21-8B), vertically orientated, and only slightly convex (contrast Fig. 3.21-8C with Fig. 3.21-1C). These features contrast with the remaining *Palaeoloxodon* spp. (Fig. 3.21) and presumably also *M. trogontherii* (see Plate 11 Fig 3 in Shpansky *et al.*, 2015) suggesting that little body mass was transmitted via the *M. lamarmorai* fibula as compared to the other species.

3.1.6.1 Variation in the presence/absence of the tibial facet

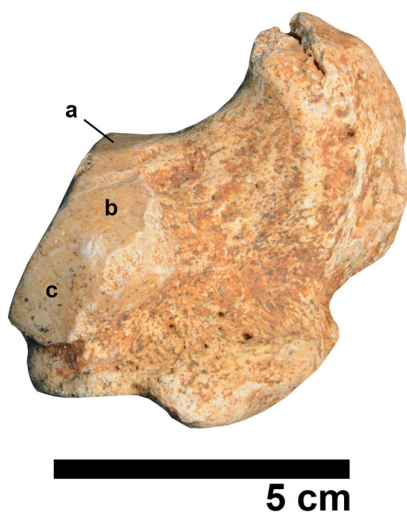


Fig. 3.20 Calcaneus of *P. ex gr. P. falconeri* from Spinagallo Cave, Sicily in lateral aspect. a) tibial facet b) Superior fibular facet and c) Inferior fibular facet (NHMB-Ty12582)^{dex}.

(iii) There is striking variation in the presence/absence of the articular facet for the tibia on the calcaneus and in its dimensions where present (Fig. 3.21-A; Fig. 3.24; Fig. 3.25; Table 3.8). *P. ex gr. P. falconeri* always possesses a more-or-less continuous tibio-fibular facet (Fig. 3.21-1A; Fig. 3.24b; Fig. 3.25; Fig. 3.26), unlike the *P. antiquus* specimens studied from Neumark-Nord 1 which lack an articular facet for the tibia. In comparison to the proportionally large tibial facet on the *P. ex gr. P. falconeri* calcaneus, the *L. africana* sample from Kenya evidences a proportionally small articular facet for the tibia (Fig. 3.24a; Fig. 3.24c), with no overlap in the ratio of the tibial facet length/distal tuber length between the two species (MWU $p<0,0001$). In '*P. melitensis*' from from Benghisa Gap, Malta there is no clearly discernible articular facet for the tibia (Fig. 3.21-4A; Adams, 1874: Pl. XVI-Fig. 5),

although the articular facet for the fibula tapers much farther towards the medial side of the calcaneus than in *P. antiquus* (presumably without articulating with the tibia). This contrasts with similar-sized *Palaeoloxodon* sp. 1 from Luparello Fissure, Sicily in which the tibial facet is always present. In *Palaeoloxodon* sp. 1 from Luparello Fissure and *P. ex gr. P. falconeri* the ability of the tibia to articulate with the calcaneus is likely attributable to three factors: a) The astragalus is more proximo-distally compressed in *Palaeoloxodon* sp. 1 (Fig. 3.15-2C; Fig. 3.16; Fig. 3.17b) and in *P. ex gr. P. falconeri* (Fig. 3.15-1C; Fig. 3.16); b) The caudal side of the *Cochlea tibia* may sometimes extend more distally (Fig. 4.39a) than in *P. antiquus* (Fig. 4.35d), or c) a greater range in flexion of the ankle-joint. iv) Ratio length/breadth of the distal end of the tuber - Differences are statistically significant between *P. antiquus* vs. *P. ex gr. P. falconeri* ($p=0,000$), indicating that the distal end is relatively longer in *P. antiquus* (Fig. 3.22b). Differences are not statistically significant between *P. ex gr. P. mnaidriensis* and *P. ex gr. P. falconeri* ($p=0,058$), though sample-size is small for the former.

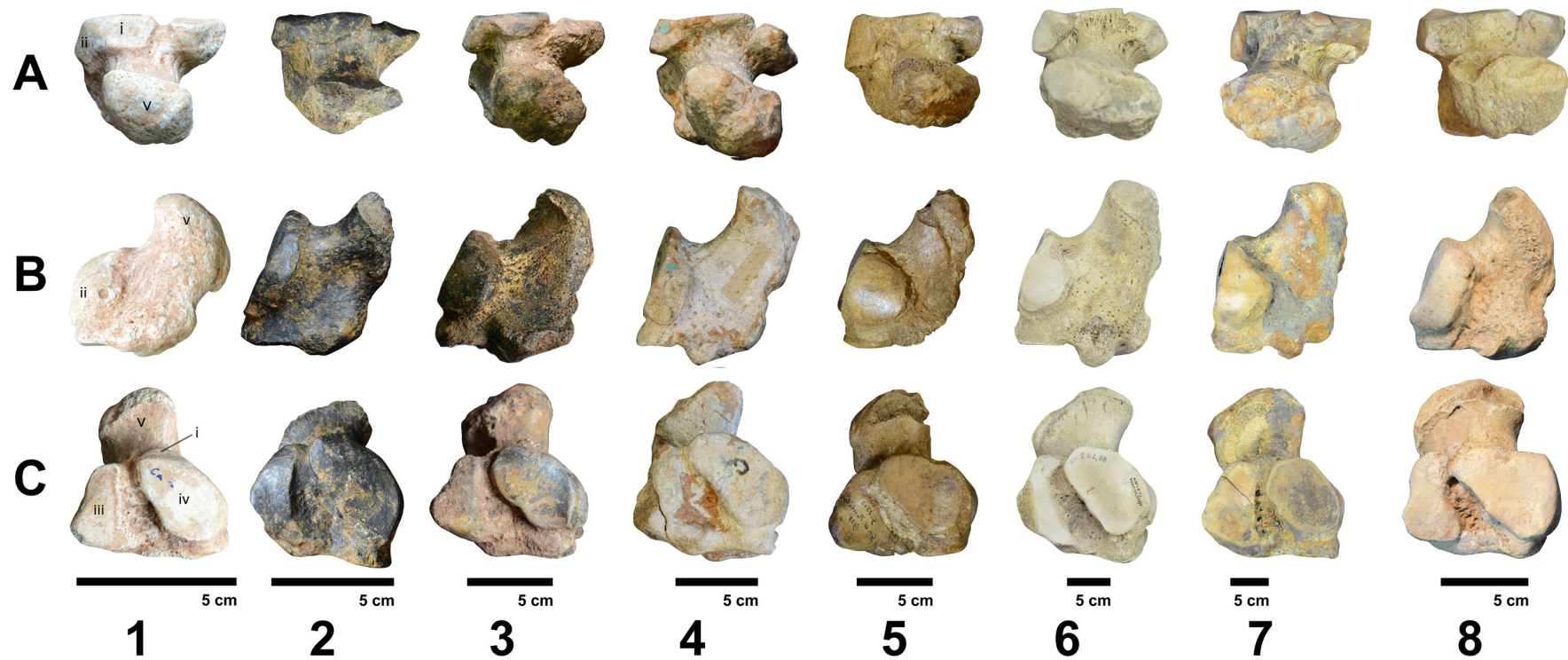


Fig. 3.21 Calcaneus of *Palaeoloxodon* spp. and *M. lamarmorai*. A) superior B) lateral and C) frontal aspects. 1) *P. ex gr. P. falconeri* from Spinagallo Cave, Sicily (MPRU)^{sin}. 2) *Palaeoloxodon* sp. 1 from Luparello Fissure (IPH-2961)^{sin}. 3) *Palaeoloxodon* sp. 1 from Luparello Fissure, Sicily (GMP-GL103)^{sin}. 4) *Palaeoloxodon* sp. from Benghisa Gap, Malta (NHMUK-44451)^{dex}. 5) *P. ex gr. P. mnaidriensis* from Puntali Cave, Sicily (NHMB-G2343)^{dex}. 6) Young *P. antiquus* from Neumark-Nord 1, Germany (LVH-NN-E22 and 2007: 25,277,58)^{sin}. 7) *P. antiquus* from Neumark-Nord 1, Germany (LVH-NN-E10 and 2007: 25.272,85)^{dex}. 8) *M. lamarmorai* from Gonnesa, Sardinia (NHMB-Tyi207i)^{sin} Anatomical features: (i) tibial facet (ii) fibular facet (iii) medial facet for astragalus (iv) lateral facet for astragalus (v) tuber.

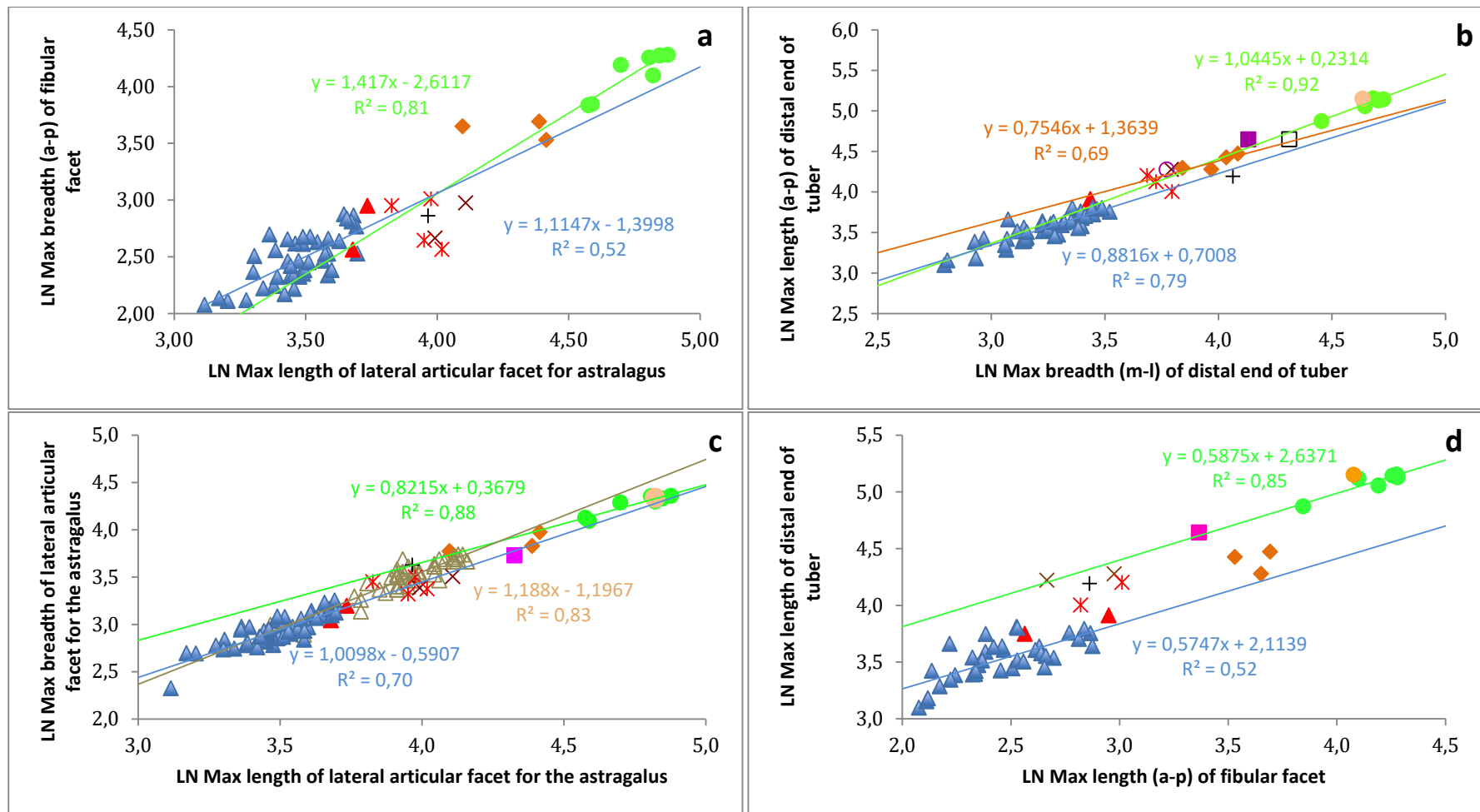


Fig. 3.22 Scatterplots of the dimensions of the calcaneus. a) Max length of lateral articular facet for astragalus vs. max articular breadth of the fibular facet. b) Max breadth vs. max length of the distal end of tuber. c) Max length vs. max breadth of the lateral articular facet for the astragalus. d) Max breadth (a-p) of fibular facet vs. max breadth of distal end of tuber. Refer to Fig. 3.3 for symbol legend. [Data: *P. tiliensis* from Theodorou, 1983: 214]

or between *Palaeoloxodon* sp. 1 and *P. ex gr. P. falconeri* ($p=0,437$). In *M. lamarmorai* the distal end of the tuber is also wide (contrast Fig. 3.21-1C with Fig. 3.21-8C) and does not project as far as in *Palaeoloxodon* spp., particularly in comparison to *P. ex gr. P. falconeri* (Fig. 3.21-1B).

3.1.6.2 PCA of the *Palaeoloxodon* spp. calcaneus

In order to investigate the possible existence of patterns underlying the data between different species Principal Components Analysis was carried out. Principal Component 1 accounts for most of the variation (88%, see Table 3.7a), and describes the amount of shape variation that may be explained by size. The output also indicates there are two distinct clusters (belonging to *P. ex gr. P. falconeri* from Sicily and *P. antiquus* from Neumark-Nord 1, Germany), with one outlier belonging to *P. antiquus* from Riano (the only specimen with a tibial facet, Fig. 3.23a). One variable (the max length of the tibial facet) is perpendicular to the other variables, indicating it is independent of these.

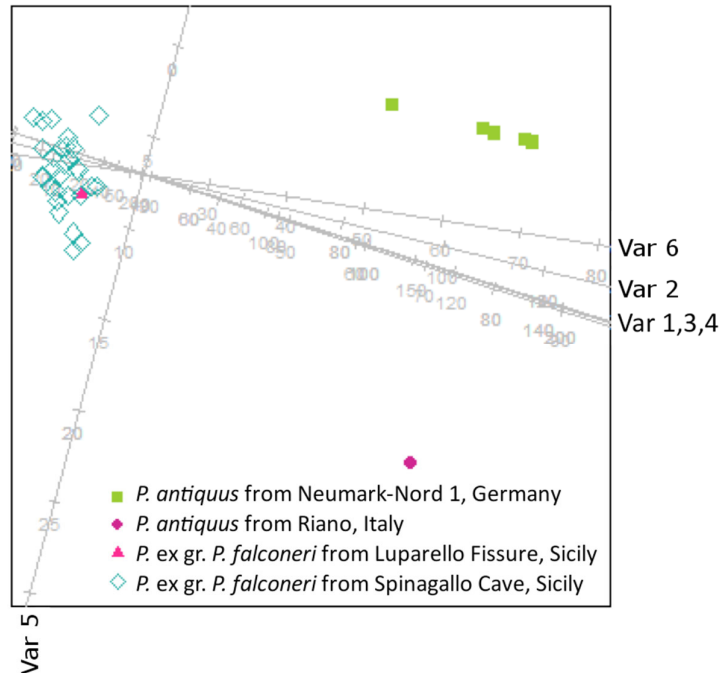


Fig. 3.23a Principal Component Analysis of the calcaneus. Refer to Table 3.7a for axes variable labels and component loading.

Importance of components:	PC1	PC2	PC3	PC4	PC5	PC6
Standard deviation	2.30	0.83	0.10	0.07	0.05	0.05
Proportion of Variance	0.88	0.11	0.00	0.00	0.00	0.00
Cumulative Proportion	0.88	1.00	1.00	1.00	1.00	1.00
Rotation:						
Var 1 - Max length of distal end of tuber	0.43	-0.14	0.35	-0.44	0.03	0.69
Var 2 - Max breadth of distal end of tuber	0.43	-0.10	0.08	-0.43	-0.51	-0.59
Var 3 - Max length of lateral art. facet for astragalus	0.43	-0.14	0.35	0.78	-0.26	0.04
Var 4 - Max breadth of lateral art. facet for astragalus	0.43	-0.14	0.06	0.00	0.81	-0.36
Var 5 - Max length (a-p) of tibial facet	-0.26	-0.96	-0.06	-0.01	-0.02	0.00
Var 6 - Max length (a-p) of fibular facet	0.43	-0.07	-0.86	0.09	-0.08	0.22

Table 3.7a Principal Component Analysis output for the calcaneus (see Fig. 3.23a).

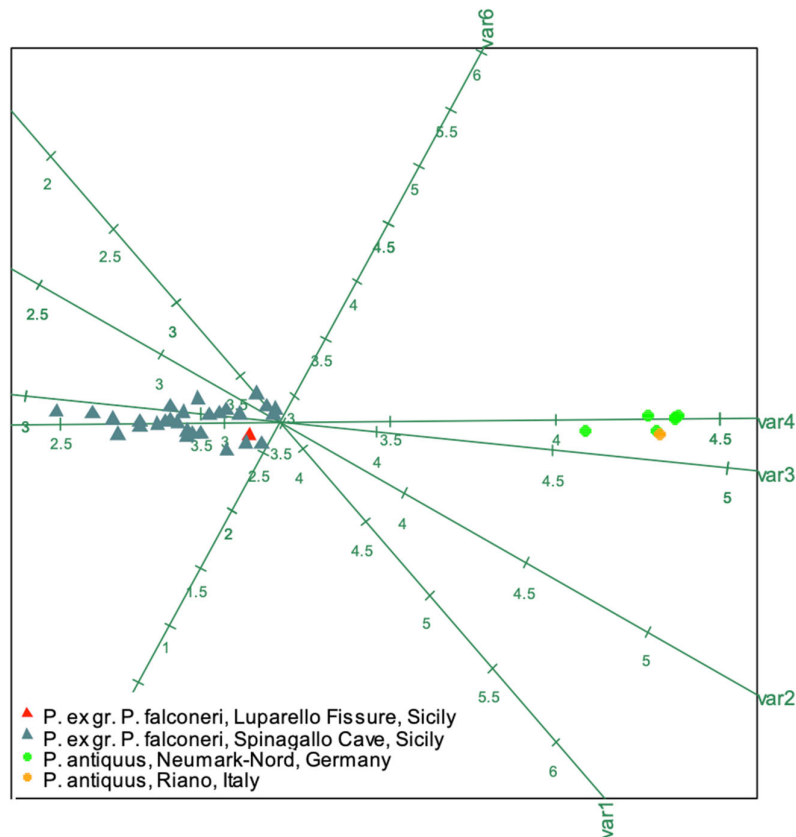
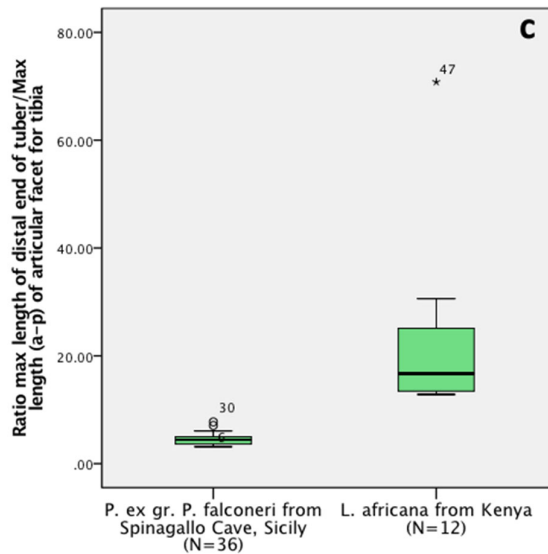
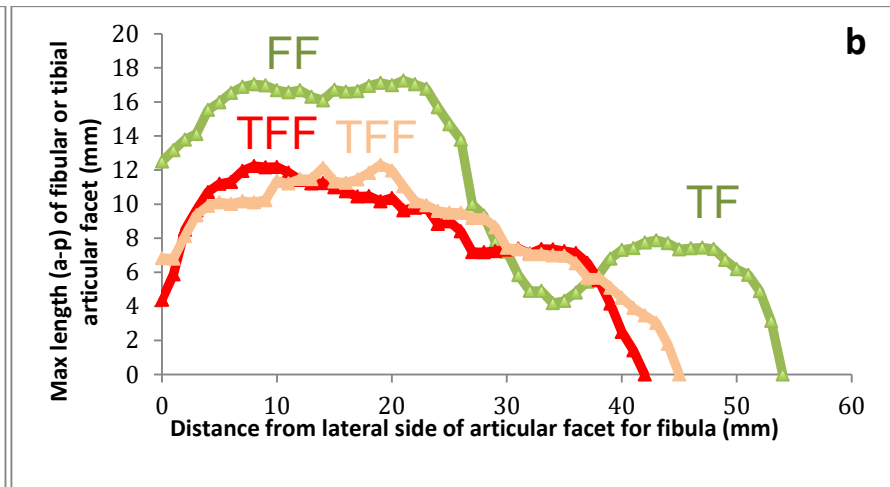
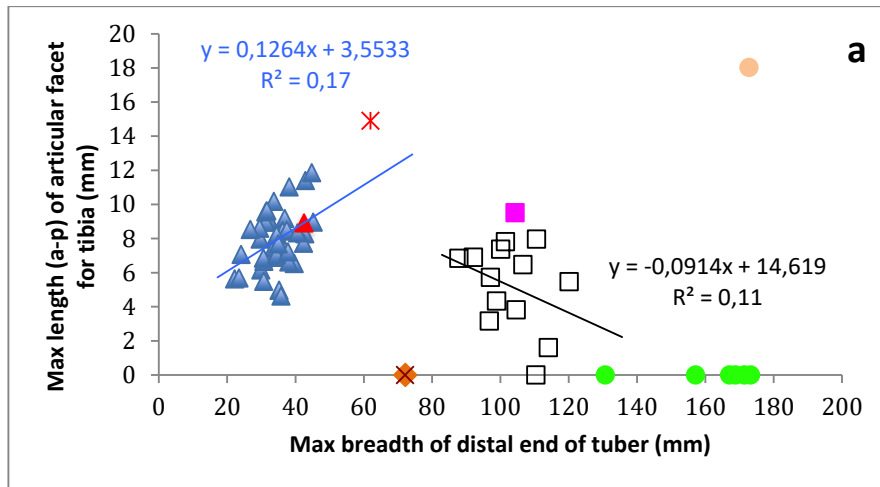


Fig. 3.23b Standardized and log-transformed Principal Component Analysis of the calcaneus. Refer to Table 3.7b for axes variable labels and component loading.

Importance of components:	PC1	PC2	PC3	PC4	PC5
Standard deviation	2,22	0,15	0,13	0,11	0,07
Proportion of Variance	0,99	0,00	0,00	0,00	0,00
Cumulative Proportion	0,99	0,99	1,00	1,00	1,00
Rotation:					
Var 1 - Max length of distal end of tuber	0,45	-0,52	0,37	0,26	-0,57
Var 2 - Max breadth of distal end of tuber	0,45	-0,25	0,39	-0,37	0,67
Var 3 - Max length of lateral art. facet for astragalus	0,45	-0,05	-0,62	-0,58	-0,28
Var 4 - Max breadth of lateral art. facet for astragalus	0,45	0,00	-0,46	0,68	0,35
Var 6 - Max length (a-p) of fibular facet	0,45	0,82	0,33	0,01	-0,17

Table 3.7b Standardized and ln-transformed Principal Component Analysis output for the calcaneus (see Fig. 3.23b). Note that variable 5 [Max length (a-p) of tibial facet] because the value is 0 in most specimens (and cannot be ln-transformed).

When the data are standardized and log-transformed and variable 5 (max length of the tibial facet) is removed (0 values are not logged), the *P. antiquus* individual from Riano is no longer an outlier, but plots closely with *P. antiquus* from Germany (Fig. 3.23b; Table 3.7b), indicating a similar overall morphology. Variables 1 and 2 [the length and breath of the distal end of the tuber] are moving in the same direction, as are Variables 3 and 4 [the length and breath of the lateral articular facet of the astragalus]. Variable 6 [Max length (a-p) of the fibular facet – see Fig. 3.21-B] now moves in a different direction to variables 1-4 on its own (Fig. 3.23b), indicating they are not closely related.



d Fig. 3.24 Morphology of the calcaneus' articular facet for the tibia and fibula a) Scatterplot of the dimensions of the articular facet for the tibia (where absent the length is plotted as 0). Refer to Fig. 3.3 for symbol legend. b) Three individuals of *P. ex gr. P. falconeri* illustrating intraspecific variability in the morphology of the tibial and fibular facets (FF=fibular facet, TF=tibial facet, TFF=tibio-fibular facet, refer to Fig. 2.25 for measurement protocol).

c) Box-and-whisker plot of the ratio of the tibial facet length/distal tuber length. d) Calcaneus of *P. tiliensis* (THEODOROU *et al.*, 2007) from Tilos, Island, Greece in lateral aspect (Megalo Chorio Museum, Tilos)^{sin}.

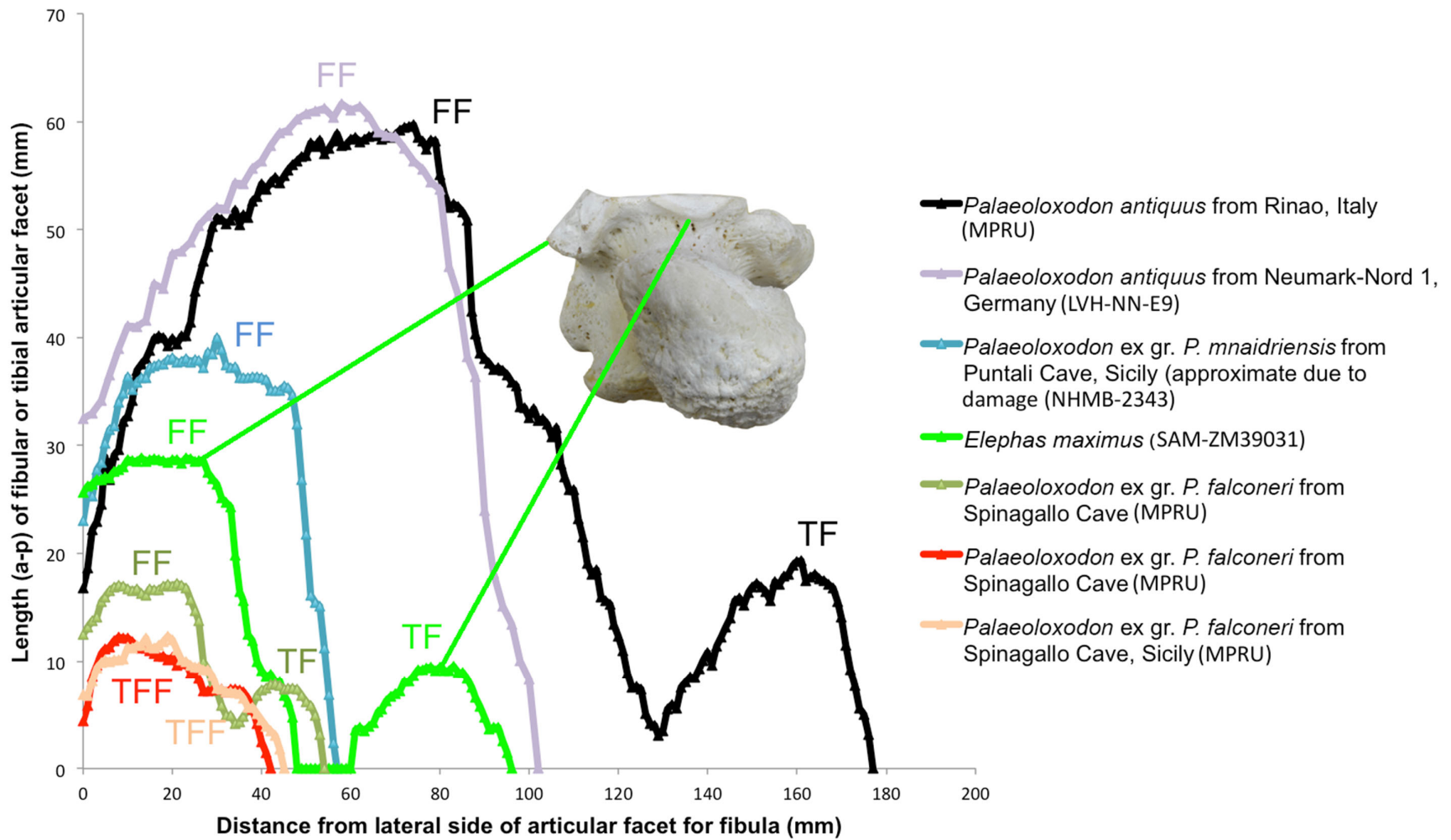


Fig. 3.25 Calcaneus intra- and inter-specific differences between the morphology of the tibial and fibular facets (FF=fibular facet, TF=tibial facet, TFF=tibio-fibular facet, refer to Fig. 2.21 for measurement protocol). The calcaneus image is illustrated in superior aspect. Two *P. antiquus* and three *P. ex gr. P. falconeri* individuals are included to illustrate intraspecific variability.

Species	Tibial facet		Morphology of tibio-fibular facet	Sites
	Present	Absent		
<i>P. antiquus</i>	0	6	No tibial facet	Neumark-Nord
	1	0	Small tibial facet, almost completely separated from fibular facet	Riano, Italy
<i>P. ex gr. P. mnaidriensis</i>	0	3	No tibial facet	Puntali Cave, Sicily
<i>Palaeoloxodon</i> sp.	0	(1)	No clearly distinguishable tibial facet, although fibular facet tapers	Benghisa Gap, Malta
<i>Palaeoloxodon</i> sp. 1	5	0	Tibial and fibular facets almost completely separated in GMP-GL103 and almost completely continuous in IPH-F2961	Luparello Fissure, Sicily
<i>P. ex gr. P. falconeri</i>	36	0	More-or-less completely continuous tibio-fibular facet	Spinagallo
	1	0		Luparello
<i>L. africana</i>	12	1	Facets completely separated	Kenya

Table 3.8 Differences in the articular facet for the tibia on the calcaneus between species (or morphotypes) listed from largest to smallest for *Palaeoloxodon* spp.

v) Separation between the tibial and fibular facets - The degree of separation between these articular facets varies greatly between species (Table 3.8). The tibial and fibular facets may be a) completely separated (as seen in *L. africana* and *E. maximus*), or b) separated by a narrow tibio-fibular bridge (*P. antiquus* from Riano, Fig. 3.25; *Palaeoloxodon* sp. 1 from Luparello Fissure, Fig. 3.21-3A). Finally, the tibio-fibular facet may be more-or-less continuous as in *P. ex gr. P. falconeri* (Fig. 3.21-1A; Fig. 3.24b; Fig. 3.25). In comparing *Palaeoloxodon* sp. 1 from Luparello Fissure with *P. ex gr. P. falconeri* there are also subtle, but significant differences, particularly with regard to the probable anagenesis between these two species (see results following in Section 3.7.1).

3.1.6.3 Dimensional and morphological differences between the calcaneus of *Palaeoloxodon* sp. 1 from Luparello Fissure and *P. ex gr. P. falconeri*

Ratio	Figure	MWU p-value
Max length (a-p) of fibular facet/min length (a-p) of tibio-fibular bridge	a	0,008*
Max length (a-p) of fibular facet/max length (a-p) of tibial facet	b	0,744
Max length of tibial facet/min length of tibio-fibular bridge	c	0,118
Max length of distal end of tuber/Min length (a-p) of tibio-fibular bridge	d	0,020*

Table 3.9 MWU-test pairwise p-values of *Palaeoloxodon* sp. 1 from Luparello Fissure and *P. ex gr. P. falconeri* from Spinagallo Cave, Sicily. Significant values are indicated with an asterisk (*).

In comparing calcanei, it is also noteworthy that although there are close morphological similarities between larger *Palaeoloxodon* sp. 1 from Luparello Fissure and smaller *P. ex gr. P. falconeri* (from Luparello Fissure and Spinagallo Cave) there are also morphological differences in the tibio-fibular facet on the calcaneus (contrast Fig. 3.21-1A with Fig. 3.21-3A; Table 3.9). In terms of absolute dimensions the maximum length of the tibial facet of

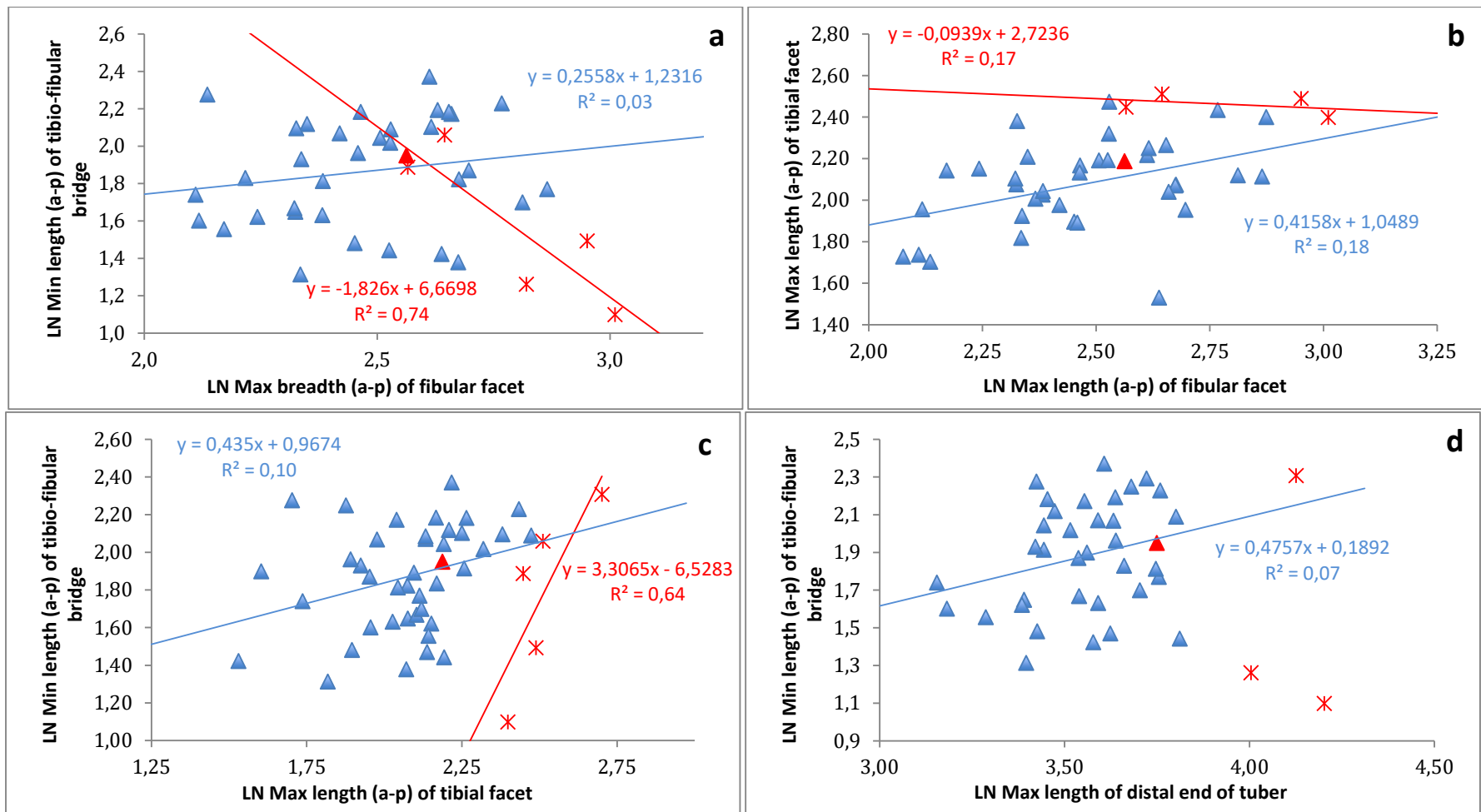


Fig. 3.26 Scatterplots of the dimensions of the calcaneal tibial and fibular facets in *P. ex gr. P. falconeri* and *Palaeoloxodon* sp. 1 from Luparello Fissure and Spinagallo Cave, Sicily. a) Max length (a-p) of fibular facet vs. min length (a-p) of the tibio-fibular bridge b) Max length (a-p) of fibular facet vs. max length (a-p) of tibial facet c) Max length (a-p) of articular facet for the tibia vs. max length of tibio-fibular bridge d) Max length of distal end of tuber vs. max length (a-p) of tibial facet minus min length of tibio-fibular bridge (a-p). Refer to Fig. 3.3 for symbol legend.

Palaeoloxodon sp. 1 from Luparello Fissure is significantly larger than that of *P. ex gr. P. falconeri* from Spinagallo Cave (MWU $p < 0,001$) whereas the minimum length of the tibio-fibular bridge is not significantly different (MWU $p = 0,732$, see also Fig. 3.26c). This indicates that the *Palaeoloxodon* sp. 1 specimens sometimes evidence a greater degree of separation between the tibial and fibular facets (Fig. 3.21-3A) than in *P. ex gr. P. falconeri* (Fig. 3.26c; Fig. 3.21-1A; Table 3.9). Considering *Palaeoloxodon* sp. 1 from Luparello Fissure may be the ancestral chronospecies of *P. ex gr. P. falconeri* as hypothesized by Vaufrey (1929: 89), the greater separation between the tibial and fibular facets in *Palaeoloxodon* sp. 1 may reflect the fact that the tibial facet became proportionally larger during anagenesis in Sicilian *Palaeoloxodon* chronospecies, before merging more completely with the fibular facet in *P. ex gr. P. falconeri* (see also Scarborough *et al.*, 2016: 117). Thus the slope of the trendline in Fig. 3.26c may suggest a weak ontogenetic trend towards a relatively larger tibial facet in *P. ex gr. P. falconeri* from Spinagallo Cave with increasing ontogenetic age, while the more positive slope of the *Palaeoloxodon* sp. 1 trendline may reflect morphological change during anagenesis in the latter species, indicating a trend towards a relatively bigger tibio-fibular bridge with a decrease in absolute size (Fig. 3.26c).

Vaufrey based his conclusion of an anagenetic relationship between *Palaeoloxodon* sp. 1 and *P. ex gr. P. falconeri* at Luparello Fissure on extensive excavations from which he reported the lower stratigraphic position of larger remains (referred by him to '*Elephas antiquus melitensis*') and the higher position of smaller remains ('*Elephas antiquus falconeri*'). Imbesi (1956), in contrast, reported the remains of a larger and smaller elephant as being present in the same strata. However, Imbesi's excavations and stratigraphic records are more limited (*ibid.*). Furthermore, the Luparello Fissure assemblage includes numerous specimens ranging from marginally larger to much larger than the late Middle Pleistocene *P. ex gr. P. falconeri* specimens from Spinagallo Cave (Fig. 3.22; Fig. 3.26), which includes more than a hundred individuals (Ambrosetti, 1968). This suggests Vaufrey's stratigraphic observations concerning the lower position of the larger remains are correct, and further supports an anagenetic relationship between larger *Palaeoloxodon* sp. 1 and smaller *P. ex gr. P. falconeri* from Luparello fissure. Vaufrey's stratigraphic and the morphological observations of this thesis therefore lend tentative support to the hypothesis that *P. ex gr. P. falconeri* evolved *in situ* on Sicily (or its northern palaeo-island), and later colonized Malta, possibly during an early or late Middle Pleistocene glacial lowstand (Scarborough *et al.*, 2016).

3.1.6.4 Possible ontogenetic allometry in the calcaneus of *P. antiquus* and *L. africana*

Since the calcaneus of *P. ex gr. P. falconeri* and *Palaeoloxodon* sp. 1 from Luparello Fissure are morphologically highly derived with respect to *P. antiquus* (particularly with regard to the articular facet for the tibia, see Fig. 3.24; Table 3.8), and pedomorphism is evident in *P. ex gr. P. falconeri* and likely also *Palaeoloxodon* sp. 1 from Luparello Fissure (see Chapter 4, Section 4.2.4 part ii), might there also be pedomorphism in the insular calcaneus of these two insular taxa?

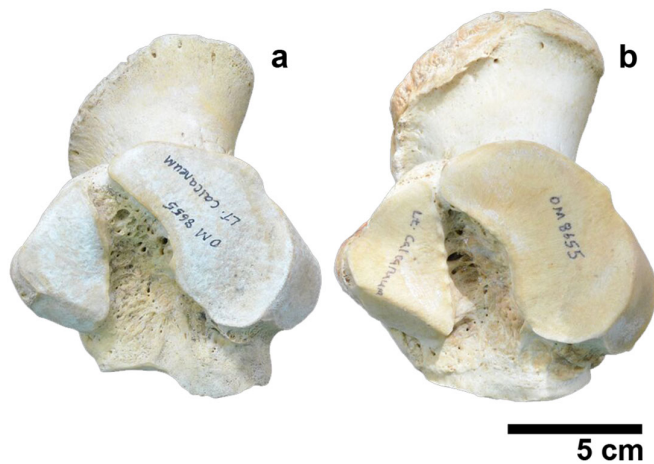


Fig. 3.27 *L. africana* calcaneus from Kenya in frontal aspect. a) Juvenile with unfused tuber^{sin}. b) Adult with fused tuber^{sin} (both specimens are accessioned as KNM-OM8655 but belong to different individuals).

Three morphological features were noted in *L. africana* and *P. antiquus* which may be candidates for further study with regard to ontogenetic allometry, although

observations were severely limited because of very few juvenile *L. africana* specimens in the NMK, presumably because they are not fully ossified, and likewise in *P. antiquus* in the LVH, likely due to taphonomic or other reasons. However, possible evidence of ontogenetic allometry were noted in (i) the morphology of the articular facet for the os t. IV. In juvenile *L. africana* this facet is concave, and seen in frontal aspect has a sinusoidal profile (Fig. 3.27a), similar to young *P. antiquus* (Fig. 3.21-6C). This contrasts with the morphology of the adults of both these species. Other possible features which may display ontogenetic allometry include: (ii) The curvature of the medial articular facet for the astragalus, which may display greater curvature in the direction of its greatest length in juveniles as compared to adults, and (iii) The angle between the articular facet for the fibula and the lateral articular facet for the astragalus, which may be slightly more obtuse in juvenile *L. africana* (Fig. 3.27a) than in adult *L. africana* (Fig. 3.27b) and young *P. antiquus* (Fig. 3.21-6A) than in adult *P. antiquus* (Fig. 3.21-7A).

In *P. ex gr. P. falconeri* the articular facet for the os t. IV tends to be more-or-less flat viewed in frontal aspect (Fig. 3.21-1C), contrasting with the sinusoidal profile of juvenile *L. africana* (Fig. 3.27a) and young *P. antiquus* (Fig. 3.21-6C). This tentatively suggests that the *P. ex gr. P. falconeri* calcaneus is unlikely to be pedomorphic. However, the curvature was not quantified, which would be appropriate for future research (see Chapter 5). Furthermore, it should not completely be ruled out that there is some pedomorphism in the calcaneus of *P. ex gr. P. falconeri* due to the fact that the calcaneus in neonate *L. africana* was not available for comparison (due to the fact that the bone was fully unossified in the KNM collection).

With regard to *Palaeoloxodon* sp. 1 only two well-preserved calcanei were measureable from Luparello Fissure (Fig. 3.21-2; Fig. 3.21-3). One of these displays a curved articular facet for the os t. IV (Fig. 3.21-2C) that has some resemblance to the morphology of juvenile *L. africana* (Fig. 3.27a) and young *P. antiquus* (Fig. 3.21-6C). However, the ontogenetic stage of this *Palaeoloxodon* sp. 1 specimen (Fig. 3.21-2) cannot be inferred from epiphyseal fusion due to damage to the epiphysis of the tuber, but it is smaller than the other well-preserved calcaneus from Luparello Fissure (Fig. 3.21-3). The morphology of this specimen may therefore reflect a juvenile morphology rather than pedomorphism in *Palaeoloxodon* sp. 1.

Although there is considerable variability in the relative size of the tibial facet within the sample of *L. africana* there is no clear evidence of ontogenetic allometry in the size of the facet (Fig. 3.24a). The presence of a large tibial facet in *Palaeoloxodon* sp. 1 from Luparello Fissure and *P. ex gr. P. falconeri* is therefore not clearly related to paedomorphism, although more data are needed on *L. africana* and *P. antiquus* calcaneus ontogeny.

3.1.7 Central tarsal

Proximally, the central tarsal articulates with the astragalus (Fig. 3.2; Fig. 3.31-A). There is a small plantar area adjoining it for articulation with the calcaneus (Fig. 3.31a; Fig. 3.33a; Fig. 3.33b; see bone in articulation in Fig. 3.2-2Ac; Fig. 3.2-2Bc; Fig. 3.2-2Cc). The distal surface has four narrow articular facets from medial to lateral for articulation with four tarsal bones. In *L. africana* the facets for os t. I/II are clearly separated, the facets for the os t. II/III being separated by a groove while the facets for the os t. III/IV are separated by a ridge (Fig. 3.31-B; Smuts and Bezuidenhout, 1994: 60). Between species, the central tarsal differs in (i) proximo-distal height, (ii) curvature viewed cranially, and (iii) the max breadth (m-l) of the central tarsal vs. max breadth (m-l) of the articular facet for the astragalus. Further differences include (iv) the max breadth (m-l) vs. max length (a-p) of the articular facet for the astragalus, (v) max length vs. max breadth of the articular facet for the calcaneus, and (vi) the morphology of the distal articular facets.

(i) Ratio of the cranial height (pr-d)/max breadth (m-l) - Viewed cranially, the central tarsal is much taller in *P. antiquus* (Fig. 3.31-1c) and *L. africana* (Fig. 3.31-2c) than in *M. lamarmorai* (Fig. 3.31-3c) and *P. ex gr. P. falconeri* (Fig. 3.31-4c, see also Fig. 3.2). The tall *P.* central tarsal of *P. antiquus* especially contrasts with the low height of *P. ex gr. P. falconeri*. Differences are statistically significant between *P. ex gr. P. falconeri* and *P. tiliensis* (MWU $p < 0,000$), *P. ex gr. P. falconeri* and *P. antiquus* from Neumark-Nord 1 (MWU $p = 0,006$), *P. ex gr. P. falconeri* and *L. africana* (MWU $p = 0,002$), but not between *P. antiquus* and *P. tiliensis* (MWU $p = 1,000$), and *P. antiquus* and *L. africana* (MWU $p = 0,343$). However, sample-size was small for *P. antiquus* and *L. africana*, so that more data are needed to evaluate intraspecific variability in these species.

(ii) Curvature viewed cranially - The central tarsal's curvature is greatest in *P. antiquus* (Fig. 3.31-1c, 1d) and least in the *P. ex gr. P. falconeri* (Fig. 3.31-4c, 4d), decreasing as mass decreases in the four figured specimens. (iii) Ratio max breadth (m-l) of the central tarsal/max breadth (m-l) of the articular facet for the astragalus - Significant differences were found between *P. antiquus* and *P. ex gr. P. falconeri* (MWU $p = 0,002$; Fig. 3.32), *P. antiquus* and *L. africana* (MWU $p = 0,042$) and *P. ex gr. P. falconeri* and *P. tiliensis* (MWU $p = 0,000$). Differences were not significant between *P. antiquus* and *P. tiliensis* (MWU $p = 0,843$) and between *L. africana* and *P. ex gr. P. falconeri* (MWU $p = 0,725$). In *M. trogontherii* from the published literature there is a wide central tarsal relative to the breadth of its articular facet for the astragalus.

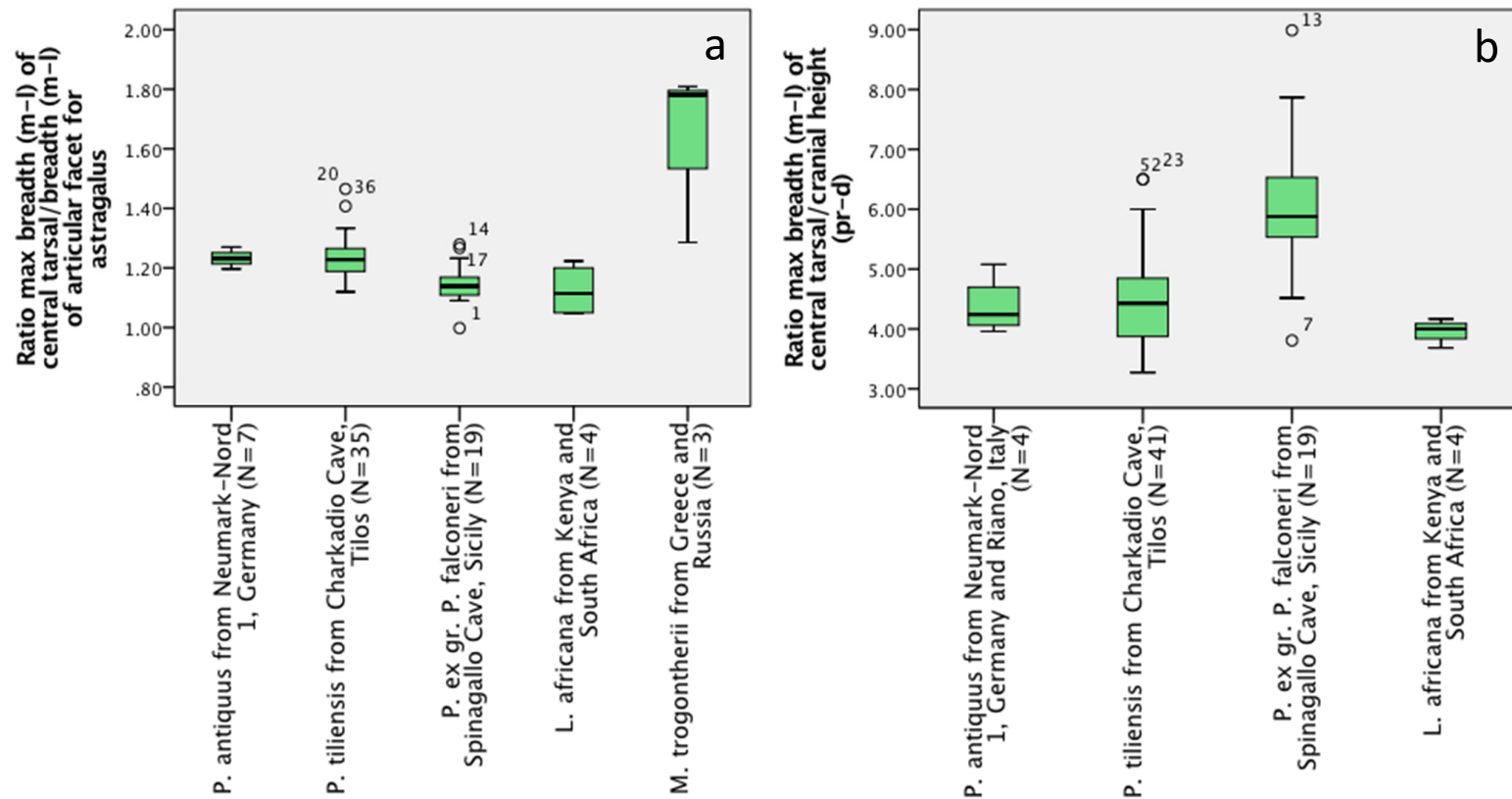


Fig. 3.28 a) Box-and-whisker plot of the ratio of the central tarsal's max breadth (m-l)/breadth (m-l) of articular facet for astragalus. b) Box-and-whisker plot of the ratio of max breadth of the central tarsal/cranial height (pr-d). Refer to Fig. 3.32 and Fig. 3.33c for scatterplots.

iv) Ratio of the max breadth (m-l)/max length (a-p) of the articular facet for the astragalus -

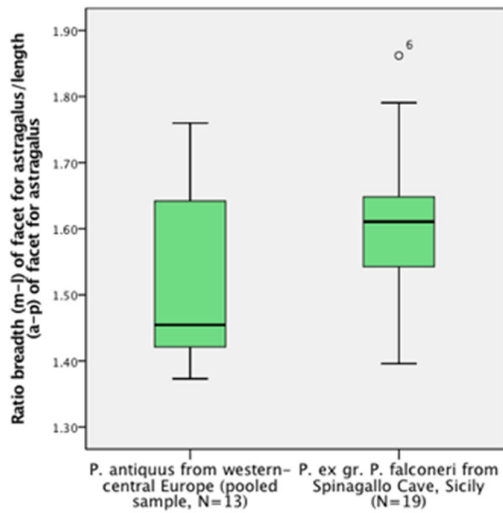


Fig. 3.27 Box-and-whisker plot of the central tarsal's breadth (m-l) of the articular facet for the astragalus/length (a-p) of the articular facet for the astragalus.

Differences are not significantly different between *P. antiquus* and *P. ex gr. P. falconeri* (MWU $p=0,152$). In *P. antiquus* there is a greater range of variability in the pooled European sample compared to the sample from Neumark-Nord 1, Germany, although these differences are not statistically significant (MWU $p=1,000$). The mean ratio of max breadth/max length of the central tarsal's articular facet for the astragalus is 1,61 in *P. ex gr. P. falconeri* from Spinagallo Cave, Sicily (N=19) and 1,49 in *P. antiquus* from all European sites (N=9). This indicates a tendency for a narrower (a-p) articular facet for the astragalus in *P. ex gr. P. falconeri*, as might be expected from the previous observation that the astragalus tends to be narrower in this species (Fig. 3.16).

However, the ratio is not significantly different between *P. ex gr. P. falconeri* from Spinagallo Cave and *P. antiquus* from Neumark-Nord 1 (MWU $p=0,152$) and between *P. ex gr. P.*

falconeri and also *P. antiquus* from the pooled sample of European sites including NN 1 (Fig. 3.29; MWU $p=0,099$).

v) Ratio max length (pr-d or a-p depending on morphology)/max breadth (m-l) of the articular facet for the calcaneus - In *P. ex gr. P. falconeri* from Spinagallo Cave there are large intraspecific differences in the allometry and particularly the orientation of the articular facet for the calcaneus. In some individuals this facet is absent altogether, and in others it is large (3.33a, b). A caudally projecting articular facet for the calcaneus is represented in two examples out of a total of 19 undamaged *P.*

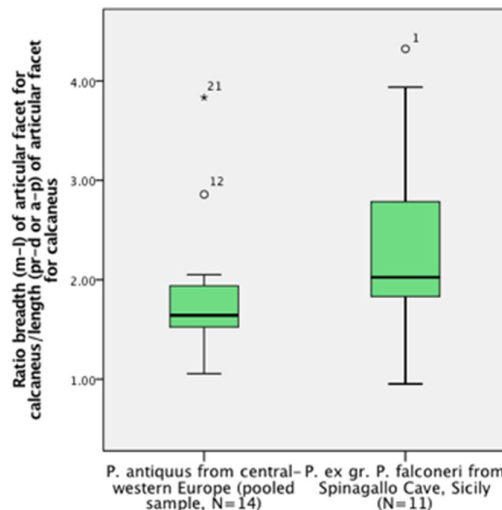


Fig. 3.30 Box-and-whisker plot of variability in the central tarsal's articular facet for the calcaneus (ratio m-l breadth/a-p length). a) *P. antiquus* from NN 1 Germany vs. pooled sample of *P. antiquus* from Gröbern I, Gröbern II, Riano, Italy and Blanzac, France. [Data: *P. antiquus* not from NN1 is from Kroll, 1991: 58].

ex gr. P. falconeri specimens (see Fig. 3.33a; Fig. 3.33b). In *P. antiquus* the articular facet for the calcaneus also varies in orientation, and noticeably projects caudally in the young individual from NN1 (LVH-NN-E22). Differences are however not significant between *P. antiquus* and *P. ex gr. P. falconeri* (MWU $p=0,442$).

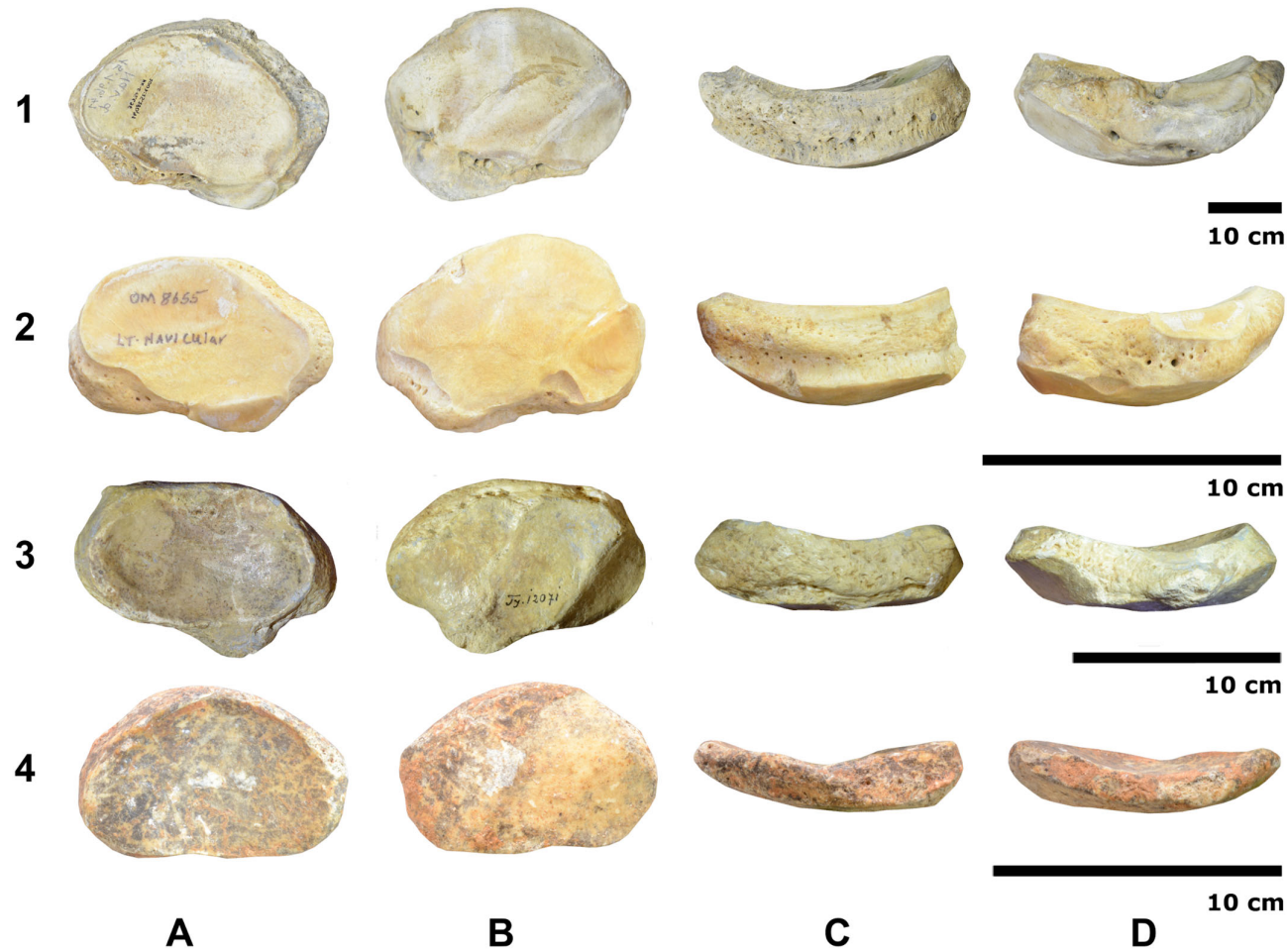


Fig. 3.31 Central tarsal of 1) *P. antiquus* from Neumark-Nord 1, Germany (LVH-NN-E.15.1.96 and 2007: 25.280,41)^{dex} 2) *L. africana* from Kenya (KNM-OM8655)^{sin} 3) *M. lamarmorai* from Gonnese, Sardinia (NHMB-Tyi207i)^{sin} 4) *P. ex gr. P. falconeri* from Spinagallo Cave, Sicily (MPRU) A) dorsal B) plantar C) cranial and D) caudal aspects.

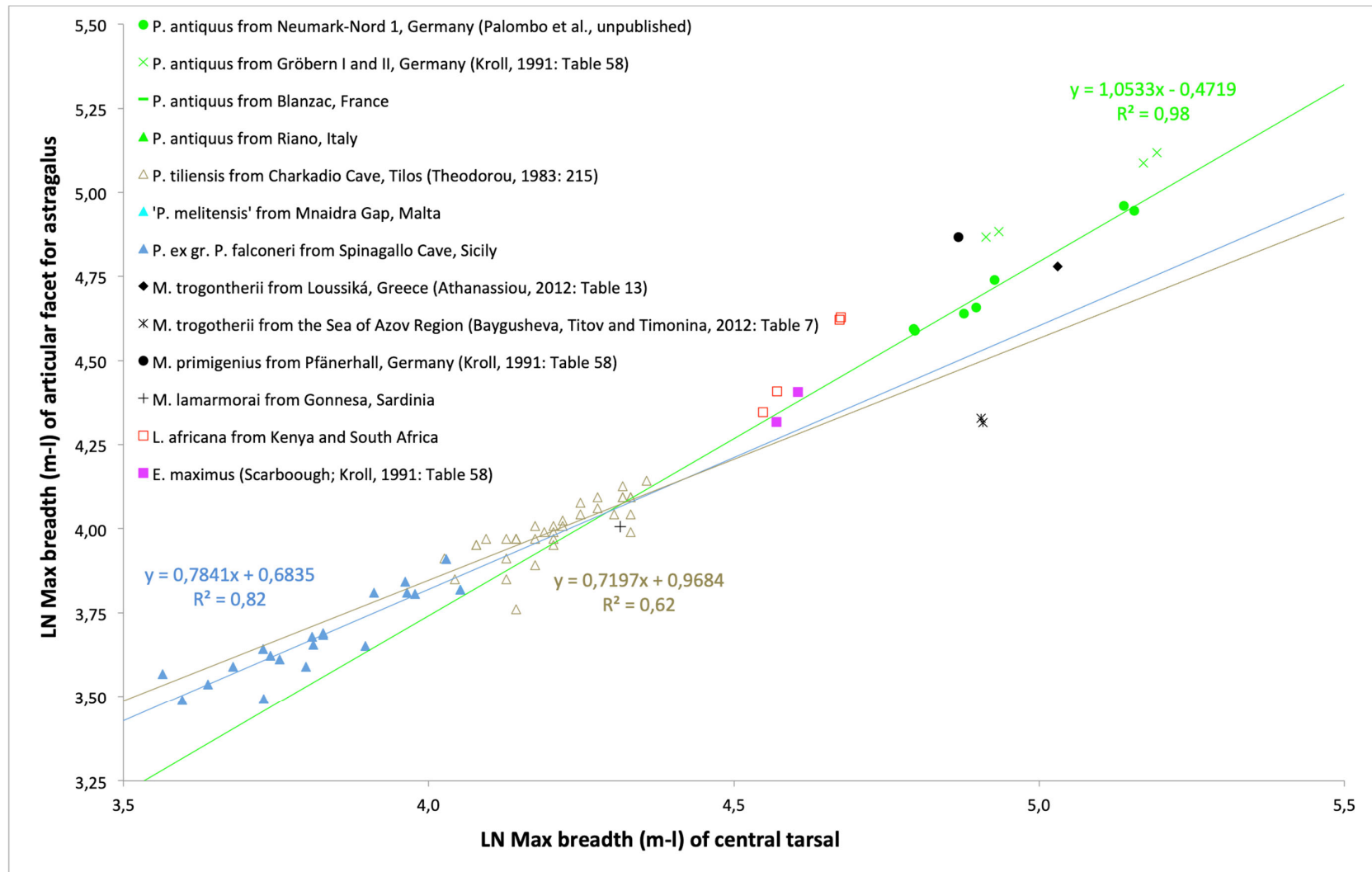


Fig. 3.32 Scatterplot of the central tarsal max breadth (m-l) vs. max breadth (m-l) of articular facet for the astragalus. The green linear trendline is for *P. antiquus* from Neumark-Nord 1 only.

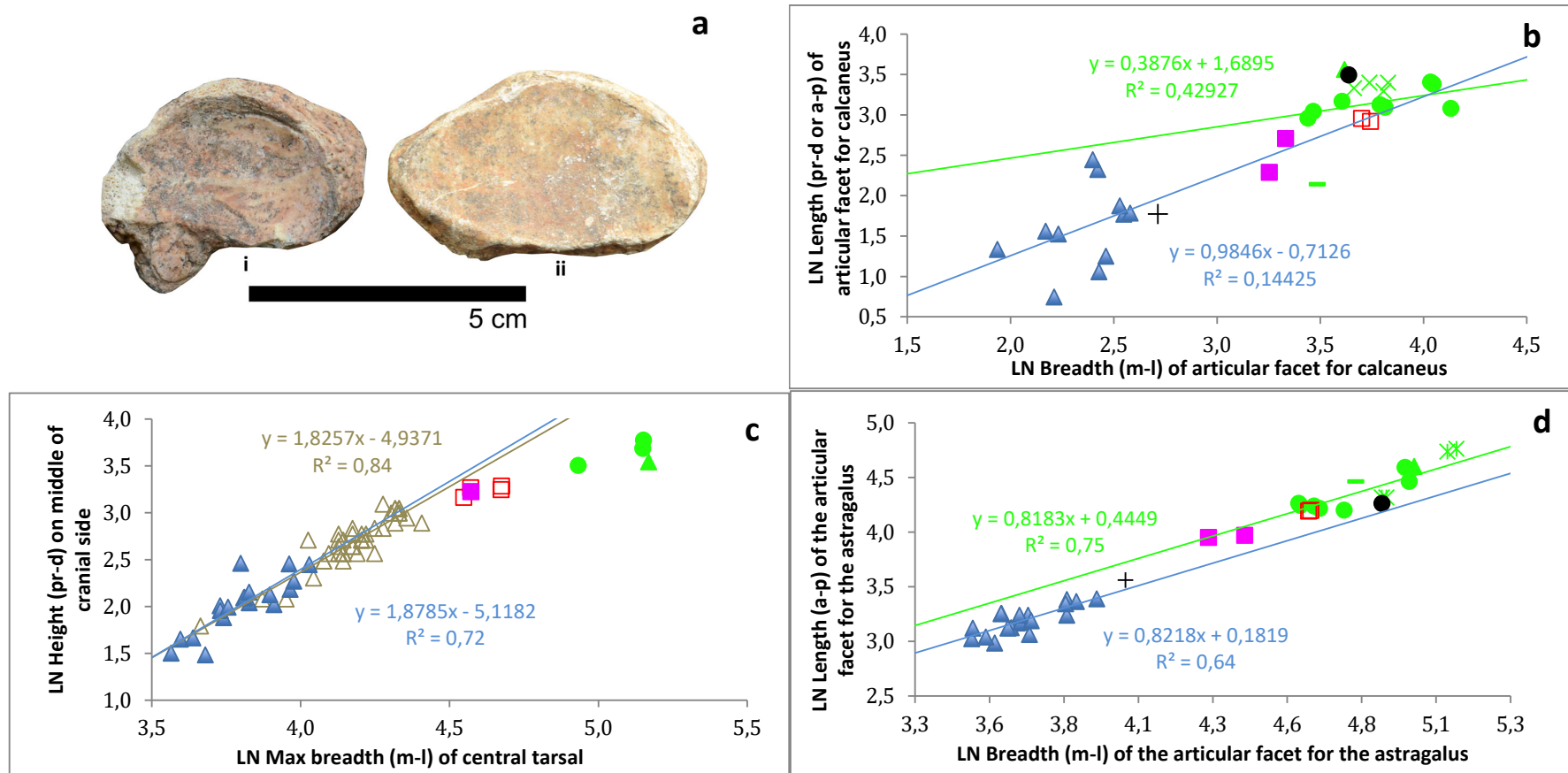


Fig. 3.33 Morphology and dimensions of the central tarsal. a) Variability of the central tarsal's articular facet for the calcaneus in *P. ex gr. P. falconeri* from Spinagallo Cave, Sicily (dorsal aspect, MPRU). (i) caudally projecting facet (ii) proximo-distally orientated facet. b) Scatterplot of the max breadth (m-l) of articular facet for the calcaneus vs. max length (pr-d) of articular facet for calcaneus (note that specimens with no articular facet are not included in the plot). c) Scatterplot of the max breadth (m-l) vs. thickness (pr-d). d) Scatterplot of the breadth (m-l) of articular facet for astragalus vs. length (a-p) of articular facet for astragalus. Refer to Fig. 3.32 for symbol legend and data sources (Note: *P. antiquus* measurements from NN1 includes original data and data from Palombo *et al.*, unpublished).

(vi) The morphology of the distal articular facets - Plantarly there are four articular facets, for the os t. I-IV. In the illustrated *P. ex gr. P. falconeri* the entire distal surface is taken up a continuous articular surface (Fig. 3.31-4B), whereas in *P. antiquus* and *L. africana* small areas of the surface are non-articular, likely for the insertion of tendons (Fig. 3.31-B1, B2). One possibility is that the absence of areas for the insertion of tendons in *P. ex gr. P. falconeri* may relate to a functional threshold of tendon thickness.

3.1.8 Os tarsale IV

The os t. IV is the largest of the distal tarsals, situated on the lateral side of the hindfoot (Fig. 3.2). Viewed in dorsal aspect, the bone is triangular, with the apex facing posteriorly (Fig. 3.34-B; Fig. 3.35-A). On its proximal surface there are two articular surfaces, a smaller concave facet for the central tarsal and a large convex surface for the calcaneus. Distally the bone articulates with the mt III, mt IV and mt V (Fig. 3.2; Fig. 3.35-B). On the medial border there are two facets, proximally and distally, for articulation with the os t. III (Smuts and Bezuidenhout, 1994: 61; *ibid.* Fig. 14). Interspecifically, the os t. IV differs in several respects, including (i) cranial height, (ii) depth of the niche for the articulation of the mt IV/V, (iii) the degree of separation between the articular facets for the central tarsal and the calcaneus, (iv) the presence/absence of a semi-circular depression for the insertion of a tendon in the caudal region of the dorsal surface, (v) the presence/absence of a fissure for the insertion of a tendon on the plantar surface, (vi) the superposition (pr-d) of the proximal and distal articular facets for the os t. III and (vi) ratio max anterior breadth (m-l)/max thickness (a-p).

(i) Cranial height - Among different species there is a wide range in cranial height (Fig. 3.35-C), being short in *P. ex gr. P. falconeri* (Fig. 3.35-1C), and also short but to a lesser degree in *Palaeoloxodon* sp. 1 from Luparello Fissure and *P. melitensis* from Benghisa Gap, Malta. In contrast, the os t. IV is tall in young *P. antiquus* (Fig. 3.35-4C) and adult *P. antiquus* (Fig. 3.35-5C) from Neumark-Nord 1, *M. lamarmorai* (Fig. 3.35-6C) and *L. africana* (Fig. 3.35-7C). (ii) Depth of the niche for the articulation of the mt IV/V - Separation between the articular facets for the mt IV and the mt V is more visible in *P. ex gr. P. falconeri* where there is a narrow line running antero-posteriorly (Fig. 3.35-1B). Viewed cranially, the same feature is seen as a deep niche (Fig. 3.2-3Bf; Fig. 3.34; Fig. 3.35-1C) and the angle between the articular facets appear to be more pronounced in *P. ex gr. P. falconeri* from Spinagallo Cave than in all other species (Fig. 3.34-A; Fig. 3.35-1C).

(iii) The degree of separation between the articular facets for the central tarsal and the calcaneus - Viewed dorsally the articular surface varies considerably (Fig. 3.35-A), with the articular facets for the central tarsal and calcaneus being separated in young *P. antiquus* (Fig. 3.35-4A), and frequently contiguous during late ontogeny (Fig. 3.35-5A). In *P. ex gr. P. falconeri* one large individual has separated facets (Fig. 3.34-1B), and a small individual has contiguous facets (Fig. 3.34-1B) typical of juvenile and adult morphology respectively in continental elephants. In *M. trogontherii* from Greece and China there is a groove separating the articular facets for the central tarsal and calcaneus (Athanasidou, 2012: Fig. 18-h; Chen and Tong, 2017: Fig 3-G1) that is absent in the *M. lamarmorai* holotype (Fig. 3.35-6A).

(iv) The presence/absence of a semi-circular depression for the insertion of a tendon in the caudal region of the dorsal surface - In two species, *Palaeoloxodon* sp. 1 from Luparello Fissure, Sicily and *Palaeoloxodon* sp. from Benghisa, Malta, a circular groove is visible on the posterior part of the proximal articular surface. The insertion is deep in *Palaeoloxodon* sp. (Fig. 3.35-3A; Adams, 1874: 85, pl. xvii. Fig. 5) and shallow in *Palaeoloxodon* sp. 1 (Fig. 3.35-2A). This contrasts markedly with *P. ex gr. P. falconeri* in which there is no depression for the insertion of a tendon (Fig. 3.35-1A). In *H. sapiens* four ligaments attach on the dorsal surface, the calcaneocuboid, cubonavicular, cuneocuboid and cubometatarsal ligaments (Standring, 2005: 2435). More research is needed to determine which ligaments attach in proboscideans, but it is possible interspecific differences in (iii) and (iv) are caused by differences in the attachments of the same ligaments as in humans.

(v) The presence/absence of a fissure for the insertion of a tendon on the plantar surface - Plantarily there is a deep groove in the posterior region for the insertion of a tendon, which is present in young and adult *P. antiquus* (Fig. 3.35-4B; 5B), *L. africana* (Fig. 3.35-7B; Smuts and Bezuidenhout, 1994: Fig. 14) and *E. maximus* (SAM-ZM39031) which is not visible in any of the figured dwarf specimens. (Fig. 3.35-1B; 2B; 3B; 6B). Nonetheless, only single examples were examined for *Palaeoloxodon* sp. 1 from Luparello Fissure, *Palaeoloxodon* sp. from Malta and *M. lamarmorai*, so that variability in this intraspecific feature

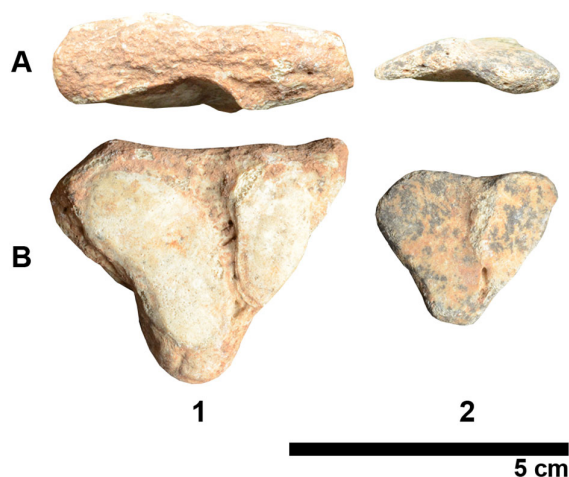


Fig. 3.34 *P. ex gr. P. falconeri* os t. IV from Spinagallo Cave, Sicily. A) Frontal aspect B) Dorsal aspect. 1) Large specimen with separated articular facets for the central tarsal and calcaneus 2) Small specimen with contiguous facets for the central tarsal and calcaneus.

is unknown. However, all the *P. ex gr. P. falconeri* specimens from Spinagallo Cave lack a groove, suggesting its absence relative to *P. antiquus* may be autapomorphic in the former species

With regard to the identity of the tendon(s) in question, in *H. sapiens* the long plantar ligament, slips from the tendons of *tibialis posterior*, and the *flexor hallucis brevis* attach to the proximomedial part of the plantar surface (Standring, 2005: 2435). Proximally, the medial calcaneocuboid ligament, which is the lateral limb of the bifurcated ligament, is also attached to this surface (Standring, 2005: 2435). Additionally, the *Peroneus longus* winds around the lateral margin of the os t. IV, entering a groove on its plantar aspect, although it inserts into the medial os t. IV (and the base of the mt I) (Standring, 2005: 2407, Fig. 115.35).

(vi) The superposition (pr-d) of the proximal and distal articular facets for the os t. III - Seen in medial aspect there are two articular facets for the os t. III. In the figured examples,

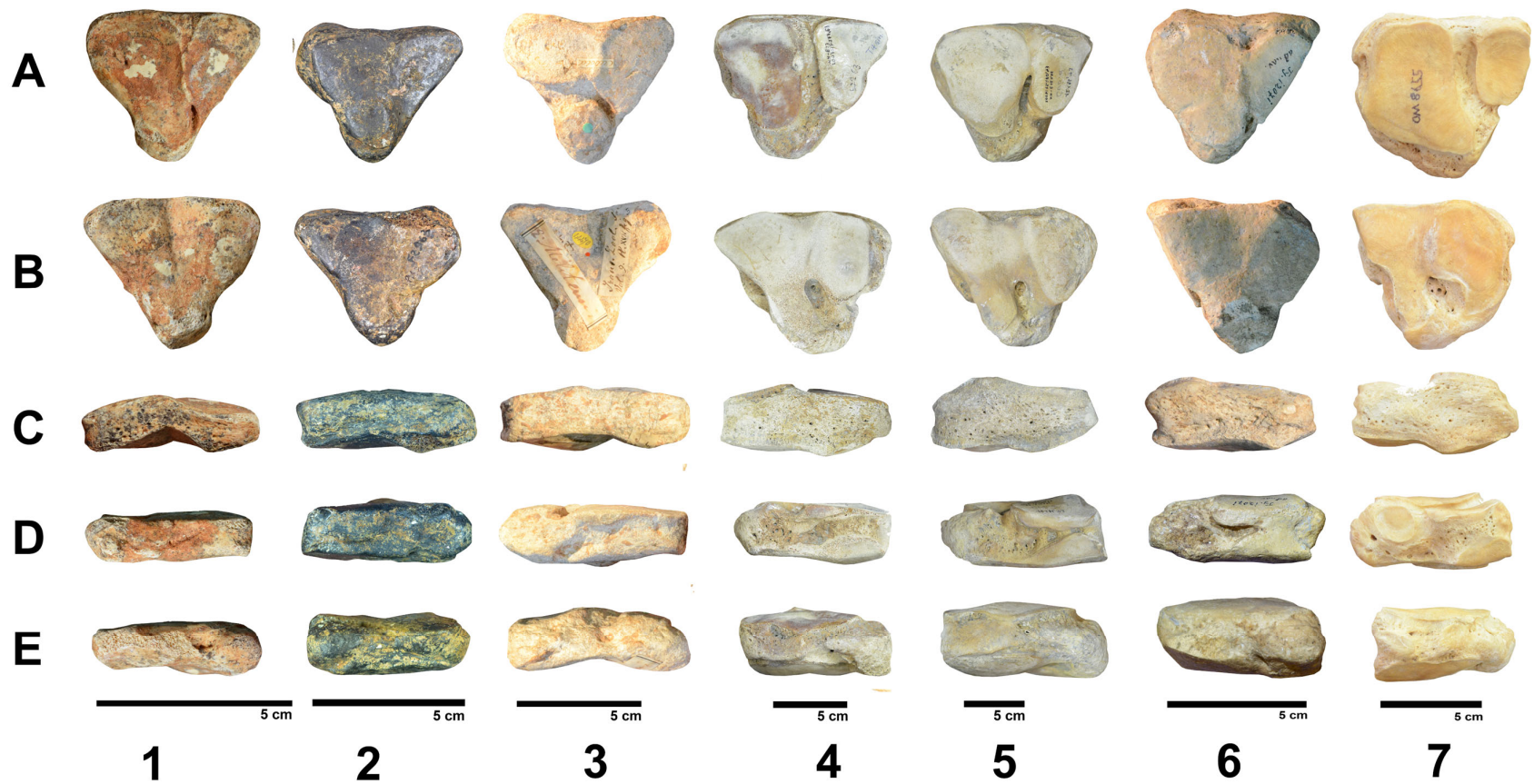


Fig. 3.35 Os t. IV of 1) *P. ex gr. P. falconeri* from Spinagallo Cave, Sicily (MPRU-SpC-TIV-4). 2) *Palaeoloxodon* sp. 1 from Luparello Fissure, Sicily (IPH-F2963)^{sin}. 3) *Palaeoloxodon* sp. from Benghisa, Malta (NHMUK-44470)^{sin}. 4) Young *P. antiquus* from Neumark-Nord 1, Germany (LVH-NN-E22)^{sin}. 5) Adult *P. antiquus* from Neumark-Nord 1, Germany (LVH-NN-E15.1.96,43 and 2007: 25.280,43)^{dex}. 6) *M. lamarmorai* from Gonnesa, Sardinia (NHMB-Tyi207i)^{sin}. 7) *L. africana* from Kenya (KNM-OM8655)^{sin}. A) dorsal B) plantar C) frontal D) medial and E) lateral aspects.

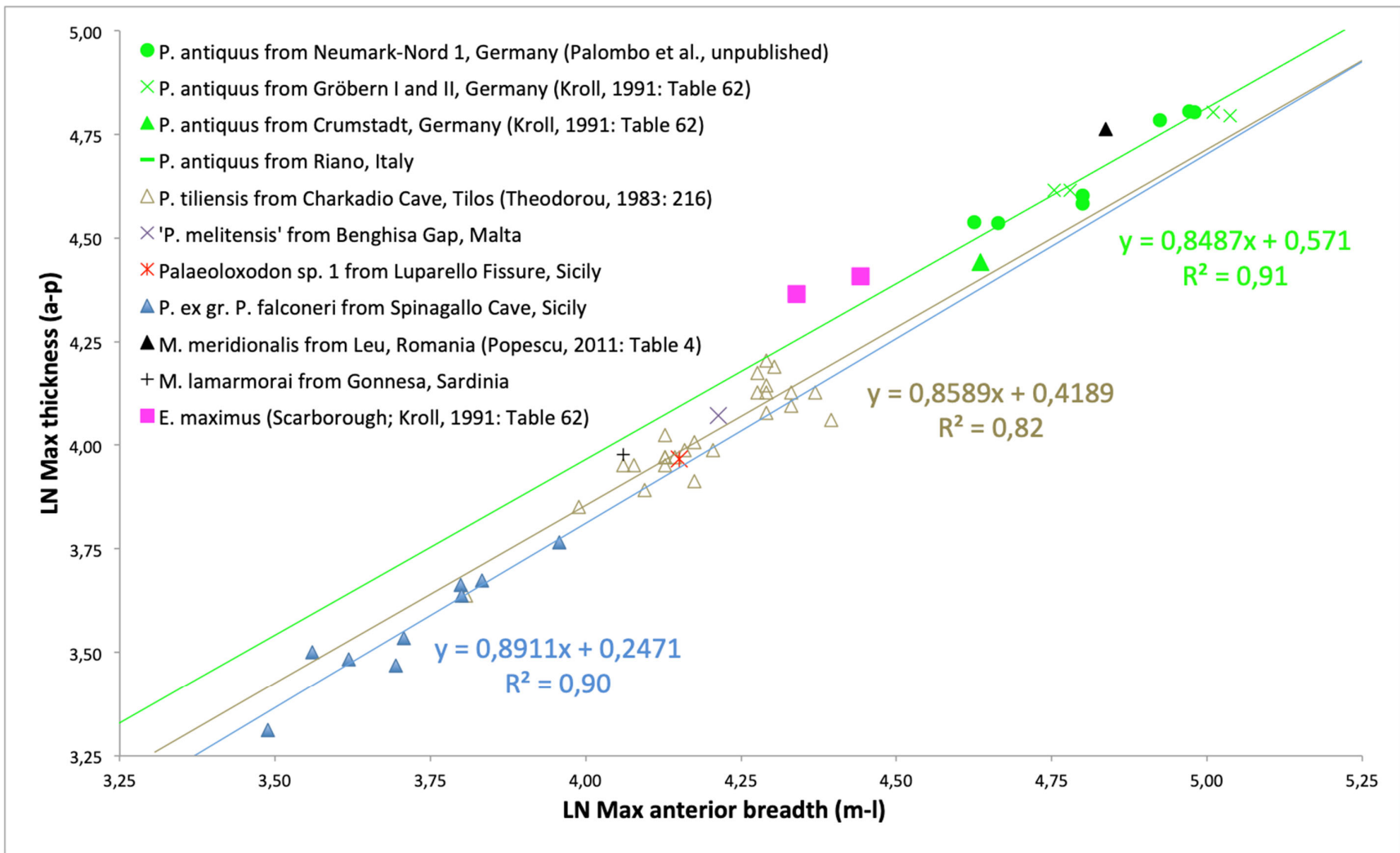


Fig. 3.36 Scatterplot of the os t. IV's anterior breadth (m-l) vs. max thickness (a-p). Note: the green trendline is fitted to *P. antiquus* from Neumark-Nord 1 only

the proximal articular facet is aligned directly above the distal articular facet in adult *P. antiquus* (Fig. 3.35-5D) and *M. lamarmorai* (Fig. 3.35-6D). In contrast, the proximal articular facet for the os t. III is situated caudally, and the distal facet cranially in *L. africana* (Fig. 3.35-7D), and young *P. antiquus* (Fig. 3.35-4D) and *Palaeoloxodon* sp. from Benghisa Gap, Malta (Fig. 3.35-3D). (vi) Ratio max anterior breadth (m-l)/max thickness (a-p) - Differences are not significant between *P. antiquus* and *P. tiliensis* (Fig. 3.36; MWU $p=0,865$), or between *P. antiquus* and *P. ex gr. P. falconeri* (MWU $p=0,955$), or between *P. tiliensis* and *P. ex gr. P. falconeri* (MWU $p=0,788$). Although there is overlap in this ratio between *P. antiquus* and dwarf *Palaeoloxodon* spp., *P. antiquus* has a tendency to be slightly thicker (Fig. 3.36). Although sample size is small, the bone is also thicker (a-p) in young *E. maximus* the other Elephantinae species (Fig. 3.36).

The tendons which insert on the os t. IV cannot be identified with certainty, although comparisons may be made with *H. sapiens*. Ontogenetic scaling has also been described in select tendons of *E. maximus* (Miller *et al.*, 2008: 472).

3.1.9 Metapodials

Intraspecific variability in the *P. ex gr. P. falconeri* metapodials from Spinagallo Cave - The *P. ex gr. P. falconeri* metapodials sometimes evidence a greater range of intraspecific variability than in the tarsals and carpals of the same species (contrast R^2 values of Fig. 3.38a-d with Fig. 3.13; Fig. 3.14a-d; Fig. 3.17a-d). The sometimes greater range of intraspecific variability may be due to ontogenetic allometry, or possibly due to the fact that the metapodials interact more directly than the carpals and tarsals with variable substrates and topography. The high degree of variability weakens the strength of statistical testing between species (Mann-Whitney U tests), although measurements combined with anatomical observations nonetheless reveal marked morphological differences.

3.1.9.1 Metacarpal III

(i) Ratio max height (pr-d)/diaphysis midshaft breadth (m-l) - Differences are statistically significant between *P. antiquus* vs. *P. ex gr. P. falconeri* (MWU $p=0,005$), indicating a tendency towards a wide diaphysis in the latter species (Fig. 3.38a). (ii) Ratio max height (pr-d)/min diaphysis thickness (a-p) - Differences are not statistically significant between *P. antiquus* vs. *P. tiliensis* (MWU $p=0,432$), but are significant between *P. antiquus* vs. *P. ex gr. P. falconeri* (MWU $p=0,000$), indicating a thicker diaphysis in *P. ex gr. P. falconeri*, and significant between *P. ex gr. P. falconeri* vs. *P. tiliensis* (MWU $p=0,000$), again due to a thicker diaphysis in *P. ex gr. P. falconeri* (Fig. 3.38c). (iii) Ratio min diaphysis breadth (m-l)/min diaphysis thickness (a-p) - Differences are not statistically significant between *P. antiquus* vs. *P. tiliensis* (MWU $p=0,454$), but are significant between *P. antiquus* vs. *P. ex gr. P. falconeri* (MWU $p=0,016$) and also between *P. tiliensis* vs. *P. ex gr. P. falconeri* (MWU $p=0,000$).

(iv) Max height (pr-d) vs. cross-sections (breadth m-l/thickness a-p) of the diaphysis - In order to better understand to what extent intraspecific variability relates to any trends in ontogenetic allometry cross-sections of the diaphysis were compared in relation to height (pr-d) (Fig. 3.38d). In *P. tiliensis* as height (pr-d) increases relative diaphysis thickness decreases. In contrast, in *P. antiquus* and *P. ex gr. P. falconeri* as height (pr-d) decreases relative diaphysis thickness decreases, indicating different ontogenetic trends between species.

Morphological differences between the *M. lamarmorai* and *Palaeoloxodon* spp. mc III - This differs primarily in two respects compared with *Palaeoloxodon* spp. and its reputed ancestor *M. meridionalis*. (i) Firstly, the *M. lamarmorai* mc III broadens distally (Fig. 3.1-C1; Fig. 3.37c), more than in *M. meridionalis* (Mol *et al.*, 1999: Fig. 4B, see Fig. 3.37) and *P. antiquus* (Fig. 3.1-A1) in which the mc III is more parallel-sided in cranial aspect. (ii) Secondly, seen in cranial aspect the angle between the articular facets for the os c. III and os c. IV (or the vertical axis of the mc III) differs between species, being more inclined (sloping downwards from the medial to lateral side) in *M. lamarmorai* (Fig. 3.1-C1; Fig. 3.37c) than in *P. antiquus* (Fig. 3.1-A1) and *M. meridionalis* (see Mol *et al.*, 1999: Fig. 4). In both (i) and (ii) however, there is greater similarity between *M. lamarmorai* and *Anancus arverensis* (CROIZET and JOBERT 1828) (Fig. 3.37b; Mol *et al.*, 1999: Fig. 4B).

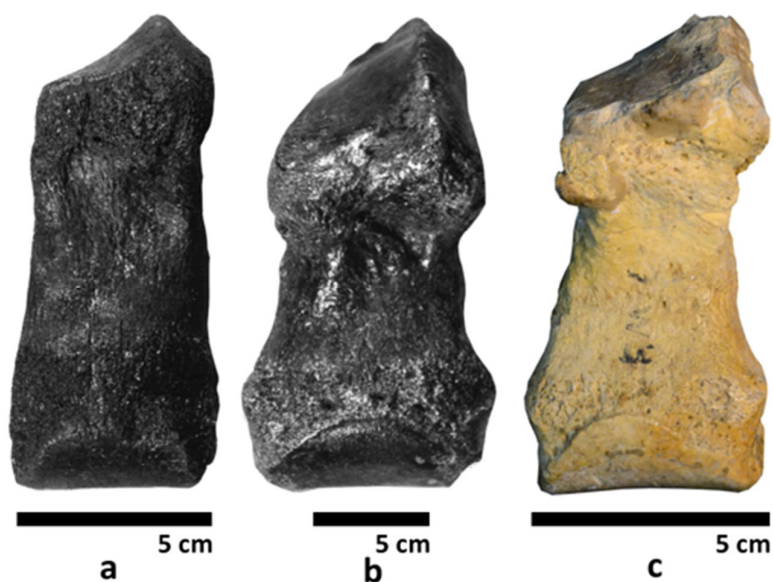


Fig. 3.37 Mc III in cranial aspect of a) *M. meridionalis* from the Oosterschelde Estuary, Netherlands b) *Anancus arverensis* (CROIZET and JOBERT 1828) from the Oosterschelde Estuary, Netherlands c) *M. lamarmorai* from Gonnese, Sardinia (NHMB)^{sin} (Figs a and b reproduced from Mol *et al.*, 1999: Fig. 4B).

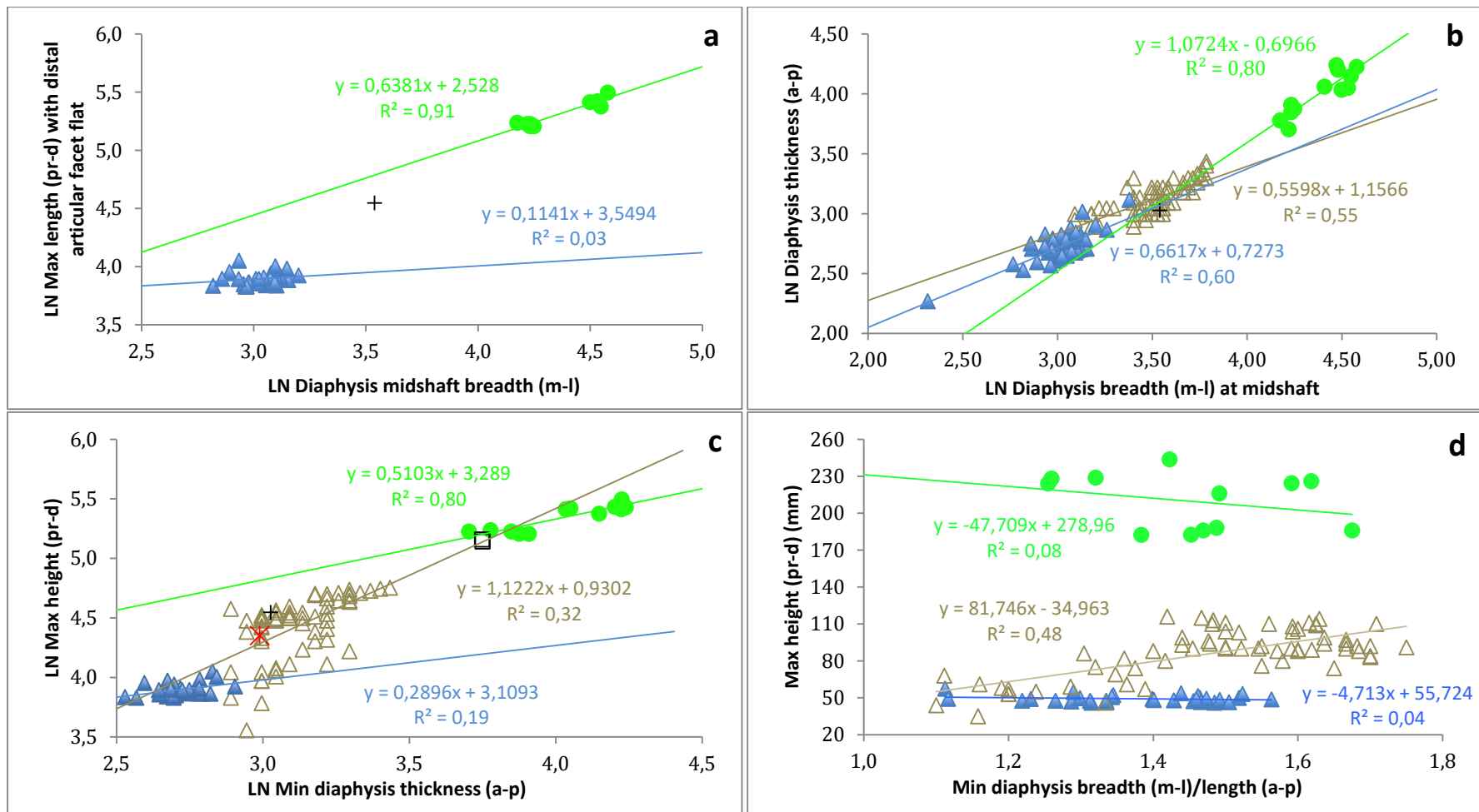


Fig. 3.38 Scatterplots of the dimensions of the mc III a) Diaphysis breadth (m-l) at midshaft vs. max length (pr-d). b) Diaphysis breadth (m-l) at midshaft vs. diaphysis thickness (a-p). c) Min diaphysis thickness (a-p) vs. max length (pr-d). d) Max height (pr-d) vs. diaphysis dimensions. Refer to Fig. 3.3 for symbol legend. [Data: *P. tiliensis* from Theodorou, 1983: 209; *P. antiquus* from Palombo *et al.*, unpublished]

3.1.9.2 Metacarpal IV

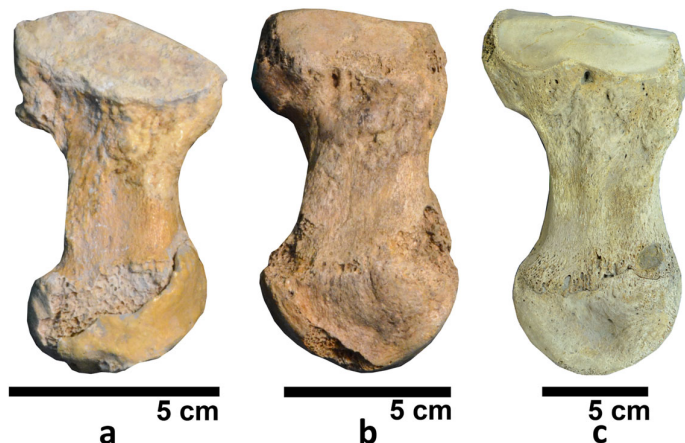


Fig. 3.39 Mc IV in medial aspect a) *M. lamarmorai* from Gonnese, Sardinia (NHMB-Ty.i2071, distal end reconstructed)^{sin.} b) *P. ex gr. P. mnaidriensis* from Puntali Cave (NHMB-G.234i)^{sin.} c) Young *P. antiquus* from Neumark-Nord 1, Germany (LVH-E22,66).

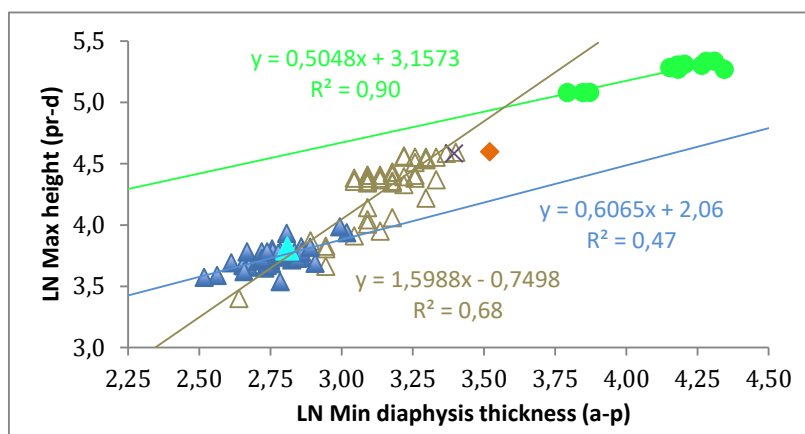


Fig. 3.40 Scatterplot of the dimensions of the mc IV. Min diaphysis thickness (a-p) vs. max height (pr-d). Refer to Fig. 3.3 for symbol legend. [Data: *P. tiliensis* from Theodorou, 1983: 210; *P. antiquus* from Palombo et al., unpublished].

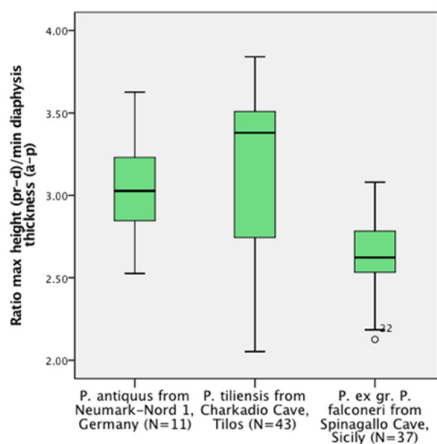


Fig. 3.41 Box-and-whisker plot of the ratio of the mc IV max height (pr-d)/min diaphysis thickness (a-p).

Max height (pr-d)/min diaphysis thickness (a-p) - Differences are not statistically significant between *P. antiquus* vs. *P. tiliensis* (Fig. 3.40; Fig. 3.41; MWU $p=0,233$). In contrast, differences are significant between *P. antiquus* vs. *P. ex gr. P. falconeri* (MWU $p=0,000$), indicating a thicker bone in the latter species. Significant differences also exist between *P. ex gr. P. falconeri* vs. *P. tiliensis* (MWU $p=0,000$), again indicating a thicker bone in *P. ex gr. P. falconeri*. Posture of the bone - When the angle formed between the proximal articular surface and the long-axis of the bone is compared one observes that posture is more digitigrade in *P. antiquus* and *P. ex gr. P. mnaidriensis* from Puntali Cave, Sicily than in *M. lamarmorai* (Fig. 3.39), implying biomechanical differences in function.

3.1.9.3 Metatarsal IV

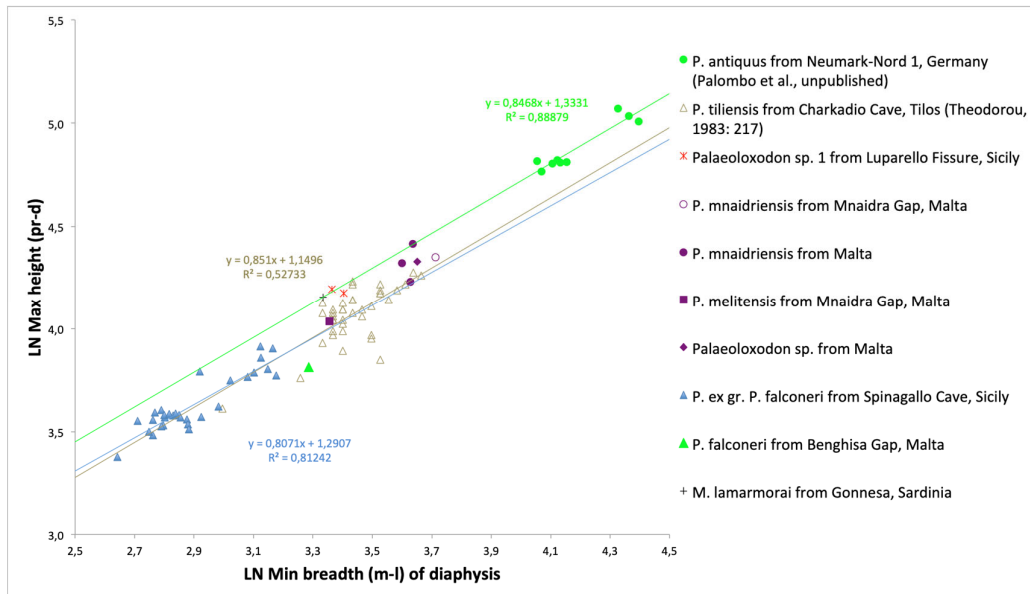


Fig. 3.42 Scatterplot of the min breadth (m-l) vs. max height (pr-d) of the mt IV.

Ratio max height (pr-d)/min diaphysis breadth (m-l) - Differences are not statistically significant between *P. antiquus* vs. *P. mnaidriensis* (Fig. 3.42; MWU $p=0,940$), or *P. antiquus* vs. *P. tiliensis* (MWU $p=0,060$), or *P. antiquus* vs. *P. ex gr. P. falconeri* (MWU $p=0,100$). Differences are however significant between *P. ex gr. P. falconeri* vs. *P. tiliensis* (MWU $p=0,000$), indicating a relatively taller bone in *P. ex gr. P. falconeri*.

3.2 DISCUSSION

The infrequent preservation of carpals and tarsals in the Spinagallo Cave assemblage - Carpals and tarsals are infrequently represented relative to the long-bones (see Ambrosetti, 1968: Table VIII; Table IX). This is particularly evident in the radial carpal, most likely due to its small absolute size and relatively large surface area (see Fig. 3.1; Fig. 3.9a-e). Since this bone has a proportionally large surface area (causing greater exposure to weathering), its infrequency thus likely resulted from taphonomic processes (see Von Endt and Ortner, 1984).

Variability in the *P. ex gr. P. falconeri* ulnar carpal - Previously, four size-frequency modes were identified in the much larger sample-size of long bones from Spinagallo Cave, (modes A, B, C, and D, see Ambrosetti, 1968: Figs 40, 42-48, 52; see also Raia *et al.*, 2001: 297). These were ascribed to A) juvenile females and males B) individuals in which a reduction in growth rate occurred as maturity approached*, C) adult females and D) adult males (Ambrosetti, 1968: 325).

*Ambrosetti attributed this size-frequency mode to a reduction in growth rate based on the observation that the growth-rate is known to decrease significantly in extant elephants during puberty, which may be coupled with an increase in mortality during this period.

Whether or not the modes in Fig. 3.4a are comparable to Ambrosetti's modes is debatable, since some allowance must be given for the smaller sample of ulnar carpi relative to the long bone assemblage. (Note that missing, mounted and damaged ulnar carpi were not included in this study, Ambrosetti, 1968: Table VIII reported 56 ulnar carpi, of which 45 were examined). However, since proboscideans typically display marked sexual size dimorphism, and sexual dimorphism has never been identified in the foot bone assemblage, it would be informative to distinguish between males and females.

Whether or not the two separate modes evident in Fig. 3.4b are attributable to sexual dimorphism or not is a possibility which requires more data to evaluate. From the PCA it may be concluded that the length/breadth of the ulnar carpal and the length/breadth of individual articular facets is generally correlated. Whether or not there may be sexual dimorphism in the allometry of the ulnar carpal's articular facet for the ulna could nonetheless not be definitively answered on the basis of the available evidence (cf. possible sexual dimorphism in *P. antiquus* in Palombo and Villa, 2003: 300). The diameter of the articular facet for the ulna is unrelated to all the other variables, and might perhaps relate to sexual dimorphism, although more data among extant Elephantinae species of known sex and age is needed to evaluate this possibility (which may be possible in future with greater *L. africana* or *P. antiquus* sample-size, cf. Marano and Palombo, 2013). As to why one *P. ex gr. P. falconeri* specimen (MPRU-SpC-UC35) has an unusually wide articular facet for the ulna is unknown, although variable UC9 (the breadth of the articular facet) in the PCA is moving in a direction of its own, unrelated to the other variables. One possibility therefore may be that variability in the breadth of the facet is attributable to ecophenotype, although age and sex may also influence morphology.

Variability in the *P. ex gr. P. falconeri* central tarsal - Large intraspecific differences were observed in morphology, with two out of nineteen individuals evidencing a posteriorly projecting articular facet for the calcaneus. The infrequency of this feature suggests it may be ecophenotypic/idiosyncratic rather than sexually dimorphic, since it is statistically improbable that a sample-size of 19 does not include both males and females (see Ambrosetti, 1968: 325 regarding the presence of males and females in the Spinagallo Cave assemblage).

3.2.1 Evolution and functional significance of the calcaneus' tibio-fibular facet

A striking morphological feature that appears to be autapomorphic in probable chronospecies *Palaeoloxodon* sp. 1 from Luparello Fissure and *P. ex gr. P. falconeri* is the presence of a tibio-fibular facet on the calcaneus. As to how this feature evolved is an interesting question since the facet is present in only one continental *P. antiquus* sampled. Its presence and morphology in insular species therefore likely resulted from several stages during anagenesis: (i) A continental *P. antiquus* population (and its insular sub-population) in which a small facet was occasionally present, (ii) an insular population of *Palaeoloxodon* sp. in which the presence of the facet likely increased in frequency, either due to selection, a bottle-neck effect or genetic drift. (iii) Finally, once always present it possibly increased in

relative size, perhaps representing an example of so-called intensification of function (*sensu* Mayr, 2001: 204).

Regarding the functional significance, the presence of a tibial facet suggests there may have been greater flexion in the ankle-joint than in other species. It has previously been suggested that body mass in *P. ex gr. P. falconeri* may have been shifted posteriorly relative to *P. antiquus*, based on the observation that the hip region is taller than the shoulder region in the former species (Larramendi and Palombo, 2015). Whether or not the shift in mass posteriorly has anything to do with the presence of the calcaneus' articular facet for the tibia is however uncertain.

Without additional data relating form, function and habitat in extant elephants the functional and taxonomic significance of the presence/absence of the tibial facet on the calcaneus in fossil insular and continental elephants are however difficult to fully understand. Nonetheless, the presence of a tibial facet in the *P. antiquus* specimen from Riano and its absence in the examined specimens from Neumark-Nord 1 may potentially be partly ecophenotypic because of the differences in topography between the two sites (the Riano surrounds being hillier in comparison to the Neumark-Nord 1 region). The sample of *L. africana* from different parts of Kenya in which the tibial facet is present also includes a single example in which the facet is absent (sample of N=13). The intraspecific presence/absence of the calcaneal tibial facet may also be an artefact of the small sample-size, although intraspecific differences among European *Palaeoloxodon* populations have also been reported (see Saegusa and Gilbert, 2008; Palombo and Ferretti, 2010; Anzidei *et al.*, 2012 for discussion). Pending a more exhaustive analysis of mainland elephants, the significance of the occasional presence/absence of the tibial facet within species remains an open question.

It is perhaps also noteworthy that the one calcaneus of *P. tiliensis* (THEODOROU *et al.*, 2007) examined also has a tibial facet (Fig. 3.24), suggesting that homoplasy may exist with *Palaeoloxodon* sp. 1 from Luparello Fissure and *P. ex gr. P. falconeri*. Tilos, like Sicily (and its palaeoislands) is an island where there may have been strong selection for elephants to reach inaccessible areas, such as the steep relief and rocky substrates of the higher elevations (cf. Theodorou, 1988).

3.2.2 Adaptive mechanisms in the tarsals of insular *Palaeoloxodon* spp.

Heterochrony in the calcaneus - On the basis of the morphological evidence examined here, there is little to suggest pedomorphism in the calcaneus of *P. ex gr. P. falconeri*, although in *Palaeoloxodon* sp. 1 from Luparello Fissure it cannot be discounted that there is some resemblance to the juvenile morphology of *P. antiquus* and *L. africana*. However, linear measurements are not particularly suitable for quantifying the ontogenetic allometry in the calcaneus, particularly with regard to ontogenetic changes in the morphology of the articular facet of the os t. IV. More research is therefore needed to reliably evaluate whether or not pedomorphism is completely absent in the calcaneus of *Palaeoloxodon* sp. 1 from Luparello Fissure and in *P. ex gr. P. falconeri*.

Possible evidence of stabilizing selection in *P. ex gr. P. falconeri* tarsals relative to *P. antiquus* - Interestingly, although samples-sizes for *P. antiquus* are generally smaller than in *P. ex gr. P. falconeri* from Spinagallo Cave, there is sometimes still a smaller range in variability in *P. ex gr. P. falconeri* than in *P. antiquus*, such as evidenced in the articular facets of the astragalus and in the radial carpal. If one assumes that variability in the Neumark-Nord 1 sample is representative of the ancestor of *P. ex gr. P. falconeri*, the smaller range of intraspecific variability in *P. ex gr. P. falconeri* may suggest a bottleneck effect or perhaps constitute evidence of stabilizing selection in *P. ex gr. P. falconeri* (cf. Scarborough *et al.*, 2016: 116). However, with regard to the assumption that *P. antiquus* variability in the NN1 sample is representative, only limited comparisons have been made in this thesis between NN1 and other sites, excluding various other Middle and southern European sites (such as from Germany, Spain and Italy). Furthermore, there may be some suggestions of *P. antiquus* variability between sites as seen in Fig. 3.32 and Fig. 3.33b, although more research is needed to better understand *P. antiquus* variability in the appendicular skeleton before the possibility of stabilizing selection in *P. ex gr. P. falconeri* can be more fully evaluated.

3.2.3 Limitations of classifying developmental stages in foot bones

As pointed out in Chapter 2, for disassociated calcanei and metapodials which possess epiphyses which fuse over the course of ontogeny, it is possible to obtain some measure of ontogenetic stage. In practice this cannot be as frequently achieved as in the long-bones, which tend to be better-preserved due to taphonomic process: the tuber of the calcaneus in dwarf elephants is often damaged (Fig. 3.1-2; Fig. 3.2-5), and in metapodials the epiphyses tend to be fully-fused or completely unfused. However, a measure of ontogenetic equivalence was accounted for in metapodials in which the bivariate plots included measurements of the maximum height including epiphyses (Fig. 3.38a; Fig. 3.38c; Fig. 3.38d; Fig. 3.40; Fig. 3.42). Particularly for the footbones without epiphyses which therefore contain an unknown level of ontogenetic variation, conclusions about static adult allometry and evolutionary allometry (see Table 2.9) need to be treated with more caution.

3.2.4 Gross manual and pedal functional morphology and possible autapomorphies

In this section the functional morphology of the manus and pes of each species is considered as a whole, focussing on morphological features that are likely to be autapomorphic and have altered the function of the foot with respect to *P. antiquus*. The discussion below proceeds from the smallest to largest species.

(i) Manus of *P. ex gr. P. falconeri* (Fig. 3.1-B) - In terms of gross anatomy, one of the most frequently cited differences in manus anatomy between species is carpal structure. Carpal structure is termed *serial* where each distal carpal corresponds to a bone of the proximal row, and *aserial* where the breadth (m-l) of the intermediate carpal exceeds the underlying os c. III (Fig. 3.1; see Lister, 1996b: 207; Palombo and Villa, 2003: 299; Ambrosetti, 1968: Fig. 39; see also Trevisan, 1948; Dubrovo and Jakubowski, 1988, Lister, 1996b; but see also Ferretti and Croitor, 2001: 106). The carpus of *P. ex gr. P. falconeri* was described as markedly aserial relative to *P. antiquus* based on a single *P. ex gr. P. falconeri* foot preserved in

anatomical connection (Ambrosetti, 1968: 318; *ibid*: Fig. 39; see also reconstructed foot in Fig. 3.1-B1). Although there is no reason to doubt that the *P. ex gr. P. falconeri* carpus may in fact have a tendency to be more aserial with respect to *P. antiquus*, two important considerations were not taken into account by Ambrosetti, namely: (i) Carpus structure varies within species, and *P. antiquus* carpus structure has been described as both serial and aserial (Andrews and Cooper, 1928; Dubrovo and Jakubowski, 1988; Palombo and Villa, 2003: 299); (ii) Secondly, there is much variability in the breadth (m-l) of the *P. ex gr. P. falconeri* os c. III (Fig. 3.11), suggesting that there may be more variability in *P. ex gr. P. falconeri* carpus structure than previously recognised (see Ambrosetti, 1968: 318; *ibid*: Fig. 39).

Element		<i>P. antiquus</i> from Neumark-Nord 1, Germany	<i>P. ex gr. P. falconeri</i> from Spinagallo Cave, Sicily
Radial carpal		Less long (a-p) articular facet for the os c. II	Long (a-p) articular facet for the os c. II
Ulnar carpal		Ulnar facet wider	Ulnar facet less wide
Os c. III	Max thickness (a-p)/max cranial breadth (m-l)	More thick (a-p)	Less thick (a-p)
	Max length (a-p)/max breadth (m-l) of the articular facet for the mc III	Broader	Less broad
	Max cranial breadth (m-l)/max caudal breadth (m-l)	Greater caudal breadth	Less broad caudally
	Max cranial height (pr-d)/max thickness (a-p)	Taller in <i>P. antiquus</i> than the other Elephantinae species	Less tall

Table 3.10 Summary observations comparing the morphology of select carpals in *P. antiquus* from Neumark-Nord 1, Germany and *P. ex gr. P. falconeri* from Spinagallo Cave, Sicily.

According to Ambrosetti the distal end of the radius plays a greater role in articulation with the proximal carpals in *P. ex gr. P. falconeri* compared with *P. antiquus* (Ambrosetti, 1968: 311). However, no statistically significant differences were found in the articular facet for the radius on the intermediate carpal between these species, and the length/breadth of the radial carpal's articular facet is not significantly different. Ambrosetti's conclusion may therefore have been biased due to small sample-size and visual rather than metric comparison between *P. antiquus* and *P. ex gr. P. falconeri*.

(ii) Pes of *P. ex gr. P. falconeri* (Fig. 3.2-B) - The pes is highly derived and displays autapomorphies in the calcaneus, astragalus and os t. IV (Table 3.11). Limited medio-lateral displacement of the calcaneus is suggested by the wide articular facet for the fibula, and increased flexion in the ankle-joint is suggested by the calcaneus' large articular facet for the tibia which also suggests that body mass is shifted more from the astragalus posteriorly onto the calcaneus. The tuber projects far posteriorly (Fig. 3.2-B2; Fig. 3.2-B3), which may (perhaps) be an indication that the *gastrocnemius* and *soleus* muscles which attach to the end

of the tuber had more leverage than in *P. antiquus*. Another morphological feature with possible functional significance includes the deep plantar niche on the os t. IV for the proximal articular surfaces of the mt IV and mt V (see position of os t. IV in anatomical reconstruction in Fig. 3.2-B3f and Fig. 3.2-B1f; the deep plantar niche in Fig. 3.34A; Fig. 3.35-1C), which likely limited displacement of the proximal articular surfaces of these metatarsals compared with *P. antiquus* (Fig. 3.35-4c; Fig. 3.35-5c). The absence of areas for the insertion of tendons on the distal surface of the central tarsal of *P. ex gr. P. falconeri* is difficult to explain, but may potentially be a consequence of functional constraints relating to a size-reduction threshold for maintenance of function in tendons (cf. Hanken and Wake, 1993). Overall, compared with *P. antiquus*, it is likely that the joint excursion angle of the ankle-joint was increased, whereas medio-lateral displacement was reduced (by the synostotically fused tibia-fibula and the calcaneus' large articular facet for the fibula).

	<i>P. antiquus</i> from Neumark-Nord 1, Germany	<i>P. ex gr. P. falconeri</i> from Spinagallo Cave, Sicily
Central tarsal	Wide articular facet for the astragalus, more curved in cranial aspect	Narrow articular facet for the astragalus. Articular facet for calcaneus sometimes less prominent
Os t. IV	Shallow niche for articulation with the mt IV and mt V	Deep niche for articulation with the mt IV and mt V
Astragalus	Large articular facet for the central tarsal	Narrow articular facet for the central tarsal
Calcaneus	Typically no tibial facet	Large and more-or-less continuous tibio-fibular facet

Table 3.11 Summary observations comparing tarsal morphology in *P. antiquus* from Neumark-Nord 1, Germany and *P. ex gr. P. falconeri* from Spinagallo Cave, Sicily.

(iii) Manus of *Palaeoloxodon* sp. 1 from Luparello Fissure - The sample from Luparello Fissure is small, but several allometric proportions fall outside of the range of variability in other *Palaeoloxodon* species, including the proportions of the ulnar carpal's articular facet for the ulna, which is considerably wider (m-l) in *Palaeoloxodon* sp. 1 from Luparello Fissure than in *P. ex gr. P. falconeri* (Fig. 3.6b). Interestingly, although sample-size is again small, this articular facet is also relatively narrow in *Palaeoloxodon* sp. from Malta. Since the two islands differ much in topography, one possibility is that this is related to a wider articular facet restricting medio-lateral movement ('low-gear locomotion'), or perhaps genetic drift or a bottleneck effect that may have occurred when Malta was colonised from Europe via Sicily.

iv) Pes of *Palaeoloxodon* sp. 1 from Luparello Fissure - The calcaneus is highly derived with a tibio-fibular facet, with a tendency to evidence greater separation between the tibial and fibular facets than in *P. ex gr. P. falconeri* (the functional significance of which is discussed below). The wide range in absolute size from Luparello Fissure and variation in the morphology of its tibio-fibular facet strongly suggest the presence of anagenesis within the assemblage.

v) Manus of *P. ex gr. P. mnaidriensis* - The small sample-size and absence of several elements made it difficult to investigate the functional morphology of the forefoot. One particularly noticeable morphological feature however includes the Zà Minica Cave (see

Fabiani, 1932b) radial carpal's absence of a clearly defined proximal articular facet for the intermediate carpal. This contrasts with its presence in all other Elephantinae species examined in this thesis (Fig. 3.9a,b,d,e), as well as in examples figured the literature (Andrews and Cooper, 1928: Plate III-1A, 1B, 1C, 1D; Smuts and Bezuidenhout, 1993: Fig 16-2; Halámková, 2006: Plate 12; Athanassiou, 2012: Fig. 16-c). Also of note is the Puntali Cave os. c. III's wide and parallel-sided shape which has no projection on the caudo-lateral end (Fig. 3.12-3E), a feature which is more evident in other species (especially *P. antiquus* and *P. ex gr. P. falconeri*). Few, if any functional inferences may be made about the manus as a whole due to the absence of several elements and small sample-sizes (N=2 for the radial carpal, and N=1 for the os. c. III). It is still noteworthy that the radial carpal's absence of a proximal articular facet for the intermediate carpal (which is absent in both *P. ex gr. P. mnaidriensis* specimens from Zà Minica Cave), is present in all other specimens of Elephantidae species studied by the author, perhaps suggestive that this feature might be autapomorphic for *P. ex gr. P. mnaidriensis* if additional samples substantiate this observation.

(vi) Pes of *P. ex gr. P. mnaidriensis* - Features which are likely morphologically derived with respect to *P. antiquus* are present in the calcaneus, including the large lateral articular facet between the astragalus and calcaneus, as well as the large articular facet for the fibula on the calcaneus. These suggest a greater proportion of mass was transmitted on the lateral side of the hindfoot than in *P. antiquus* from Neumark-Nord 1, and perhaps a more restricted motion in the medio-lateral direction. One of the possible functional significances for this would be adaptation for the avoidance of twisting the ankle due to the hilly topography of Sicily.

(vii) Manus of *M. lamarmorai* (Fig. 3.1-C) - Only the distal carpus is represented, but the os. c. III is noticeably broad (m-l) and parallel-sided (m-l), contrasting with *P. antiquus* (Fig. 3.1-A) and the morphology of the carpals are allegedly more similar to *M. meridionalis* than *P. antiquus* (Palombo *et al.*, 2012: 164). *Brachydactyly in the metapodials of the manus* - The toes of the *M. lamarmorai* manus (Fig. 3.1-C1) are more splayed than in *P. antiquus* (Fig. 3.1-A1) and *P. ex gr. P. falconeri* (Fig. 3.1-B1). Two of the possible reasons for more splayed toes possibly include: a) They may be more suitable for walking on certain substrates, such as marshy ground or unconsolidated sand (Benz, 2005: 101); b) The body mass in *M. lamarmorai* may be shifted more towards the forelimbs than in *Palaeoloxodon* spp. requiring different functional anatomy, Since foot size generally scales with mass (Cumming and Cumming, 2003) and *M. meridionalis* and *M. trogontherii* both had arched backs and likely supported more of their mass through the forelimbs (see Larramendi, 2016: Appendix), it is possible that *M. lamarmorai* also had an arched back which shifted more mass onto the forelimbs relative to *P. antiquus*.

(viii) Pes of *M. lamarmorai* (Fig. 3.2-C) - The *M. lamarmorai* calcaneus differs from all the others species (genera *Mammuthus*, *Palaeoloxodon*, *Loxodonta* and *Elephas*) examined in possessing expanded lateral articular facets between the astragalus-calcaneus (Fig. 3.21-8C; Fig. 3.15-7B) and a very narrow articular facet for the fibula (Fig. 3.2-C3b; Fig. 3.21-8B).

The fibular facet is only slightly convex and vertically orientated compared with the other species, suggesting that little body mass was transmitted via the fibula. This suggests much of the body mass was transmitted compressionally by the astragalus-calcaneus, and perhaps only small medio-lateral forces were involved during locomotion. Perhaps the large articular facet between the astragalus-calcaneus also compensated for the transmission of little body mass via the fibular facet, reducing medio-lateral displacement. The calcaneus' broad tuber (Fig. 3.2-C2b) provided a large attachment surface for the *gastrocnemius* and *soleus* muscles (Caloi *et al.*, 2004: 237). Although it is not known to what extent there is variability since the pes is only represented by one individual, a conspicuous feature in *M. lamarmorai* is that the os t. III (Fig. 3.2-C1e) does not articulate with the mt IV. In continental mammoths for which feet are illustrated in the literature, the os t. III also does not articulate with the mt IV, as seen in *M. meridionalis* (Halámková, 2006: Plate 31), *M. trogontherii* (Shpansky *et al.*, 2012: Plate 11-Fig. 3) and *M. primigenius* (Mol and de Vos 1995; Fig. 5). In contrast, the os t. III articulates with the mt IV in *P. antiquus* (Fig. 3.2-A1e), and to a lesser extent in *P. ex gr. P. falconeri* (Fig. 3.2-B1e; Caloi *et al.*, 2004: 237).

With regard to the posture in the metapodials *M. lamarmorai* appears semi-plantigrade (slightly flat-footed) compared to *Palaeoloxodon* spp. In extant elephants the toes are digitigrade in the forefoot and semiplantigrade in the hindfoot (Mikota *et al.*, 1994: 137). The reasons for these differences may include adaptations to different topographies, differences in ecological niche, or the type of locomotion (cursorial vs. non-cursorial, refer to discussion in Chapter 5). However, it is possible that evolutionary history may also have influenced posture, as demonstrated in the toes of *Anancus* and *Mammuthus* found in the same region, but displaying different toe postures (see Mol *et al.*, 1999: Fig. 5). While comparing *M. lamarmorai* with *Palaeoloxodon* species is useful for functional and ecological analysis, further comparisons with continental mammoths (*M. trogontherii* or *M. meridionalis*) are needed for evolutionary analysis.

3.3 CONCLUSIONS

The purpose of this Chapter was to test Hypothesis I (*The feet of elephants from Sicily differ significantly in terms their morphology compared with their ancestral species and contemporary P. antiquus*) by comparing Elephantinae species from Sicily, Malta and Europe. As predicted in Chapter 1, the allometry of the articular facets of insular *Palaeoloxodon* spp. are significantly different to those of *P. antiquus*, particularly the articular facets of the ankle-joint of *P. ex gr. P. falconeri*, and, to a lesser extent in the forefoot.

Anatomy of the manus in relation to Hypothesis I - This chapter examined the overall morphology and allometry of articular facets of select carpals, and has demonstrated large morphological differences in the articular facets of the radial carpal between *P. antiquus* and *P. ex gr. P. mnaidriensis* (Fig. 3.9). Additionally, the sole os c. III belonging to *P. ex gr. P. mnaidriensis* from Puntali Cave widens anteriorly, as does the *M. lamarmorai* type-specimen, differing from other *Palaeoloxodon* spp. The presence of differences in the carpals of insular

species compared with mainland *P. antiquus*, while not fully understood, do not clearly evidence selection for low-gear locomotion.

Anatomy of the pes in relation to Hypothesis I – Large differences were found in the anatomy of the ankle-joint between *P. antiquus* and *P. ex gr. P. falconeri*, particularly in the calcaneus. The functional significance of the articular facet for the tibia on the calcaneus however remains only partially understood, but likely increased the range of flexion in the ankle-joint, and may have acted as a braking mechanism for walking downslope. The relatively wide articular facet for the fibula on the calcaneus in *P. ex gr. P. falconeri* and synostosis between the tibia-fibula possibly evidence low-gear adaptations in the hindfoot of this species. These observations also tend to suggest reduced medio-lateral mobility and increased antero-posterior mobility in the hindfoot of *P. ex gr. P. falconeri*. Additionally, several features in the tarsals tentatively suggest a reduction in body mass may be one of the contributing causes of morphological changes in the feet of *P. ex gr. P. falconeri* (see Section 5.4.1).

CHAPTER 4

Insular adaptations in limb musculoskeletal anatomy

This chapter investigates the morphology of the shoulder joint and of the long bones in continental and insular Elephantinae, using a combination of bivariate allometry and anatomical descriptions of bone morphology, including the morphology of muscle attachment scars on the long bones. The purpose of the chapter is to test Hypothesis II and Hypothesis III (see Table 4.1) and to provide a better understanding of how the long bones differ between different species of the genus *Palaeoloxodon*. To begin with, the chapter provides a brief overview of previous studies on the bivariate and multivariate allometry of the long bones belonging to insular *Palaeoloxodon* spp. The chapter further compares the allometry of the scapula, and allometry and morphology of each of the long bones. The chapter concludes with a discussion on the reasons for major morphological differences between species in each of the skeletal elements examined.

Hypothesis	Description	Elements	Predictions
Hypothesis II	Heterochrony causing dwarfism resulted in pedomorphic morphologies in the limbs of <i>P. ex gr. P. falconeri</i>	Humerus, ulna, femur, tibia	The long bones of <i>P. ex gr. P. falconeri</i> more closely resemble juvenile <i>L. africana</i> than adult <i>L. africana</i> in terms of bivariate allometry and overall morphology
Hypothesis III	As mass decreases in dwarf elephant species' gait becomes more agile in the a-p direction	Scapula	In comparing <i>P. ex gr. P. falconeri</i> and <i>P. antiquus</i> , the glenoid fossa is deeper, and longer in the a-p direction relative to the m-l direction in the former species

Table 4.1 Hypotheses and predictions tested in Chapter 4. Hypothesis II is primarily metrically examined in the tibia of *P. ex gr. P. falconeri*.

Previous allometric studies of the long bones of insular *Palaeoloxodon*

The interspecific bivariate and multivariate allometry of the long bones of Sicilian and Maltese *Palaeoloxodon* spp. has been described before, notably by Herridge (Herridge, 2010: 281-310; 319-320; 334-341; 350-351), in a study including the bivariate ontogenetic allometry of *L. africana*, *E. maximus* and *P. tiliensis* (Herridge, 2010: Fig. 6.11). This study examined adult static-allometry*¹ and evolutionary allometry/interspecific juvenile morphology² and comparisons with a combined juvenile and adult sample³.

These results demonstrated that the long bones of continental European *Palaeoloxodon* spp. and Mediterranean insular species are broadly similar in terms of ontogenetic and static-adult allometry patterns (Herridge, 2010: 319; see also Raia *et al.*, 2001). Furthermore, patterns of intraspecific ontogenetic allometry were characterised by isometry, and static-adult allometry by negative allometry (a relative increase in slenderness with absolute size). Interspecific limb-bone allometry on the other hand (between full-sized and dwarf taxa and for full-sized taxa alone), appeared to be explained by shared *grade-shifted* ontogenetic trajectories (see Herridge, 2010: 350). The differences in scaling predicted by different

*Refer to Table 2.5 for categories of allometric comparisons. ¹Herridge, 2010: Table 6.20; Fig. A11.1; Table A12.1; Table 6.21; Fig. A11.2; Table A12.2; Table 6.22; A11.3; Table A12.3; Table 6.23; A11.4; A12.4 ²Herridge, 2010: Table 12.5; Table A12.6; Table A12.7; Table A12.8. ³Herridge, 2010: Table A12.9; Table A12.10; Table A12.11; Table A12.11.

models (see Chapter 2) were furthermore found to be generally small (Herridge, 2010: Tables 6.10; 6.13; 6.20; see Raia *et al.*, 2001).

Although interspecific patterns in bivariate and multivariate allometry have been investigated before, the musculo-skeletal morphology of the long bones has never been described in detail in Sicilian *Palaeoloxodon* spp. Similarly, although the scapula has been described in continental and insular Elephantinae species (e.g. Andrews and Cooper, 1928: 3, Fig. 1-2; Trevisan 1948; Maccagno, 1962a: 107; Ambrosetti, 1968: 307-308; Roth, 1982: 199-202; Kroll, 1991: 19; Smuts and Bezuidenhout, 1993: 2-3; Bonfiglio *et al.*, 1996: 380), there are few measurements of Elephantinae species in the published literature with which to compare Sicilian *Palaeoloxodon* spp. This chapter therefore investigates the bivariate allometry of the glenoid fossa of the scapula, followed by an examination of the bivariate allometry and musculo-skeletal morphology of the humerus, ulna, femur and tibia.

4.1 RESULTS

4.1.1 Bivariate allometry of the scapula's glenoid fossa

The blade of the scapula is proportionately seldom intact in the Spinagallo Cave assemblage (Ambrosetti, 1968: Fig. 28), which is consistent with its greater fragility (Accordi and Colaccichi, 1962: 226) and specimens without a fused glenoid fossa are nearly entirely absent (likely attributable to the porosity and fragility of the juvenile scapula). However, the glenoid fossa, being the most robust part of the scapula is evidently frequently preserved completely, most likely due to its robusticity (see also Adams, 1874 Pl. XII), so that the sample-size for *P. ex gr. P. falconeri* from Spinagallo Cave is large (Fig. 4.1). Unlike the long bones it was not useful to subdivide epiphyseal fusion stages of the glenoid fossa (other than discriminating between fused and unfused specimens) since virtually only completely-fused examples are represented in fossil assemblages.

4.1.1.1 Intraspecific variability in *P. ex gr. P. falconeri*, *P. antiquus* and *L. africana*

(i) *P. ex gr. P. falconeri* from Spinagallo Cave - Chord length (a-p) and surficial length* (a-p) were found to be highly correlated (Fig. 4.1d, $R^2=0.97$). In contrast chord breadth (m-l) vs. surficial length (a-p) are less highly correlated (Fig. 4.1b, $R^2=0.75$), as is the case in chord length (a-p) vs. chord breadth (m-l) (Fig. 4.1c, $R^2=0.79$). (ii) *P. antiquus* from Neumark-Nord 1 - The sample is more biased towards older individuals (see Marano and Palombo, 2013: Table 3), such that a limited range in ontogeny represented (Fig. 4.2b-d). (iii) *L. africana* from Kenya - In contrast to the aforementioned samples, in *L. africana* juvenile specimens without fused epiphyses were also sampled in order to more adequately investigate a greater range in ontogeny than possible in the fossil assemblages. Measurements on the unfused glenoid fossa are nevertheless only approximately comparable to measurements on the glenoid fossa with fused epiphyses as the dimensions are slightly smaller for the former.

*Refer to Fig. 2.11 for measurement descriptions.

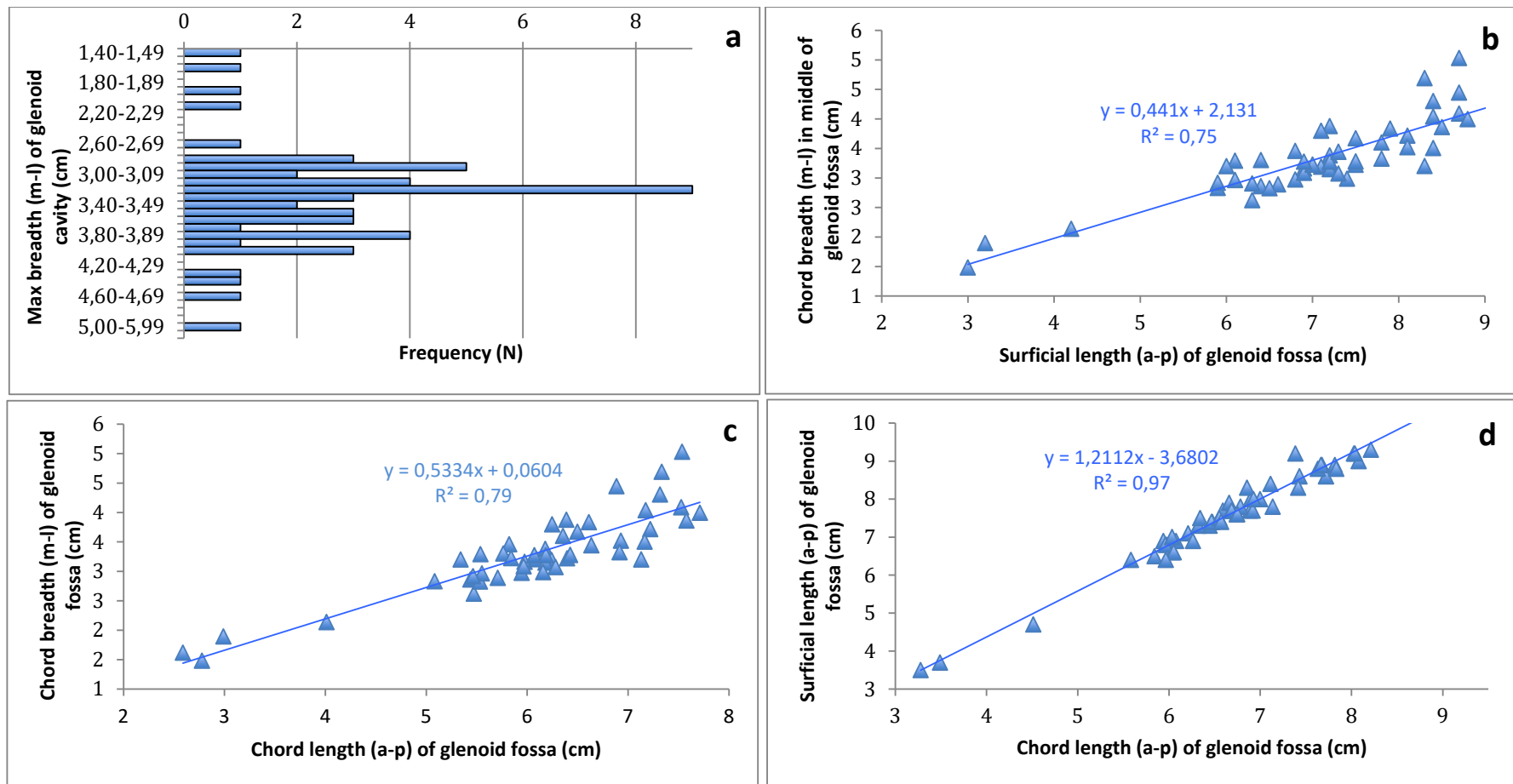


Fig. 4.1 Dimensions of the scapula's glenoid fossa in *P. ex gr. P. falconeri* from Spinagallo Cave, Sicily (all specimens belonging to older individuals with fused fossae including articular surface). a) Size-frequency histogram of the max breadth of the glenoid fossa. b) Scatterplot of the chord breadth (m-l) vs. surficial length (a-p). c) Scatterplot of the chord length (a-p) vs. chord breadth (m-l). d) Scatterplot of the chord length (a-p) vs. surficial length (a-p). For the significance of the size-maxima A-D in Fig. 4.1a see Section 4.2.1 and cf. Ambrosetti, 1968: Figs 40, 42-48, 52.

- *P. antiquus* from Neumark-Nord 1, Germany (fused glenoid epiphyses)
- ▲ *P. ex gr. P. falconeri* from Spinagallo Cave, Sicily (fused glenoid epiphyses)
- *L. africana* from Kenya (fused glenoid epiphyses)
- × *L. africana* from Kenya (unfused glenoid epiphyses)

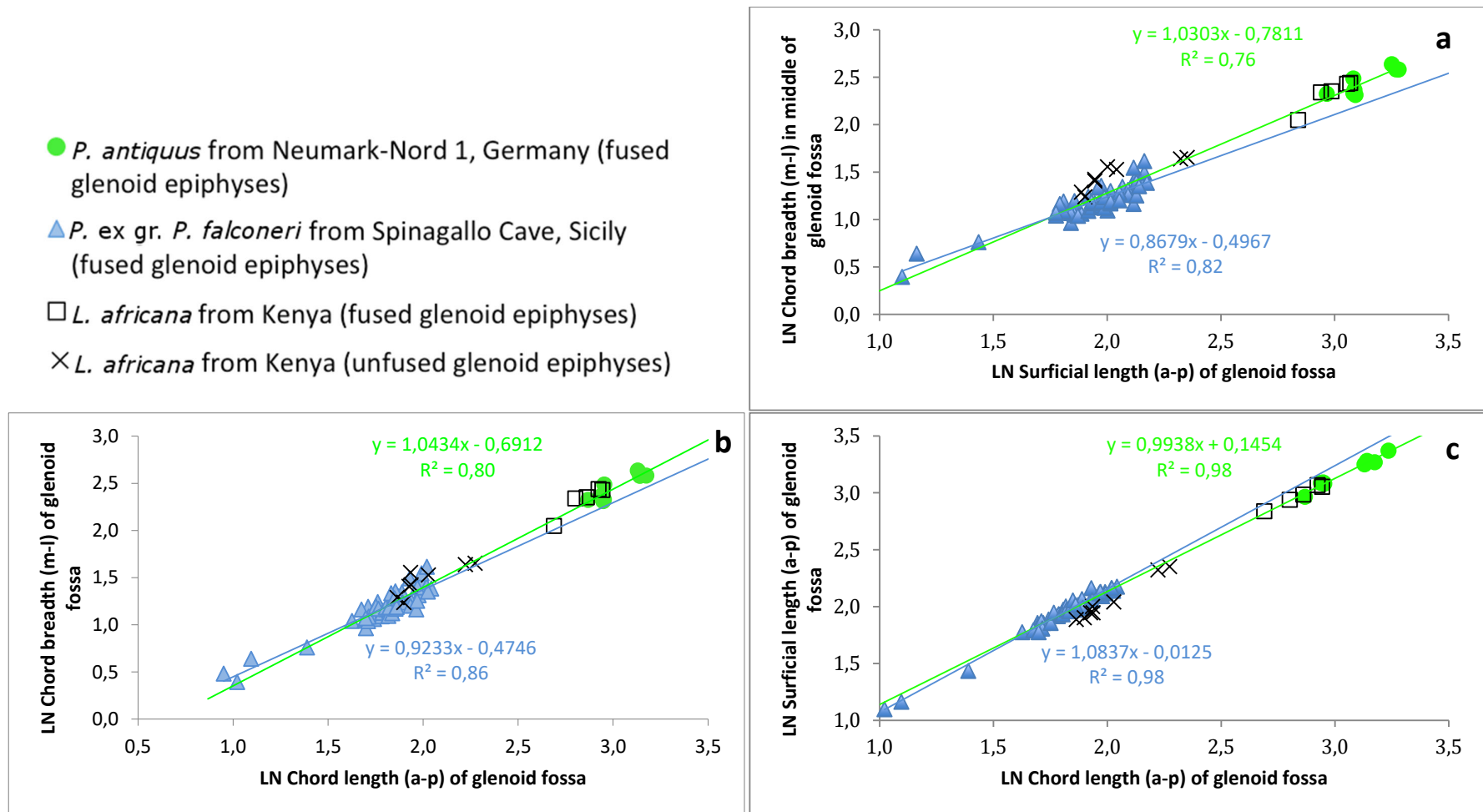


Fig. 4.1 Scatterplots of the dimensions of the scapula's glenoid fossa a) Surficial length (a-p) vs. chord breadth (m-l). b) Chord length (a-p) vs. surficial length (a-p). c) Chord length (a-p) vs. chord breadth (m-l). Note that comparisons between *L. africana* specimens with unfused and fused with epiphyses are only more-or-less comparable.

Measurements in juvenile *L. africana* are therefore only included in order to investigate whether major changes occur during ontogeny in *L. africana*. The results nevertheless indicate that allometry is broadly similar for juvenile and adult *L. africana* (Fig. 4.2).

4.1.1.2 Interspecific bivariate allometry

The results demonstrate statistically significant differences between *P. ex gr. P. falconeri* vs. *L. africana* with fused epiphyses (Table 4.2), reflecting a relatively broad glenoid fossa in *L. africana* (Table 4.2; Fig. 4.2a, b) although sample-size is small for the latter species.

	Surficial length (a-p)/chord breadth (m-l)	Chord length (a-p)/chord breadth (m-l)	Surficial length (a-p)/chord length (a-p)
Figures	Fig. 4.2a	Fig. 4.2b	Fig. 4.2c
<i>P. antiquus</i> vs. <i>L. africana</i>	0,524	0,354	0,518
<i>P. antiquus</i> vs. <i>P. ex gr. P. falconeri</i>	0,028*	0,057	0,133
<i>P. ex gr. P. falconeri</i> vs. <i>L. africana</i>	0,040*	0,340*	0,502

Table 4.2 Mann-Whitney U-test p-values on interspecific bivariate allometric comparisons of the scapula's glenoid fossa. Refer to Fig. 4.2 for the associated scatterplots. Note that the calculated MWU p-values exclude *L. africana* individuals in Fig. 4.2 with unfused glenoid epiphysis.

In contrast, there are no statistically significant differences between *P. antiquus* and *L. africana* (Table 4.2), although sample-size is again small for *L. africana* with fused epiphyses (Fig. 4.2). Between *P. antiquus* vs. *P. ex gr. P. falconeri* the ratio of surficial length (a-p)/chord breadth (m-l) is significantly different (Table 4.2), reflecting a relatively greater surficial length (a-p) in *P. ex gr. P. falconeri*. The ratio of the surficial length (a-p)/chord length (a-p) is however not significant between *P. antiquus* and *P. ex gr. P. falconeri* as might be expected from Hypothesis III, although the comparison of the mean reveals a slightly deeper glenoid fossa in *P. ex gr. P. falconeri* (Fig. 4.2) although differences are not statistically significant (MWU p=0,133). There is thus little support for Hypothesis III which predicted that the glenoid fossa in *P. ex gr. P. falconeri* would evidence greater depth and antero-posterior length than *P. antiquus*, increasing the range in rotation of the humeral head.

4.1.2 Anatomy of the humerus

The humerus presents proximal and distal epiphyses and the diaphysis (Fig. 4.3-4.8). The head is elongated craniocaudally and articulates with the scapula (Fig. 4.4e). The *Sulcus intertubercularis* is situated cranially to the head and flanked laterally by the cranial part of the major tubercle (Fig. 4.4e). From each of the tubercles there is a ridge for muscular attachment that runs onto the body of the humerus (Fig. 4.4a). The deltoid tuberosity is represented by a prominence in the proximal third of the lateral surface of the shaft (Fig. 4.4a). On the caudolateral side of the tuberosity there is a niche for the insertion of the deltoid

4.1.2.1 Cranial profile of the humerus

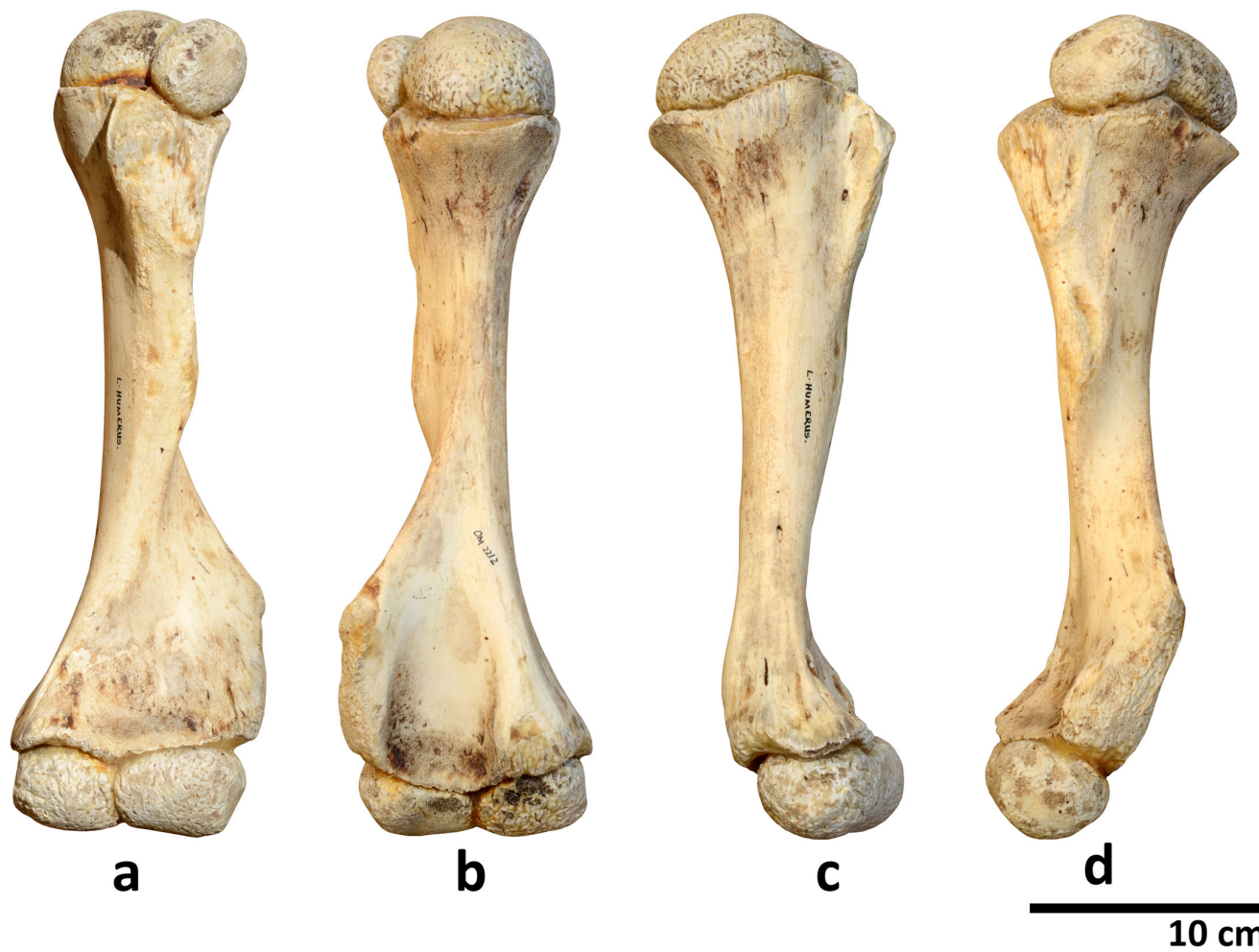


Fig. 4.2 Humerus of juvenile *L. africana* from Kenya a) cranial b) caudal c) medial d) lateral (KNM-OM2212)^{sin}. Refer to Table 2.8 for ontogenetic metadata.

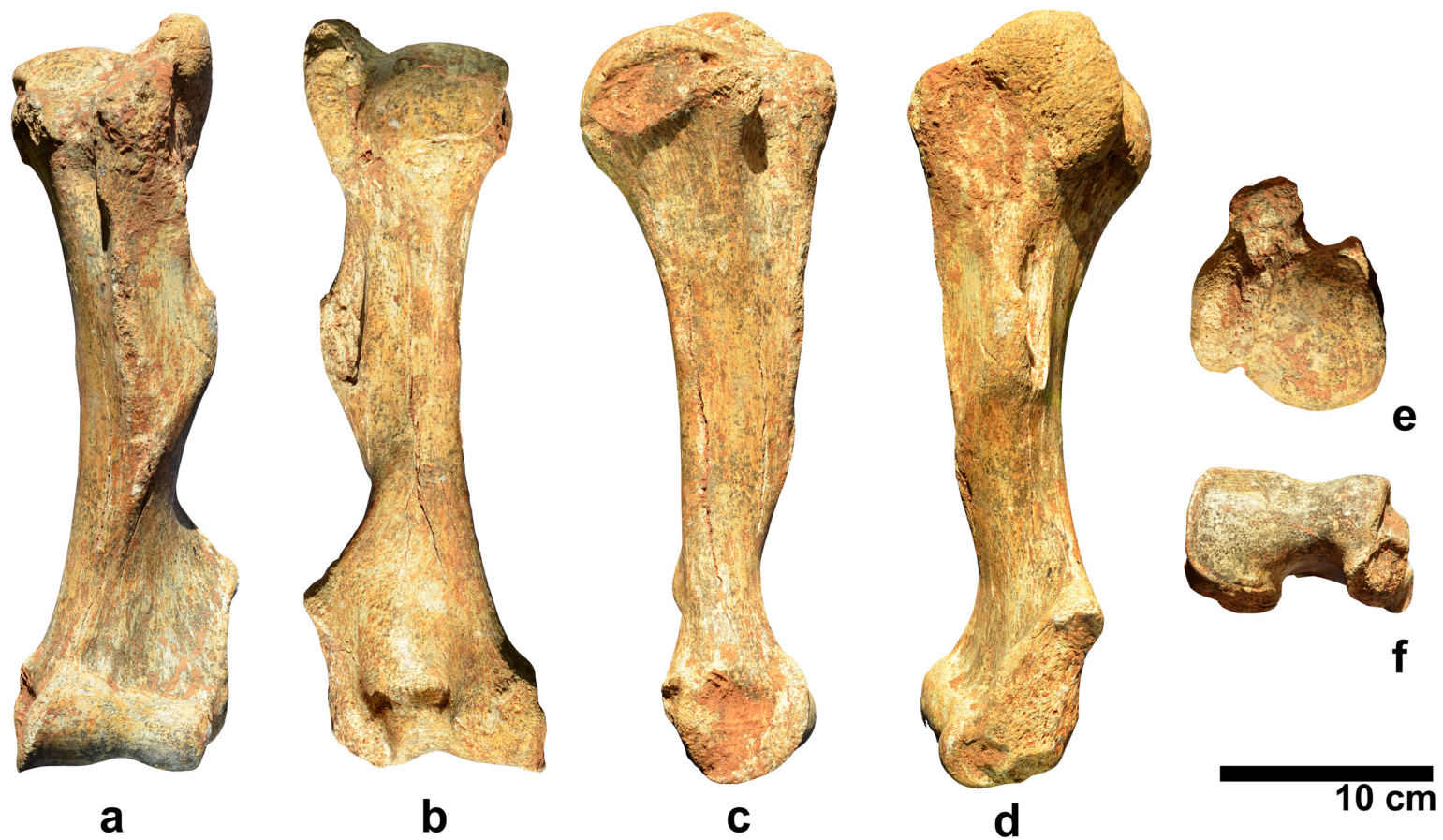


Fig. 4.3 Humerus of *P. ex gr. P. falconeri* from Spinagallo Cave, Sicily a) cranial b) caudal c) medial d) lateral e) superior f) inferior (UCat)^{dex}.



Fig. 4.4 Humerus (partially reconstructed) of *Palaeoloxodon* sp. 1 from Luparello Fissure, Sicily a) cranial b) caudal c) medial d) lateral e) superior f) inferior (IPH-F2932)^{sin}.



Fig. 4.5 Humerus of *P. ex gr. P. mnaidriensis* from Puntali Cave, Sicily a) cranial b) medial c) lateral d) caudal e) superior f) inferior (GMP-560. 104)^{sin}.

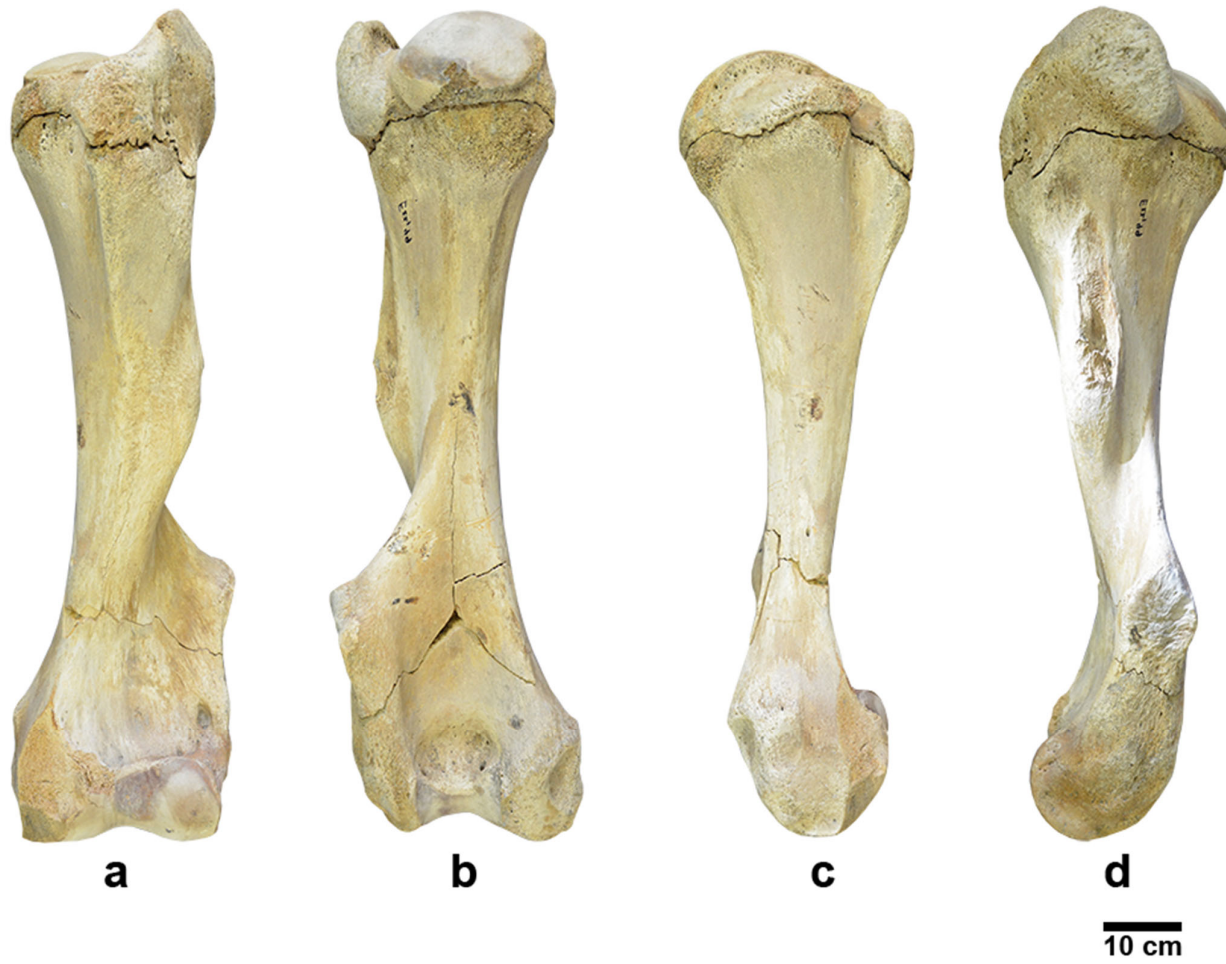


Fig. 4.6 Humerus of young *P. antiquus* from Neumark-Nord 1, Germany a) cranial b) caudal c) medial d) lateral (LVH-NN-E22)^{dex}. Refer to Marano and Palombo, 2013: Table 3 for ontogenetic metadata.

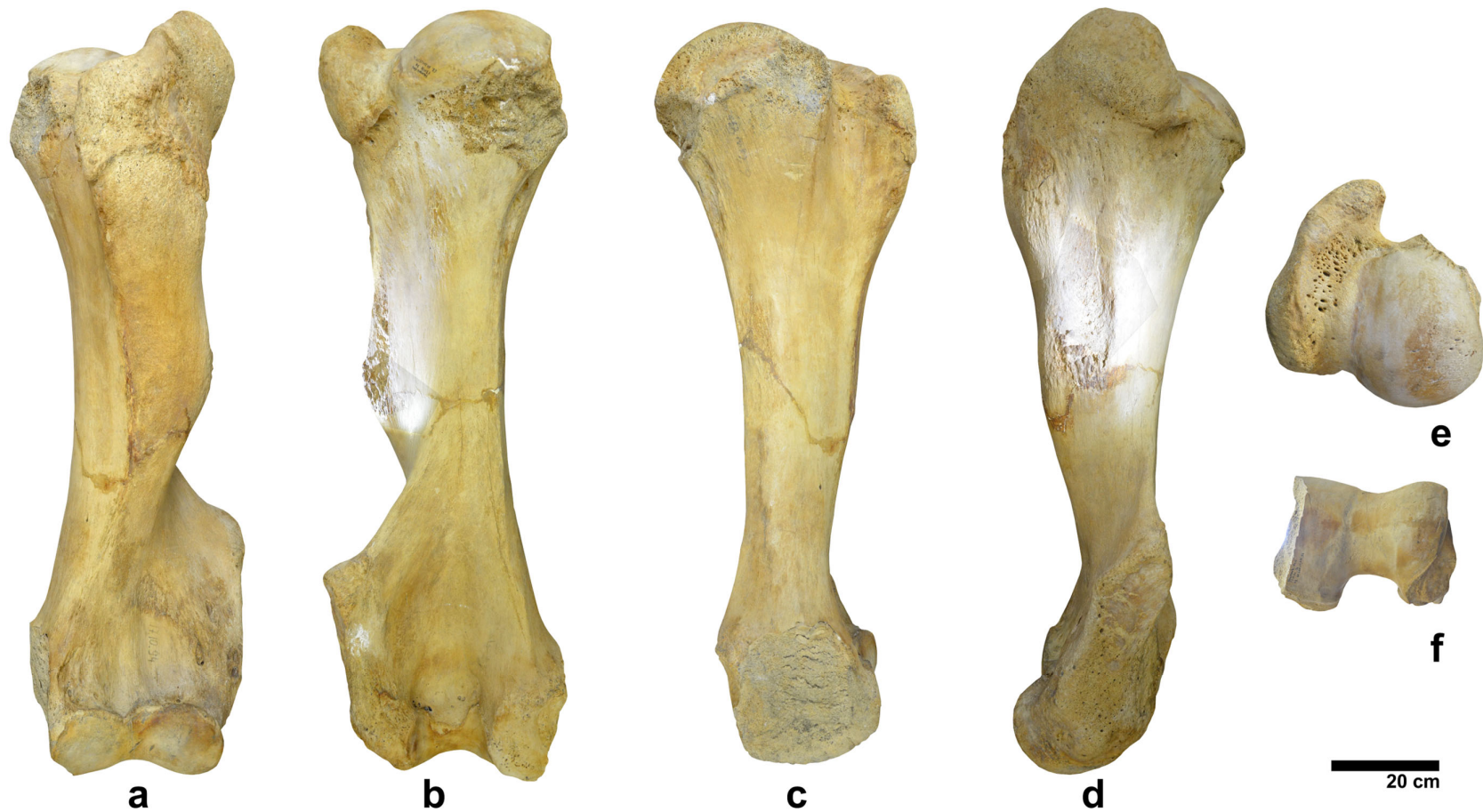


Fig. 4.7 Humerus of adult *P. antiquus* from Neumark-Nord 1, Germany a) cranial b) caudal c) medial d) lateral e) superior f) inferior (LVH-NN-E9)^{sin}. Note that the medial side of the proximal and distal epiphyses are partly missing. Refer to Marano and Palombo, 2013: Table 3 for ontogenetic metadata.

muscle (the deltoid fossa, see Fig. 4.4b, d). The distal extremity (*Condylus humeri*) has an articular surface, the *trochlea*, which is divided into a smaller medial and a larger lateral part (Fig. 4.4f). The *Epicondylus lateralis* is massive and situated directly above the condyle, consisting of a tuberos distal part that flattens and narrows proximally (Fig. 4.4a). The medial condyle is smaller than the lateral epicondyle and the epicondyles caudally flank a wide shallow *Fossa olecrani* (Fig. 4.4b), which deepens directly above the condyle (Kroll, 1991: 20-21; Smuts and Bezuidenhout, 1993: 3-4).

In comparing the cranial profile, three features differ noticeably between species: (i) Min breadth (m-l) of the diaphysis - In both *P. antiquus* (Fig. 4.8a, b) and *L. africana* the diaphysis is wider in the adult than in young individuals. The wide diaphysis in *P. ex gr. P. falconeri* (Fig. 4.4a, b) contrasts with the slender diaphysis of young *P. antiquus* (Fig. 4.7a, b) and juvenile *L. africana* (Fig. 4.3a, b; see also metric analyses following). (ii) Lateral projection of the deltoid tuberosity - This projects farther laterally in *P. ex gr. P. falconeri* (Fig. 4.4a) than in young and adult *P. antiquus* (Fig. 4.7a; Fig. 4.8a), and in *P. ex gr. P. mnaidriensis*. (iii) The position of the supracondylar crest - This is situated farther distally in *P. ex gr. P. falconeri* (Fig. 4.4a) than in *P. antiquus* (Fig. 4.8a). (iv) Position of the apophysis on the distomedial side - Seen in cranial and caudal aspects, an apophysis is visible on the medial side of the distal diaphysis, which is particularly large in *P. ex gr. P. mnaidriensis* (Fig. 4.6a, b). In *P. ex gr. P. falconeri* it is situated more distally than in the other represented *Palaeoloxodon* spp. specimens (contrast Fig. 4.4a with Fig. 4.5a; Fig. 4.6a; Fig. 4.7a; Fig. 4.8a).



Fig. 4.8 Humerus of juvenile *P. ex gr. P. falconeri* from Spinagallo Cave in lateral aspect (NHMB-Ty-12559)^{sin}.

4.1.2.2 Morphology of the deltoid fossa

The deltoid is a triangular muscle arising on the scapula (lateral *Spina scapulae*, *Processus uncinatus* and the under-surface of an attached fascia), and is inserted into the outer and anterior surface of the humerus, immediately below the root of the *Tuberositas deltoidea*, with broad insertion tendon (Shindo and Mori, 1956a: 89 and Fig. 7; see also Rispoli *et al.*, 2009). As such the deltoid is involved in the adduction and abduction of the humerus (pulling towards and away from the midline of the body respectively).

Intraspecifically the morphology of the deltoid differs considerably between juvenile and adult *P. ex gr. P. falconeri*. In adult *P. ex gr. P. falconeri*, the muscular insertion presents a continuous fossa (Fig. 4.4b, d), whereas it is divided into separate areas in juvenile *P. ex gr. P. falconeri* (Fig. 4.9). In the juvenile there are two deep and clearly separated insertion scars demarcated by a ridge, the anterior scar being broader and terminating more proximally than the posterior scar which tapers distally and is less broad (Fig. 4.9). These morphological differences between young and old presumably relate to the

separation of muscular attachment areas.

Interspecifically, the morphology of the deltoid fossa is also clearly visible in all adults of the species examined (Figs. 4.3b, d; 4.4b, d; 4.5b, d; 4.7b, d; 4.8b, d) with the exception of *Palaeoloxodon* sp. 1 from Luparello Fissure in which the fossa is shallow and barely visible (Fig. 4.5b, d). Morphologically, the deltoid fossa also differs interspecifically (Table 4.3), including in (i) orientation, (ii) depth, (iii) proximo-distal position along the shaft, and iv) rugosity.

(i) Orientation of the deltoid fossa - Among the represented specimens the fossa faces caudolaterally in adult *P. antiquus* (Fig. 4.8d) and adult *P. ex gr. P. mnaidriensis* (Fig. 4.6d). In contrast, the fossa faces caudally in the represented adult *P. ex gr. P. falconeri* (Fig. 4.4d), and in juvenile *L. africana* (Fig. 4.3d). (ii) Depth of the deltoid fossa - A deep muscle scar is evident in *P. ex gr. P. falconeri* from Spinagallo Cave (Fig. 4.4b, d), and *P. ex gr. P. mnaidriensis* from Puntali Cave (Fig. 4.6 b, d) and in *P. antiquus* from Neumark-Nord 1 (Fig. 4.7b, d; Fig. 4.8b, d). In contrast, the deltoid fossa in *Palaeoloxodon* sp. 1 from Luparello Fissure is extremely shallow, to the point of being barely identifiable (Fig. 4.5b, d). (iii) Proximo-distal position of the deltoid fossa - The deltoid fossa terminates above the diaphysis midpoint in the represented adult *P. ex gr. P. falconeri* (Fig. 4.4b, d), but extends more distally in *P. ex gr. P. mnaidriensis* from Puntali Cave (Fig. 4.6b, d). (iv) Rugosity of the deltoid fossa - The attachment area for the insertion of the deltoid is rugose in *P. ex gr. P. mnaidriensis* (Fig. 4.6b, d) and young and adult *P. antiquus* (Fig. 4.7b, d; Fig. 4.8b, d), but less so in *P. ex gr. P. falconeri* (Fig. 4.4b, d) and *Palaeoloxodon* sp. 1 from Luparello Fissure (Fig. 4.5b, d). In juvenile *P. ex gr. P. falconeri* (Fig. 4.9) and juvenile *L. africana* (Fig. 4.3b, d) the surface of the deltoid fossa appears smooth.

Species	Depth	Observations on position and morphology
Adult <i>P. antiquus</i>	Deep	Broad (a-p) compared to <i>P. ex gr. P. mnaidriensis</i> and <i>P. ex gr. P. falconeri</i> .
Adult <i>P. ex gr. P. mnaidriensis</i>	Deep, becoming deeper towards deltoid tuberosity	Tapering from widest (proximally) to narrowest (distally), extending far distally beyond the deltoid tuber
Adult <i>Palaeoloxodon</i> sp. 1	Shallow	Nearly invisible due to shallowness
Adult <i>P. ex gr. P. falconeri</i>	Deep	Faces posteriorly
Juvenile <i>P. ex gr. P. falconeri</i>	Deep	Two concave regions separated by a ridge, the one more cranio-proximally, the other more caudo-distally

Table 4.3 Interspecific differences in the morphology of the deltoid fossa (after Figs 4.3-4.8; Fig. 4.9). Note that adults are denoted by completely fused and obliterated epiphyseal lines and juveniles by unattached epiphyses. Refer to Section 6.2 for a discussion on the idiosyncratic and subjective nature of these observations (due to small sample-size).

4.1.2.3 Interspecific bivariate allometry

(i) Ratio of max height (pr-d) including epiphyses/min diaphysis breadth (m-l) - Differences are not significant between *P. antiquus* vs. *L. africana* (MWU $p=0,571$), whereas there are significant differences between *P. antiquus* vs. *P. ex gr. P. falconeri* (MWU $p=0,019$), reflecting a wider diaphysis in *P. ex gr. P. falconeri*, and also *P. ex gr. P. falconeri* vs. *L. africana* (MWU $p=0,018$), reflecting a more slender diaphysis in *L. africana*. (ii) Ratio of diaphysis height (pr-d)/min diaphysis breadth (m-l) - Differences are statistically significant between *P. ex gr. P. falconeri* and *L. africana*, where the sample for both species includes fused and unfused specimens (MWU $p=0,000$), reflecting a tendency towards a more slender diaphysis in *L. africana* (Fig. 4.12a), although there is overlap between species. Differences are also statistically significant between juvenile and adult *L. africana* (Fig. 4.12a; Table 4.4), reflecting a more slender diaphysis in the juvenile than adult. Similarly, *P. ex gr. P. falconeri* evidences a more slender diaphysis in the juvenile than adult (Fig. 4.12a; Table 4.4), indicating similar ontogenetic trends in both species. Juvenile *L. africana* (with unfused epiphyses) is however clearly less similar to adult *P. ex gr. P. falconeri* than adult *L. africana*, contrary to the predictions of Hypothesis II.

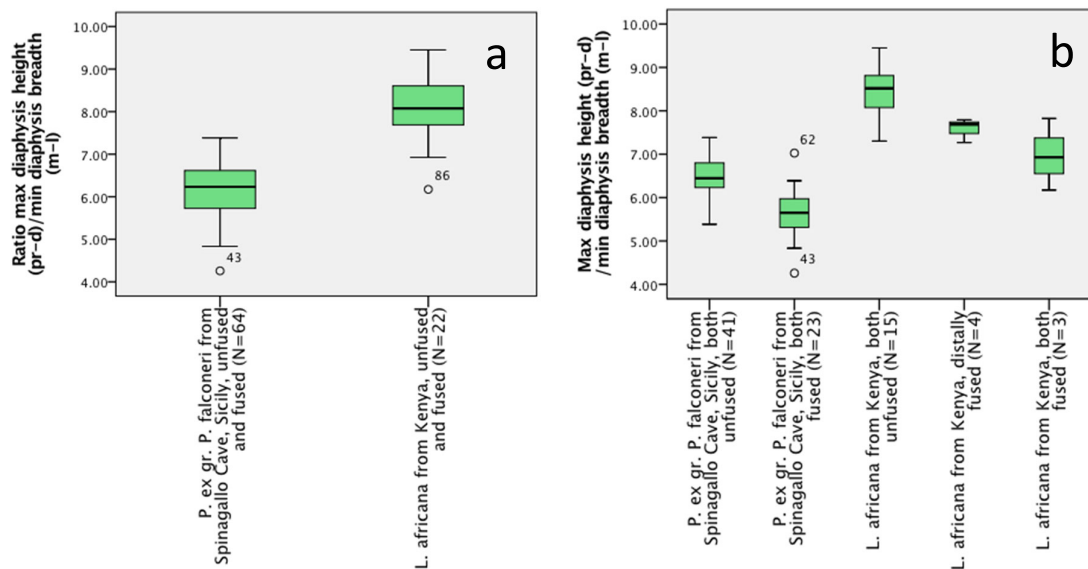


Fig. 4.9 Box-and-whisker plot of the ratio of the humerus' max diaphysis height (pr-d)/min diaphysis breadth (m-l). a) Pooled samples of unfused and fused epiphyses. b) Samples divided into groups with unfused and fused epiphyses.

	Max diaphysis height (pr-d)/min diaphysis breadth (m-l)
<i>L. africana</i> neither/ <i>L. africana</i> distal	0,006*
<i>L. africana</i> neither/ <i>L. africana</i> both	0,010*
<i>L. africana</i> distal/ <i>L. africana</i> both	0,629
<i>P. ex gr. P. falconeri</i> neither/ <i>P. ex gr. P. falconeri</i> both	0,000*
<i>L. africana</i> both/ <i>P. ex gr. P. falconeri</i> both	0,000*
<i>L. africana</i> neither/ <i>P. ex gr. P. falconeri</i> neither	0,000*
<i>L. africana</i> neither/ <i>P. ex gr. P. falconeri</i> both	0,000*
<i>L. africana</i> distal/ <i>P. ex gr. P. falconeri</i> both	0,000*

Table 4.4 Pair-wise Mann-Whitney U-test results for the humerus' diaphysis height (pr-d) vs. min diaphysis breadth (m-l). The sample with the relatively wider diaphysis is indicated with bold text. Statistically significant values are indicated with an asterisk (*).

- *Palaeoloxodon antiquus* pooled European sample
- *Palaeoloxodon antiquus* from Neumark-Nord 1, Germany
- ◆ *Palaeoloxodon ex gr. P. mnaidriensis* from Puntali Cave, Sicily
- ✱ *Palaeoloxodon* sp. 1 from Luparello Fissure, Sicily
- ▲ *Palaeoloxodon ex gr. P. falconeri* from Spinagallo Cave, Sicily
- *Loxodonta africana* from Kenya

Fig. 4.11 Figure legend for taxa in Fig. 4.12

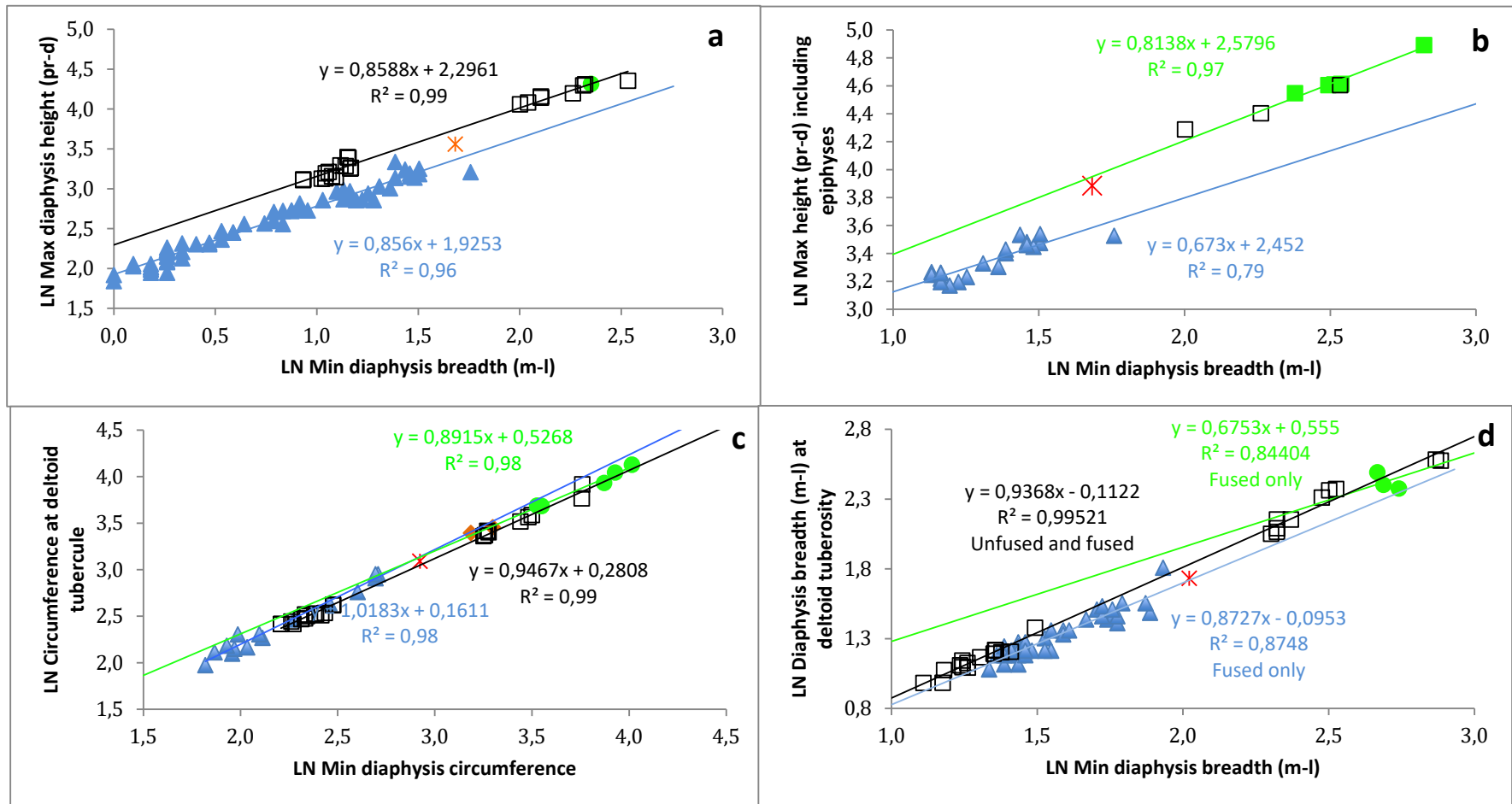


Fig. 4.12 Scatterplots of the dimensions of the humerus. a) Min diaphysis breadth (m-l) vs. max diaphysis height (pr-d). b) Min diaphysis breadth (m-l) vs. max height (pr-d) including epiphyses. The height (pr-d) value for *Palaeoloxodon* sp. 1 is approximate. c) Min diaphysis circumference vs. circumference at deltoid tuberosity. d) Min diaphysis breadth (m-l) vs. diaphysis breadth (m-l) at deltoid tuberosity. Refer to Fig. 3.3 for symbol legend. [Data: *P. antiquus* from Palombo *et al.*, unpublished; including Christiansen, 2004: 544 for Fig. 4.12b; *P. ex gr. P. falconeri* from Ambrosetti, 1968: 364 except Fig. 4.12c which is original data for *P. ex gr. P. falconeri*].

(iii) Ratio diaphysis breadth (m-l) at deltoid tuberosity/min diaphysis breadth (m-l) -

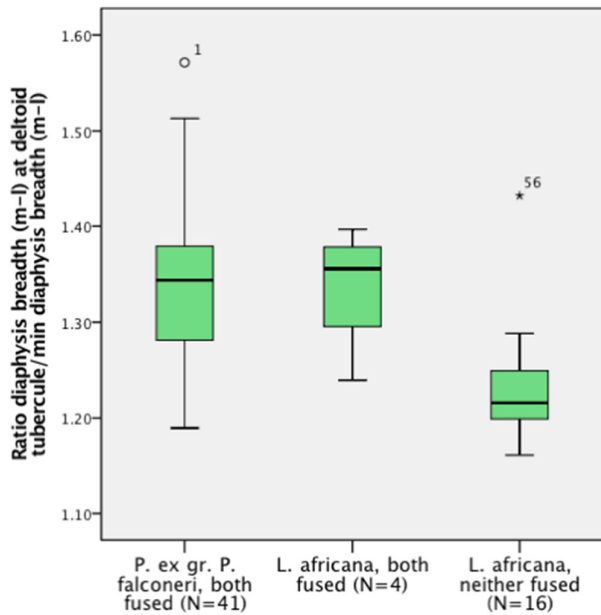


Fig. 4.13 Box-and-whisker plot of the ratio of the humerus' diaphysis breadth (m-l) at deltoid tubercle (m-l)/min diaphysis breadth (m-l).

Differences are not statistically significant between *P. antiquus* and *P. ex gr. P. falconeri* with fused epiphyses (Fig. 4.12d; MWU $p=0,189$), nor between *P. antiquus* and *L. africana* with fused epiphyses (MWU $p=0,200$) nor between *L. africana* and *P. ex gr. P. falconeri* with fused epiphyses (MWU $p=0,863$). Differences are however significant between *L. africana* with unfused epiphyses and *L. africana* with fused epiphyses (MWU $p=0,022$), reflecting a relatively greater breadth of the deltoid tuberosity in the adult. Differences are also statistically significant between *L. africana* with unfused epiphyses and *P. ex gr. P. falconeri* with fused epiphyses (MWU $p=0,000$), reflecting a relatively broader diaphysis at the deltoid tuberosity in *P. ex gr. P. falconeri*.

Differences between *P. ex gr. P. falconeri* with fused epiphyses and *L. africana* with fused epiphyses are not statistically significant (MWU $p=0,863$), although sample-sizes are small for *L. africana* with fused epiphyses. iv) Ratio of circumference at deltoid tuberosity/min diaphysis circumference - Although only small sub-sample sizes belonging to different epiphyseal fusion stages were obtained (due to limited time), the data suggests there are relatively small differences between species (Fig. 4.12c).

4.1.3 Anatomy of the ulna-radius

The ulna is larger than the radius, which articulates with it so that the proximal part is placed craniomedially and the shaft spirals laterally over the cranial surface of the ulna, articulating distally with the medial aspect of the ulna via the *Circumferentia articularis* (Smuts and Bezuidenhout, 1993: 4 and Fig. 13). The *Tuber olecrani* is massive, especially caudolaterally. The *Processus coronoideus medialis* is larger than the *Processus coronoideus lateralis* which are both concave for articulation with the humerus. Proximally, there is a deep concavity, the *Incisura radialis*. In some *L. africana* individuals a clear line runs along the lateral border from the vicinity of a ligamentous tuberosity on the lateral coronoid process, running obliquely in a caudodistal direction, fading out towards the distal extremity (Smuts and Bezuidenhout, 1993: 6). Distally there is a roughly oval articular surface, *Circumferentia articularis*, for articulation with the radius. The distal extremity of the ulna articulates mainly with the ulnar carpal, and caudally with the accessory carpal. Directly distally to the articular surface for the radius is an articular surface for the intermediate carpal bone (Smuts and Bezuidenhout, 1993: 7). Distally the ulna articulates with the intermediate carpal, ulnar carpal

and caudally with the accessory carpal (Palombo and Villa, 20013: Fig. 7), and the radius articulates with the intermediate carpal and radial carpal.

Cranial and medial profiles of the ulna - In cranial aspect the diaphysis of juvenile *L. africana* displays an hourglass-shaped profile (Fig. 4.15a) compared with the more parallel-sided diaphysis of adult *L. africana* (Fig. 4.15b). In the juvenile, the proximal epiphysis is also wide compared with adult *L. africana*. Seen in medial aspect the juvenile *L. africana* ulna evidences a slender diaphysis (Fig. 4.16a), and although unossified distally, the distal diaphysis indicates that the unossified distal epiphysis would have been robust in the juvenile. Both the juvenile *L. africana* ulna and femur in medial aspect therefore share a more curved diaphysis and wider distal end than in the adult (see Fig. 4.16a; Fig. 4.18c).

4.1.3.1 Radio-ulnar synostosis

Synostosis between the ulna-radius is frequent in adult *P.* ex gr. *P. falconeri* (Fig. 4.14; see also fusion developing in proximal and distal areas of Fig. 4.15c) and *P.* ex gr. *P. mnaidriensis* from Puntali Cave (Fig 4.14e; Fig 4.15e), although the frequency with which synostosis occurs has not been determined in the Spinagallo Cave assemblage due to specimen damage and breakage. The single represented ulna belonging to *Palaeoloxodon* sp.



Fig. 4.14 Distal ulna-radius of *P.* ex gr. *P. falconeri* from Spinagallo Cave. Radius (left) and ulna (right) in cranial aspect (UCat).

1 from Luparello Fissure (though slightly damaged) shows no obvious signs of having been synostotically fused (Fig. 4.15d; Fig. 4.16d; see also Vaufrey, 1929: Plate VIII, Fig. 13), although the species is likely ancestral to *P.* ex gr. *P. falconeri* (Scarborough *et al.*, 2016). In contrast to synostosis between the tibia-fibula (Fig. 4.36), synostosis in the ulna-radius may occur more-or-less completely along the length of the diaphysis (and epiphyses) in both *P.* ex gr. *P. mnaidriensis* (Fig. 4.16e) and *P.* ex gr. *P. falconeri* (Fig. 4.14), likely proceeding with the deposition of cancellous bone along a proximo-distally orientated bony ridge often evident on the diaphysis of unfused ulnae belonging to *P.* ex gr. *P. falconeri*. In contrast to the ulna-radius, the tibia-fibula are only joined at the proximal and distal ends, whereas the ulna-radius tends to be fused (partially or completely) along the diaphysis (and epiphyses). Viewed in cranial aspect in some ulnae belonging to *P.* ex gr. *P. falconeri* a prominent bony ridge runs proximo-distally along the diaphysis long-axis on the cranial side, twisting torsionally along the surface of the medial side of the diaphysis, and though less prominent, is also sometimes present in *L. africana* (Smuts and Bezuidenhout, 1993: Fig. 14).

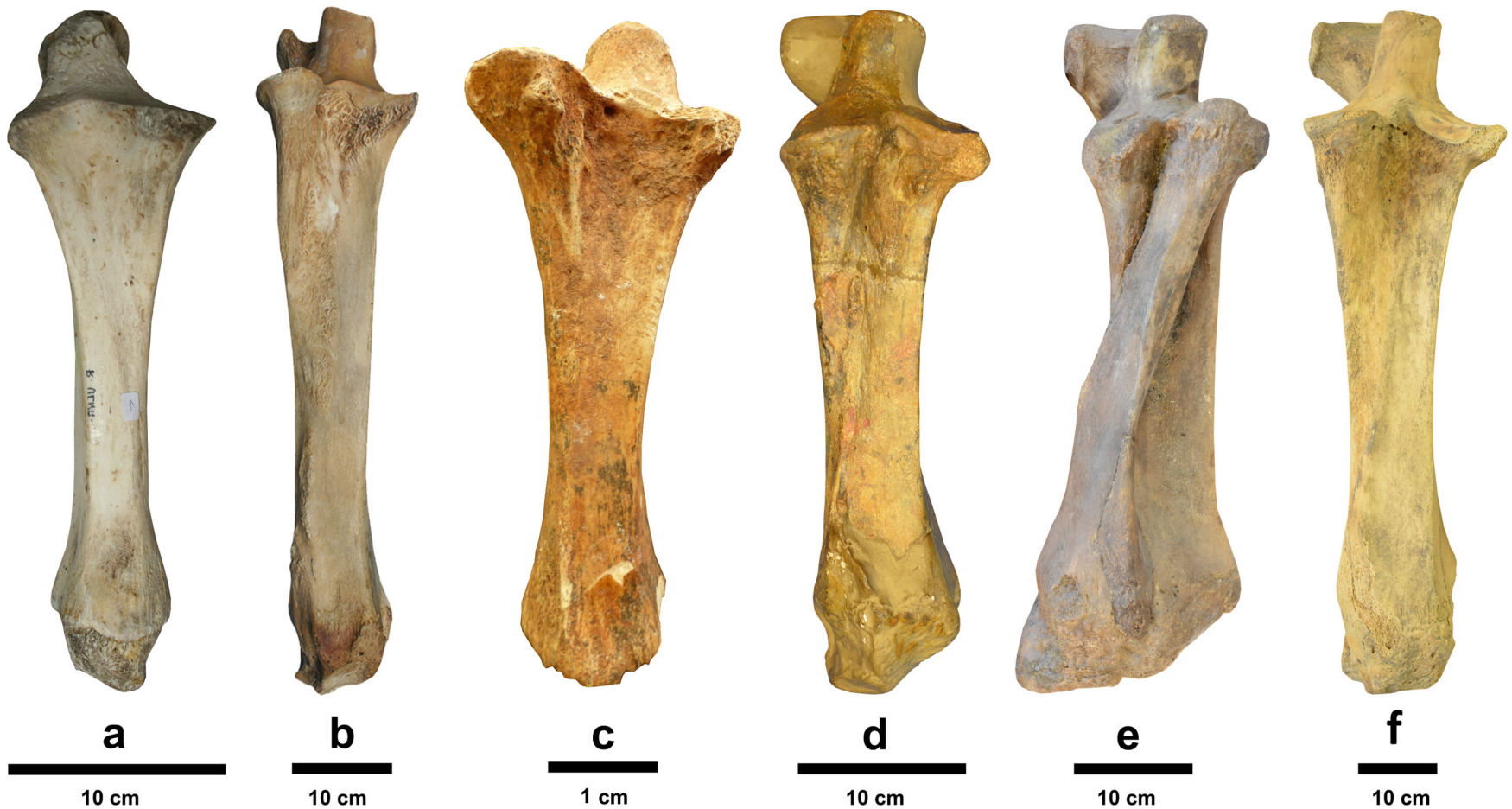


Fig. 4.15 Comparison of the ulna in cranial aspect a) Juvenile *L. africana* from Kenya (KNM-OM2212)^{dex}. b) Adult *L. africana* from Kenya (KNM-OM8655)^{sin}. c) *P. ex gr. P. falconeri* from Spinagallo Cave, Sicily (UCat). d) *Palaeoloxodon* sp. 1 from Luparello Fissure, Sicily (IPH-F2929, partially reconstructed)^{dex}. e) Adult *P. ex gr. P. mnaidriensis* from Puntali Cave, Sicily (GMP-105?)^{sin}. f) Adult *P. antiquus* from Neumark-Nord 1, Germany (LVH-NN-14.10.94 and 2003: 55,12). Refer to Table 2.8 for *L. africana* ontogenetic metadata and Marano and Palombo, 2013: Table 3 for *P. antiquus* metadata.



Fig. 4.16 Comparison of the ulna in medial aspect a) Juvenile *L. africana* from Kenya (KNM-OM2212)^{dex}. b) Adult *L. africana* from Kenya (KNM-OM8655)^{sin}. c) *P. ex gr. P. falconeri* from Spinagallo Cave, Sicily (UCat). d) *Palaeoloxodon* sp. 1 from Luparello Fissure, Sicily (IPH-F2929, partially reconstructed)^{dex}. e) Adult *P. ex gr. P. mnaidriensis* from Puntali Cave, Sicily with synostotic radius) (GMP-105?)^{sin}. f) Adult *P. antiquus* from Neumark-Nord 1, Germany (LVH-NN-14.10.94 and 2003: 55,12). Refer to Table 2.8 for *L. africana* ontogenetic metadata metadata and Marano and Palombo, 2013: Table 3 for *P. antiquus* metadata.

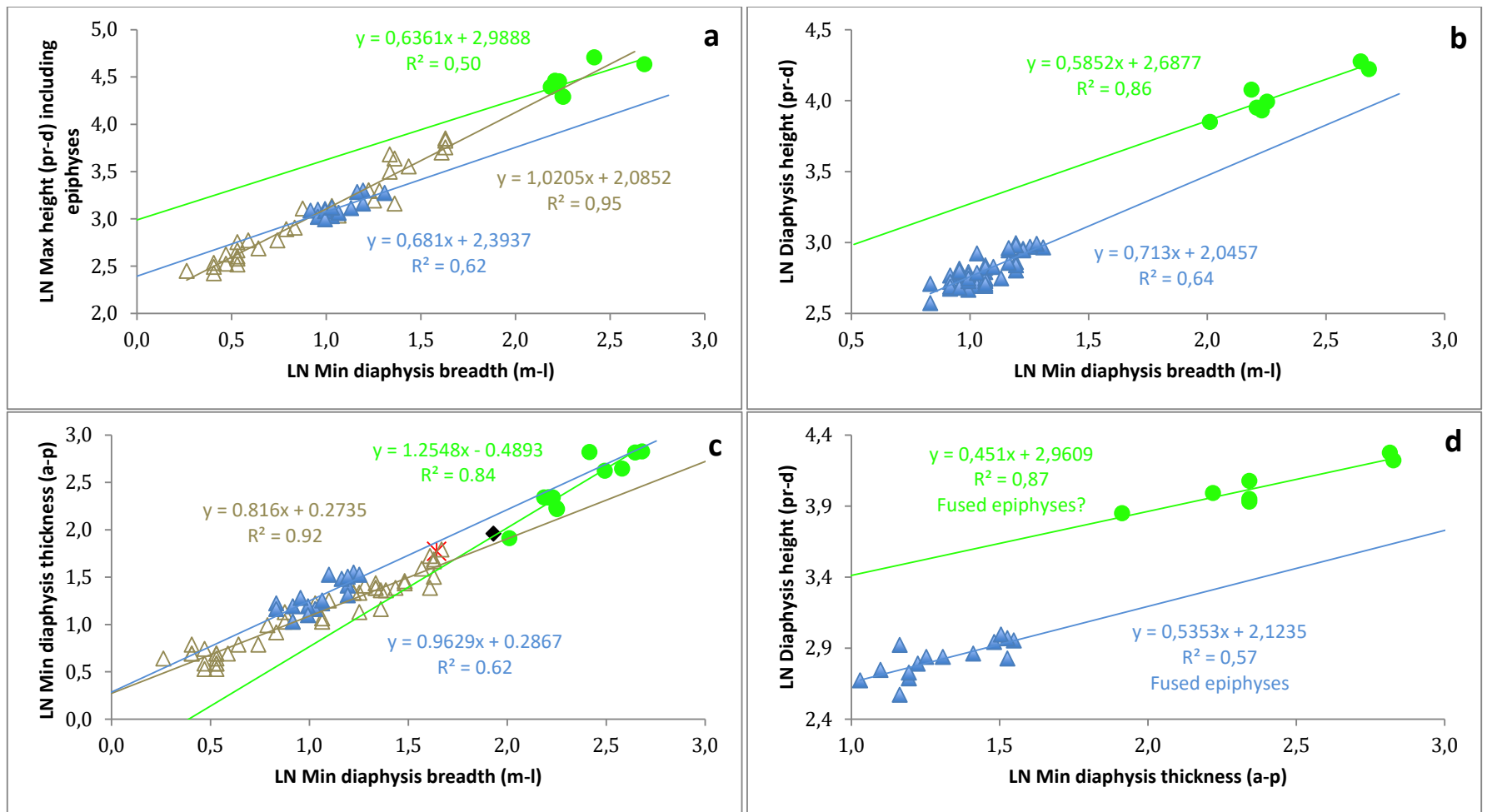


Fig. 4.17 Scatterplots of the dimensions of the ulna. a) Min diaphysis breadth (m-l) vs. max height (pr-d) including epiphyses b) Min diaphysis breadth (m-l) vs. diaphysis height (pr-d). c) Min diaphysis breadth (m-l) vs. min diaphysis thickness (a-p). d) Min diaphysis thickness (a-p) vs. diaphysis height (pr-d). Refer to Fig. 3.3 for symbol legend. [Data: *P. ex gr. P. falconeri* from Ambrosetti, 1968: 364; *P. tiliensis* from Theodorou, 1983: 203; *P. antiquus* from Palombo *et al.*, unpublished].

Proximal and distal articular surfaces of the synostotic ulna-radius - In *P. ex gr. P. falconeri* and *P. ex gr. P. mnaidriensis* synostosis of the proximal ulna-radius presents a continuous articular surface for the distal humerus. Distally, synostosis would likely have altered the motion between the distal ulna-radius and the proximal carpals (see Figs 4.14 and 3.1), by reducing movement in three directions: (i) Antero-posterior flexion - This was likely reduced as suggested by a bony margin situated cranially, which created a depression that likely prevented dorsiflexion exceeding 90°. (ii) Medio-lateral displacement - Proximally the articular surface of the intermediate carpal is saddle-shaped for articulation with the radius, and dorsolaterally there is an oblique continuation of this surface for the ulna (see Fig. 3.1; Smuts and Bezuidenhout, 1993: 7). Medio-lateral displacement of the intermediate carpal was thus likely reduced where synostosis occurred. Furthermore, because the intermediate carpal articulates medially with the ulnar carpal, and laterally with the radial carpal, medio-lateral displacement of the ulnar and radial carpals was possibly also reduced (Fig. 3.1). (iii) Proximo-distal displacement - Since synostosis between the ulna-radius eliminates proximo-distal displacement between these bones, displacement between the ulnar carpal on the lateral side and the intermediate and radial carpals on the medial side is likely to have been reduced.

Alterations in muscle attachment areas - In some *P. ex gr. P. falconeri* specimens the craniodistal surface of the synostotically fused radius displays a proximodistally-orientated ridge for the attachment of an adductor, possibly the origin of one of the extensor muscles such as *M. extensor digitorum communis*, or the *M. extensor indicis proprius* (refer to Shindo and Mori, 1956a: Fig. 7).

4.1.3.2 Interspecific bivariate allometry

(i) Ratio max height (pr-d) including epiphyses/min diaphysis breadth (m-l) - Differences are not significant between *P. antiquus* and *P. tiliensis* (MWU $p=0,438$), or between *P. antiquus* vs. *P. ex gr. P. falconeri* (Fig. 4.17a, MWU $p=0,142$) or between *P. tiliensis* vs. *P. ex gr. P. falconeri* (MWU $p=0,073$). (ii) Ratio diaphysis height (pr-d)/min diaphysis breadth (m-l) - Differences are not significant for *P. antiquus* vs. adult *P. ex gr. P. falconeri* with fused epiphyses (Fig. 4.17b; MWU $p=0,827$), or between *P. antiquus* and *P. ex gr. P. falconeri* as a pooled sample of unfused and fused epiphyses (MWU $p=0,199$). (iii) Ratio min diaphysis thickness (a-p)/min diaphysis breadth (m-l) - Differences are statistically significant between *P. antiquus* and adult *P. ex gr. P. falconeri* with fused epiphyses (Fig. 4.17c; MWU $p=0,005$) reflecting a thicker diaphysis in the latter species. (iv) Ratio diaphysis height (pr-d)/min diaphysis thickness (a-p) - Differences are not significant between *P. antiquus* and adult *P. ex gr. P. falconeri* with fused epiphyses (Fig. 4.17d; MWU $p=0,142$).

4.1.4 Anatomy of the femur

The femur is the longest bone of the skeleton (Figs 4.18-4.23). On the lateral side of the proximal extremity is the *Trochanter major*, which is divided by a smooth, shallow groove into cranial and caudal parts with its rough surface facing cranio-laterally (Fig. 4.19d). Along the cranio-lateral border of the femoral shaft, the *Trochanter tertius* is represented by the pointed distal continuation of the greater trochanter (Fig. 4.19a). The *Fossa trochanterica*, a

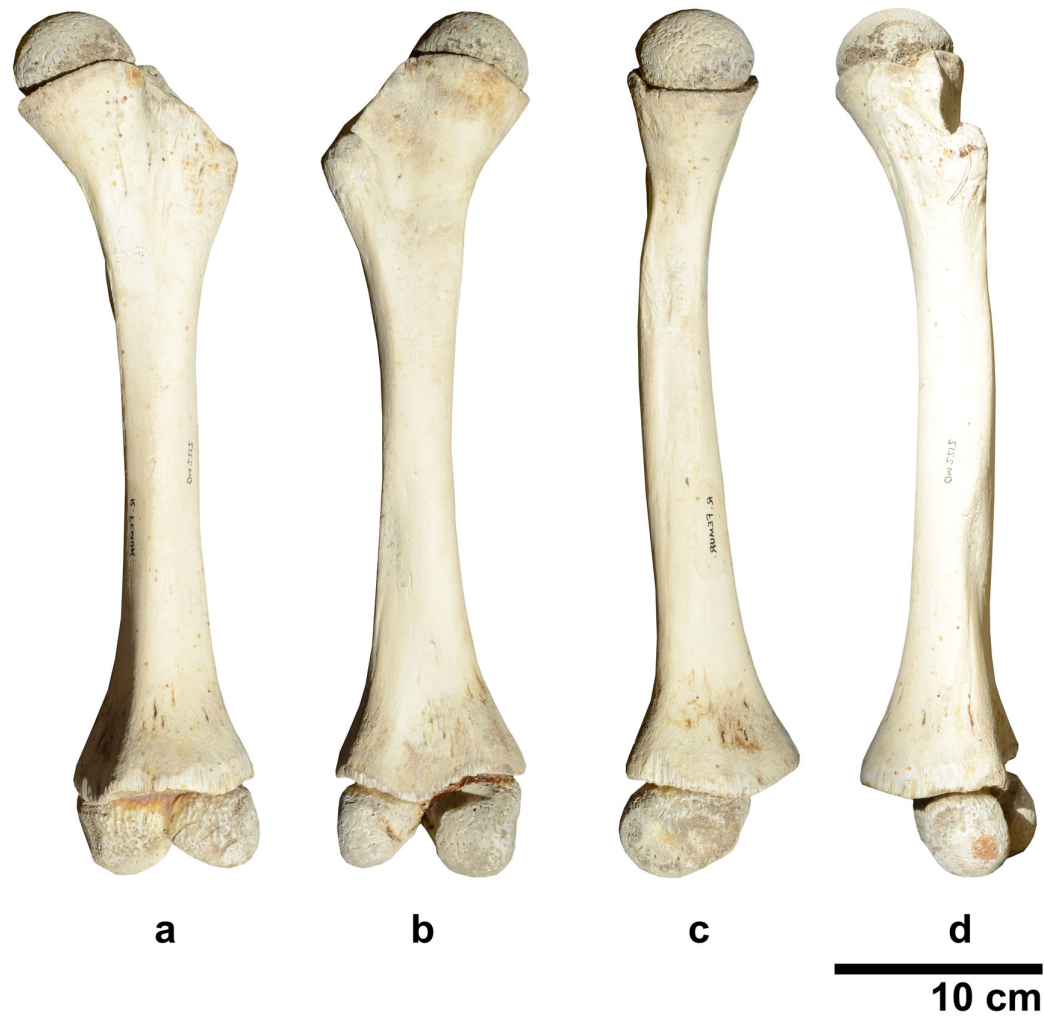


Fig. 4.18 Femur of juvenile *L. africana* from Kenya a) cranial b) caudal c) medial d) lateral (KNM-OM2212)^{dex}. Refer to Table 2.8 for ontogenetic metadata.

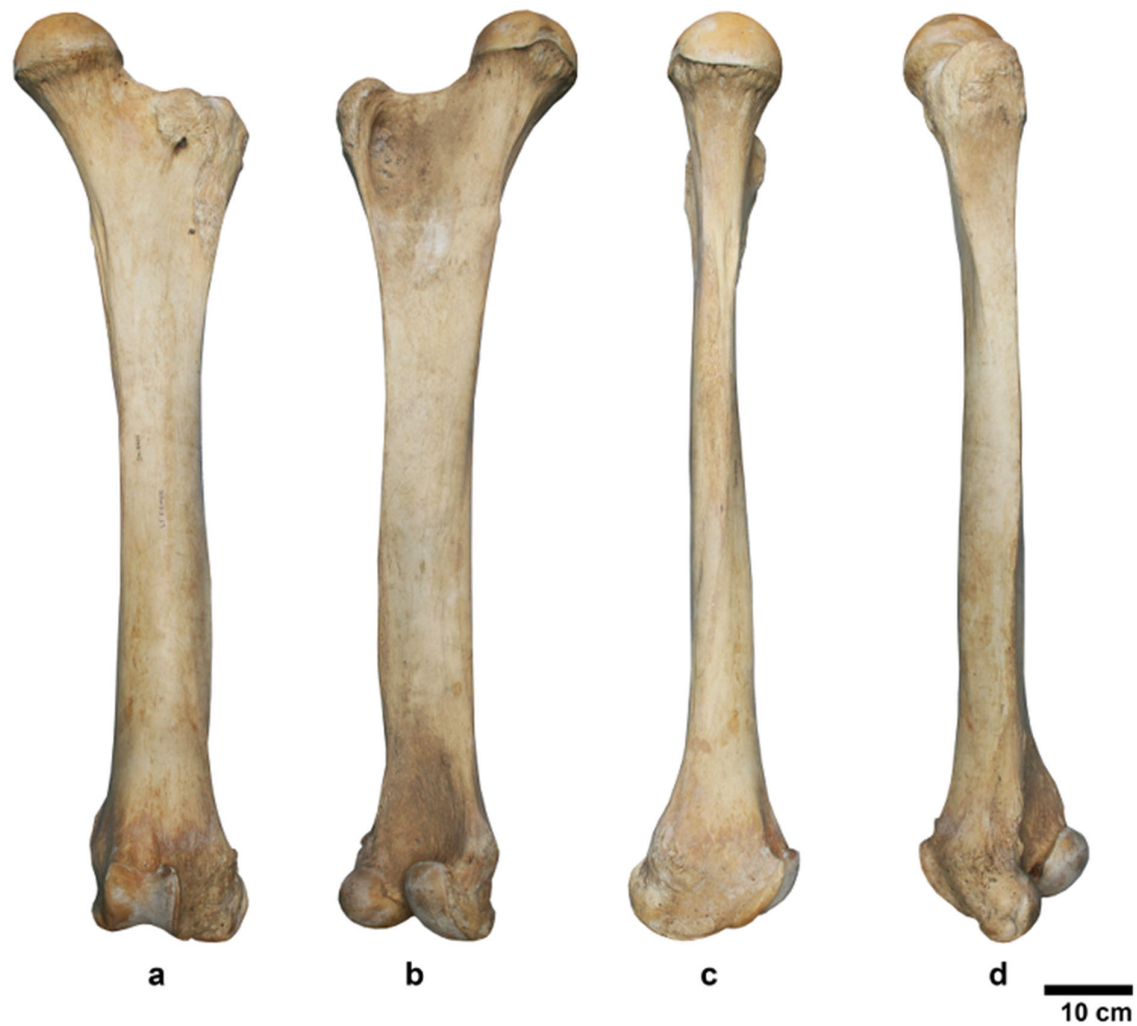


Fig. 4.19 Femur of adult *L. africana* from Kenya a) cranial b) caudal c) medial d) lateral (KNM-OM8655)^{sin}. Refer to Table 2.8 for ontogenetic metadata.

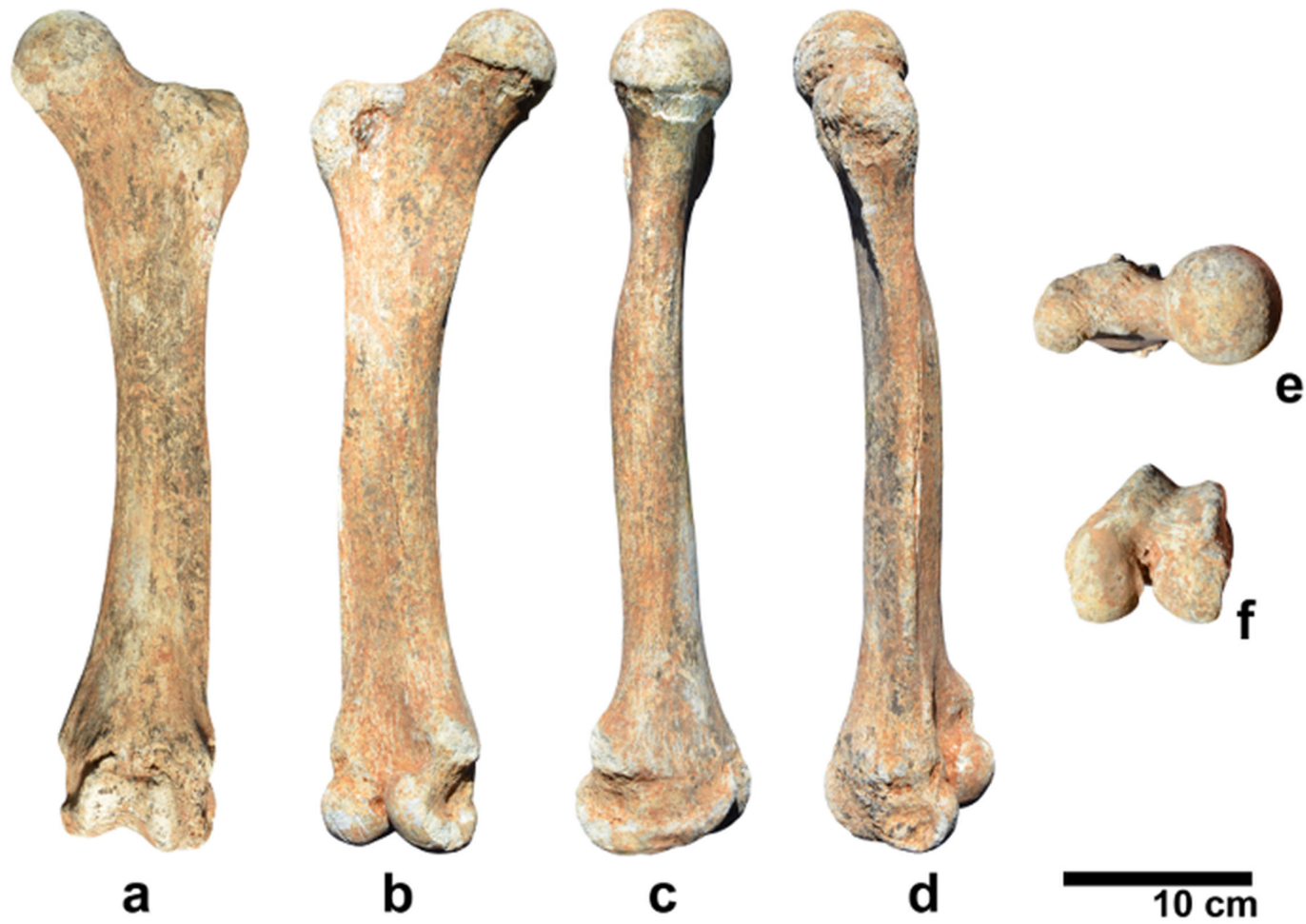


Fig. 4.20 Femur of *P. ex gr. P. falconeri* from Spinagallo Cave, Sicily a) cranial b) caudal c) medial d) lateral e) superior f) inferior (UCat)^{sin}.

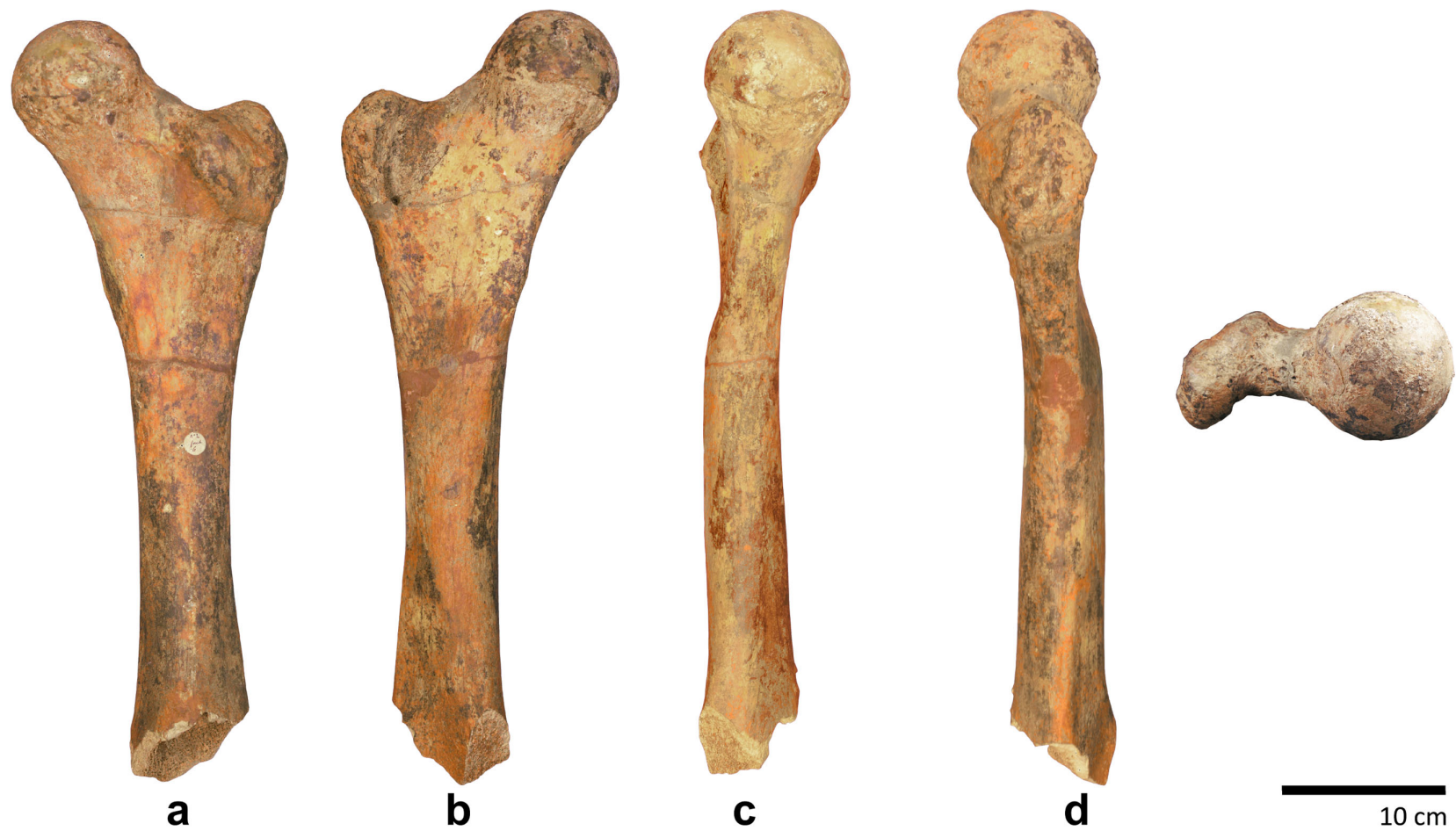


Fig. 4.21 Femur of *Palaeoloxodon* sp. 1 from Luparello Fissure, Sicily. a) cranial b) caudal c) medial d) lateral e) superior (IPH)^{sin}.

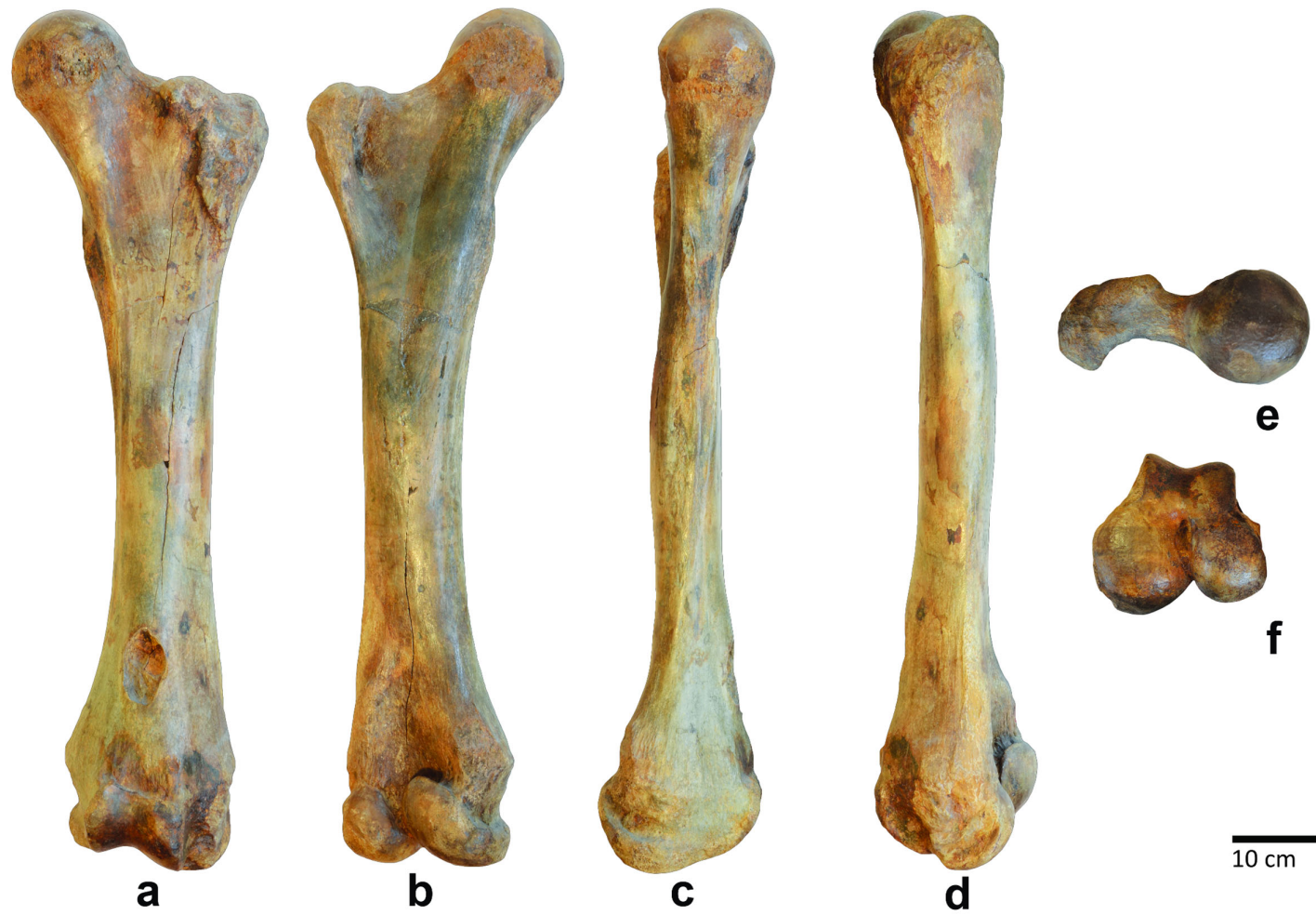


Fig. 4.22 Femur of *P. ex gr. P. mnaidriensis* femur from Puntali Cave, Sicily a) cranial b) caudal c) medial d) lateral e) superior f) inferior (GMP-L.M.O.782)^{sin.}

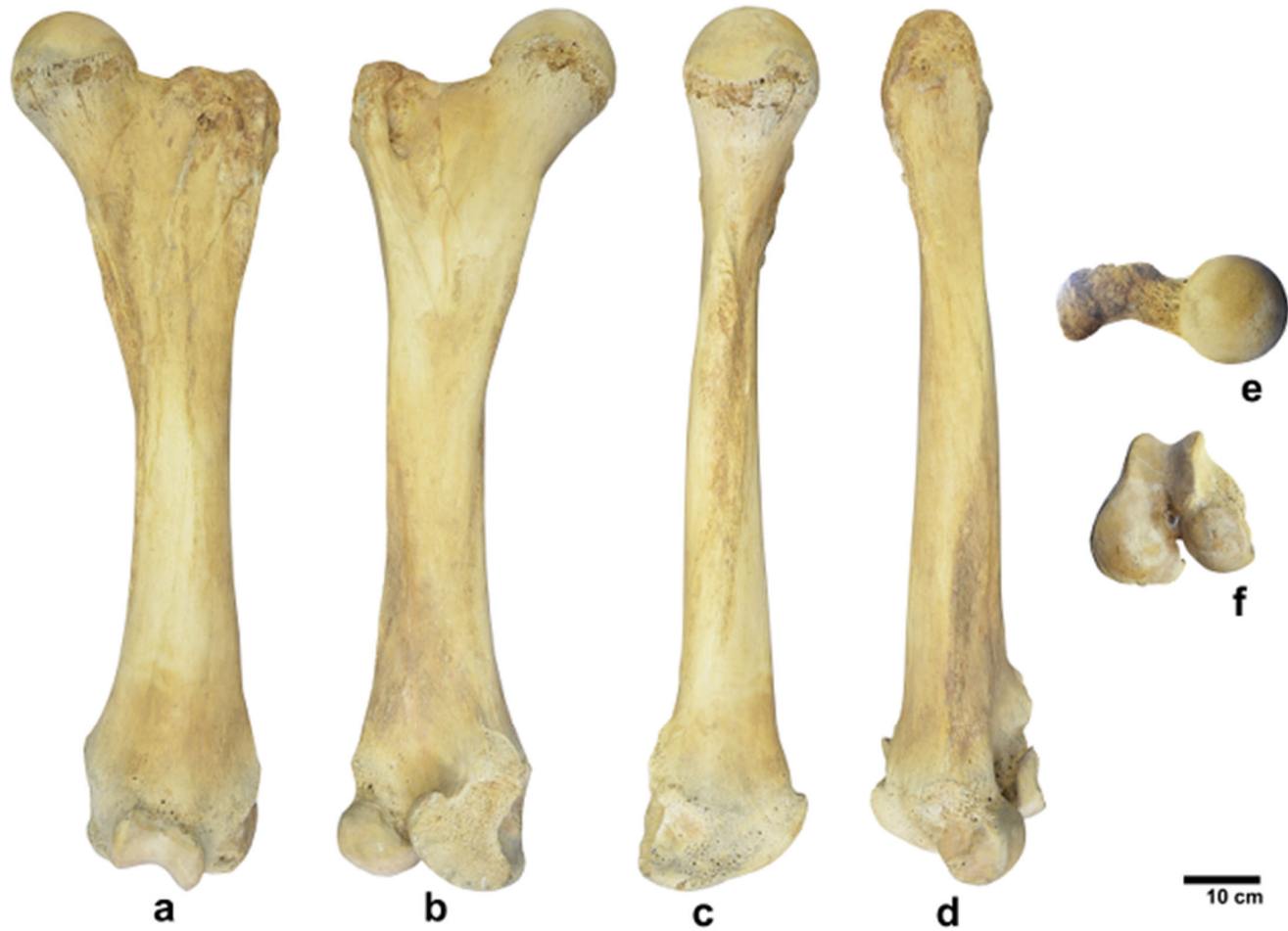


Fig. 4.23 Femur of *P. antiquus* from Neumark-Nord 1, Germany a) cranial b) caudal c) medial d) lateral e) superior f) inferior (LVH-NN-E8 and 2003.55,5-6)^{sin}. Refer to Marano and Palombo, 2013: Table 3 for ontogenetic metadata.

deep depression facing caudomedially is on the caudal aspect of the major trochanter (Fig. 4.19b). The *Trochanter minor* is a rough, elongated area along the proximal third of the medial border of the diaphysis. Muscular ridges are visible distally to the lesser trochanter, continuing along the medial border of the shaft (Smuts and Bezuidenhout, 1994: 56).

A rough elevated area occurs on the shaft cranially to the lesser trochanter (Fig. 4.19a). On the cranial surface of the diaphysis there is a longitudinal muscular line arising near the greater trochanter and petering out in the distal quarter (Fig. 4.19a). On the caudal surface of the diaphysis there is also a rough surface (*Facies aspera*), along the second quarter of its length (Fig. 4.19b). Distally there are the lateral and medial condyles for articulation with the tibia, and between the condyles was a narrow gap (*Fossa intercondylaris*, see Fig. 4.19f). The medial condyle is larger and faces caudolaterally, and the lateral condyle is orientated sagittally and faces caudally (Fig. 4.19b) Craniocaudally is the *Trochlea ossis femoris* that articulates with the patella (Fig. 4.19a, f, refer to Kroll, 1991: 27-28; Smuts and Bezuidenhout, 1994: 53; 56).

Ontogenetic and interspecific differences in the femur were compared (Figs 4.18-4.23; Figs 4.24-4.26). The femur differs interspecifically in eight respects: (i) allometry of the diaphysis midshaft, (ii) the femur length (pr-d) vs. diaphysis midshaft breadth (m-l), (iii) the femur length (pr-d) vs. diaphysis midshaft length (a-p), (iv) diaphyseal vs. epiphyseal robusticity, (v) the cranial profile, (vi) the longitudinal curvature of the diaphysis in the subtrochanteric region, and in the muscular attachments of the femur, including the (vii) position and morphology of the *Trochanter major* and the (viii) position and morphology of the *Trochanter minor*.

4.1.4.1 Cranial and medial profiles

(i) Cranial profile - In comparing cranial profiles a particularly prominent difference is seen between juvenile and adult *L. africana*. Although the minimum breadth of the two specimens is identical, the proximal and especially the distal end of the diaphysis are wide in juvenile *L. africana*. Although to a much lesser extent, the proximal and distal ends also appear to be broader (m-l) in young compared with adult *P. antiquus*. Adult *P. ex gr. P. falconeri* in contrast with juvenile *L. africana* does not have broad proximal and distal ends.

(ii) Proximo-distal curvature of the diaphysis in the subtrochanteric region - Viewed in medial aspect (and to a lesser degree in lateral aspect), at roughly one third of its length below the proximal end, the diaphysis curves posteriorly, although there is much interspecific variation and ontogenetic variability in the degree of curvature (Fig. 4.18c; Fig. 4.19c; Fig. 4.20c; Fig. 4.21c; Fig. 4.22c; Fig. 4.23c; Fig. 4.24). In adult *L. africana* the diaphysis is characterized by only slight curvature (Fig. 4.19c), compared with adult *P. antiquus* (Fig. 4.23c) and adult *P. ex gr. P. mnaidriensis* (Fig. 4.22c) where diaphysis curvature is greater. In contrast to adult *L. africana*, adult *P. ex gr. P. mnaidriensis* and adult *P. antiquus*, the curvature of the diaphysis is much greater in adult *P. ex gr. P. falconeri* (Fig. 4.20c) and juvenile *L. africana* (Fig. 4.18c), as well as adult *Palaeoloxodon* sp. 1 from Luparello Fissure (Fig. 4.21c), although the position along the diaphysis at which this curvature occurs differs slightly, being more proximally situated in juvenile *L. africana* (Fig. 4.18c) than in adult *P. ex*

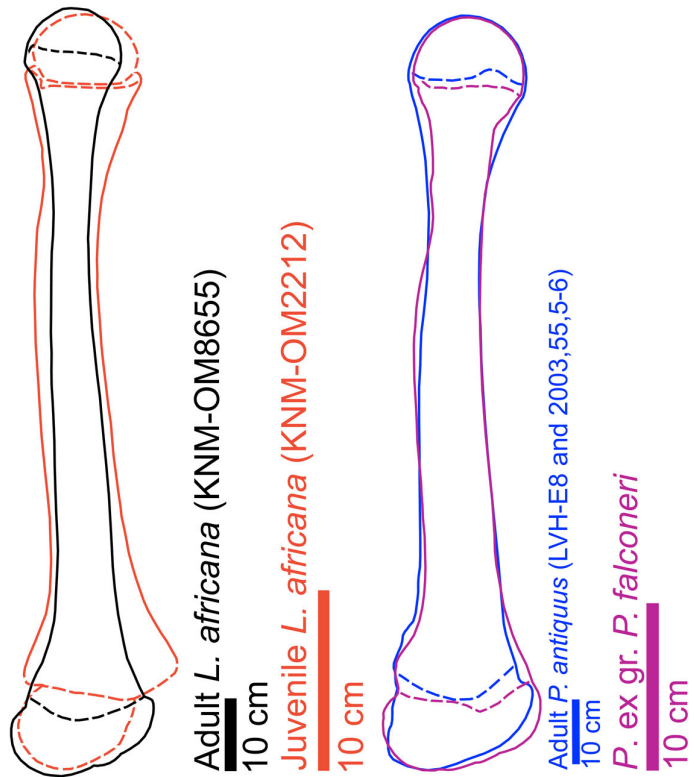


Fig. 4.24 Ontogeny and phylogeny in the femur diaphysis (medial aspect). Note: the position of the sutural lines is approximate due to partial obliteration in individuals with fused epiphyses. The stippled epiphyses in juvenile *L. africana* indicate the epiphyseal bodies are present, but the epiphyseal cortex is absent.

gr. *P. falconeri* (Fig. 4.20c). Slightly proximally to the curved region, the diaphysis narrows in adult *Palaeoloxodon* sp. 1 (Fig. 4.21c) and adult *P. ex gr. P. falconeri* (Fig. 4.20c), different to juvenile *L. africana* in this regard (Fig. 4.18c). There are therefore some differences, although an overall greater resemblance between the morphology of the femur diaphysis in juvenile *L. africana* and adult *Palaeoloxodon* sp. 1 and adult *P. ex gr. P. falconeri* (cf. Hypothesis II).

4.1.4.2 Position and morphology of muscle scars

(iii) Position and surface morphology of the *Trochanter major* - The *Trochanter major* is a rugose area situated towards

the lateral side of the cranial surface of the proximal femur, and marks the position of the insertion of the *Quadratus femoris* muscle (Fig. 4.19a). This muscle originates on the pelvis (on the posterior side of the hip joint), and inserts on the femur, and is a strong external rotator and adductor of the thigh, also acting in stabilizing the femoral head in the acetabulum. In the figured *Palaeoloxodon* sp. 1 (Fig. 4.21) and *P. ex gr. P. mnaidriensis* (4.22a) the *Trochanter major* is more raised and rugose in its profile compared with adult *P. antiquus* (Fig. 4.23a). (iv) Position and surface morphology of the *Trochanter minor* - The *Trochanter minor* is a rugose area on the medial side of the proximal femur into which the tendon for the *Psoas major* and the *Iliacus* inserts (Fig. 4.19a). The *Psoas major* originates on the lumbar region of the vertebral column, and contributes to the flexion in the hip joint (it lifts the upper leg towards the trunk). In the figured *P. ex gr. P. mnaidriensis* the *Trochanter minor* projects medially (Fig. 4.22a), whereas in *P. ex gr. P. falconeri* the projection extends less far medially (Fig. 4.20a). The *Trochanter major* also differs in rugosity, being rugose in adult *P. antiquus* (Fig. 4.23a, c) and adult *L. africana* (Fig. 4.19a, c), less rugose in *P. ex gr. P. mnaidriensis* (Fig. 4.22c), and relatively smooth in *Palaeoloxodon* sp. 1 from Luparello Fissure (Fig. 4.21c), *P. ex gr. P. falconeri* (Fig. 4.20c) and juvenile *L. africana* (Fig. 4.18c).

4.1.4.3 Interspecific bivariate allometry

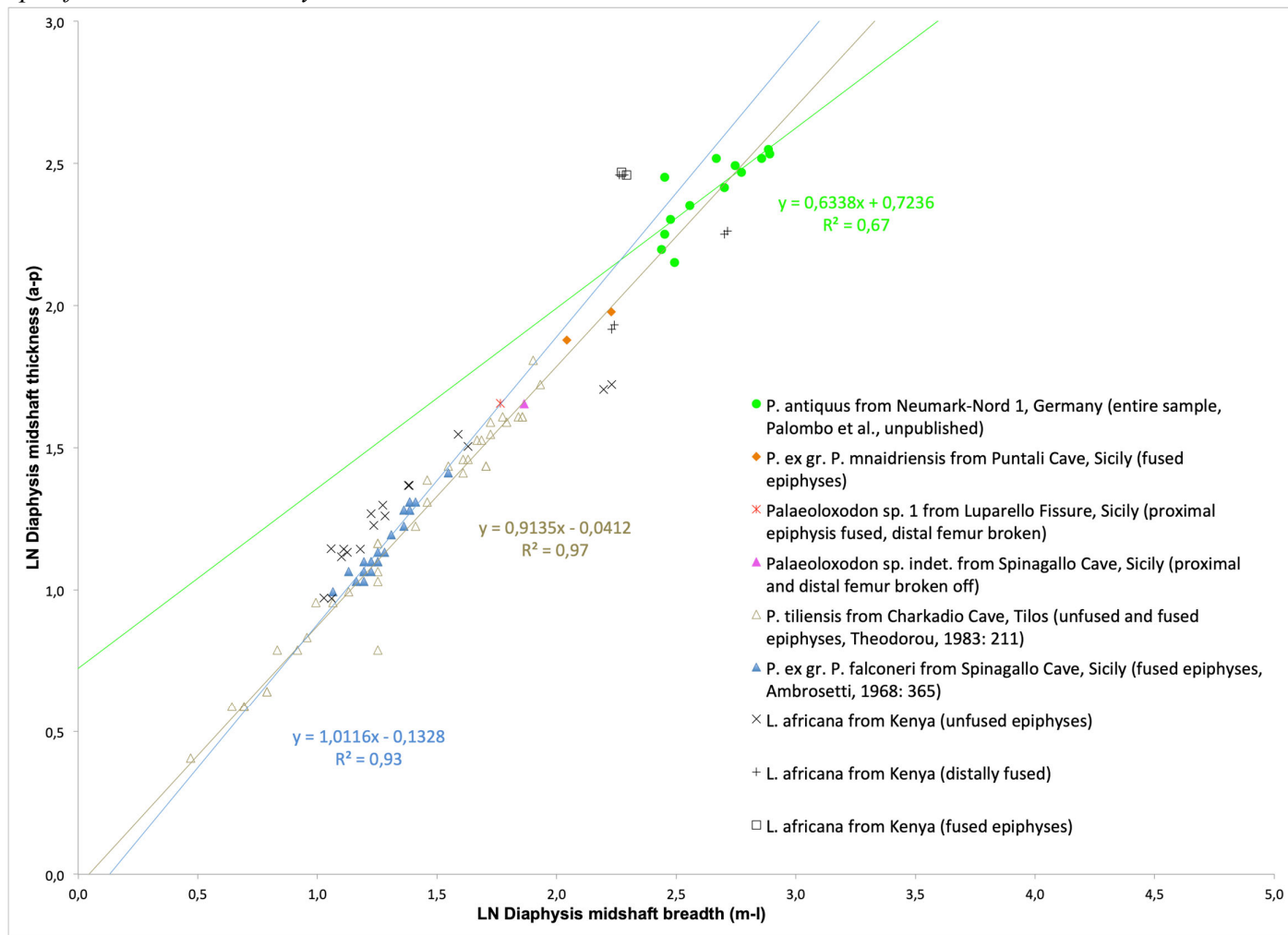


Fig. 4.25 Scatterplot of the femoral diaphysis dimensions (medio-lateral breadth vs. antero-posterior thickness).

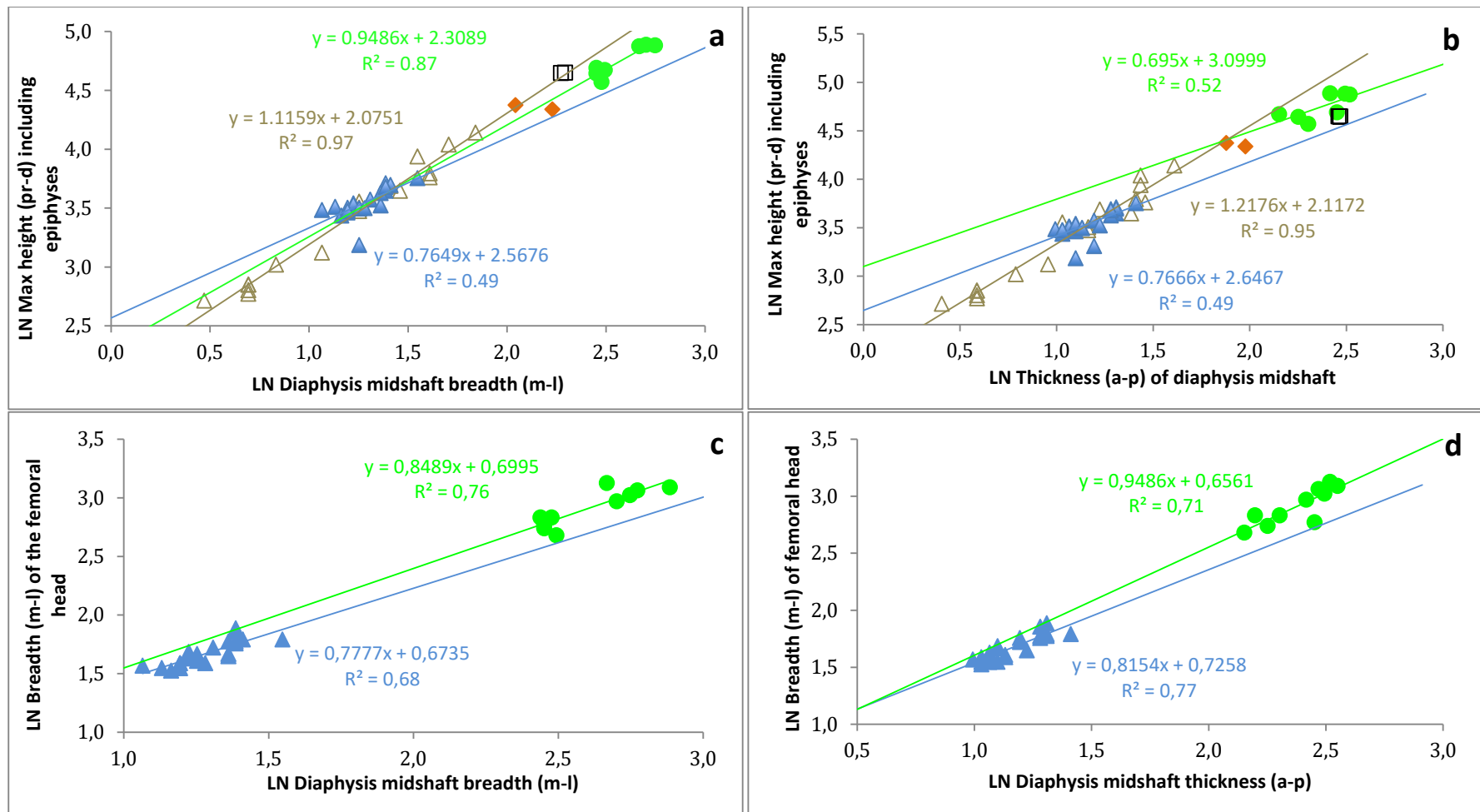


Fig. 4.26 Scatterplots of the dimensions of the femur a) Diaphysis midshaft breadth (m-l) vs. max height (pr-d) including epiphyses. b) Diaphysis midshaft thickness (a-p) vs. max height (pr-d) including epiphyses. c) Diaphysis midshaft breadth (m-l) vs. breadth (m-l) of femoral head. d) Diaphysis midshaft thickness (a-p) vs. breadth (m-l) of femoral head. Refer to Fig. 3.3 for symbol legend. [Data: *P. tiliensis* from Theodorou, 1983: 211, *P. antiquus* from Palombo *et al.*, unpublished].

v) Absolute dimensions and ratio of diaphysis breadth (m-l)/diaphysis thickness (a-p) – In terms of absolute size, one femur from Spinagallo Cave is unusual in its size, falling between the size of the smaller *P. ex gr. P. falconeri* and larger *P. ex gr. P. mnaidriensis* specimens, but being similar in size to the single distally-broken specimen from Luparello Fissure with a fused proximal epiphysis (see Fig. 4.25). The diaphysis has a tendency to be wider in *P. antiquus* from Neumark-Nord 1 in comparison to *P. ex gr. P. falconeri*, *P. tiliensis* and *L. africana* (Fig. 4.27). However *L. africana* has a particularly large range in intraspecific allometry, particularly in the larger specimens, with several outliers (Fig. 4.27).

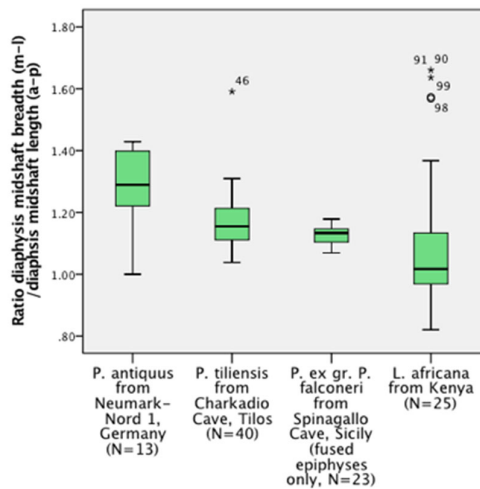


Fig. 4.27 Box-and-whisker plot of the ratio of the femur's diaphysis midshaft breadth (m-l)/diaphysis midshaft thickness (a-p).

(vi) Ratio max height (pr-d) including epiphyses/diaphysis midshaft breadth (m-l) - Differences are not significant between *P. antiquus* vs. *P. tiliensis* (MWU $p=0,383$), but are significant between *P. antiquus* vs. *P. ex gr. P. falconeri* (MWU $p=0,001$) and also between *P. ex gr. P. falconeri* vs. *P. tiliensis* (MWU $p=0,025$), indicating a progressive reduction in robusticity from *P. antiquus*, to *P. tiliensis*, and to *P. ex gr. P. falconeri*. (vii) Ratio max height including epiphyses (pr-d)/diaphysis midshaft thickness (a-p) - Differences are not statistically significant between *P. antiquus* vs. *P. ex gr. P. falconeri* (Fig. 4.22b, MWU $p=0,789$) or *P. antiquus* vs. *P. tiliensis* (MWU

$p=0,418$) or *P. ex gr. P. falconeri* vs. *P. tiliensis* (MWU $p=0,187$).

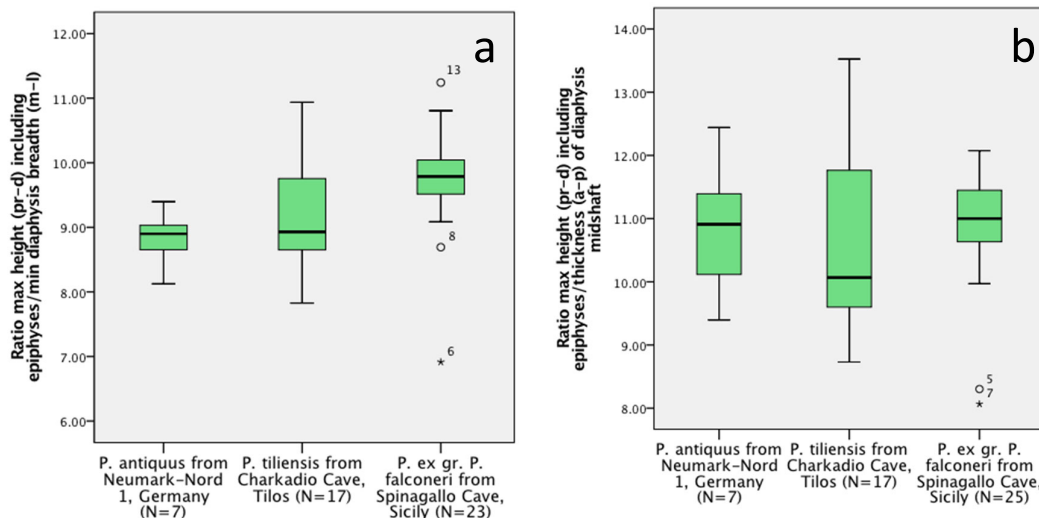


Fig. 4.28 a) Box-and-whisker plot of the ratio of the femur's max height (pr-d) including epiphyses vs. min diaphysis breadth (m-l). b) Box-and-whisker plot of the ratio of the femur's max height (pr-d) including epiphyses vs. thickness (a-p) of diaphysis midshaft.

(viii) Ratio breadth (m-l) of femoral head/diaphysis midshaft thickness (a-p) - Differences are not statistically significant between *P. ex gr. P. falconeri* and *P. antiquus* (MWU $p=0,162$), although *P. antiquus* has a tendency to have a relatively wider femoral head. (ix) Ratio breadth (m-l) of femoral head/diaphysis midshaft breadth (m-l) - Differences are statistically significant between *P. ex gr. P. falconeri* and *P. antiquus* (MWU $p=0,007$), reflecting a relatively wider femoral head in *P. ex gr. P. falconeri*.

4.1.5 Anatomy of the tibia

The tibia is relatively short, and proximally there are two concave condyles for articulation with the femur (Fig. 4.31e). The medial condyle, *Condylus medialis*, is larger and than the lateral condyle, and situated more cranially and is slanted upwards mediocranially whereas the lateral condyle, *Condylus lateralis*, slanted upwards medially (Fig. 4.31b, Fig. 4.31e). There is a deeply indented tibial tuberosity at the proximal end visible in cranial aspect (Fig. 4.31a). The medial and lateral tubercles are situated in a sagittal plane, with the medial tubercle situated more cranially than the lateral tubercle (Fig. 4.31e). A sagittal crest (*Eminentia intercondylaris*) is represented by a cranial and a caudal prominence (Fig. 4.31a, Fig. 4.31e). On the caudolateral aspect of the lateral condyle there is a round articular facet for the fibula, the *Facies articularis fibularis* (Fig. 4.31f). About halfway down the medial surface a prominent rough area for muscular attachment occurs (Fig. 4.31a). In caudal aspect the proximal half of the diaphysis was concave, with a rough surface below the condyles (the popliteal notch). The medial border forms a rounded, prominent ridge and the less prominent lateral border is rough for muscular attachment. On the caudal surface of the *Malleolus medialis* there is a groove, the *Sulcus malleolaris* (Fig. 4.31b). The distal articulation (*Cochlea tibiae*) is concave, consisting of a concave medial and a smaller, flattened lateral area (Fig. 4.31e). Adjacent to this and at an angle is the articular facet for the fibula (Fig. 4.31f; Smuts and Bezuidenhout, 1994: 57-58; Kroll, 1991: 28-29).

4.1.5.1 Interspecific variation in the tibia

The tibia was compared metrically (Fig. 4.37; Fig. 4.38; Fig. 4.41; Table 4.5), and in terms of its basic morphology (Figs 4.29-4.35). Morphologically noteworthy characteristics include (i) robusticity of the epiphyses relative to the diaphysis (Fig. 4.29-4.35), (ii) synostosis between the tibia-fibula (Fig. 4.36), (iii) the presence/absence and size of the *Linea muscularis* on the craniomedial surface of the diaphysis (Fig. 4.29a; Fig. 4.30a; Fig. 4.31a; Fig. 4.32a; Fig. 4.33a; Fig. 4.34a; Fig. Fig. 4.35a). (iv) Finally the shape of the *Tuberositas tibiae* differs between represented species (ibid.).

4.1.5.2 Cranial profile and external characteristics

In contrasting adult *P. ex gr. P. falconeri* with adult *P. antiquus*, the former species has robust epiphyses and a more slender diaphysis, which also narrows more towards the distal end in contrast to the more parallel-sided diaphysis of *P. antiquus* (Fig. 4.31a, b; Fig. 4.35a, b). In contrasting juvenile *L. africana* with adult *L. africana*, although the epiphyses are not ossified in the juvenile, they were evidently more robust than in the adult. Finally, in

comparing *Palaeoloxodon* sp. 1 with all other species, the diaphysis is extremely robust, as are the epiphyses.

In *P. ex gr. P. falconeri* synostosis sometimes occurs at the proximal and distal ends of the tibia-fibula. Unlike in the ulna-radius where fusion occurs along the diaphysis shaft (Ambrosetti, 1968: Plate XI), synostosis only occurs proximally and distally. Proximally, synostosis does not alter the morphology of the articulation with the femur, but distally immobilizes the union between the tibia-fibula which articulates with the astragalus-calcaneus. Further, the morphology of the *Tuberositas tibiae* also varies, being V-shaped in the represented specimens of adult *P. antiquus* from Germany (Fig. 4.35a) and Sicily (Fig. 1.4d), contrasting with the U-shaped Sicilian dwarfs represented in this thesis, as seen in *P. ex gr. P. falconeri* (Fig. 1.4a; Fig. 4.31a; Fig. 4.36a), *Palaeoloxodon* sp. 1 from Luparello Fissure (Fig. 1.4b; Fig. 4.32a; see also Vaufray, 1929: Plate VIII, Fig. 11) and *P. ex gr. P. mnaidriensis* from Puntali Cave (Fig. 1.4c; Fig. 4.33a; see also Mangano and Bonfiglio, 2012: Fig. 9 for San Teodoro Cave). Finally, the presence of a proximo-distally orientated *Linea muscularis* on the craniomedial diaphysis surface varies: In the specimens figured, the line is visible in juvenile *L. africana* (Fig. 4.29a) and the adults of *L. africana* (Fig. 4.30a), *P. ex gr. mnaidriensis* (Fig. 4.33a) and *P. antiquus* (Fig. 4.35a). However, the presence of the line is also intraspecifically variable.

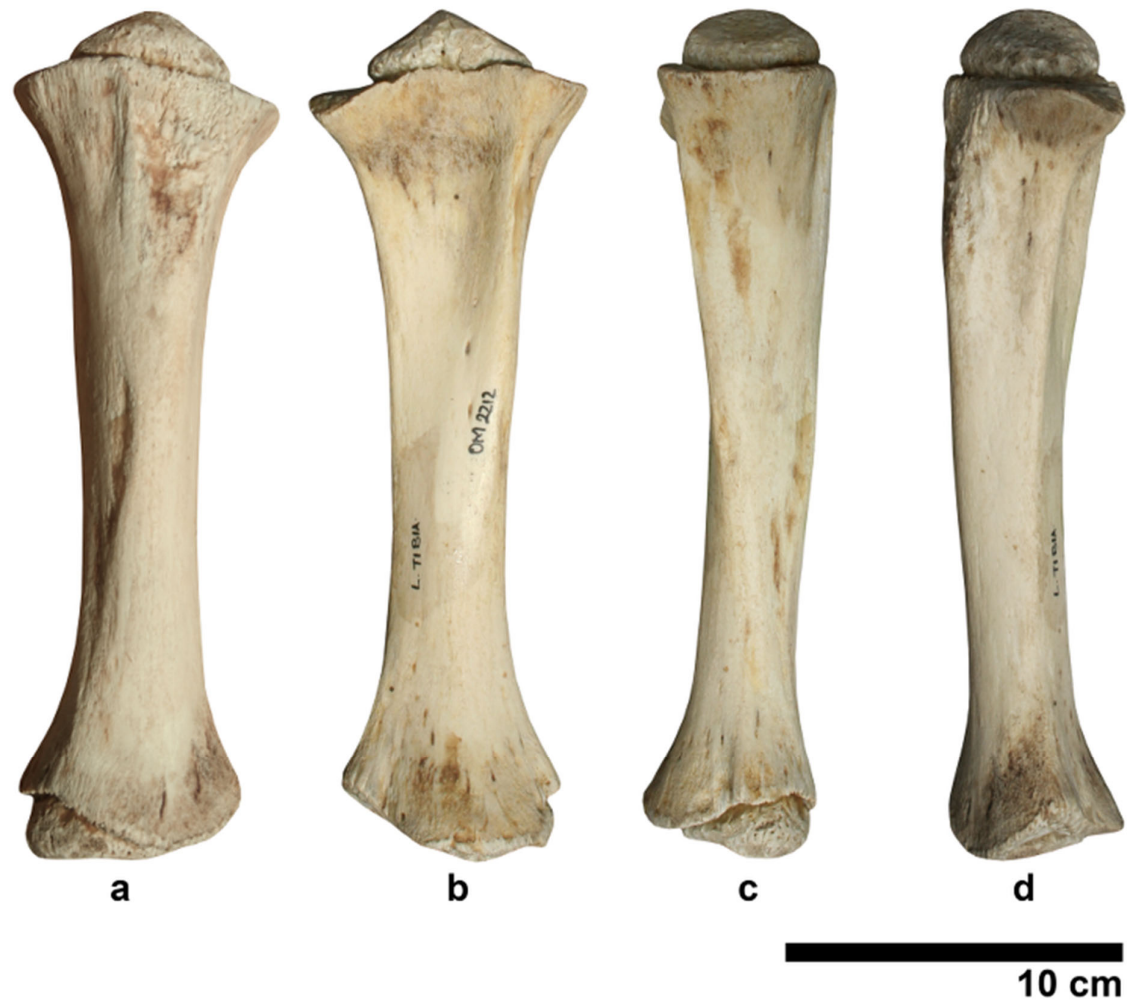


Fig. 4.29 Tibia of juvenile *L. africana* from Kenya a) cranial b) caudal c) medial d) lateral (KNM-OM2212)^{sin}. Refer to Table 2.8 for ontogenetic metadata.

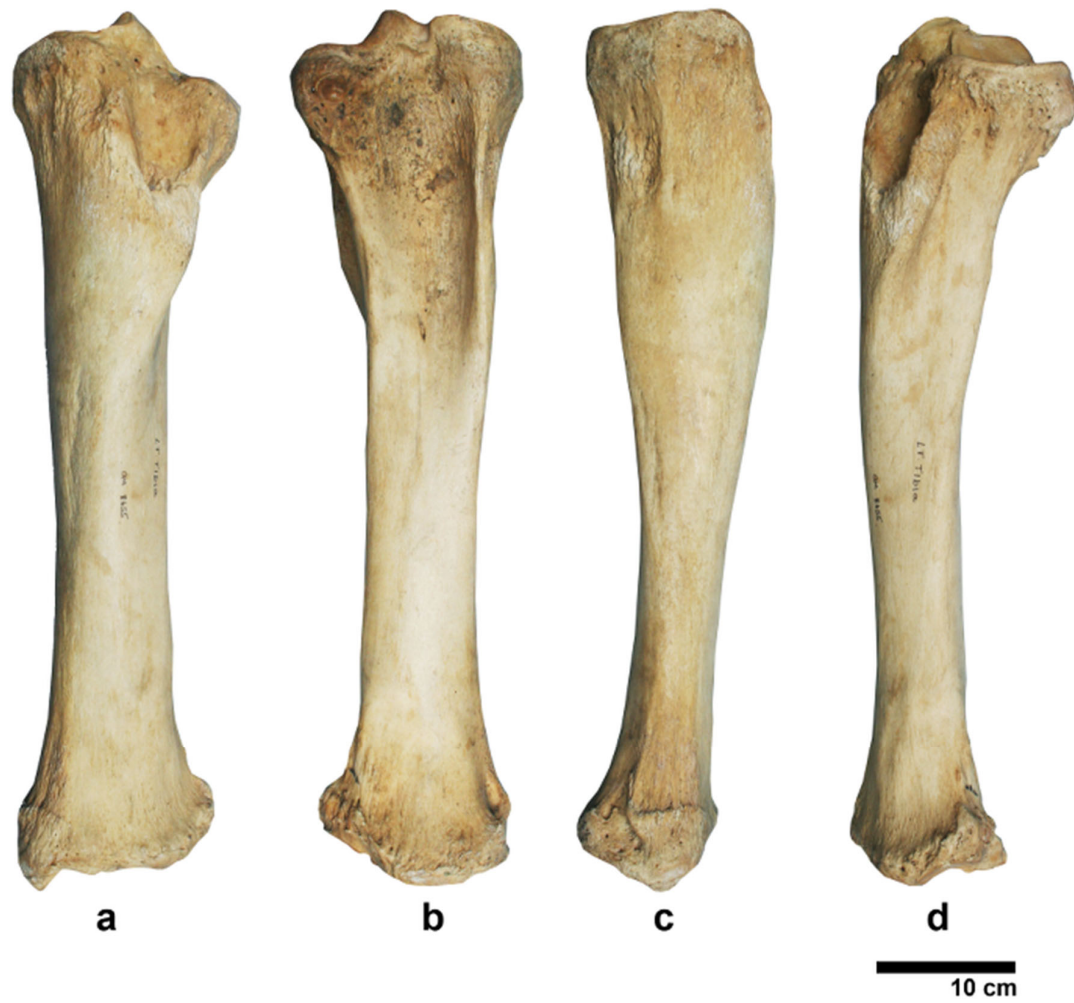


Fig. 4.30 Tibia of adult *L. africana* from Kenya a) cranial b) caudal c) medial d) lateral (KNM-OM8655)^{sin}. Refer to Table 2.8 for ontogenetic metadata.

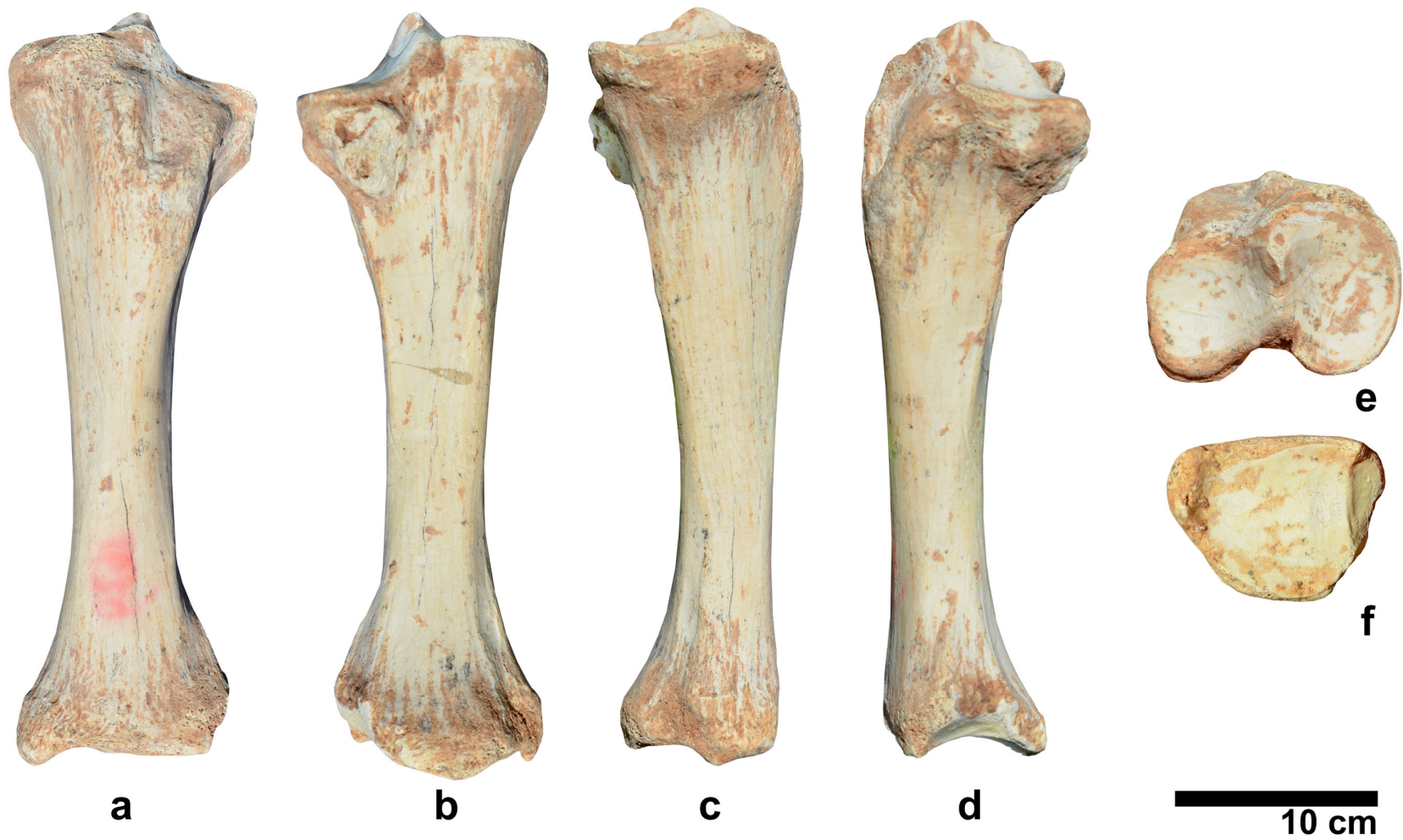


Fig. 4.31 Tibia of *P. ex gr. P. falconeri* from Spinagallo Cave, Sicily a) cranial b) caudal c) medial and d) lateral e) superior f) inferior (MPRU)^{dex}.

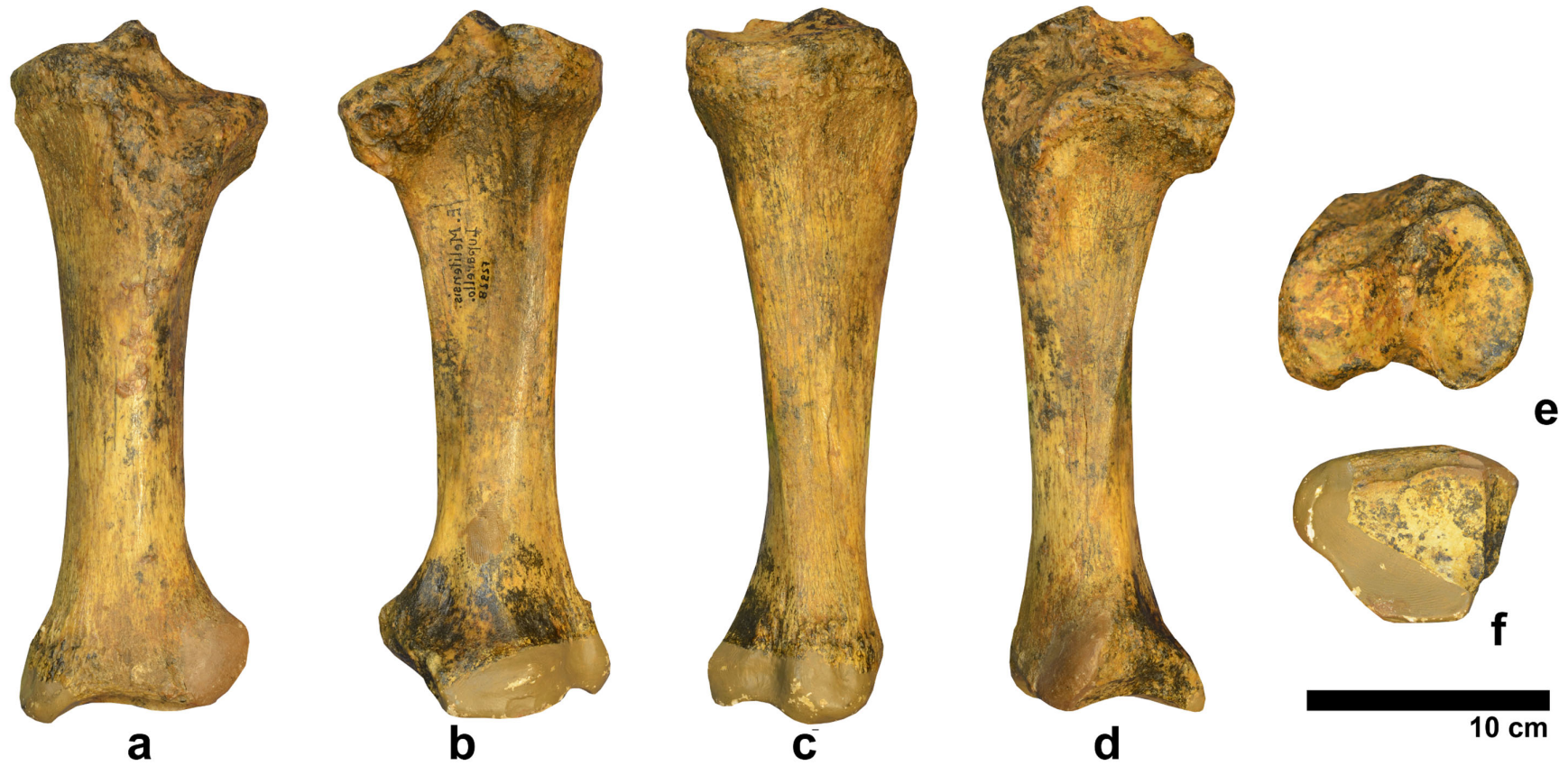


Fig. 4.32 *Tibia* of *Palaeoloxodon* sp. 1 from Luparello Fissure, Sicily a) cranial b) caudal c) medial d) lateral e) superior f) inferior (IPH-F2928)^{dex}.
Note that the distal epiphysis is partially reconstructed.



Fig. 4.33 Tibia of *P. ex gr. P. mnaidriensis* from Puntali Cave, Sicily a) cranial b) caudal c) medial and d) lateral (GMP-GPM12)^{sin}.

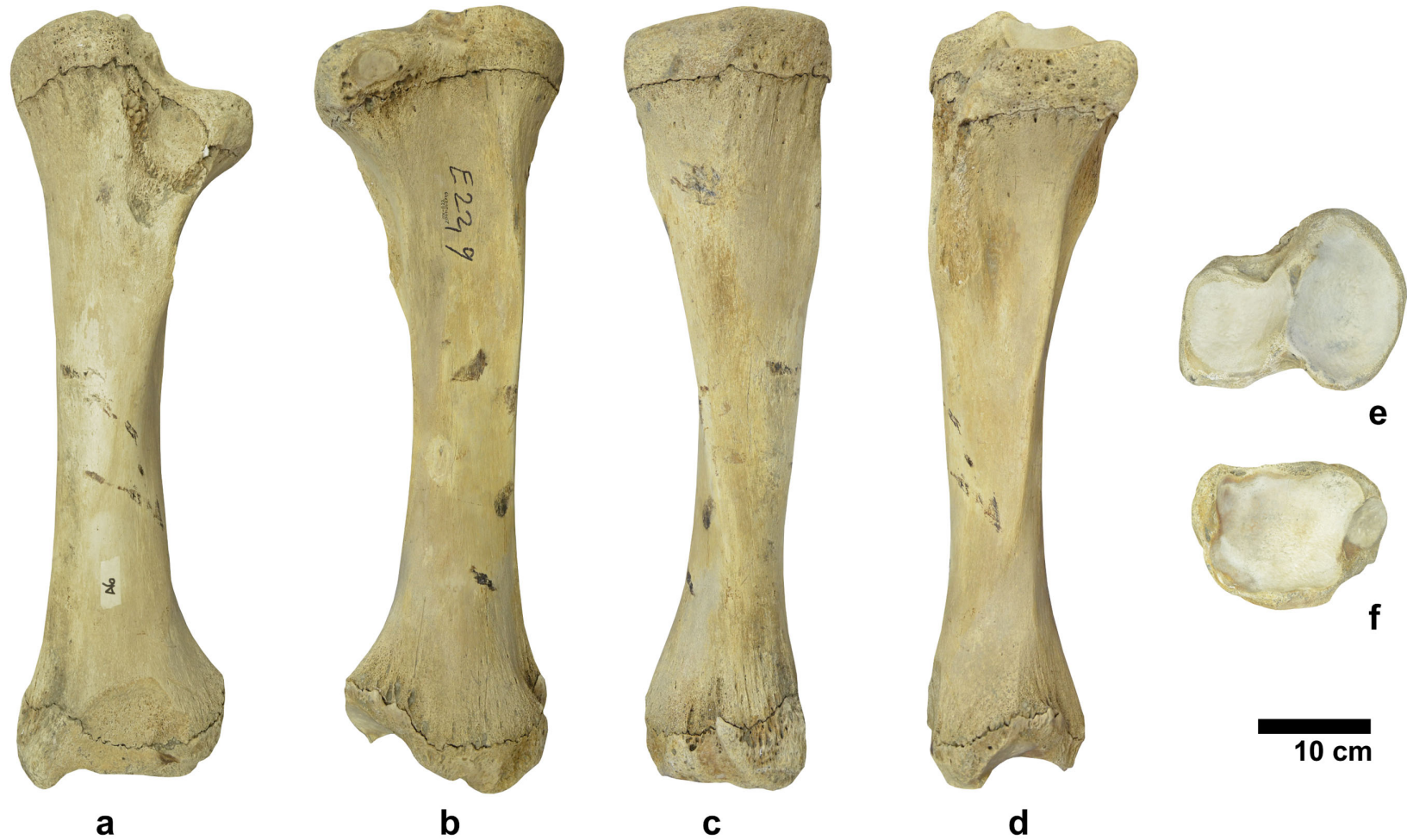


Fig. 4.34 Tibia of young *P. antiquus* from Neumark-Nord 1, Germany a) cranial b) caudal c) medial d) lateral e) superior f) inferior (LVH-NN-E22)^{sin}. Refer to Marano and Palombo, 2013: Table 3 for ontogenetic metadata.



Fig. 4.35 Tibia of adult *P. antiquus* from Neumark-Nord 1, Germany a) cranial b) caudal c) medial d) lateral e) superior f) inferior (LVH-NN-E8,47 and 2003: 55,7)^{dex}. Refer to Marano and Palombo, 2013: Table 3 for ontogenetic metadata.

4.1.5.3 Bivariate allometry in adult *Palaeoloxodon* spp.



Fig. 4.36 Synostotically fused tibia-fibula of *P. ex gr. P. falconeri* from Spinagallo Cave
a) cranial aspect b) Inferior aspect (UCat-T60)^{sin}.

P. antiquus vs. *P. ex gr. P. falconeri* - Differences are statistically significant for the ratio of the max height (pr-d) including epiphyses vs. max breadth (m-l) of distal epiphysis (Table 4.5) and also for the max height (pr-d) including epiphyses vs. thickness (a-p) of distal epiphysis (Table 4.5). *P. antiquus* vs. *P. ex gr. P. mnaidriensis* - Differences are statistically significant for the ratio between max height (pr-d) including epiphyses/max breadth (m-l) of the distal epiphysis Fig. 4.37b; Table 4.5), reflecting a relatively broader (m-l) distal epiphysis in *P. ex gr. P. mnaidriensis*. Other bivariate ratios between the species are not statistically significant (Fig. 4.37a; Fig. 4.38a; Table 4.5). *P. ex gr. P. mnaidriensis* vs. *P. ex gr. P. falconeri* - Differences are not statistically significant between the two species where compared (Fig. 4.37a, b; Fig. 4.38a; Table 4.5). *L. africana* vs. *Palaeoloxodon* spp. - Although sample-size is small, the tibia of *L. africana* is clearly much more slender than in *Palaeoloxodon* spp. (Fig. 4.37a, b; Fig. 4.38).

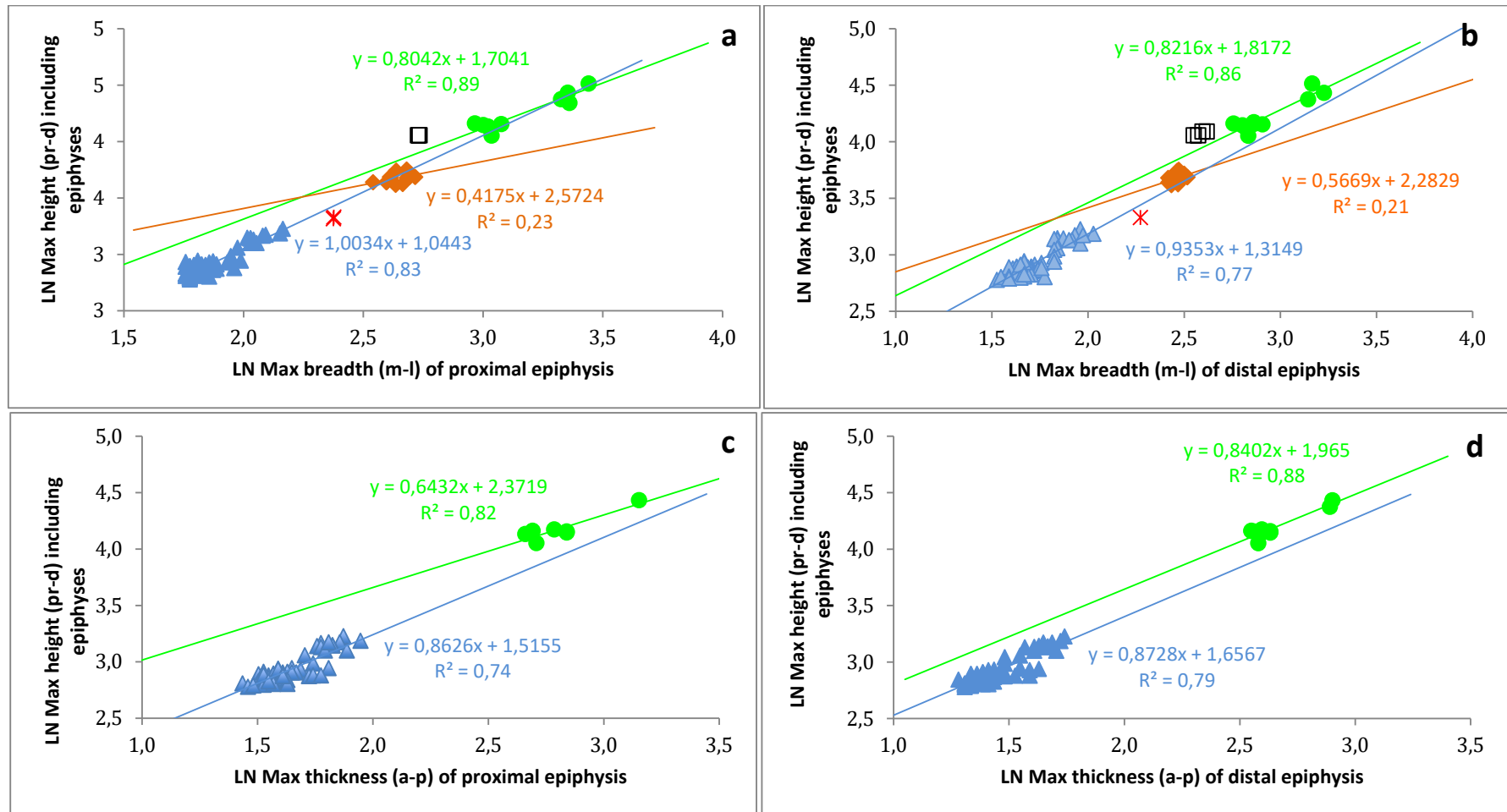


Fig. 4.37 Scatterplots of the dimensions of the tibia. a) Max breadth (m-l) of proximal epiphysis vs. max height (pr-d) including epiphyses. b) Max breadth (m-l) of distal epiphysis vs. max height (pr-d) including epiphyses. c) Max thickness (a-p) of proximal epiphysis vs. max height (pr-d) including epiphyses. d) Diaphysis midshaft breadth (m-l) vs. max height (pr-d) including epiphyses. Note that values are approximate for *Palaeoloxodon* sp. 1 due to specimen damage. Refer to Fig. 3.3 for symbol legend. [Data: *P. ex gr. P. falconeri* from Ambrosetti, 1968: 366; *P. antiquus* from Palombo *et al.*, unpublished].

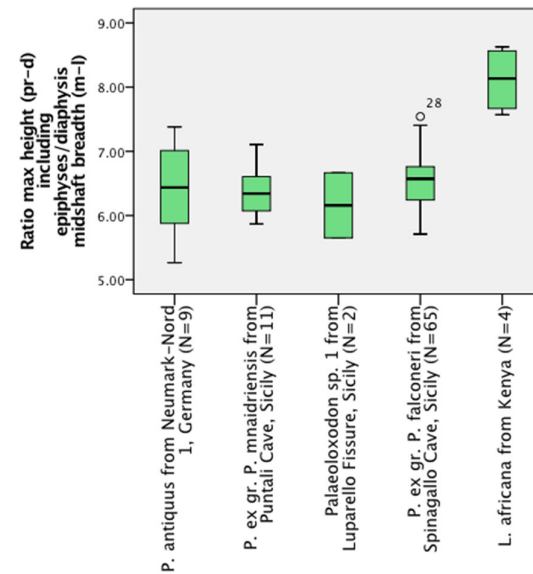
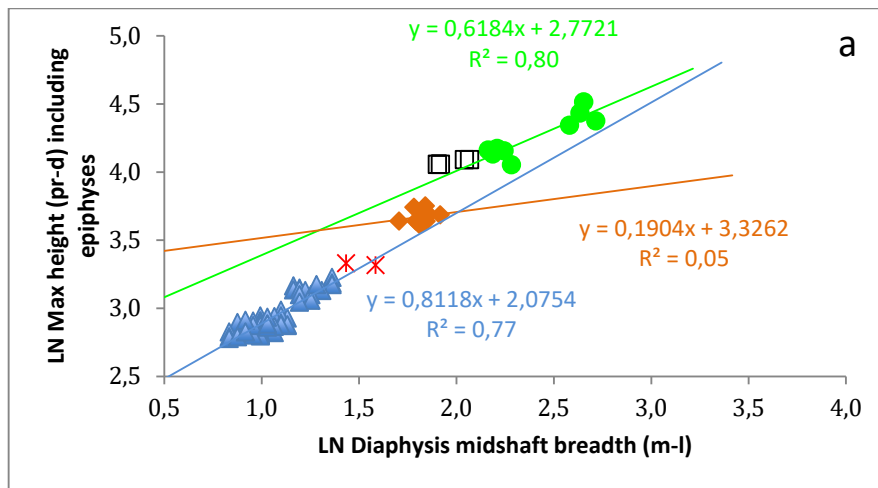


Fig. 4.38 a) Scatterplot of the tibial max height (pr-d) including epiphyses vs. diaphysis midshaft breadth (m-l). Note that values are approximate for *Palaeoloxodon* sp. 1 due to specimen damage. Refer to Fig. 3.3 for symbol legend. [Data: *P. ex gr. P. falconeri* from Ambrosetti, 1968: 366; *P. antiquus* from Palombo *et al.*, unpublished]. b) Box-and-whisker plot of the tibia's max height (pr-d) including epiphyses/diaphysis midshaft breadth (m-l).

Bivariate ratio	Fig.	MWU p-value	<i>P. antiquus</i> vs. <i>P. ex gr. P. falconeri</i>	MWU p-value	<i>P. antiquus</i> vs. <i>P. ex gr. P. mnaidriensis</i>
Max height (pr-d) including epiphyses/max breadth (m-l) of proximal epiphysis	4.37a	0,155	Not significant	0,058	Not significant
Max height (pr-d) including epiphyses/max breadth (m-l) of distal epiphysis	4.37b	0,001*	<i>P. ex gr. P. falconeri</i> distal epiphysis is relatively broader	0,009*	<i>P. ex gr. P. mnaidriensis</i> distal epiphysis is relatively broader
Max height (pr-d) including epiphyses/max thickness (a-p) of proximal epiphysis	4.37c	0,112	Not significant	-	-
Max height (pr-d) including epiphyses/thickness (a-p) of distal epiphysis	4.37d	0,002*	<i>P. ex gr. P. falconeri</i> distal epiphysis is relatively thicker	-	-
Max height (pr-d) including epiphyses/diaphysis midshaft breadth (m-l)	4.38a	0,637	Not significant	1,000	Not significant

Table 4.5 Mann-Whitney pairwise p-values of allometric differences in the tibia of *P. antiquus* from Neumark-Nord 1, Germany and *P. ex gr. P. falconeri* from Spinagallo Cave, Sicily, and *P. ex gr. P. mnaidriensis* from Puntali Cave, Sicily. Statistically significant values are indicated with an asterisk (*). For the regression table refer to Appendix E.

4.1.5.4 Contrasting ontogenetic series in *P. ex gr. P. falconeri* and *L. africana*

Due to its robusticity, the tibia is one of the most frequently represented elements in fossil assemblages, and is the most frequently represented element from Spinagallo Cave (Ambrosetti, 1968: 285). Thus the tibia was chosen for detailed study, particularly with regard to testing Hypothesis II (*Heterochrony causing dwarfism resulted in pedomorphic morphologies in the limbs of P. ex gr. P. falconeri* from Spinagallo Cave). In the next section the ontogenetic allometry of *P. ex gr. P. falconeri* and *L. africana* are compared, beginning with an examination of the large assemblage from Spinagallo Cave. Thereafter the specific prediction of Hypothesis II is tested that juvenile *L. africana* (with unfused epiphyses) is morphologically more similar to adult *P. ex gr. P. falconeri* (with fused epiphyses) than adult *L. africana*. This is tested using bivariate allometric comparisons and Mann Whitney U tests. Allometric differences are also illustrated using box-and-whisker plots.

4.1.5.5 Intraspecific variability in *P. ex gr. P. falconeri* from Spinagallo Cave

In contrast with previous studies (Ambrosetti, 1968; Herridge, 2010), the allometry of the tibia sample from Spinagallo Cave was sampled across the entire ontogenetic range. In most bivariate comparisons, ontogenetic allometry scales with approximate isometry (Fig. 4.40). However, in several cases there are allometric trends which depart from isometry during ontogeny: (i) Ratio of the min diaphysis breadth/max diaphysis height - The diaphysis has a tendency to become relatively taller (pr-d) during ontogeny (Fig. 4.40). (ii) Ratio of the max breadth (m-l) of the proximal end of the diaphysis/min diaphysis breadth (m-l) - The proximal end has a tendency to become relatively wider during ontogeny (Fig. 4.40). (iii) The ratio of the max breadth (m-l) of the proximal end of the diaphysis/max diaphysis height (pr-d) - In all



Fig. 4.39 Distal tibia of *P. ex gr. P. falconeri* from Spinagallo Cave, illustrating morphological variability in the *Cochlea tibiae*.

the bivariate scatterplots there is more morphological variability represented by epiphyseal fusion stage 5 (and to some extent in 2, 3 and 4) compared with epiphyseal fusion stage 0 (Fig. 4.40). A wide range in size is however also represented in epiphyseal fusion stage 0 (in which the epiphysis is unfused and unattached, see Fig. 4.40). Although not compared metrically, the morphology of the *Tuberositas tibiae* also varies significantly, extending more distally on the posterior side in some specimens than others (Fig.

4.39).

Following the prediction of Hypothesis II the allometry of the tibia of juvenile *L. africana* (with unfused epiphyses) is expected to be more similar to that of adult *P. ex gr. P. falconeri* (with fused epiphyses) than that of adult *L. africana*. In order to investigate whether there is any evidence of paedomorphism therefore, the allometry of the two species was compared using pairwise Mann-Whitney U tests, using subsamples of *P. ex gr. P. falconeri* and *L. africana* categorised as juveniles (with unfused epiphyses) and adults (with fused epiphyses). Below three bivariate ratios are examined: (i) Ratio of the diaphysis height (pr-d)/breadth (m-l) of the proximal diaphysis; (ii) Ratio of the diaphysis height/breadth (m-l) of the distal diaphysis; (iii) Ratio max breadth (m-l) of proximal diaphysis/max breadth (m-l) of distal diaphysis .

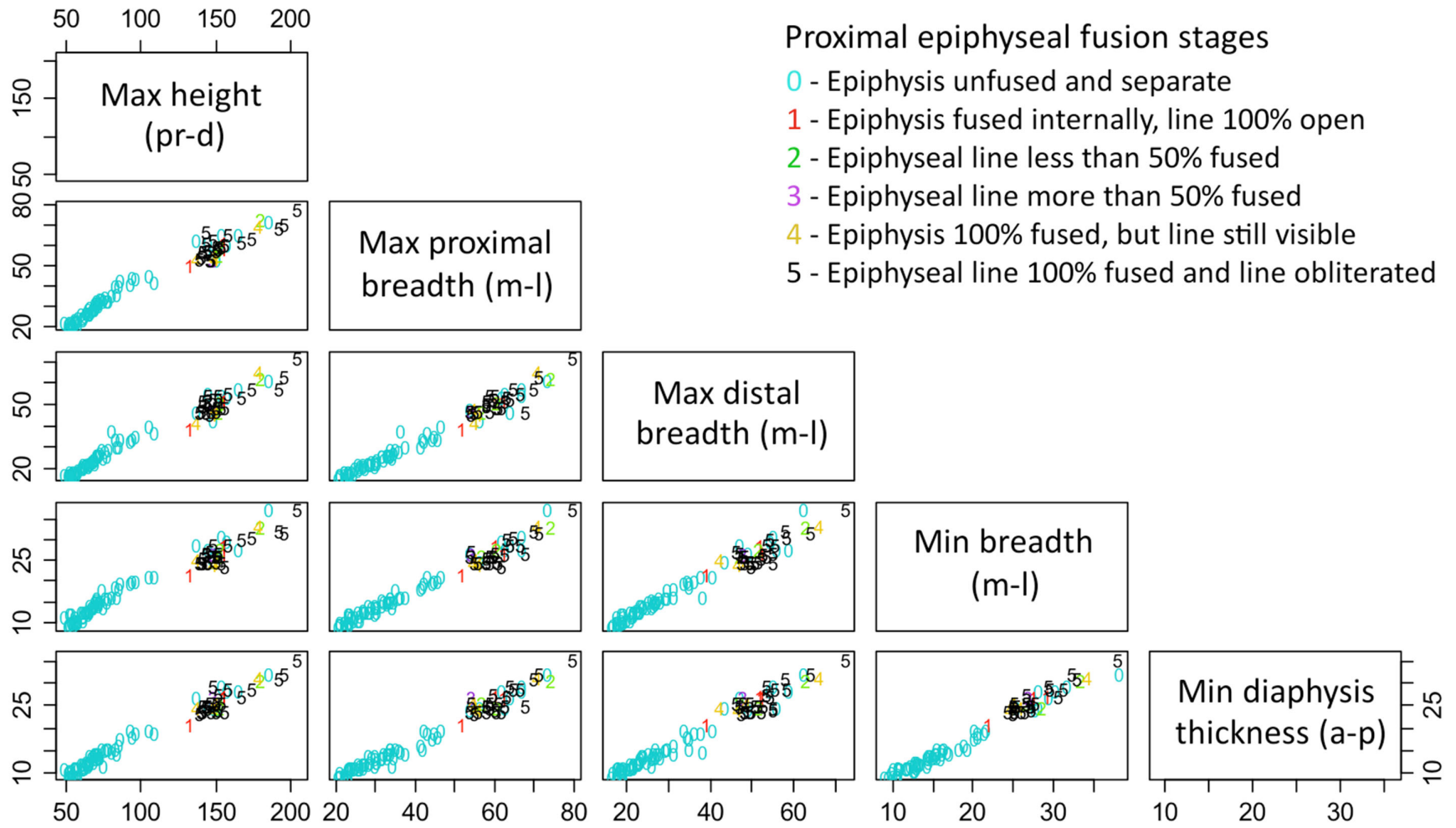


Fig. 4.40 Scatterplots of the dimensions of the *P. ex gr. P. falconeri* tibia diaphysis from Spinagallo Cave (UCat collection). Epiphyseal fusion stages are scored following Herridge, 2010: Fig. 5.2. Note that all measurements are taken on the diaphysis (in mm), even where the epiphysis is present (in fusion stages 1-5) in order to compare a wide range in ontogeny.

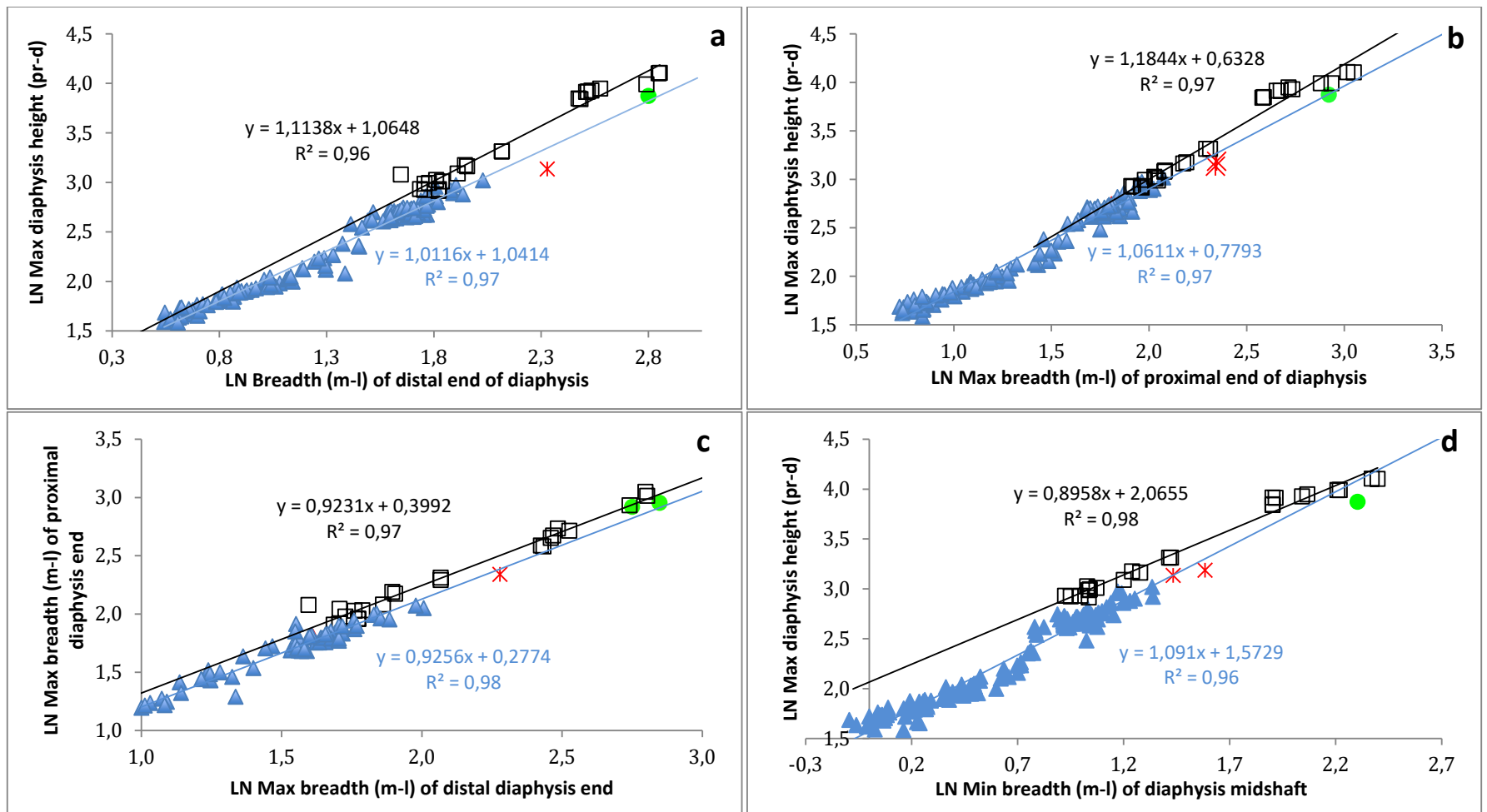


Fig. 4.41 Scatterplots of the interspecific bivariate allometry of the tibia. a) Max breadth (m-l) of distal end of diaphysis vs. max diaphysis height (pr-d). b) Max breadth (m-l) of proximal end of diaphysis vs. max diaphysis height (pr-d). c) Max breadth (m-l) of distal end of diaphysis vs. max breadth (m-l) of proximal end of diaphysis. d) Breadth (m-l) at diaphysis midshaft vs. max diaphysis height (pr-d). Ontogenetic stages: sample includes unfused and fused epiphyses in *P. ex gr. P. falconeri* and *L. africana*. Refer to Fig. 3.3 for symbol legend.

(i) Ratio of the diaphysis height (pr-d)/breadth (m-l) of the proximal end of the diaphysis

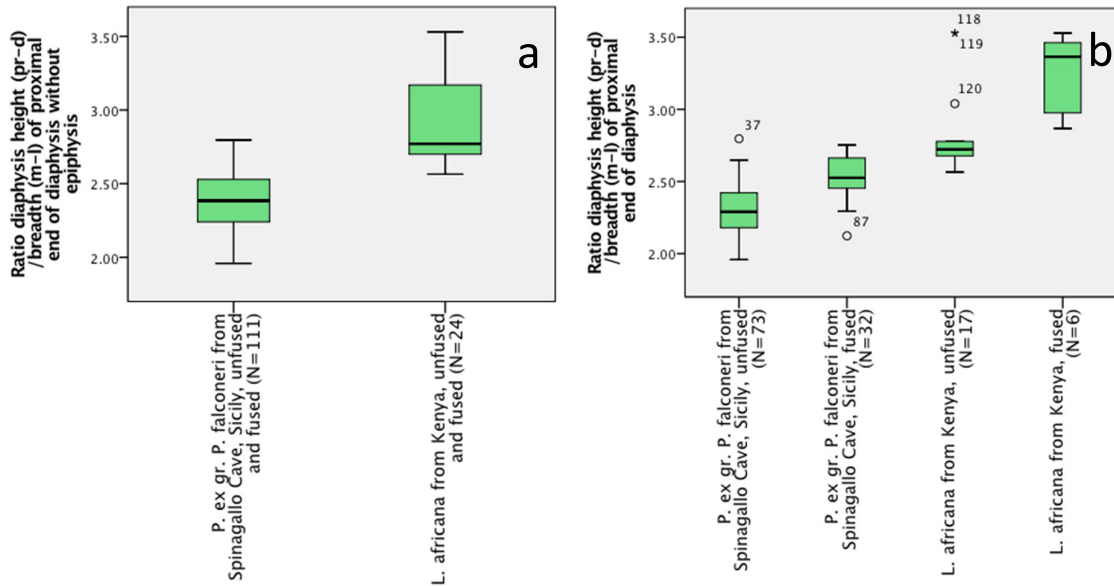


Fig. 4.42 Box-and-whisker plot of the ratio of the tibia's diaphysis height (pr-d)/breadth (m-l) of the proximal end of diaphysis without the epiphysis a) Pooled samples of unfused and fused epiphyses. b) Samples divided into groups with fused and unfused epiphyses. For dental stages of unfused and fused samples refer to Table 2.28.

Differences are statistically significant between *L. africana* and *P. ex gr. P. falconeri* when all ontogenetic stages are compared together (MWU $p=0,000$), reflecting that the *L. africana* diaphysis has a tendency to be more slender than in *P. ex gr. P. falconeri*. However, in both adult *L. africana* and adult *P. ex gr. P. falconeri* the diaphysis is relatively taller in the fused sample than the unfused sample (Fig. 4.42; see MWU p -values in Table 4.6). Further, the allometry of juvenile *L. africana* with unfused epiphyses is more similar to that of adult *P. ex gr. P. falconeri* than that of adult *L. africana*. In conclusion, although there are significant statistical differences between juvenile *L. africana* and adult *P. ex gr. P. falconeri*, and there is overlap in the allometry of these two samples, there is a tendency for juvenile *L. africana* to be more similar in terms of bivariate allometry than adult *L. africana* to adult *P. ex gr. P. falconeri*.

(ii) Ratio of the diaphysis height/breadth (m-l) of distal end of the diaphysis - Relative to the diaphysis height, the distal end has a tendency to be broader in *P. ex gr. P. falconeri* than in *L. africana* (Fig. 4.43; Table 4.6). However, the allometry of juvenile *L. africana* is more similar to adult *P. ex gr. P. falconeri* than that of adult *L. africana* (Fig. 4.43; Table 4.6). Although there are smaller differences in the ratio between *P. ex gr. P. falconeri* and *L. africana* (comparing all ontogenetic stages) differences are nonetheless statistically significant (MWU $p=0,003$). When different subsamples are compared, in both *P. ex gr. P. falconeri* and *L. africana* the proximal end appears to be slightly broader in the sample with unfused epiphyses than in the sample with fused epiphyses (Fig. 4.43; Table 4.6). However, the allometry is less similar between juvenile *L. africana* and adult *P. ex gr. P. falconeri* than it is between adult *L. africana* and adult *P. ex gr. P. falconeri* (Fig. 4.43; Table 4.6).

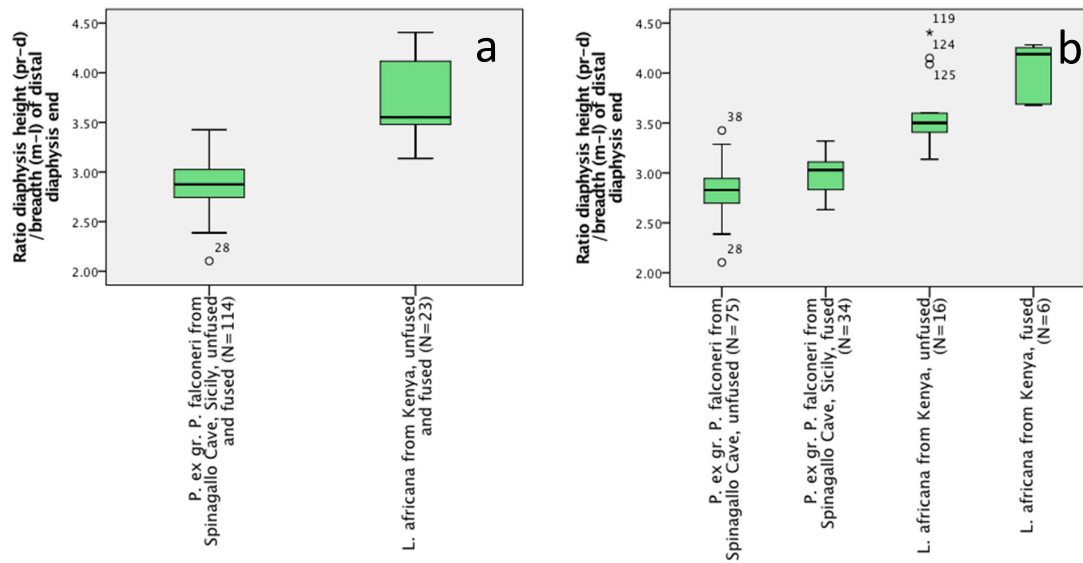


Fig. 4.43 Box-and-whisker plot of the ratio of the tibia's diaphysis height (pr-d)/breadth (m-l) of the distal end of diaphysis without the epiphysis a) Pooled samples of unfused and fused epiphyses. b) Samples divided into groups with fused and unfused epiphyses. For dental stages of unfused and fused samples refer to Table 2.28.

(iii) Ratio max breadth (m-l) of proximal diaphysis end/max breadth (m-l) of distal diaphysis end

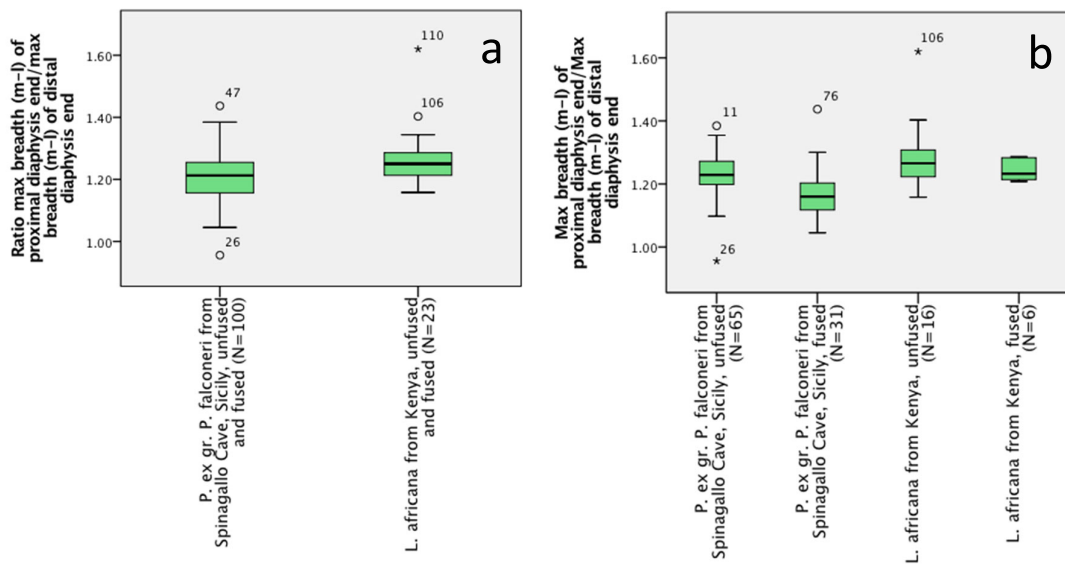


Fig. 4.44 Box-and-whisker plot of the ratio of the tibia's max breadth (m-l) of the proximal end of diaphysis without the epiphysis/max breadth (m-l) of distal diaphysis end without epiphysis a) Pooled samples of unfused and fused epiphyses b) Samples divided into groups with fused and unfused epiphyses. For dental stages of unfused and fused samples refer to Table 2.28.

Bivariate ratio	Samples compared	MWU p-value	<i>L. africana</i> (N)	<i>P. ex gr. P. falconeri</i> (N)	Figs
Ratio diaphysis height (pr-d)/breadth (m-l) of proximal end of diaphysis	Juvenile <i>P. ex gr. P. falconeri</i> /Adult <i>P. ex gr. P. falconeri</i>	0,000	-	73 unfused 32 fused	Fig. 4.41; Fig. 4.42
	Juvenile <i>L. africana</i> /Adult <i>L. africana</i>	0,006	17 unfused 6 fused	-	
	Juvenile <i>L. africana</i> /Adult <i>P. ex gr. P. falconeri</i>	0,000	17	32	
Ratio diaphysis height (pr-d)/breadth (m-l) of distal diaphysis end	Juvenile <i>P. ex gr. P. falconeri</i> /Adult <i>P. ex gr. P. falconeri</i>	0,000	-	75 unfused 34 fused	Fig. 4.41a; Fig. 4.43
	Juvenile <i>L. africana</i> /Adult <i>L. africana</i>	0,005	16 unfused 6 fused	-	
	Juvenile <i>L. africana</i> /Adult <i>P. ex gr. P. falconeri</i>	0,000	16	34	
	Adult <i>L. africana</i> /Adult <i>P. ex gr. P. falconeri</i>	0,000	6	34	
Ratio max breadth (m-l) of proximal diaphysis end/max breadth (m-l) of distal diaphysis end	Juvenile <i>P. ex gr. P. falconeri</i> /Adult <i>P. ex gr. P. falconeri</i>	0,000	-	65 unfused 31 fused	Fig. 4.41c; Fig. 4.44
	Juvenile <i>L. africana</i> /Adult <i>L. africana</i>	0,005	16 unfused 6 fused	-	
	Juvenile <i>L. africana</i> /Adult <i>P. ex gr. P. falconeri</i>	0,000	16	31	

Table 4.6 Allometry of the tibia in *L. africana* and *P. ex gr. P. falconeri*. Adults are individuals with both fused proximal and distal epiphyses (fusion stages 1-5), and juveniles are with both proximal and distal epiphyses unfused and unattached (fusion stage 0). For dental stages of unfused and fused samples refer to Table 2.8. For the regression table refer to Appendix E.

4.1.6 Scaling in *Palaeoloxodon* limb bones

Data were obtained from adult *Palaeoloxodon* long-bones (Appendix F, Fig. 6.1) belonging to the ca. 1m-tall *P. ex gr. P. falconeri* to the ca. 3,4m-tall *P. antiquus* (Table 2.1), a range in mass from ca. 165-300 kg to 6,000-12,000 kg respectively (Larramendi, 2016; Larramendi and Palombo, 2015: 104; Romano *et al.*, 2019). R^2 values are greater 0,97 for all long-bones. As outlined in chapter 2. An isometric relationship would generate a slope equal to 1.0 (with negative and positive allometry exhibiting slopes less and greater than one,

respectively). In contrast, according to the predictions of elastic similarity one would expect a slope gradient = 0,67. Thus, if a line plotted through all the data (including all species) falls within the 95% confidence interval elastic similarity applies.

The results (Table 4.7) indicate isometry in the adult humerus, ulna and femur, but not in the tibia. Elastic similarity was however rejected in all four long-bones. Seeing sample-sizes are very small for adult *L. africana*, the species was excluded entirely from the scaling analysis (McMahon, 1973; 1975).

Element	Fig.	N (<i>Palaeoloxodon</i>)	R ²	Low CI	Upp CI	Isometry	Elastic similarity
Humerus	6.1a	26	0.975	0.968	1.107	Yes	No
Ulna	6.1b	53	0.971	0.973	1.073	Yes	No
Femur	6.1c	49	0.973	0.935	1.032	Yes	No
Tibia	6.1d	87	0.979	0.928	0.988	No	No

Table 4.7 Scaling in the long-bones *Palaeoloxodon* spp. Refer to Appendix F for data. All values were calculated in SPSS.

4.2 DISCUSSION

The purpose of the chapter was to test (i) Hypothesis III (*As mass decreases in dwarf elephants gait becomes more agile in the antero-posterior direction*); (ii) Hypothesis II (*Heterochrony causing dwarfism resulted in paedomorphic morphologies in the limbs of P. ex gr. P. falconeri from Spinagallo Cave*) and (iii) To provide an improved understanding of how the long bones differ between different species of the genus *Palaeoloxodon*. In evaluating the data, this assessment demonstrated that the morphology of the bones of insular *Palaeoloxodon* spp. differs considerably from those of *P. antiquus* and *L. africana*. In contrast, the articular surface of the glenoid fossa was found to be similar between *P. antiquus* and *P. ex gr. P. falconeri*. In the next section differences in the morphology of each of the long bones in the limbs are discussed, as well as the absence of differences in the glenoid fossa, and concludes with a discussion concerning the differences documented between *Palaeoloxodon* sp. 1 and *P. ex gr. P. falconeri*.

4.2.1 Scapula's glenoid fossa

Size-frequency distribution in the scapula's glenoid fossa from Spinagallo Cave - Despite the large sample-size, the four size-frequency modes characteristic of the Spinagallo Cave long-bone assemblages (see Ambrosetti, 1968: Figs 40, 42-48, 52) is not clearly identifiable in the scapula's glenoid fossa (Fig. 4.1a). These four modes in the long bones were attributed to A) juveniles B) the onset of maturity, C) adult females and D) adult males (Ambrosetti, 1968: 325). Reasons for this discrepancy in the size-frequency distributions between long bones and the scapula's glenoid fossa may therefore include: (i) Scapulae with unfused glenoid fossa were almost absent, and not included in the sample; (ii) At least seven specimens were excluded from the study (UCat; MPRU; NHMB) due to being on display as part of mounted skeletons or unavailable. Unfortunately it was not recorded how many scapulae were originally identified from the Spinagallo Cave assemblage (Ambroestti, 1968), but the measured sample is likely to be almost complete.

The measurements indicate relatively little change in allometry during ontogeny in the glenoid fossa of *P. antiquus*, *P. ex gr. P. falconeri* or *L. africana* (Fig. 4.1b-d; Fig. 4.2a-c), although previous studies among Elephatinae species have briefly described ontogenetic changes in the allometry, including in the depth of the glenoid fossa, although without metric comparisons (Roth, 1982: 199; Roth, 1984; Maschenko, 2006: 136). However, the samples studied in this thesis could not evaluate ontogenetic allometry in young individuals and only produced broadly comparable measurements in juvenile *L. africana* due to the fact that the articular surface is unossified.

Flexion between the glenoid fossa and humerus of *P. ex gr. P. falconeri* - Several features in the appendicular anatomy of *P. ex gr. P. falconeri* have been described as evidence for a more cursorial locomotion with morphological adaptations similar to proboscideans from open environments (Caloi and Palombo, 1994; Palombo, 1996, 2003; Palombo, 2004: 362). For example, the acromion process in the scapula is more robust and in a lower position than the metacromion (Palombo, 2003: 288). *P. ex gr. P. falconeri* is supposedly more saggital in its locomotion and the legs allegedly have greater antero-posterior mobility in the sagittal plane than other elephants (Palombo and Petronio, 1989: 96; Caloi and Palombo, 1994: 154). Furthermore, the tibia minimum diaphysis breadth (m-l) is less than the diaphysis thickness (a-p), which has never been observed in the Elephantimorpha (*sensu* Shoshani and Tassy, 2005: Table 2), but is typical of cursorial mammals (Larramendi and Palombo, 2015 citing Christiansen, 2007). However, no statistically significant differences in the glenoid fossa were observed between *P. antiquus* and *P. ex gr. falconeri*, indicating that the proximal forelimb does not suggest increased agility in *P. ex gr. falconeri*. Hypothesis III is therefore rejected.

Nevertheless, without the support of additional features the absence of a deeper glenoid fossa does not completely rule out the possibility of a more agile gait in anterior-posterior direction in *P. ex gr. P. falconeri*, since there are other anatomical features (such as the position of the attachment of the shoulder muscles on the scapula) which are relevant to gait. However, it may be concluded that there is no evidence for a different gait between *P. antiquus* and *P. ex gr. P. falconeri* on the basis of the depth of the glenoid fossa.

4.2.2 Humerus

Humerus morphology between species was compared in terms of (i) the morphology of the deltoid fossa, and (ii) bivariate allometry:

(i) The morphology of the deltoid fossa - *Differences in deltoid fossa morphology between juvenile and adult P. ex gr. P. falconeri* - As to why the juvenile presents two depressions whereas the adult presents only one is an intriguing question. Dissection in *E. maximus* indicates there are two regions for the insertion of the deltoid muscle on the diaphysis of the humerus (Shindo and Mori, 1956a: Fig. 8), the anterior insertion being broader and more proximally situated, and the posterior insertion terminating farther distally. One possibility is therefore that the two scars in juvenile *P. ex gr. P. falconeri* may also represent anterior and posterior insertion scars of the deltoid muscle. In *H. sapiens* (in which the anatomy of the

deltoid has been described in greater detail), the muscle is usually divided into three groups of fibres (horizontally cut through the muscle's inferior part; see Kapandji, 1982: 60 citing Fick, 1911), namely the anterior, middle and posterior components (fibres I-II, III and IV-VII respectively, see Kapandji, 1982: Figs 63-64), which contribute at different stages of the movement of the limb (Kapandji, 1982: 60, Fig. 65). It should nevertheless not be completely ruled out that the two fossae in juvenile *P. ex gr. P. falconeri* represent separate muscles entirely (possibly the *Pectoralis major* and *deltoid*) rather than separate insertions of the deltoid. Whatever the identification of the muscle(s) attaching in juvenile *P. ex gr. P. falconeri*, morphological differences between juvenile and adult suggest differences in functional morphology. Although less pronounced, there are also differences in the morphology of the muscle insertions between *L. africana* with unfused (Fig. 4.3d) and fused epiphyses, although the significance of ontogenetic differences is yet to be explained since gaits appear similar in juvenile and adult elephants (Hutchinson *et al.*, 2006: 3812, 3818; see also Ren *et al.*, 2008). Dissection of *L. africana* or *E. maximus* juveniles and adults would therefore likely aid in more reliably identifying the origin of the insertion scars seen in *P. ex gr. P. falconeri* as well as the possible causes of ontogenetic differences.

Interspecific variability in deltoid fossa - The variable morphology in the deltoid fossa (or its associated tuberosity) among different genera of the Elephantinae has previously been noted (Falconer in Busk, 1867: 258; Haughton, 1932; Kroll, 1991: 20; van den Bergh, 1999: Fig. 59; Ferretti and Croitor, 2001; Ferretti, 2008; Kevrekidis and Mol, 2015), although most of these studies did not analyse interspecific differences in morphology in detail. Here large interspecific differences were also described within the genus *Palaeoloxodon*, in terms of the deltoid's (i) depth, (ii) orientation and (iii) position, suggesting there may be significant differences in the biomechanics of the shoulder joint between insular species of *Palaeoloxodon*.

(i) *Depth* - A deep deltoid fossa was evident in both young and adult *P. antiquus* from Neumark-Nord 1, Germany, although it was not evaluated whether this trait may be autapomorphic in *P. antiquus* as previously suggested (Kroll, 1991: 20). As to why the deltoid fossa is shallow to the point of being barely present in *Palaeoloxodon* sp. 1 from Luparello Fissure, Sicily (Fig. 4.5b, d) is an important question with regard to interpreting functional morphology, considering that most aponeurotic attachments are associated with rugose scarring (Bryant and Seymour, 1990) and that the near-absent fossa contrasts with all other Elephantinae specimens examined by the author (belonging to *Palaeoloxodon* spp., *M. primigenius*, *L. africana* and *E. maximus*). However, nothing is known about the range of variation in *Palaeoloxodon* sp. 1 since only one specimen is represented from Luparello Fissure. It is therefore impossible to ascertain whether or not the absence of a clearly discernible fossa is attributable to the specimen representing an extreme end-point of variability in *Palaeoloxodon* sp. 1, or possibly relates to a *bona fide* autapomorphic difference. However, given that the two *Palaeoloxodon* sp. 1 tibiae also contrast markedly in terms of their massive robusticity compared with all other Elephantinae species examined, it is possible that the near-absence of the deltoid fossa is autapomorphic in *Palaeoloxodon* sp. 1. Regardless of the uncertain functional significance, if a shallow deltoid fossa is

autapomorphic, it suggests significant differences in locomotion between hypothesized chronospecies *Palaeoloxodon* sp. 1 and *P. ex gr. P. falconeri*.

Biomechanical significance of interspecific variation in deltoid fossa morphology - (i) *Depth* - A deep deltoid fossa suggests more force was applied to this area of the humerus during locomotion than in examples with a shallow fossa, or may perhaps indicate habitual flexion of the forelimbs (see Ferretti and Croitor, 2001: 106) in accordance with Wolff's law (which states that bone adapts to the loads under which it is placed). (ii) *Deltoid fossa orientation* - Photographs indicate the orientation of the deltoid fossa varies: a laterally-facing deltoid fossa suggests the deltoid muscle applied relatively more force to the humerus during abduction (movement drawing the limb away from the midline of the body). In contrast, a caudally-facing deltoid fossa suggests relatively more force may have been applied during flexion (movement in the sagittal plane) which may be consistent with the previous suggestion that the forelimb is capable of greater flexion in *P. ex gr. P. falconeri* than in *P. antiquus* (Larramendi and Palombo, 2015: 103) and the suggestion that torsion of the limbs was less far from the sagittal plane than in continental forms (Caloi and Palombo, 1994: 153). However, another possible biomechanical significance of a caudally-facing deltoid fossa is in down-slope locomotion (Sicily being hilly), when the deltoid muscle is involved in 'braking' (cf. Agenbroad, 2003: 6).

Although differences between species are reflected in the photographs, time did not permit me to examine to what extent the position, depth and orientation of the deltoid fossa vary between species. Furthermore, it is currently not known to what extent habitat, topography, ontogenetic stage, sex and idiosyncratic locomotory habits may contribute to intraspecific variability in deltoid fossa morphology. Intraspecific morphological variability has been reported in the literature before (e.g. Ferretti, 2008: 101), and muscle ridges may be more prominent on the long bones of male proboscideans (Averianov, 1996: 265; Smuts and Bezuidenhout, 1994: 53). Additional description and metric data in *L. africana* and *E. maximus* of known age, sex and habitat would therefore certainly help to clarify the possible biomechanical significance of the interspecific variation in deltoid fossa morphology here described among isolated specimens of insular *Palaeoloxodon* spp.

(ii) Interspecific bivariate allometry - Interspecifically, the humerus was compared in terms of the ratio of the max diaphysis height (pr-d)/min diaphysis breadth (m-l). Statistically significant differences were found between *L. africana* with unfused epiphyses and *L. africana* with both proximally and distally fused epiphyses. However, the *L. africana* humerus with proximally and distally fused, and distally fused epiphyses is more similar in terms of bivariate allometry to adult *P. ex gr. P. falconeri* than that with unfused epiphyses, contrary to the predictions of Hypothesis II. In fact the opposite of what was predicted appears to be the case, that juvenile *L. africana* is less similar to adult *P. ex gr. P. falconeri*. Juvenile *L. africana* evidences a much more slender diaphysis than adult *P. ex gr. P. falconeri*. In contrast, according to Ambrosetti, the position of the supracondylar crest in *P. ex gr. P. falconeri* has a greater resemblance to a juvenile specimen of *P. antiquus* than adults belonging to the same species (Ambrosetti, 1968: 308).

4.2.3 Ulna and radius

In terms of bivariate allometry, differences are not statistically significant between *P. antiquus* vs. *P. ex gr. P. falconeri* in terms of the ratios of (i) max height (pr-d) including epiphyses/min diaphysis breadth (m-l), (ii) diaphysis height (pr-d)/min diaphysis breadth (m-l), (iii) diaphysis height (pr-d)/min diaphysis thickness (a-p). In contrast, statistically significant differences exist in terms of min diaphysis thickness (a-p)/min diaphysis breadth (m-l) between *P. antiquus* and adult *P. ex gr. P. falconeri* with fused epiphyses (Fig. 4.17c), reflecting a thicker diaphysis in the latter species.

However, the greatest morphological difference between species is the presence/absence of radio-ulnar synostosis which is common in several insular *Palaeoloxodon* spp., particularly in *P. ex gr. P. falconeri* from Spinagallo Cave, and occurs in about 30% of *P. ex gr. P. mnaidriensis* specimens from Puntali Cave (Ambrosetti, 1968: 316; van der Geer *et al.*, 2010: 363; Ferretti, 2008: 101; *ibid.* Fig. 10). Additionally the single *M. lamormarai* type-specimen from Sardinia also has a fused ulna-radius (Palombo *et al.*, 2012: 164; *ibid.* Figs 9-10).

In contrast, radio-ulnar synostosis is extremely rare in continental proboscideans but is occasionally reported in gerontic individuals (Harington *et al.*, 2012). To the author's knowledge, only a single example of distal radio-ulnar synostosis is reported in *P. antiquus* is known (from Neumark-Nord 1, see Palombo, 2010: 233; *ibid.* Fig. 21). Seeing that Sicily is an island with mountainous terrain, it has previously been proposed that synostosis may be the consequence of selection for a more secure gait, reducing displacement (Caloi and Palombo, 1994: 153, see also Palombo *et al.*, 2012: 164 for Sardinian *M. lamarmorai*). Here it was described in greater detail how synostosis likely reduced the displacement of the proximal carpals relative to the distal ulna-radius, particularly with regard to medio-lateral motion so that the explanation that synostosis is a locomotory adaptation appears true. However, it is not known to what extent displacement occurs between the ulna and radius in extant elephants in which the distal ulna-radius are joined via a tendon, so that the biomechanical significance of the fused ulna-radius in insular elephants remains only partially understood. Thus it should not be ruled out that synostosis is alternatively primarily a by-product of selection for some other factor, such as a genetic mechanism causing dwarfism.

With regard to the prominent muscle-scar ridge sometimes present on the radius of *P. ex gr. P. falconeri* more research is needed to identify the muscle in question. Regardless of uncertain identification however, the prominent insertion suggests proportionally more force was applied to the distal limb in some *P. ex gr. P. falconeri* individuals compared with *P. antiquus* (in which a similar scar has thus far never been described). The precise functional significance is thus impossible to pinpoint without identifying the muscle, but one possibility is that the presence of the muscle-scar relates to muscular reorganization in *P. ex gr. P. falconeri* as a result of synostosis.

4.2.4 Femur

(i) Interspecific bivariate allometry and absolute dimensions - With regard to absolute dimensions, one specimen of note is the individual from Spinagallo Cave falling outside the

range of *P. ex gr. P. falconeri*, but similar in size to *Palaeoloxodon* sp. 1 from Luparello Fissure. The proximal and distal ends of the specimen are missing, but the distolateral side is slightly expanded and has a flattened crest (the same feature as seen for example in Fig. 4.19a, d; see also Maschenko *et al.*, 2011: Fig. 5B), suggesting it may belong to a subadult or adult individual. This specimen may therefore be attributable to a species intermediate in size between the smaller *P. ex gr. P. falconeri* and larger *P. ex gr. P. mnaidriensis*, such as *Palaeoloxodon* sp. 1 from Luparello Fissure (Fig. 4.21), or alternatively to a small *P. ex gr. P. mnaidriensis* individual, a question that would be better-resolved if more measurements of *P. ex gr. P. mnaidriensis* were included in future.

In terms of interspecific allometry *Palaeoloxodon* spp. differ in terms of diaphyseal robusticity. In comparing max height vs. diaphysis midshaft breadth a progressive reduction in robusticity was found from *P. antiquus*, to *P. tiliensis*, to *P. ex gr. P. falconeri*. This conclusion contrasts with the previous deduction that there is a ‘shortening and thickening’ in the femur of dwarf proboscideans (van der Geer *et al.*, 2010: 361, although without citing metric evidence). In comparing the breadth (m-l) of the femoral head vs. diaphysis midshaft breadth (m-l) a relatively wider femoral head is evidenced in *P. ex gr. P. falconeri* relative to *P. antiquus*. Additionally, the femoral diaphysis is relatively thicker (a-p) in *P. ex gr. P. falconeri* compared with *P. antiquus*, indicating a rounder diaphysis cross-section in the dwarf species. Although not compared metrically, a rounder cross-section in *P. ex gr. P. falconeri* may mirror a more rounded cross-section seen in insular *M. exilis* as compared with its continental ancestor and contemporary *M. columbi* (see Agenbroad, 2002: 521). As to why *L. africana* evidences a particularly large range in terms of the ratio of diaphysis breadth (m-l)/diaphysis thickness (a-p), particularly in the larger specimens (with some specimens being nearly round in cross-section, and others being wider medio-laterally) is an intriguing question. Perhaps this relates in part to an increase in sexual dimorphism with age. Another contributing factor may have been that the *L. africana* sample also includes a greater range in ontogeny compared with the other sampled species. Furthermore, it is also possible that a more tubular structure has something to do with the biomechanical requirements of weight-bearing, although more research is needed to evaluate the different possibilities.

(ii) Longitudinal diaphysis curvature in the subtrochanteric region - The morphology of the femur is derived in *P. ex gr. P. falconeri* (Fig. 4.20c) and *Palaeoloxodon* sp. 1 from Luparello Fissure (Fig. 4.21c) with respect to *P. antiquus* (Fig. 4.23c; Fig. 4.24), bearing in mind that the morphology of *Palaeoloxodon* sp. 1 is here described based on only one proximal femur examined by the author (but see also Vaufrey, 1929: Plate VIII Fig. 10). Of particular note is the curved diaphysis of *P. ex gr. P. falconeri*, and a similar curvature also described for the first time in *Palaeoloxodon* sp. 1 from Luparello Fissure. Curvature in *P. ex gr. P. falconeri* has previously been suggested to be associated with a reduction in body mass (Herridge, 2010: 259), a suggestion which is congruent with the observation that longitudinal femur curvature (viewed in lateral aspect) exhibits a slight but significant trend towards reduced curvature as body mass increases, a phenomenon observed across a wide range in mass of quadrupedal mammals (curvature scaling with $\propto M^{-0.09}$, see Biewener, 1983; Carrano, 2001), in order to compensate for the increased peak stresses experienced by the bone due to scaling effects in large, graviportal animals.

However, a decrease in mass between *P. antiquus* to *P. ex gr. P. falconeri* (from ca. 13 tons to ca. 168-300 kg, see Larramendi and Palombo, 2015: 104; Larramendi, 2016: Table 8) *permits* rather than *explains* the increase in curvature in *P. ex gr. P. falconeri*. However, since close similarity was observed in the morphology between juvenile *L. africana* and adult *P. ex gr. P. falconeri* diaphysis, the evolutionary mechanism causing an increase in curvature may therefore relate to paedomorphism. Furthermore, morphological differences in diaphysis curvature have been described between juvenile and adult *E. maximus* and compared with dwarfed *M. exilis* and continental *Mammuthus columbi* FALCONER 1857, refer to Roth, 1982: 202; 206). It is therefore possible that a curved femur in *Palaeoloxodon* sp. 1 from Luparello Fissure and *P. ex gr. P. falconeri* is an apomorphy that resulted from paedomorphism that was permitted by the massive reduction in mass. Whether or not the suggested presence of paedomorphism in *Palaeoloxodon* sp. 1 and *P. ex gr. P. falconeri* is related to a mechanism such as delayed termination of the descendant ontogenies, while both size and shape retain the ancestral growth rates resulting in progenesis (see Klingenberg, 1998: 87) is therefore intriguing.

(iii) Interspecific variation in musculature - The morphology of the *Trochanter minor* varies greatly in the figured specimens, being well-developed in *P. antiquus* and *L. africana* compared with *P. ex gr. P. falconeri*. However, it is not known to what extent the musculature in the figured left femur of *P. antiquus* from Neumark-Nord 1 (Fig. 4.23) may be representative of the species as a whole. This particular individual (LVH-NN-E8 HK 2007:55, an adult female aged 37-40 African Elephant Years with shoulder height ca. 2,9m) displayed severe pathology of the vertebral column and invasive arthritis of the right femur and pelvic girdle, (Marano and Palombo, 2011), such that the musculature may in part have been influenced by the need to place more weight on the left, healthy femur. However, it is also possible that the rugose musculature in *P. antiquus* is an apomorphy in the adult relating to the requirements of mass and bone/muscle area: bone and muscle stresses are fairly constant across a size range from 0,04-300 kg because of the increase in limb muscle mechanical advantage. Above this size mammals exhibit more pronounced skeletal allometry (Biewener, 2005). However, too few specimens were examined from Neumark-Nord 1 in order to infer what the typical morphology of the *Trochanter minor* is in *P. antiquus*.

4.2.5 Tibia

Bivariate allometry of the tibia was particularly examined in terms of the ontogenetic allometry of *L. africana* compared with the allometry of adult *P. ex gr. P. falconeri*.

(i) Interspecific bivariate allometry - *P. antiquus* vs. *P. ex gr. P. falconeri* – Relative to its max height including the epiphyses, in *P. ex gr. P. falconeri* distal epiphysis is relatively broader. Likewise, the distal epiphysis is relatively thicker (a-p) in *P. ex gr. P. falconeri*. Adult *P. ex gr. P. falconeri* demonstrates robust epiphyses and a more slender diaphysis. *P. antiquus* vs. *P. ex gr. P. mnaidriensis* – Relative to its max height (pr-d) including epiphyses the distal epiphysis is relatively broader (m-l) in *P. ex gr. P. mnaidriensis*. In contrast, no statistically significant differences were found between *P. ex gr. P. mnaidriensis* vs. *P. ex gr. P. falconeri*. Furthermore, although sample-sizes were small, the tibia of *L. africana* is clearly much more slender than in *Palaeoloxodon* spp. In contrasting juvenile *L. africana* with adult

L. africana, although the epiphyses are not ossified in the juvenile, they appear more robust (medio-laterally wide) than in the adult. *Palaeoloxodon* sp. 1 from Luparello Fissure, although sample-size is very small, appears to be extremely robust, both in terms of its diaphysis and epiphyses (compared with Elephantinae species in general), possibly reflecting an autapomorphic trait.

(iii) Allometric variability in *P. ex gr. P. falconeri* - In the bivariate scatterplots there is a tendency towards more morphological variability in the later epiphyseal fusion stages (2, 3, 4 and especially 5) compared with epiphyseal fusion stage 0 in which the epiphyses are unattached. Considering that two of the size-frequency modes in the long bones of the Spinagallo Cave assemblage likely represent males and females it is likely that the increase in scatter in the larger specimens reflects an increase in sexual dimorphism with age (Fig 4.38).

(iv) Distal articulation of the *P. ex gr. P. falconeri* tibia - The morphology of the distal articulation of the tibia (*Cochlea tibiae*) varies considerably in *P. ex gr. P. falconeri*, and depending on the morphology, would have to a greater or lesser extent limited the (a) antero-posterior and (b) medio-lateral displacement of the astragalus-calcaneus. (c) The curvature of the *Cochlea tibiae* varies considerably in *P. ex gr. P. falconeri*, and where very concave (extending farther distally on the caudal side), likely acted as a braking mechanism while walking downslope, by limiting displacement of the astragalus in the anterior to posterior direction. Whether or not the greater curvature seen in the one represented *P. ex gr. P. falconeri* (Fig. 4.39a) is typical of the species or not, or explains some of the variability in the size of the calcaneus' tibial facet (Fig. 3.24b, c) remains an open question.

It is however possible that a greater curvature of the *Cochlea tibiae* evolved in concert with the calcaneus' tibial facet which is autapomorphic in this species. A concave *Cochlea tibiae* (Fig. 4.39a) likely articulated with the calcaneus to a greater extent in *P. ex gr. P. falconeri*, limiting antero-posterior displacement of the astragalus-calcaneus. One of the possible functional significances of a concave *Cochlea tibiae* may therefore have been to limit displacement when walking directly down slopes.

(v) Distal tibio-fibular synostosis in *P. ex gr. P. falconeri* - Distal tibio-fibular synostosis in insular proboscideans is an oft-cited example of a locomotory adaptation to steep relief (Ambrosetti, 1968: 316; Sondaar, 1977: 686; Caloi and Palombo, 1994: 153; Scarborough *et al.*, 2016). Distal tibio-fibular synostosis would have limited movement of the astragalus-calcaneus, particularly movement from the medial to lateral direction, more than if the distal tibia-fibula were only joined with a tendon.

(vi) Ontogenetic allometry in *L. africana* and heterochrony in the adult *P. ex gr. P. falconeri* tibia - In two of the three ratios compared between *L. africana* and *P. ex gr. P. falconeri*. juvenile *L. africana* is more similar to adult *P. ex gr. P. falconeri* than adult *L. africana*. It is therefore unclear whether or not the greater similarity in the two ratios is attributable to paedomorphism in *P. ex gr. P. falconeri* or not. While it cannot be ruled out that a mechanism other than paedomorphism may account for the closer similarity between

juvenile *L. africana* and adult *P. ex gr. P. falconeri*, than between adult *L. africana* and adult *P. ex gr. P. falconeri*, paedomorphism is a viable explanation.

Bivariate ratio	Comparison of the mean	Remarks
Ratio diaphysis height (pr-d)/breadth (m-l) of proximal end of diaphysis	Juvenile <i>L. africana</i> mean is more similar to adult <i>P. ex gr. P. falconeri</i>	Adult <i>L. africana</i> falls within the extreme range of juvenile <i>L. africana</i>
Ratio diaphysis height (pr-d)/breadth (m-l) of distal diaphysis end	Juvenile <i>L. africana</i> is more similar to adult <i>P. ex gr. P. falconeri</i>	Adult <i>L. africana</i> falls within the extreme range of juvenile <i>L. africana</i>
Ratio max breadth (m-l) of proximal diaphysis end/max breadth (m-l) of distal diaphysis end	Adult <i>L. africana</i> is more similar to adult <i>P. ex gr. P. falconeri</i>	-

Table 4.7 Summary of results from Table 4.6 comparing the allometry of the tibia.

(vii) Morphological differences between the long bones of *Palaeoloxodon* sp. 1 and *P. ex gr. P. falconeri* - In comparing the long bones of the two likely chronospecies there are both close similarities in morphology (likely apomorphic traits) as well as differences (likely autapomorphic traits), bearing in mind that sample-size is small for *Palaeoloxodon* sp. 1. Close morphological similarities include the curvature of the femur diaphysis in the subtrochanteric region, whereas notable differences include i) the depth of the deltoid fossa on the humerus, which is extremely shallow in *Palaeoloxodon* sp. 1 and deep in *P. ex gr. P. falconeri* and ii) the robusticity of the tibia, which is very robust in *Palaeoloxodon* sp. 1 in terms of its diaphysis breadth (m-l), as well as the breadth of its proximal and distal ends (Fig. 4.32).

This observation that there are both close morphological similarities in the long bones of *Palaeoloxodon* sp. 1 and *P. ex gr. P. falconeri* (not shared with *P. antiquus*), as well as differences between *Palaeoloxodon* sp. 1 and *P. ex gr. P. falconeri* mirrors previous observations of Chapter 3 where the existence of both morphological similarities and differences in the foot bones was documented. As to why there are both close morphological similarities and differences between the likely chronospecies is interesting. One possibility is that the difference in mass between the heavier *Palaeoloxodon* sp. 1 and lighter *P. ex gr. P. falconeri* (weighing up to ca. 300 kg, see Larramendi and Palombo, 2015), the threshold at which morphological changes are hypothesized to be less constrained by mass (Biewener, 1989; 1990). Thus, a possible cause for morphological differences may be associated with reduced mass in *P. ex gr. P. falconeri*.

Another possibility is that natural selection favoured a different functional morphology in *P. ex gr. P. falconeri*, perhaps allowing the species to expand its ecological niche as a result of locomotory adaptations permitted by reduced mass. Another factor that potentially played a role in the evolution of morphological differences is that Sicily's environment changed as it may have transitioned from two palaeo-islands to a single island during the period of *Palaeoloxodon* anagenesis likely represented at Luparello Fissure.

4.2.6 Scaling

As to why isometry is not evidenced in the tibia, but in the other long bones (Table 4.7) is an interesting question. The tibia sample did not include *P. tiliensis* because the published measurements were not comparable (Fig. 4.38a). The humerus sample (Fig. 4.12a; Appendix F) consisted mainly of *P. ex gr. P. falconeri* and *P. antiquus* (with only one *Palaeoloxodon* sp. 1 individual), so that the sample was biased towards very small and very large species. A previous study (although based on diaphysis lengths, not total lengths including epiphyses) found the adult *Palaeoloxodon* humerus evidenced isometry (Herridge, 2010: Table 6.12), the adult *Palaeoloxodon* ulna evidenced isometry (Herridge, 2010: Table 6.13), the adult *Palaeoloxodon* femur evidenced negative allometry (Herridge, 2010: Table 6.10), and the adult *Palaeoloxodon* tibia evidenced negative allometry (Herridge, 2010: Table 6.11). However, all long-bones evidenced isometry in adult samples when other genera were included (Herridge, 2010: Tables 6.10-6.13). Differences with previously published results no doubt reflect the availability/choice of sample, especially for *P. antiquus*, and perhaps also differences in diaphyseal measurements.

4.3 SUMMARY AND CONCLUSIONS

The purpose of this chapter was to test Hypothesis II and III (see Table 4.1), the outcomes of which are summarized below:

Hypothesis II: Paedomorphism in the long bones - Hypothesis II predicted that paedomorphic morphologies would be evident in the limbs of *P. ex gr. P. falconeri* from Spinagallo Cave). Hypothesis II is supported in the femur, and in two out of three indicators in the tibia of *P. ex gr. P. falconeri* (*contra* van der Geer, 2014: 174), based on its morphological resemblance with juvenile *L. africana*. In the tibia two out of three bivariate ratios displayed greater similarity in terms of allometry between juvenile *L. africana* and adult *P. ex gr. P. falconeri* than between adult *L. africana* and adult *P. ex gr. P. falconeri*, which is consistent (though not necessarily indicative) of paedomorphism. However, paedomorphism may explain the similarity between juvenile *L. africana* and adult *P. ex gr. P. falconeri*.

In the femur the curvature of the diaphysis in the subtrochanteric region was found to demonstrate a resemblance between adult *P. ex gr. P. falconeri* and juvenile *L. africana*, suggesting increased subtrochanteric curvature is possibly related to paedomorphism. Although it was previously noted that the humerus of *P. ex gr. P. falconeri* displays morphological similarity to juvenile *P. antiquus* (Ambrosetti, 1968: 308-309), the contrast between the robust diaphysis in adult *P. ex gr. P. falconeri* and juvenile *L. africana* suggests the greater robusticity in adult *P. ex gr. P. falconeri* is not attributable to paedomorphism. It may also be concluded that at some morphological features peculiar to the long bones of juvenile *L. africana* are not present in adult *P. ex gr. P. falconeri*, such as the wide proximal and distal ends of the femur, perhaps due to natural selection in the latter species.

Additionally, although only one femur was available for study in *Palaeoloxodon* sp. 1 from Luparello Fissure, its distinctive morphology suggests it was paedomorphic (being the first time paedomorphism has been tentatively identified in *Palaeoloxodon* sp. 1). This suggests

paedomorphism causing a curved femur diaphysis is likely a synapomorphy in *Palaeoloxodon* sp. 1 and its more derived chronospecies *P. ex gr. P. falconeri*. Thus paedomorphism is reflected in the *P. ex gr. P. falconeri* cranium and femur, and possibly also in the tibia and humerus (Ambrosetti, 1968: 308-309; Accordi and Palombo 1971; Palombo, 2001a; 2003; Palombo and Giovinazzo, 2005; Benoit, 2015; Larramendi and Palombo, 2015). The observations of this chapter therefore provide additional evidence of the important role the mechanism of paedomorphism plays in insular endemic dwarf mammals adapting to insular environments (van Heteren and de Vos, 2007: 78; Maglio, 1973; see also van den Bergh, 1999: 201; Roth, 1992; Lister, 1996a; Herridge, 2010: 325).

Hypothesis III: Morphological trends in relation to a reduction in mass - Hypothesis III predicted evidence of greater flexion in the shoulder-joint of *P. ex gr. P. falconeri*, and that the glenoid fossa of the scapula was deeper and longer in the antero-posterior direction relative to the medio-lateral direction. However, no statistically significant differences in the allometry of the glenoid fossa were found between *P. antiquus* and *P. ex gr. falconeri*. Hypothesis III was therefore rejected. Interestingly, the lack of an increase in flexion in the shoulder joint contrasts with the suggested increase in flexion in the ankle-joint in *P. ex gr. P. falconeri*, although more research is needed to explain this difference. In conclusion, Hypothesis III is rejected, indicating no significant changes in the joint between the scapula and humerus or its agility.

CHAPTER 5

DISCUSSION

In this chapter the key findings of Chapters 3 and 4 are summarized and discussed. The chapter is divided into two parts, Part I: Discussion on Hypotheses and Part II: Discussion on Chronology and Systematics. The Chapter begins with a review of the hypotheses previously outlined in Chapter 1 in light of the results obtained in this study (see Table 5.1). Additionally, the implications of the morphological observations of the systematics of *Palaeoloxodon* sp. 1 from Luparello Fissure are considered.

Hypothesis	Tested in	Hypothesis description	Hypothesis supported?
Hypothesis I	Carpals and tarsals	The feet of elephants from Sicily differ significantly in terms their morphology compared with their ancestral species (and contemporary) <i>P. antiquus</i> .	Supported in hindfoot by calcaneus morphology.
Hypothesis II	Long bones, carpals and tarsals	Paedomorphism is evident in the limbs of <i>P. ex gr. P. falconeri</i> from Spinagallo Cave	Suggested in femur and possibly tibia, unlikely in calcaneus and os t. IV
Hypothesis III	Scapula	As mass decreases gait becomes more flexed	Not supported in scapula of <i>P. ex gr. P. falconeri</i>

Table 5.1 Outcomes of the Hypotheses as stated in Chapter 1.

PART I: DISCUSSION ON HYPOTHESES

5.1 Hypothesis III in the scapula

Hypothesis III predicted that *As mass decreases, gait becomes more flexed*. In Chapter 4 the allometry of the scapula's glenoid fossa was compared between *P. antiquus* and *P. ex gr. P. falconeri*, although little difference was found in the anatomical features compared (Table 4.2). Contrary to the predictions of Hypothesis III, there were no statistically significant differences in the allometry of the scapula's glenoid fossa in terms of depth or length between *P. antiquus* and *P. ex gr. P. falconeri*. It is therefore concluded that the morphology of the joint between the scapula and the humerus displays little evidence to support a more agile form of locomotion as hypothesized for *P. ex gr. P. falconeri*, and as previously hypothesised in dwarf species (see Roth, 1992: 273; Lister 1996a: 290; Herridge, 2010: 258). Whether or not body mass influences the morphology of the glenoid fossa in other Elephantinae species is an open question, but it appears not to be the case in *P. ex gr. P. falconeri*.

5.2 Hypotheses II and III in the long bones

The morphology and gross anatomy of the long bones was compared in Elephantinae species from Sicily (*P. ex gr. P. mnaidriensis*, *Palaeoloxodon* sp. 1, *P. ex gr. P. falconeri*) and their continental comparators (*P. antiquus* from Germany and *L. africana* from Kenya). Large morphological differences between different continental *P. antiquus* and different insular *Palaeoloxodon* spp. were documented in terms of bivariate allometry and the morphology of muscle scars.

5.2.1 Morphology of the humerus

Interspecifically the humerus was compared in terms of (i) the morphology of the deltoid fossa, and (ii) its bivariate allometry:

(i) The morphology of the deltoid fossa varies greatly between species, particularly in terms of depth and orientation (Table 4.3), suggesting significant differences in the biomechanics of the upper forelimb, while bearing in mind that only a limited number of specimens were compared between species. Large morphological differences are particularly evident between *Palaeoloxodon* sp. 1 and *P. ex gr. P. falconeri*, which displays a much deeper deltoid fossa than its likely ancestral chronospecies, again bearing in mind *Palaeoloxodon* sp. 1 is only represented by a single specimen. The deeper deltoid fossa in *P. ex gr. P. falconeri* compared to *Palaeoloxodon* sp. 1 cannot be attributed to the allometry of muscle volume in relation to the work a muscle is required to perform, since the work that a muscle needs to perform is proportional to an animal's mass (third power of linear size). A large animal therefore needs proportionately more muscle fibres than a small one (muscle strength is in part proportional to cross-sectional area rather than directly to muscle volume, see Biewener, 2003: 36; Hutchinson, 2004).

(ii) Interspecifically the humerus allometry differs noticeably in terms of bivariate allometry (Table 4.4). Juvenile *L. africana* was less similar to adult *P. ex gr. P. falconeri* than adult *L. africana* in terms of the ratio of the max diaphysis height (pr-d)/min diaphysis breadth (m-l) (contrary to the predictions of Hypothesis II, see below). There are also significant differences in terms of the ratio of max height (pr-d) including epiphyses/min diaphysis breadth (m-l) between *P. antiquus* vs. *P. ex gr. P. falconeri*, reflecting a wider diaphysis in *P. ex gr. P. falconeri*, and between *P. ex gr. P. falconeri* vs. *L. africana*, reflecting a more slender diaphysis in *L. africana*. Differences are however not significant between *P. antiquus* vs. *L. africana*. *P. ex gr. P. falconeri* has a very robust diaphysis and laterally projecting deltoid tuberosity, contrasting with the slender humerus of juvenile *L. africana*, thereby underlining the fact that the robust diaphysis of *P. ex gr. P. falconeri* is not related to pedomorphism (as expected from Hypothesis II). The robusticity of the *P. ex gr. P. falconeri* diaphysis must therefore relate to a factor other than pedomorphism.

Element	Species and provenance				
	<i>P. antiquus</i>	<i>P. ex gr. P. mnaidriensis</i>	<i>Palaeoloxodon</i> sp. 1	<i>P. ex gr. P. falconeri</i>	Adult <i>L. africana</i>
	Neumark-Nord 1, Germany	Puntali Cave, Sicily	Luparello Fissure, Sicily	Spinagallo Cave, Sicily	Kenya
Humerus	Deep and rugose deltoid fossa	Deep deltoid fossa	Deltoid fossa extremely shallow	Wide diaphysis breadth (m-l) and thickness (a-p), deep deltoid fossa	Slender diaphysis in juveniles, robust in adults
Ulna	Almost never synostotically fused	Synostotic fusion not uncommon	Not synostotically fused	Thick diaphysis (a-p), broad diaphysis (m-l), often synostotically fused with radius	Never synostotically fused
Femur	Slight curvature in subtrochanteric region, diaphysis tends to be broad (m-l) relative to thickness (a-p).	Slight curvature in subtrochanteric region	Curved diaphysis in subtrochanteric region	Curved diaphysis in subtrochanteric region, diaphysis arched as seen in cranial aspect	Diaphysis parallel-sided
Tibia	Robust diaphysis and epiphyses. No synostosis with fibula.	Robust diaphysis and epiphyses. No synostosis with fibula	Very robust diaphysis and epiphyses relative to <i>P. antiquus</i> and <i>L. africana</i>	Robust epiphyses, more slender diaphysis narrowing distally. Synostotic fusion with fibula common	More slender diaphysis and epiphyses. No synostosis with fibula

Table 5.2 Summary of qualitative morphological differences in the long bones between Sicilian *Palaeoloxodon* spp. and European *P. antiquus* (results from Chapter 4). The morphological features in insular *Palaeoloxodon* are described relative to *P. antiquus*. Note: N=1 for *Palaeoloxodon* sp. 1 from Luparello Fissure (refer to Table 2.4 for materials).

In terms of the ratio of the min diaphysis breadth (m-l) at the deltoid tuberosity/min diaphysis breadth (m-l) differences are significant between *L. africana* with unfused epiphyses and *L. africana* with fused epiphyses, reflecting a relatively greater breadth of the deltoid tuberosity in the adult. Differences are also statistically significant between *L. africana* with unfused epiphyses and *P. ex gr. P. falconeri* with fused epiphyses, reflecting a relatively broader deltoid tuberosity in *P. ex gr. P. falconeri*. In specimens with fused epiphyses however, differences are not statistically significant between *P. antiquus* and *P. ex gr. P. falconeri*, nor between *P. antiquus* and *L. africana* nor between *L. africana* and *P. ex gr. P. falconeri*. Nevertheless, it should be borne in mind that sample-sizes for *L. africana* with fused epiphyses are small.

Finally, with regard to the co-existence of morphological traits, there appears to be no obvious common factor underlying autapomorphies in *P. ex gr. P. falconeri*: a very robust diaphysis in *P. ex gr. P. falconeri* (unlike juvenile *L. africana*) is not related to pedomorphism, and the much deeper deltoid fossa in *P. ex gr. P. falconeri* than in *Palaeoloxodon* sp. 1 suggests differences in the biomechanics of the upper forelimb. It may be concluded that multiple selection forces likely played a role in the evolution of *P. ex gr. P. falconeri*'s locomotion.

5.2.2 Morphology of the ulna-radius

The ulna-radius was found to vary primarily in (i) the robusticity of the diaphysis, (ii) radio-ulnar synostosis and (iii) the presence of muscle scars:

(i) In terms of the bivariate allometry of the diaphysis, differences were statistically significant between *P. antiquus* and adult *P. ex gr. P. falconeri* with fused epiphyses in terms of the ratio of the min diaphysis thickness (a-p)/min diaphysis breadth (m-l), reflecting a thicker diaphysis in the latter species. Differences were however not significant between *P. antiquus* vs. *P. ex gr. P. falconeri* for the ratio of the max height (pr-d) including epiphyses/min diaphysis breadth (m-l), and the ratio diaphysis height (pr-d)/min diaphysis breadth (m-l) as well as the ratio diaphysis height (pr-d)/min diaphysis thickness (a-p).

(ii) Synostosis is frequently found in the long bones of insular elephants (the ulna-radius and tibia-fibula of *P. ex gr. P. falconeri* and ulna-radius of *P. ex gr. P. mnaidriensis*), but not in continental species (*P. antiquus* and *L. africana*). Further, synostosis in the distal tibia-fibula and ulna-radius would have limited medio-lateral displacement of the feet (Ambrosetti, 1968: 316) suggesting possible evidence of low-gear locomotion in *P. ex gr. P. falconeri* and to a lesser degree in *P. ex gr. P. mnaidriensis*. Synostosis in the proximal and distal ulna-radius may relate to low-gear locomotion. Synostosis is also found in the ulna-radius of the dwarf hippopotamus from Cyprus (Houtekamer and Sondaar, 1979). (iii) Alterations in muscle attachment areas - In some *P. ex gr. P. falconeri* specimens the cranio-distal surface of the synostotically fused radius displays a proximodistally-orientated ridge for the attachment of an adductor, possibly the origin of one of the extensor muscles.

In terms of the co-occurrence of morphological traits, although more research is needed to identify the muscle described in (iii) above, one possible explanation for the muscle-scar's presence is muscular reorganization as a result of synostosis in *P. ex gr. P. falconeri*. Since synostosis would not have permitted any muscles to pass between the ulna-radius, a robust muscle attachment may reflect the fact that proportionally more force was applied to the surface of the bone as a result.

5.2.3 Morphology of the femur

Interspecifically the femur was compared in terms of (i) its overall anatomy, particularly with regard to the subtrochanteric region of the diaphysis, and (ii) its bivariate allometry, particularly the diaphyseal robusticity:

(i) A curved diaphysis in the subtrochanteric region appears to be autapomorphic in adult *P. ex gr. P. falconeri*, and possibly in adult *Palaeoloxodon* sp. 1 from Luparello Fissure, although only one specimen was examined in the latter species. In contrast, the diaphysis is less curved in adult *P. antiquus* from Neumark-Nord 1, Germany and adult *P. ex gr. P. mnaidriensis* from Puntali Cave. Since the femur diaphysis is sometimes (though not always) curved in the subtrochanteric region in juvenile *L. africana*, but a much more vertical orientation in adults belonging to the same species, the greater curvature seen in *Palaeoloxodon* sp. 1 and *P. ex gr. P. falconeri* is suggested to relate to pedomorphism.

(ii) The diaphysis has a tendency to be wider (m-l) relative to its thickness (a-p) in *P. antiquus* than in all the insular *Palaeoloxodon* spp., and also to be taller (pr-d) relative to its diaphysis midshaft thickness (a-p), which is consistent with the previous observation that dwarf proboscideans have short limbs in relation to body length (Herridge, 2010: 258; Sondaar, 1977: 682; Roth, 1984; 1990; van der Geer *et al.*, 2010: 313 although often qualitatively described). Furthermore, in comparing its max height vs. diaphysis midshaft breadth a progressive reduction in robusticity was seen from *P. antiquus*, to *P. tiliensis*, to *P. ex gr. P. falconeri*.

Compared to *P. antiquus* the femur diaphysis of *P. ex gr. P. falconeri* has a tendency to be slightly broader (m-l), and thicker (a-p) in relation to its length (Fig. 4.27a; Fig. 4.27b; Fig. 4.28), indicating greater robusticity in the dwarf species, as is commonly held to be the case among dwarf elephants (van der Geer *et al.*, 2010: 361; Caloi and Palombo, 1994; Ferretti, 2008: 101; Herridge, 2010: 292; see also Roth, 1982: 215; Caloi and Palombo, 1994). In comparing the breadth (m-l) of femoral head vs. diaphysis midshaft breadth (m-l) there is a relatively wider femoral head in *P. ex gr. P. falconeri* compared to *P. antiquus*. Additionally the femur diaphysis is relatively thicker (a-p) in *P. ex gr. P. falconeri* compared with *P. antiquus*, indicating a rounder diaphysis cross-section in the dwarf species. Although not compared metrically, this may mirror a more rounded cross-section seen in the diaphysis of insular *M. exilis* compared to its continental ancestor and contemporary *M. columbi* (see

Agenbroad, 2002: 521). It would therefore be informative to investigate the extent (or lack thereof) of homoplasy between the two dwarf species.

In contrast to its medial aspect however, in cranial aspect juvenile *L. africana*'s wide proximal and distal ends of the diaphysis differ from the less wide ends in adult *P. ex gr. P. falconeri*. Considering the aforementioned evidence of paedomorphism, one possible explanation for this difference may be that wide proximal and distal diaphysis ends (and their epiphyses) would be over-built in a dwarf species which does not continue to grow beyond the vertical height of the neonate of its ancestor, particularly in a species such as *P. ex gr. P. falconeri* for which there may have been selection for rapid somatic maturation (see Section 1.4.1). Negative selection for slender epiphyses in *P. ex gr. P. falconeri* may therefore possibly account for the absence of this juvenile trait in the dwarfed species. However, an alternative hypothesis is that the proximal and distal epiphyses in juvenile *P. antiquus* (currently not represented from the fossil record), may not have been as wide in juvenile *L. africana*.

As to why *L. africana* displays a particularly large range in terms of diaphysis breadth/thickness in the larger specimens is uncertain: In some *L. africana* specimens the diaphysis cross-section is nearly round, whereas in others the cross-section of the diaphysis is wide in the medio-lateral direction. The greater variability in larger individuals no doubt relates in part to an increase in sexual dimorphism during ontogeny (cf. Roth, 1984: 132). Possibly a wider range in habitat than in other species also contributed to the wider range in morphological variability in the Kenyan *L. africana* sample.

In terms of the co-occurrence of morphological traits, the curved diaphysis in the subtrochanteric region in the adult *Palaeoloxodon* sp. 1 and *P. ex gr. P. falconeri* is likely paedomorphic, based on its similarity with juvenile *L. africana*. However, the two *Palaeoloxodon* species also contrast morphologically with juvenile *L. africana*'s wide proximal and distal ends. Thus it appears that paedomorphic traits do not necessarily co-occur in the long-bones of a dwarf species, in this case possibly because robust proximal and distal ends would be over-built in the dwarf. Although a curved femur diaphysis likely reflects paedomorphism, a biomechanical reason for a curved diaphysis should also be considered: curved bones add skeletal resilience by acting as pre-stressed beams/pre-buckled struts (Milne, 2016). Models have shown that longitudinal and flexor muscle forces produce bending strains that counter strains resulting from the pull of the triceps muscle in curved bones in the forelimb (Milne, 2016), and a curved femur might, *a priori*, play a similar biomechanical role.

5.2.4 Morphology of the tibia

Three features were observed which vary greatly between species: (i) bivariate allometry, particularly as it relates to diaphyseal and epiphyseal robusticity, and (ii) tibio-fibular synostosis. Additionally, the (iii) bivariate ontogenetic allometry of *L. africana* was contrasted with that of *P. ex gr. P. falconeri* in order to evaluate the possible presence of paedomorphism in the latter species.

(i) Bivariate allometry in relation to diaphyseal and epiphyseal robusticity - *P. antiquus* vs. *P. ex gr. P. falconeri* – Differences are statistically significant for the ratio of the max height (pr-d) including epiphyses vs. max breadth (m-l) of distal epiphysis, reflecting a relatively broader distal epiphysis *P. ex gr. P. falconeri*, and also for the max height (pr-d) including epiphyses vs. thickness (a-p) of distal epiphysis, reflecting a relatively thicker distal epiphysis in *P. ex gr. P. falconeri*. *P. antiquus* vs. *P. ex gr. P. mnaidriensis*. Differences are statistically significant for the ratio between max height (pr-d) including epiphyses/max breadth (m-l) of distal epiphysis, reflecting a relatively broader (m-l) distal epiphysis in *P. ex gr. P. mnaidriensis*. In comparing *Palaeoloxodon* sp. 1 from Luparello Fissure with *P. ex gr. P. falconeri*, the extreme epiphyseal and diaphyseal robusticity of the former species contrasts with the lesser robusticity of the latter, indicating large changes in morphology with a relatively modest reduction in absolute size between likely chronospecies. As to why *Palaeoloxodon* sp. 1 exhibits such pronounced robusticity compared with *P. ex gr. P. falconeri* still requires further explanation. It has however previously been suggested that once dwarfism reached an evolutionary stable state within a population, selection for more gracile individuals may have become more important (Herridge, 2010: 338), as perhaps reflected in this case. Nevertheless, it must be borne in mind that *Palaeoloxodon* sp. 1 is only represented by two tibiae from Luparello Fissure, Sicily.

In contrasting adult *P. ex gr. P. falconeri* with adult *P. antiquus*, the former species has robust epiphyses and a more slender diaphysis. Furthermore, in contrasting juvenile *L. africana* with adult *L. africana*, although the epiphyses are absent in the juvenile, they were evidently more robust than in the adult as indicated by the wide diaphysis ends. Finally, in comparing *Palaeoloxodon* sp. 1 with all other species, both the diaphysis and epiphyses are extremely robust. It is also notable that in comparing *Palaeoloxodon* sp. 1 from Luparello Fissure with *P. ex gr. P. falconeri*, the extreme epiphyseal and diaphyseal robusticity in the former relative to the latter indicates large changes in morphology with a relatively modest reduction in absolute size between likely chronospecies.

(ii) Tibio-fibular synostosis - Synostosis in the distal tibia-fibula may relate to low-gear locomotion in *P. ex gr. P. falconeri* by restricting medio-lateral displacement of the astragalus and calcaneus (Ambrosetti, 1968: 316; Sondaar, 1977: 686; Caloi and Palombo, 1994: 153; Scarborough *et al.*, 2016). *Palaeoloxodon* sp. 1 tibiae from Luparello Fissure are both not synostotically fused as is often the case in adult *P. ex gr. P. falconeri*, although sample-size is too small (N=2) to know whether or not this is typical for the former species.

(iii) Evaluating heterochrony in the *P. ex gr. P. falconeri* tibia - In two of the three bivariate ratios compared between *L. africana* and *P. ex gr. P. falconeri*, juvenile *L. africana* is more similar to adult *P. ex gr. P. falconeri* than adult *L. africana*. Whether or not the greater similarity in the two ratios is attributable to paedomorphism in *P. ex gr. P. falconeri* or not is therefore an important question. While it cannot be ruled out that a mechanism other than paedomorphism may account for the closer similarity between juvenile *L. africana* and adult *P. ex gr. P. falconeri*, than between adult *L. africana* and adult *P. ex gr. P. falconeri*, paedomorphism is a viable explanation.

Bivariate ratio	Comparison of the mean	Remarks
Ratio diaphysis height (pr-d)/breadth (m-l) of proximal end of diaphysis	Juvenile <i>L. africana</i> mean is more similar to adult <i>P. ex gr. P. falconeri</i>	Adult <i>L. africana</i> falls within the extreme range of juvenile <i>L. africana</i>
Ratio diaphysis height (pr-d)/breadth (m-l) of distal diaphysis end	Juvenile <i>L. africana</i> is more similar to adult <i>P. ex gr. P. falconeri</i>	Adult <i>L. africana</i> falls within the extreme range of juvenile <i>L. africana</i>
Ratio max breadth (m-l) of proximal diaphysis end/max breadth (m-l) of distal diaphysis end	Adult <i>L. africana</i> is more similar to adult <i>P. ex gr. P. falconeri</i>	-

Table 5.3 Summary of the results from Table 4.6 comparing the allometry of the tibia in *L. africana* and *P. ex gr. P. falconeri*.

Regarding the co-existence of morphological traits, in two of the three bivariate ratios compared (between *L. africana* and *P. ex gr. P. falconeri*), juvenile *L. africana* was more similar to adult *P. ex gr. P. falconeri* than adult *L. africana*, such that paedomorphism is one possible explanation for their similarity. The epiphyses were also observed to be wider in juvenile *L. africana* than in the adult of the same species.

5.3 Hypothesis II in *P. ex gr. P. falconeri* from Spinagallo Cave

Hypothesis II predicted that *Heterochrony causing dwarfism resulted in paedomorphic morphologies in the limbs of P. ex gr. P. falconeri from Spinagallo Cave*. In order to investigate the validity of this hypothesis bivariate ontogenetic series were studied in the *L. africana* humerus and the tibia. In Chapter 4 it was shown that humerus bivariate allometry (max diaphysis height vs. min diaphysis breadth) is less similar in young than adult *L. africana* compared with adult *P. ex gr. P. falconeri*, and also that adult *L. africana* is more similar to adult *P. ex gr. P. falconeri* than young *L. africana* with respect to the tibia's ratio max breadth (m-l) of proximal diaphysis end/max breadth (m-l) of distal diaphysis end (Table 4.7).

In contrast, the medial profile of the femur suggests that there is often greater morphological similarity between the femur diaphysis in juvenile *L. africana* compared with adult *P. ex gr. P. falconeri* from Spinagallo Cave and *Palaeoloxodon* sp. 1 from Luparello Fissure, most likely reflecting paedomorphism. This is the first time evidence of

paedomorphism has been presented in the latter species. This conclusion contrasts with the previous assertion that *P. ex gr. P. falconeri*'s limbs are not paedomorphic, based on the observation that extant juvenile elephants have proportionally long limbs whereas in adult *P. ex gr. P. falconeri* the limbs are short in relation to body length (van der Geer, 2014: 174, see also Roth, 1984; Sondaar, 1977: 682).

Feature	Species and provenance			
	<i>P. ex gr. P. mnaidriensis</i>	<i>Palaeoloxodon</i> sp. 1	<i>P. ex gr. P. falconeri</i>	<i>M. lamarmorai</i>
	Puntali Cave, Sicily	Luparello Fissure, Sicily	Spinagallo Cave, Sicily	Gonnesa, Sardinia
Curved diaphysis in subtrochanteric region	?	Paedomorphic	Paedomorphic	-
Crooked plantar facet of calcaneus	Not paedomorphic	?	Not paedomorphic	Not paedomorphic
Globular cranium	Not paedomorphic	-	Paedomorphic	-

Table 5.4 The presence/absence of paedomorphic features in Siculo-Maltese *Palaeoloxodon* spp. and *M. lamarmorai* from Sardinia. (For cranial morphology refer to Accordi and Palombo, 1971; Palombo, 2001a; 2003; Palombo and Giovinazzo 2005; van der Geer *et al.*, 2018). Note that sample-sizes vary among species.

However, relatively long limb bones in extant juvenile elephants which become less slender during ontogeny (negative allometric growth), may either relate to maturation of the skeleton's (biomechanical?) properties or reflect the need for younger animals to move relatively faster in order to keep pace with much larger adults in the same social group (Main and Biewener, 2004: 309; Biewener, 2005: 1665, 1669; Roth, 1982: 225; see also Herridge, 2010: 338). Thus relatively long legs particularly have adaptive value when birth occurs while a herd is migrating in order to keep up with faster adults (Pennycuick, 1975: 784). However, *P. ex gr. P. falconeri* evolved in a predator-free environment (Table 1.3; Table 2.3), where no ecological pressure was exerted in order to reduce predation risk in younger animals. Further, long-distance migration likely did not occur, so that relaxed selection likely permitted the absence of long limbs.

In contrast, short limbs may be of adaptive significance to low-gear locomotion (cf. Sondaar, 1977: 682; Sondaar, 2005: 236), since low-gear locomotion is associated with shorter stride length and increased power (Herridge, 2010: 339; see also Sondaar, 1977: 683) although the possibility that short limbs in *P. ex gr. P. falconeri* might be a by-product of selection for a particular developmental processes associated with dwarfism unrelated to selection for low-gear locomotion should not be ruled out.

The absence of evidence of paedomorphism in the feet of *P. ex gr. P. falconeri* - The os c. III, os t. IV and calcaneus all exhibit significant morphological differences between juvenile and adult *L. africana* and between the young and adult *P. antiquus* from Neumark-Nord 1,

Germany. If the same elements were paedomorphic in adult *P. ex gr. P. falconeri*, one would therefore expect a morphological resemblance with juvenile *L. africana* and the young *P. antiquus* individual. However, this is not the case. In contrast, paedomorphism is reflected in the cranium (Palombo, 2001a) and likely femur (see Chapter 4) of *P. ex gr. P. falconeri*. As to why paedomorphisms which might be expected are both present but also absent is a thought-provoking question. One possibility is that during the earlier stages of insular evolution in the fore-runners of *P. ex gr. P. falconeri*, paedomorphisms were reflected in the foot-bones mentioned above which later disappeared due to selection pressures which favoured specific functional morphologies in order to adapt to the insular environment. If this was the case, it may at least partially explain the select absence of paedomorphism in the species *P. ex gr. P. falconeri*. However, until the morphology in the early fore-runners of *P. ex gr. P. falconeri* is known this hypothesis will remain untested.

5.4 Hypothesis I in the carpals and tarsals

Hypothesis I (The feet of elephants from Sicily differ significantly in terms their morphology compared with their ancestral species (and contemporary *P. antiquus*). This hypothesis was tested in Chapter 3 in select foot bones (ulnar, radial, intermediate, and accessory carpals, os c. III, astragalus, central tarsal, os t. IV, calcaneus) comparing *Palaeoloxodon* spp. from Sicily, Favingana, Malta, and *M. lamarmorai* from Sardinia with *P. antiquus* from Germany.

Anatomy of the manus - Between *P. antiquus* and *P. ex gr. P. falconeri* the morphology of the os c. III differs in terms of the articular facets for the os c. IV and os c. II, being separated by a rough groove in *P. antiquus*, which contrasts with the continuous articular facet in *P. ex gr. P. falconeri*. In terms of the os c. III's bivariate allometry, statistically significant differences were also found in bivariate ratios between the two species: (i) Max thickness (a-p)/max cranial breadth (m-l) - *P. ex gr. P. falconeri* is relatively less thick (a-p). (ii) Max length (a-p)/max breadth (m-l) of the articular facet for the mc III – this has a tendency to be broader in *P. antiquus*. (iii) Max cranial breadth (m-l)/max caudal breadth (m-l) - A greater caudal breadth is evident in *P. antiquus*. (iv) Max cranial height (pr-d)/max thickness (a-p) – The bone was found to be taller in *P. antiquus* than the other Elephantinae species.

There is nothing which would strongly suggest low-gear locomotion in the fore-foot may have played a role in the differences in allometry. The intermediate carpal tends to be slightly wider (m-l) in *P. antiquus* and *P. ex gr. P. mnaidriensis* than in *P. ex gr. P. falconeri* from Spinagallo Cave.. The evidence also indicates that the relative length of the radial carpal's articular facet for the radius is greater in *P. antiquus*. However, there appears to be little difference in the angle between the radial carpal's articular facets for the radius and os c. II which would be expected if there were major differences in digitigrady between species (see Maccagno, 1962a: 111; *ibid* Fig. 25).

iv) Morphology of the calcaneus - The calcaneus differs greatly in the proportions of its articular facets between species, and a new method was developed (see Section 2.9.3) for

measuring and describing the articular facets for the fibula and tibia. An absolute reduction in element size (as seen in *P. antiquus*, *Palaeoloxodon* sp. 1 and *P. ex gr. P. falconeri*) was accompanied by an increase in the relative size of the articular facet for the tibia, and the articular facet for the fibula becomes relatively larger in proportion to the tuber. *P. ex gr. P. mnaidriensis* has no articular facet for the tibia and a large fibular facet. In *M. lamarmorai* the specimen is damaged so that it is unknown whether there was a tibial facet, but the fibular facet is very narrow.

Anatomy of the pes - In Chapter 3 it was shown that the tarsals of Siculo-Maltese *Palaeoloxodon* spp. are highly derived and that there is considerable morphological variation between insular species (Table 5.5). (i) *Morphology of the astragalus* - The astragalus has a tendency to be less thick in insular dwarfs, particularly in *P. ex gr. P. falconeri*, and the articular facet for the central tarsal tends to decrease in a-p thickness as mass decreases. The bone suggests differences in the posture of the hindfoot. (ii) *Morphology of the central tarsal* - There are large differences in the morphology of the central tarsal between species, which has a tendency to be narrower in the antero-posterior direction, particularly in *P. ex gr. P. falconeri*, as might be expected from the larger articular facet for the astragalus. As with the os t. IV, but unlike the carpals of the forefoot, the height of the bone (pr-d) is low. (iii) *Morphology of the os t. IV* - In *P. ex gr. P. falconeri* the bone is low (pr-d) compared with other species and a deep niche exists for the mt IV and mt V.

5.4.1 Tarsal morphology in relation to body mass

It was possible to compare tarsal morphology across a wide range in body mass, from ca. 165-300 kg *P. ex gr. P. falconeri* to ca. 4,500-12,000 *P. antiquus* (see Larramendi and Palombo, 2015: 104; Larramendi, 2016 for mass estimates). In comparing *Palaeoloxodon* spp. in order of decreasing mass (*P. antiquus*, *P. ex gr. P. mnaidriensis*, *Palaeoloxodon* sp. 1 and *P. ex gr. P. falconeri*), six morphological trends were noted: (i) an increase in relative size of the tibial facet on the calcaneus (ii) a antero-posterior narrowing of the articular facet for the central tarsal on the astragalus*, and (iii) a corresponding antero-posterior narrowing of the central tarsal's articular facet for the astragalus. Photographic comparisons also suggest a reduction in the proximo-distal height of the distal tarsals, including (iv) the os t. IV and (v) the central tarsal, as well as (vi) a decrease in the curvature of the central tarsal. (vii) Finally, the groove for the insertion of the tendon on the distal surface of the os t. IV is also absent in all the insular species (*Palaeoloxodon* sp.).

*Although there appears to be a trend in a reduction in the relative size of the astragalus' articular facet for the central tarsal with a decrease in mass in Sicilian *Palaeoloxodon* spp., *P. tiliensis* baulks this trend, suggesting factors other than mass reduction may explain this exception.

Element	Species and provenance				
	<i>P. antiquus</i>	<i>P. ex gr. P. mnaidriensis</i>	<i>Palaeoloxodon</i> sp. 1	<i>P. ex gr. P. falconeri</i>	<i>M. lamarmorai</i>
	Neumark-Nord 1, Germany	Puntali Cave, Sicily	Luparello Fissure, Sicily	Spinagallo Cave, Sicily	Gonnesa, Sardinia
Central tarsal	Long articular facet (a-p) for astragalus	-	-	Narrow articular facet (a-p) for astragalus	Narrow articular facet (a-p) for astragalus
Astragalus	Wide articular facet (pr-d) with a considerable range in dimensions	Likely narrow articular facet (pr-d) for central tarsal	Narrow articular facet (pr-d) for central tarsal	Narrow articular facet (pr-d) for central tarsal	Very large articular facet for calcaneus, narrow articular facet for the central tarsal
Calcaneus	Typically no tibial facet	Wide articular facet for the fibula, no tibial facet	Greater separation between articular facets for tibia and fibula	Large and continuous tibio-fibular facet, with articular facet for fibula distinguishable as proximal and distal facets	Very large lateral articular facet for astragalus, very narrow articular facet for fibula
Os t. IV	Relatively thick (pr-d). Presence of groove on plantar surface. Groove on plantar surface for tendon is present.	-	Proximally there is a very shallow circular groove for the insertion of a tendon. Groove on plantar surface for tendon is absent.	Low height (pr-d). Plantarly niche exists for the mt IV and mt V. Groove on plantar surface for tendon is absent.	Groove on plantar surface for tendon is absent.

Table 5.5 Summary of the metric and qualitative morphological differences in the tarsals between *P. antiquus*, Sicilian *Palaeoloxodon* spp., and Sardinian *M. lamarmorai*. The morphological features in insular *Palaeoloxodon* are described relative to *P. antiquus*. Note: N=1 for the *M. lamarmorai* type-specimen from Sardinia (refer to Table 2.7 for materials).

1 from Luparello Fissure, Sicily, *P. ex gr. P. falconeri* from Spinagallo Cave, Sicily, *Palaeoloxodon* sp. from Benghisa Gap, Malta and *M. lamarmorai* from Gonnese, Sardinia), while present in continental species (*P. antiquus*, *L. africana* and *E. maximus*).

Whether or not the aforementioned morphological changes imply causation or only correlation in relation to reduced mass is an interesting question. Differences in the allometry of articular facets certainly reflect differences in the way body mass is distributed in insular dwarf elephants compared with their ancestors*, and it has been suggested that a reduction in mass may permit greater mobility in the antero-posterior direction as reflected in the *P. ex gr. P. falconeri* astragalus-calcaneus (Scarborough *et al.*, 2016).

As pointed out in Chapter 3 the absence of a tendon in insular dwarfs may also relate to a functional threshold, due to the fact that loss of function may occur when the volume of a tendon is decreased beyond a certain limit. A similar cause has been invoked to explain the relatively low number of molar plates and proportionally thick enamel of *P. ex gr. P. falconeri*, which could not be reduced below a critical minimum thickness required for mastication (Maglio, 1973: 83; Mol *et al.*, 1996: 83).

In contrast, there is no immediately obvious reason why a decrease in the height of the distal tarsals would be related to a reduction in mass, save the possibility that proportionally less strength is required in the bone due to the fact that mass decreases at a faster rate in dwarf elephants than absolute height. However, another possibility is that a reduction in the height of these elements is related to the side-effects of the dwarfing process including developmental constraint or non-adaptive causes such as genetic drift or coincidence unrelated to a reduction in mass (cf. Scarborough *et al.*, 2016: 117).

Due to the fact that the central tarsal and os t. IV were not present in juvenile *L. africana* collection in the NMK (presumably due to the lack of ossification) they were not studied. However, photographic evidence suggests the central tarsal of juvenile *M. trogontherii* from China is low (see Chen and Tong, 2017: Fig. 3-A3 and B3) compared with that of adult *M. trogontherii* (see Chen and Tong, 2017: Fig. 3-C3), suggesting a low central tarsal may be a juvenile trait among Elephantinae. As such, it is possible that a low central tarsal in adult *P. ex gr. P. falconeri* may be paedomorphic, although metric analysis of *L. africana* specimens obtained from dissection as well as the skeletons of adults will likely be necessary evaluate this possibility.

*As mentioned in Chapter 2, articular facet area may scale with (i) mass-induced forces or (ii) muscle-induced forces. In the former case one would expect facet area to scale with positive allometry to body mass, and in the latter one would expect facets to scale isometrically with body mass (Yapuncich and Boyer, 2014). The dimensions of the calcaneus' lateral articular facet for the astragalus (length vs. breadth which give some idea of the area of the articular facet) were measured across a wide range in body mass (Fig. 3.1c), and suggest approximate isometry. However, without exact measurements of the actual area of articular facets and a knowledge of body mass it is impossible to distinguish reliably between mass-induced and muscle-induced forces.

5.4.2 Low-gear locomotion in the feet of *P. ex gr. P. falconeri*

In Chapter 3 qualitative and quantitative morphological comparisons between insular *P. ex gr. P. falconeri* and non-insular species demonstrated that there is no explicit evidence of reduced medio-lateral movement in the forefoot which might be associated with low-gear locomotion (Fig. 3.6; Fig. 3.7; Fig. 3.8; Fig. 3.12; Fig. 3.14; Table 3.6). However, it is possible that two morphological features in the calcaneus and one in the os t. IV may have to do with low-gear locomotion. It was shown that the calcaneus has a wide articular facet for the fibula (Fig. 3.22d), which likely limited medio-lateral displacement of the ankle-joint, particularly in *P. ex gr. P. mnaidriensis* and *P. ex gr. P. falconeri*. It is also possible that the articular facet for the fibula functioned as a breaking mechanism when walking downslope in *Palaeoloxodon* sp. 1, *P. ex gr. P. falconeri*. As discussed below, synostosis in the distal tibia-fibula and proximal and distal ulna-radius may relate to low-gear locomotion.

From what we know of observations in extant elephants, they generally avoid steeper slopes due to the higher energy costs and danger (Wall *et al.*, 2006; Ngene *et al.*, 2012: 167). In one study *L. africana* avoided a hill of 300m, with elephant densities decreasing exponentially with increasing hill slope (Wall *et al.*, 2006). There are also reports of accidental deaths by climbing elephants, especially calves, due to falling down from these foothills (see image between p. 240-241 in Douglas-Hamilton and Douglas-Hamilton, 1975; Joshi, 2009: 64). Behaviour such as in climbing slopes to reach a favourite food is also more typical in adventurous males than females (Joshi, 2009: 64). Thus, while there are exceptions, elephants are usually considered reluctant climbers and actively avoid steep or rocky substrates (Wall *et al.*, 2006; Edkins *et al.*, 2007; Roever *et al.*, 2012; Birn-Jeffery and Higham, 2014).

Although African elephants are sometimes described as being good climbers (Rankin, 1882: 279; Kistler, 2006: 115-116 and references therein), they climb slowly and with great caution when relief is steep (Selous, 1881: 81; Rankin, 1882; Kistler, 2006: 116), sometimes creating paths which zigzag back and forth parallel to the contours of steep terrain (Selous, 1881: 100). This behaviour includes moving large blocks aside in order to render a more secure footing, often testing doubtful spots with their forefeet before trusting them with their full weight (Selous, 1881: 100). *E. maximus* has also been observed negotiating atop hills described as being hazardous and mounting hillocks, as well as sliding back down (Joshi, 2009: 63). This kind of behaviour has for example sometimes been observed while reaching for a favourite food-plant (Joshi, 2009: 64).

PART II: DISCUSSION ON CHRONOLOGY AND SYSTEMATICS

5.5 Preliminary U-Th dating of *Palaeoloxodon* sp. from Alcamo Quarry, Sicily

Two U-Th ages obtained from Alcamo Quarry, western Sicily tentatively indicate an age of 551 and 514 ka (Appendix B), the only radiometric dates preliminarily associated with Middle Pleistocene *Palaeoloxodon* sp. However, these dates are associated with large error bars (>80 ka), and may theoretically indicate an infinite age (i.e. potentially not suitable for U-Th dating). This uncertainty is due to the high detrital thorium content of the samples (Appendix B), and further confirmation of these dates is therefore needed. Ideally more samples would be obtained from multiple places up and down the exposed profile (Fig 5.1a), and include purer samples and/or alternative methods (see suggestions for further research below).

5.6 New insights into *Palaeoloxodon* sp. 1 from Luparello Fissure, Sicily

The metric and morphological analyses of the appendicular anatomy of *Palaeoloxodon* sp. 1 presented in Chapters 3 and 4 shed new light on this species, including on (i) the approximate chronological position of the species, (ii) the morphological differences between *Palaeoloxodon* sp. 1 and *P. ex gr. P. falconeri*, and (iii) and also provide some tentative insights into its systematics and taxonomy. These results are summarised in the section below.

5.6.1 The uncertain chronological position of *Palaeoloxodon* sp. 1

On the basis of its stratigraphic position, size and morphology it has been argued that *Palaeoloxodon* sp. 1 is likely the ancestral chronospecies of *P. ex gr. P. falconeri* (Scarborough *et al.*, 2016). Since *P. ex gr. P. falconeri* from Spinagallo Cave has been OSL and U-series dated to the Middle Pleistocene (cf. Herridge *et al.*, 2014; Herridge *et al.*, in prep.), *Palaeoloxodon* sp. 1 is likely older than the ages from Spinagallo Cave (366-233 ka). Nevertheless, further geochronological evidence is needed to evaluate this suggestion. Regardless of its uncertain absolute age however, future refinements in the current Pleistocene biochronology of Sicily may require a new biochronological phase for *Palaeoloxodon* sp. 1 since it does not belong to the *Elephas falconeri* Faunal Complex (*sensu* Bonfiglio *et al.*, 2002: Table 1) by definition, or the Spinagallo Faunal Complex (Marra, 2013 as represented at Spinagallo Cave)*.

*The requirements for a biochronological phase include either/and (i) the arrival of new taxa, their (ii) co-occurrence, (iii) phyletic evolutionary stages, and (iv) extinction. However, the age of *Palaeoloxodon* sp. 1 is unknown, and the palaeogeography of Sicily is therefore also unclear, either consisting of two (Early Pleistocene), or one (much of Middle Pleistocene) islands (see Fig. 1.2). Further, the species still lacks a binomial name. Thus future refinements in Sicilian biochronology may potentially be based on the presence of (i) *Palaeoloxodon* sp. 1, (ii) from Luparello Fissure, (iii) of late Early or early Middle Pleistocene age from (iv) the northern palaeoisland of Sicily or the whole of Sicily (see palaeogeography in Fig. 1.2).

5.6.2 Morphological differences between *Palaeoloxodon* sp. 1 and *P. ex gr. P. falconeri*

Since Sicilian *Palaeoloxodon* sp. 1 from Luparello Fissure is likely the ancestral chronospecies of *P. ex gr. P. falconeri* (Scarborough *et al.*, 2016: 117-118; 120), comparing their anatomy provides insights into the order by which morphological novelties appear. Notably, *Palaeoloxodon* sp. 1 from Luparello Fissure and *P. ex gr. P. falconeri* from Spinagallo Cave share several close morphological similarities, but also significant differences (Table 5.6). Notable differences between the species likely include (i) the depth of the deltoid fossa (ii) the degree of separation between the calcaneus' tibial and fibular facets, and iii) the robusticity of the tibia, although sample-sizes are small for the long-bones. These morphological differences suggest locomotion underwent significant changes in the phyletic lineage's evolution, and that relatively moderate changes in size were accompanied by significant changes in morphology. Whether or not large changes in morphology also reflect rapid evolution or not is a question which can however only be answered with recourse to securer dating.

Element	Morphological feature	Species and provenance			
		<i>P. antiquus</i>	<i>Palaeoloxodon</i> sp. 1	<i>P. ex gr. P. falconeri</i>	<i>Palaeoloxodon</i> sp. 1 vs. <i>P. ex gr. P. falconeri</i>
		Neumark-Nord 1, Germany	Luparello Fissure, Sicily	Spinagallo Cave, Sicily	-
Femur	Curvature of diaphysis in subtrochanteric region	Curved	Very curved	Very curved	Similarity
Tibia	Robusticity of the diaphysis and epiphyses	Robust diaphysis and epiphyses	Extremely robust diaphysis and extremely robust epiphyses	Robust diaphysis and epiphyses	Difference
Os t. IV	Presence/absence of groove for tendon on plantar surface	Present	Absent	Absent	Similarity
Calcaneus	Presence of tibial facet	Absent	Present	Present	Similarity
Humerus	Depth of deltoid fossa	Deep	Shallow	Deep	Difference
Ulnar carpal	Breadth (m-l) of articular facet for the ulna	Broad	Broad	Less broad	Difference

Table 5.6 Features in the appendicular skeleton demonstrating both close morphological similarities and differences between *Palaeoloxodon* sp. 1 and *P. ex gr. P. falconeri* (shared and derived features). Note that sample-sizes for *Palaeoloxodon* sp. 1 are small (see Tables 2.4, 2.5, 2.6, 2.7) and that possible autapomorphic morphological differences are therefore considered tentative.

5.6.3 Systematics and taxonomy of *Palaeoloxodon* sp. 1

The smallest elephant remains from Luparello Fissure have been referred to *Elephas* or *Palaeoloxodon falconeri* based on their similarity with Maltese remains (Vaufrey, 1929;

Imbesi, 1956; Palombo and Ferretti, 2005 *inter alios*). Larger remains from Luparello Fissure in contrast have been referred to *Elephas* or *Palaeoloxodon melitensis* or *mnaidriensis*, (refer to synonymy in Appendix A) based on the similar size (Vaufrey, 1929) and tooth morphology (Herridge, 2010), although it has been shown that morphological differences in the calcaneus exist, either relating to ecophenotype, or due to the presence of separate species. Taxeopody of *Palaeoloxodon* sp. 1 - Most studies of insular proboscidean appendicular anatomy exclude the morphology of the foot bones in relation to systematics and taxonomy (e.g. Roth, 1982; van den Bergh, 1999; Herridge, 2010), either because foot bones are considered taxonomically uninformative (Herridge, 2010: 29), and (very likely) in part due to the anatomical complexity of the foot and depth of anatomical knowledge it requires, as well as the lack of associated elements. *P. mnaidriensis* from Malta and *Palaeoloxodon* sp. 1 from Luparello Fissure, Sicily have not been distinguished as separate species or ecomorphs on the basis of tooth morphology (Herridge, 2010). Chapter 3 however demonstrated that *Palaeoloxodon* sp. 1 from Luparello Fissure and *P. ex gr. P. falconeri* are morphologically highly derived in the calcaneus relative to *P. antiquus*, and may also display other autapomorphies in the tarsals (see Table 5.6).

Remarks on morphological differences between *Palaeoloxodon* sp. from Bnghisa Gap, Malta and *Palaeoloxodon* sp. 1 from Luparello Fissure - Due to the fact that teeth are among the most frequently preserved fossil elephant remains and tooth morphology is interspecifically variable, systematics and taxonomy within the Elephantinae places a strong emphasis on dental rather than appendicular autapomorphies (e.g. Osborn, 1936; Aguirre, 1969b: 1369; Maglio, 1973; Todd, 2005; 2010; Herridge, 2010) while acknowledging certain limitations in delimiting proboscidean species based on dental morphology (see e.g. Roth, 1989)*. The systematics and taxonomy of Siculo-Maltese elephants also follows this tradition (Bonfiglio and Berdar, 1979; Bagnasco, 1994; Simonelli, 1995; Palombo, 2003; Ferretti, 2008; Guenther, 1988; Herridge, 2010), often largely ignoring or explicitly considering the postcranial remains to be uninformative with regard to systematics and taxonomy (e.g. Herridge, 2010: 29; 397).

This thesis has however demonstrated highly significant differences in the functional morphology of the calcaneus between insular *Palaeoloxodon* species, which may be particularly relevant when distinguishing species of similar size, such as with regard to *Palaeoloxodon* sp. 1 from Luparello Fissure, Sicily and *Palaeoloxodon* sp. from Bnghisa Gap, Malta. Furthermore, the possibility that Maltese *P. mnaidriensis* may not be the ancestral chronospecies of *P. falconeri* (*contra* Herridge, 2010: Fig. 7.1) merits consideration since there is a greater resemblance between the calcaneus morphology of *Palaeoloxodon* sp. 1 from Luparello Fissure and *P. ex gr. P. falconeri* from Spinagallo Cave than *Palaeoloxodon* sp. from Bnghisa Gap, Malta (see Scarborough *et al.*, 2016: Fig. 9). However, the taxonomy and chronometric age of calcanei from neither Luparello Fissure nor Bnghisa Gap is currently secure, so that more research is needed to clarify the alleged conspecificity between

*The names of many genera belonging to the Elephantinae (those derived from the Greek root *odontos*) describe the shape of their teeth, e.g. *Loxodonta*, meaning *slanted tooth*.

Sicilian and Maltese *Palaeoloxodon* sp. from Luparello Fissure and Bnghisa Gap (see Proposals for further research in Section 6.2).

The key conclusions based on the calcaneus morphology of *Palaeoloxodon* sp. from Sicily and Malta therefore include: i) Similar-sized Maltese *Palaeoloxodon* sp. from Bnghisa Gap and Sicilian *Palaeoloxodon* sp. 1 from Luparello Fissure may belong to separate species. ii) *Palaeoloxodon* sp. 1 from Luparello Fissure is likely the ancestral chronospecies of *P. ex gr. P. falconeri* from Sicily and Malta. iii) Further, the morphology of the calcaneus is more useful for systematics and taxonomy than previously recognised, and may also prove a valuable tool for taxonomic assessment of the Elephantidae in general. The large differences in calcaneus morphology between different *Palaeoloxodon* spp. therefore suggest the calcaneus merits more emphasis with regard to dwarf elephant systematics and taxonomy than has thus far been given (*contra* Herridge, 2010: 29). Whether or not allopatric speciation during an interglacial highstand (see Siddall *et al.* 2003; Herridge, 2010: 354 for bathymetry) may account for differences in morphology between insular elephants on Sicily and Malta is thus something that requires investigation, given that allopatry in other taxa likely occurred between the two islands (see Gliozzi *et al.*, 1993: 326).

5.6.4 Concluding remarks on *Palaeoloxodon* sp. 1

Based on the morphological observations in the limbs and feet it was tentatively concluded that *Palaeoloxodon* sp. 1 is: (i) Likely the ancestral chronospecies of *P. ex gr. P. falconeri*; (ii) there are several large differences in appendicular morphology compared to *P. ex gr. P. falconeri*; (iii) The taxon may exhibit several possible autapomorphies including a shallow deltoid fossa on the humerus; a tibia with extremely robust diaphysis and epiphyses (compared with other Elephantinae species), and a femur which likely exhibits pedomorphism in the curvature of the diaphysis, and a calcaneus with a tibial facet; (iv) Furthermore, *Palaeoloxodon* sp. 1 is possibly a separate species to similar-sized *Palaeoloxodon* sp. from Bnghisa Gap, Malta (although the alternative, that ecophenotype accounts for different morphologies cannot be ruled out). (v) Large remains from Luparello Fissure are possibly referable to a new species of *Palaeoloxodon*, although more research is needed, particularly on the re-discovered material (Appendix D).

CHAPTER 6

CONCLUSIONS

This Chapter briefly summarizes the results and discussion of the previous three chapters, in light of the Hypotheses stated in Chapter 1, and is divided into three parts, 6.1 (Concluding Remarks), 6.2 (Proposals for further research) and 6.3 (The major findings of this study).

6.1 Concluding remarks

This thesis provides new insights into the appendicular anatomy of the insular dwarf descendants of *P. antiquus*, including endemic species from Sicily, Malta and Favignana islands, and the tentative identification of one new species from Sicily and another from Favignana island. Additionally new insights are provided into the appendicular anatomy of a dwarf mammoth from Sardinia. These new insights broadly fall into several categories, including (i) functional morphology, (ii) the presence/absence of paedomorphism, (iii) evolutionary history and (iv) taxonomy of dwarf elephants.

Comparisons across a wide spectrum in body mass suggest that morphological changes in the tarsals may in part be attributable to reduced mass in dwarf *Palaeoloxodon* species. Fossil *Palaeoloxodon* spp. represent the greatest range of body mass in any terrestrial mammalian phylum, thereby providing an excellent means of investigating how mass and appendicular anatomy are related, and for testing evolutionary hypotheses about mass and anatomy. Paedomorphism is likely present in the femur of the chronospecies *Palaeoloxodon* sp. 1 from Luparello Fissure and *P. ex gr. P. falconeri*. There is also similarity in morphology between the tibia of juvenile *L. africana* and *P. ex gr. P. falconeri*, perhaps reflecting paedomorphism. However, it appears that paedomorphism is not clearly reflected in the tarsals and carpals of *P. ex gr. P. falconeri*, and the considerable morphological changes in the tarsals relative to *P. antiquus* are therefore likely the result of natural selection, relaxed selection or genetic drift.

Morphological differences between species indicate functional differences, including some possible evidence of low-gear locomotion, which may be reflected in the morphology of the *P. ex gr. P. falconeri* calcaneus. Postcranial morphological adaptations in *Palaeoloxodon* species on islands fit within a broader context of adaptation to insular environments (Millien, 2006), and particularly within the context of other insular endemics with locomotory adaptations to their insular environments. As such insular *Palaeoloxodon* phyla fit a larger pattern of endemic mammals evolving locomotory adaptations to the specific requirements of their local environments (Boekschoten and Sondaar, 1966; Leinders and Sondaar, 1974: 112; Sondaar, 1977: 683-687; 1994; Houtekamer and Sondaar, 1979; Caloi and Palombo, 1994, 1995; Köhler and Moyà-Solà, 2001; Quintana *et al.*, 2011: 238; van der Geer *et al.*, 2010: 361-363; Scarborough *et al.*, 2016).

In closing, and with regard to future work, it is worth noting that due to intense selection pressures to which elephants were subjected during the Pleistocene, their wide range in mass, and repeated process of adaptation to uniquely different insular environments, the study of insular endemic *Palaeoloxodon* spp. offers unique insights into the pattern and process of natural selection on islands, with broad implications for adaptation and evolutionary biology. As such, insular proboscideans have the potential to provide many exciting new avenues for

research into the causes and correlates of island evolution which other taxa are less likely to do, or may only do less clearly.

Summary of results on Hypotheses

Of the three hypotheses which were tested (see Chapter 1), Hypotheses I and II found support, whereas III was not supported. The outcomes of Hypotheses I and II however indicate that insularity has profound effects on the appendicular morphology of dwarf elephants, particularly in *P. ex gr. P. falconeri*. The results of the hypotheses are summarized as follows:

1. Paedomorphism is likely reflected in the femur of *Palaeoloxodon* sp. 1 and *P. ex gr. P. falconeri*.
2. Paedomorphism is one possible explanation for morphological features in the *P. ex gr. P. falconeri* tibia.
3. Paedomorphism is not clearly reflected in the carpals and tarsals of *P. ex gr. P. falconeri*.
4. Morphological changes are clearly evidenced in the articular facets of the feet of insular *Palaeoloxodon* species, particularly in some tarsals of *P. ex gr. P. falconeri*, most notably the highly derived calcaneus.
5. There is no clear evidence in the scapula's glenoid fossa of a more agile gait in *P. ex gr. P. falconeri* compared with *P. antiquus*.

Summary of results on chronology and phylogeny

In addition, several novel conclusions were drawn on the Pleistocene chronology and phylogeny:

6. *Palaeoloxodon* sp. 1 from Luparello Fissure is likely the ancestral chronospecies of *P. ex gr. P. falconeri*.
7. *P. ex gr. P. falconeri* likely evolved on Sicily during the later phase of its evolution (although the early stages are still unknown) and subsequently colonized Malta.
8. A Sicilian dwarf elephant (*Palaeoloxodon* sp.) likely evolved its extremely reduced body mass by roughly 0,5 Ma, based on preliminary U-Th dating results of travertine at Alcamo Quarry, but awaits further confirmation because of high detrital Thorium.
9. The morphology of the calcaneus appears to be taxonomically informative among the Elephantinae, particularly with regard to the phylogeny of *Palaeoloxodon* sp. 1 and *P. ex gr. P. falconeri*.

6.2 Proposals for further research

Several aspects of this thesis require further investigation:

(i) 2D morphometrics of the long bones in cranial aspect - Photographic comparisons revealed ontogenetic and interspecific differences in the shape in the humerus, femur, tibia (Figs 4.9; 4.24; 4.37). In order to more accurately assess (and quantify) these differences 2D morphometrics would be useful in addition to photography by circumventing distortion due to parallax effects (Stephan, 2015).

(ii) Morphometry of the deltoid fossa - Hypothesis III predicted that gait becomes more agile as mass decreases in insular proboscideans, although no evidence was found in the scapula's glenoid fossa of a different gait in *P. ex gr. P. falconeri*. If *P. ex gr. P. falconeri* is more cursorial than its ancestor however, one would predict the distal termination of the deltoid fossa to be more proximally situated than in *P. antiquus*, due to the fact that the upper leg-muscles are more bunched-up proximally in cursorial quadrupeds, requiring less work for each stride (Hildebrand, 1988: 483). This therefore provides a testable hypothesis, and as part of this study differences in the morphology of the fossa were described, although it is not known to which extent the observed differences were idiosyncratic, and the differences described are also somewhat subjective without being measured. As part of this study it was attempted to measure the position of the distal termination of the deltoid fossa on the humerus. However, this was found to be problematic due to the indistinct tapering-out of the deltoid fossa's distal termination. In order to quantify this hand-held laser-scanning would possibly enable the measuring the depth of the deltoid fossa as a function of its distance from the proximal end of the articular head (see materials in Table 2.4; Ambrosetti, 1968: 364; Theodorou, 1983: 202; Di Patti *et al.*, 1995: 15-16, 34, 59; Marano and Palombo, 2013: Table 3). Laser scanning would also assist in potentially scoring/coding these characters, and the frequency of each character state reported for each taxon, also providing a better indication of the range of myological variation observed (in depth and orientation) of the deltoid fossa (see Table 4.3).

(iii) Morphometry of the femur - In this study the morphological similarity between the longitudinal curvature of the diaphysis in the subtrochanteric region of juvenile *L. africana* was suggested to reflect paedomorphism in *Palaeoloxodon* sp. 1 and *P. ex gr. P. falconeri* based on photographic comparisons. It would however be possible to quantify the curvature in an ontogenetic series of *L. africana* using 3D scanning (or geometric morphometrics) and compare curvature with adult insular *Palaeoloxodon* spp. of different sizes (see methods in Wibowo, 2016: 60). This would enable a test of the hypothesis that there is a clinal trend towards increased curvature in the femur in a) an ontogenetic series from adult to juvenile *L. africana* (see materials in Table 2.8), and b) in a series of decreasing adult size in *Palaeoloxodon* spp., from *P. antiquus*, *P. ex gr. P. mnaidriensis*, *Palaeoloxodon* sp. 1, and ending with *P. ex gr. P. falconeri* (see materials in Table 2.4). Furthermore, it would be possible to include *P. tiliensis* from Tilos, *Palaeoloxodon* sp. from Malta and *P. kreutzburgi* from Crete in order to investigate whether or not the femur is more crooked in other

Palaeoloxodon dwarfs compared with *P. antiquus*, since if a more crooked femur than in *P. antiquus* is found in additional species it would suggest that similar heterochronic mechanisms resulting in paedomorphism may underpin dwarfism on separate islands (see materials in Table 2.4; Lydekker, 1886: 145; Adams, 1874: 58, plate. xiv Fig. 1; Ambrosetti, 1968: 365; Theodorou, 1983: 211; Palombo and Petronio, 1989: Fig. 2; Di Patti *et al.*, 1995: 18-19, 34, 58; Marano and Palombo, 2013: Table 3). Finally, it would also be possible to compare the femur of continental *M. columbi* with dwarfed *M. exilis* from the California Channel Islands as part of such a study (see materials in Roth, 1982: 21-22; Agenbroad and Mead, 1994; Agenbroad, 2002; 2009: Table 2).

(iv) Morphometry of the astragalus' articular facet for the tibia in relation to biomechanics - Initially, it was attempted to measure the articular facet for the tibia. Unfortunately, this proved difficult due to the fact that the bone has rounded edges (Fig. 3.15-A), making it difficult to define between which two points a measurement should be taken. Difficulties with repeatability were also encountered due to interspecific morphological differences. However, due to the fact that the astragalus is the main point of articulation for the ankle joint, and that its morphology differs between species, a thorough study of its size and shape is clearly merited. This would be especially relevant for comparing the biomechanics of the articulation between the astragalus and tibia (see methods in Püschel *et al.*, 2017).

(v) Morphometry of the calcaneus and its application to systematics in the Elephantidae - In Chapter 3 large interspecific morphological differences were described in the calcaneus' articular facets for the tibia and fibula, using a new biometric method developed in this study (see p. 54). There is however much potential for improving this method using 3D scanning, which would improve measurement accuracy, particularly with regard to calculating the surface areas of the tibial and curved fibular facet. 3D scanning of the tibial facet would further be useful for estimating the maximum range of flexion in the ankle-joint of *Palaeoloxodon* sp. 1 and *P. ex gr. P. falconeri*, which is particularly relevant to comparing functional morphology between species. Furthermore, morphometric analysis would likely be of great relevance to the systematics and taxonomy among the Elephantidae, including in non-insular proboscideans (see materials in Scarborough *et al.*, 2016: Table 1).

(vi) U-Th dating at Alcamo Quarry - The travertine deposit at Alcamo (see Appendix B) is particularly suitable for radiometric dating for several reasons. Unlike nearly all previously excavated cave deposits on Sicily and Malta (for which there are often extremely limited stratigraphic records), the stratigraphic provenance is directly observable for *in situ* fossils within the travertine matrix. Undated *Palaeoloxodon* sp. material at the site are also present in the section several metres above the samples dated in Appendix B, and therefore useful for investigating a potentially finely-resolved time-range of dwarf *Palaeoloxodon* sp. remains. Furthermore, the site may also have potential for oxygen isotope ($\delta^{18}\text{O}$) chrono-stratigraphic correlation and magnetostratigraphy. Alcamo Quarry is therefore potentially one of the most suitable Middle Pleistocene Sicilian sites with *Palaeoloxodon* sp. at which to undertake more extensive chronometric dating.

(vii) Morphological description and metric analysis of the *Palaeoloxodon* spp. assemblage from Luparello Fissure - A very wide clinal range in absolute size is represented in the *Palaeoloxodon* spp. remains from Luparello Fissure, suggesting that anagenesis is reflected in the assemblage. However, a large portion of the assemblage from Luparello Fissure (including 156+ *Palaeoloxodon* sp. remains preliminarily identified by the author from storage in the IPH Vaufrey collection) have thus far never been identified, catalogued, described or measured. The Luparello Fissure assemblage therefore has great potential for further study, particularly with regard to the morphological evolution of the suggested chronospecies *Palaeoloxodon* sp. 1 and *P. ex gr. P. falconeri* and the uncertain taxonomy of larger *Palaeoloxodon* sp. 1 (see also discussion in Scarborough *et al.*, 2016) regarding the integrity of the Siculo-Maltese *P. mnaidriensis* hypodigm). Furthermore, comparisons between *Palaeoloxodon* sp. 1 from Luparello Fissure and the large remains from the Comiso limnic deposits may prove highly informative with regard to the evolution of Middle Pleistocene dwarf elephants (see Bonfiglio and Inasacco, 1992: 202; Bonfiglio *et al.*, 2000: 175; Bonfiglio *et al.*, 2001: Fig. 3)

(viii) Taphonomy of the Spinagallo Cave *Palaeoloxodon* spp. assemblage - The *P. ex gr. P. falconeri* sample from Spinagallo Cave displays an extensive range in absolute size (in specimens with fused epiphyses), variation which has been attributed to sexual dimorphism and ontogeny (Ambrosetti, 1968: 329ff). However, the excavators originally described larger remains (*Elephas melitensis*) as coming from the lower strata of the cave's main deposit (Accordi and Colaccichi, 1962: 222; see also Palombo, 2001b: 487). According to the excavators "there was a rather well defined succession of the fossil specimens: the smallest form (*E. falconeri*) was prevalent in the upper part, whilst in the inferior part the greatest number of the remains belonged to *E. melitensis* (intermediate dwarf form)" (Accordi and Colaccichi, 1962: 221). Furthermore, personal observation suggested a tendency for many of the largest specimens to share a similar taphonomy (large specimens often being a distinctive dark-red or purplish colour, contrasting with white, blue-grey and mottled specimens), perhaps reflecting a provenance from the dark red layer near the base of the deposit (see Accordi and Colaccichi, 1962: 222; *ibid.*, Fig. 2). Whether or not evidence of anagenesis is seen in the bone taphonomy is therefore a question which may be answerable by comparing the biometrics of specimens of known ontogenetic stage with a more rigorous categorization of their taphonomy (e.g. using the bones' Munsell colour and mineralization via X-ray fluorescence). It therefore cannot be ruled out that Ambrosetti's mode D (the largest specimens, see Ambrosetti, 1968: 329ff) belong to the infrequently represented forerunners of *P. ex gr. P. falconeri* rather than the end-point of *P. ex gr. P. falconeri* size.

6.3 The major findings of this study

This thesis has identified previously undocumented morphological differences in different *Palaeoloxodon* species, reflecting adaptation to the Siculo-Maltese palaeoarchipelago, providing new insights into the anatomy of the feet, the role of heterochrony in the evolution of dwarfism, and the relationship between body mass, environment and functional morphology among the Elephantidae.

In addition, this thesis suggests the presence of a new taxon: Sicilian remains from Luparello Fissure which are likely ancestral to *P. ex gr. P. falconeri* (*contra* Herridge, 2010: Fig. 7.1), thus contributing to our understanding of diversity in the genus *Palaeoloxodon*. Methodologically, a novel emphasis is placed on the use and potential for further study of calcaneus morphology with regard to Elephantinae systematics and taxonomy (*contra* Herridge, 2010: 29), contrasting with previous results which placed a stronger emphasis on tooth morphology (Bonfiglio and Berdar, 1986; Bagnasco, 1994; Simonelli, 1995; Herridge, 2010 *inter alios*). *Palaeoloxodon* remains from Faraglione Cave, Favignana still require further study in order to explain its small size relative to *P. ex gr. P. mnaidriensis* from Puntali Cave, Sicily.

Finally, this thesis further underscores how insular proboscideans are a window into evolutionary processes, and have the potential to provide many new and unique insights into the processes surrounding adaptation and extinction. Future studies of insular proboscideans may therefore provide the key to resolving some of the important and currently unanswered questions of island biogeography (see Patiño, *et al.* 2017), and have much potential for improving our understanding of the drivers and correlates of mammalian macroevolution.

References cited

- Abbate, R. 1974. L'*Elephas falconeri* Busk in Sicilia. *Speleologia Siciliana* 1: 12-14.
- Abbate, R. 2007. Le Grotte di Baida (Palermo): Geomorfologia e palaeontologia. *Thalassia Salentina* 5-17.
- Abercrombie, M., Hickman, M., Johnson, M.L. and Thain, T. 1990. *The New Penguin Dictionary of Biology* (8th ed.). London: Penguin Books, 600 pp.
- Accordi, B. 1962. Some data on the Pleistocene stratigraphy and related pigmy mammalian fauna of eastern Sicily. *Quaternaria* 6: 415-429.
- Accordi, B. 1963. Rapporti fra il "Milazziano" della costa iblea (Sicilia sud-orientale) e la comparsa di *Elephas mnaidriensis*. *Geologica Romana* 2: 295-304.
- Accordi, B., Campisi, B. and Colacicchi, R. 1959. Scoperta di un giacimento pleistocenico a elefanti nani e ghiro gigante nella grotta di Spinagallo (SR). *Atti della Accademia Gioenia di Scienze Naturali in Catania* (series 6) 12: 167-182.
- Accordi, B. and Colacicchi, R. 1962. Excavations in the Pygmy Elephants Cave of Spinagallo (Siracusa). *Geologica Romana* 1: 217-229.
- Accordi, B. and Maccagno, A.M. 1962. Researches in the Pleistocene of Riano (Roma). *Geologica Romana* 1: 25-32.
- Accordi, F.S. and Palombo, M.R. 1971. Morfologia endocranica degli elefanti nani pleistocenici di Spinagallo (Siracusa) e comparazione con l'endocranio di *Elephas antiquus*. *Atti della Accademia Nazionale dei Lincei, classe di scienze fisiche, matematiche, e naturali* 51(1-2): 111-124.
- Adams, A.L. 1865. History of the discovery of the fossil elephant of Malta with a description of the fissure in which it was originally found. *Geological Magazine* 2: 488-491.
- Adams, A.L. 1870. *Notes of a Naturalist in the Nile Valley and Malta: A narrative of exploration and research in connection with the natural history, geology and archæology of the Lower Nile and Maltese Islands*. Edinburgh: Edmonston and Douglas, 295 pp.
- Adams, A.L. 1874. On the dentition and osteology of the Maltese fossil Elephants, being a description of remains discovered by the author in Malta between the years 1860 and 1866. *Transactions of the Zoological Society of London* 9(1): 1-124.
- Agenbroad, L.D. 2001. Channel Islands (USA) pygmy mammoths (*Mammuthus exilis*) compared and contrasted with *M. columbi*, their continental ancestral stock. *Proceedings of the 1st International Congress of the World of Elephants*. 6-20 October 2001. Rome: Consiglio Nazionale delle Ricerche. 473-475.
- Agenbroad, L.D. 2002. New localities, chronology, and comparisons for the pygmy mammoth (*Mammuthus exilis*): 1994-1998. *Proceedings of the 5th California Island Symposium*. 29 March-1 April 1999. Santa Barbara: Santa Barbara Museum of Natural History. 518-524.
- Agenbroad, L.D., 2003. New absolute dates and comparisons for California's *Mammuthus exilis*. *DEINSEA* 9: 1-16.
- Agenbroad, L.D. 2009. *Mammuthus exilis* from the California Channel Islands: Height, Mass, and Geologic Age. *Proceedings of the 7th California Islands Symposium* 5-8 February 2008. Arcata, California: Institute for Wildlife Studies. 15-19.
- Agenbroad, L.D. and Mead, J.I. Eds. 1994. *The Hot Springs Mammoth Site: A Decade of Field and Laboratory Research in Paleontology, Geology, and Paleoecology*. Rapid City, SD: Fenske Printing, 457 pp.
- Agenbroad, L.D., Morris, D. and Roth, V.L. 1999. Pygmy mammoths (*M. exilis*) from Santa Rosa Island, Channel Islands National Park, California, USA. *DEINSEA* 6: 89-102.
- Aguirre, E. 1969a. Revisión sistemática de los *Elephantidae* por su morfología y morfometría dentaria. *Estudios Geológicos* 25 (3-4): 317-367.

- Aguirre, E.E. 1969b. Evolutionary history of the elephant. *Science* 164: 1366-76.
- Aiba, H., Baba, K. and Matsukawa, M. 2010. A new species of *Stegodon* (Mammalia, Proboscidea) from the Kazusa Group (lower Pleistocene), Hachioji City, Tokyo, Japan and its evolutionary morphodynamics. *Palaeontology* 53(3): 471-490.
- Airaghi, C. 1928. Mammiferi pliocenici dell'isola di Coo (Dodecaneso). *Atti della Società Italiana di Scienze Naturali e del Museo Civico di Storia Naturale in Milano* 67: 125-135.
- Aitken, M. J. 1990. *Science-based dating in Archaeology*. London: Longman, 274 pp.
- Albayrak, E. 2012. Fossil Elephants of Turkey. *Hacettepe Journal of Biology and Chemistry, Special Issue* 365-370.
- Albayrak, E. and Lister, A.M. 2012. Dental remains of fossil elephants from Turkey. *Quaternary International* 276: 198-211.
- Alexander, R.McN. 1977. Allometry of the limbs of antelopes (Bovidae). *Journal of Zoology* 183: 135-146.
- Alexander, R.McN., Maloiy G.M.O., Hunter, B., Jayes, A.S. and Nturibi, J. 1979a. Mechanical stresses in fast locomotion of buffalo (*Syncerus caffer*) and elephant (*Loxodonta africana*). *Journal of Zoology* 189:135-144.
- Alexander, R.McN., Jayes, A.S., Maloiy, G.M.O., Wathuta, E.M. 1979b. Allometry of the limb bones of mammals from shrews (*Sorex*) to elephant (*Loxodonta*). *Journal of Zoology* 189: 305-314.
- Aloisi, A., Di Ferro, M., Lentini, E., Mangano, G. and Mineo, S. Eds. with Meli, G. (coordinating editor). 2006. *Il travertino di Alcamo: Proposta per l'istituzione di un geosito*. Palermo: Walter Farina, 71 pp.
- Ambrosetti, P. 1968. The Pleistocene dwarf elephants of Spinagallo (Siracusa, south-eastern Sicily). *Geologica Romana* 7: 277-398.
- Ambrosetti, P. 1972. L'elefante fossile della Sardegna. *Bollettino della Società Geologica Italiana e del Servizio Geologico d'Italia* 91: 127-131.
- Anastasakis, G.C. and Dermitzakis, M. 1990. Post middle Miocene palaeogeographic evolution of the central Aegean Sea and detailed Quaternary reconstruction of the region; its possible influence on the distribution of the Quaternary mammals of the Cyclades Islands. *Neues Jahrbuch für Geologie und Paläontologie Monatshefte* 1: 1-16.
- Antonoli, F., Lo Presti, V., Morticelli, M.G., *et al.*, 2016. Timing of the emergence of the Europe-Sicily bridge (40–17 cal ka BP) and its implications for the spread of modern humans. *Geological Society of London Special Publications* 411(1): 111-144.
- Anca, F. and Gemmellaro, G.G. 1867. *Monografia degli elefanti fossili di Sicilia*. Palermo: Giovanni Lorscheider, 23pp.
- Andrews, C.W. 1908. *A guide to the elephants (recent and fossil) exhibited in the Department of geology and palaeontology in the British museum (Natural history)*. London: Department of Geology, British Museum (Natural History), 46 pp.
- Andrews, C.W. and Cooper, C.E. 1928. *On a specimen of Elephas antiquus from Upnor*. London: British Museum of Natural History, 25 pp.
- Anonymous. 1862. Section C - Geology. *The Parthenon* no. 25, October 18, 1862: 780.
- Anonymous. 1827. A review of Frédéric Cuvier and Étienne Geoffroy Saint-Hilaire's *Histoire Naturelle des Mammifères*. *The Zoological Journal (London)* 3: 140-143.
- Antoine, P.O., Welcomme, J.L., Marivaux, L., Baloch, I., Benammi, M. and Tassy, P. 2003. First record of Paleogene Elephantoidea (Mammalia, Proboscidea) from the Bughti Hills of Pakistan. *Journal of Vertebrate Paleontology* 23: 977-980.
- Anzidei, A.P., Bulgarelli, G.M., Catalano, P., Cerilli, E., Gallotti, R., Lemorini, C., Milli, S., Palombo, M.R., Pantano, W. and Santucci, E. 2012. Ongoing research at the late Middle Pleistocene site of La Polledrara di Cecanibbio (central Italy), with emphasis on human-elephant relationships. *Quaternary International* 255: 171-187.

- Argnani, A. 2009. Evolution of the southern Tyrrhenian slab tear and active tectonics along the western edge of the Tyrrhenian subducted slab. *Geological Society of London, Special Publications* 311: 193-212.
- Arpe, L., Karhu, J.A. and Vartanyan, S.L. 2009. Bioapatite $^{87}\text{Sr}/^{86}\text{Sr}$ of the last woolly mammoths - Implications for the isolation of Wrangel Island. *Geology*: 347-350.
- Athanassiou, A. 2012. A skeleton of *Mammuthus trogontherii* (Proboscidea, Elephantidae) from NW Peloponnese, Greece. *Quaternary International* 255: 9-28
- Athanassiou, A., Herridge, V., Reese, D.S., Iliopoulos, G., Roussiakis, S., Mitsopoulou, V., Tsiolakis, E., Theodorou, G. 2015. Cranial evidence for the presence of a second endemic elephant species on Cyprus. *Quaternary International* 379: 47-57.
- Athanassiou, A., Lyras, G. and van der Geer, A.A.E. 2017. Pleistocene insular Proboscidea of the Eastern Mediterranean: an update and revision of available samples. *Abstract book of the 7th International Conference of Mammoths and their Relatives*. 17-23 September 2017. Taichung (Taiwan): National Museum of Natural Science. PE2-2.
- Athanassiou, A., van der Geer, A.A.E. and Lyras, G.A. 2019. Pleistocene insular Proboscidea of the Eastern Mediterranean: A review and update. *Quaternary Science Reviews* 218. XXX.
- Averianov, A. O. 1996. Sexual dimorphism in the mammoth skull, teeth, and long bones. In *The Proboscidea*. J. Shoshani, & P. Tassy, Eds. Oxford Oxford: University Press. 260-267.
- Bada, J.L., Belluomini, G., Bonfiglio, L., Branca, M., Burgio, E. and Delitala, L. 1991. Isoleucine epimerization ages of Quaternary Mammals of Sicily. *Il Quaternario* 4(1a): 49-54.
- Bagnasco, L. 1994. *Nuovi contribute alla revision delle specie di elefanti nani del Quaternario Siciliano: Un approccio biometrico alla morfologia dentaria*. Unpublished thesis, Universita degli Studi di Palermo.
- Basile, B. and Chilardi, S. Eds. 1996. *Siracusa, le ossa dei giganti: lo scavo paleontologico di Contrada Fusco*. Siracusa: Arnaldo Lombardi, 199 pp.
- Bate, D.M.A. 1903. Preliminary Note on the Discovery of a Pigmy Elephant in the Pleistocene of Cyprus. *Proceedings of the Royal Society of London* 71: 498-500.
- Bate, D.M.A. 1907. On elephant remains from Crete, with description of *Elephas creticus* sp. n. *Proceedings of the Zoological Society of London* 77(2): 238-50.
- Baygusheva, V.S., Titov, V.V. and Timonina, G.I. 2012. Two skeletons of *Mammuthus trogontherii* from the Sea of Azov Region. *Quaternary International* 276-277: 242-252.
- Beden, M. 1980. *Elephas recki* Dietrich, 1915 (Proboscidea, Elephantidae): évolution au cours de Plio-Pléistocène en Afrique Orientale. *Géobios* 13: 891-901.
- Belluomini, G. and Bada, J.L. 1985. Isoleucine epimerization ages of the dwarf elephants of Sicily. *Geology* 13: 451-452.
- Benedetto, G. and Giordano, A. 2008. Sicily. In *Mediterranean Island Landscapes: Natural and Cultural Approaches*. I.N. Vogiatzakis, G. Pungetti & A.M. Mannion, Eds. Dordrecht: Springer.. 117-142.
- Benoit, J. 2015. A new method of estimating brain mass through cranial capacity in extinct proboscideans to account for the non-neural tissues surrounding their brain. *Journal of Vertebrate Paleontology* DOI: [10.1080/02724634.2014.991021](https://doi.org/10.1080/02724634.2014.991021).
- Benton, M.J., Csiki, Z., Grigorescu, D., Redelstorff, R., Sander, P.M., Stein, K. and Weishampel, D.B. 2010. Dinosaurs and the island rule: Dinosaurs from Hațeg Island. *Palaeogeography, Palaeoclimatology, Palaeoecology* 293: 438-454.
- Benz, A. 2005. *The elephant's hoof: Macroscopic and microscopic morphology of defined locations under consideration of pathological changes*. PhD thesis, University of Zürich, 146 pp. Available online at <http://www.upali.ch/diss.pdf>.

- Bertram, J.E.A. 2016. Design for Prodigious Size without Extreme Body Mass. In J.E.A. Bertram, Ed. *Understanding Mammalian Locomotion: Concepts and Applications*. 349-367.
- Biewener, A.A. 1982. Bone strength in small mammals and bipedal birds: do safety factors change with body size? *Journal of Experimental Biology* 98: 289-301
- Biewener, A.A. 1983. Allometry of quadrupedal locomotion: the scaling of duty factor, bone curvature and limb orientation to body size. *Journal of Experimental Biology* 105: 147-171.
- Biewener, A.A. 1989. Scaling body support in mammals: limb posture and muscle mechanics. *Science* 245: 45-48.
- Biewener, A.A. 1990. Biomechanics of mammalian terrestrial locomotion. *Science* 250: 1097-1103.
- Biewener, A.A. 2000. Scaling of terrestrial support: differing solutions to mechanical constraints of size. In *Scaling in Biology*. J.H. Brown and G.B. West, Eds. Oxford: Oxford University Press, pp. 51-66.
- Biewener, A.A. 2003. *Animal Locomotion*. Oxford: Oxford University Press, 296 pp.
- Biewener, A.A. 2005. Biomechanical consequences of scaling. *The Journal of Experimental Biology* 208: 1665-1676.
- Birn-Jeffery, A.V. and Higham, T.E. 2014. The Scaling of Uphill and Downhill Locomotion in Legged Animals. *Integrative and Comparative Biology* 54(6): 1159-1172.
- Blueweiss, L., Fox, H. Kudzma, V., Nakashima, D., Peters, R., Sams, S. 1978. Relationships between body size and some life history parameters. *Oecologia* 37(2): 257-272.
- Blumenbach, J.F. 1797. (5th ed.) *Handbuch der Naturgeschichte*. Göttingen: Dieterich, 714 pp.
- Blumenbach, J.F. 1799. (6th ed.) *Handbuch der Naturgeschichte*. Göttingen: Dieterich, 708 pp.
- Boekschoten, G.J. and Sondaar P.Y. 1966. The Pleistocene of the Katharo Basin (Crete) and its Hippopotamus. *Bijdragen tot de Dierkunde* 36: 17-44.
- Boekschoten, G.J. and Sondaar, P.Y. 1972. On the fossil Mammalia of Cyprus. *Proceedings of the Koninklijke Nederlandse Akademie van Wetenschappen Series B* 75: 306-338.
- Bonavia, C.G. 1999. The early stages of the Maltese Pleistocene mammalian sequence, evidence from the Maghlaq Quaternary deposits. In *Facets on Maltese Prehistory*. A. Mifsud and C. Savonia-Ventura, Eds. Malta: Prehistory Society of Malta, 33-40.
- Bonfiglio, L. 1992. Middle and Upper Pleistocene mammal faunas in the islands of Sicily and Malta: analogies and palaeogeographic implications. *International Union for Quaternary Research Newsletter* 14: 52-56.
- Bonfiglio, L. 2013. Notes and Discussions on Marra, A.C. Evolution of Endemic Species, Ecological Interactions and Geographical Changes in an Insular Environment: A Case Study of Quaternary Mammals of Sicily (Italy, EU). *Geosciences* 3: 616-625^[1]_[SEP]
- Bonfiglio, L. and Berdar, A. 1979. Gli elefanti delle ghaie pleistoceniche di Messina. *Quaternaria* 21: 139-177.
- Bonfiglio, L. and Berdar, A. 1986. Gli elefanti del Pleistocene superiore di Archi (RC): nuove evidenze di insularità della Calabria meridionale durante il ciclo Tirreniano. *Bollettino della Società Paleontologica Italiana* 25(1): 9-34.
- Bonfiglio, L. and Burgio, E. Significato paleoambientale e cronologico delle mammalofaune Pleistoceniche della Sicilia in relazione all'evoluzione paleogeografica. *Il Quaternario* 5: 223-234.
- Bonfiglio, L. and Insacco, G. 1992. Palaeoenvironmental, paleontologic and stratigraphic significance of vertebrate remains in Pleistocene limnic and alluvial deposits from southeastern Sicily. *Palaeoecology, Palaeoclimatology, Palaeoecology* 95: 195-208.

- Bonfiglio, L. and Piperno, M. 1996. Early Faunal and Human Populations. In *Early Societies in Sicily: new developments in archaeological research*. Accordia specialist studies on Italy. R. Leighton, Ed. London: University of London. 21-29.
- Bonfiglio, L., Di Geronimo, I.S., Insacco, G. and Marra, A.C., 1996. Large Mammal remains from Middle Pleistocene deposits of Sicily: new stratigraphic evidence from western edge of the Hyblean Plateau (southeastern Sicily). *Rivista Italiana di Paleontologia e Stratigrafia* 102(3): 375-384.
- Bonfiglio, L., Marra, A.C. and Masini, F. 2000. The contribution of Quaternary vertebrates to palaeoenvironmental and palaeoclimatological reconstructions in Sicily. *Geological Society, London, Special Publications* 181: 171-184.
- Bonfiglio, L., Marra, A.C., Masini, F. and Petruso, D. 2001. Depositi a vertebrati e ambienti costieri pleistocenici della Sicilia e della Calabria meridionale. *Biogeographia* 22: 29-43.
- Bonfiglio, L., Mangano, G., Marra, A.C., Masini, F., Pavia, M., Petruso, D. 2002. Pleistocene Calabrian and Sicilian bioprovinces. *Geobios* 24: 29-39.
- Bonfiglio, L., Di Maggio, C., Marra, A.C., Masini, F. and Petruso, D. 2003. Bio-chronology of Pleistocene vertebrate faunas of Sicily and correlation of vertebrate bearing deposits with marine deposits. *Il Quaternario* 16: 107-114.
- Bonfiglio, L., Esu, D., Mangano, G., Masini, F., Petruso, D., Soligo, M. and Tuccimei, P. 2008. Late Pleistocene vertebrate-bearing deposits at San Teodoro Cave (Northeastern Sicily): Preliminary data on faunal diversification and chronology. *Quaternary International* 190: 26-37. ^[11]_[SEP]
- Bonnan, M.F. 2005. Pes Anatomy in Sauropod Dinosaurs: Implications for Functional Morphology, Evolution, and Phylogeny. In *Thunder-Lizards: The Sauropodomorph Dinosaurs*. V. Tidwell & K. Carpenter, K, Eds. Bloomington: Indiana University Press. 346-380.
- Böttger, T. 2010. Anwendung stabiler Isotope leichter Elemente für paläoklimatische Untersuchungen limnischer Sedimentfolgen. In *Elefantenreich: eine Fossilwelt in Europa*. D. Höhne, and W. Schwarz, Eds. Halle (Saale): Landesamt für Denkmalpflege und Archäologie Sachsen-Anhalt. 93-97.
- Bourliere, F. 1975. Mammals small and large: the ecological implications of size. In *Small Mammals, their Productivity and Population Dynamics*. F.B. Gollay, K. Petrusewicz & L. Ryszkowskie, Eds. Cambridge: Cambridge University Press. 1-8.
- Bover, P., Fornós, J.J. and Alcover, J.A. 2005. Carpal bones, carpal fusions and footprints of *Myotragus*: clues for locomotion and behavior. *Monografies de la Societat d'Història Natural de les Balears* 12: 325-336.
- Bover, P., Quintana, J. and Alcover, J.A. 2008. Three islands, three worlds: Paleogeography and evolution of the vertebrate fauna from the Balearic Islands. *Quaternary International* 182(1): 135-144.
- Bover, P., Quintana, J. and Alcover, J.A. 2010. A new species of *Myotragus* Bate, 1909 (Artiodactyla, Caprinae) from the Early Pliocene of Mallorca (Balearic Islands, western Mediterranean). *Geological Magazine* 147: 871-885.
- Bowell, R.J., Warren, A., Redmond, I., 1996. Formation of cave salts and utilization by elephants in the Mount Elgon region, Kenya. In *Environmental Geochemistry and Health*. J.D. Appleton, R. Fuge & G.J.H. McCall, Eds. London: The Geological Society. 63-80.
- Boyce, M.S. 1988. Evolution of life histories: theory and patterns from mammals. In *Evolution of Life Histories of Mammals*. M.S. Boyce, Ed. New Haven: Yale University Press. 3-30.
- Branca, S., Coltelli, M., De Beni, E. and Wijbrans, J. 2008. Geological evolution of Mount Etna volcano (Italy) from earliest products until the first central volcanism (between 500

- and 100 ka ago) inferred from geochronological and stratigraphic data. *International Journal of Earth Sciences* 97: 135-152.
- Branca, S., Coltelli, M. and Groppe, G. 2011. Geological evolution of a complex basaltic stratovolcano: Mount Etna, Italy. *Italian Journal of Geosciences* 130(3): 306-317.
- Braun, I.M., and Palombo, M.R. 2012. *Mammuthus primigenius* in the cave and portable art: an overview with a short account on the elephant fossil record in Southern Europe during the last glacial. *Quaternary International* 276: 61-76.
- Brookes, J. 1828. *A catalogue of the anatomical and zoological museum of Joshua Brookes*, part 1. London: R. Taylor, 76 pp.
- Bryant, H.N. and Seymour, K.L. 1990. Observations and comments on the reliability of muscle reconstruction in fossil vertebrates. *Journal of Morphology* 206(1): 109-117.
- Burgio, E. Oliva, N. and Scalone, E. 1983. La Collezione Vertebratologica della Grotta dei Puntali Presso Carini (Palermo). *Naturalista Siciliano* 7(1-4) : 67-79.
- Burgio, E. and Cani, M., 1988. Sul ritrovamento di Elefanti fossili ad Alcamo (Trapani, Sicilia). *Naturalista Siciliano* 12: 87-97.
- Burgio, E. and Di Patti, C. 1990. I vertebrate fossili della Grotta di San Teodoro (Acquedolci-Sicilia). *Naturalista Siciliano* (Series IV) 14: 1-19.
- Burgio, E. 1997. Le attuali conoscenze sui mammiferi terrestri quaternari della Sicilia. In *Prima Sicilia: Alle Origini Della Società Siciliana*. S. Tusa, Ed. Palermo: Edilprint. 55-72.
- Burgio, E. and Costanza, M. 1999. La collezione vertebratologica della Grotta di Luparello (Palermo). *Naturalista Siciliana* 3-4: 359-379.
- Burgio, E., Costanza, M. and Di Patti, C. 2002. I depositi a vertebrati continentali del Pleistocene della Sicilia occidentale. *Naturalista Siciliano* (Series IV) 26: 229-282.
- Busk, G. 1867. Description of the Remains of three extinct Species of Elephant, collected by Capt. Spratt, C. B., R. N., in the Ossiferous Cavern of Zebbug, in the Island of Malta. *Transactions of the Zoological Society of London* 6(5): 227-306.
- Caloi, L. and Palombo, M.R. 1990. Pleistocene herbivores of Mediterranean islands: adaptations. *Hystrix* (n.s.) 2: 87-100.
- Caloi, L. and Palombo, M.R. 1994. Functional aspects and ecological implications in Pleistocene endemic herbivores of Mediterranean Islands. *Historical Biology* 8(1-4): 151-172.
- Caloi, L., Kotsakis, T., Palombo, M.R. and Petronio, C. 2004. The Pleistocene dwarf elephants of Mediterranean islands. In *The Proboscidea: Evolution and Palaeoecology of Elephants and Their Relatives*. J. Shoshani & P. Tassy, Eds. Oxford: Oxford University Press. 234-239.
- Campione, N.E. and Evans, D.C. 2012. A universal scaling relationship between body mass and proximal limb bone dimensions in quadrupedal terrestrial tetrapods. *BMC Biology* 10(1): '1-21'.
- Chesi, F., Delfino, M. and Insacco, G. 2007. Middle Pleistocene Giant Tortoises from Sicily. In *Proceedings of the 7th Giornate di Paleontologia della Società Paleontologica Italiana*. 6-10 June 2007. Milan: University of Milan Printing Press. 19.
- Colomba, M.S., Gregorini A., Liberto F., Reitano A., Giglio S. and Sparacio, I. 2011. Monographic revision of the endemic *Helix mazzullii* De Cristofori & Jan, 1832 complex from Sicily and re-introduction of the genus *Ercetella* Monterosato, 1894 (Pulmonata, Stylommatophora, Helicidae). *Zootaxa* 3134: 1-42.
- Capasso Barbato, L., Minieri, M.R. and Petronio, C. 1988. Resti di mammiferi endemici nelle grotte del Faraglione di Favignana (Egadi, Trapani). *Il Naturalista Siciliano* 4 (3-4): 99-105.
- Carrano, M.T. 2001. Implications of limb bone scaling, curvature and eccentricity in mammals and non-avian dinosaurs. *Journal of Zoology* 254(1): 41-55.

- Case, T.J. 1978. A general explanation for insular body size trends in terrestrial vertebrates. *Ecology* 59: 1-18.
- Cayeux, L. 1908. Découverte de l'*Elephas antiquus* à l'île de Délos (Cyclades). *Comptes rendus hebdomadaires des séances de l'Académie des Sciences* 147: 1089-1090.
- Charnov, E.L., 1993. *Life History Invariants: Some Explorations of Symmetry in Evolutionary Ecology*. Oxford: Oxford University Press, 167 pp.
- Chatwin, B., 2016. It's Not All Heterochrony. In *The Shape of Life: Genes, Development, and the Evolution of Animal Form*. R.A. Raff, Ed. Chicago: University of Chicago Press, p. 255-291.
- Chen, X. and Tong, H. 2017. On the hindfoot bones of *Mammuthus trogontherii* from Shanshenmiaozui in Nihewan Basin, China. *Quaternary International* ^[SEP] 445: 50-59.
- Chiappini, L. 2006. *Gli elefanti fossili del Museo di Storia Naturale e del Territorio dell'Università di Pisa. Revisione sistematica e proposta di un nuovo progetto espositivo integrato*. University of Pisa: Tesi di laurea vecchio ordinamento, 79 pp. Available online at: <https://etd.adm.unipi.it/t/etd-09062006-113051/>
- Chiba, S. 2004. Ecological and morphological patterns in communities of land snails of the genus *Mandarina* from the Bonin Islands. *Journal of Evolutionary Biology* 17: 131-143.
- Chilardi, S. 2001. Large-sized and middle-sized elephants from the Pleistocene of Sicily: the case of Contrada Fusco (Siracusa, Southeastern Sicily). *Proceedings of the 1st International Congress of the World of Elephants* Rome: Consiglio Nazionale delle Ricerche. 476-478.
- Christiansen, P. 1999. Long bone scaling and limb posture in non-avian theropods: evidence for differential limb allometry. *Journal of Vertebrate Paleontology* 19(4): 666-80.
- Christiansen, P. 2004. Body size in proboscideans, with notes on elephant metabolism. *Zoological Journal of the Linnean Society* 140: 523-549.
- Christiansen, P. 2007. Long-bone geometry in columnar-limbed animals: allometry of the proboscidean appendicular skeleton. *Zool. Journal of the Linnean Society* 149: 423-436.
- Clauss, M., Dittmann, M T., Dennis, W.H., Zerbe, P. and Codron, D. 2014. Low scaling of a life history variable: analysing eutherian gestation periods with and without phylogeny-informed statistics. *Mammalian Biology* 79: 9-16.
- Cock, A. G. 1966. Genetical aspects of metrical growth and form in animals. *The Quarterly Review of Biology* 41: 131-190. ^[SEP]
- Croizet, J.B. and Jobert, A.C.G. 1828. *Recherches sur les ossemens fossils du Département du Puy de Dôme*. Paris: Principaux Libraires, 224 pp.
- Cumming, D.H.M. and Cumming, G. S. 2003. Ungulate community structure and ecological processes: body size, hoof area and trampling in African savannas. *Oecologia* 134: 560-568.
- Custodio, C.C., Lepiten, M.V. and Heaney, L.R. 1996. *Bubalus mindorensis*. *Mammalian Species* 520: 1-5.
- Darwin, C.R. 1859. *On the Origin of Species by Means of Natural Selection, or the Preservation of Favoured Races in the Struggle for Life*. London: John Murray, 502 pp.
- Davies, P. and Lister, A. 2001. *Palaeoloxodon cypriotes*, the dwarf elephant of Cyprus: size and scaling comparisons with *P. falconeri* (Sicily-Malta) and mainland *P. antiquus*. *Proceedings of the 1st International Congress of the World of Elephants*. 6-20 October 2001. Rome: Consiglio Nazionale delle Ricerche. 479-480.
- Davies, P. 2002. *The Straight-tusked Elephant (Palaeoloxodon antiquus) in Pleistocene Europe*. Unpublished PhD thesis, University of London.
- Deperet, C. and Mayet, L. 1923. Monographie des éléphants pliocènes de l'Europe et de l'Afrique du Nord. II. *Annales de l'Université de Lyon, Paris n.s. I (Sciences, Médecine)* 42: 89-221.

- De Beni, E., Branca, S., Coltelli, M., Groppelli, G. and Wijbrans, J.R. 2011. $^{40}\text{Ar}/^{39}\text{Ar}$ isotopic dating of Etna volcanic succession. *Italian Journal of Geosciences* 130(3): 292-305.
- De Gregorio, A. 1899. Deux nouveaux dépôts d'*Elephas antiquus* dans le Quaternaire des environs de Palerme. *Annales de Géologie et de Paléontologie* 26 Livraison, Palermo.
- de Vos, J., van der Made, J., Athanassiou, A., Lyras, G., Sondaar, P.Y. and Dermitzakis, M. D. 2002. Preliminary note on the Late Pliocene fauna from Vaterá (Lesbos, Greece). *Annales Géologiques des Pays Helléniques* 39: 37-70.
- Diamond, J. 1991. A new species of rail from the Solomon Islands and convergent evolution of insular flightlessness. *The Auk* 108.3: 461-470.
- Dick, T.J. and Clemente, C.J. 2017. Where have all the giants gone? How animals deal with the problem of size. *PLoS Biology* 15: e2000473.
- Dietrich, W.O. 1915. *Elephas antiquus* Recki n.f. aus dem Diluvium Deutsch-Ostafrikas nebst Bemerkungen über die stammesgeschichtlichen Veränderungen des Extremitätenskeletts der Proboscider: wissenschaftliche Ergebnisse der Oldoway-Expedition 1913. Leipzig: Friedländer & Sohn 80 pp.
- Di Maggio, C. Incandela, A., Masini, F. Petruso, D., Renda, P., Simonelli, C. and Boschian G. 1999. Oscillazioni eustatiche, biocronologia dei depositi continentali quaternari e neotettonica nella Sicilia nord-occidentale (Penisola di San Vito Lo Capo - Trapani): un approccio interdisciplinare. *Il Quaternario* 12(1): 25-49.
- Di Patti, C., Galletti, L. and Patricolo, V. 1995. *Catalogo dei Fossili Siciliani 1. Provincia di Palermo*. Palermo: Osservatorio Paleontologico Gemmellaro, 91 pp.
- Di Patti, C. and Mannino, G. 2006. *I vertebrati fossili della piana di Carini: la paleontologia, la storia, la preistoria e le collezioni*. Palermo: Regione Siciliana Assessorato Territorio e Ambiente, 97 pp.
- Dirks, W., Bromage, T.G. and Agenbroad, L.D. 2012. The duration and rate of molar plate formation in *Palaeoloxodon cypriotes* and *Mammuthus columbi* from dental histology. *Quaternary International* 255: 79-85.
- Douglas-Hamilton, I. and Douglas-Hamilton, O. 1975. *Among the Elephants*. New York: Penguin Books, 285 pp.
- Doukas, C.S. and Athanassiou, A. 2003. Review of the Pliocene and Pleistocene Proboscidea (Mammalia) from Greece. *DEINSEA* 9: 97-110.
- Dubrovo, I.A. and Jakubovski, G. 1988. The carpus morphology of the forest elephant (*Palaeoloxodon*) and its significance for taxonomy. *Prace Muzeum Ziemi* 40: 65-83.
- Edkins, M.T., Kruger, L.M., Harris, K. and Midgley, J.J. 2007. Baobabs and elephants in Kruger National Park: nowhere to hide. *African Journal of Ecology* 46: 119-125.
- Ehrlich, P.R. 1986. Which animal will invade? In *Ecology of Biological Invasions of North American and Hawaii*. H.A. Mooney & J.A. Drake, Eds. New York: Springer Verlag. 79-95.
- Estes, R.D. 2012. *The behaviour guide to African mammals*. London: The University of California Press, 611 pp.
- Fabiani, R. 1928. Cenni sulle raccolte di Mammiferi Quaternari del Museo Geologico della R. Università di Palermo e sui risultati dei nuovi saggi esplorativi. *Bollettino dell'Associazione Mineraria Siciliana* 4(5): 25-34.
- Fabiani, R. 1932a. Giacimento a resti di elefanti scoperto presso Via Libertà a Palermo. *Il Naturalista siciliano* 28(8): 99.
- Fabiani, R. 1932b. Risultati di alcuni scavi nella Grotta della "Za Minica" presso Capaci (Palermo). *Atti della Reale Accademia delle Scienze Lettere e Belle Arti* 17: 1-8.
- Falconer, H. and Cautley, P.T. 1847. *Fauna Antiqua Sivalensis, Being the Fossil Zoology of the Sewalik Hills in the North of India*. London: Smith Elder and Co., pp. 25-80.

- Falconer, H. 1857. On the Species of Mastodon and Elephant occurring in the fossil state in Great Britain. Part I. Mastodon. *Quarterly Journal of the Geological Society* 13.1-2: 307-360.
- Falconer, H. in Murchison, C. 1868. On the fossil remains of *Elephas melitensis*, an extinct pigmy species of elephant; and of other Mammalia, &c. from the ossiferous caves of Malta. In *Palaeontological Memoirs and Notes of the Late Hugh Falconer: Mastodon, Elephant, Rhinoceros, Ossiferous Caves, Primeval Man and His Contemporaries (Vol. II)*. C. Murchison, Ed. London: Robert Hardwicke, pp. 292-308.
- Fanelli, M. 1963. *Studio osteometrico delle ossa lunghe degli elefanti nani di Spinagallo*. Unpublished thesis, Università degli Studi di Roma.
- Fehlmann, M. and Brinkmann, W. 2014. New material of *Mammuthus primigenius* (Proboscidea, Elephantidae) from the Late Pleistocene of Niederweningen, Canton Zurich, Switzerland. *Abstract book of the 6th International Conference on Mammoths and their Relatives*. May 5-12, 2014. Grevena-Siatista, Greece. Published in *Scientific Annals, School of Geology, Aristotle University of Thessaloniki, Greece [Special issue]*. 102: 54.
- Ferretti, M.P. 2008. The dwarf elephant *Palaeoloxodon mnaidriensis* from Puntali Cave, Carini (Sicily; late Middle Pleistocene): Anatomy, systematics and phylogenetic relationships. *Quaternary International* 182: 90-108.
- Ferretti, M.P. and Croitor, R.V. 2001. Functional morphology and ecology of Villafranchian Proboscideans from Central Italy. *Proceedings of the 1st International Congress of the World of Elephants*. 6-20 October 2001. Rome: Consiglio Nazionale delle Ricerche. 103-108.
- Fick, R. 1911. *Handbuch der Anatomie und Mechanik der Gelenke*. Jena: Gustav Fischer, 512 pp.
- Fogliani, F., Prampolini, M., Micallef, A., Angeletti, L., Vandelli, V., Deidun, A., Soldati, M. and Taviani, M. 2016. Late Quaternary coastal landscape morphology and evolution of the Maltese Islands (Mediterranean Sea) reconstructed from high-resolution seafloor data. J. Harff, G. Bailey, F. Luth, Eds. In *Geology and Archaeology: Submerged Landscapes of the Continental Shelf. Geological Society Special Publications* 411(1): 77-95.
- Foster, J.B. 1964. The evolution of mammals on islands. *Nature* 202: 234-235.
- Furlani, S., Antonioli F., Biolchi S., Gambin T., Gauci R., Lo Presti V., Anzidei M., Devoto S., Palombo M.R. and, Sulli, A., 2013. Holocene Sea Level Change in Malta. *Quaternary International* 288: 146-157.
- Garcia G.J.M. and da Silva J.K.L. 2006. Interspecific allometry of bone dimensions: a review of the theoretical models. *Physics of Life Reviews* 3: 188-209.
- Garland, T. 1983. Scaling the Ecological Cost of Transport to Body Mass in Terrestrial Mammals. *The American Naturalist* 121(4): 571-587.
- Gheerbrant, E. and Tassy, P. 2009. L'origine et l'évolution des éléphants. *Comptes Rendus Palevol* 8: 281-294.
- Gliozzi, E., Malatesta, A., Scalone, E., 1993. Revision of *Cervus elaphus siciliae*, Pohlig 1893, Late Pleistocene endemic deer of the siculo-maltese district. *Geologica Romana* 29: 307-354.
- Godfrey, L.R., and Sutherland, M.R. 1995 What's growth got to do with it? Process and product in the evolution of ontogeny. *Journal of Human Evolution* 29: 405-431
- Gould, S.J. 1977. *Ontogeny and Phylogeny*. Cambridge, Massachusetts: Belknap Press. 501 pp.
- Graham, R.W. et al. 2016. Timing and causes of mid-Holocene mammoth extinction on St. Paul Island, Alaska. *Proceedings of the National Academy of Sciences (USA)*. 113(33): 9310-9314.

- Grant, P.R. 1999. *Ecology and Evolution of Darwin's Finches*. Princeton: Princeton University Press, 492 pp.
- Grasso, M. and Lentini, F. 1982. Sedimentary and tectonic evolution of the eastern Hyblean Plateau (Southeastern Sicily) during Late Cretaceous to Quaternary time. *Palaeogeography, Palaeoclimatology, Palaeoecology* 39: 261-280.
- Gray, J.E. 1821. On the natural arrangements of vertebrate animals. *London Medical Repository* 15(88): 296-310.
- Guenther, E.W. 1988. Auf Mittelmeer-Inseln während des Pleistozäns lebende Säuger und ihre morphologischen Abänderungen. *Schriften des Naturwissenschaftlichen Vereins für Schleswig-Holstein* 57: 91-108.
- Gvirtzman, Z. and Nur, A. 1999. The formation of Mount Etna as the consequence of slab rollback. *Nature* 401: 782-785.
- Hanken, J and Wake, D.B. 1993. Miniaturization of Body Size: Organismal Consequences and Evolutionary Significance. *Annual Review of Ecology and Systematics* 24: 501-519
- Halámková, L. 2006. *Fosilní sloni se zvláštním zřetelem na mamuty*. PhD thesis, Masarykova univerzita v Brně, 151 pp. Available online at: http://is.muni.cz/th/19122/prif_d/DIZERTACE.pdf, 151 pp.
- Hardin, G. 1960. The Competitive Exclusion Principle. *Science* 131: 1292-1297.
- Harrington, C.R., Mol, D. and van der Plicht, J. 2012. The Muirkirk Mammoth: A Late Pleistocene woolly mammoth (*Mammuthus primigenius*) skeleton from southern Ontario, Canada. *Quaternary International* 255: 106-113.
- Haynes, G. 1985. Age profiles in Elephant and Mammoth Bone Assemblages. *Quaternary Research* 24: 333-345.
- Haynes, G. 1987. Proboscidean die-offs and die-outs: Age profiles in fossil collections. *Journal of Archaeological Science* 14(6): 659-668.
- Haynes, G. 1991. *Mammoths, Mastodonts, and Elephants*. Cambridge: Cambridge University Press, 395 pp.
- Haughton, S.H. 1932. On some South African fossil Proboscidea. *Transactions of the Royal Society of South Africa*. 21(1): 1-18.
- Herridge, V.L. 2010. *Dwarf elephants on Mediterranean islands: a natural experiment in parallel evolution*. University College London PhD thesis, 480 pp. Available online at http://discovery.ucl.ac.uk/133456/1/133456_Vol.1.pdf
- Herridge, V.L. 2012. A taxonomic tangle: how an elephant's name came to be forgotten. *Evolve* 13: 29-33.
- Herridge, V.L. and Hutchinson, J.R. 2007. Dwarfing a giant: Allometry and ontogeny of elephant limb bones. *Journal of morphology* (Abstract) 268(12): 1083.
- Herridge, V.L. and Lister, A.M. 2012. Extreme Insular Dwarfism Evolved in a Mammoth. *Proceedings of the Royal Society Series B* 279(1741): 3193-3200.
- Herridge, V.L., D. Nita, Schwenninger, J., Mangano, G., Bonfiglio, L., Lister, A.M. and Richards, D. 2014. A new chronology for Spinagallo Cave (Sicily): Implications for the evolution of the insular dwarf elephant *Palaeoloxodon falconeri*. *Abstract book of the 6th International Conference on Mammoths and their Relatives*. May 5-12, 2014. Grevena-Siatista, Greece. Published in *Scientific Annals, School of Geology, Aristotle University of Thessaloniki, Greece [Special issue]*. 102: 70.
- Hildebrand, M. 1988. (3rd ed.) *Analysis of Vertebrate Structure*. New York: John Wiley & Sons, 701 pp.
- Honea, K. 1975. Prehistoric remains on the Island of Kythnos. *American Journal of Archaeology* 79: 277-279.
- Hooijer, D.A. 1967. Indo-Australian Insular Elephants. *Genetica* 38: 143-162.

- Houtekamer, J. L. and Sondaar, P. Y. 1979. Osteology of the forelimb of the Pleistocene dwarf hippopotamus from Cyprus with special reference to phylogeny and function. *Proceedings Koninklijke Nederlandse Akademie van Wetenschappen Series B* 82(4): 411-448.
- Hunt, C.O. and Schembri, P.J. 1999. Quaternary environments and biogeography of the Maltese Islands. In *Facets of Maltese prehistory*. A. Mifsud & C. Savona Ventura, Eds. Malta: The Prehistoric Society of Malta. 41-75.
- Hutchinson, J.R. 2004. Biomechanical modeling and sensitivity analysis of bipedal running ability. I. Extant taxa. *Journal of Morphology* 262: 421-440.
- Hutchinson, J.R., Schwerda, D., Famini, D.J., Dale, R.H.I., Fischer, M.S. and Kram, R. 2006. The locomotor kinematics of Asian and African elephants: changes with speed and size. *Journal of Experimental Biology* 209: 3812-3827.
- Hutchinson, J.R., Miller, C., Fritsch, G. and Hildebrand, T. 2008. The anatomical foundation for multidisciplinary studies of animal limb function: examples from dinosaur and elephant limb imaging studies. In *Anatomical Imaging Techniques: Towards a New Morphology*. H. Endo & R. Frey, Eds. Berlin: Springer-Verlag. 23-38.
- Hutchinson, J.R., Delmer, C., Miller, C.E., Hildebrandt, T., Pitsillides, A.A. and Boyde, A. 2011. From flat foot to fat foot: Structure, Ontogeny, Function and Evolution of Elephant "Sixth Toes". *Science* 334: 1699-1703.
- Huxley, J.S. and Teissier, G. 1936. Terminology of relative growth. *Nature* 137: 780-781.
- ICZN, 1999. *International Code of Zoological Nomenclature*. London: The International Trust for Zoological Nomenclature. Available: <http://www.nhm.ac.uk/hosted-sites/iczn/code/index.jsp>
- Illiger, C.D. 1811. *Prodromus systematis mammalium et avium additis terminis zoographicis utriusque classis*. Berlin: Salfeld, 301 pp.
- Imbesi, M. 1956. Sugli elefanti nani della grotta di Luparello (Palermo). *Actes du IV Congrès International du Quaternaire: Rome-Pise, 1953*: 443-447.
- Inuzuka, N. 1977. On the origin of *Palaeoloxodon naumanni* - A comparative osteology of the cranium. *Journal of the Geological Society of Japan* 83: 639-655.
- Inuzuka, N. and Takahashi, K. 2004. Discrimination between the genera *Palaeoloxodon* and *Elephas* and the independent taxonomical position of *Palaeoloxodon* (Mammalia: Proboscidea). *Zona Arqueológica* 4(2): 234-244.
- Jachmann, H. 1988. Estimating age in African elephants: a revision of Laws' molar evaluation technique. *African Journal of Ecology* 26: 51-56.
- Johnson, D.L. 1980. Problems in the Land Vertebrate Zoogeography of Certain Islands and the Swimming Powers of Elephants. *Journal of Biogeography* (7)4: 383-398.
- Jones, K.E. 2015. Evolutionary Allometry of the Thoracolumbar Centra in Felids and Bovids *Journal of Morphology* 276: 818-831.
- Jordana, X., Marín-Moratalla, N., DeMiguel, D., Kaiser, T.M., and Köhler, M. 2012. Evidence of correlated evolution of hypsodonty and exceptional longevity in endemic insular mammals. *Proceedings of the Royal Society B* 279(1741): 3339-3346.
- Joshi, R. 2009. Asian Elephant's *Elephas maximus* Behaviour in the Rajaji National Park, North-West India: Eight Years with Asian Elephant. *Nature and Science* 7(1): 49-77.
- Kadmon, R. and Pulliam, H.R. 1993. Island biogeography: effect of geographical isolation on species composition. *Ecology* 74: 977-981.
- Kalb, J.E., Froehlich, D.J. and Bell, G.L. 2004a. Phylogeny of African and Eurasian Elephantoida of the late Neogene. In *The Proboscidea: Evolution and Palaeoecology of Elephants and Their Relatives*. J. Shoshani & P. Tassy, Eds. Oxford: Oxford University Press. 101-116.

- Kalb, J.E., Froehlich, D.J. and Bell, G.L. 2004b. Palaeobiogeography of the late Neogene African and Eurasian Elephantoida 117-123. In *The Proboscidea: Evolution and Palaeoecology of Elephants and Their Relatives*. J. Shoshani & P. Tassy, Eds. Oxford: Oxford University Press. 117-123.
- Kapandji, I.A. 1982. (5th ed.) *The Physiology of the Joints: annotated diagrams of the mechanics of the human joints (Volume One Upper Limb)*. Edinburgh: Churchill Livingstone, 283 pp.
- Kevrekidis, C. and Mol, D. 2016. A new partial skeleton of *Elephas (Palaeoloxodon) antiquus* Falconer and Cautley, 1847 (Proboscidea, Elephantidae) from Amyntaio, Macedonia, Greece. *Quaternary International* 406: 35-56.
- Kistler, J. 2006. *War Elephants*. Westport, Connecticut: Praeger, 333 pp.
- Klingenberg, C.P. 1996. Multivariate allometry. In *Advances in Morphometrics*. L.F. Marcus, Ed. New York: Plenum Press. 23-49.
- Klingenberg, C.P. 1998. Heterochrony and allometry: the analysis of evolutionary change in ontogeny. *Biological Reviews* 73: 79-123.
- Klingenberg, C.P. and Zimmermann, M. 1992. Static, ontogenetic, and evolutionary allometry: a multivariate comparison in nine species of water striders. *The American Naturalist* 140: 601-620.
- Köhler, M. 2010. Fast or slow? The evolution of life history traits associated with insular dwarfing. In *Islands and Evolution*. V. Pérez-Mellado & C. Ramon, Eds. Menorca: Institut Menorq d'Estudis. 261-280.
- Köhler, M. and Moyà-Solà, S. 2001. Phalangeal adaptations in the fossil insular goat *Myotragus*. *Journal of Vertebrate Paleontology* 21(3): 621-624.
- Köhler, M. and Moyà-Solà, S. 2009. Slow life history and physiological plasticity: survival strategies of a large mammal in a resource-poor environment. *Proceedings of the National Academy of Sciences (USA)* 106: 20354-20358.
- Köhler, M. and Moyà-Solà, S. 2010. Reply to Meiri and Raia: Small offspring size and fast life history all the way? *Proceedings of the National Academy of Sciences (USA)* 107(8): E28.
- Köhler, M., Palombo, M.R., Pretus, J.L., Jordana, X., Moncunill-Solé, B., Madurell-Malapeira, J., Marín-Moratalla, N. and Bromage, T.G. 2013. Bone histology of the dwarf elephant *Palaeoloxodon falconeri* from Sicily. *Abstract book of the 2nd International Symposium on Paleohistology 2013*. 18-20 July 2013. Bozeman, Montana, USA.
- Kokshenev V.B. 2003. Observation of mammalian similarity through allometric scaling laws. *Physica A: Statistical Mechanics and its Applications* 322: 491-505.
- Kokshenev, V.B., Silva J.K.L. and Garcia, G.J.M. 2003. Long-bone allometry of terrestrial mammals and the geometric-shape and elastic-force constraints of bone evolution. *Journal of Theoretical Biology* 224: 551-6.
- Kokshenev, V.B. and Christiansen, P. 2010. Salient features in the locomotion of proboscideans revealed via the differential scaling of limb long bones. *Biological journal of the Linnean Society* 100(1): 16-29.
- Kolb, C., Scheyer, T.M., Lister, A.M., Azorit, C., de Vos, J., Schlingemann, M.A.J., Rössner, G.E., Monaghan, N.T. and Sánchez-Villagra, M.R. 2015. Growth in fossil and extant deer and implications for body size and life history evolution. *BMC Evolutionary Biology* 15:19.
- Konishi, S. 2000. Skeletal restruction of *Stegodon aurorae* (Proboscidea, Mammalia) and its feature: case study in the Taqa specimen. *Earth Science* 54: 268-78.
- Kotsakis, T. 1977. I resti di anfibi e rettili pleistocenici della Grotta di Spinagallo (Siracusa, Sicilia). *Geologica Romana* 16: 211-229.

- Kotsakis, T. 1979. Sulle mammalofaune quaternarie siciliane. *Bollettino della Società Geologica Italiana e del Servizio Geologico d'Italia* 99: 263-276.
- Kotsakis, T. 1980. Short account on the elephant remains of the Simonelli cave. *Accademia Nazionale dei Lincei*. 249: 115-121.
- Kotsakis, T. 1984. *Crocidura esui* n.sp. (Soricidae, Insectivora) du Pléistocène de Spinagallo (Sicile orientale, Italie). *Geologica Romana* 23: 51-64.
- Kotsakis, T. and Petronio, C. 1980. I chiroterri del Pleistocene superiore della grotta di Spinagallo (Siracusa, Sicilia). *Bollettino del Servizio Geologico d'Italia* 101: 49-76.
- Kroll, W. 1991. *Der Waldelefant von Crumstadt: Ein Beitrag zur Osteologie des Waldelefanten, Elephas (Palaeoloxodon) antiquus Falconer & Cautley (1847)*. Unpublished doctoral thesis, Tierärztliche Fakultät der Ludwig-Maximilians-Universität München, 104 pp.
- Kuss, S.E. 1965. Eine Pleistozäne Säugetierfauna der Insel Kreta. *Berichte der naturforschenden Gesellschaft zu Freiburg im Breisgau* 55: 271-348.
- Larramendi, A. 2016. Shoulder height, body mass and shape of proboscideans. *Acta Palaeontologica Polonica* 61(3): 537-574.
- Larramendi, A. and Palombo, M.R. 2015. Body Size, Biology and Encephalization Quotient of *Palaeoloxodon* ex gr. *P. falconeri* from Spinagallo Cave (Hyblean plateau, Sicily). *Hystrix* 26(2): 102-109.
- Larramendi A., Palombo M.R. and Marano F. 2017. Reconstructing the life appearance of a Pleistocene giant: size, shape, sexual dimorphism and ontogeny of *Palaeoloxodon antiquus* (Proboscidea: Elephantidae) from Neumark-Nord 1 (Germany). *Bollettino della Società Paleontologica Italiana* 56: 299-317.
- Lawlor, T.E. 1982. The evolution of body size in Mammals: evidence from insular population in Mexico. *American Naturalist* 119(1): 54-72.
- Laws, R.M. 1966. Age criteria for the African elephant *Loxodonta africana*. *East African Wildlife Journal* 4: 1-37.
- Leinders, J.J.M. and Sondaar, P.Z. 1974. On functional fusions in footbones of ungulates. *Zeitschrift für Säugetierkunde* 39(2): 109-115.
- Leinders, J.J.M. 1979. On the osteology and function of the digits of some ruminants and their bearing on taxonomy. *Zeitschrift für Säugetierkunde* 44: 305-318.
- Linnæus, C. 1758. (10th ed.) *Systema naturæ per regna tria naturæ, secundum classes, ordines, genera, species, cum characteribus, differentiis, synonymis, locis*. Stockholm: Salvius, 881 pp.
- Liscaljet, N. 2007. A pygmy elephant's shadow is greater with the setting sun. A survey of the Mediterranean insular elephants and a biometrical comparison of the Philippine elephant material. Unpublished MA Thesis, Leiden University, the Netherlands.
- Liscaljet, N. 2012. Napakaliit trompa: New pygmy proboscidean remains from the Cagayan Valley (Philippines). *Quaternary International* 276-277: 278-286.
- Lister, A.M. 1996a. Dwarfing in island elephants and deer: processes in relation to time of isolation. *Symposium of the Zoological Society of London* 69: 277-292.
- Lister, A.M. 1996b. Evolution and taxonomy of Eurasian mammoths. In *The Proboscidea: Trends in Evolution and Paleoecology*. J. Shoshani & P. Tassy, Eds. Oxford: Oxford University Press. 203-213.
- Lister, A.M. 1999. Epiphyseal fusion and postcranial age determination in the woolly mammoth, *Mammuthus primigenius* (Blum.). *DEINSEA* 6: 79-88.^[17]_[SEP]
- Lister, A.M. 2004 Ecological interactions of elephantids in Pleistocene Eurasia: *Palaeoloxodon* and *Mammuthus*. In N. Goren-Inbar & J.D. Spelth, Eds. *Human palaeoecology in the levantine corridor* Oxford: Oxbow. 53-60.

- Lister, A.M. 2013. The role of behaviour in adaptive morphological evolution of African proboscideans *Nature* 500: 331-334.
- Lister, A.M and Bahn, P. (1st ed.) 1994. *Mammoths: Giants of the Ice Age*. Macmillan, 168 pp.
- Lister, A.M and Bahn, P. 2009 (revised ed.) *Mammoths: Giants of the Ice Age*. Berkely: University of California Press, 192 pp.
- Lister, A.M., and Sher, A.V. 2001. The origin and evolution of the woolly mammoth. *Science* 294(5544): 1094-1097.
- Lister, A.M., Sher, A.V., van Essen, H. and Wei, G. 2005. The pattern and process of mammoth evolution in Eurasia. *Quaternary International* 126–128:49-64.
- Lister, A.M. and Stuart, A.J. 2010. The West Runton mammoth (*Mammuthus trogontherii*) and its evolutionary significance. *Quaternary International* 228: 180-209.
- Lomolino, M.V. 2005. Body size evolution in insular vertebrates: generality of the island rule. *Journal of Biogeography* 32: 1683-1699.
- Lomolino, M.V. Sax, D.F., Palombo, M.R. and van der Geer, A.A. 2012. Of mice and mammoths: evaluations of causal explanations for body size evolution in insular mammals. *Journal of Biogeography* (39): 842-854.
- Lomolino, M.V., van der Geer, A.A., Lyras, G.A., Palombo, M.R., Sax, D.F. and Rozzi, R. 2013. Of mice and mammoths: generality and antiquity of the island rule. *Journal of Biogeography* 40: 1427-1439.
- Long, E.S., Courtney, K.L., Lippert, J.C. and Wall-Scheffler, C.M. 2019. Reduced body size of insular black-tailed deer is caused by slowed development. *Oecologia* 189:675–685.
- Losos, J.B., Warheit, K.I. and Schoener, T.W. 1997. Adaptive differentiation following experimental island colonization in *Anolis* lizards. *Nature* 387:70-73.
- Losos, J.B., Jackman, T.R., Larson, A., de Queiroz, K. and Rodriguez-Schettino, L. 1998. Contingency and determinism in replicated adaptive radiations of island lizards. *Science* 279: 2115-2118.
- Losos, J.B. and Ricklefs, R.E. 2009. Adaptation and diversification on islands. *Nature* 457(12): 830-836.
- Losos, J.B. and Ricklefs, R.E. Eds. 2010. *The theory of island biogeography revisited*. Princeton: Princeton University Press, 476 pp.
- Lundquist, C.F. and Varnedoe, W.W. 2006. Salt ingestion caves. *International Journal of Speleology* 35(1): 13-18.
- Lydekker, R. 1886. *Catalogue of the Fossil Mammalia in the British Museum (Natural History): Part IV containing the Order Ungulata, Suborder Proboscidea*. London: British Museum (Natural History), 235 pp.
- MacArthur, R.H. and Wilson, E.O. 1967. *The Theory of Island Biogeography*. Princeton: Princeton University Press, 203 pp.
- Maccagno, A.M. 1962a. Gli elefanti fossili di Riano (Roma). *Geologica Romana* 1: 3-131.
- Maccagno, A.M., 1962b. *L'Elephas meridionalis* NESTI di contrada 'Madonna della Strada', Scoppito (L'Aquila). *Atti della Reale Accademia delle scienze fisiche e matematiche di Napoli* 4(1): 1-132.
- Madurell-Malapeira, J., Palombo, M.R. and Sotnikova, M. 2015. *Cynotherium malatestai*, sp. nov. (Carnivora, Canidae) from the early middle Pleistocene deposits of Grotta dei Fiori (Sardinia, Western Mediterranean). *Journal of Vertebrate Paleontology* 35(4): DOI: [10.1080/02724634.2014.943400](https://doi.org/10.1080/02724634.2014.943400).
- Maglio, V.J. 1973. Origin and evolution of the Elephantidae. *American Philosophical Society Transactions* 63: 1-149.
- Magri, O. 2006. A geological and geomorphological review of the Maltese Islands with special reference to the coastal zone. *Territoris* 6: 7-26.

- Mai, H.D. and Hoffman, J. 2010. Die Vegetation von Neumark-Nord - eine Rekonstruktion anhand karpologischer Reste. In *Elefantenreich: eine Fossilwelt in Europa*. D. Höhne & W. Schwarz, Eds. Halle (Saale): Landesamt für Denkmalpflege und Archäologie Sachsen-Anhalt. 141-149.
- Main, R.P. and Biewener, A.A. 2004. *In vivo* bone strain through ontogeny: a comparison of two vertebrate taxa. *Journal of Morphology* (Abstract) 260: 309.
- Major, F.C.J. 1883. Die Tyrrenis: Studien über geographische Verbreitung von Tieren und Pflanzen im westlich Mittelmeergebiet. *Kosmos* 13: 81-106.
- Major C.I.F. 1902. On the pigmy Hippopotamus from the Pleistocene of Cyprus. *Proceedings of the Zoological Society of London* 1902, 107-112.
- Malatesta, A. 1954. Primo dente di elefante fossile rinvenuto in Sardegna. *Quaternaria* 1: 97-105.
- Malatesta, A. 1957. Terreni, faune e industrie quaternarie nell'Arcipelago delle Egadi. *Quaternaria*: 4: 165-190.
- Maloiy, G.M.O., Alexander, R. McN., Njau, R. & Jayes, A.S. 1979. Allometry of the legs of running birds. *Journal of Zoology* 187: 161-167.
- Mangano, G. and Bonfiglio, L. ¹_{SEP} 2012. First finding of a partially articulated elephant skeleton from a Late Pleistocene hyena den in Sicily (San Teodoro Cave, North Eastern Sicily, Italy). *Quaternary International* 276-277: 53-60.
- Mania, D. 2010a. Die Umwelt der Elefanten von Neumark-Nord. In *Elefantenreich: eine Fossilwelt in Europa*. D. Höhne & W. Schwarz, Eds. Halle (Saale): Landesamt für Denkmalpflege und Archäologie Sachsen-Anhalt. 187-194.
- Mania, D. 2010b. Der Fossilbericht von den Waldelefanten im Seebecken von Neumark-Nord. In *Elefantenreich: eine Fossilwelt in Europa*. D. Höhne & W. Schwarz, Eds. Halle (Saale): Landesamt für Denkmalpflege und Archäologie Sachsen-Anhalt. 201-218.
- Mania, D. and Mai, D. H. 2010. Der Klimacharakter der Warmzeit von Neumark-Nord 1. In *Elefantenreich: eine Fossilwelt in Europa*. D. Höhne & W. Schwarz, Eds. Halle (Saale): Landesamt für Denkmalpflege und Archäologie Sachsen-Anhalt. 175-185.
- Marano, F. and Palombo, M.R. 2011. A pathologic straight-tusked elephant female from Neumark Nord (Germany). *Il Quaternario* 24(1): 93-101.
- Marano, F. and Palombo, M.R. 2013. Population structure in straight-tusked elephants: a case study from Neumark Nord 1 (late Middle Pleistocene?, Sachsen-Anhalt, Germany). *Bollettino della Società Paleontologica Italiana* 52(3): 207-218.
- Marano, F. and Palombo, M.R. 2014. Dimorphic traits in the dwarf elephant “*Palaeoloxodon falconeri*” from Spinagallo Cave (Siracusa, south-eastern Sicily). *Abstract book of the 6th International Conference on Mammoths and their Relatives*. May 5-12, 2014. Grevena-Siatista, Greece. Published in *Scientific Annals, School of Geology, Aristotle University of Thessaloniki, Greece [Special issue]*. 102: 112-113.
- Marra, A.C. 2005. Pleistocene mammals of Mediterranean islands. *Quaternary International* 129(1): 5-14.
- Marra, A.C. 2009. Pleistocene mammal faunas of Calabria (Southern Italy): biochronology and palaeobiogeography. *Bollettino della Società Paleontologica Italiana* 48(2): 113-122.
- Marra, A.C. 2013. Evolution of Endemic Species, Ecological Interactions and Geographical Changes in an Insular Environment: A Case Study of Quaternary Mammals of Sicily (Italy, EU). *Geosciences* 3: 114-139.
- Maschenko, E.N. 2006. New data on the morphology of a foetal mammoth (*Mammuthus primigenius*) from the Late Pleistocene of southwestern Siberia. *Quaternary International* 142-143: 130-146.

- Maschenko, E.N., Gablina, S.S., Tesakov, A.S., Simakova, A.N. 2006. The Sevsk woolly mammoth (*Mammuthus primigenius*) site in Russia: Taphonomic, biological and behavioral interpretations. *Quaternary International* 142-143: 147-165.
- Maschenko, E.N. Schvyreva, A.K. and Kalmykov, N.P. 2011. The second complete skeleton of *Archidiskodon meridionalis* (Elephantidae, Proboscidea) from the Stavropol Region, Russia. *Quaternary Science Reviews* 30: 2273-2288.
- Masini, F., Petruso, D., Bonfiglio, L. and Mangano G. 2008. Origination and extinction patterns of mammals in three central Western Mediterranean islands from the Late Miocene to Quaternary. *Quaternary International* 182: 63-79.
- Masseti, M. 1994. On the Pleistocene Occurrence of *Elephas (Palaeoloxodon) antiquus* in the Tuscan Archipelago, Northern Tyrrhenian Sea (Italy). *Hystrix* (n.s.) 5(1-2): 101-105.
- Masseti, M. 2009. Mammals of the Mediterranean islands: homogenization and the loss of biodiversity. *Mammalia* 73: 169-202.
- Masseti, M. 2012. Atlas of terrestrial mammals of the Ionian and Aegean islands. Berlin: Walter de Gruyter, 303 pp.
- Masters, J.C., Génin, F., Silvestro, D., Lister, A.M., & DelPero, M. 2014. The red island and the seven dwarfs: Body size reduction in Cheirogaleidae. *Journal of Biogeography* 41: 1833-1847.
- Matschie, P. 1900. Über geographische Abarten des afrikanischen Elefanten. *Sitzungsberichte der Gesellschaft Naturforschender Freunde zu Berlin* 8: 189-97.
- Matsumoto, H. 1918. On a new archetypal fossil elephant from Mt. Tomuro, Kaga. *Science Report of the Tohoku Imperial University, 2nd Series (Geology)* 3: 51-56.
- Matsumoto, H. 1924. Preliminary note on fossil elephants in Japan. *The Journal of the Geological Society of Tokyo* 31(371): 255-72.
- Mayr, E. 1963. *Animal Speciation and Evolution*. Cambridge, Massachusetts: Harvard University Press, 797 pp.
- Mayr, E. 2001. *What evolution is*. New York: Basic Books, 318 pp.
- McGowan, C. 1994. *Diatoms to Dinosaurs: The Size and Scale of Living Things*. Washington: Island Press, 288 pp.
- McKay, G.M. 1973. Behavior and ecology of the Asiatic elephant in southeastern Ceylon. *Smithsonian Contributions to Zoology* 125:1-113.
- McKinney, M.L., McNamara, K.J. and Zachos, L.G., 1990. Heterochronic hierarchies: application and theory in evolution. *Historical Biology* 3(4): 269-287.
- McKinney, M.L. and McNamara, K.J., 1991. Classifying and Analyzing Heterochrony. In *Heterochrony: The Evolution of Ontogeny*. Boston: Springer, pp. 13-46.
- McMahon, T.A. 1973. Size and shape in biology. *Science* 179: 1201-1204.
- McMahon, T.A. 1975. Allometry and biomechanics: limb bones in adult ungulates. *The American Naturalist* 109: 547-563.
- McMahon, T.A. 1984 *Muscles, Reflexes and Locomotion*. Princeton: Princeton University Press.
- McMahon, T.A. and Bonner, J.T. 1983. *On Size and Life*. New York: Scientific American Library.
- McNab, B.K. 1994. Energy Conservation and the Evolution of Flightlessness in Birds. *The American Naturalist* 144(4): 628-642.
- McNamara, K.J. 1997. *Shapes of time: the evolution of growth and development*. Baltimore: Johns Hopkins University Press, 342 pp.
- McNamara, K.J. 2002. What is heterochrony? In *Human Evolution Through Developmental Change*. N. Minugh-Purvis & K.J. McNamara, Eds. Baltimore: Johns Hopkins University Press. 1-4.

- Meiri, S., Dayan, T. and Simberloff, D. 2004. Body Size of Insular Carnivores: Little Support for the Island Rule. *The American Naturalist* 163(3): 469-479.
- Meiri, S., Dayan, T. and Simberloff, D. 2006. The generality of the island rule reexamined. *Journal of Biogeography* 33: 1571-1577.
- Meiri, S., Raia, P. and Phillimore, A.B. 2011. Slaying dragons: limited evidence for unusual body size evolution on islands. *Journal of Biogeography* 38: 89-100.
- Meiri, S. and Raia, P. 2010. Reptilian all the way? *Proceedings of the National Academy of Sciences (USA)* 107(8): E27.
- Melis, R., Palombo, M.R. and Mussi, M. 2001. *Mammuthus lamarmorae* (Major, 1883) remains in the pre-Tyrrhenian deposits of San Giovanni in Sinis (Western Sardinia; Italy). *Proceedings of the 1st International Congress of the World of Elephants*. 6-20 October 2001. Rome: Consiglio Nazionale delle Ricerche. 481-485.
- Melis, R. and Palombo, M.R. 2002. Sedimentary sequences and paleoclimate evidences in the Middle-Late Pleistocene of Sardinia. *AIQUA, Stato delle conoscenze e nuovi dati, Bari 24-25 giugno 2002*: 26-27.
- Melis, R., Palombo, M.R. and Mussi, M. 2002. The Stratigraphic sequence of Gonnese (SW Sardinia): palaeoenvironmental, palaeontological, and archaeological evidence. In *World Islands in Prehistory: International Insular Investigations*. W.H. Waldren & J.A. Ensenyat, Eds. Oxford: BAR International Series. 445-453. [SEP]
- Meyer, M. *et al.*, 2017. Palaeogenomes of Eurasian straight-tusked elephants challenge the current view of elephant evolution. *eLife* DOI: [10.7554/eLife.25413](https://doi.org/10.7554/eLife.25413).
- Micallef, A., Foglini, F., Le Bas, T., Angeletti, L., Maselli, V., Pasuto, A. and Taviani, M. 2012. Submerged Palaeolandscape of the Maltese islands: morphology, evolution and relation to quaternary environmental change. *Marine Geology* 335: 129-147.
- Mikota, S. K., Sargent, E. L. and Ranglack, G. S. Eds. 1994. *Medical Management of the Elephant*. West Bloomfield: Indira Publishing House. 298 pp.
- Miller, C.M., Basu, C., Fritsch, G., Hildebrandt, T., and Hutchinson, J.R. 2008. Ontogenetic scaling of foot musculoskeletal anatomy in elephants. *Journal of The Royal Society Interface* 5: 465-476.
- Millien, V. 2006. Morphological Evolution Is Accelerated among Island Mammals. *PLoS Biology* 4(10): 1863-1868.
- Milne, N. 2016. Curved bones: An adaptation to habitual loading. *Journal of Theoretical Biology* 407: 18-24.
- Mitzopoulos, M.K. 1961. Über einen pleistozänen Zwergelefanten von der Insel Naxos (Kykladen). *Praktiká Akadēmias Athinón* 36: 332-340.
- Mol, D. 1984. Over de hand van de mammoet en een bijzonder middenhandsbeen van dit dier. *Cranium* 1: 11-19.
- Mol, D. and Agenbroad, L. 1994. Metapodials and shoulder height of *Mammuthus columbi* compared with Eurasian *Mammuthus* species. In *The Hot Springs Mammoth Site: a Decade of Field and Laboratory Research in Paleontology, Geology, and Paleoecology*. L.D. Agenbroad and J.I. Mead, Eds. Rapid City, South Dakota: Fenske. 224-252.
- Mol, D. and de Vos, J. 1995. De linker achterpoot van de wolharige mammoet; een museumstuk. *Grondboor & Hamer* 49(5): 124-127.
- Mol, D., De Vos, J. van den Berg, G.D. Sondaar, P.Y. 1996. The taxonomy and ancestry of the fossil Elephants of Crete: Faunal turnover and a comparison with proboscidean faunas of Indonesian islands. In *Pleistocene and Holocene fauna of Crete and its first settlers*. D.S. Reese, Ed. Madison, USA: Prehistory Press. 81-98.
- Mol, D., van den Bergh, G.D. and de Vos, J. 1999. Fossil proboscideans from The Netherlands, the North Sea and the Oosterschelde Estuary. *DEINSEA* 6: 119-146.

- Moncunill-Solé, B., Jordana, X. and Köhler, M. 2018. Where did *Mikrotia magna* originate? Drawing ecogeographical inferences from body mass reconstructions. *Geobios* 51: 359-366.
- Moyá-Solá, S. 1979. Morfología funcional del tarso en el género *Myotragus* Bate 1909 (*Artiodactyla*, *Rupicaprini*). *Acta Geologica Hispanica* 13(3): 87-91.
- Muhs, D.R., Simmons, K.R., Groves, L.T., McGeehin, J.P., Schumann, R.R. and Agenbroad, L.D. 2015. Late Quaternary sea-level history and the antiquity of mammoths (*Mammuthus exilis* and *Mammuthus columbi*), Channel Islands National Park, California, USA. *Quaternary Research* 83: 502-521.
- Nagel, R.M., Forstenpointner, G., Soley, J.T. and Weissengruber, G.E. 2018. Muscles and fascial elements of the antebrachium and manus of the African elephant (*Loxodonta africana*, Blumenbach 1797): starring comparative and functional considerations. *Anatomia, Histologia, Embryologia* 47: 195-205.
- Nesti, F. 1825. Sulla nuova specie di elefante fossile del Valdarno all'Illustrissimo sig. Dott. Prof. Ottaviano Targioni Tozzetti. (Lettere sopra alcune ossa fossili del Valdarno non per anco descritte.). *Nuovo Giornale de' Letterati* 11(24): 195-216.
- Ngene, S.M., Skidmore, A.K., Van Gils, H., Van Wieren, S.E., Prins, H.H.T., Douglas-Hamilton, I., and Toxopeus, A.G. 2012. Intensity of elephant occupancy in Marsabit protected area, Kenya: effects of biophysical and anthropogenic factors. In *Elephants: Ecology, Behavior and Conservation*. In M. Aranovich & O. Dufresne, Eds. New York: Nova Science Publishers. 153-172.
- Nowak, R.M. 1999. (6th ed.) *Walker's mammals of the world*. Baltimore: The Johns Hopkins University Press. 1919 pp.
- Osborn, H.F. 1925. The elephants and mastodonts arrive in America. *Journal of the American Museum of Natural History* 15(1): 3-23.
- Osborn, H.F. 1931. *Palaeoloxodon antiquus italicus* sp. nov., Final Stage in the '*Elephas antiquus*' Phylum. *American Museum Novitates* 460: 1-24.
- Osborn, H.F. 1934. The Thirty-Nine Distinct Lines of Proboscidean Descent, and Their Migration into All Parts of the World except Australia. *Proceedings of the American Philosophical Society* 74 (4): 273-285.
- Osborn, H.F. 1936. *The Proboscidea: a monograph of the discovery, evolution, migration and extinction of the mastodonts and elephants of the world (Vol. I): Moeritherioidea, Deinotherioidea, Mastodontoidea*. New York: American Museum Press, 802 pp.
- Osborn, H.F. 1942. *The Proboscidea: a monograph of the discovery, evolution, migration and extinction of the mastodonts and elephants of the world (Vol. II): Stegodontoidea, Elephantoidea*. New York: American Museum Press, 1675 pp.
- Packard, G.C. and Boardman, T.J. 2008. Model selection and logarithmic transformation in allometric analysis. *Physiological and Biochemical Zoology* 81: 496-507.^[1]_{SEP}
- Palkovacs, E.P. 2003. Explaining adaptive shifts in body size on islands: a life history Approach. *OIKOS* 103: 37-44.
- Palombo, M.R. 1994. Gli elefanti del Pliocene superiore e del Pleistocene dell'Italia centrale peninsulare, alcune considerazioni. *Studi Geologici Camerti* (Special volume, Biostratigrafia dell'Italia central). 447-457.
- Palombo, M.R., 1996. Large Pleistocene mammals of the Mediterranean islands. *Vie et Milieu* 46 (3/4): 365-374.
- Palombo, M.R. 2001a. Pedomorphic features and allometric growth in the skull of *Elephas falconeri* from Spinagallo (Middle Pleistocene, Sicily). *Proceedings of the 1st International Congress of the World of Elephants*. 6-20 October 2001. Rome: Consiglio Nazionale delle Ricerche. 492-496.

- Palombo, M.R. 2001b. Endemic elephants of the Mediterranean Islands: knowledge, problems and perspectives. *Proceedings of the 1st International Congress of the World of Elephants*. 6-20 October 2001. Rome: Consiglio Nazionale delle Ricerche. 486-491.
- Palombo, M.R. 2003. *Elephas? Mammuthus? Loxodonta?* The question of the true ancestor of the smallest dwarfed elephant of Sicily. *DEINSEA* 9: 273-291.
- Palombo, M.R. 2004. Dwarfing in insular mammals: the endemic elephants of Mediterranean islands. In *Miscelánea en homenaje a Emiliano Aguirre, Vol. II: Paleontología*. E. Baquedano & S.R. Jara, Eds. Madrid: Museo Arqueológico Regional. 354-371.
- Palombo, M.R. 2006. Biochronology of the Plio-Pleistocene Terrestrial mammals of Sardinia: The state of the art. *Hellenic Journal of Geosciences* 41: 47-66.
- Palombo, M.R. 2007. How can endemic proboscideans help us understand the “island rule”? A case study of Mediterranean islands. *Quaternary International* 169-170: 105-124.
- Palombo, M.R. 2009a. Biochronology, paleobiogeography and faunal turnover in western Mediterranean Cenozoic mammals. *Integrative zoology* 4(4): 367-386.
- Palombo, M.R. 2009b. Body size structure of Pleistocene mammalian communities: what support is there for the “island rule”? *Integrative Zoology* 4: 341-356.
- Palombo, M.R. 2010. Elephants in miniature. In *Elefantenreich: eine Fossilwelt in Europa*. In D. Höhne & W. Schwarz, Eds. Halle (Saale): Landesamt für Denkmalpflege und Archäologie Sachsen-Anhalt. 275-292.
- Palombo, M.R. 2012. Intra-specific variation of stylohyoid bones in *Palaeoloxodon*: A case study of Neumark-Nord 1 (Geiseltal, Sachsen-Anhalt, Germany) straight-tusked elephants. *Quaternary International* 276-277: 77-92.
- Palombo, M.R. 2014. Deconstructing mammal dispersals and faunal dynamics in SW Europe during the Quaternary. *Quaternary Science Reviews* 96: 50-71.
- Palombo, M.R. 2017. Discrete dispersal bioevents of large mammals in Southern Europe in the post-Olduvai Early Pleistocene: A critical overview. *Quaternary International* 431(Part B): 3-19.
- Palombo, M.R. 2018. Insular mammalian fauna dynamics and Paleogeography: a lesson from the Western Mediterranean islands. *Integrative Zoology* 13: 2-20.
- Palombo, M.R. and Petronio, C. 1989. Morphostructural Characters of *Elephas (Palaeoloxodon) creutzburgi* (Kuss, 1965) femur from Simonelli Cave (Rethymnon, Crete). *Hystrix n.s.* 1: 95-105.
- Palombo, M.R. and Villa, P. 2003. Sexually dimorphic characters of *Elephas (Palaeoloxodon) antiquus* from Grotte Santo Stefano (Viterbo, Central Italy). *DEINSEA* 9: 293-315.
- Palombo, M.R., Ginesu, S., Melis, R.T., Sias, S., 2005. The endemic elephants from Sardinia: an unsolved problem. *Monografies de la Societat d'Història Natural de les Balears* 12: 245-254.
- Palombo, M.R. and Ferretti, M.P. 2005. Elephant fossil record from Italy: knowledge, problems, and perspectives. *Quaternary International* 126-128: 107-136.
- Palombo, M.R. and Giovinazzo, C. 2005. *Elephas falconeri* from Spinagallo Cave (South-Eastern Sicily, Hyblean Plateau, Siracusa): a preliminary report on brain to body weight comparison. In *Proceedings of the International Symposium on Insular Vertebrate Evolution: the Palaeontological Approach., 16-19 September 2005. Mallorca. Monografies de la Societat d' Història Natural de les Balears.* 12: 255-264.
- Palombo, M.R., Allbayrak, E. and Marano, F. 2010. The straight-tusked elephants from Neumark-Nord. A glance into a lost world. In *Elefantenreich: eine Fossilwelt in Europa*. D. Höhne & W. Schwarz, Eds. Halle (Saale): Landesamt für Denkmalpflege und Archäologie Sachsen-Anhalt. 219-247.

- Palombo, M.R., Ferretti, M.P. 2010. What about the taxonomical status of European straight-tusked elephants? *Quaternaire Hors-série 3*: 27-28.
- Palombo, M.R., Ferretti, M.P., Pillola, G.L. and Chiappini, L.A. 2012. A reappraisal of the dwarfed mammoth *Mammuthus lamarmorai* (Major, 1883) from Gonnesa (south-western Sardinia, Italy). *Quaternary International* 255: 158-170.
- Palombo, M.R. and Rozzi, R. 2014. How correct is any chronological ordering of the Quaternary Sardinian mammalian assemblages? *Quaternary International* 328: 136-155.
- Palombo, M.R. Zedda, M. and Melis, R.T. 2017. A new elephant fossil from the late Pleistocene of Alghero: The puzzling question of Sardinian dwarf elephants. *Comptes Rendus Palevol* 16: 841-849.
- Palombo, M.R., Ferretti, M.P., Larramendi, A. and Zhang, H. 2017. How many Palaeoloxodon species in Eurasia? Disentangling phylogenetic, dimorphic, ontogenetic, allometric and environmentally-driven characters. *Abstract book of the 7th International Conference of Mammoths and their Relatives*. 17-23 September 2017. Taichung (Taiwan): National Museum of Natural Science. PE2-5.
- Panagiotopoulou, O., Pataky, T.C., Hill, Z. and Hutchinson, J.R. 2012. Statistical parametric mapping of the regional distribution and ontogenetic scaling of foot pressures during walking in Asian elephants (*Elephas maximus*). *The Journal of Experimental Biology* 215, 1584-1593.
- Patiño, J., et al. 2017. A roadmap for island biology: 50 fundamental questions after 50 years of The Theory of Island Biogeography. *Journal of Biogeography* 44(5): 963-983.
- Paul, G. 2009. The nearly columnar limbs of elephants are very different from the more flexed, spring action limbs of running mammals and birds. *Journal of Experimental Biology* 212(1), 152-153.
- Pavia, M. 1999. The Middle Pleistocene Avifauna of Spinagallo Cave (Sicily, Italy): preliminary report. *Smithsonian Contributions to Paleobiology* 89: 125-127.
- Pavia, M., 2000. *Le avifaune pleistoceniche dell'Italia meridionale*. Ph.D. Thesis, Università di Torino, 155 pp.
- Pavia, M. 2004. A new large Barn Owl (Aves, Strigiformes, Tytonidae) from the Middle Pleistocene of Sicily, Italy, and its taphonomical significance. *Geobios* 37: 631-641.
- Pedley, M. 2011. The Calabrian Stage, Pleistocene highstand in Malta: a new marker for unravelling the Late Neogene and Quaternary history of the islands. *Journal of the Geological Society, London* 168: 913-925.
- Pélabon, C., Bolstad, G.H., Egset, C.K., Cheverud, J.M., Pavlicev, M. and Rosenqvist, G. 2013. On the Relationship between Ontogenetic and Static Allometry. *The American Naturalist* 181(2): 195-212.
- Pennycuik, C.J. 1975. On the running of the gnu (*Connochaetes taurinus*) and other animals. *Journal of Experimental Biology* 63: 775-799.
- Pettitt, P.B., Davies, W., Gamble, C.S. and Richards, M.B. 2003. Palaeolithic radiocarbon chronology: quantifying our confidence beyond two half-lives. *Journal of Archaeological Science* 30: 1685-1693.
- Petronio, C. 1970. I roditori pleistocenici della Grotta di Spinagallo (Siracusa). *Geologica Romana* 9: 149-194.
- Petronio, C. 1995. Resti inediti di Ippopotami della Grotta dei Puntali (Carini, Palermo). *Geologica Romana* 31: 265-272.
- Petrova, E.A., Masutin, V.V. and Zhuykova, I.A. 2017. Two incomplete skeletons of woolly mammoth (*Mammuthus primigenius*) from the late Pleistocene in the Kirov Region, European Russia. *Russian Journal of Theriology* 16(2): 157-175
- Piccoli, G. and Del Pup, G. 1967. I resti di elefante nano *Elephas falconeri* della grotta "Luparello" (Palermo) conservati nell'Istituto Geologico di Padova. *Atti e Memorie*

- dell'Accademia Patavina di Scienze, Lettere ed Arti. *Memorie della Classe di Scienze Morali, Lettere ed Arti* 79: 243-260.
- Piccoli, G., Formentin, O.L., and Del Pup, G.W. 1970. Studi su resti di crani di *Elephas mnaidriensis* Adams del Pleistocene di Sicilia. *Memorie dell'Istituto di Geologia e Mineralogia dell'Università di Padova* 27: 1-33.
- Pillola, G.L. and Zoboli, D. 2017. Dwarf mammoth footprints from the Pleistocene of Gonnese (southwestern Sardinia, Italy). *Bollettino della Società Paleontologica Italiana* 56(1): 57-64.
- Piperno, M., Lefèvre, D., Raynal, J.P. and Tagliacozzo, A. 1998. Notarchirico. An early middle pleistocene site in the venosa basin. *Anthropologie* 36: 85-90.
- Pohlig, H., 1893. Eine Elephantenhöhle Siciliens und der erste Nachweis des Cranialdomes von *Elephas antiquus*. *Abhandlungen der Königlich Baierischen Akademie der Wissenschaften* 18: 73-100.
- Pohlig, H. 1885. Über eine Hipparionen-Fauna von Maragha in Nordpersien, über fossile Elephantenreste Kaukasiens und Persiens und über die Resultate einer Monographie der fossilen Elephanten Deutschlands und Italiens. *Zeitschrift der deutschen geologischen Gesellschaft*: 1022-1027.
- Popescu^[1]_{SEP}, A. 2011. The tarsals of *Mammuthus meridionalis* (Nesti, 1825) from Leu (Dolj County, Romania). *Geo-Eco-Marina* 211-217.
- Poulakakis, N., Mylonas, M., Lymberakis, P. and Fassoulas, C. 2002a. Origin and taxonomy of the fossil elephants of the island of Crete (Greece): problems and perspectives. *Palaeogeography, Palaeoclimatology, Palaeoecology* 186:163-183.
- Poulakakis, N., Theodorou, G.E., Zouros, E. and Mylonas, M. 2002b. Molecular Phylogeny of the Extinct Pleistocene Dwarf Elephant *Palaeoloxodon antiquus falconeri* from Tilos Island, Dodekanesia, Greece. *Journal of Molecular Evolution* 55: 364-374.
- Prampolini, M., Fogliini, F., Biolchi, S., Devoto, S., Angelini, S. and Soldati, M. 2017. Geomorphological mapping of terrestrial and marine areas, northern Malta and Comino (central Mediterranean Sea). *Journal of Maps* 13: 457-469.
- Promislow, D.E.L. and Harvey, P.H. 1990. Living fast and dying young: a comparative analysis of life-history variation among mammals. *Journal of Zoology* 220: 417-43.
- Püschel, T.A., Gladman, J.T., Bobe, R. and Sellers, W.I. 2017. The evolution of the platyrrhine talus: A comparative analysis of the phenetic affinities of the Miocene platyrrhines with their modern relatives. *Journal of Human Evolution* 111: 179-201
- Pushkina, D. 2007. The Pleistocene easternmost distribution in Eurasia of the species associated with the Eemian *Palaeoloxodon antiquus* assemblage. *Mammal Review* 37(3): 224-245.
- Quintana, J., Köhler, M. and Moyà-Solà, S. 2011. *Nuralagus rex*, gen. et sp. nov., an endemic insular giant rabbit from the Neogene of Minorca (Balearic Islands, Spain). *Journal of Vertebrate Paleontology* 31: 231-240.
- Raia, P., Carotenuto, F., Passaro, F., Fulgione, D. and Fortelius, M. 2012. Ecological Specialization in Fossil Mammals Explains Cope's Rule. *The American Naturalist* 179(3): 328-337.
- Raia, P., Barbera, C. and Conte, M. 2001. Scaling of proximal limb bones between *Elephas antiquus* and its insular descendant *Elephas falconeri*. *Proceedings of the 1st International Congress of the World of Elephants*. 6-20 October 2001. Rome: Consiglio Nazionale delle Ricerche. 473-475.
- Raia, P., Barbera, C. and Conte, M. 2003. The fast life of a dwarfed giant. *Evolutionary Ecology* 17: 293-312.
- Raia, P. and Meiri, S. 2006. The Island Rule in Large Mammals: Paleontology Meets Ecology. *Evolution* 60(8): 1731-1742.

- Ramsay, E.C. and Henry, R.W. 2008. Anatomy of the Elephant Foot. In *The Elephant's Foot: Prevention and Care of Foot Conditions in Captive Asian and African Elephants*. B. Csuti, E.L. Sargent & U.S. Bechert, Eds. Ames: Iowa State University Press. 9-12.
- Rankin, L.K. 1882. The Elephant Experiment in Africa: A Brief Account of the Belgian Elephant Expedition. *Proceedings of the Royal Geographical Society and Monthly Record of Geography* 4(5): 273-289.
- Redmond, I., 1982. Salt-mining elephants of Mount Elgon. *Swara* 5: 28-31.
- Reggiani, P. 1999. The elephant *Archidiskodon meridionalis* (Nesti, 1825) from the lower Pleistocene of Steggio (Possagno, Treviso, north-east Italy). *Bollettino della Società Paleontologica Italiana* 38(1): 109-119.
- Reggiani, P. 2001. Morphological differences in *Mammuthus meridionalis* and *Palaeoloxodon antiquus* carpal bones. *Proceedings of the 1st International Congress of the World of Elephants*. 6-20 October 2001. Rome: Consiglio Nazionale delle Ricerche. 661-664.
- Ren, L., Butler, M., Miller, C., Paxton, H., Schwerda, D., Fischer, M. S. and Hutchinson, J. R. 2008. The movements of limb segments and joints during locomotion in African and Asian Elephants. *Journal of Experimental Biology* 211: 2735-2751.
- Rispoli, D.M., Athwal, G.S., Sperling, J.W. and Cofield, R.H. 2009. The anatomy of the deltoid insertion. *Journal of Shoulder and Elbow Surgery* 18: 386-390.
- Rhodes, E. J., 1996. ESR dating of tooth enamel. In *Siracusa, le ossa dei giganti: lo scavo paleontologico di Contrada Fusco*. B. Basile & S. Chilardi, Eds. Siracusa: Arnaldo Lombardi. 39-44.
- Roever, C.L., van Aarde, R.J. and Leggett, K. 2012. Functional responses in the habitat selection of a generalist megaherbivore, the African savannah elephant. *Ecography* 35(11): 972-982.
- Rohland, N., Malaspinas, A.S., Pollack, J.L., Slatkin, M., Matheus, P. and Hofreiter, M. 2007. Proboscidean mitogenomics: Chronology and mode of elephant evolution using mastodon as outgroup. *PLoS Biology* 5(8): 1663-1671.
- Romano, M., Manucci, F. and Palombo, M.R. 2019. The smallest of the largest: new volumetric body mass estimate and in-vivo restoration of the dwarf elephant *Palaeoloxodon ex gr. P. falconeri* from Spinagallo Cave (Sicily). *Historical Biology* DOI: 10.1080/08912963.2019.1617289.
- Roth, V.L. 1982. *Dwarf mammoths from the Santa Barbara, California Channel Islands: size, shape, development and evolution*. Ph.D. thesis, Yale University. Ann Arbor: University Microfilms, 277 pp.
- Roth, V.L. 1984. How elephants grow: heterochrony and the calibration of developmental stages in some living and fossil species. *Journal of Vertebrate Paleontology* 4: 126-145. 14(4): 567-588.
- Roth, V.L. 1989. Fabricational noise in elephant dentitions *Paleobiology* 15: 165-179.
- Roth, V.L. 1990. Insular dwarf elephants: a case study in body mass estimation and ecological inference. In *Body size in mammal palaeobiology: Estimation and Biological Implications*. J. Damuth & B.J. MacFadden, Eds. Cambridge: Cambridge University Press. 151-180.
- Roth, V.L. 1992. Inferences from allometry and fossils: dwarfing of elephants on islands. In *Oxford Surveys in Evolutionary Biology*. D. Futuyma & J. Antonovics, Eds. Oxford: Oxford University Press, 259-288.
- Roth, V.L. 1993. *Dwarfism and variability in the Santa Rosa island mammoth: An interspecific comparison of limb-bone sizes and shapes in elephants*. In *Proceedings of the 3rd California Islands Symposium: Recent Advances in Research on the California Islands*. F.G. Hochberg, Ed. Santa Barbara: Santa Barbara Museum of Natural History. 433-442.

- Roth, V.L. 2001. Ecology and evolution of dwarfing in insular elephants. *Proceedings of the 1st International Congress of the World of Elephants*. 6-20 October 2001. Rome: Consiglio Nazionale delle Ricerche. 473-475.
- Roth, V.L. and Shoshani, J. 1988. Dental identification and age determination in *Elephas maximus*. *Journal of Zoology* 214(4): 567-588.
- Rozzi, R. and Palombo, M.R. 2014. Lights and shadows in the evolutionary patterns of insular bovids. *Integrative Zoology* 9: 213-228.
- Saegusa, H. and Gilbert, W.H. 2008. Elephantidae. In *Homo erectus: Pleistocene evidence from the Middle Awash, Ethiopia*. W.H. Gilbert and B. Asfaw, Eds. Berkeley: University of California Press, pp. 193-226.
- Saunders, J.J. 1999. Morphometrical analyses of *Mammuthus columbi* from the Dent Site, Weld County, Colorado. *DEINSEA* 6: 55-78.
- Savona-Ventura, C. and Mifsud, A. 1998. Ghar Dalam cave: a review of the sediments on the cave floor stratigraphy. *Xjensa* 3: 5-12.
- Savona-Ventura, C. and Mifsud, A. 1999. A review of the Pleistocene Deposits in the Southwestern Coast of Malta. *Xjensa* 4(2): 10-17.
- Scarborough, M.E., Palombo, M.R. and Chinsamy-Turan, A. 2014. Locomotory adaptations in the astragalus-calcaneus of Siculo-Maltese dwarf elephants. *Abstract book of the 6th International Conference on Mammoths and their Relatives*. May 5-12, 2014. Grevena-Siatista, Greece. Published in *Scientific Annals, School of Geology, Aristotle University of Thessaloniki, Greece [Special issue]*. 102: 179.
- Scarborough, M.E., Palombo, M.R. and Chinsamy, A. 2016. Insular adaptations in the astragalus-calcaneus of Sicilian and Maltese dwarf elephants. *Quaternary International* 406: 111-122.
- Schaurer, K. 2010. Wie sahen sie aus? Zur Rekonstruktion des *Elephas (Palaeoloxodon) antiquus* aus den Seeablagerungen von Neumark-Nord. In *Elefantenreich: eine Fossilwelt in Europa*. D. Höhne & W. Schwarz, Eds. Halle (Saale): Landesamt für Denkmalpflege und Archäologie Sachsen-Anhalt. 296-311.
- Schmidt-Nielsen, K. 1984. *Scaling: Why is Animal Size So Important?* Cambridge: Cambridge University Press, 241 pp.
- Schoch, W. 2010. Die Holzfunde von Neumark-Nord 1. In *Elefantenreich: eine Fossilwelt in Europa*. D. Höhne & W. Schwarz, Eds. Halle (Saale): Landesamt für Denkmalpflege und Archäologie Sachsen-Anhalt, pp.157-170.
- Schulter, D. 2000. *The Ecology of Adaptive Radiation*. Oxford University Press.
- Seifert-Eulen, M. 2010. Die Vegetation der Warmzeit aus dem Becken NN1 von Neumark-Nord aufgrund der Pollenanalyse. In *Elefantenreich: eine Fossilwelt in Europa*. D. Höhne & W. Schwarz, Eds. Halle (Saale): Landesamt für Denkmalpflege und Archäologie Sachsen-Anhalt. 127-135.
- Selous, F.C. 1907. *A Hunter's Wanderings in Africa: A narrative of nine years spent amongst the game of the far interior of South Africa*. London: MacMillan and co., 504 pp.
- Sen, S., Barrier, E. and Crété, X. 2014. Late Pleistocene Dwarf Elephants from the Aegean Islands of Kassos and Dilos, Greece. *Annales Zoologici Fennici* 51(1-2): 27-42.
- Sen, S. 2017. A review of the Pleistocene dwarfed elephants from the Aegean islands, and their paleogeographic context. *Fossil Imprint* 73(1-2): 76-92.
- Serpelloni, E., Vannucci, G., Pondrelli, S., Argnani, A., Casula, G., Anzidei, M., Baldi, P. and Gasperini, P. 2007. Kinematics of the Western Africa-Eurasia plate boundary from focal mechanisms and GPS data. *Geophysics Journal International* 169: 1180-1200.^[1]_[SEP]
- Shackleton, N.J. 1995. New data on the evolution of Pliocene climatic variability. *Paleoclimate and evolution, with emphasis on human origins*. Yale University Press, New Haven 242-248.

- Shindo, T and Mori, M. 1956a. Musculature of the Indian Elephant. Part I. Musculature of the Forelimb *Okajimas Folia Anatomica Japonica* 28: 89-113.
- Shindo, T. and Mori, M. 1956b. Musculature of the Indian Elephant. Part II. Musculature of the Hindlimb. *Okajimas Folia Anatomica Japonica* 28: 114-147.
- Shoshani, J. 1998. Understanding proboscidean evolution: a formidable task. *Tree* 13(12): 480-487.
- Shoshani, J. and Tassy, P. Eds. 2004. *The Proboscidea: Evolution and Palaeoecology of Elephants and Their Relatives*. Oxford: Oxford University Press, 472 pp.
- Shoshani, J. and Tassy, P. 2005. Advances in proboscidean taxonomy & classification, anatomy & physiology, and ecology & behavior. *Quaternary International* 126-128: 5-20.
- Shoshani, J., Sanders, W.J. and Tassy, P. 2001. Elephants and other Proboscideans: a summary of recent findings and new taxonomic suggestions. *Proceedings of the 1st International Congress of the World of Elephants*. 6-20 October 2001. Rome: Consiglio Nazionale delle Ricerche. 676-679.
- Shoshani J., Ferretti, M.P., Lister A.M., Saegusa, H., Agenbroad, L.D., Mol, D., and Takahashi, K. 2007. Relationships within the Elephantinae using hyoid characters. *Quaternary International* 169-170: 174-185.
- Shpansky, A.V., Vasiliev, S.K. and Pecherskaya, K.O. 2015. The Steppe Elephant *Mammuthus trogontherii* (Pohlig) from the Irtysh Region Near Omsk. *Paleontological Journal* 49(3): 304-325.
- Siddall, M., Rohling, E.J. and Almogi-Labin, A. 2003. Sea-level fluctuations during the last glacial cycle. *Nature* 423: 853-858.
- Silva, M. 1998. Allometric scaling of body length: elastic or geometric similarity in mammalian design. *Journal of Mammalogy* 79: 20-32.
- Simonelli, C. 1995. *Un approccio biometrico alla morfologia dentaria per la revisione della specie Elephas mnaidriensis*. Facoltà di Scienze Matematiche, Fisiche e Naturali, Università degli Studi di Palermo.
- Singer, R. and Crawford, J.R. 1958. The significance of the archaeological discoveries at Hopefield, South Africa. *The Journal of the Royal Anthropological Institute of Great Britain and Ireland* 88(1): 11-19.
- Smith, F. A. *et al.* 2010. The Evolution of Maximum Body Size of Terrestrial Mammals *Science* 330: 1216-1219.
- Smuts, M.M.S. and Bezuidenhout, A. J. 1993. Osteology of the thoracic limb of the African elephant (*Loxodonta africana*). *Onderstepoort Journal of Veterinary Research* 60(1): 1-14.
- Smuts, M.M.S. and Bezuidenhout, A. J. 1994. Osteology of the pelvic limb of the African elephant (*Loxodonta africana*). *Onderstepoort Journal of Veterinary Research* 61(1): 51-66.
- Soergel, W. 1912. *Elephas trogontherii* Pohl. und *Elephas antiquus* Falc., ihre Stammesgeschichte und ihre Bedeutung für die Gliederung des deutschen Diluviums. *Palaeontographica* 60: 1-114.
- Sondaar, P. Y. 1977. Insularity and its effect on mammal evolution. In *Major patterns in vertebrate evolution*. M.K. Hecht, P.C. Goody, and B.M. Hecht, Eds. London: Plenum Press. 671-707.
- Sondaar, P.Y., van der Geer, A.A.E. 2002. Plio-Pleistocene terrestrial vertebrate faunal evolution on Mediterranean islands, compared to that of the Palearctic mainland. *Annales Géologiques des Pays Helléniques* 39A: 165-180.
- Spence, A.J. 2009. Scaling in Biology. *Current Biology* 19: R57-R61.
- Spoor, C.F. 1988. The limb bones of *Myotragus balearicus* Bate 1909. *Proceedings of the Koninklijke Nederlandse Akademie van Wetenschappen, series B* 91: 295-309.

- Spratt, T.A.B. 1867. On the bone caves near Crendi, Zebbug and Mellihha on the island of Malta. *Quarterly Journal of the Geological Society, London* 23: 283-297.
- Sprovieri, R. 1982. Considerazioni sul Plio-Pleistocene della Sicilia. In *Guida alla Geologia della Sicilia Occidentale*. R. Catalano & B. D'Argenio, Eds. Rome: Società Geologica Italiana. 115-118.
- Standring, S. (Ed.). 2005. *Gray's Anatomy: The Anatomical Basis of Clinical Practice* (39th Edition). London: Churchill Livingstone. 1600 pp.
- Stearns, S.C. 1992. *The Evolution of Life Histories*. Oxford: Oxford University Press, 249 pp.
- Ștefănescu, S. 1924. Sur la présence de l'*Elephas planifrons* et de trois mutations de l'*Elephas antiquus* dans les couches géologiques de Roumanie. *Comptes Rendus de l'Académie des Sciences* 179: 1418-1419.
- Stephan, C.N. 2015. Perspective distortion in craniofacial superimposition: Logarithmic decay curves mapped mathematically and by practical experiment. *Forensic Science International* 257 DOI: <http://dx.doi.org/doi:10.1016/j.forsciint.2015.09.009>.
- Stuart, A.J. 1982. *Pleistocene Vertebrates in the British Isles*. London: Longman, 212 pp.
- Stuart, A.J. 2005. The extinction of woolly mammoth (*Mammuthus primigenius*) and straight-tusked elephant (*Palaeoloxodon antiquus*) in Europe. *Quaternary International* 126-128: 171-177.
- Suc, J.P. 1984. Origin and evolution of the Mediterranean vegetation and climate in Europe. *Nature* 307 : 429-432.
- Suc, J.P., Bertini, A., Combourieu-Nebout, N., Diniz, F., Leroy, S., Russo-Ermolli, E., Zheng, Z., Bessais, E. and Ferrier, J. 1995. Structure of West Mediterranean vegetation and climate since 5.3 ma. *Acta Zoologica Cracoviensia* 38: 3-16.
- Symeonidis, N., Bachmayer, F. and Zapfe, H. 1974. Entdeckung von Zwergelafanten auf der Insel Rhodos (Ausgrabungen 1973). *Annalen des Naturhistorischen Museum, Wien* 78: 193-202.
- Symeonidis, N.K., Theodorou, G.E., Gianopoulos, V.I. 2000. The new species *Elephas chaniensis* from the submerged Pleistocene deposits of Vamos Cave at Chania, Crete. *Bulletin de la Société Spéléologique de Grèce* 22: 95-108 (in Greek). Takahashi, K. Chang, C.H. and Cheng, Y.N. 2001. Proboscidean fossils from the Japanese Archipelago and Taiwan Islands and their relationship with the Chinese mainland. *Proceedings of the 1st International Congress of the World of Elephants*. 6-20 October 2001. Rome: Consiglio Nazionale delle Ricerche. 473-475.
- Tassy, P. 1988. The classification of Proboscidea: how many cladistic classifications? *Cladistics* 4: 43-57.
- Theodorou, G., 1983. *The fossil dwarf elephants of Charkadio Cave of Tilos Island, Dodecanese, Greece* (PhD thesis in Greek, edition offset). Athens: University of Athens, 240 pp.
- Theodorou, G. 1988. Environmental factors affecting the evolution of island endemic: the Tilos example from Greece. *Modern Geology* 13: 183-188.
- Theodorou, G., Symeonidis, N. and Stathopoulou, E. 2007. *Elephas tiliensis* n. sp. from Tilos island (Dodecanese, Greece). *Hellenic Journal of Geosciences* 42: 19-32.
- Thouless, C.R. 1995. Long distance movements of elephants in northern Kenya. *African Journal of Ecology* 33(4): 321-334.
- Thouless, C.R. 1996. Home ranges and social organization of female elephants in northern Kenya. *African Journal of Ecology* 34(3): 284-297.
- Tikhonov, A., Agenbroad, L. and Vartanyan, S. 2003. Comparative analysis of the mammoth populations on Wrangel Island and the Channel Islands. *DEINSEA* 9: 415-420.

- Todd, N.E. and Roth, V.L. 1996. Origin and radiation of the Elephantidae. In *The Proboscidea: Evolution and Palaeoecology of Elephants and Their Relatives*. J. Shoshani, & P. Tassy, Eds. Oxford: Oxford University Press, pp. 193-202.
- Todd, N.E. 2005. Reanalysis of African *Elephas recki*: implications for time, space and taxonomy. *Quaternary International* 126-128: 65-72.
- Todd, N.E. 2010. New Phylogenetic Analysis of the Family Elephantidae Based on Cranial-Dental Morphology. *The Anatomical Record* 293:74-90.
- Tong, H. 2012. New remains of *Mammuthus trogontherii* from the Early Pleistocene Nihewan beds at Shanshenmiaozui, Hebei. *Quaternary International* 255: 217-230.
- Tsoukala, E. And Lister, A. 1998. Remains of straight-tusked elephant, *Elephas (Palaeoloxodon) antiquus* Falc. (1847) ESR-dated to oxygen isotope Stage 6 from Grevena. *Bollettino della Società Paleontologica Italiana* 37(1): 117-139.
- Trevisan, L. 1948. Lo Scheletro di *Elephas antiquus italicus* di Fonte Campamile (Viterbo). *Palaeontographia Italica* 44(2): 2-78.
- Tsoukala, E., Mol, D., Pappa, S., Vlachos, E., van Logchem, W., Vaxevanopoulos, M. and Reumer, J. 2011. *Elephas antiquus* in Greece: New finds and a reappraisal of older material (Mammalia, Proboscidea, Elephantidae). *Quaternary International* 245: 339-349.
- Tsubamoto T. 2014. Estimating body mass from the astragalus in mammals. *Acta Paleontologica Polonica* 52:259-265.
- van den Bergh, G. D. 1999. The Late Neogene elephantoid-bearing faunas of Indonesia and their palaeozoogeographic implications; a study of the terrestrial and faunal succession of Sulawesi, Flores and Java, including evidence for early hominid dispersal east of Wallace's line. *Scripta Geologica* 117: 1-419.
- van den Bergh, G.D., Sondaar, P.Y., de Vos, J. and Aziz, F. 2004. The proboscideans of the South-East Asian Islands. In *The Proboscidea: Evolution and Palaeoecology of Elephants and Their Relatives*. J. Shoshani & P. Tassy, Eds. Oxford: Oxford University Press. 240-248.
- van den Bergh, G.D., Awe, R.D., Morwood, M.J. Sutikna, T., Jatmiko, E., and Saptomo, W. 2008. The youngest *Stegodon* remains in south-east Asia from the Late Pleistocene archaeological site Liang Bua, Flores, Indonesia. *Quaternary International* 181(1): 16-48.
- van der Geer, A.A.E. 1999. On the astragalus of the Miocene endemic deer *Hoplitomeryx* from the Gargano (Italy). *DEINSEA* 7: 325-336.
- van der Geer, A.A.E. 2005a. Island ruminants and the evolution of parallel functional structures. *Quaternaire hors série 2*: 231-240.
- van der Geer, A.A.E. 2005b. The postcranial of the deer *Hoplitomeryx* (Pliocene; Italy): another example of adaptive radiation on Eastern Mediterranean islands. *Monografies de la Societat d'Història Natural de les Balears* 12: 325-336.
- van der Geer, A.A.E. 2014. Parallel patterns and trends in functional structures in extinct island mammals. *Integrative Zoology* 9: 167-182.
- van der Geer, A., Lyras, G., de Vos, J. and Dermitzakis, M. 2010. *Evolution of Island Mammals: Adaptation and Extinction of Placental Mammals on Islands*. Oxford: Wiley-Blackwell, 496 pp.
- van der Geer, A.A.E., Lyras, G.A., van den Hoek Ostende, L.W., de Vos, J. and Drinia, H. 2014. A dwarf elephant and a rock mouse on Naxos (Cyclades, Greece) with a revision of the palaeozoogeography of the Cycladic Islands (Greece) during the Pleistocene. *Palaeogeography, Palaeoclimatology, Palaeoecology* 404: 133-144.
- van der Geer, A.A.E., van den Bergh, G.D., Lyras, G.A., Prasetyo, U.W., Due, R.A., Setiyabudi, E. and Drinia, H. 2016. The effect of area and isolation on insular dwarf proboscideans. *Journal of Biogeography* DOI: [10.1111/jbi.12743](https://doi.org/10.1111/jbi.12743)

- van der Geer, A.A.E., Lyras, G.A., Mitteroecker, P. and MacPhee, R.D.E. 2018. From Jumbo to Dumbo: Cranial Shape Changes in Elephants and Hippos During Phyletic Dwarfing. *Evolutionary Biology* 45: 303-317.
- van der Made, J. 2008. New endemic large mammals from the Lower Miocene of Oschiri (Sardinia): Observations on evolution in insular environment. *Quaternary International* 182: 116-134.
- van der Made, J. 2010. The evolution of the elephants and their relatives in the context of a changing climate and geography. In *Elefantenreich: eine Fossilwelt in Europa*. D. Höhne, & W. Schwarz, Eds. Halle (Saale): Landesamt für Denkmalpflege und Archäologie Sachsen-Anhalt. 341-360.
- van der Made, J. and Mazo, A.V. 2003. Proboscidean dispersals from Africa towards Western Europe. *DEINSEA* 9: 437-453.
- van der Merwe, N.J., Bezuidenhout, A.J. and Seegers, C.D. 1995. The skull and mandible of the African elephant (*Loxodonta africana*). *The Onderstepoort journal of veterinary research* 62(4): 245-260.
- van Heteren, A.H. and de Vos, J. 2007. Heterochrony as a typical island adaptation in *Homo floresiensis*. *Proceedings of the International Seminar on Southeast Asian Paleoanthropology: Recent advances on Southeast Asian Paleoanthropology and Archaeology*. Yogyakarta, Indonesia: Gadjah Mada University. 95-106.
- Van Valen, L.M. 1973. Pattern and the balance of nature. *Evolutionary Theory* 1: 31-49.
- Vartanyan, S.L., Garutt, V.E., Sher, A.V. 1993. Holocene dwarf mammoths from Wrangel island in the Siberian arctic. *Nature* 362: 337-340.
- Vartanyan, S.L., Arslanov, K.A., Karhu, J.A., Possnert, G., and Sulerzhitsky, L.D., 2008. Collection of radiocarbon dates on the mammoths (*Mammuthus primigenius*) and other genera of Wrangel Island, northeast Siberia, Russia. *Quaternary Research* 70: 51-59.
- Vaufrey, R. 1929. Les éléphants nains des îles méditerranéennes et la question des isthmes pléistocènes. *Archives de l'Institut de Paléontologie Humaine, Paris* 6: 1-220.
- Vaufrey R. 1930. Les isthmes pléistocènes en Méditerranée. *Bulletin de l'Association de géographes français* 41(7): 37-43.
- Veltre, D.W., Yesner, D.R., Crossen, K.J., Graham, R.W. and Coltrain, J.B. 2008. Patterns of faunal extinction and paleoclimatic change from mid-Holocene mammoth and polar bear remains, Pribilof Islands, Alaska. *Quaternary Research* 70: 40-50.
- Viljoen, P.J. 1989. Spatial distribution and movements of elephants (*Loxodonta africana*) in the northern Namib Desert region of the Kaokoveld, South West Africa/Namibia. *Journal of Zoology* 219(1): 1-19.
- Viljoen, P.J. and Bothma, J.P. 1990. Daily movements of desert-dwelling elephants in the northern Namib Desert. *South African Wildlife Research* 20: 69-72.
- Von Endt, D.W. and Ortner, D.J. 1984. Experimental effects of bone size and temperature on bone diagenesis. *Journal of Archaeological Science* 11(3): 247-253.
- Wassersug, R.J., Yang, H., Sepkoski, J.J. and Raup, D.M. 1979. The evolution of body size on islands: a computer simulation. *American Naturalist* 114:287-295.
- Wall, J., Douglas-Hamilton, I. and Vollrath, F. 2006. Elephants avoid costly mountaineering. *Current Biology* 16(14): R527-R529.
- Weissengruber, G.E. and Forstenpointner, G. 2004. Musculature of the crus and pes of the African elephant (*Loxodonta africana*): insight into semiplantigrade limb architecture. *Anatomy and Embryology* 208: 451-461.
- Weissengruber, G.E., Egger, G.F., Hutchinson, J.R., Groenewald, H.B., Elsässer, L., Famini, D. and Forstenpointner, G. 2006. The structure of the cushions in the feet of African elephants (*Loxodonta africana*). *Journal of Anatomy* 209: 781-792.

- West, J.B. 2001. Snorkel breathing in the elephant explains the unique anatomy of its pleura. *Respiration Physiology* 126(1): 1-8.
- West, J.B., Fu, Z., Gaeth, A.P., Short, R.V. 2003. Fetal lung development in the elephant reflects the adaptations required for snorkeling in adult life. *Respiratory Physiology & Neurobiology* 138: 325-333.
- Western, D. 1979. Size, life history and ecology in mammals. *African Journal of Ecology* 17: 185-204.
- Whittaker, R.J., Fernandez-Palacios, J.M., 2006. (2nd ed.) *Island Biogeography: Ecology, Evolution, and Conservation*. Oxford: Oxford University Press.
- Wibowo, U.P. 2016. *Walking with Indonesian elephants: attribution of isolated proboscidean femurs and tibias to genus based on morphological differences*. Master of Philosophy thesis, School of Earth and Environmental Sciences, University of Wollongong. Available online at: <http://ro.uow.edu.au/theses/4803>.
- Woodward, H. 1903. Cave Hunting in Cyprus. *Geological Magazine* 10(6): 241-246.
- Yamada, F. and Cervantes, F.A. 2005. *Pentalagus furnessi*. *Mammalian Species* 782: 1-5.
- Yapuncich, G.S. and Boyer, D.M. 2014. Interspecific scaling patterns of talar articular surfaces within primates and their closest living relatives. *Journal of Anatomy* 224: 150-172.
- Yapuncich, G.S., Gladman, J.T. and Boyer, D.M. 2015. Predicting euarchontan body mass: a comparison of tarsal and dental variables. *American Journal of Physical Anthropology* 157: 472-506.
- Yellin-Dror, A., Grasso, M., Ben-Avraham, Z. and Tibor, G. 1997. The subsidence history of the northern Hyblean plateau margin, southeastern Sicily. *Tectonophysics* 282: 277-289.
- Zammit Maempel, G. 1989. Ghar Dalam cave and deposits. Malta: Mid-Med Bank, 74 pp.
- Zoboli, D., Pillola, G.L. and Palombo, M.R. 2018. The remains of *Mammuthus lamarmorai* (Major, 1883) housed in the Naturhistorisches Museum of Basel (Switzerland) and the complete “Skeleton-Puzzle”. *Bollettino della Società Paleontologica Italiana* 57(1): 45-57.

APPENDIX A

Systematics and taxonomy

The systematics and taxonomy of insular elephants, and Siculo-Maltese elephants in particular is complex and confusing (Herridge, 2010; 2012). Siculo-Maltese elephants have variously been ascribed to the genera *Elephas* LINNAEUS 1758, *Loxodonta* (ANONYMOUS 1827), *Mammuthus* (BROOKES 1828) and *Palaeoloxodon* (MATSUMOTU 1924)* (see below). Here the taxonomic validity of *Palaeoloxodon* for all Siculo-Maltese elephants is outlined, and the relevant type-series listed in Table A1.1.

There is also some confusion in the literature with regard to the taxonomic rank and phylogeny of *Palaeoloxodon*, which, on the basis of morphology has variously been considered (i) a junior synonym of *Elephas* (Shoshani and Tassy, 2004: 350; Maglio, 1973) (ii) a subgenus of *Loxodonta* (Matsumoto, 1924; Singer and Crawford, 1958), (iii) a sister-taxon of *L. cyclotis* (Meyer *et al.*, 2017), (iv) an African subgenus of *Elephas* (Beden, 1980: 892), (v) an Eurasian subgenus of *Elephas* (e.g. Palombo, 2007; Saegusa and Gilbert, 2008: 198) and (vi) an Afro-Eurasian genus (Osborn, 1942; Ferretti, 2008 *inter alios*). Although uncertainty still exists regarding the phylogenetic relationship between and specific attribution to *Palaeoloxodon* vs. *Elephas* (Shoshani and Tassy, 2005: 8), autapomorphies (especially in the cranium and hyoid) demonstrate monophyly in *Palaeoloxodon* (see Inuzuka, 1977; Shoshani *et al.*, 2001; Davies, 2002; Inuzuka and Takahashi, 2004: 235; Ferretti, 2008; Shoshani and Tassy, 2005; Shoshani *et al.*, 2007; Herridge and Lister, 2012: supplementary; Herridge, 2010: 89). As such, *Palaeoloxodon* would be considered a *bona fide* genus:

Class MAMMALIA Linnaeus 1758
Order PROBOSCIDEA Illiger 1811
Suborder ELEPHANTIFORMES Tassy 1988
Superfamily ELEPHANTOIDEA Gray 1821
Family ELEPHANTIDAE Gray 1821
Subfamily ELEPHANTINAE Gray 1821
Tribe ELEPHANTINI Gray 1821
Genus *PALAEOLOXODON* (Matsumoto 1924)

However, a recent nuclear and mtDNA study of *P. antiquus* from Neumark-Nord and Weimar-Ehringsdorf suggests the *P. antiquus* may more closely related to *L. cyclotis* than *E. maximus* (Meyer *et al.*, 2017), which if true indicates a major taxonomic revision of the Elephantinae is required. Nevertheless, fossil evidence (morphology and chronology) has been argued to discredit this claim (Larramendi *et al.*, 2017: 310-11), so that *Palaeoloxodon* is provisionally used herein until this matter is further resolved: Siculo-Maltese elephants were first referred to the genus *Palaeoloxodon* in 1942 (Osborn, 1942: 913, 1171) and as many as six *Palaeoloxodon* spp. may be represented on the Siculo-Maltese palaeo-archipelago comprising Sicily, Malta and Favignana. Four likely species and one alleged subspecies are known from Sicily, three likely species from Malta, and one possible species from Favignana Island (Table 1.1; Table 1.2).

*Following taxonomic convention, the names of binomial authorities are placed in parentheses () where the original taxon name has been amended.

Due to taxonomic lumping (see e.g. Vaufrey, 1929 *inter alios*), particularly with regard to similar-sized *Palaeoloxodon* spp. from Sicily and Malta which may belong to separate species (see Herridge, 2010; Scarborough *et al.*, 2016), the systematic taxonomy presented here only includes material where the type-locality is named, or the publication cites the original excavation report. An exception is made for *P. falconeri* for which autapomorphies have been well-described (Adams, 1874; Ambrosetti, 1968; Herridge, 2010). The partial synonymy listed provides the most complete review for the species listed; however, due to the extensive literature (particularly Italian works which were difficult to obtain from South Africa), the synonymy presented is only partially complete. In addition to named species with designated type-collections, partial synonymies are also presented for the taxa with no type-locality or type-series listed in Table A1.1, using the largest and historically most important localities.

A1 Partial synonymy of Siculo-Maltese taxa with notes on systematic uncertainties

Taxon	Type localities	Type-series
<i>P. mnaidriensis</i>	Mnaidra Gap, Malta	Adams, 1874; Lydekker, 1886: 138-151; Osborn, 1942: 1264-1265; Herridge, 2010: Table A6.3, Table A6.4
<i>P. falconeri</i>	Zebbug Fissure, Malta	Busk, 1867; Lydekker, 1886: 151-167; Osborn, 1942: 1263-1264; Herridge, 2010: Table A6.1, Table A6.4

Table A1.1 Type-series of insular *Palaeoloxodon* spp. studied in this thesis.

A1.1 *Palaeoloxodon mnaidriensis* (ADAMS 1874) from Mnaidra Gap, Malta

- 1870 *Elephas mnaidrae* - Adams, pp. 224-228, 230, Plate II: Fig. 2
- 1874 *Elephas mnaidriensis* - Adams, p. 116, Plate 1 Figs 1-2, Fig. 9, Figs 14, 15, 16, Plate VII Fig. 1, Fig. 2.2a, Plate VIII Fig. 1.1a, Figs 2-5, Fig. 7, Fig. 8.8a, Plate X Figs 1-4, Fig. 6, Fig. 7.7a, Plate XI Figs 1-3, Figs 5-8, Plate XIV Fig. 1, Fig. 2.2a, Plate XV Fig. 1, Fig. 2.2a, Figs 3-4, Figs 7-8, Plate XVI Fig. 1-2, Fig. 4, Plate XVII Figs 1-4, Figs 12-13, Plate XVIII Fig. 1, Fig. 3, Plate XIX Fig. 2, Fig. 5(?), Figs 10-11, Fig 13(?), Fig. 14(?), Fig. 15(?), Plate XX Fig. 1,1, Fig. 4, Fig. 7-9, Fig. 10, Figs 12-13, Fig. 15, Fig. 22, Plate XXI Fig. 16
- 1925 *Loxodonta (Pilgrimia) mnaidrae* - Osborn, pp. 6, 23
- 1929 *Elephas mnaidriensis* - Vaufrey, Fig. 28.1, Fig. 28.4, Fig. 28.5, Fig. 28.10
- 1942 *Palaeoloxodon mnaidriensis* - Osborn, Fig. 27, Fig. 1132(6)
- 2008 *Palaeoloxodon mnaidriensis* - Ferretti, p. 105
- 2010 *Palaeoloxodon mnaidriensis* - Herridge, Fig. 4.8a-d

A1.2 *Palaeoloxodon falconeri* (BUSK 1867) from Malta and Sicily

- 1862 *Elephas melitensis* - Anonymous (Malta)
- 1867 *Elephas melitensis* - Falconer in Busk, pp.?
- 1867 *Elephas falconeri* - Busk (Malta), pp.?
- 1867 *Elephas melitensis* - Anca and Gemmellaro, p. 4 (Malta, unspecified)
- 1868 *Elephas Melitensis* - Falconer in Murchison, pp. 251 (note), 284, 299, 302, 303, 304, 307, Plate XI, Figs 1-3, Plate XII, Figs 1-4 (Zebbug Fissure, Malta)
- 1886 *Elephas melitensis* - Lydekker, pp. 151, 152, Fig. 27, Fig. 28 (Benghisa Gap, Mnaidra Gap, Zebbug Fissure, Malta)
- 1903 *Elephas Falconeri* - Woodward, p. 246 (Malta, unspecified)
- 1908 *Elephas falconeri* - Andrews, p. 39 (Malta, unspecified)
- 1925 *Loxodonta (Pilgrimia) falconeri* - Osborn, pp. 6, 23, (Malta, unspecified)
- 1929 *Elephas Falconeri* - Vaufrey, p. 76 (Zebbug Fissure, Malta)
- 1936 *Loxodonta (Pilgrimia) falconeri* - Osborn, pp. 32 (Malta, unspecified)
Palaeoloxodon falconeri - ibid. Fig. 1.25 (Malta, unspecified)
- 1942 *Palaeoloxodon falconeri* - Osborn, pp. 913, 1171, (Malta and Sicily)
- 1956 *Elephas Falconeri* - Imbesi, pp. 443, 445, caption of Fig. 3 (Luparello Fissure, Sicily)
Elephas antiquus Falconeri - ibid. p. 447
- 1962 *Elephas falconeri* - Accordi and Colaccichi, pp. 217, 219, 221, 222, 223, 224, 226, 228, 229, Fig. 3, Fig. 4, Fig. 5 (Malta and Spinagallo Cave, Sicily)
Elephas melitensis pp. 219, 221, 222, 223, 226, 228, 229 (Malta and Spinagallo Cave, Sicily)
- 1968 *Elephas falconeri* - Ambrosetti, various pages between 278-397, Figs 6-15, Figs 17-29, Fig. 34, Fig. 41, Plates I-XV (Spinagallo Cave, Sicily)
- 1973 *Elephas falconeri* - Maglio, pp. 31-33, 42, 66, 83, 94, 107, 118, Fig. 2A, Fig. 18C (Malta and Sicily)
- 1985 *Elephas (Palaeoloxodon) falconeri* - Belluomini and Bada, pp. 451-452, Fig. 2 (Malta and Sicily)
- 1988 *Palaeoloxodon antiquus falconeri* - Guenther, Fig. 3 (unspecified)
- 1992 *Elephas falconeri* - Bonfiglio and Insacco, pp. 198, 200, 202, 203, 206, Table 2, Plate 1 (Malta and Sicily)
- 1994 ?*Mammuthus falconeri* - Lister and Bahn, p. 34
- 1996 *Elephas falconeri* - Bonfiglio *et al.*, 1996, pp. 375, 377, 380, 381 (Malta and Sicily)
- 1996 ?*Mammuthus falconeri* - Mol *et al.*, p. 83 (unspecified)
- 1999 *Mammuthus falconeri* - van den Bergh, pp. 301, 302, 341, 342 (Sicily, unspecified)
- 2000 *Elephas falconeri* - Bonfiglio *et al.*, pp. 171, 173, 175, 176, 177, 178, 180, Table 1
- 2002a *Elephas falconeri* - Poulakakis *et al.* pp. 172, 179 (Sicily, unspecified)
- 2002 *Elephas falconeri* - Bonfiglio *et al.*, pp. 30, 33, 34, 35, 37, Table 1, Table 2 (Malta and Sicily, various sites)
- 2003 *Elephas falconeri* or '*Elephas*' *falconeri* - Palombo, pp. 273, 274, 275, 277, 278, 280, 283, 284, 287, 288, 289, Fig. 1, Fig. 2, Fig. 3, Fig. 4, Fig. 5, Fig. 6, Fig. 7A-B, Fig. 8, Fig. 9, Fig. 11 Fig. 12A-B (Malta and Sicily, various sites)
- 2007 *Elephas falconeri* - Abbate, pp. 5, 13, Fig. 7, Fig. 10, Fig. 11 (Sicily, various sites)

- 2010 *Elephas falconeri* - Benton *et al.*, 2010, pp. 442, 443 (Spinagallo Cave, Sicily)
- 2010 *Palaeoloxodon falconeri* - van der Geer *et al.*, pp. 11, 84, 85, 86, 87, 95, 97, 98, 306, 307, 308, 310, 311, 312, 313, 358, 359, 363, 364, 366, 378, 384, 386, 387, 388, Fig. 7.3 (artificial cast), Fig. 20.1 (artificial cast), Fig. 27.5, Plate 11 (artificial cast?) (Malta and Sicily)
- 2010 *Palaeoloxodon falconeri* - Herridge, various pages between 3-463, Fig. 1.1, Fig. 2.2, Fig. 4.7, (Malta and Sicily)
- 2012 *Elephas falconeri* - Dirks *et al.*, p. 83 (Spinagallo Cave, Sicily)
- 2013 *Palaeoloxodon falconeri* - Lomolino *et al.*, 2013, pp. 1428, 1434, 1436, Table 1, Fig. 6 (Spinagallo Cave, Sicily)
- 2016 *Palaeoloxodon falconeri* (Malta), *Palaeoloxodon* ex gr. *P. falconeri* (Sicily) - Scarborough *et al.*, pp. 112, 114-120, Fig. 7-5, Fig. 9-6

Although *P. melitensis* is the senior synonym for the smallest Maltese elephant (following the International Code of Zoological Nomenclature's Principal of Priority, article 81.2.3), the conditional suppression in favour of the junior synonym, *P. falconeri*, which should be maintained and applied to both *P. falconeri* and '*P. melitensis*' material from Malta has been recommended (Herridge, 2010: 192-193; see also Ambrosetti, 1968: 339; Herridge, 2012: 32-33). Further, although *P. falconeri* is a valid species name, the type-series from Malta consists of juveniles (Herridge, 2010: 130), and is therefore a *nomen dubium* according to the ICZN, which requires the designation of a neotype (article 75.6). Although there are some phenetic morphological differences between Sicilian assemblages (Spinagallo Cave and Luparello Fissure) and Maltese assemblages (Herridge, 2010: 148; 347), *P. falconeri* material from both islands shares autapomorphies, so that the designation of a neotype from Spinagallo Cave is recommended pending a submission and decision on this suggestion (Herridge, 2010: 193). However, lacking any compelling evidence of genetic interchanges among Maltese and Sicilian populations and to avoid any confusion, in this thesis *P. falconeri* was applied exclusively to Maltese material, and *P. ex gr. P. falconeri* to Sicilian material although it most likely a single species with a disjunct distribution.

A2 Partial synonymy of Siculo-Maltese taxa of uncertain systematic position

Taxon	Reference localities	Reference collections
<i>Palaeoloxodon</i> sp. 1	Luparello Fissure, Sicily	Vaufrey, 1929; Burgio <i>et al.</i> , 2002: 252; Scarborough <i>et al.</i> , 2016: Table 1
<i>P. antiquus leonardi</i>	Via Libertà, Palermo, Italy	GMP humerus and mandible
<i>P. ex gr. P. mnaidriensis</i>	Puntali Cave, Carini, Sicily	Burgio <i>et al.</i> , 1983: 73-74; Burgio and Di Patti, 1990; Di Patti <i>et al.</i> , 1995: 9-20; Palombo and Ferretti, 2005; Ferretti 2008; Herridge, 2010; Scarborough <i>et al.</i> , 2016: Table 1
<i>Palaeoloxodon</i> sp. 2	Faraglione Cave, Favignana Island	Capasso Barbato <i>et al.</i> , 1988: Figs 2-3

Table A1.2 Published reference material of *Palaeoloxodon* spp. from Sicily and Favignana Island for which the taxonomic status may require revision.

In addition to the species listed above, material from Sicily and Favignana islands likely includes new taxa still in need of taxonomic revision. In order to aid clarifying their systematic position partial synonymies are provided for the taxa in Table A1.2.

A2.1 *Palaeoloxodon antiquus leonardi* (AGUIRRE 1969a) from Via Libertà, Sicily

- 1932a *Elephas mnaidriensis* - Fabiani, p. 99
- 1968 *Elephas* cf. *antiquus* - Ambrosetti, 1968, pp. 342, 358
- 1969a *Palaeoloxodon antiquus leonardi* - Aguirre, pp.?
- 1991 *Elephas* cfr. *antiquus* - Bada *et al.*, p. 51
- 2001 *Palaeoloxodon antiquus leonardi* - Chilardi, p. 477
- 2004 *Elephas antiquus leonardi* - Caloi *et al.*, 2004, p. 234
- 2004 *Elephas antiquus leonardi* - Palombo, p. 357
- 2005 *Elephas (Palaeoloxodon) antiquus leonardii* - Palombo and Ferretti, p. 123
- 2010 *Palaeoloxodon antiquus*-sized taxon - Herridge, pp. 53, 80
- 2010 *Elephas mnaidriensis?* - van der Geer *et al.*, pp. 84, 90
- 2016 *Palaeoloxodon leonardi* - van der Geer *et al.*, in press
- 2016 *Palaeoloxodon antiquus leonardi?* - Scarborough *et al.*, 2016, p. 112

A2.2 *Palaeoloxodon* ex gr. *P. mnaidriensis* (ADAMS 1874) from Puntali Cave, Sicily

- 1893 *Elephas Melitae* - Pohlig, pp. 89, 92, 93, 94, 96, 97, 99, 100, Plate I: Figs 1-3, Plate II: Figs 1-3, Plate III: Figs 1-3, Plate IV: Fig. 1, Plate V: Fig. 1
Elephas (antiquus) Melitae - *ibid.* pp. 81
- 1912 *Elephas antiquus insularis* - Soergel, p. 1
- 1928 *Elephas (antiquus) mnaidriensis* - Fabiani, p. 34
- 1929 *Elephas antiquus mnaidriensis* - Vaufrey, Fig. 27.3, Fig. 30.5, Fig. 39, Fig. 40
Elephas mnaidriensis - *ibid.* p. 28, Fig. 30.5
- 1942 *Palaeoloxodon mnaidriensis* - Osborn, Fig. 1121, Fig. 1122
- 1963 *Elephas mnaidriensis* - Accordi, p. 301
- 1968 *Elephas mnaidriensis* - Ambrosetti, pp. 333, 341, 355, Fig. 53, Fig. 54
- 1969a *Loxodonta mnaidriensis* - Aguirre, pages?
- 1979 *Palaeoloxodon mnaidriensis* - Bonfiglio and Berdar, p. 151
- 1983 *Elephas mnaidriensis* - Burgio *et al.*, p.71, Fig. 3
- 1985 *Elephas (Palaeoloxodon) mnaidriensis* - Belluomini and Bada, pp. 451-452
- 1988 *Elephas (Palaeoloxodon) mnaidriensis* - Capasso Barbato *et al.*, pp. 102-103
- 1995 *Elephas (Palaeoloxodon) mnaidriensis* - Petronio, pp. 265-267
- 2005 *Elephas (Palaeoloxodon) “mnaidriensis”* - Palombo and Ferretti, p. 123, Fig. 13A-B
- 2008 *Palaeoloxodon mnaidriensis* - Ferretti, Fig. 3A-D, Fig. 4A-F, Fig. 5A-D, Fig. 6A-E, Fig. 7A-D, Fig. 8, Fig. 9A-J, Fig. 10A-L, Fig. 11A-D
- 2010 *Elephas mnaidriensis* - van der Geer *et al.*, Fig. 7.4
- 2010 *Palaeoloxodon mnaidriensis* - Herridge, p. 69, Fig 4.8e-h
- 2013 *Palaeoloxodon* sp. nov. - Bonfiglio, p. 616
- 2016 *Palaeoloxodon* ex gr. *Palaeoloxodon mnaidriensis* - Scarborough *et al.*, p. 115, Table 2, Fig. 7(2), Fig. 9(2)

Although the species name *E. (recte P.) mnaidriensis* was originally applied to Maltese material only (Adams, 1874), it was later applied to the material from Puntali Cave (Vaufrey, 1929). According to Herridge the Puntali Cave elephant is however a separate species to *P. mnaidriensis* (Herridge, 2010: 195; *ibid.* Table 7.1). According to Ferretti (2008) however, cranial autapomorphies are required to reliably settle the question as to the integrity of the Siculo-Maltese *P. mnaidriensis* hypodigm. Considering that recent research suggests the presence of a new species, but the issue is not yet definitely resolved, the Puntali Cave material is here provisionally referred to as *P. ex gr. P. mnaidriensis* in contrast to Maltese *P. mnaidriensis* derived from the type-locality of Mnaidra Gap in Section A1.3.

A2.3 *Palaeoloxodon* sp. 1 from Luparello Fissure, Sicily

- 1899 *Elephas antiquus* - De Gregorio (note: author does not distinguish between larger *Palaeoloxodon* sp. 1 and smaller *P. ex gr. P. falconeri* from Luparello Fissure)
- 1928 *Elephas (antiquus) melitensis* - Fabiani, p. 34
- 1929 *Elephas melitensis* - Vaufrey, pp. 52, 53, 77, 84, 112, 136, 141, 142, 143, 208, Fig. 7 annotation, Fig. 12, Fig. 20.6, Fig. 20.7, Fig. 22.5, Fig. 22.7, Fig. 23.1, Fig. 23.2, Fig. 23.4, Fig. 23.5, Fig. 23.7, Fig. 26 (middle), Plate V: Figs 1-9, Plate VII: Figs 4-9, Fig. 12, Fig. 14, Plate VIII: Figs 4-12
Elephas antiquus melitensis, *ibid.* Fig. 27.2
- 1930 *Elephas melitensis* - Vaufrey, p. 38
- 1942 *Palaeoloxodon melitensis* - Osborn, p. 1268 (pp. 1269, 1271 are reproductions of Vaufrey, 1929)
- 1956 *Elephas melitensis* - Imbesi, pp. 443, 445, 446, caption to Fig. 3
Elephas antiquus melitensis - *ibid.* p. 447
- 1968 *Elephas mnaidriensis* - Ambrosetti, p. 339
- 2004 *Elephas melitensis*-sized species - Caloi *et al.*, p. 239
- 2010 *Palaeoloxodon mnaidriensis?* - Herridge, pp. 192, 195
- 2010 *Elephas falconeri* - van der Geer *et al.*, p. 87
- 2014 *Palaeoloxodon 'melitensis'* - van der Geer *et al.*, pp. 135-138
- 2016 *Palaeoloxodon* sp. - Scarborough *et al.*, Table 1, pp. 114-118, 120, Fig. 7.4, Fig. 9.4, Fig. 9.5

Although large elephant remains from Luparello Fissure are often considered conspecific with Maltese remains, the Maltese *P. mnaidriensis* (Adams 1874) hypodigm may not encompass material from Luparello Fissure as previously suggested (*contra* Herridge, 2010: 192; 195; see Scarborough *et al.*, 2016), so that it is treated as a possible new species here. However, a difficulty presents itself in that there is more-or-less continuous variation in absolute size and also in morphology between larger *Palaeoloxodon* sp. 1 and smaller *P. ex gr. P. falconeri*. As a preliminary, albeit somewhat arbitrary solution to referring material to each species category one may therefore designate material that has a size exceeding the largest examples of *P. ex gr. P. falconeri* from Spinagallo Cave to *Palaeoloxodon* sp. 1 until the systematics of *Palaeoloxodon* sp. 1 is further clarified.

A2.4 *Palaeoloxodon* sp. 2 from Faraglione Cave, Favignana Island

1988 *Elephas* (*Palaeoloxodon*) sp. - Capasso Barbato *et al.*, Fig. 2a-b, Fig. 3a-e

2010 *Elephas* '*mnaidriensis*'? - van der Geer *et al.*, p. 90

A3 Phylogeny of Siculo-Maltese elephants

The phylogeny of elephants from Sicily, Malta and Favignana includes both anagenetic and cladogenetic taxa, the taxonomy of which is complicated due to several factors, including the clinal variation sometimes evidenced in the size and morphology of insular dwarf chronospecies (cf. Aiba *et al.*, 2010; van der Geer *et al.*, 2010: 368-370; Scarborough *et al.*, 2016). Clinal variation is further compounded by poor chronological control, largely stemming from the fact that Siculo-Maltese cave sites were excavated during the 19th century without detailed stratigraphic records being made and limited radiometric dating (Herridge, 2010: 357-377). The systematics and taxonomy of elephants from the Siculo-Maltese palaeo-archipelago therefore requires further clarification, particularly with regard to the material listed in Table A1.2. Nevertheless, a tentative evolutionary history based on the literature cited in this thesis and its original observations may be inferred, and is presented below.

Sicily (or its palaeo-islands) was likely colonized independently twice (possibly thrice) by *P. antiquus* or its descendants from Calabrian palaeo-islands, with each lineage in turn becoming extinct. The first lineage, and the one with the longest temporal representation on Sicily, was likely found there from the late Early Pleistocene (or early Middle Pleistocene) to the late Middle Pleistocene (Bonfiglio and Insacco, 1992: 202; Marra, 2013), although the presence of *P. antiquus* and early stages of endemic evolution are not yet reported. Morphological features in the species *P. ex gr. P. falconeri* indicate *P. antiquus* was the most likely ancestor of this phyletic lineage (Palombo, 2003; 2004; Herridge, 2010). This same phyletic lineage likely includes fossils belonging to two chronospecies from Luparello Fissure, namely the earlier and larger *Palaeoloxodon* sp. 1, followed by the ca. 1m-tall species *P. ex gr. P. falconeri* which became extinct during the late Middle or early Late Pleistocene. The cause and timing of *P. ex gr. P. falconeri* extinction on Sicily are uncertain, but may have had to do with the colonization of the island by mainland competitors or hyenas (Bonfiglio *et al.*, 2000: 175), or alternatively (though perhaps less likely) due to violent volcanism (see Herridge, 2010: 58).

Metric and qualitative phenetic morphological differences have also been reported in *P. ex gr. P. falconeri* remains from different parts of Sicily (Spinagallo Cave in the extreme south-east and Luparello Fissure in the extreme north-west, see Fig. 1.2), which has previously been considered to possibly indicate evolutionary independence due to geographic isolation (Herridge, 2010: 195). However, more recent dating of the Spinagallo Cave assemblage places its age within the late Middle Pleistocene (cf. Herridge *et al.*, 2014; Larramendi and Palombo, 2015: 102-103), ruling out the possibility of two separate palaeo-islands at this time. Nevertheless, the absolute age of the *P. ex gr. P. falconeri* remains from Luparello

Fissure remains unknown (Herridge, 2010: 347), such that there may be a difference in age between remains from different sites.

Following (or possibly contemporaneous with) the extinction of *P. ex gr. P. falconeri* on Sicily the second colonisation of the island by *P. antiquus* likely occurred during the Late Middle Pleistocene (Bonfiglio *et al.*, 2003), persisting until the Late Pleistocene. Three phyletic evolutionary stages have been hypothesized, represented as *Palaeoloxodon antiquus* (FALCONER and CAUTLEY 1847), the allegedly slightly size-reduced *Palaeoloxodon antiquus leonardi* AGUIRRE 1969a (represented at Via Libertà, Palermo, although the remains belonging to a single individual fall within the dimensional range of mainland *P. antiquus*, Palombo, pers. comm.), and finally the ca. 2m-tall endemic *P. ex gr. P. mnaidriensis* from Puntali Cave. A possible third colonization of Sicily that may have occurred during the late Middle Pleistocene has also been hypothesized on the basis of some very large individuals from Contrada Fusco in eastern Sicily (Palombo and Ferretti, 2005: 124). Whether or not this alleged third colonisation took place while *P. ex gr. P. mnaidriensis* was still present on Sicily is uncertain, and unlike the previous two colonisations the alleged colonisation probably never resulted in the evolution of an endemic species.

Palaeoloxodont elephants further colonized Malta and Favignana islands, using Sicily as a stepping-stone (*sensu* MacArthur and Wilson, 1967). Currently three taxa are recognised from Malta, *Palaeoloxodon falconeri* (BUSK 1867), *Palaeoloxodon mnaidriensis* (ADAMS 1874) and *Palaeoloxodon* sp. from Għar Dalam Cave (Herridge, 2010: 135), although the dating of most Maltese material is poorly constrained. However Maltese *P. mnaidriensis* or its ancestor may have colonised Malta during the Middle Pleistocene from Sicily, and *P. ex gr. P. falconeri* (or a slightly earlier phyletic representative) likely arrived from Sicily. Furthermore, Malta may have been colonized again during the late Middle Pleistocene or early Late Pleistocene by *Palaeoloxodon* sp. indet. from Sicily. Finally, scanty remains of a small elephant of Late Pleistocene age from Favignana, an Aegadian island off the west-coast of Sicily, may have been descended from *P. ex gr. P. mnaidriensis* as described from Puntali Cave, although further research is required to ascertain its age and taxonomic position (see Palombo, 2001b: 487).

**A4 Partial synonymy of *Mammuthus lamarmorai* (MAJOR 1883) from
Gonnesa, Sardinia**

- 1883 *Elephas Lamarmorae* - Major, p. 7
1903 *Elephas lamarmoræ* - Bate, p. 246
1929 *Elephas melitensis* - Vaufrey, p. 112, 141, 143, 194, 195, 209
1942 *Palæoloxodon lamarmorae* - Osborn, pp. 1266, 1457, 1476, 1542, 1595, 1603
1968 *Elephas lamarmorae* - Ambrosetti, p. 283
1999 *Mammuthus lamarmorai* - ICZN
2001 *Mammuthus lamarmorae* - Melis *et al.*, p. 481
2012 *Mammuthus lamarmorae* - Liscaljet, p. 283
2012 *Mammuthus lamarmorai* - Palombo *et al.*, Fig. 1-2, Fig. 4, Fig. 6-11, Fig. 14
2016 *Mammuthus lamarmorai* - Scarborough *et al.*, 2016, p. 112
2018 *Mammuthus lamarmorai* – Zoboli *et al.*, pp. 45-47, 52, 55-56, Fig. 3, Plate 1, Plate 2,
Plate 3, Plate 4,

For type-material from Gonnesa, Sardinia refer to Chiappini, 2006; Palombo *et al.*, 2012;
Zoboli *et al.*, 2018.

APPENDIX B

**Preliminary results of Uranium-Thorium dating at
Alcamo Quarry, Sicily**



Fig B1 a) Alcamo Quarry sampling location, with the author pointing to the associated exposed *Palaeoloxodon* sp. tusk. b) Close-up of exposed tusk in section, with sample removed from immediately to the left of the tusk.

Site description – The site is an abandoned travertine quarry located in the town of Alcamo, in the Province of Trapani of north-western Sicily. The limestone deposit (up to 20m thick) formed in the presence of cold-water springs, and consists of a Middle Pleistocene sandy travertine which was deposited near a coastal plain (Aloisi *et al.*, 2006: 22, 63), up to ca. 8m of which is currently exposed in a vertical section (Fig. 5.1a). Numerous Middle Pleistocene vertebrate and plant macrofossils have been recovered from the travertine quarry and surrounds of Alcamo (Chesi *et al.*, 2007; Aloisi *et al.*, 2006: 26, 29-30, 32-33). Fissures within the travertine are also infilled with red-earth including the remains of later *P.* ex gr. *P. mnaidriensis* belonging to either the Maccagnone or San Teodoro FC (see Aloisi *et al.*, 2006: 45-46, 64).

Pleistocene vertebrate fossils previously recovered from the travertine belong to the Middle Pleistocene Spinagallo FC, and include giant tortoise remains provisionally referred to the subfamily Testudininei indet. *Palaeoloxodon* remains recovered from within the travertine include long-bones, tusks and exceptionally-preserved endocasts) which have been attributed to *P.* ex gr. *P. falconeri* (see Burgio and Cani, 1988; Palombo and Giovinazzo, 2005; Aloisi *et al.*, 2006: 26-27, 31). Additional *Palaeoloxodon* remains are visible *in situ* within the section

exposed by mining (Aloisi *et al.*, 2006: 46), including a tusk exposed in section (Fig. 5.1) which has previously been referred to *P. ex gr. P. falconeri* (Aloisi *et al.*, 2006: 46).

Taxonomic affinity of the associated fossil tusk - Although all the elephant remains previously quarried from within the travertine and those still *in situ* have previously been ascribed to *E./P. falconeri*, remains from the Alcamo travertine are sometimes large relative to remains of *P. ex gr. P. falconeri* from Spinagallo Cave (Palombo, pers comm 2014, see metric study on the Spinagallo Cave assemblage in Ambrosetti, 1968), although metric data on limb bones are lacking from Alcamo. The *in situ* tusk (Fig. 5.1) which has previously been referred to *P. ex gr. P. falconeri* (Aloisi *et al.*, 2006: 46) measures 5cm in diameter, falling within the upper size-range of the maximum tusk diameter of *P. ex gr. P. falconeri* from Spinagallo Cave (see Ambrosetti, 1968: Fig. 16). However, the circumference of the proboscidean tusk varies along its length, as well as increasing in circumference during ontogeny, so that the tusk's referral to *P. ex gr. P. falconeri* on the basis of metrics and the associated fauna from similar layers of the Alcamo travertine awaits further verification.

Material and methods - A ca. 5 X 2 cm sample of travertine was collected from the lower area of one of the exposed sections (Fig. 5.1a) using a Dremel Drill with diamond-tipped rotary saw from the left of the matrix of the isolated exposed tusk in Fig. 5.1. Isotopic ratios were obtained using multi-collector inductively coupled plasma mass spectrometry (MC-ICPMS) techniques by Robyn Pickering and John Hellstrom (Department of Earth Sciences, University of Melbourne).

Results - The resulting ages were calculated for four-subsamples and are presented in Table B1a and B1b Two subsamples (AQ1.1 and AQ1.2) did not produce viable results due to high detrital Thorium content. The two viable results however produced a corrected age range of 514.370 to 551.303 ka, tentatively indicating a Middle Pleistocene age (see Section 5.5 for a discussion of these results in relation to elephant evolution).

Discussion - Under ideal conditions, U-Th dating operates under the assumption that newly deposited calcite contains no Thorium, and that all ^{230}Th is derived from the radioactive decay of ^{238}U . However, the Alcamo deposit consists of a sandy travertine, so that clastic inclusions (e.g. dust) cause the age to appear too old (Aitken, 1990: 127). However, U-Th ages may be adjusted with reference to the ratio of $^{230}\text{Th}/^{232}\text{Th}$, since this ratio provides a measure of detrital contamination due to the fact that ^{232}Th is not derived from the radioactive decay of ^{238}U . Due to the high content of contaminating detrital Thorium, the ages calculated from AQ1.3 and AQ1.4 may only be treated as provisional. The most reliable date (sample AQ1.3) produced a corrected age of 514,37 ka (which is in agreement with the previous suggestions of its Middle Pleistocene age of Alcamo fossils, see Aloisi *et al.*, 2006: 63), but may only be treated as tentative (see Section 5.5).

Sample ID	Lab number	Mass/g	238 ng/g	2SE	238/V	230/238A	95% ext.	234/238A	95% ext.
AQ1.1	UMD130821-537	0.0512	27	2	0.23	1.3724	0.0121	1.2173	0.0034
AQ1.2	UMD130821-538	0.0540	18	1	0.16	1.1954	0.0100	1.1283	0.0056
AQ1.3	UMD130821-539	0.0562	47	4	0.39	1.0392	0.0072	1.0346	0.0030
AQ1.4	UMD130821-553	0.0687	26	2	0.31	1.0630	0.0071	1.0495	0.0031

Table B1 a). Preliminary U-Th results from the Alcamo Quarry travertine deposit, western Sicily associated with an *in situ Palaeoloxodon* sp. tusk. Note that viable results were only obtained from subsamples AQ1.3 and AQ1.4, and require further verification due to the large associated errors.

Sample ID	Lab number	Age/Ka	95%err	232/238A	2SE	230/232i	2sd	230/232A	Age cr Ka	2se	[4/8]i Corr	2se
AQ1.1	UMD130821-537	0.000	0.000	2.463427	0.023324	0.60	0.60	0.6	125.192	1767.270	1.3580	0.2260
AQ1.2	UMD130821-538	0.000	0.000	0.306794	0.002675	0.60	0.60	3.9	797.245	326.690	2.4244	1.8981
AQ1.3	UMD130821-539	514.370	80.416	0.215046	0.003729	0.60	0.60	4.8	513.106	119.592	1.1495	0.0695
AQ1.4	UMD130821-553	551.303	104.643	0.365258	0.003893	0.60	0.60	2.9	543.820	158.034	1.2373	0.2353

Table B1 b) Preliminary U-Th results from the Alcamo Quarry travertine deposit, western Sicily associated with an *in situ Palaeoloxodon* sp. tusk. Note that viable results were only obtained from subsamples AQ1.3 and AQ1.4, and require further confirmation due to the large associated errors.

APPENDIX C

Insular endemic mammals with alleged evidence of low-gear locomotion

Order	Species	Island	Short limbs in relation to body length	Relative shortening of distal limbs	Tibio-fibular synostosis	Radio-ulnar synostosis	Restricted movement in patella	Short and stiff vertebral column	Short manus and pes with splayed phalanges	Foot-bones tightly bound by tendons	Fusions in manus	Fusions in pes	Robust metapodials or phalanges	Short metapodials or phalanges	Movement-restricting articular facets in foot bones	References
Proboscidea	<i>P. ex gr. P. falconeri</i>	Sicily, Malta	x	x	x	x										Sondaar, 1977: 686; van der Geer <i>et al.</i> , 2010: 313; Ambrosetti, 1968: 308-316; Larramendi and Palombo, 2015: 105
	<i>P. ex gr. P. mnaidriensis</i>	Sicily				x										Ferretti, 2008: 101
	<i>Stegodon aurorae</i>	Japan	x													Van der Geer <i>et al.</i> , 2010: 313
	<i>S. florensis insularis</i>	Flores				x										Van der Geer, 2014: 170
	<i>M. lamarmorai</i>	Sardinia				x										Palombo <i>et al.</i> , 2012: 164, 168
Artiodactyla	<i>Hippopotamus creutzburgi</i>	Crete											x	x		Boeckschoten and Sondaar, 1966: 31, 35; Sondaar, 1977: 686-687; Spaan <i>et al.</i> , 1994
	<i>Phanourios minutes</i>	Cyprus			x	x						x		x	?	Boeckschoten and Sondaar, 1972: 331; Leinders and Sondaar, 1974: 112; Sondaar, 1977: 685; Van der
	<i>Myotragus balearicus</i>	Majorca, Menorca							x		x					Sondaar, 1977: 684; Moyá-Solá, 1979; Leinders, 1979; Spoor, 1988: 307; Caloi and Palombo, 1994: 161; Köhler and Moyá-Solá, 2001; Bover <i>et al.</i> , 2005; Bover <i>et al.</i> , 2008: 138
	<i>M. palomboi</i>	Mallorca						x								Bover <i>et al.</i> , 2010: 878; 880-883
	<i>Bubalus mindorensis</i>	Mindoro	x										x			Rozzi and Palombo, 2014: 220 citing Custodio <i>et al.</i> , 1996
	<i>Hoplitomeryx</i>	Gargano				x	x					x				Van der Geer, 1999: 328; Van der Geer, 2005a: 236-238; Van der Geer, 2005b: 332; Van der Geer, 2014:
	<i>Hyotherium? insularis</i>	Sardinia											x	x		van der Made, 2008: 120
<i>Candiacervus sp.</i>	Crete				x										Van der Geer, 2005a: 236; Van der Geer, 2014	
Lagomorpha	<i>Nuralagus rex</i>	Minorca						x	x				x			Quintana <i>et al.</i> , 2011
	<i>Pentalagus furnessi</i>	Amami Ōshima											x	x		Yamada and Cervantes, 2005: 1; Moncunill-Solá <i>et al.</i> , 2018: 360
Primates	<i>Homo floresiensis</i>	Flores	x													van Heteren, 2012: 176

Table C1 Insular endemic mammals displaying alleged evidence of low-gear locomotion (*sensu* Sondaar, 1977) and their alleged specific morphofunctional adaptations.

APPENDIX D

**Preliminary catalogue of the unaccessioned
Palaeoloxodon sp. remains from Luparello Fissure, Sicily
in the Vaufrey collection
(Insitut de Paléontologie Humaine, Paris)**

Crate #	Sachet #	Preliminary species identification	Element	Preservation
1	279	<i>Palaeoloxodon</i> sp. 1?	Tooth	-
1	280	<i>Palaeoloxodon</i> sp. 1?	Tooth	-
1	282	<i>Palaeoloxodon</i> sp. 1?	Tooth	-
1	287	<i>Palaeoloxodon</i> sp. 1?	Tooth	Fragment
3	149	<i>Palaeoloxodon</i> sp. 1?	Vertebra	-
3	150	<i>Palaeoloxodon</i> sp. 1?	Vertebra	-
3	152	<i>Palaeoloxodon</i> sp. 1?	Vertebra	-
3	154	<i>Palaeoloxodon</i> sp. 1?	Vertebra	-
3	155	<i>Palaeoloxodon</i> sp. 1?	Vertebra	-
3	156	<i>Palaeoloxodon</i> sp. 1?	Vertebra	-
3	157	<i>Palaeoloxodon</i> sp. 1?	Vertebra	-
3	158	<i>Palaeoloxodon</i> sp. 1?	Vertebra	-
3	160	<i>Palaeoloxodon</i> sp. 1?	Vertebra	-
3	161	<i>Palaeoloxodon</i> sp. 1?	Vertebra	-
3	162	<i>Palaeoloxodon</i> sp. 1?	Vertebra	-
3	165	<i>Palaeoloxodon</i> sp. 1?	Vertebra	-
3	166	<i>Palaeoloxodon</i> sp. 1?	Vertebra	-
3	170	<i>Palaeoloxodon</i> sp. 1?	Vertebra	-
4	288	<i>Palaeoloxodon</i> sp. 1?	Vertebra	-
4	290	<i>Palaeoloxodon</i> sp. 1?	Vertebra	-
4	296	<i>Palaeoloxodon</i> sp. 1?	Vertebra	-
4	301	<i>Palaeoloxodon</i> sp. 1?	Vertebra	-
3	164	<i>Palaeoloxodon</i> sp. 1?	Acetabulum	
4	289	<i>Palaeoloxodon</i> sp. 1?	Femur	Diaphysis
4	291	<i>Palaeoloxodon</i> sp. 1?	Femur	Distal epiphysis
4	298	<i>Palaeoloxodon</i> sp. 1?	Femur	Distal epiphysis
4	314	<i>Palaeoloxodon</i> sp. 1?	Femur	Distal
4	326	<i>Palaeoloxodon</i> sp. 1?	Femur	Missing distal end
3	163	<i>Palaeoloxodon</i> sp. 1?	Femur	Head (fused)
3	167	<i>Palaeoloxodon</i> sp. 1?	Femur	Proximal, head fused
3	151	<i>Palaeoloxodon</i> sp. 1?	Tibia	Medial side of prox. part
3	153	<i>Palaeoloxodon</i> sp. 1?	Tibia	Proximal
4	293	<i>Palaeoloxodon</i> sp. 1?	Patella	-
4	294	<i>Palaeoloxodon</i> sp. 1?	Patella	-
4	295	<i>Palaeoloxodon</i> sp. 1?	Patella	-
4	299	<i>Palaeoloxodon</i> sp. 1?	Patella	-
4	300	<i>Palaeoloxodon</i> sp. 1?	Patella	-
4	303	<i>Palaeoloxodon</i> sp. 1?	Patella	-
4	305	<i>Palaeoloxodon</i> sp. 1?	Patella	-
1	259	<i>Palaeoloxodon</i> sp. 1?	Os t. III?	-
1	252	<i>Palaeoloxodon</i> sp. 1?	Os t. IV	-
1	237	<i>Palaeoloxodon</i> sp. 1?	Astragalus	-
1	238	<i>Palaeoloxodon</i> sp. 1?	Astragalus	-

Table D1 Preliminary identification of unaccessioned *Palaeoloxodon* spp. remains from Luparello Fissure, Sicily, excavated by Raymond Vaufrey in 1925/1926 (Vaufrey, 1929: 1).

Crate #	Sachet #	Preliminary species identification	Element	Preservation
1	239	<i>Palaeoloxodon</i> sp. 1?	Astragalus	-
1	240	<i>Palaeoloxodon</i> sp. 1?	Astragalus	-
1	241	<i>Palaeoloxodon</i> sp. 1?	Astragalus	-
1	242	<i>Palaeoloxodon</i> sp. 1?	Astragalus	-
1	243	<i>Palaeoloxodon</i> sp. 1?	Astragalus	-
1	251	<i>Palaeoloxodon</i> sp. 1?	Astragalus	-
1	257	<i>Palaeoloxodon</i> sp. 1?	Astragalus	Fragment
1	247	<i>Palaeoloxodon</i> sp. 1?	Calcaneus	-
1	248	<i>Palaeoloxodon</i> sp. 1?	Calcaneus	-
1	249	<i>Palaeoloxodon</i> sp. 1?	Calcaneus	-
1	250	<i>Palaeoloxodon</i> sp. 1?	Calcaneus	-
3	168	<i>Palaeoloxodon</i> sp. 1?	Ulna	Proximal
1	260	<i>Palaeoloxodon</i> sp. 1?	Ulnar carpal	-
1	261	<i>Palaeoloxodon</i> sp. 1?	Ulnar carpal	-
1	262	<i>Palaeoloxodon</i> sp. 1?	Ulnar carpal	-
1	278	<i>Palaeoloxodon</i> sp. 1?	Ulnar carpal	-
1	266	<i>Palaeoloxodon</i> sp. 1?	Intermediate carpal	-
1	269	<i>Palaeoloxodon</i> sp. 1?	Intermediate carpal	-
1	270	<i>Palaeoloxodon</i> sp. 1?	Intermediate carpal	-
1	271	<i>Palaeoloxodon</i> sp. 1?	Intermediate carpal	-
1	255	<i>Palaeoloxodon</i> sp. 1?	Os c. III?	-
1	252	<i>Palaeoloxodon</i> sp. 1?	Os c. IV	-
1	283	<i>Palaeoloxodon</i> sp. 1?	Os c. IV	-
1	284	<i>Palaeoloxodon</i> sp. 1?	Os c. IV	-
1	285	<i>Palaeoloxodon</i> sp. 1?	Os c. IV	-
1	286	<i>Palaeoloxodon</i> sp. 1?	Os c. IV	-
1	-	<i>Palaeoloxodon</i> sp. 1?	Os c. IV	-
1	275	? <i>Palaeoloxodon</i> sp.	Mandibular ramus?	-
1	272	<i>Palaeoloxodon</i> sp.	Tooth	Fragment
1	277	<i>Palaeoloxodon</i> sp.	Tooth	Fragment
1	265	? <i>Palaeoloxodon</i> sp.	Tooth	Fragment
1	267	? <i>Palaeoloxodon</i> sp.	Tooth	Fragment
1	268	? <i>Palaeoloxodon</i> sp.	Tooth	Fragment
3	159	<i>Palaeoloxodon</i> sp.	Femur	Unatt. head
4	292	<i>Palaeoloxodon</i> sp.	Patella	-
4	302	<i>Palaeoloxodon</i> sp.	Patella	-
2	203	<i>Palaeoloxodon</i> sp.	Radius	Distal
4	323	<i>Palaeoloxodon</i> sp.	Phalange	-
1	276	<i>Palaeoloxodon</i> sp.	Metapodial	-
2	224	<i>Palaeoloxodon</i> ex gr. <i>P. falconeri</i>	Vertebra?	Corpus?
4	319	<i>Palaeoloxodon</i> ex gr. <i>P. falconeri</i>	Vertebra	Corpus
2	195	<i>Palaeoloxodon</i> ex gr. <i>P. falconeri</i>	Vertebra?	Corpus?
2	174	<i>Palaeoloxodon</i> ex gr. <i>P. falconeri</i> ?	Pelvis?	-
2	180	<i>Palaeoloxodon</i> ex gr. <i>P. falconeri</i>	Femur	-
2	184	<i>Palaeoloxodon</i> ex gr. <i>P. falconeri</i>	Femur	-
2	186	<i>Palaeoloxodon</i> ex gr. <i>P. falconeri</i>	Femur	Distal

Table D1 continued.

Crate #	Sachet #	Preliminary species identification	Element	Preservation
2	189	<i>Palaeoloxodon ex gr. P. falconeri</i>	Femur	Missing distal end
2	204	<i>Palaeoloxodon ex gr. P. falconeri</i>	Femur	-
2	208	<i>Palaeoloxodon ex gr. P. falconeri</i>	Femur	-
2	209	<i>Palaeoloxodon ex gr. P. falconeri</i>	Femur	-
2	211	<i>Palaeoloxodon ex gr. P. falconeri</i>	Femur	-
2	220	<i>Palaeoloxodon ex gr. P. falconeri</i>	Femur	-
2	223	<i>Palaeoloxodon ex gr. P. falconeri</i>	Femur	Proximal
2	225	<i>Palaeoloxodon ex gr. P. falconeri</i>	Femur	Proximal
2	229	<i>Palaeoloxodon ex gr. P. falconeri</i>	Femur	Proximal
2	236	<i>Palaeoloxodon ex gr. P. falconeri</i>	Femur	Unattached head
2	171	<i>Palaeoloxodon ex gr. P. falconeri?</i>	Tibia	-
2	176	<i>Palaeoloxodon ex gr. P. falconeri</i>	Tibia	-
2	-	<i>Palaeoloxodon ex gr. P. falconeri</i>	Tibia	-
2	187	<i>Palaeoloxodon ex gr. P. falconeri</i>	Tibia	Proximal
2	193	<i>Palaeoloxodon ex gr. P. falconeri</i>	Tibia	-
2	196	<i>Palaeoloxodon ex gr. P. falconeri</i>	Tibia	-
2	197	<i>Palaeoloxodon ex gr. P. falconeri</i>	Tibia	-
2	200	<i>Palaeoloxodon ex gr. P. falconeri</i>	Tibia	-
2	202	<i>Palaeoloxodon ex gr. P. falconeri</i>	Tibia	-
2	218	<i>Palaeoloxodon ex gr. P. falconeri</i>	Tibia	-
2	230	<i>Palaeoloxodon ex gr. P. falconeri</i>	Tibia	-
2	232	<i>Palaeoloxodon ex gr. P. falconeri</i>	Tibia	-
2	235	<i>Palaeoloxodon ex gr. P. falconeri</i>	Tibia	-
2	277	<i>Palaeoloxodon ex gr. P. falconeri</i>	Tibia	-
3	169	<i>Palaeoloxodon ex gr. P. falconeri</i>	Tibia	-
4	321	<i>Palaeoloxodon ex gr. P. falconeri</i>	Patella	-
4	322	<i>Palaeoloxodon ex gr. P. falconeri</i>	Patella	-
4	235	<i>Palaeoloxodon ex gr. P. falconeri</i>	Patella	-
4	317	<i>Palaeoloxodon ex gr. P. falconeri</i>	Os. t. III	-
1	257	<i>Palaeoloxodon ex gr. P. falconeri</i>	Calcaneus	-
2	173	<i>Palaeoloxodon ex gr. P. falconeri</i>	Humerus	-
2	177	<i>Palaeoloxodon ex gr. P. falconeri</i>	Humerus	-
2	183	<i>Palaeoloxodon ex gr. P. falconeri</i>	Humerus	-
2	-	<i>Palaeoloxodon ex gr. P. falconeri</i>	Humerus	-
2	188	<i>Palaeoloxodon ex gr. P. falconeri</i>	Humerus?	Proximal?
2	190	<i>Palaeoloxodon ex gr. P. falconeri</i>	Humerus	-
2	194	<i>Palaeoloxodon ex gr. P. falconeri</i>	Humerus?	Distal?
2	198	<i>Palaeoloxodon ex gr. P. falconeri</i>	Humerus	Proximal
2	199	<i>Palaeoloxodon ex gr. P. falconeri</i>	Humerus	-
2	205	<i>Palaeoloxodon ex gr. P. falconeri</i>	Humerus	Proximal
2	207	<i>Palaeoloxodon ex gr. P. falconeri</i>	Humerus	Diaphysis
2	222	<i>Palaeoloxodon ex gr. P. falconeri</i>	Humerus	-
2	234	<i>Palaeoloxodon ex gr. P. falconeri</i>	Humerus	-
2	175	<i>Palaeoloxodon ex gr. P. falconeri</i>	Ulna	-

Table D1 continued.

Crate #	Sachet #	Preliminary species identification	Element	Preservation
2	186	<i>Palaeoloxodon ex gr. P. falconeri</i>	Ulna?	Distal?
2	192	<i>Palaeoloxodon ex gr. P. falconeri</i>	Ulna	-
2	206	<i>Palaeoloxodon ex gr. P. falconeri</i>	Ulna	-
2	210	<i>Palaeoloxodon ex gr. P. falconeri</i>	Ulna	-
2	212	<i>Palaeoloxodon ex gr. P. falconeri</i>	Ulna	-
2	214	<i>Palaeoloxodon ex gr. P. falconeri</i>	Ulna	Proximal
2	216	<i>Palaeoloxodon ex gr. P. falconeri</i>	Ulna	Proximal
2	226	<i>Palaeoloxodon ex gr. P. falconeri</i>	Ulna	-
2	228	<i>Palaeoloxodon ex gr. P. falconeri</i>	Ulna	Proximal
2	231	<i>Palaeoloxodon ex gr. P. falconeri</i>	Ulna	-
1	273	<i>Palaeoloxodon ex gr. P. falconeri</i>	Ulna-radius	Proximal radius
4	320	<i>Palaeoloxodon ex gr. P. falconeri</i>	Ulnar carpal	-
1	254	<i>Palaeoloxodon ex gr. P. falconeri</i>	Os c. III	-
1	255	<i>Palaeoloxodon ex gr. P. falconeri</i>	Os c. III	-
1	258	<i>Palaeoloxodon ex gr. P. falconeri</i>	Os c. III	-
1	264	<i>Palaeoloxodon ex gr. P. falconeri</i>	Os c. III	-
1	256	<i>Palaeoloxodon ex gr. P. falconeri</i>	Os c. IV	-
4	318	<i>Palaeoloxodon ex gr. P. falconeri</i>	Os c. IV	-
4	324	<i>Palaeoloxodon ex gr. P. falconeri</i>	Phalange	-
2	189	<i>Palaeoloxodon ex gr. P. falconeri</i>	Frag indet	-
2	191	<i>Palaeoloxodon ex gr. P. falconeri</i>	Frag	-

Table D1 continued.

The specimens listed in Table D1 were accidentally discovered in the basement of the IPH by the author in 2014, where they were being used as a teaching collection. With the possible exception of specimens reported by the excavator (Vaufrey, 1929) and the astragalus and calcaneus from this collection (Scarborough *et al.*, 2016), the remains in Appendix D have not been published before. Refer to Appendix A (Section A2.3) regarding the systematics and taxonomy of *Palaeoloxodon* sp. 1. Note that the preliminary species identification in this appendix is based on size, with *Palaeoloxodon* sp. 1 being larger than *P. ex gr. P. falconeri* although there is likely clinal variation in the size of specimens, and metric and statistical comparisons are still lacking for most specimens.

APPENDIX E

Regression table

Fig.	Taxon	Provenance	N	R ²	b	95% Low CI	95% Upp CI	t	P	Intercept
3.6a	<i>P. ex gr. P. falconeri</i>	Spinagallo Cave, Sicily	35	0.677	0.900	0.680	1.120	8.308	0.000	-0.423
	<i>Palaeoloxodon sp. 1</i>	Luparello Fissure, Sicily	4	0.030	0.160	-2.594	2.914	0.250	0.826	2.860
b	<i>P. ex gr. P. falconeri</i>	Spinagallo Cave, Sicily	36	0.750	0.839	0.670	1.008	10.087	0.000	0.479
	<i>Palaeoloxodon sp. 1</i>	Luparello Fissure, Sicily	4	0.724	1.899	-1.667	5.465	2.921	0.149	-3.931
3.8a	<i>P. ex gr. P. falconeri</i>	Spinagallo Cave, Sicily	14	0.776	0.931	0.616	1.245	6.449	0.000	0.389
	<i>P. antiquus</i>	NN1, Germany	15	0.878	0.940	0.730	1.150	9.675	0.000	0.466
c	<i>P. ex gr. P. falconeri</i>	Spinagallo Cave, Sicily	38	0.801	0.834	0.693	0.974	12.050	0.000	0.426
	<i>P. antiquus</i>	NN1, Germany	14	0.856	0.933	0.692	1.174	8.449	0.000	0.933
d	<i>P. ex gr. P. falconeri</i>	Spinagallo Cave, Sicily	36	0.945	1.104	0.971	1.237	16.863	0.000	-0.418
	<i>P. antiquus</i>	NN1, Germany	14	0.924	0.953	0.781	1.124	12.115	0.000	0.210
3.10a	<i>P. ex gr. P. falconeri</i>	Spinagallo Cave, Sicily	7	0.956	0.941	0.127	1.754	2.973	0.031	0.348
	<i>P. antiquus</i>	NN1, Germany	5	0.639	0.903	0.549	1.257	8.115	0.004	0.591
b	<i>P. ex gr. P. falconeri</i>	Spinagallo Cave, Sicily	7	0.715	0.945	0.259	1.632	3.539	0.017	0.395
	<i>P. tiliensis</i>	Charkadio Cave, Tilos	44	0.805	0.871	0.737	1.004	13.156	0.000	0.796
	<i>P. antiquus</i>	NN1, Germany	5	0.915	0.818	0.361	1.275	5.696	0.011	1.108
c	<i>P. ex gr. P. falconeri</i>	Spinagallo Cave, Sicily	6	0.688	1.140	0.074	2.206	2.970	0.041	-0.929
	<i>P. antiquus</i>	NN1, Germany	4	0.843	1.008	-0.316	2.331	3.276	0.082	-0.280
d	<i>P. ex gr. P. falconeri</i>	Spinagallo Cave, Sicily	9	0.319	0.600	-0.184	1.383	1.810	0.113	1.440
	<i>P. antiquus</i>	NN1, Germany	4	0.950	1.377	0.411	2.342	6.135	0.026	-1.094
E	<i>P. ex gr. P. falconeri</i>	Spinagallo Cave, Sicily	6	0.882	1.479	0.727	2.232	5.460	0.005	-3.129
	<i>P. antiquus</i>	NN1, Germany	4	0.769	1.386	-0.925	3.696	2.581	0.123	-3.461
3.13	<i>P. ex gr. P. falconeri</i>	Spinagallo Cave, Sicily	21	0.925	1.194	1.031	1.357	15.335	0.000	-1.444
	<i>P. tiliensis</i>	Charkadio Cave, Tilos	43	0.868	1.268	1.112	1.424	16.449	0.000	-1.748
	<i>P. antiquus</i>	NN1, Germany	13	0.635	0.716	0.356	1.076	4.376	0.001	0.944
3.14a	<i>P. ex gr. P. falconeri</i>	Spinagallo Cave, Sicily	21	0.774	0.772	0.572	0.973	8.057	0.000	1.246
	<i>P. antiquus</i>	NN1, Germany	13	0.844	0.872	0.623	1.122	7.708	0.000	0.924
B	<i>P. ex gr. P. falconeri</i>	Spinagallo Cave, Sicily	21	0.925	1.194	1.031	1.357	15.335	0.000	-1.444
	<i>P. tiliensis</i>	Charkadio Cave, Tilos	43	0.868	1.268	1.112	1.424	16.449	0.000	-1.748
	<i>P. antiquus</i>	NN1, Germany	13	0.635	0.716	0.356	1.076	4.376	0.001	0.944
C	<i>P. ex gr. P. falconeri</i>	Spinagallo Cave, Sicily	20	0.857	1.002	0.800	1.204	10.403	0.000	-0.094
	<i>P. antiquus</i>	NN1, Germany	6	0.864	0.555	0.250	0.861	5.041	0.007	0.555
D	<i>P. ex gr. P. falconeri</i>	Spinagallo Cave, Sicily	18	0.578	0.829	0.454	1.204	4.685	0.000	0.015
	<i>P. tiliensis</i>	Charkadio Cave, Tilos	29	0.669	0.964	0.697	1.232	7.389	0.000	-0.326
	<i>P. antiquus</i>	NN1, Germany	13	0.870	1.071	0.797	1.346	8.583	0.000	-0.728
3.16/ 3.17b	<i>P. ex gr. P. falconeri</i>	Spinagallo Cave, Sicily	51	0.806	1.054	0.905	1.202	14.287	0.000	-0.979
	<i>Palaeoloxodon sp. 1</i>	Luparello Fissure, Sicily	6	0.676	0.752	0.029	1.476	2.886	0.045	0.218
	<i>P. tiliensis</i>	Charkadio Cave, Tilos	53	0.785	1.049	0.895	1.203	13.639	0.000	-0.833
	<i>P. mnaidriensis</i>	Mnaidra Gap, Malta	3	0.835	0.733	-3.399	4.865	2.253	0.266	0.281
3.17c	<i>P. antiquus</i>	NN1, Germany	6	0.972	1.286	0.984	1.587	11.841	0.000	-2.195
	<i>P. ex gr. P. falconeri</i>	Spinagallo Cave, Sicily	53	0.842	0.985	0.865	1.104	16.506	0.000	-0.544
	<i>P. tiliensis</i>	Charkadio Cave, Tilos	56	0.822	0.950	0.829	1.071	15.769	0.000	-0.242
3.17d	<i>P. antiquus</i>	NN1, Germany	6	0.944	0.833	0.551	1.115	8.193	0.001	0.361
	<i>P. ex gr. P. falconeri</i>	Spinagallo Cave, Sicily	13	0.899	0.838	0.652	1.025	9.915	0.000	0.901
	<i>Palaeoloxodon sp. 1</i>	Luparello Fissure, Sicily	6	0.696	1.110	0.092	2.128	3.028	0.039	-0.109
3.22b	<i>P. mnaidriensis</i>	Mnaidra Gap, Malta	4	0.990	1.485	1.033	1.937	14.142	0.005	-1.731
	<i>P. antiquus</i>	NN1, Germany	5	0.869	0.993	0.285	1.701	4.464	0.021	0.443
	<i>P. ex gr. P. falconeri</i>	Spinagallo Cave, Sicily	47	0.795	0.909	0.771	1.048	13.216	0.000	0.616
	<i>Palaeoloxodon sp. 1</i>	Luparello Fissure, Sicily	3	0.999	-1.801	-2.339	-1.263	-42.560	0.015	10.838
3.22c	<i>P. ex gr. P. mnaidriensis</i>	Puntali Cave, Sicily	4	0.692	0.755	-0.777	2.287	2.119	0.168	1.364
	<i>P. antiquus</i>	NN1, Germany	8	0.922	1.044	0.624	1.465	6.891	0.002	0.231
	<i>P. ex gr. P. falconeri</i>	Spinagallo Cave, Sicily	52	0.717	0.999	0.820	1.177	11.251	0.000	-1.785
	<i>Palaeoloxodon sp. 1</i>	Luparello Fissure, Sicily	4	0.063	-0.241	-3.082	2.599	-0.366	0.750	1.677
3.22c	<i>P. ex gr. P. mnaidriensis</i>	Puntali Cave, Sicily	3	0.581	0.449	-4.393	5.291	1.178	0.448	1.930
	<i>P. tiliensis</i>	Charkadio Cave, Tilos	49	0.831	1.188	1.031	1.177	15.200	0.000	-3.872
	<i>P. antiquus</i>	NN1, Germany	7	0.889	0.828	0.535	1.120	6.918	0.000	0.340

Table E1 Regression table (all values calculated in SPSS version 19.0 or later).

Fig.	Taxon	Provenance	N	R ²	b	95% Low CI	95% Upp CI	t	P	Intercept
3.22d	<i>P. ex gr. P. falconeri</i>	Spinagallo Cave, Sicily	38	0.561	0.606	0.425	0.788	6.776	0.000	2.041
	<i>P. ex gr. P. mnaidriensis</i>	Puntali Cave, Sicily	3	0.006	-0.096	-15.332	15.140	-0.080	0.949	4.742
	<i>P. antiquus</i>	NN1, Germany	7	0.687	0.534	0.119	0.948	3.312	0.021	2.877
3.24a	<i>P. ex gr. P. falconeri</i>	Spinagallo Cave, Sicily	36	0.156	0.509	0.096	0.922	2.504	0.017	0.249
	<i>L. africana</i>	Kenya	13	0.089	-1.570	-5.120	1.980	-0.986	0.348	8.909
3.26a	<i>P. ex gr. P. falconeri</i>	Spinagallo Cave, Sicily	35	0.034	0.260	-0.234	0.754	1.071	0.292	1.223
	<i>Palaeoloxodon sp. 1</i>	Luparello Fissure, Sicily	5	0.737	-1.826	-3.831	0.179	-2.898	0.063	6.670
B	<i>P. ex gr. P. falconeri</i>	Spinagallo Cave, Sicily	37	0.177	0.416	0.104	0.728	2.707	0.011	1.049
	<i>Palaeoloxodon sp. 1</i>	Luparello Fissure, Sicily	4	0.172	-.094	-0.720	0.533	0-.645	0.585	6.681
C	<i>P. ex gr. P. falconeri</i>	Spinagallo Cave, Sicily	41	0.102	0.435	0.011	0.859	2.079	0.044	0.967
	<i>Palaeoloxodon sp. 1</i>	Luparello Fissure, Sicily	5	0.640	3.306	-1.247	7.860	2.311	0.104	-6.528
d	<i>P. ex gr. P. falconeri</i>	Spinagallo Cave, Sicily	35	0.071	0.476	-0.134	1.085	1.587	0.122	0.189
	<i>Palaeoloxodon sp. 1</i>	Luparello Fissure, Sicily	3	0.000	0.058	-83.297	83.412	0.009	0.994	1.318
3.32	<i>P. ex gr. P. falconeri</i>	Spinagallo Cave, Sicily	19	0.816	0.818	0.619	1.017	8.679	0.000	1.553
	<i>P. tiliensis</i>	Charkadio Cave, Tilos	35	0.624	0.720	0.522	0.918	7.396	0.000	2.365
	<i>P. antiquus</i>	NN1, Germany	7	0.981	1.053	0.887	1.220	16.241	0.000	-1.472
3.33b	<i>P. ex gr. P. falconeri</i>	Spinagallo Cave, Sicily	11	0.144	0.985	-0.824	2.793	1.232	0.249	-0.713
	<i>P. antiquus</i>	All sites	14	0.184	0.676	-0.218	1.569	1.647	0.125	0.640
c	<i>P. ex gr. P. falconeri</i>	Spinagallo Cave, Sicily	19	0.722	1.887	1.288	2.487	6.641	0.000	-5.153
	<i>P. tiliensis</i>	Charkadio Cave, Tilos	41	0.838	1.818	1.560	2.077	14.218	0.000	-4.907
	<i>P. antiquus</i>	Germany and Italy	4	0.321	.634	-2.172	3.440	0.972	0.433	0.396
d	<i>P. ex gr. P. falconeri</i>	Spinagallo Cave, Sicily	19	0.643	0.822	0.509	1.135	5.539	0.000	0.182
	<i>P. antiquus</i>	NN1, Germany	7	0.747	0.818	0.271	1.366	3.843	0.012	0.445
3.36	<i>P. ex gr. P. falconeri</i>	Spinagallo Cave, Sicily	9	0.900	0.891	0.625	1.157	7.916	0.000	0.247
	<i>P. tiliensis</i>	Charkadio Cave, Tilos	25	0.819	0.859	0.685	1.033	10.187	0.000	0.419
	<i>P. antiquus</i>	Central and Western Europe	14	0.700	0.701	0.412	0.989	5.290	0.000	1.259
3.38a	<i>P. ex gr. P. falconeri</i>	Spinagallo Cave, Sicily	30	0.035	0.114	-0.117	0.345	1.013	0.320	3.549
	<i>P. antiquus</i>	NN1, Germany	9	0.913	0.638	0.462	0.815	8.551	0.000	2.528
b	<i>P. ex gr. P. falconeri</i>	Spinagallo Cave, Sicily	46	0.599	0.662	0.497	0.826	8.100	0.000	0.727
	<i>P. tiliensis</i>	Charkadio Cave, Tilos	66	0.546	0.560	0.432	0.687	8.775	0.000	1.157
	<i>P. antiquus</i>	NN1, Germany	12	0.799	1.072	0.693	1.452	6.300	0.000	-0.697
c	<i>P. ex gr. P. falconeri</i>	Spinagallo Cave, Sicily	30	0.192	0.290	0.064	0.516	2.621	0.014	3.109
	<i>P. tiliensis</i>	Charkadio Cave, Tilos	65	0.320	1.122	0.710	1.535	5.439	0.000	0.930
	<i>P. antiquus</i>	NN1, Germany	12	0.800	0.510	0.330	0.690	6.316	0.000	3.289
3.40	<i>P. ex gr. P. falconeri</i>	Spinagallo Cave, Sicily	37	0.474	0.606	0.387	0.826	5.622	0.000	2.060
	<i>P. tiliensis</i>	Charkadio Cave, Tilos	43	0.684	1.599	1.256	1.942	9.415	0.000	-0.750
	<i>P. antiquus</i>	NN1, Germany	11	0.897	0.505	0.376	0.634	8.871	0.000	3.157
3.42	<i>P. ex gr. P. falconeri</i>	Spinagallo Cave, Sicily	30	0.812	0.807	0.657	0.957	11.012	0.000	1.291
	<i>P. tiliensis</i>	Charkadio Cave, Tilos	40	0.527	0.851	0.586	1.116	6.511	0.000	1.150
	<i>P. mnaidriensis</i>	Malta	4	0.056	0.374	-4.282	5.031	0.346	0.762	2.966
	<i>P. antiquus</i>	NN1, Germany	9	0.889	0.847	0.579	1.115	7.480	0.000	1.333
4.2a	<i>P. ex gr. P. falconeri</i>	Spinagallo Cave, Sicily	48	0.818	0.868	0.747	0.989	14.401	0.000	-0.497
	<i>P. antiquus</i>	NN1, Germany	8	0.764	1.030	0.457	1.603	4.401	0.005	-0.781
	<i>L. africana (fused)</i>	Kenya	5	0.899	1.616	0.618	2.614	5.155	0.014	-2.490
b	<i>P. ex gr. P. falconeri</i>	Spinagallo Cave, Sicily	51	0.981	1.084	1.041	1.127	50.739	0.000	-0.013
	<i>P. antiquus</i>	NN1, Germany	9	0.979	0.994	0.864	1.124	18.115	0.000	0.145
	<i>L. africana (fused)</i>	Kenya	5	0.983	0.897	0.681	1.114	13.183	0.001	0.426
c	<i>P. ex gr. P. falconeri</i>	Spinagallo Cave, Sicily	49	0.861	0.923	0.814	1.032	17.072	0.000	-0.475
	<i>P. antiquus</i>	NN1, Germany	8	0.809	1.043	0.536	1.550	5.037	0.002	-0.691
	<i>L. africana (fused)</i>	Kenya	5	0.899	1.463	0.561	2.365	5.160	0.014	-1.837
4.12a	<i>P. ex gr. P. falconeri</i>	Spinagallo Cave, Sicily	64	0.964	0.856	0.814	0.898	40.884	0.000	1.925
	<i>L. africana</i>	Kenya	22	0.986	0.859	0.812	0.906	38.046	0.000	2.296
b	<i>P. ex gr. P. falconeri</i>	Spinagallo Cave, Sicily	20	0.792	0.673	0.814	0.898	8.281	0.000	2.452
	<i>P. antiquus</i>	NN1, Germany	5	0.966	0.814	0.535	1.092	9.295	0.003	2.580
d...	<i>P. ex gr. P. falconeri</i>	Spinagallo Cave, Sicily	41	0.875	1.002	0.880	1.125	16.508	0.000	0.291

Table E1 continued.

Fig.	Taxon	Provenance	N	R ²	b	95% Low CI	95% Upp CI	t	P	Intercept
...d	<i>P. antiquus</i>	NN1, Germany	4	0.844	1.250	-0.385	2.884	3.290	0.081	-0.254
	<i>L. africana</i> (unfused + fused)	Kenya	25	0.995	1.062	1.031	1.094	69.136	0.000	0.128
4.17a	<i>P. ex gr. P. falconeri</i>	Spinagallo Cave, Sicily	15	0.618	0.681	0.360	1.001	4.590	0.001	2.394
	<i>P. tiliensis</i>	Charkadio Cave, Tilos	47	0.948	0.102 1	0.930	1.112	22.925	0.000	2.085
	<i>P. antiquus</i>	NN1, Germany	7	0.502	0.636	-0.092	1.364	2.245	0.075	2.989
b	<i>P. ex gr. P. falconeri</i> (fused)	Spinagallo Cave, Sicily	43	0.987	0.713	0.546	0.880	8.644	0.000	2.046
	<i>P. ex gr. P. falconeri</i> (unfused + fused)	Spinagallo Cave, Sicily	10 2	0.987	0.889	0.860	0.917	61.735	0.000	0.000
	<i>P. antiquus</i>	NN1, Germany	7	0.931	0.585	0.320	0.850	5.681	0.002	2.688
c	<i>P. ex gr. P. falconeri</i>	Spinagallo Cave, Sicily	17	0.963	0.963	0.551	1.375	4.980	0.000	0.287
	<i>P. tiliensis</i>	Charkadio Cave, Tilos	47	0.816	0.816	0.747	0.885	23.721	0.000	0.274
	<i>P. antiquus</i>	NN1, Germany	12	1.255	1.255	0.871	1.639	7.286	0.000	-0.489
d	<i>P. ex gr. P. falconeri</i>	Spinagallo Cave, Sicily	15	0.575	0.535	0.260	0.811	4.197	0.001	2.124
	<i>P. antiquus</i>	NN1, Germany	7	0.871	0.451	0.251	0.651	5.798	0.002	2.961
4.25	<i>P. ex gr. P. falconeri</i>	Spinagallo Cave, Sicily	23	0.935	1.012	0.891	1.132	17.397	0.000	-0.133
	<i>P. tiliensis</i>	Charkadio Cave, Tilos	40	0.972	0.914	0.863	0.964	36.385	0.000	-0.041
	<i>P. antiquus</i>	NN1, Germany	13	0.673	0.634	0.341	0.927	4.761	0.001	2.051
	<i>L. africana</i>	Kenya (all stages)	25	0.862	0.835	0.690	0.979	11.969	0.000	0.199
4.26a	<i>P. ex gr. P. falconeri</i>	Spinagallo Cave, Sicily	23	0.493	0.765	0.413	1.117	4.515	0.000	2.568
	<i>P. tiliensis</i>	Charkadio Cave, Tilos	17	0.975	1.116	1.018	1.214	24.170	0.000	2.075
	<i>P. antiquus</i>	NN1, Germany	7	0.871	0.949	0.529	1.369	5.806	0.002	2.309
b	<i>P. ex gr. P. falconeri</i>	Spinagallo Cave, Sicily	25	0.489	0.767	0.428	1.105	4.688	0.000	2.647
	<i>P. tiliensis</i>	Charkadio Cave, Tilos	17	0.954	1.218	1.070	1.365	17.640	0.000	2.117
	<i>P. antiquus</i>	NN1, Germany	7	0.518	0.695	-0.076	1.466	2.316	0.068	3.100
c	<i>P. ex gr. P. falconeri</i>	Spinagallo Cave, Sicily	24	0.679	0.778	0.541	1.014	6.829	0.000	0.673
	<i>P. antiquus</i>	NN1, Germany	10	0.760	0.849	0.460	1.238	5.036	0.001	0.699
d	<i>P. ex gr. P. falconeri</i>	Spinagallo Cave, Sicily	24	0.770	0.815	0.619	1.012	1.012	0.000	0.726
	<i>P. antiquus</i>	NN1, Germany	10	0.711	0.949	0.455	1.442	4.432	0.002	0.656
4.37a	<i>P. ex gr. P. falconeri</i>	Spinagallo Cave, Sicily	59	0.828	1.003	0.882	1.125	16.587	1.003	1.044
	<i>P. ex gr. P. mnaidriensis</i>	Puntali Cave, Sicily	12	0.235	0.417	-0.113	0.948	1.752	0.417	2.572
	<i>P. antiquus</i>	NN1, Germany	9	0.894	0.804	0.557	1.051	7.692	0.804	1.704
b	<i>P. ex gr. P. falconeri</i>	Spinagallo Cave, Sicily	59	0.769	0.935	0.799	1.071	13.770	0.935	1.315
	<i>P. ex gr. P. mnaidriensis</i>	Puntali Cave, Sicily	10	0.211	0.567	-0.327	1.461	1.463	0.567	2.283
	<i>P. antiquus</i>	NN1, Germany	10	0.860	0.822	0.551	1.092	7.013	0.822	1.817
c	<i>P. ex gr. P. falconeri</i>	Spinagallo Cave, Sicily	58	0.740	0.863	0.726	1.000	12.609	0.000	1.515
	<i>P. antiquus</i>	NN1, Germany	8	0.847	0.594	0.342	0.846	5.762	0.001	2.507
d	<i>P. ex gr. P. falconeri</i>	Spinagallo Cave, Sicily	66	0.792	0.873	0.761	0.984	15.615	0.000	1.657
	<i>P. antiquus</i>	NN1, Germany	9	0.884	0.840	0.568	1.112	7.301	0.000	1.965
4.38a	<i>P. ex gr. P. falconeri</i>	Spinagallo Cave, Sicily	65	0.770	0.812	0.700	0.924	14.511	0.000	2.075
	<i>P. ex gr. P. mnaidriensis</i>	Puntali Cave, Sicily	11	0.049	0.190	-0.442	0.823	0.681	0.513	3.326
	<i>P. antiquus</i>	NN1, Germany	9	0.808	0.618	0.349	0.888	5.426	0.001	2.772
4.41a	<i>P. ex gr. P. falconeri</i> (unfused)	Spinagallo Cave, Sicily	75	0.956	0.942	0.895	0.952	39.712	0.000	1.093
	<i>P. ex gr. P. falconeri</i> (fused)	Spinagallo Cave, Sicily	34	0.704	0.776	0.595	0.595	8.734	0.000	1.457
	<i>L. africana</i> (unfused)	Kenya	16	0.920	1.146	0.952	0.895	12.673	0.000	0.999
	<i>L. africana</i> (fused)	Kenya	6	1.000	0.563	0.551	0.551	127.397	0.000	2.528
b	<i>P. ex gr. P. falconeri</i> (unfused)	Spinagallo Cave, Sicily	65	0.974	0.938	0.899	0.977	48.232	0.000	0.264
	<i>P. ex gr. P. falconeri</i> (fused)	Spinagallo Cave, Sicily	31	0.767	0.706	0.558	0.854	9.771	0.000	0.640
	<i>L. africana</i> (unfused)	Kenya	16	0.906	0.820	0.668	0.972	11.601	0.000	0.587
	<i>L. africana</i> (fused)	Kenya	6	0.980	1.066	0.855	1.278	13.977	0.000	0.045
c	<i>P. ex gr. P. falconeri</i> (unfused)	Spinagallo Cave, Sicily	73	0.975	0.974	0.922	1.027	36.847	0.000	0.865
	<i>P. ex gr. P. falconeri</i> (fused)	Spinagallo Cave, Sicily	32	0.835	0.883	0.665	1.100	8.302	0.000	1.140
	<i>L. africana</i> (unfused)	Kenya	17	0.984	1.255	1.131	1.380	21.490	0.000	0.475
	<i>L. africana</i> (fused)	Kenya	6	0.991	0.518	0.420	0.616	14.662	0.000	2.532

Table E1 continued.

APPENDIX F

Scaling in *Palaeoloxodon* long-bones

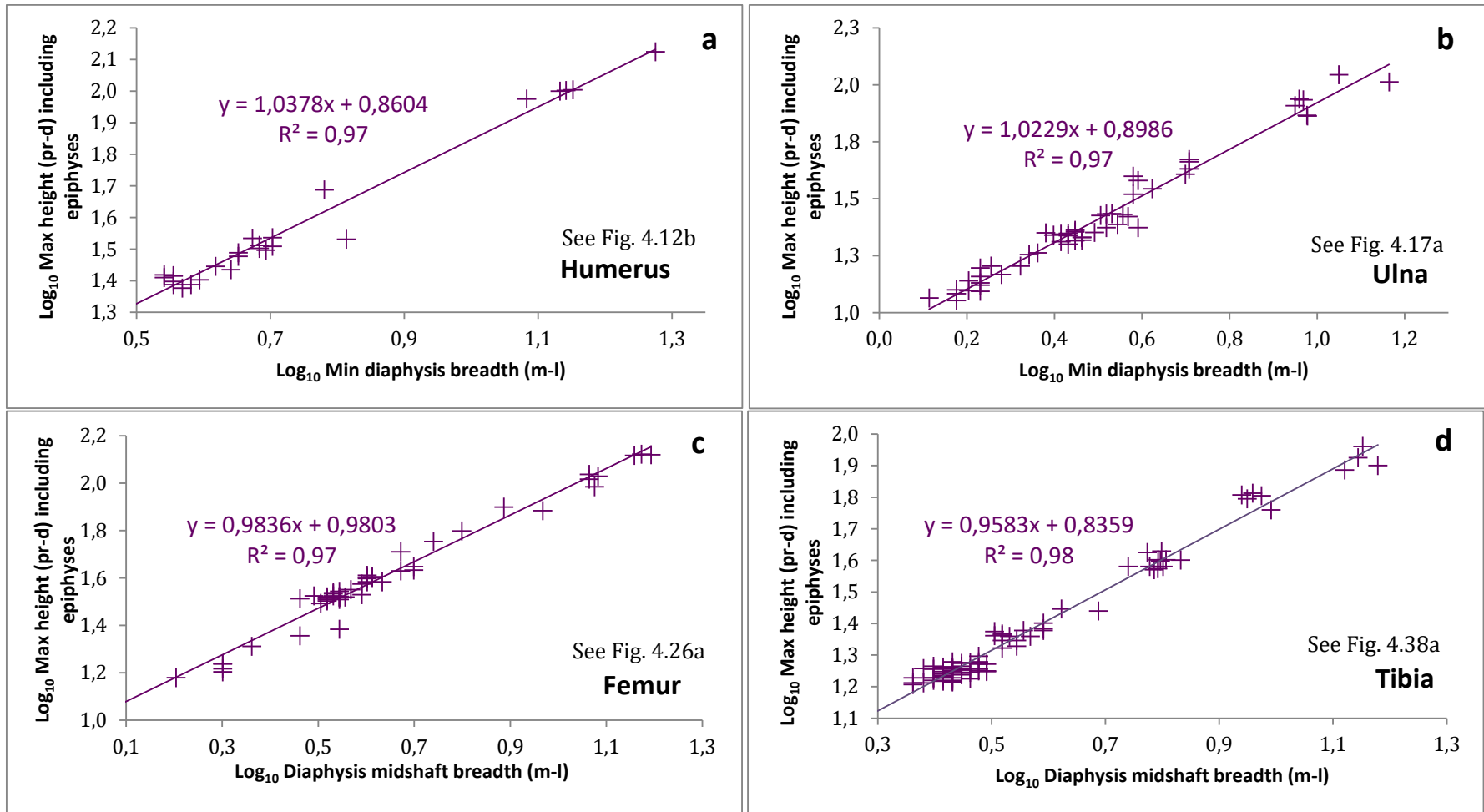


Fig. 6.1 Bivariate regression of *Palaeoloxodon* long-bone allometry for testing McMahon's elastic similarity hypothesis (McMahon, 1973; 1975; 1984; McMahon and Bonner, 1983; see p. 47 regarding methodology). Refer to Table 4.8 for statistical results. (Note \log_{10} - \log_{10} axes are used rather than \ln - \ln axes used elsewhere in this thesis order to compare with McMahon's predictions).